BIOACTIVITY-GUIDED ISOLATION AND STRUCTURE ELUCIDATION OF ANTIMALARIAL TRITERPENES FROM *Combretum zenkeri*ENGL & DIELS AND *Combretum racemosum*P. BEAUV. LEAVES

BY

Wande Michael OLUYEMI

Matric No: 159805

B. Sc. Industrial Chemistry (AAU, Akungba), M. Sc. Pharmaceutical Chemistry (Ibadan)

A Thesis in the Department of Pharmaceutical Chemistry
Submitted to the Faculty of Pharmacy
In partial fulfilment of the requirements for the Degree of

DOCTOR OF PHILOSOPHY

of the

UNIVERSITY OF IBADAN

FEBRUARY, 2020

ABSTRACT

Medicinal plants are rich sources of antimalarial compounds. Combretaceae family is known from ethnobotanical survey to possess broad spectrum of activities against different diseases including malaria. The increasing trend of resistance to many antimalarial agents including artemisinin and its derivatives has necessitated the need for new drug candidates. This study was, therefore, designed to validate the antimalarial potential of selected Combretaceae species, investigate the most active plant extracts by bioactivity-guided isolation and structure elucidation of the active principles.

Methanol and acetone extracts of the leaves of ten Combretaceae species, collected from the University of Ibadan Botanical Garden, were obtained by Soxhlet method. These extracts were screened for inhibition of β-hematin synthesis monitored with UV-Visible spectrophotometer at 405 nm. The most active methanol extracts, *Combretum racemosum* (CRM) [FHI/108887] and *Combretum zenkeri* (CZM) [FHI/110277] were screened against chloroquine-sensitive D10 and chloroquine-resistant W2 *Plasmodium falciparum* strains using lactate dehydrogenase assay with chloroquine as the standard. Both extracts were successively partitioned into chloroform and *n*-butanol by solvent-solvent partitioning, fractions obtained were also investigated for anti-plasmodial activity. The chloroform fractions were subjected to flash and column chromatographic techniques for bioactive compound isolation. Isolated compounds were characterised by NMR and MS techniques (1D and 2D NMR, ESI-MS and HR-ESIMS) and subjected to anti-plasmodial screening. Structure-activity relationship (SAR) study of the isolated compounds was conducted. The IC_{50} was calculated by curve-fitting analysis. Statistical analyses were conducted using a two-tailed Student's t test at $\alpha_{0.05}$.

The CZM (IC_{50}: 2.92±0.846 mg/mL) and CRM (IC_{50}: 3.96±0.132 mg/mL) crude extracts had significant activities. The CRM [D10: IC_{50}= 64.18±2.69 µg/mL (R^2 = 0.99); W2: IC_{50}= 65.80±14.85 µg/mL (R^2 = 0.96)] and CZM [D10: IC_{50}= 68.98±1.00 µg/mL (R^2 = 0.95); W2: IC_{50}= 69.68±3.09 µg/mL (R^2 = 0.99)] crude extracts showed antiplasmodial activity. The CRM chloroform fraction (D10: IC_{50}= 33.80±1.52 µg/mL; W2: IC_{50}= 27.82±2.85 µg/mL) showed higher activity relative to the n-butanol fraction (D10: IC_{50}= 78.08±7.29 µg/mL; W2: IC_{50}= 78.12±14.98 µg/mL). The chloroform fraction of CZM (D10: IC_{50}= 12.57±1.57 µg/mL; W2: IC_{50}= 12.14±0.95 µg/mL); also had higher activity than n-butanol fraction (D10: IC_{50}=

61.98±3.25 µg/mL; W2: IC_{50}= 61.26±8.64 µg/mL). Phytochemical isolation from the *C. racemosum* chloroform fraction led to the identification of four ursane-type triterpenes: 19α-hydroxyasiatic acid, 6β, 23-dihydroxytormentic acid, madecassic acid, nigaichigoside F1; four oleanane-type triterpenes: arjungenin, combregenin, terminolic acid, arjunglucoside I, and abscisic acid. All isolated compounds exhibited antiplasmodial activity (17.19±4.34 ≤ IC_{50} ≤ 134.70±13.21 µg/mL) with madecassic acid showing significant activity [D10: IC_{50}= 27.62±11.56 µg/mL (R^2 = 0.96); W2: IC_{50}= 17.19±4.34 µg/mL (R^2 = 0.98)]; however, chloroquine standard showed higher activity (D10: IC_{50}= 0.01±0.002 µg/mL; W2: IC_{50}= 0.22±0.03 µg/mL) than madecasic acid. The chloroform fraction of *C. zenkeri* led to the isolation of two triterpenes, ursolic and oleanolic acids, with known antimalarial activities. The SAR showed that dehydroxylation at 6β- and/or 19α-positions in these triterpenes increased the antiplasmodial activity, while the geminal-dimethyl substitutions at position C-20 did not significantly impact the bioactivity.

The antiplasmodial potential of *Combretum racemosum* and *Combretum zenkeri* was validated. Madecassic acid showed potential for antimalarial drug development.

Keywords: *Combretum zenkeri*, *Combretum racemosum*, Antiplasmodial activity, Triterpenes, Madecassic acid

Word count: 500

ACKNOWLEDGEMENTS

My profound gratitude goes to my supervisor, Dr. B.B. Samuel, who helped me understand my potentials and made my interest for research deepened. The lessons that prepared me for my Ph.D studies were taught to me by him during my master's programme. I appreciate your unflinching support and balanced critique of this work.

I gratefully appreciate my H.O.D., Prof. S.O. Idowu for his intelligent contribution in making my thesis smart and focused, and also for his effort in putting me through the appropriate statistics for my work. A well-deserved appreciation to all my postgraduate studies' lecturers, Prof. C.P. Babalola, Prof. S.O. Idowu, Prof. A.O. Adegoke, Dr. O.M.Adegbolagun and Dr. B.B. Samuel, who all taught me all I learned in my postgraduate education. Their impact is so much felt in my life like a foot-print on the rock; you are all inspirational and positive role models.

I thank the following technical staff in the Pharmaceutical Chemistry department: Mr. O. Adegboyega, Mr. T. Ale, Mr. M. Obitokun, Mr. A. Rasaq, you all contributed in a way to the success of this work. All my friends and colleagues in B.B. Samuel's natural products chemistry research group, Chinedu, Yemi, Maria, Faith, Omolara, Francis, Soliu, Fisayo, Olumide, Funke, Wale, Ayo, Elizabeth, Esther, it was interesting working with you guys.

I am highly grateful to the Association of African Universities (AAU) for the grant awarded to me in 2015 helping me to commence the preliminary studies of this work, which include the biological screening of the ten Combretaceae plants. I am also indebted to The Austrian Agency for International Cooperation in Education, Science and Research (OeAD-GmbH)-Ernst Mach for the scholarship awarded to me to carry out the phytochemical isolation part of this work in University of Vienna, Austria.

Many thanks to Prof. Liselotte Krenn, my host at the Phytochemistry/biodiscovery unit, Pharmacognosy department, University of Vienna, Austria for your indepth contributions to the completion of the phytochemical isolation part of this work. All the research trainings you gave me have shaped my competence and uncovered my potentials. Thank you for all the care and generosity shown to me. All members of phytochemistry/biodiscovery group of University

of Vienna, I say a big thank you for the warm reception you gave me during my stay. All the times that I spent in the group were fabulous moments!

I acknowledge and profoundly appreciate Prof. Hanspeter Kaelig of the Department of Organic Chemistry, Faculty of Chemistry University of Vienna, Austria for taking time out of your very busy schedules to carry out the NMR experiments of all my compounds isolated and also for the assistance you gave in elucidation of the structures. I acknowledge the contribution of Dr. Martin Zehl of the Department of Analytical Chemistry, Faculty of Chemistry, University of Vienna. You are highly appreciated for helping to carry out the mass spectrometer analysis of all my compounds in your laboratory.

My unreserved gratitude goes to Prof. Donatella Taramelli of Dipartimento di ScienzeFarmacologiche e Biomolecolari, Università degliStudi di Milano, Milan, Italyand her co-wokers for the assistance they rendered to ensure the antiplasmodial assay part of this work was conducted in her laboratory. When all hope was lost for this important part of the study to be achieved in Vienna, you saved the situationby agreeing to collaborate with us and make this work possible.

I am grateful to my Pastor and Pastor (Mrs) Fola Taiwo of Redeemed Christian Church of God, Chapel of His Glory Parish, Vienna for the fatherly and motherly care you showed to me. Thank you sir and ma for giving me the chance to serve my Master Jesus Christ in different capacity under your leadership during my stay in Vienna. It was indeed a training ground for me. You boycotted all protocols in order for me to utilize my short period of stay to serve the Lord in the workforce of the church. I can't forget that these services became a huge blessing to my Ph.D research work. Also, Deacon and Deaconess Richard Egobi, you are well appreciated for all your kind gestures and concerns. You are such an inspiration to me. Thanks for driving me home after church programs some of the times. My gratitude also goes to the families of Mr. Habeeb (Daddy Ayomide) and Mr. Iretiola (Daddy Nifemi) of Chapel of His Glory Parish, Vienna. Thanks for making me like your own family and for always inviting me to your houses and when leaving you will always pack foods and many other things for me to take along. I saved a lot of money because of your kind hearts. Many thanks to all members of the Sunday school, prayer and ushering Departments of Chapel of His Glory Parish, Vienna for your love and brotherly kindness. My story in Vienna can not be complete without

specially acknowledging and appreciating my kinsmen, my dear family friends in Vienna, Mr. and Mrs. Mike Adeleke Peacemaker. You gave me a warm welcome and helped my easy settling down in Vienna. Your house was like my second home; you made my stay in Vienna memorable. Thank you people for always asking how the research was going and for all the suiting encouragements.

I also show a deep appreciation to Pastor Kehinde Olofinkoya, my uncle in Vienna. Though I met you so late, about two months to my departure from Austria. However, within the short time we enjoyed together, you left on my heart indelible marks by the extreme love you and your family showed to me.

I appreciate all members of Christ Apostolic Church Students' Association Postgraduate Fellowship University of Ibadan (CACSAPGFUI) for their supports, prayers and encouragement throughout the period of this work.

My profound gratitude goes to my family friends, Folami and Folashade Ogunrinade, you are brother and sister from another mother. You called in virtually every week to check the progress of this work.

I am deeply grateful to my father and mother-in-law- late Elder and Deac. Olaniyi Famakinwa, all my brothers-in-law and sisters-in-law:the Famakinwas, Oduyemis, Adeloyes, Orogbades and Aderetisfor all their support given, their prayers, encouragement and for always checking and pushing for the work to be completed.

My profound gratitude goes to all my siblings for their supports in one way or the other during the course of this work. You guys have always stood by me, prayed for me, and I also drew so much strength from your words of encouragements. Mrs. Folasade Oni, Mrs. Olabisi Olalekan, Pastor Olajide Oluyemi, Engr. Olakunle Oluyemi, Olalekan Oluyemi, Oluseye Akinola and Motunrayo Akinola- it is a good thing to have you all as lovely siblings. Also, my dear niece-Omowumi Feyisayo Oni, thank you for always praying for the success of my Ph.D thesis. I say thank you to my daddy, Mr. Philip Oluyemi, for your support and asking about the progress of this work.

To my dear mummy, the rare gem in my life, Mrs. Victoria Aduke Oluyemi. Words are not enough to describe your sacrifice and commitment to my academic achievement. You promised to keep backing me until I am strong enough to stand on my own. You gave me the push that was needed to commence this Ph.D journey, and you supported me physically, emotionally, prayerfully and financially, all for it to be a success. I know I am so much indebted to you mum. Many thanks to you for believing in me.

To my most loving and admirable darling wife, Mrs Ayoola A. Oluyemi (RAS, MNSAP, MASAN), my God's gift- Ayomi, as I foundly call you. Your many sacrifices was instrumental to the success of this work. I left you back in Nigeria to far away Austria to complete this Ph.D work, though it was not easy for you during the several months of loneliness, but you supported the decision so that I could achieve my dream. You stood by me, and gave me the needed encouragement. My unreserved appreciation to you, sweetheart, for all your prayers and support.

To the most important One in my life, God Almighty. You gave words and revelations concerning this Ph.D, You favoured and supported it every stepof the way. You are the only reason why this is possible. I return all glory, honour and adoration to You, my God and Maker.

DEDICATION

This research work is dedicated to:

1. The Almighty God, the creator of heaven and earth; my help in the time of need.

2. My extraordinary mother, Mrs. Victoria Aduke Oluyemi, who has been my godmother and instrument in God's hand to help my academic pursuit to this highest degree.

CERTIFICATION

This is to certify that this project work was carried out byWande MichaelOLUYEMI in the Department of Pharmaceutical Chemistry, Faculty of Pharmacy, University of Ibadan, under my supervision.

…… ……

Supervisor **Date**

Dr. B.B. Samuel
B.Pharm, M.Sc, Ph.D, MPSN
Pharmaceutical Chemistry Department
Faculty of Pharmacy
University of Ibadan

TABLE OF CONTENTS

LIST OF TABLES

LIST OF FIGURES

LIST OF APPENDICES

CHAPTER ONE

1.0 GENERAL INTRODUCTION

1.1 RESEARCH CONTEXT AND OBJECTIVES

Malaria is an ancient infection and hasbeen enlistedamong the most fatal parasite-causing diseases in the globe since antiquity. Ithas remained, over previous decades, one crucial health complication which affects the health oflots of persons, predominantly in sub-Saharan Africadeveloping countries(Njoroge and Bussmann, 2006). The women with pregnancy and below age fivechildren are most prone to the malaria burden as a result of their weak immune system. The blood is infected when the female *Anopheles* mosquitoes transfer*Plasmodium* parasite from one person to another, thereby leading to the epidemicity of the disease. This epidemic is characterised by factors such as hot and humid climate, frequently combined with bad environmental habits, which are particularly associated with tropical regions.In 2015, a concerted effort was ensued to fight against malaria to accelerate progress towards malaria elimination and improve the situation for more robust investment towards malaria with 2016-2030 as set target for actualisation (WHO GST and WHO RBM AIM, 2015). However, in 2016 an estimated cases of *falciparum* malaria grew to 216 million cases globally from 211 million in 2015; a 2.4% increase which has caused a draw-back in the recent progress made in malaria eradication (WHO, 2017). Likewise in same 2016, more than 20% decrease in malaria cases was estimated in 16 countries out of the 91 countries endemic with malaria burden compared with 2015, however, an estimated rise of the same magnitude was observed in 25 countries with Africa and Latin America regions accounting for the largest proportion of these countries (WHO, 2017).The occurrence of malaria cases in 2017 was showed to be about 219 million, and consequently led to the death of nearly 435,000 persons corresponding toincidence in the preceding year (WHO, 2018). Severe anaemia and cerebral malaria is responsible for elevated degree of lethal outcome in young children.

Malaria infection has thrived for centuries, also, the efforts to control the widespread of the menace has increased over the years. The control of malaria has involved different approaches,examples include, insecticide treated bed nets (ITNs), effective drugs therapy usage as well asindoor residual spraying of insecticide (IRS)(Babamale *et al*., 2015; WHO, 2017). Presently, Artemisinin-based combination therapies (ACTs) remains the initial treatments for cases of malariathat is uncomplicated in many of the prevalent regions(WHO, 2015). Though,ACTs are expensive for the endemic low income region people (Mutabingwa, 2005), and the low-cost monotherapies like chloroquine and sulphadoxine has developed orare rapidly developing resistance from malaria parasite, resulting to increased mortality rate (RBM-WHO, 2006).Unfortunately, it has been reported that artemisinin as well as its derivativesare susceptible to increasing situations of resistance of *Plasmodium* parasite (Dondorp *et al.*, 2009).

The herbal medicines, which are sourced from medicinal plants, form major parts of therapies that are formulated to treat malaria. Apparently, some patients resort to the use of herbal preparations as their first choice of medication and some use them complementarily with the orthodox drugs. Meanwhile, it is well known that ethnomedicinal practice has shown to be a successful way the people living in developing countries readily access healthcare, where medicinal plants is being used for malaria prevention and treatment (Willcox and Bodeker, 2004; Willcox, 2011). The prominent use of herbal products may be hinged on the fact of its availability, relative affordability, as well as therapeutic effectiveness (Willcox and Bodeker, 2004). In Nigeria, the use of herbs is an age-long practice in which several of these plants are employed in the malaria management and cure as well as several other infections or ailments and they are documented appropriately(Adebayo and Krettli, 2011). Preparation of several of these plants into formulated herbal products are presently being carried out by accredited trado-medical practitioners, who marketed them in herbal clinics, retail outlets and pharmacy storeslocated mostly in the cities. As a result of this, the traditional method to the treatment of malaria is brought closer to people dwelling in urban areas that have no direct access to the plant products as a result of urbanisation, ethno-diversification among several reasons.

1.1.1Statement of the problem

Malaria has continued to show to be a crucial general health problem which affects several lots ofpersons, especiallythose in the sub-Sahara African developing countries. Many of the drug products in malaria treatment including artemisinin have suffered resistance, because of this, development of alternative treatment is necessary and very urgent. Plants of medicinal use, including those of the Combretacae family, have been utilised in ethnomedicine fortreating malaria and a number of other diseases by huge numbers of people in sub-Saharan African countrieswho get some recovery by their use.All the same,there is little or no scientifical information to support the therapeutic claims of greater number of these plants. In the same effect, just a little number ofplants from Combretaceae family have demonstrated to beusefulin treating malaria; only few were so far exploredto be able to derive useful activeingredients for treating malaria.

1.1.2Research question

It should be mentioned that the effect of malaria ismajor acrossAfrica, Asia as well as Latin America. Asia provided artemisinin forthe people and quinine was given by Latin America. The question on the minds of many researchers is that when will Africa utilise its biodiversitycoupled with a very large ethnomedicine to offer a new antimalarial drug to humanity?Following this fundamental question, answers will be provided to the two major research questions of this study.

Medicinal plants from thefamily of Combretaceae have been used in treating malaria, and several persons get some relief in their use in spite of the unavailability of scientific proof of antimalarial effect of many of these plants. Do the extracts of thesemedicinal plantsunder investigation have antiplasmodial property? What are the antiplasmodial principles present in these extracts?

1.1.3Research aim and the objectives

Thisresearch work was designed to validate the antimalarial efficacy of selected ethnomedicinally important plants from Combretaceae family, investigate the promising ones by abioactivity-guided isolation and structure elucidation of their active principles.

The objectives included to:

i. to collect and authenticate plants of the Combretaceae family
ii. screen acetone and methanol crude extracts of selected plants from Combretaceae family for antimalarial efficacy by application of the β-hematin synthesis inhibition
iii. select the most promising extract(s) from (i) and validate the antimalarial activity of its/their organic fractions
iv. carry out the isolation, characterisation and structure elucidation of the compounds from the most potent fractions and carry out their antiplasmodial test.

CHAPTER TWO

2.0 LITERATURE REVIEW

2.1MALARIA

The Italian originated the word malaria‘mala aria’ which signifies ‘bad air’. The English calledit malaria, ‘ague’ and ‘marsh fever’. Malaria has been known since antiquity; the records of showing its identifiable accounts were documented in several Egyptian Papyri. Fever, splenomegaly, as well as the usage of oil of the Balamites tree as repellant of mosquitoes were mentioned in the Ebers Papyrus (3550 BC). *Plasmodium* parasites are the cause of malaria infection, showing acute symptoms ranging from recurrent fever, headache, muscle and joint pain, vomiting, jaundice and anaemia to critical complications likesevere anaemia,acidosis, kidney failure, respiratory distress and cerebral malaria.

2.1.1Malaria parasites of humans

Female *Anopheles* mosquitoes which are the causative vector of malaria through blood infection transmit*Plasmodium* parasitesfrom one person toanother.Four of the five species of *Plasmodium* parasites (*P. falciparum*, *P. malariae*, *P. vivax* as well as *P. ovale*), which are the reason for human malaria, are known to be the *Plasmodium* species in people transfered from one individual to the other through female *Anopheles*mosquitoe’s bite. *Plasmodium knowlesi*, the fifth *Plasmodium* species, is found in persons when an *Anopheles* mosquito transfer infection through a bite from monkey to humans, so is not transmittedfrom human to human. *Plasmodium falciparium* showed to be the most deadly among the five *Plasmodium*species that human malaria originates from(WHO, 2015).*Plasmodium vivax* and *P. malariae*have among others almost obviously becomethe most widely distributed in the world. They have been recognized and identifiedby Europeans ever sinceprehistoriceras as theepisodic fevers(Anderson, 1927). These wereunconnected with the critical and frequently deadlyappearances of the recurring fevers (*P. falciparum*), which is characterised with display of asevere febrile occurrence, or paroxysm(Dobson, 1994).Currently, *P. malariae* no longer has the prevalence it used to show but *P. vivax* as well as*P. falciparum*are now parasites of

malariafrequently encountered.*Plasmodium vivax* is sometimes still located in few temperate regions, where its prevalence was widely present in the past. However, itsoccurrence remains frequentacross most of the tropics and subtropics. Due to the limitation of temperature on *P. falciparum* transmission, the occurrence is usually in temperate, tropical and subtropicalregions.Presently, *P. falciparum* has remained widely prevalent in the tropics.
Thereason for virulent malaria in humans which originated from*P. falciparum*, has been linked to *Gorilla gorilla*, thereby indicatingthat infections in human originated from this species (Liu*etal*., 2010).

2.1.2The economic and social burden of malaria

The human malaria disease is due to*Plasmodium*parasites, when it is transferred by *Anopheles*mosquitoes from one individual to the other. In adults, its frequent manifestations are high body temperature, aches and pains, headaches, weaknessand loss of appetite.It may show additional signs in children like nausea and vomiting. It is a severeailmentthat affectsall categories of persons but its effects are severer among pregnant women andchildren. Historically, malaria killed more warriors than warfare. Malaria has indeed contributed major part in the rise and falls of nations and has caused the death of numerous of people globally. It is estimated that human societies have shown lesser growth and development where malaria thrives most. The remarkable link between poverty and malaria is demonstrated by the spread of lower economic growth incountries where malaria is most prevalent. Malaria hampers development through many ways, includingworkers' productivity,investment and savings,fertility problem, growth rate of population, absenteeism, premature death and medical costs (Sachs and Malaney, 2002). Although, progress has been made in the last few years through several programmes and interventions towards eliminating the parasite (WHO, 2017). However, with the rapidly growing population in malaria-endemic regions, and in the absence of proactive political will from government, and sustaining of the current active intervention approaches, the sum of malaria incidence may likely increase over the succeeding twenty years. It is estimated that malaria shows economic burden in most endemic developing countries, due to the incurring of non-private as well as privatemedical expensesconnected with the illness as a main focus, as well as amount of the earnings that is foregone due to death from malaria. Private medical expenses areindividualexpenses on prophylaxis, diagnosis, and disease treatment.Factors considered as private medical cost include the expenses on bed nets,

price of antimalarial drugs,transportation expenses to medical facilities, doctor's feesas well as the requiredcare provided. Public expenses on both prevention and disease treatment is showed as non-private medical costs. Thesecontain governmentexpenses on mosquitoes control, facilities for healthcare, research and education. The estimation of the foregone earnings is calculated by the rate of absent workdays due to malaria and ailment related to malaria, based on estimation of wages. In the instance of premature death as a result of the infection, estimation of the foregone earnings is done based on the cumulativeworth of future salaries of the victim based on projected incomes if he/she should be alive. Beyond direct medical costs and foregone earnings, malaria can enforce economic burdens through other ways. The first is the occurrence that lead to changes in household behavior as a result ofthe illness, which may causewide social burdenleading to adverse effect on demography, migration, schooling and savings. Secondly, macroeconomic costs that is as a result of the prevalent manner of the disease. These among others include effect of malaria on commercial activities, foreign direct investment and tourism. These burdens are consequential and particularly critical for the people in the lowest income categories. Malaria is one among primary reasons of preventable death, predominantly among pregnant women and children, and this has raised serious health concern in Africa.Africa possesses the largest percentage of cases of malaria in the world, it shares a huge economic burden(Oluyole *et al*., 2011). Each month, malarial treatment cost between $2 and $25 and between $15 and $20 on prevention among family circles in Africa with consequent loss of resources (Oluyole *et al*., 2011). Thereducedproduction output and lost incomes due to declined quality of life, hospitalisations, treatment and other occurrences which are all human and economic costslinked to malaria are huge(Erhun *et al*., 2005). Malaria set limitationson the socio-economic growth of a country prevalent with it apart frombeing a challengeto the health of many(Sachs and Malaney 2002).

In Nigeria, available documentations showed that around 50% of the populace is down withat least one incident of malaria yearly while 2–4 attacks of malariaon the average is observed in under 5 children (Adedotun *et al*., 2010).About 7% of average family's monthly incomeis consumed because of cost of treatingmalariaas well as other ailments, and treatingmalaria casesonly constituted 2.91% to these; this alluded to the reality that more than 40% of the overallcost of health incurred by homes monthlyin Nigeria in comparison with other illnesses put together is because of malaria(Onwujekwe *et al*., 2000).

2.1.3The life cycle of malariaPlasmodium

The *Plasmodium*utilises two kinds of host (Figure 2.1): an invertebrate such as mosquitoes and a vertebrate such as reptiles, birds, or mammals. Theultimate host is the invertebrate where thesexual reproduction actualises. The intermediate host is the tissues of the vertebrate where the asexual reproduction occur.

Vertebrate phases: there is injection of saliva having sporozoites into the bloodstream of a vertebrate by mosquito with the infection whenin the process of taking blood-meal. After injection into the blood circulation, sporozoites cease to be visible in the circulating blood within one hour and infiltrate the parenchyma of the liver within one or two days(Figure 2.2). The reason sporozoites penetrate hepatocytes and never any other body cells is because a protein (circumsporozoite protein) which covers the surface of the sporozoite carries a ligand which attaches to receptors on basolateral domain of the membrane of liver cell. A series of asexual reproduction identified as the preerythrocytic cycle is initiated at the entry into the hepatocyte. The parasite metamorphosises into a feeding trophozoite in the liver cell. Schizogony begins after about a week, depending on species, at the maturation of trophozoites. There is first the formation of numerous daughter nuclei, converting the parasitesinto schizonts.

The amount of merozoites formed at the completion of the cycle is as well dependent on species: the estimation shows*P.malariae* forms 2,000 whereas*P.vivax* or *P.ovale* forms 10,000then30,000 is formed for *P.falciparum*(Garnham,1966). Erythrocytic cycle is initiated by the time merozoites depart from hepatic cells andinfiltrateerythrocytes. Entering the erythrocyte, the merozoite again converts into a trophozoite. A large food vacuole is formed by a host cytoplasm ingested by a trophozoite, making the young plasmodium have the look of a ring of cytoplasm (signet ring stage Figure 2.3) with the nucleus displaced to one side (like a signet ring). The food vacuoles of the trophozoite become less noticeable as it grows, but hemozoin pigment granules are deposited. The parasite quickly develops into a schizont. At a phase (segmenter stage) in the erythrocytic schizogony the nucleus divides several times and cytoplasm surrounds each nuclei.When merozoites finish developing, there

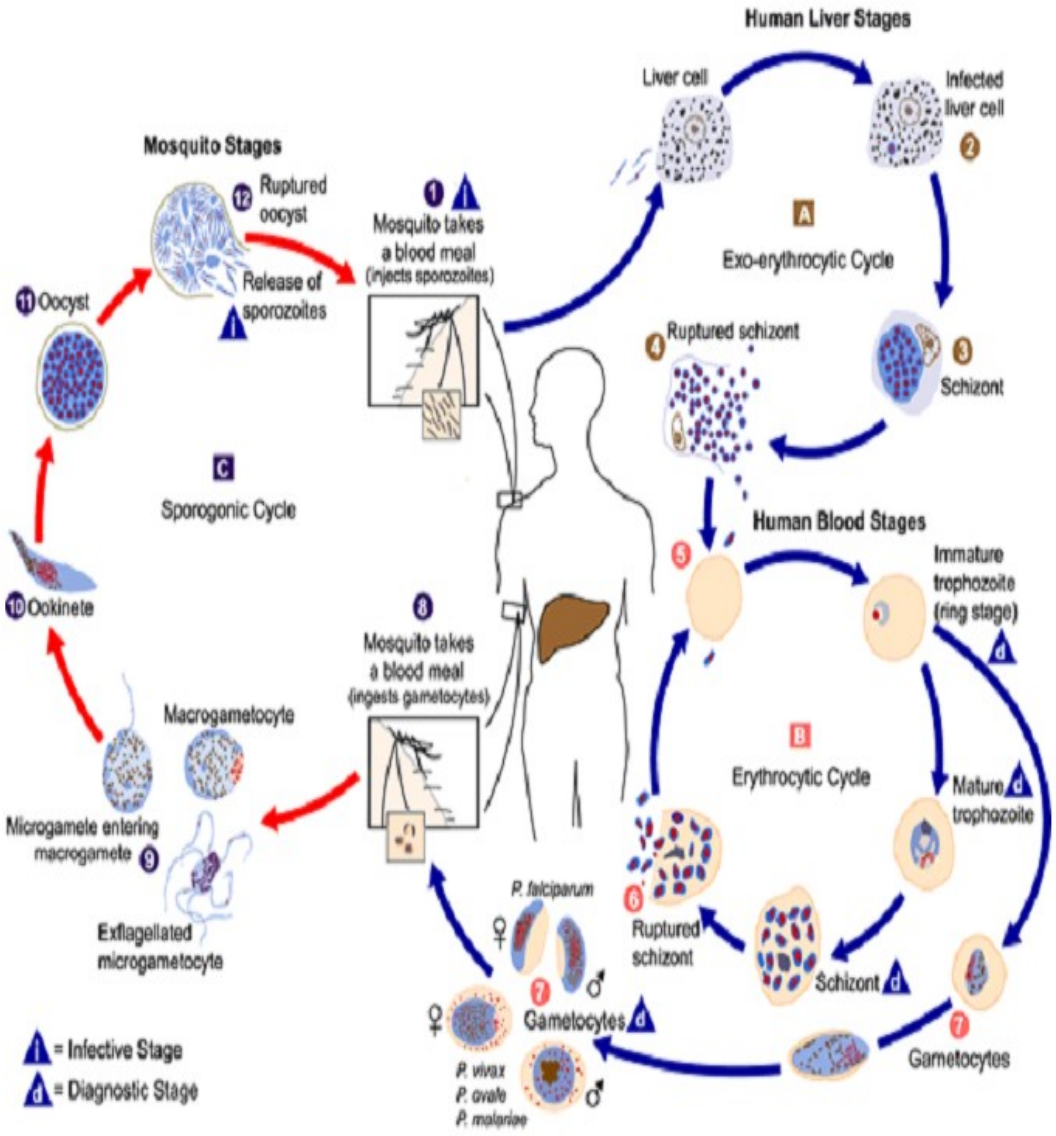

Figure 2.1: Life cycle of the malaria parasite (National Center of Infectious Disease, 2006).

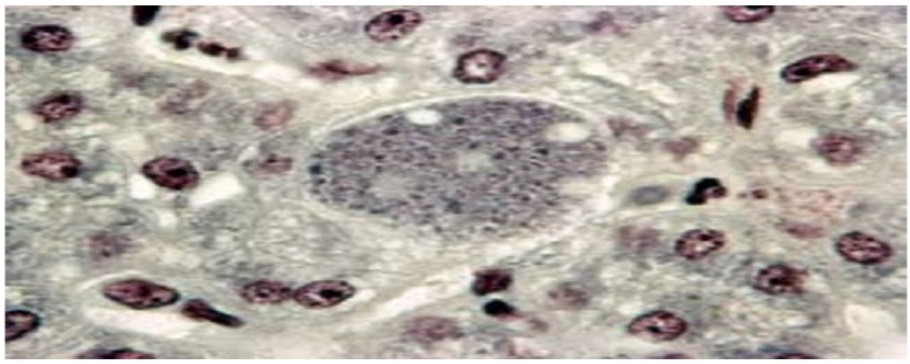

Figure 2.2: Exoerythrocytic stages of malaria in liver parenchymal cell.

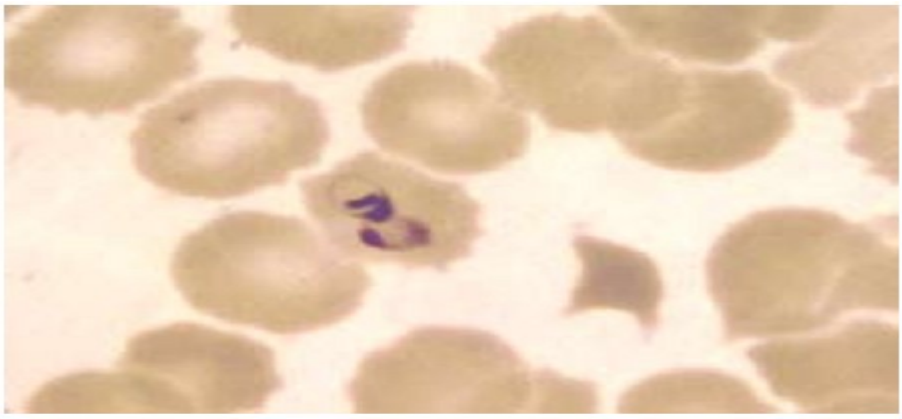

Figure 2.3: Signet ring stage of Plasmodium spp

is rupture of the host cell, parasite metabolic wastes and residual body, including hemozoin is released. Malaria symptoms are partly characterised by the metabolic wastes released. The rupture of the parasitised cells is synchronised such that they all rupture at definite intervals. It

is this periodicity which accounts for the bouts of fever at regular intervals, caused by a metabolic waste.

Invertebrate phases: Some of the merozoites, after some time, move into the erythrocytes and develop into gametocytes (microgametocytes and macrogametocytes). No further development occurs until theiringestion by a mosquito while it is sucking blood of an individual with infection. In the stomach of the mosquito, the development of the gametocytes into gametes takes place after emerging from the erythrocytes. Macrogametocyte matures to produce a single macrogamete, recognisable by a more peripherally located nucleus. The nucleus of the microgametocyte divides three times, each nucleus passing into the membrane surrounding the axoneme of each of eight flagella which have developed from the microgametocyte surface. This development is known as exflagellation, results in the formation of eight flagella-like microgametes which now break free from the gametocyte. The whole process takes place within 15 to 20 minutes.

A macrogamete is fertilised by one microgamete resulting in the formation of a zygote called an ookinete which enters between the stomach wall's cells and migrate facing the hemocoel, where it develops and form an oocyst. The nucleus of the oocyst splits several times, the first division being a reduction division to produce a number sporoblasts. This then divides further producing several sporozoites in thousands. Theformed oocyst spurts at maturation and there isrelease of sporozoites into the mosquito's hemocoel. Some of them penetrate the salivary gland and are injected with saliva into the bloodstream when the mosquito bites man to suck blood. They then invade the liver cells and the life cycle starts all over again (White *et al*., 2014).

2.1.4The pathogenesis, pathology and pathophysiology of malaria

The intracellular occupation of *Plasmodium*in the environment of the host cell allows asignificant modification. At the end of exo-erythrocytic schizogony, which ushers in the start of erythrocytic phase, there is asexual multiplication and discharge of merozoites into the blood circulation from hepatocytes and directed to host erythrocytes after the red blood cells ruptured. Thefresh merozoites produced undergo a repeat of similar process in the newerythrocytes (Bousema *et al*., 2014). There is need for egress of infected erythrocyte before reinvasion of fresh erythrocyte. Between the merozoites surface proteins (MSPs) andhost erythrocytes receptors,there is occurrence of numerous molecular interactionsduring

egress and internalisation process (Cowman *et al*., 2012). Moreover, when the parasite enters into the host cell there is modulation of the host environment to make it suitable and avoid the host defense. There are well-defined signaling mechanism which are employed by the parasite to mediate the modulation processes, and the description of this is shown at molecular and cellular levels (Parker *et al*., 2004). During disease pathogenesis, the roles and participation of cytokines in signaling pathways is already resolved; in spite ofthis, some proteins still remained uncharacterised. From drug discovery point of view, it will be helpful to understand the tactics employed by parasite to flourish well in the host by thestudy of diverse signaling mechanism in the course of the asexual erythrocytic phase (Miller *et al*., 2002), whichaffords novel contribution in developing an efficient antimalarial therapeutic strategy. In knockout study conductedon *P. berghei*PKG (PfPKG), it was demonstrated that at late liver sporozoites (LS) phase, hepatic cell lines (HePG2) can be infected by the parasite, but it was unsuccessful for it to be released as merosome from the hepatocytes. There is induction of protective immune response in the host by sporozoites at this stage(Falae *et al*., 2010). Thus, it reveals the importance of cyclic guanosine monophosphate (cGMP) signaling when merosome isformed and released.The exact function of protein kinase G (PKG) and what prompts its stimulation is not clear up till now. A thorough understanding of the signaling implicated in liver sporozoites would afford opportunity for disease pathologies controlin erythrocytic phase which could be an advantage in the preerythrocytic vaccine development andthe search forfuture malaria medication (Falae *et al*., 2010). Cyclic guanosine monophosphate (cGMP) showed to demonstrate a crucial function in gametogenesis;coupled with this,it has been established thatits functionality is well expressed during the ring and schizogony stage (Deng and Baker, 2002).

Changes in membrane permeability and thorough modification in erythrocytes are part of major processes involved during malaria (Sherman *et al*., 2004). The level of parasitemia in the host is established to be rightlyconnected to adenosine triphosphate (ATP) level released (Eaton and Brewer, 1969). The *Plasmodium*parasite becomes ineffectual to infect the new erythrocytes when there is any decrease in the level of ATP in the medium (Glushakova *et al*., 2013). The preventionof the parasite entrance via inhibitor-mediated purinergic receptor blockade and apyrase addition established the importance of ATP in the host invasion by parasite. The phosphorylation of skeleton protein such as spectrin which is existing in

erythrocyte mediates purinergic signaling response (Glushakova *et al*., 2013). The new permeation pathway is induced by purinoceptor signaling, therefore, there is reduction of membrane permeability via purinoceptors antagonist, suramin,and this leads to decline in parasite growth in*in vivo* as well as*in vitro*(Tanneur *et al*., 2006). After the host is infected with malaria, host-induced inflammation is mediated by ATP (Cruz *et al*., 2012).

The development of future antimalarial agentis possible by targeting the human kinase. This serves as an advantage as several kinase inhibitors had showed to be successful as anti-cancer agents in clinical trials stages. If this type of inhibitors showto kill the parasite, therefore they can serve as antimalarial agents at alesser cost,thereby reducing the wholeprolongeddrug development process. Also, the circumvention of the problem of drug resistance could be aided by targeting host protein (Sicard *et al*., 2011).

Calcium ion (Ca^{2+}) is one of the keymolecules that serve as secondary messenger which is required in the signal transduction. Several of its functionality in various facets of parasite lifecycleare for instance indevelopment, secretion, invasion, egress, growth and motility (Glushakova *et al*., 2013). Consequently, maintenance of Ca^{2+} homeostasis is important to the continued existence of the parasite. Ca^{2+} ions help in the regulation of diverse cellular actions when they bind to the effector molecules. However,the characterisation of the Ca^{2+}-dependent signaling components is not easy because of the absenceof effector molecules homology betweenhigher eukaryotes and*Plasmodium*(Prole and Taylor, 2011).

Malaria severity is accompanied with pathological symptoms which correspond to the increase in pro-inflammatory cytokines level.At the release of liver schizonts, infected persons indicated rise in the pro-inflammatory cytokines production, includinginterferon (IFN)-γ,interleukin (IL)-8 as well as IL-12(Schofield and Grau, 2005). Therefore, flaw in the inflammatory response will lead to disease severity(Schofield and Grau, 2005).In a severe malaria case study, increased levels of Toll-like receptor TLR2, TLR4as well as TLR8 were observed (Sobota *et al*., 2016). As a result of this, they could be good candidates for elucidatinginherent immune response mechanism in the process of parasite infection; inthis case, TLR ligands can be employed in therapeutic intervention (Gowda, 2007). Majority of thepathologies involved in malaria are connected with the cellular interaction between parasitic proteins and host (Miller *et al*., 2002; Ho and White, 1999).So, paying attention to the cytoadhesion response will assist in review of pathogenesis mechanisms.

A huge stock of proteins is transmitted on the surface of infected red blood cell (RBC) at the trophozoite phase. The attachement of these proteins to the endothelial cell, other infected RBC or new RBCs is what leadstosequestration of infected red blood cell in different tissue. Consequentially, it decreases the blood movement and circumvents the main movement to avoid the splenic clearance (Dondorp *et al*., 2000). The association of infected RBCs with intercellular adhesion molecule 1 (ICAM-1)in *P. falciparum* infectionis part of the explanations for progression in cerebral pathologies(Turner, 1997; Gray *et al*., 2003). There is increased level of the expression of ICAM-1during the inflammatory response. The infected RBCgrouping as well as their sticking to ICAM-1 has beenproposed as the reason whychildren that show severe malaria indicate intestinal bacterial infection(Church, 2016). Therefore, the development of anti-adhesion therapeutic agents combined with antimalarial agents are necessary to fight the infection (Bell and Boehm, 2013). The use of anti-adhesion therapeutic agents couldafford a noveloutlook in the decrease of the interactions associated with severe pathologies of malaria.

2.2Therapeutic potential of medicinal plants for drug discovery

The use of medicinal herbs for therapeutic purpose has evolved over several decades. Indigenous plants and herbs have been used for centuries across the world by traditional practitioners for treatingnumerousdiseases and they have demonstratedstrong pharmacological actions. Medicinal plants have been useful to humans since many centuries in the past for diverse diseases and have delivered valuable drugs likecardiotonics (digoxin),antihypertensives (reserpine),antineoplastics (vinblastine and taxol), analgesics (morphine), antitussives (codeine) and antimalarials (quinine and artemisinin). Medicinal plantsdrug discovery remain a means of providing novel and vital agents against several ailments including cancer, cardiovascular diseases, neurological disordersas well as malaria (Ramawat *et al*., 2009).

For thousands of years, they have undergone development and adaptation to resistinsects, bacteria, fungi as well as weather to yieldcharacteristic secondary metabolites. Bioactive constituents from them were utilised as primary source of drugs(McRae *et al*., 2007).Traditional medicines from plant source is still dependent upon by eighty percent (80%)

of general publicas means of primary health management, and eighty percent of the drugs resulting from plants justified the original traditional applicationof the plant source (Fabricant and Farnsworth, 2001). The traditional use of medicinal plantsfor treating several diseases have been for ages(Dias *et al*., 2012). They areconsidered to be the source of many active ingredients of drugs. In the application to discovery of drug, this is generallyacknowledged to be correct (Sneader, 1996). Despite the dominance of chemical synthesislately as a mode of discovering and producing medicines, the prospect of plants with bioactivity to offer new agents for treating and preventing diseases is still huge (Raskin *et al*., 2002). The persistence of killer diseases like diabetes and arthritis, coupled with the harmful side effects of synthesised drugs, prompted a change in interest from allopathy to natural/alternative systems of medicine. Ghosh *et al.*(2008) opined that natural products discovered from plantsrepresent astriking source of bioactive molecules compared with chemical synthesis,as they are from natural source and not costly. Likewisedrugs from plants may not possessthe same mechanisms like synthetic ones, also could be of medical relevance in health managementenhancement (Eloff, 1998). Successful development of natural products and synthetic products of natural origin for treating human diseases in nearly all therapeutic areas has been achieved (Newman and Cragg, 2007). Morphine turned out to be the foremost bioactive molecule derived purely from a plant in 1805, though its structure unknowntill 1923.*Atropa belladonna*, *Coffeaarabica*, *Erythroxylum coca*, *Ephedra* species, *Papaversomniferum*, *Physostigma venenosum* and*Cinchona succirubra* are plant species from where some alkaloids such as atropine, caffeine, cocaine, ephedrine, morphine,physostigmine andquinine, respectively were among several others isolated in the 19th century.As a result of this, biologically active agentsderived from plants werewidely used later, both in their modified as well as original forms, as drugs (Salim *et al*., 2008). Medicinal plants are enriched withsecondary metabolites, and it is due to the existenceof these compounds in them that they are called ‘drug/medicinal’ plants. These secondary plant productsapply anintense physiological action on human biological systems; thereforerecognised as the active principles of plants. Presently, there are 125 isolated drugs from roughly 100 plant species that are useful clinically. It was shown that around 5000 plants have been investigated extensively as potential origins of new drugs (Tantry, 2009). Majority of the world’s biodiversities are not

yetexplored for pharmacological potentials, therefore, several beneficial lead compounds areexpectedto be discovered from plants (Cragg and Newman, 2005).

2.2.1Ethnomedicinal healthcare practices

Ethnomedicinal practices were the backbone of majority of drugs in early times;laterchemical, pharmacological and clinical studies became necessary for drug development (Butler, 2004). The isolation of quite a lot of alkaloid compounds including morphine was from*Papaver somniferum* L. (opium poppy).*Digitalis purpurea* L. (foxglove) was in the 10th century recorded to be in use in Europe, but digitoxin, a cardiotonic glycoside, which is the active ingredient was isolatedin the 1700s. This compound showed to increase cardiac conduction, thus enhancing cardiac contractibility strength. Quinine, an antimalarial agent from the bark of *C. succirubra*, for many yearswas used for treating malaria, cancer, throat as well as mouth diseases among others. A global cultivation of the plant was done by the British in the mid-1800s which led to the bark to be formally used for malaria treatment. Medicinal plants are said to be bases of several types of biologically active molecules having different therapeutic properties. Traditional medicine is indigenous to diverse cultures and is as a result of practices based on experiences and beliefs utilised in preventing diseases and health maintenance. The use of traditional medicine is widespread and it is based on centuries-old practices based on beliefs and local traditions at the time when modern scientific medicine had not become popular and accepted. Plant utilised in treating a specific disease was often identified by "signature codes" earlier before it was realised that molecules with pharmacological activityavailable in medicinal plants are responsible for their observed efficacy. For instance, jaundice was cured using goldenrod with a yellow colour, liverworts were utilised for ailments of the liver,herbs with red colour were utilised in treatingdiseases of the blood, toothworts for toothache, also pileworts for hemorrhoids (Sneader, 2005).

Based on traditional and ethnobotanical use, medicinal plants provide source of information for active components isolation, for example, some as direct therapeutic agents, starting molecule for semisynthesis and also as taxonomic markers for identification (Balunas and Kinghorn, 2005; Gurib-Fakim, 2006). Traditional medicine is continually in high demand to treat several diseases, which is accessed through the traditional medicine practitioners and herbalists. Traditional medicinal drug comprises only medicines which predominantly utilise medicinal plants concoction for treatment; this preparation comprises medicinal plants,

minerals and organic matters among others (Samy and Gopalakrishnakone, 2007). The management and cure of ailments have been one of the major concerns of mankind over the years (Tantry, 2009). In developing countries, traditional system of healing is fundamentally centered on the use of phytomedicines, which showed to be avital aspect of their history and culture (Arif *et al*., 2009). In the traditional systems of medicine (TSM),the use of plants with medicinal properties has played significant role, particularly as means to discover novel drugable molecules. Isolation of compounds with the aid of several separation procedures, chemical properties and spectra characterisation are necessary to determine its chemical nature (Ramawat *et al*., 2009).The prospect of plants for therapeutic effect has been thoroughlyexploredover long decades (Raina *et al*., 2014).

2.2.2Natural products derived from medicinal plants

For several decades, most of the new drugs have showed to be generated from natural products and their derivatives (Lahlou, 2007). Natural products have been long shown to be developed source for new drug molecules discovery as a result of their possession of chemical diversity whichshow action on numeroustargets in the biological system (Bhutani and Gohil, 2010). Moleculesknown to be the major natural products are categorised as secondary metaboliteswhich include flavonoids, terpenes, alkaloids, sterols, lignins, essential oils, tannins, phenolics, e.t.c.,are known asresults of secondary metabolism (Ramawat *et al*., 2009). The individuality of plant species is expressed by organism-specific mechanism of biosynthesis of compounds known as secondary metabolites by organism(Maplestone *et al*., 1992). Colegate and Molyneux (2008) alluded that secondary metabolites are generated either due to adaptation of organism to its surroundings or are generated for them as potentialmechanism of defense in combating predators and helpsupport thoseorganismsto survive. The secondary metabolites biosynthesis resulted from photosynthesis, Krebs cycle and glycolysis, which arefundamental processes yielding intermediates which, in the end, afford the production of secondary metabolites similarlyidentified as natural products. Two major biosynthetic pathways are responsible for the synthesis of most secondary metabolites: (1) a collection of aromatic amino acids, which are transformed to become different molecules likealkaloids and phenolics (lignins, quinones, tannins), are generated through shikimic acid pathway(Mustafa and Verpoorte, 2007), also (2) a huge collection of terpenoids are generated through acetyl-CoA mevalonic acid pathway (Eisenreich *et al*., 2004). These compounds of

plant source, according to Wood-Sheldon *et al.*(1997),play good roles for elucidating their functions in managing and treatingdiverse diseases.*Anthriscus sylvestris* roots for instanceafforded a lignin which displayedeffect against insects (Kozawa *et al.*, 1982). Natural products have provided distinct structural diversity compared to normal combinatorial chemistry, which offers potentials for the discovery ofmostly newlead compounds with low molecular weights (Dias *et al*., 2012). One important feature of products from natural source are the huge structure and chemical diversity. As a matter of fact, natural products or their derivatives provide 45% of today's most purchased drugs. Several plants of medicinal properties have been subjected to detailed chemical investigations for isolation of pure bioactive molecules which have specific pharmacological potentials. This has afforded the discovery of drugs along with their applications (Table 2.1). These biologically active compounds are used as therapeutic agents, starting materials and new reagents for molecular biology research (Phillipson, 2007). Discovering drugs from plants is an herculeanprocess and one which consumes time. The typical examples of drugs discovered from plant such as quinine, morphine, digoxin, etc., which substituted the extracts of their individual plants largely show the point that a single potent agent was responsible for the biological activity (Bhutani and Gohil, 2010). Once the medicinal plant is chosen for a single drug molecule based on a literature survey and known phytochemical relationships, collection and botanical identification follows. The plant material is dried in a coolroom withairflow orin a controlled temperature oven. The dried plant material should then be pulverised to give a satisfactory mesh size and made to undergo a suitable extraction process as per standard operating procedures. Forbioactive studies, different extracts of varying polarities are prepared and subjected to a preliminary screening programme. The extracts are made to undergo standard chromatographic techniques for fractionation and isolation of bioactive molecules (Tantry, 2009).

Arteether was introduced as artemotil in 2000. It was derived from artemisinin previously isolated from*Artemisia annua* and both are approved antimalarial medicines (Newman and Cragg, 2007). Apomorphine, an effective dopamine agonistused in treating Parkinson's disease was derived from morphine from*P. somniferum*(Deleu *et al*., 2004). Alkaloids (Facchini, 2001), terpenoids (Trapp and Croteau, 2001) and phenylpropanoids (Dixon and Paiva, 1995)have been shown to possess antitumor properties among several other plant-

derived natural products. It is already known that sixty percent of drugs used in treating tumour and infectious diseases currently available commercially or going through clinical trials are from natural source (Hamburger and Hostettmann, 1991). Paclitaxel (Taxol®), the most commonly used drug in treating breast cancer is derived from*Taxus brevifolia* bark. Taxol® is not available in abundantamounts from natural sources.The efforts for its synthesis was challenging and with huge financial cost, though successful (Nicolaou *et al*., 1994). From the needles of *T. brevifolia*, baccatin III is easily and abundantly isolated and is an instance of a structural analogue that is effectivelyconverted into Taxol® (Dewick, 2002). Severalbig drug manufacturing companies minimised natural products usein screening for drug discovery in last few decades in spite of the advantages and the past accomplishments. This isdue tosupposeddrawbacks of natural products such as the issues with inability of working fastly due to its complexities, accessibility and supply, and worries relating to intellectual property rights, as well ashopefulnessrelated to the useof pools of molecules made availablethrough combinatorial chemistry approaches (Harvey, 2008). The process of discovery of drug through natural productsgenerally demandeda series of separation rounds as well as structure elucidation and therefore time consuming. Nevertheless, because ofthe use of newly placed technologies that assure improved profits, discovery of drugs from natural product source has regainedthe Pharmaceutical company reception and thus on the brink of a comeback. The application of new technologies has reformed natural productsscreening procedures in new drug discovery,together with their chemical structure diversity as well as their biodiversity. The innatenatural products limitationsrequire the application of these technologiesto give a distinct chance to again demonstrate theirimportance indrug discovery. For new, safe and cost effective drug discovery and development programme,natural products are seen to continueas importantconstituents (Lahlou, 2013).

Table 2.1: Important biologically active compounds from medicinal plants and their bioactivity

Drug	Plant	Biological activity
Achyranthine	*Achyranthes aspera*	Diuretic
Aegelin, Marmelosin	*Aegle marmalos*	Bowel diseases
Ajmalicine	*Rauwolfia canesocence*	Hypotensive
Allicin	*Allium sativum*	Hypolipidemic
Aloin	*Aloe vera*	Demulcent, Skin diseases
Andrographolide	*Andrographis paniculata*	Hepatoprotective
Arboreol	*Gmelina arborea*	Tonic, Stomachic
Artemisinin	*Artemisia annua*	Antimalarial
Asiaticoside	*Centella asiatica*	Memory enhancer
Asparanin A, Asparanin B, Sarasapogenin	*Asparagus adscendens*	Fertility enhancer
Atropine	*Solanaceae spp.*	Anticholinergic
Bacoside	*Bacopa monneri*	Memory enhancer
Berberine	*Berberis lycium*	Antiemetic
Boeravinones	*Boerrhavia diffusa*	Hepatoprotective
Boswellic acid	*Boswellia seratta*	Antiinflammatory
Caffeine	*Camellia sinensis*	CNS stimulant
Camptothecin	*Camptotheca acuminata*	Anticancer
Cocaine	*Erythroxylum coca*	Anaesthetic
Codeine	*Papaver somniferum*	Antitussive
Colchicine	*Colchicum luteum*	Antiinflammatory
Curcumin	*Curcuma longa*	Antioxidant
Embelin	*Embelia ribes*	Anthelmintic

Ephedrine	*Ephedrae herba*	Hypertensive
Galantamine	*Galanthusworonowii*	Dementia, Anticholinesterase
Glycyrrhizin	*Glycyrrhiza glabra*	Antiviral
Hypericin	*Hypericum perforatum*	Anti-HIV
Liquiritigenin, Isoliquiritigenin	*Pterocarpus marsupium*	Anti-diabetic
Lycopene	*Lycopersicon esculentum*	Antioxidant
Monoterpenes, Sesquiterpenes	*Ocimum sanctum*	Respiratory diseases, Immunomodulatory
Morphine/Papaverine	*Papaver somniferum*	Anagelsic
Polyphenolics, Tannins	*Phyllanthus emblica*	Antioxidant
Protodioscin	*Tribulus terrestris*	Diuretic, Anabolic, Aphrodisiac
Quinine/Quinidine	*Cinchona officinalis*	Antimalarial
Reserpine	*Rauwolfia serpentina*	Hypotensive
Sennoside	*Cassia angustifolia*	Laxative
Silymarin	*Ilybium marianum*	Hepatoprotective
Taxol	*Taxus wallichiana*	Anticancer
Tinosporic acid, Cordifolioside	*Tinospora cordifolia*	Immunomodulatory
Trigonellin	*Trigonella foenum-graecum*	Anti-diabetic
Tubocurarine	*Chondodendron tomentosum*	Muscle relaxant

Tylophorine	*Tylophora indica*	Bronchodilator
Vasacine	*Adhatoda vasica*	Vasodilatory
Vinblastine/ Vincristine	*Cathranthus roseus*	Anticancer
Valepotriates	*Valeraina wallachi*	Sedative
Withanolides	*Withania somnifera*	Immunomodulatory

Source: Tantry, 2009; Bhutani and Gohil, 2010; Kumar *et al*., 2015

2.3Biological activity and antimalarial agents from plant sources

Quassinoids, alkaloids and sesquiterpene lactones have shown to possess the most significanteffect and have diverse bio-effectivenessamong the various groups of secondary

metabolites in plant responsible for antimalarial effect. Several classes of secondary metabolites which wereevaluatedfor either*in vivo* actionto inhibit *P. berghei* or*in vitro* action to inhibit*P. falciparum*are highlighted below:

Alkaloids

Alkaloids are known to be among the main classes of compounds showing antimalarial effect. Quinine, also among the foremostantimalarial drugs with utmost importanceis one of the compounds in this family of compounds and still has relevance. Alkaloids are nitrogenous bases which possess physiological activityresulting from several biogenetic precursors. Described below are some of the alkaloids from natural source which belong to diverse classes:

Naphthylisoquinoline alkaloids

Thiskindof alkaloids show to have aremarkable*in vitro* and *in vivo*inhibition of malariaparasites.*Ancistrocladus korupensis*,was reported to yield korundamine A, a novel dimeric antiplasmodial napthylisoquinoline alkaloid. It is one of thenaphthylisoquinoline dimers from plant source having high antiplasmodial effect using*in vitro* test against *P. falciparum* and showed EC_{50}= 1.1 µg/mL (Hallock *etal*., 1997).Dioncopeltine A, dioncophylline B and C identified in*Triphophyllum peltatum*, a species belonging to the same family,as well as its extractsaltogether displayedappreciably high antiplasmodial action, with dioncopeltine A showing very high and nearly total parasitaemia suppression while dioncophylline C administered (50 mg/kg daily dose for 4 days) showed complete cure onmice with infection without visible toxicity (Francois *et al*., 1997).

Quinoline alkaloids

Chimanine B, 2-*n*-propylquinoline and 2-*n*-pentylquinoline, which are other quinoline derivatives from plant sources possess anti-leishmania activities with EC_{50}25-50 µg/mL (Kayser *et al*., 1998).Quinine, belonging to this class, has shown to be a useful drug for treating malaria, but became very important again with the development and widespreadof *Plasmodium falciparum*chloroquine-resistant strains(Kayser *et al*., 1998). Chloroquine and mefloquine, though with higher antimalarial activity, was discovered as synthetic derivatives from the chemical modification of quinine as lead compound.

Bisbenzylisoquinoline alkaloids

Reports have shown the identification of many different bisbenzylisoquinolines which have antiprotozoal activity.Antimalarial activity*in vitro* (IC_{50}) of majority of bisbenzylisoquinolines have showed to be less than 1.0 µg/mL.For example, IC_{50}value of 0.15 µg/mL was reported for Pycnamine from *Trichilia sp*. But antiplasmodial effect was lacking in monomeric benzylisoquinolines, while antiplasmodial activity of isoguattouredigine, an aporhinoidisolated from *Guatteria foliosa*was determined (Kayser *et al*., 1998).

Indole alkaloids

Indole consists of a set of alkaloids which showeddiverse biological activity, and its sub-structure is broadlyspread in plant. Certain indole alkaloidsshowed antiprotozoal activity. From *Cryptolepis sanguinolenta*, Cryptolepine and related indole-quinolines,for example, showed activity*in vitro*with IC_{50s} ranging from 27-41 ng/mLagainstW2, D6 and K1*P. falciparum* strains (Kayser *etal*., 1998).

Phenanthridine and benzophenanthridine

Papaveraceae, Fumariaceae and Rutaceae are the families of plant where these class of alkaloids are mostly found (Krane *et al*., 1984). Fagaronine and nitidine with antimalarial activitiesagainst *P. falciparum* ranging from IC_{50}9-108 ng/mLare certain examples of benzophenanthridine alkaloids got from plant sources (Gakunju *et al*., 1995).

Quassinoids

The quassinoids are lactones saturated with oxygen atoms showing majorly20 carbon skeleton termedpicrasane. But quassinoids with 18, 19 as well as 25 carbon skeletons have as well been discovered. They possess differingamounts of unalike groups containing oxygen atoms showing anextensive biological activity reportedfor them. From biosynthesis point of view, they are similar to triterpenoids and sharesimilar metabolic precursors. Simalikalactone D, of this class of compound, isolated from *Simaba guianensis* (Simaroubaceae) had antiplasmodial activity showing IC_{50}< 1.7 ng/mL. The antimalarial potential of some other isolated compounds from this class, for example,brucein A, B and C, bruceantin as well as brusatol was determined. The methylene-oxygen bridge in this classof compounds is responsible for their antiplasmodial action(Cabral *et al*., 1993).

Terpenoids

Monoterpenes

Monoterpenes are types known as antiprotozoal drugs. From *Oxandra espinata*, Piquerol A (IC_{50}= 100 µg/mL)isolatedshowedrelatively very low efficacyagainst *P. falciparum*compared to several other compounds (Kayser *et al*., 1998).

Sesquiterpenes

Thediscovery of artemisinin, anantimalarial sesquiterpene lactone with endoperoxide component, motivated the antiplasmodialinvestigation of other peroxides from plant source.

The 1,2,4 trioxane ring of artemisinin plays a vital part in its antiplasmodial action. The actual mechanism of activity of this class of drugs is yet to be elucidated. After being administeredit forms a free radicalat the release of singlet oxygen, as active cytotoxins become toxic to the *Plasmodium* and cause its death. Other sesquiterpenes that show antiplasmodial activity have also been reported in addition to sesquiterpene endoperoxides.Francois *et al*.(1996) reported the antimalarial activity of neurolenin A and B, germacranolide sesquiterpene lactonesisolated from *Neuroleaena lobata* (Asteraceae).

Diterpenes

Diterpenes from many medicinal plant are part of the most widely spread terpenoids in plant and are also well-known for possession of various biological activity (Kayser *et al*., 1998).A number of these diterpenes, according to Oketch-Rabah *et al*. (1998), have together high antiparasitic effect but highlytoxic to mammalian cells.From *Vernonia brachycalyx* (Asteraceae), 16, 17-dihydrobrachy-calyxolide, a macrocyclic germacrane dilactone, isolated possessed antiplasmodial activity (IC_{50} = 17 µg/mL on *P. falciparum*) but as wellshowed human lymphocytes proliferation inhibition atsimilar concentration signifyingoverall toxicity (Oketch-Rabah *et al*., 1998).From *Microglossa pyrifolia* (Asteraceae), theisolated antiplasmodial diterpenes are 6-*E*-geranylgeraniol-19-oic acid (IC_{50}:12.9 µg/mL) and phytol(IC_{50}:8.5 µg/mL) with high antiplasmodial activity reported for these compounds (Kohler *et al*., 2002).

Triterpenes

Naturally occurring triterpenes and saponins have been reported to possess biological activity, likewise have showed human toxicity.Regardless of the fact that the bioactivity of triterpenes has been established, Kayser *et al*.(1998) reported that it was until the late 1970s before the first antiprotozoal activity was documented. Betulinic acid which wasidentified as the antiplasmodial compoundisolated from *Ancistrocladus heyneanus* (Ancistrocladaceae) and*Triphyophyllum peltatum* (Dioncophyllaceae)also shown to possess antineoplastic activity. Bringmann *et al*.(1997) reported it to showagainst *P. falciparum* an *in vitro* activity (IC_{50} 10.46 µg/mL)and (CC_{50}>20 µg/mL) moderate toxicity. Factors such as low bioavailability, haemolytic toxicity when administered orally as well as decreased gastrointestinal tract absorption are said to be responsible for the limitations for the use of saponins as drug molecules.A steroidal saponin known as muzanzagenin which was isolated from *Asparagus africanus* (Liliaceae)showed to exhibit antiplasmodial effect of EC_{50}61 µM against *P. falciparum* K39 strain (Oketch-Rabah *et al*., 1997a).

Limonoids

Limonoids are class of compounds that are richly found in plant family, Meliaceae. Nimbolide tested against*P. falciparum* K1 with activity (IC_{50} = 0.95 ng/mL) was isolated from*Azadirachta indica*, a plant commonly utilised for malaria treatment.This was the first antiplasmodial compound from this plant (Rochanakij *et al*., 1985). Gedunin (IC_{50}0.72-1.74 µg/mL) showedafterwards to also possess *in vitro* activity against *P. falciparum*(McKinnon *et al*., 1997).

Phenolics

From *Vernonia brachycalyx* (Asteraceae), Oketch-Rabah *et al*.(1997b) reported the isolation of phenols like 2'-epicycloisobrachycoumarinone epoxide and its stereoisomer and these showedactivity against *P. falciparum* chloroquine-resistant and chloroquine-sensitive strains to possess comparable antiplasmodial activity (IC_{50}= 0.11 and 0.15 µg/mL, respectively).

Flavonoids

A number of flavonoids have been reportedfrom numerous plant species with their antimalarial potential established.Renewed interest was shown in this class of compoundafter

antiplasmodial flavonoids was identified from *Artemisia annua* (Asteraceae). As part of intense effort towards antiplasmodial drugs research programme, additional *Artemisia* species were screened in Thailand. As a result of this,from *Artemisia indica* (Asteraceae), Chanphen *et al*.(1998) reported that there was isolation of exiguaflavanone A (EC_{50}= 4.6µg/mL) and B (EC_{50}= 7.1 µg/mL)which showed*in vitro* activityagainst *P. falciparum*.

Chalcones

A Chalcone glycoside- phlorizidin,was reported by Kayser *et al*. (1998) to have been isolated from *Micromelum tephrocarpum* (Rutaceae) and showed to display antiparasitic action. *Micromelum tephrocarpum*,due to its bitter taste, is traditionallyutilised in malaria treatment. This bitter taste islikewise characteristics of quinine as well as many other plants used in treating malaria. Licochalcone A, a very promising compound first identified from *Glycyrrhiza glabra* (Fabaceae), showedagainst *P. falciparum* 3D7 and Dd2 strains antiplasmodial effect of IC_{50} 0.1 µg/mL and 0.5 µg/mL, respectively;alsowent throughrigorous preclinical studies (Chen *et al*., 1994).

Naphthoquinones

Plumbagin, a napthoquinone from *Plumbago zeylanica*, has showed to possess against resistant (W2) and chloroquine-sensitive (D6) strains of *P. falciparum* antiplasmodial activity with IC_{50}=188.8 ng/mL and 178.12 ng/mL, respectively (Lin *et al*., 2003).

Anthraquinones and xanthonones

Anthraquinones and xanthonones are similar to naphthoquinones in structure and biological activity.Tricyclic aromatic skeleton with a *para*-quinoid substitution is seen to be the major chemical difference between the groups.Sittie *et al*.(1999) showed *in vitro* antimalarial effect (EC50 ˜ 21.4 - 82.9 µM) for anthraquinones-digitolutein, rubiadin-1-methyl ether and damnacanthal-from *Morinda lucida* (Rubiaceae)on chloroquine-resistant *P. falciparum* strain. Isolated from *Psychotria camponutans* (Rubiaceae), was benzoisoquinoline-5-10-dione, a rare anthraquinones which was reported to have against *P. falciparum* an antiplasmodial activity(EC_{50}0.84 µg/mL)(Solis *et al*., 1995).

Xanthones was as well reported for their antiplasmodial potential. Likhitwitayawuid *et al*.(1998) reported five prenylated xanthones from *Garcinia cowa* (Guttiferae)which showed significant *in vitro*action(IC_{50} 1.5-3.0 µg/mL)against *P. falciparum*. Cowaxanthone among

them demonstrated the highest antiplasmodial effect (EC_{50} = 1.5 µg/mL)more than pyrimethamine (IC_{50}2.8 µg/mL). Examples of biologically active antimalarial agents derived from plant sources are shown below in Figure 2.4.

2.4 Review of Nigerian medicinal plants with antimalarial potential

Various parts of the world have for many decades utilise traditional herbal medicines for the treating malaria.Quinine, alkaloid, which was the foremost drug to treat malaria, and was isolated from the bark of the *Cinchona* species (Rubiaceae);it is still in use until now. Baird *et al*. (1996) reported that malaria was treated with the bark of the plant by infusions as far back as 1632. Several decades after, quinine was isolated and its structure identified (Saxena *et al*., 2003), it became the foremost and very important and most widely used antimalarial drug. *Artemisia annua*, re-discovered in China in 1970s is another useful and importantmedicinal herb for treating malaria and from where antimalarial artemisinin was isolated (Klayman, 1985). From 2005 onwards, the adoption of Artemisinin-combination therapies (ACTs) in Nigeria as first-line drugs for uncomplicated malaria treatment was established (Mokuolu *et al*., 2007). Though, the use of ACTs has limitationsbecause of its high costs, toxicity and limitation in artemisinin derivatives production (Afonso *et al*., 2006). The two most effective drugs, artemisinin and quinine were respectively isolated from the medicinal plants*Artemisia annua* and *Cinchona* species, but neither of them is native to sub-Saharan Africa. Plants from tropicshave been shown to possess greater amounts of naturally occurring chemical defenses and a largerbiodiversity than the plants belonging to any other flora, hence they showed to be possible sources for novel drugs with greater effectiveness (Balick *et al*., 1996). It looks rational then to cheer the courage for researches on plants belonging to these regions, particularly since malaria and death from malaria majorlyaffects the population of sub-Saharan African counties (Figure 2.5).

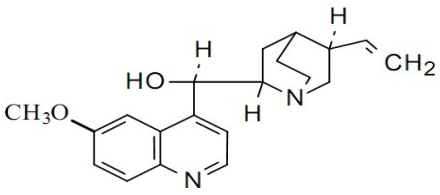

Quinine

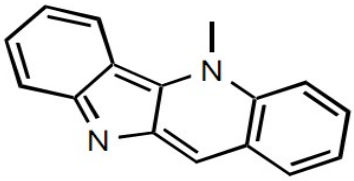

Cryptolepine

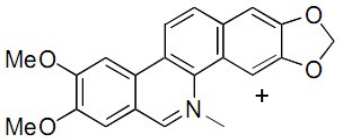

Nitidine

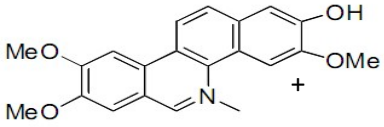

Fagaronine

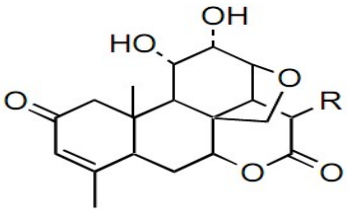

(R = O-tiglate) Simalikalactone D

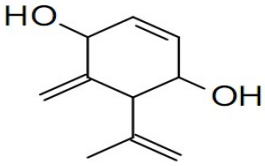

Piquerol A

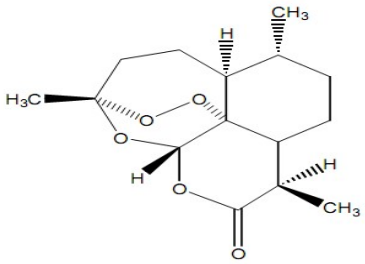

Artemisinin (Qinghaosu)

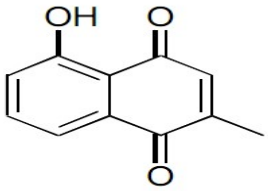

Plumbagin

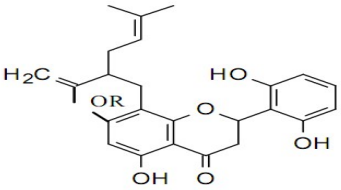

R = H R = CH_3

Exiguaflavanone A Exiguaflavanone B

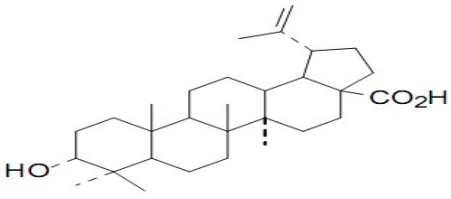

Betulinic acid

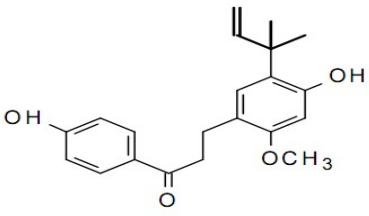

Licochalcone A

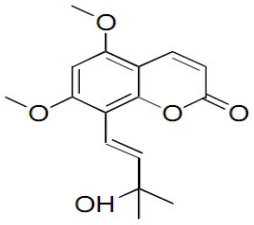

Coumarin

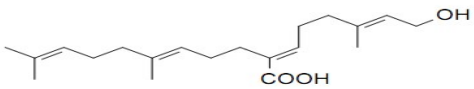

geranylgeraniol-19-oic acid

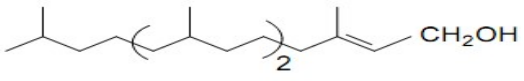

Phytol

6-*E*-

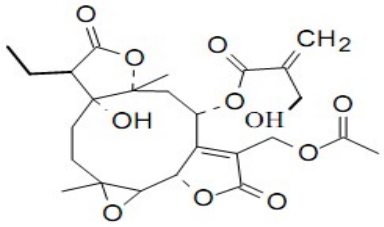

17-dihydrobrachy-calyxolide

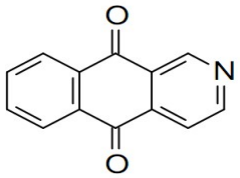

Benzoisoquinoline-5-10-dione

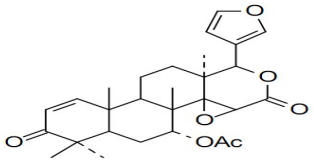

Nimbolide

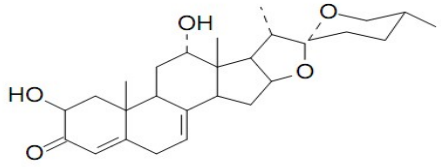

Muzanzagenin

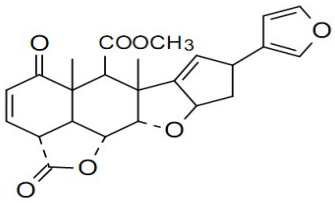

Gedunin

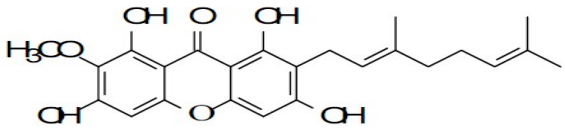

Cowaxanthone

Figure 2.4: Bioactive antimalarial agents from plant sources

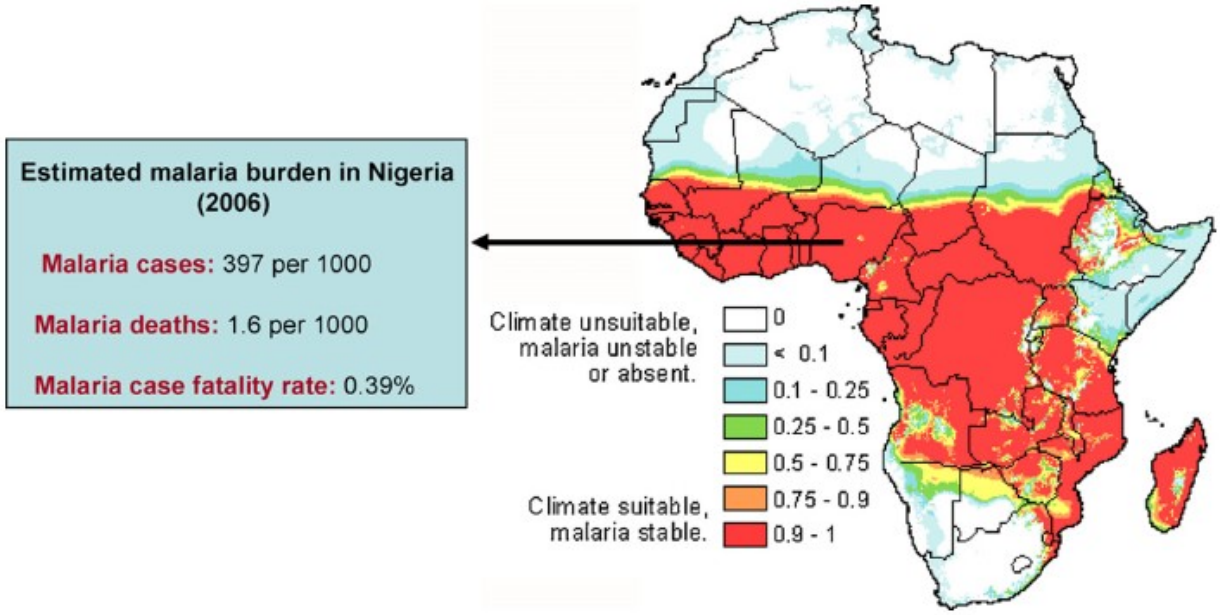

Figure2.5: Human malaria distribution in Africa and its estimated burden in Nigeria.

(http://www.mara.org.za)

2.4.1Treatment of malaria with Nigerian medicinal plants

Nigeria has a richbiodiversity with numerous of these plant species utilised for medicinal purpose by the local communities. In Southern Nigeria with existence of rain forests which is a source ofhumid climate, the perfectenvironments for continuousmalaria spread all round the year (Figure 2.6),there is high use of several of these medicinal plants for malaria treatment. Certain plantsare made useof in treatingmalaria throughout all ethnicsets in the country, for instance, *Azadirachta indica* (Meliaceae) and *Alstonia boonei* (Apocynaceae). Among the medicinal plants utilised for treating malariain Nigeria are listed in Table 2.2 and Figure 2.7. In Nigeria, plants species from Meliaceae familysuch as *Khaya senegalensis*, *Azadirachta indica* and *Khaya grandifoliola* are also utilised in treating malaria. *Azadirachta indica*commolyreferred to as "neem tree" is an ever popular tree, about25 m in height and is utilised in ethnomedicineagainst malaria by subjecting the leaves, stem bark or root to an aqueous decoction (Obih and Makinde, 1985). This plant is one of the very important species for treating malaria infection in Nigeria, because of this, it was determined that the tablet suspensions of the leaf and bark should be made. Meanwhile, Isah *et al*. (2003) reported that it showed a very reduced curative, moderate suppressive and high preventive antimalarialoutcomeagainst *P. berghei*. *Khaya grandifoliola*as well as*K. senegalensis*which frequentlyserved as shades are widely utilised for medicinal purpose. For the purpose of malaria illness treatment, the stem barks are subjected to decoctions though they appear to show adverse effects (Bumah *et al*., 2005).

Morinda lucida (Rubiaceae), is a plant mostly utilised for treatingmalaria in Nigeria (Avwioro *et al*., 2005). Generally utilised in Western part of Africa formalaria treatmentand many diseases of the tropics are the root bark, stem bark and aerialparts of the plant. Earlier report has showed seasonal difference in its activity against malaria (Makinde *et al*., 1994).The root bark of *Nauclea latifolia*, another plant of Rubiaceae family principally from the savannah,in a aqueous decoctionis utilised in treatingmalaria.

Figure 2.6: Vegetation map of Nigeria (http://www.lib.utexas.edu/maps/nigeria.html)**].**

Table 2.2: Some medicinal plants in Nigeria used for treating malaria

Plant species (Family)	Part used	Geographical region	Reference
Azadirachta indica **A. Juss. (Meliaceae)**	Leaves	All regions	Ehiagbonare (2007)
Fagara zanthoxyloides **Lam. (Rutaceae)**	Root	Southwest	Kassim *et al*. (2005)
Khaya grandifoliola **C.DC. (Meliaceae)**	Stem bark	Middle Belt, Southwest	Agbedahunsi *et al*. (1998)
Morinda lucida **Benth. (Rubiaceae)**	Leaves, stem bark	Middle Belt, Southwest	Tor-Anyiin *et al*. (2003)
Nauclea latifolia **Sm. (Rubiaceae)**	Stem bark, root	Middle Belt, Southern regions	Ajaiyeoba *et al*. (2006a)
Picralima nitida **(Staph) Th. & H.Dur. (Apocynaceae)**	Stem bark, seed	Southeast	Ezeamuzie *et al*. (1994)
Quassia amara **Linn. (Simaroubaceae)**	Leaves, Stem	Southwest	Ajaiyeoba *et al*. (1999)
Terminalia latifolia **Blanco (Combretaceae)**	Leaves	Middle Belt	Ajaiyeoba *et al*. (2006b)
Tithonia diversifolia **(Hemsl.) A.Gray (Compositae)**	Leaves	Southwest	Elufioye and Agbedahunsi (2004)

Source: Adebayo and Krettli, 2011

Figure 2.7:Nigerian medicinal plant parts scientifically validated for their antimalarial potential

2.4.2Antimalarials isolated from Nigerian medicinal plants

Compounds with antimalarial activity have been isolated from some plant used for treating malaria in Nigerian traditional medicine. Majority of the bioactive principles isolated (Table 2.2, Figure 2.8) are alkaloids, next are limonoids. Several of the bioactive principles isolated were only screened*in vitro* against *P. falciparum*, possibly due to lack of sizeable amounts isolated. Several medicinal plants had been reported to have afforded various antimalarial alkaloids: (a) from the root of *Fagara zanthoxyloides*,Kassim *et al*. (2005) testedfagaronine (IC_{50}= 0.018 µg/mL), a benzophenanthridine alkaloidwith *in vitro* activity against*P. falciparum*; (b) from *Enantia chlorantha*,Vennerstrom and Klayman(1988) reported the isolation of jatrorrhizine and palmatine, protoberberine alkaloids; (c) from *Picralima nitida*,Ansa-Asamoah *et al*.(1990) reported that some alkaloids were identified such as alstonine,picraline, akuammiline, akuammine,akuammidine, akuammicine,akuammigine, picraline, as well as alstonine. Activity similar to chloroquine and quinine against *P. falciparum* was reported for some of these alkaloids (IC_{50} 0.01 to 0.9 µg/mL) from *Picralima nitida* with alstonine showing the highest activity (Okunji *et al*., 2005).

Limonoids have as well showedactivities against malaria parasites, for instance, gedunin isolated from*A. indica* plants (MacKinnon *et al*., 1997). According to Bray *et al*.(1990) the activity looks to be due to the occurrence of an α, β-unsaturated ketone in ring A, as well due to 7α-acetate group; the observed activity is likewise contributed to by the furan ring. Butagainst*P. berghei*, gedunin did not show activity. Meldenin showed highest effect against *P. falciparum* among four other limonoids identified from*A. indica* leaves(Joshi *et al*., 1998). From *K. grandifoliola*,Bickii *et al*. (2000) reported there was isolation of limonoids that showed activity against malaria parasites (methylangolensate, gedunin, 7-deacetylkhivorin, 6-acetylswietenolideas well as 1-deacetylkhivorin). Three limonoids of mexicanolide type were identified fromthe barks, roots and seeds of *K. senegalensis*, of which fissinolide showing activity against *P. falciparum*(Khalid *et al*., 1998). Some more antimalarialcompounds from plant sources in Nigerian ethnomedicinal are: (a) azadirachtin (a tetranortriterpenoid) (Butterworth and Morgan, 1968), which showed *in vitro* activity against the development of mobile microgametes; (b) from*Spathodea campanulata* stem bark, Amusan *et al*.(1996) reported the isolation of ursolic acid which protracted the survival of mice infected with *P. berghei*and repressed infection; (c) damnacanthal,anthraquinones isolated from *Morinda*

lucida, showed to have the highest activity.Improved activity was observed against *P. falciparum*by the addition of an aldehyde moiety at C-2 position as well as a phenolic hydroxy moiety at position C-3 in a structure–activity relationship studies(Sittie *et al*., 1999); (d) from the leaves of *Tithonia diversifolia*,Tagitinin C, sesquiterpene lactone isolated showed against *P. falciparum*activity (Goffin *et al*., 2002); (e) from*Allium sativum*,Perez *et al*.(1994)reported isolation of Ajoene whichshowed activity against *P. berghei*; (f) isolation of Simalikalactone D from *Quassia amara* leaves as the possible antimalarial principle (Bertani *et al*., 2006).

2.5 Plants selected for antiplasmodial investigation

2.5.1*Combretum racemosum*

Combretum racemosum(Figure 2.9) is a liane or sometimes a scandent shrub which is widely spread in the west tropical Africa and commonly known as Christmas rose. The leaves are between 2-5 cm wide also up to 6 cm long. It is refer to as belegwe in Ivory Coast and Balanta part of Senegal call it kinde kinde. In Nigeria, it is called okoso among Edo, alagame in Igbo land and ogan pupa among Yoruba.

Onocha *et al*. (2005) reported *Combretum racemosum*as very useful medicinal plant in ethnomedicine intreating numerous diseases. In earlier ethnopharmacological investigations, this planthas indicatedantimalarial actionamong certain Combretum species utilised for treating malaria in folk medicine in some part of West Africa (Atindehou *et al*., 2004; De Morais Lima *et al*., 2012), which was also established recently in our report on antimalarial activity of selected Combretaceae plants (Wande and Babatunde, 2017). It equally showed reputation in the Nigerian traditional medicine as source of treatment for certain parasitic diseases and fever (Mgbemena *et al*., 2016).Thesereported potentials therefore becamethe motivation for this research work aiming atdefining the bioactive principles in this plant by validating its antiplasmodial properties against the strains of *P. falciparum*. Meanwhile,the active principles responsible for the antimalarial properties in this plant are yet to be known.

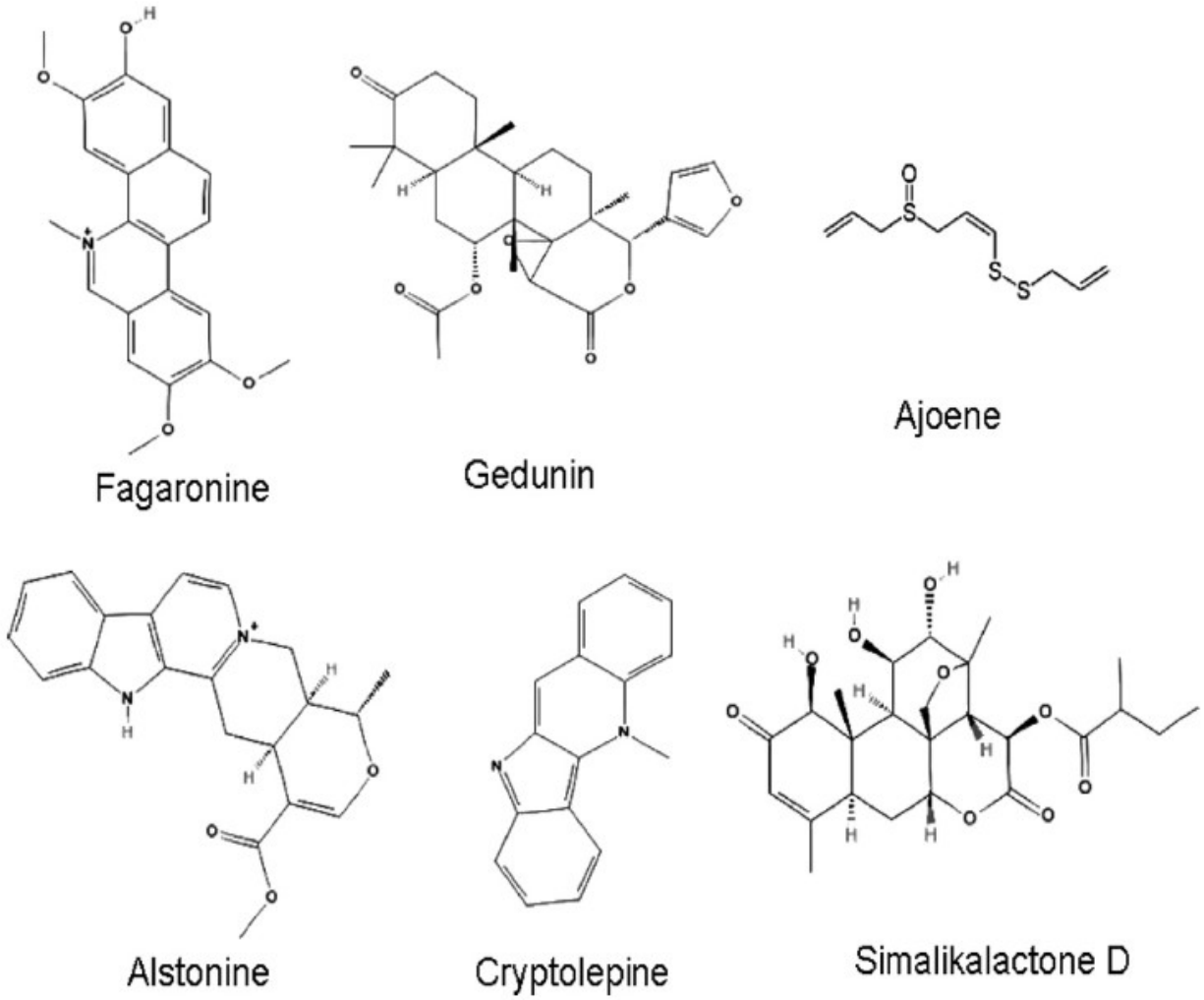

Figure 2.8: Antimalarial agents isolated from some Nigerianplants for treating malaria.

Figure 2.9: *Combretum racemosum* plant

2.5.2*Combretum zenkeri*

Combretum zenkeri Engl & Diels (Figure 2.10) is a widely distributed climbing shrub of about 3.5 to 4.5 m used in tropical West Africa from Guinea to Southern Nigeria and Cameroon. It is called ogan ibule in the South west part of Nigeria. The leaves of this plant is utilised as purgative by decoction preparation, the twig is chewed by Ivory Coast women to relieve menstrual pain, treating intestinal worms and malaria treatment (Ujowundu *et al*., 2010). *Combretum zenkeri* leaves are, in Western Nigeria, utilised for treating inflammatory diseases like rheumatoid–arthritis, and the roots used frequently in recipes for managing cancer (Gbolade *et al*., 2010; Sowemimo *et al*., 2009). In previous studies, several pharmacological investigations for *Combretum zenkeri* such as nephro-protective effect (Ogbonna *et al*., 2016), hepatoprotective effect (Okwu *et al*., 2014), anti-oxidative activity and neuroprotectiveeffect (Ujowundu *et al*., 2015) as well as cytotoxic action (Sowemimo *et al*., 2009) was validated. In our more recent report, preliminary screening of 10 Combretaceae species showed that *Combretum zenkeri* possessed antimalarial activity (Wande and Babatunde, 2017). All these pharmacological effects show *Combretum zenkeri* as a promising and important phyto-agent in the search of bioactive compounds for treating diseases. Until now, no bioactive constituent is reported to have been isolated from *Combretum zenkeri*, which prompted the investigation of its active principles in this work.

Figure 2.10: *Combretum zenkeri* plant

CHAPTER THREE

3.0 MATERIALS AND METHODS

3.1 Equipment, reagents and consumables

3.1.1 Equipment

Oven, incubator, Rayto RT-6100 microplate reader, centrifuge, pH meter, fume cupboard, micro-pipettes (10-100 µL and 100-1000 µL), weighing balance, flat bottom 96-well plates (300 µL), 2 mL eppendorf's tube, 96-well eppendorf tube racks, Buchi rotary evaporator, desiccators, Soxhlet apparatus, Laboratory blender, 5 µL capillary tubes, separatory flask, glass column chromatograph (1 cm x 100 cm, 500 mL volume), glass column chromatograph (1 cm x 60 cm, 250 mL volume), electronic automatic CC fraction collector, HPLC system (Schimadzu Corporation), Analytical HPLC Luna C_{18} column (5 µm, 250 mm x 4.6 mm ID) purchased from Phenomenex, HPLC vials, PuriFlash column 25 silica HC (120 g, 20 bar), Flash chromatography system (InterchimpuriFlash 4250), in connection with an evaporative light scattering detector (ELSD), also a photodiode array detector (PDA), as well as a Interchim software-controlled fraction collector, maXis UHR ESI-Qq-TOF mass spectrometer (Bruker Daltonics, Bremen, Germany), Avance III HDX 700 MHz NMR spectrometer (Bruker BioSpin, Germany).

3.1.2 Reagents and consumables

Methanol, ethyl acetate, chloroform, hexane, toluene, acetone, formic acid, glacial acetic acid, sulphuric acid,Acetonitrile, pre-coated TLC plates (Merck Germany), pre-coated preparative TLC plates (Merck, Germany), silica gel 60 (230-400 mesh size), Vanillin, anisaldehyde, deutarated chloroform, deuterated methanol, pyridine, bovine hemin, hydroxyethylpiperazine-N-[2-ethanesulfonic acid] (HEPES) (Sigma Aldrich, USA), HEPES (Euroclone, Celbio), Albumax (Invitrogen, Milan, Italy), L-glutamine (Euroclone, Celbio), hypoxanthine (Sigma, Italy), RPMI-1640 medium, sodium hydroxide, hydrochloric acid, sodium acetate,abscisic acid

(Sigma Aldrich, Art. no. 90769), madecassic acid (VWR, Art. no. CAYM11854). Arjungenin was generously supplied by Professor Ikhlas Khan, University of Mississippi, USA.

3.2 Preliminary investigation of medicinal plants of Combretaceae family for their antimalarial potential

3.2.1 Collection of plant and identification

The leaves of ten Combretaceae species; eight *Combretum*: *C. racemosum*, *C. zenkeri*, *C. sordidum*, *C. paniculatum*, *C. dolicopetalum*, *C. hispidum*, *C. confertum*, *C. platypterum* and two *Terminalia*: *T. mentalis*, *T. ivorensis*, were collected around the Botanical Garden, University of Ibadan and identified by Mr. Owolabi, the Curator of the Botanical Garden, University of Ibadan, Nigeria.

3.2.2 Preparation of extracts

The leaves of all the plants collected were air-dried for about 3 weeks. The air-dried leaves were milled to powder with laboratory blending machine.Extraction of fifty grams (50 g) each of the pulverized plant was carried out independently with acetone and methanol using Soxhlet apparatus. Whatman No 1 filter paper was used to filter all extracts and concentration was done under reduced pressure with Buchi rotary evaporator at 40°C. The amounts of all plant extracts were determined and they were kept in a cool and dry place till needed for analysis.

3.3 Preliminary bioactivity screening (Beta-hematin inhibition assay)

The antimalarial property of the 10 Combretaceae plants was evaluated. Eighteen extracts were tested in all. Using the method adapted by Vargas *et al.* (2011), the ability of the extracts to show *in vitro*inhibition of beta-hematin synthesis was determined.

3.3.1 Preparation of solutions and reagents

Stock concentration (50 mg/mL)of the plant extracts was prepared by weighing 500 mg of extracts of acetone and methanol in and were made up with 10 mL of acetone and methanol, respectively in volumetric flasks. Preparation of fresh bovine hematin solution was carried out (6.8 mg of bovine hemin was weighedand dissolved in 10 mL of 0.1M NaOH to become 0.68 mg/mL used for each determination). Preparation of HEPES solution was carried out(238 mg

of HEPES was weighed, 50 mL distilled water used to dissolve it to become 4.76 mg/mL and controlled to pH 7.5 used for each determination). Fifteen percent pyridine (15%) used for the assay was prepared by adding 15 mL of pyridine into 85 mL of HEPES solution. The preparation of saturated acetate solution was carried out by weighing 36 g of sodium acetate and dissolved in 20 mL of distilled water with the addition of 48 mL of acetic acid, and pre-warmed at 60 $^{\circ}$C before each use.

3.3.2 Qualitative determination of inhibition of beta-hematin formation

Each of the plant extracts (25 mg/mL) was tested in the beta-hematin synthesis inhibition. Briefly, 10 µL of each of the plant extract and chloroquine was dispensed into wells in columns of 96-well plates and were tested.Furthermore, 10 µL of 1M HCl was added to all plant extracts in the 96-well plates. Hematin solution (100 µL)freshly prepared was added into the wells in row A and B. The test plate was shaken at 900 rpm for 10 minutes, followed by addition of pre-warmed (60 $^{\circ}$C)saturated acetate solution (60 µL) (pH 5.0) to all the wells. The test plate was further incubated at 60°C for 90 minutes. Afterward, 750 µL of 15% pyridine was added to wells in the row A and C whereas 750 µL HEPES (pH 7.5) was added into wells in row B and D. Thereafter, the test plate was shaken for 10 minutesat 900 rpm,alsoleft for 15 minutes to settle down. For each sample, aliquot of 100 µL was taken out and moved in triplicate to non-sterilized 96-well plates. AUV-spectrophotometer absorbance was measured with a Rayto scientific RT-6100 microplate reader at 405 nm.

3.3.3 Beta-hematin inhibition determination

Beta-hematin synthesis inhibition assay was carried out following the process shown below. For all sample tested, there is $A_{Analysis}$ (contained all prepared solutions) which represented the sample for analysis in row A of the test plate; there is $A_{Analysis;Blank}$(different from $A_{Analysis}$by adding 750 µL of HEPES (4.76 mg/mL) instead of pyridine, after incubation) which represented the control in row B of the test plate. Also, for all sample tested, there was preparation of $A_{CLT;Blank}$(in the absence of hematin and HEPESbut with 750 µL of 15% pyridine)which represented a blank control in row C and its blank ($A_{CLTBlank;Blank}$) in the absence of hematin and 750 µL of 15% pyridine but with 750 µL of HEPES which was presented in row D of the test plate.

The residual absorbance ($\Delta A_{Analysis}$) of the sample due to β-hematin inhibition was determinedby the following formula:

$\Delta A_{Analysis} = A_{Analysis} - A_{Analysis;Blank}$

The sample residual absorbance ($\Delta A_{CLT;Blank}$) independent from the β-hematin inhibition complex was determined by the following formula:

$\Delta A_{CLT;Blank} = A_{CLT;Blank} - A_{CLTBlank;Blank}$

The resulting β-hematin synthesis inhibition as shown by the analysed sample was determinedby the following formula:

$I_{Analysis} = \Delta A_{Analysis} - \Delta A_{CLT;Blank}$

A positive value for $I_{Analysis}$ showeda positive assay (sample was active) while a value that showed negative demonstrated no inhibition (not active sample).

3.3.4 Determination of 50% inhibitory concentration (IC_{50})

The above experiment was repeated for six other concentrations (12.5 to 0.39 mg/mL) in seven prominently active extracts tested and chloroquine. The extracts and chloroquine were tested in triplicates in 96-well plates. Non-linear regression in a commercially available statistical package Prism Graphpad® (7.0) was used to determine the IC_{50} values.

3.3.5 Statistical analysis

Results were communicated as means ± SEM and the analysis conducted using prism Graphpad® (7.0). Comparisons were made between positive control (chloroquine) and treatment groups of various concentrations using one-way analysis of variance (ANOVA) followed by Dunnett's multiple comparison tests. The mean of IC_{50} values obtained for the extracts were compared with the IC_{50} value obtained for chloroquine using paired t-test. P-values of 0.05 were considered statistically significant.

3.4 Bulk collection, identification and preparation

Combretum racemosum and *Combretum zenkeri* were taken for further phytochemical investigations based on their appropriate antiplasmodial properties to elicit the main biologically active compounds.

3.4.1 Bulk collection, identification and authentication

The fresh leaves of *Combretum racemosum*(voucher number: 108887) and *Combretum zenkeri*(voucher number: 110277) were collected from the University of IbadanBotanical Curator. The plants identification wasdone by Mr. Owolabi, the Botanical Garden warden. The Voucher specimens were submitted to Forestry Research Institute of Nigeria (FRIN), Ibadan for authentication and documentation.

3.4.2 Preparation of extracts

The *C. racemosum* and *C. zenkeri* leaves collected were air-dried for about 3 weeks. The air-dried leaves were milled to powder with milling machine. Methanol with the aid of Soxhlet apparatus was used to extract the pulverised*C. racemosum*leaves (1.5 kg) and *C. zenkeri*leaves (1.5 kg).All extractswere filtered by Whatman No 1 filter paper and concentration to dryness was done under reduced pressure with Buchi rotary evaporator at 40°C. The extracts were placed in desiccators to remove residual solvents. The weight of the crude methanol extracts was determined andthey were kept in a cool and dry place till needed for analysis.

3.5 TLC profiling of the methanol extracts of *C. racemosum* and *C. zenkeri*

The TLC spray reagents was prepared according to the following procedures: (a) natural products (NP) reagent was prepared by dissolving 0.5 g diphenylboric acid aminoethyl ester in 50 mL methanol, (b) polyethylene glycol (PEG) reagent was prepared by dissolving 2.5 g PEG in 50 mL ethanol (spraying was done with 10 mL of NP and 8 mL of PEG reagents one after the other), (c) anisaldehyde reagent was prepared by taking 1.5 mL anisaldehyde, 30 mL glacial acetic acid, 255 mL methanol, 15 mL concentrated sulphuric acid, all added in that order.The extracts were dissolved in methanol for TLC analysis. Theextracts (5 µL) each were loaded on pre-coated TLC plates F_{254} silica gel 60. The two mobile phases: toluene/ethyl acetate 90/10 and ethyl acetate/methanol/water 100/13.5/10 were prepared inside TLC chambers, left for about 20 minutes to saturate the tank and thereafter the extracts were developed. Anisaldehyde-sulphuric acid detecting reagent was used to spray the TLC plates and subjected to heat at 110 $^{\circ}$C for optimal visualization of the chromatograms at visible light. The analysis was repeated with the same mobile phases and TLC chromatogram sprayed with natural product/polyethylene glycol 4000 detecting reagent and visualized at 366 nm.

3.6 Antiplasmodial test ofmethanol extracts of *C. racemosum* and *C. zenkeri*

3.6.1 *In vitro*culture of the strains of *Plasmodium falciparum*

Two *P. falciparum*strains namely: Chloroquine-resistant (W2)and chloroquine-sensitive (D10)were utilised for the chemosensitivity assay. The two strains were cultured based on the procedure described by Trager and Jensen in 1976 with minoradjustments(Ilboudo*et al*., 2013). The culturing of the parasites wasdonein a standard gas mixture consisting of 1% O_2, 5% CO_2, 94% N_2in human type A-positive erythrocytes at 5% hematocrit at 37°C. RPMI-1640was the medium used, and added to the medium were20mM Hepes,1% AlbuMax(lipid-rich bovine serum albumin), 2mM L-glutamineand 0.01% hypoxantine. The parasitemia was considered in between 1% and 5% for repetitive growth of parasite, and estimated in Giemsa coloured smears, as the number of infected red blood cellrelating to the total number of erythrocytes counted.

3.6.2 Plant extracts sensitivity assay

For the drug sensitivity assay, a colorimetric method was used based on the detection of parasite LDH (Markler *et al*., 1993). The dissolution of the MeOH extracts of *C. zenkeri* and *C. racemosum*was done in DMSO to a 10mg/mL concentration. The extracts were placed in 96 wells flat-bottom microplates in duplicate (Costar) and seven 1:2 serial dilutions were made directly into the plate in a volume of 100 µL (1.6 to 200 µg/mL were the final concentrations used for the extracts and ≤1% was final concentration of DMSO used, which showedno toxicity to the parasite). Asynchronous cultures with parasitemia of 1–1.5% and 2% hematocrit (1% final) were aliquoted into the plates and incubated for 72 h, in a final volume of 200 µL/well. The negative control was cultures without drugs while chloroquine (CQ) was utlised as reference compound. Using a modified method (Markler *et al*., 1993), the parasite growth was determined by measuring the *P. falciparum* lactate dehydrogenase (pfLDH)activity. By the usage of 3-acetyl pyridine adenine dinucleotide (APAD) to be a co-factor, the pfLDH activity could be easily distinguished from that of the host LDH. Briefly, the cultures were carefully re-suspendedat the end of the incubation, and aliquots of 20 µL were taken out and added toa 96-well microplate that contained 100 µL of the Malstat reagent and 25 µL of NBT/PES (Nitro Blue Tetrazolium/ Phenazineethylsulphate). The Malstat reagent is a combination of 0.125% v/v Triton X-100, 130 mM L-lactate, 30 mM Tris buffer and 0.62 mMAPAD and controlled to

pH 9 using1 M HCl. The NBT/PES reagent is made up of 1.96 mM NBT and 0.24 mM PES. Nitro Blue Tetrazolium is reduced to blue formazan and is spectrophotometrically (OD_{650}) read as a measure of pLDH activity and thus of parasite viability. The values of the % parasite growthagainst their concentrations were plotted. The IC_{50}were determined by curve-fitting analysis which was achieved using non-linear regression equationof the sigmoidal dose-response data through a four-parameter variable slope method. The analysis was performed on a Graphpad prism® (7.0). Antiplasmodial activities were determined and demonstrated to be 50% inhibitory concentrations (that is concentrations of drug that can achievethe inhibition of parasite growth by 50%). Each IC_{50} value was calculatedto be mean ± standard deviation of no less than three different analyses measured in duplicate.

3.7Preliminary solvent-solvent partitioning

Liquid-liquid fractionation was carried out on *C. racemosum* and *C. zenkeri* methanol extracts. The extracts (5 g) each were partitioned successively in a separating funnel between chloroform, ethyl acetate, n-butanol and water to produce four fractions.

3.8The TLC analysis of partitioned fractions of *C. racemosum* and *C. zenkeri*

The TLC analysis was carried out for *C. racemosum* ethyl acetate fraction (CRE), *C. racemosum* butanol fraction (CRB), *C. zenkeri* ethyl acetate fraction (CZE) and *C. zenkeri* butanol fraction (CZB). The fractions (5 µL) each were loaded on pre-coated TLC plates F_{254} silica gel 60. The mobile phase ratio 100/11/11/24 of ethyl acetate/acetic acid/formic acid/water was used to develop the fractions inside TLC chambers. Anisaldehyde-sulphuric acid detecting reagent was used to spray the TLC plate and was subjected to heat at 110 °C for optimal visualization of the chromatograms at visible light. The analysis was repeated with the same mobile phase and natural product/polyethylene glycol 4000 detecting reagent was used to spray the TLC chromatogram and visualized under UV at 366 nm. The TLC analysis was likewise carried out for *C. racemosum* chloroform fraction (CRC) and *C. zenkeri* chloroform fraction (CZC). The fractions (5 µL) each were loaded on pre-coated TLC plates F_{254} silica gel 60. The mobile phase ratio 95/1.5/0.1of chloroform/methanol/water was used to develop the fractions inside TLC chambers.Anisaldehyde-sulphuric acid detecting reagent was used to spray the TLC plate and was subjected to heat at 110 °C for optimal visualization of the chromatograms at visible light. A repetition of the TLC analysis was conductedusing mobile

phase chloroform/methanol 97/5 and anisaldehyde-sulphuric acid detecting reagent was used to spray the TLC plate and was subjected to heat at 110 °C for optimal visualization of the chromatograms at visible light and also viewed under UV at 366 nm.

3.9 Antiplasmodial activity investigation of the*C. racemosum* and *C. zenkeri* fractions

In vitro maintenance of *Plasmodium falciparum* strains was done according to procedure reported earlier in session 3.6.1.

3.9.1 Sensitivity assay of fractions

For the fractions sensitivity assay, a colorimetric method was used on the basis of parasite LDH detection (Markler *et al*., 1993). *Combretum zenkeri* and *C. racemosum*fractions were dissolved in DMSObecoming 10 mg/mL concentration. Thesolution of fractions were transfered into 96 wells flat-bottom micro-well plates in duplicate (Costar) and seven 1:2 serial dilutions were made directly in the plate in a volume of 100 µL (1.6 to 200 µg/mL were the final concentrations used for the fractions and ≤1% was final concentration of DMSO used, which showedno toxicity to the parasite. Asynchronous cultures with parasitemia of 1–1.5% and 2% hematocrit (1% final) were aliquoted into the plates and incubated for 72 h, in a final volume of 200 µL/well. The negative control was cultures without drugs while chloroquine (CQ) was utilised as reference compound. Using a modified method (Markler *et al*., 1993), the parasite growth was determined by measuring the *P. falciparum* lactate dehydrogenase (pfLDH) activity. By the usage of 3-acetyl pyridine adenine dinucleotide (APAD) to be a co-factor, the pfLDH activity could be easily distinguished from that of the host LDH.Briefly, the cultures were carefully re-suspendedat the end of the incubation, and aliquots of 20 µL were taken out and added to a 96-well microplate that contained 100 µL ofthe Malstat reagent and 25 µL of NBT/PES (Nitro Blue Tetrazolium/ Phenazineethylsulphate). The Malstat reagent is made of 0.125% v/v Triton X-100, 130 mM L-lactate, 30 mM Tris buffer and 0.62 mM APAD and controlled to pH 9 using 1 M HCl. The NBT/PES reagent is made up of 1.96 mM NBT and 0.24 mM PES. Nitro Blue Tetrazolium is reduced to blue formazan and is spectrophotometrically (OD_{650}) read as a measure of pLDH activity and thus of parasite viability. The values of the % parasite growth against their concentrations were plotted. The IC_{50}were determined by curve-fitting analysis which was achieved using non-linear regression equation of the sigmoidal dose-response data through a four-parameter variable slope method.

The analysis was performed on a Graphpad prism® (7.0). Antimalarial activity was determined and demonstratedto be 50% inhibitory concentrations (that is concentrations of drug that can achieve the inhibition of parasite growth by 50%). Each IC_{50} value was calculatedto be mean ± standard deviation of no less than three different analyses measured in duplicate.Statistical analyses were determined by means ofa two-tailed Student t test and statistical significance was set at $\alpha_{0.05}$.

3.10*Combretum racemosum* methanol extract (large scale) solvent-solvent partition

The fractionation of *C. racemosum* methanol extract (25 g) through solvent-solvent partition was carried out. This was a scale-up of the initial solvent-solvent partition previously done on *C. racemosum* methanol extract. This was carried out to get more chloroform portion for further investigation. The extract was partitioned between chloroform, n-butanol and water in a 1000 ml separatory flask. The chloroform fraction was filtered with Whatman No 1 filter paper and dried by evaporation under reduced pressure with Buchi rotary evaporator at 40 °C. The fraction was placed in a desiccator to remove residual solvents. The *C. racemosum* chloroform (CRC) fraction was weighed to determine the amount and was stored in a cool and dry place till needed for analysis.

3.11 Chromatographic fractionation of *C. racemosum* chloroform (CRC) fraction

To search for the real biologically active component(s) in this plant, 4.5 g of the chloroform fraction was fractionated using silica column flash CC (PuriFlash column 25 silica HC 120G 20 bar) using mobile phase of $CHCl_3$/MeOH/H_2O (30 mins 98%:2%:0%; 20 mins 95%:5%:0%; 11 mins 90%:9%:1%; 14 mins 52%:45%:3%; 15 mins 50%:45%:5%) in a gradient manner to yield 307 fractions pooled thereafter based on the similarities in their TLC profile to afford 20 fractions (FCR1 to FCR20). The fractions were dried under reduced pressure with Buchi rotary evaporator at 40 °C. The fractions were placed in desiccator to remove residual solvents. The amount of the fractions were determinedas wellkept in the refrigerator till needed for analysis. The elution, detection and collection procedures are shown in Figure 3.1 below:

Elution Steps

N°	Time	Flow Rate	%A	%B	%C	B.Flush
01	00 s	46.0	98	02	00	Dir.
02	20:00	46.0	98	02	00	Dir.
03	30:00	46.0	95	05	00	Dir.
04	40:00	46.0	95	05	00	Dir.
05	50:00	46.0	90	09	01	Dir.
06	01:00:00	46.0	90	09	01	Dir.
07	01:01:00	46.0	52	45	03	Dir.
08	01:10:00	46.0	52	45	03	Dir.
09	01:15:00	46.0	50	45	05	Dir.
10	01:20:00	46.0	50	45	05	Dir.
11	01:25:00	46.0	50	45	05	Dir.
12	01:30:00	46.0	50	45	05	Dir.

Detection Steps

N°	Time	Parameter	Collect	Threshold	F1
01	00 s	UV600:SIG1 ==> 254 nm	No	10	1
		UV600:SCAN ==> 200-600	Yes	10	1
		ELSD ==> 30°-1	Yes	10	1
		UV600:SIG2 ==> 330 nm	No	15	5

Collection Steps

N°	Time	Local	Volume	Mode	Action
01	00 s	Yes	15.0	All	None

Figure 3.1: Separation and elution procedure for *C. racemosum* chloroform fraction

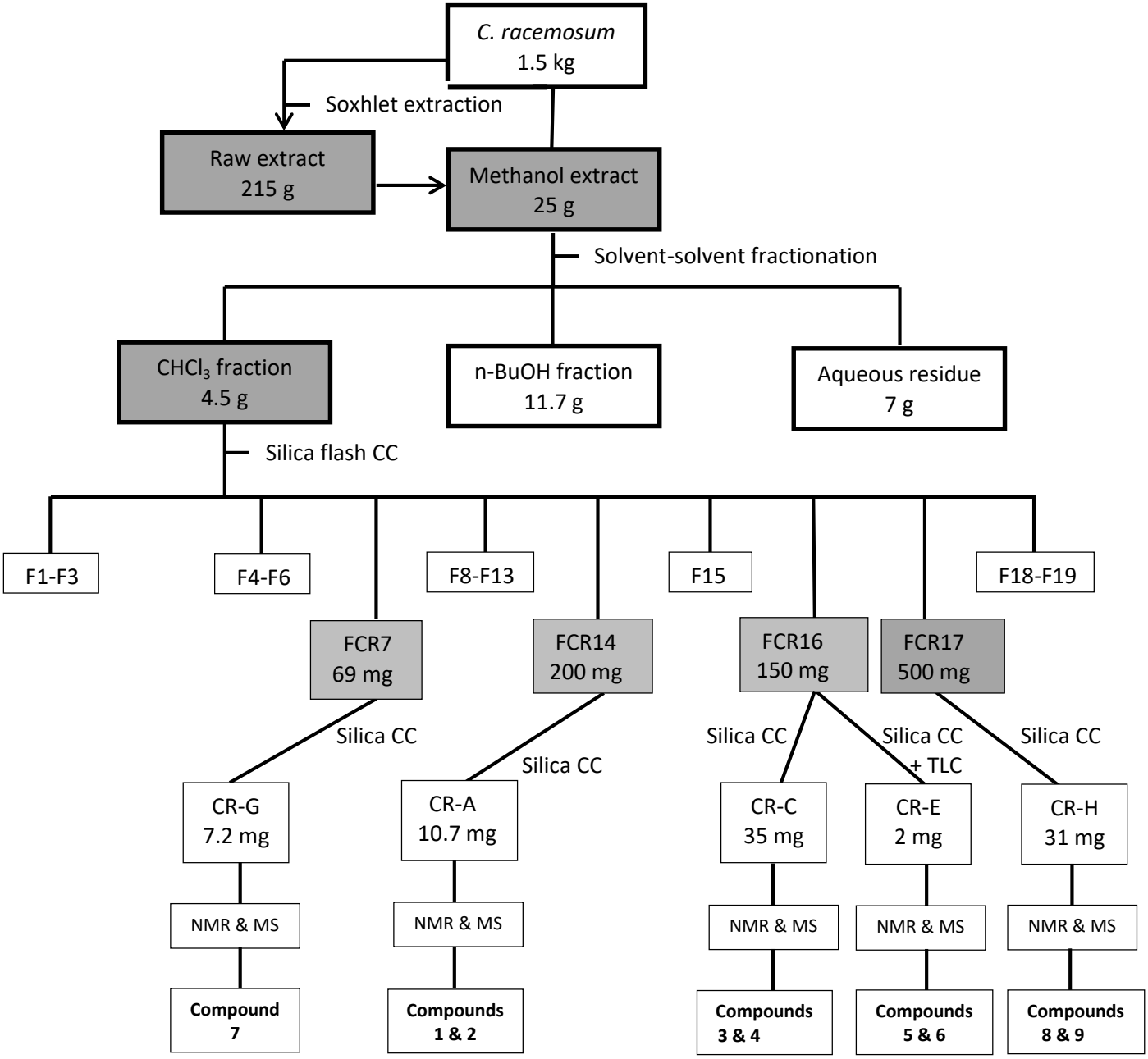

Figure 3.2: Diagramatic representation of extraction and fractionation of *C. racemosum*

3.12 Chromatographic isolation of compound CR-A

The FCR14 (200 mg) was investigated further by means of chromatographic separation on a silica glass column (1cm x 100cm; 500 mL column vol.) filled with silica gel 60 (70-230 mesh) (Merck) and eluted with gradient mobile phase ratio in an increasing polar mixture of $CHCl_3$/MeOH/H_2O 95+1.5+0.1 (46.5 hours) → 90:3:0.1 (70.5 hours) → 85:8:0.5 (75.5 hours) → 75:15:1.5 (11.5 hours) → 60:30:2.5 (17 hours). The collection tubes were arranged inside automatic electronic fraction collector with the flow rate set at 2 mL per 30 minutes for the collection of fractions. This produced 18 fractions (FCR14_1 to FCR14_18). The fractions were dried by evaporation under reduced pressure with Buchi rotary evaporator at 40 °C. The fractions were placed in desiccator to remove residual solvents. These were weighed to determine their amount and were stored in a cool and dry place till needed for analysis. The TLC of all 18 fractions was carried out. The fractions (5 µL) each were loaded on pre-coated TLC plates F_{254} silica gel 60. The fractions were developed inside TLC chambers using mobile phase ratio 80/20 of chloroform/methanol. Anisaldehyde-sulphuric acid detecting reagent was used to spray the TLC plate and was subjected to heat at 110 °C for optimal visualisation of the chromatograms at visible light. From the TLC profiles, FCR14_12 afforded compound CR-A.

Table 3.1: Elution and separation procedures for compound CR-A

Gradient			Duration	Fractionscollected	Eluent volume
$CHCl_3$	MeOH	Water	ofcollection (h)		used (mL)
95	1.5	0.1	46.5	F1-93	186
90	3	0.1	70.5	F94-234	282
85	8	0.5	75.5	F235-385	302
75	15	1.5	11.5	F386-408	46
60	30	2.5	17	F409-442	68

Note:

Column specification: 1cm diameter, 100cm length and 500mL column volume

Stationary phase: silica gel 60 (70-230 mesh size)

Flow rate: 2mL per 30 minutes

Sample amount: 200 mg

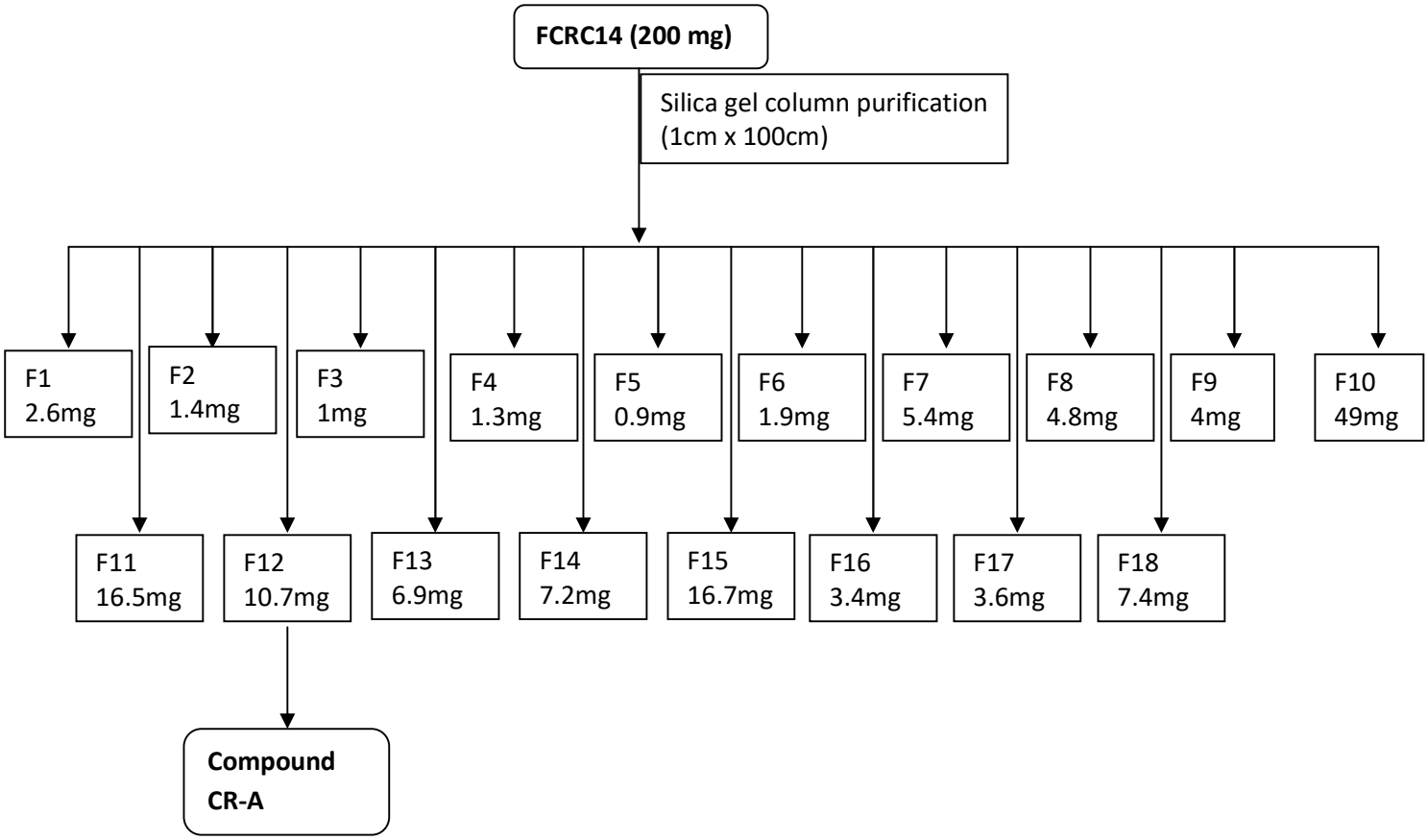

Figure 3.3: Diagramatic representation of isolation of compound CR-A

3.13 Chromatographic isolation of compound CR-C

The FCR16 (300 mg) was fractionated using silica columnflash CC (PuriFlash column 30 silica HP 25G 22 bar) with a gradient mobile phase in an increasing polar mixture of $CHCl_3$/MeOH/H_2O (10 mins 98%:2%:0%; 20 mins 95%:5%:0%; 21 mins 90%:9%:1%; 4 mins 52%:45%:3%; 19.51 mins 50%:45%:5%; 9.79 mins 0%:100%:0%) to yield 128 fractions pooled thereafter based on the similarities in their TLC profile to afford 5 fractions (FCR16_1 to FCR16_5). The fractions were dried by evaporation under reduced pressure with Buchi rotary evaporator at 40 °C. The fractions were placed in desiccator to remove residual solvents. The amounts of the fractions were determinedas wellkept in the refrigerator till needed for analysis.The TLC of all 5 fractions was carried out. The fractions (5 µL) each were loaded on pre-coated TLC plates F_{254} silica gel 60. The fractions were developed inside TLC chambers using mobile phase ratio 80/20 of chloroform/methanol. Anisaldehyde-sulphuric acid detecting reagent was used to spray the TLC plate and was subjected to heat at 110 °C for optimal visualisation of the chromatograms at visible light. The FCR16_3 (150 mg) was investigated further by means of chromatographic separation on a silica glass column (1cm x 100cm; 1000 mL column vol.) filled with silica gel 60 (70-230 mesh) (Merck) and eluted with gradient mobile phase ratio in an increasing polar mixture of $CHCl_3$/MeOH/H_2O 100:0:0 (12 hours) → 95:1.5:0 (12 hours) → 90:3:0.1 (24 hours) → 85:8:0.5 (166 hours) → 75:15:1.5 (24 hours). The collection tubes were arranged inside automatic electronic fraction collector with the flow rate set at 2 ml per 30 minutes for the collection of fractions. This produced 18 fractions (FCR16_3_1 to FCR16_3_18). The fractions were dried by evaporation under reduced pressure with Buchi rotary evaporator at 40 °C. The fractions were placed in desiccator to remove residual solvents. These were weighed to determine their amount and were stored in a cool and dry place till needed for analysis. The TLC of all 18 fractions was carried out. The fractions (5 µL) each were loaded on pre-coated TLC plates F_{254} silica gel 60. Mobile phase chloroform/methanol 80/20 was used to develop the fractions inside TLC chambers. Anisaldehyde-sulphuric acid detecting reagent was used to spray the TLC plate and was subjected to heat at 110 °C for optimal visualisation of the chromatograms at visible light. From the TLC profiles, FCR16_3_10 to FCR16_3_14 as a result of their similarities in TLC pattern afforded compound CR-C. Also, compound CR-A was once again identified from FCR16_3_1.

Elution Steps

N°	Time	Flow Rate	%A	%B	%C	B.Flush
01	00 s	15.0	98	02	00	Dir.
02	05:00	15.0	98	02	00	Dir.
03	10:00	15.0	95	05	00	Dir.
04	20:00	15.0	95	05	00	Dir.
05	30:00	15.0	90	09	01	Dir.
06	50:00	15.0	90	09	01	Dir.
07	51:00	15.0	52	45	03	Dir.
08	56:00	15.0	50	45	05	Dir.
09	01:06:00	15.0	50	45	05	Dir.
10	01:15:51	15.0	00	100	00	Dir.
11	01:25:30	15.0	00	100	00	Dir.

Detection Steps

N°	Time	Parameter	Collect	Threshold	F1
01	00 s	UV600:SIG1 ==> 254 nm	No	10	1
		UV600:SCAN ==> 200-600	Yes	10	1
		ELSD ==> 30°-1	Yes	10	1
		UV600:SIG2 ==> 330 nm	No	15	5

Collection Steps

N°	Time	Local	Volume	Mode	Action
01	00 s	Yes	15.0	All	None

Figure 3.4: Separation and elution procedure for FCRC16

Table 3.2: Elution and separation procedures for compound CR-C

Gradient			Duration	Fractionscollected	Eluent volume
$CHCl_3$	MeOH	Water	ofcollection (h)		used (mL)
100	0	0	12	Nil	
95	1.5	0	12	Nil	
90	3	0.1	24	Nil	
85	8	0.5	166	F1-332	664
75	15	1.5	24	F333-381	98

Note:

Column specification: 1cm diameter, 100cm length& 1000mL column volume

Stationary phase: silica gel 60 (70-230 mesh size)

Flow rate: 2mL per 30 minutes

Sample amount: 150 mg

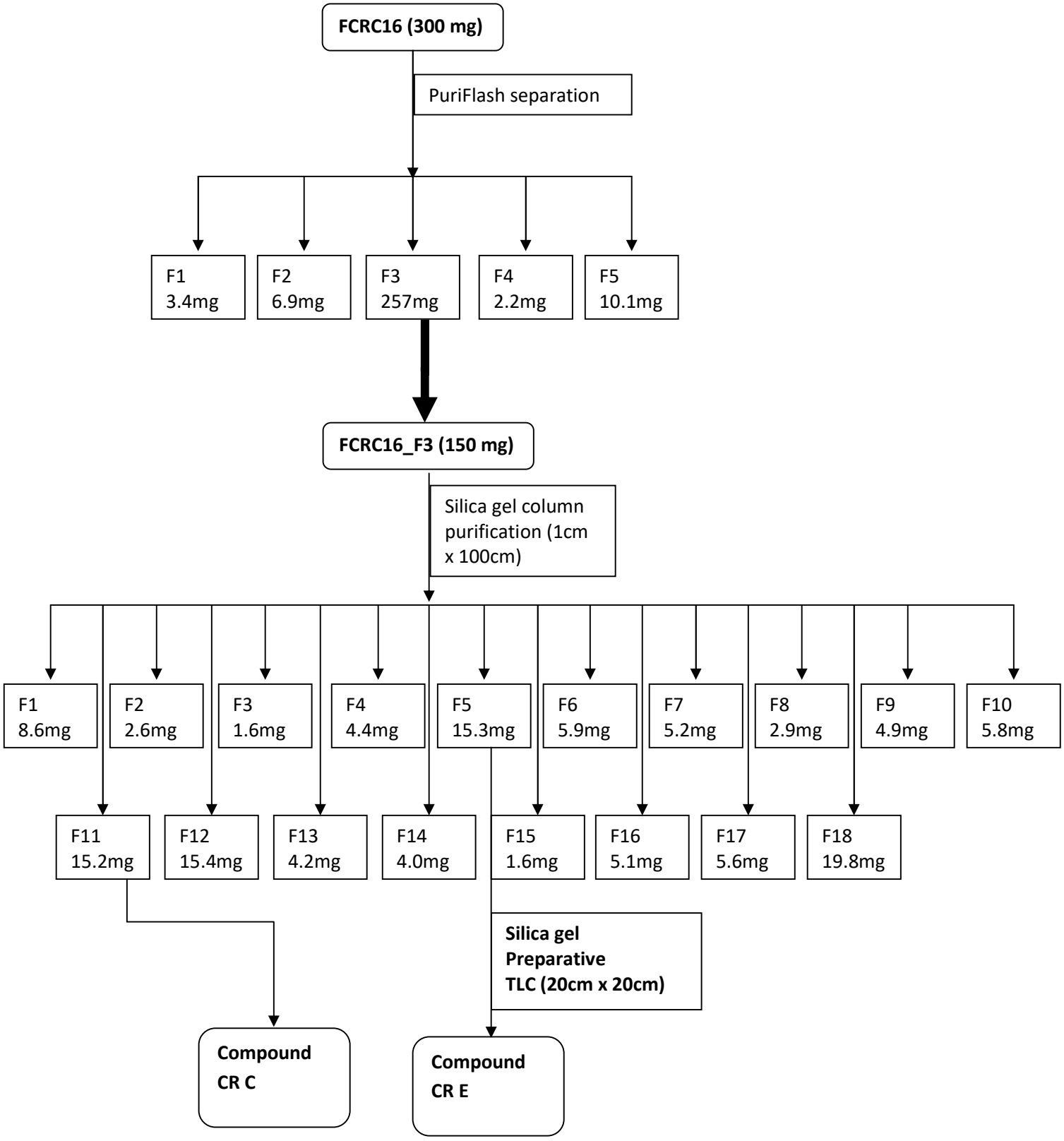

Figure 3.5: Diagramatic representation showing the isolation of compounds CR-C and CR-E

3.14 Chromatographic isolation of compound CR-E

Purification of FCR16_3_5 (15 mg) was carried out using preparative TLC plates (20cm x20cm) (Merck) under the use of aprogrammed TLC sampling machine (ATS4, CAMAG). The mobile phase toluene/ethyl acetate/formic acid (3:7:1) was used to develop the plates by making use of automated chamber(ADC2, CAMAG) for development of TLC set to 48% humidity, 24°C, and 20 minutes saturation with saturation pad. The sample applied (11 µL) each was loaded with CAMAG TLC automated machine. A total of 198 µL of the sample was applied as band on the plate. Sample was repeated on another plate by applying 15 µL each with CAMAG TLC automated machine. In this case, a total of 270 µL of thesample was applied as band on the plate. The two plates prepared were both left to dry under a stream of air. A preliminary TLC for mobile phase optimisation was carried out to select the appropriate mobile phase for the best separation. The fraction was developed on TLC with mobile phases: toluene/ethyl acetate/formic acid 3/7/1 and chloroform/ethyl acetate/formic acid 4/5/1. The two plates already prepared were developed with toluene/ethyl acetate/formic acid 3/7/1 being selected as best solvent system. After developing on TLC the two plates that contain the separated compounds were placed under vacuum dryer to evaporate the formic acid. The separation was not visible under UV or visible light, therefore, 2 cm of the plates was dipped into anisaldehyde/sulphuric acid detecting reagent to visualise the separation and the band of interest was carefully marked and scrapped. The purification afforded compound CR-E.

3.15 Chromatographic isolation of compound CR-G

The FCR7 (69 mg) was investigated further by means of chromatographic separation on a silica glass column (1cm x 100cm; 500 mL column vol.) filled with silica gel 60 (70-230 mesh) (Merck) and eluted with gradient mobile phase ratio in an increasing polar mixture of $CHCl_3$/MeOH/H_2O 100:0:0 (12 hours) → 95:1.5:0.1 (20 hours) → 90:5:0.2(26 hours) → 85:8:0.5 (64 hours). The collection tubes were arranged inside automatic electronic fraction collector with the flow rate set at 2 ml per 30 minutes for the collection of fractions. This produced 11 fractions (FCR7_1 to FCR7_11). The fractions were dried by evaporation under reduced pressure with Buchi rotary evaporator at 40 °C. The fractions were placed in desiccator to remove residual solvents. These were weighed to determine their amount and was stored in a cool and dry place till needed for analysis. The TLC of all 11 fractions was carried out. The fractions (5 µL) each were loaded on pre-coated TLC plates F_{254} silica gel 60.

Mobile phase chloroform/methanol 80/20 was used to develop the fractions inside TLC chambers. Anisaldehyde-sulphuric acid detecting reagent was used to spray the TLC plate and was subjected to heat at 110 $^{\circ}$C for optimal visualisation of the chromatograms at visible light. From the TLC profiles, FCR7_9 to FCR7_11 as a result of their similarities in TLC pattern afforded compound CR-G.

3.16 Chromatographic isolation of compound CR-H

The FCR17 (500 mg) was investigated further by means of chromatographic separation on a silica glass column (2cm x 100cm; 2000 mL column vol.) filled with silica gel 60 (70-230 mesh) (Merck) and eluted with gradient mobile phase ratio in an increasing polar mixture of EtoAc/MeOH/H_2O 100:0:0 (24 hours) → 97.5:2.5:0 (5.5 hours) → 95:5:0(39.5 hours) → 90:10:0.1(9.5 hours) → 85:15:0.1 (61.5 hours) → 75:25:0.1 (26.5 hours) → 65:30:0.2 (25 hours) → and the column was washed down with 30:65:3. The collection tubes were arranged inside automatic electronic fraction collector with the flow rate set at 2 mL per 30 minutes for the collection of fractions. This produced 14 fractions (FCR17_1 to FCR17_14). The fractions were dried by evaporation under reduced pressure with Buchi rotary evaporator at 40 °C. The fractions were placed in desiccator to remove residual solvents. These were weighed to determine their amount and was stored in a cool and dry place till needed for analysis. The TLC of all 14 fractions was carried out. The fractions (5 µL) each were loaded on pre-coated TLC plates F_{254} silica gel 60. Mobile phase ethyl acetate/methanol 75/25 was used to develop the FCR17_1 to FCR17_9 and ethyl acetate/methanol/water 80/15/5 to develop more polar FCR17_10 to FCR17_14 inside TLC chambers. Anisaldehyde-sulphuric acid detecting reagent was used to spray the TLC plate and was subjected to heat at 110 $^{\circ}$C for optimal visualisation of the chromatograms at visible light. From the TLC profiles, FCR17_4 to FCR17_6 as a result of their similarities in TLC pattern afforded compound CR-H.

Table 3.3: Elution and separation procedures for compound CR-G

Gradient			Duration	Fractionscollected	Eluent volume
$CHCl_3$	MeOH	Water	ofcollection (h)		used (mL)
100	0	0	12	Nil	
95	1.5	0.1	20	F1-40	80
90	5	0.2	26	F41-92	104
85	8	0.5	64	F93-220	256

Note:

Column specification: 2cm diameter, 100cm length and 500mL column volume

Stationary phase: silica gel 60 (230-400 mesh size)

Flow rate: 2mL per 30 minutes

Sample amount: 69 mg

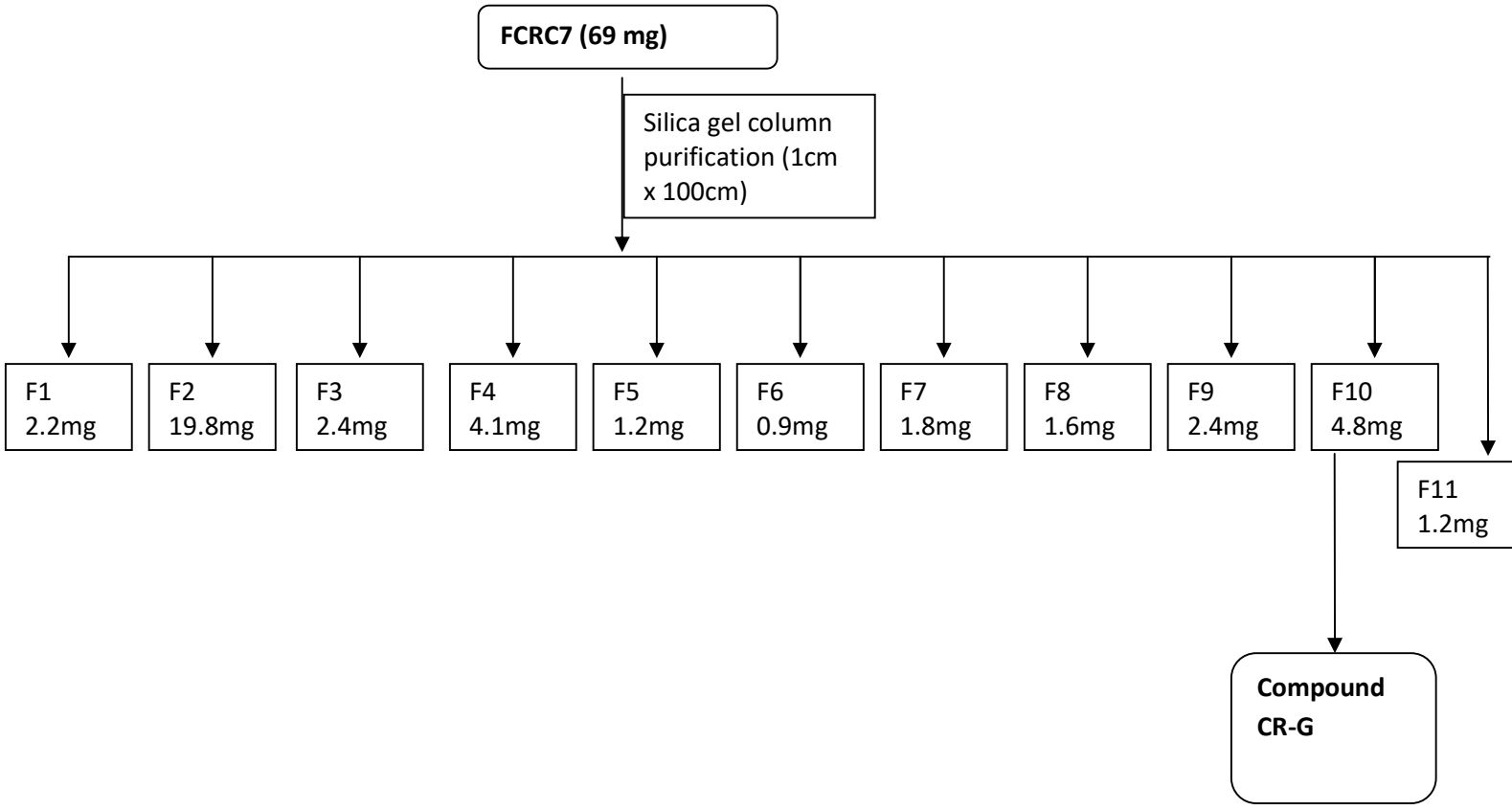

Figure 3.6: Diagramatic representation showing the isolation of compound CR-G

Table 3.4: Elution and separation procedures for compound CR-H

Gradient			Duration	Fractionscollected	Eluent volume
EtOAc	MeOH	Water	ofcollection (h)		used (mL)
100	0	0	24	Nil	
97.5	2.5	0	5	F1-11	22
95	5	0	39.5	F12-90	158
90	10	0.1	9.5	F91-109	38
85	15	0.1	61.5	F110-232	246
75	25	0.1	26.5	F233-285	106
65	30	0.2	25	F286-335	100
30	65	3	Columnwash	Columnwash	

Note:

Column specification: 2.5cm diameter, 100cm lengthand 2000mL column volume

Stationary phase: silica gel 60 (70-230 mesh size)

Flow rate: 2mL per 30 minutes

Sample amount: 500 mg

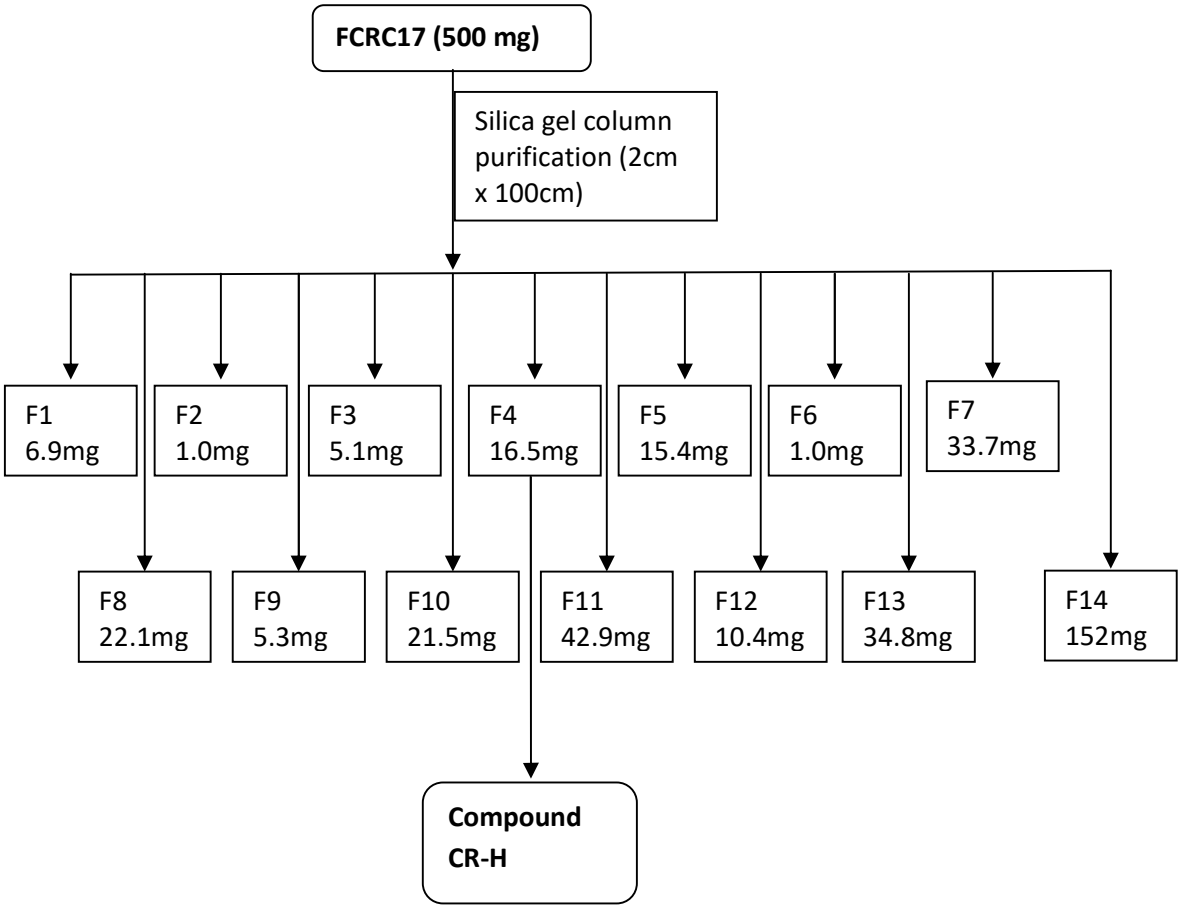

Figure 3.7: Diagramatic representation showing the isolation of compound CR-H

3.17 Chromatographic fractionation of *C. zenkeri* chloroform fraction

More *C. zenkeri* chloroform fraction was afforded by weighing 10 g of *C. zenkeri* methanol extract and 300 mL chloroform was added to it, was put on supersonic bath for 15 minutes to extract the chloroform portion. For more chloroform extractible, this was done two more times, supernatant was filtered and evaporated to dryness at a reduced pressure on a rotary evaporator. The fraction was put in desiccator for complete dryness of the solvent residue. Afterwards 600 mg of the chloroform fraction was used for chromatographic separation. In order to search out the actual biologically active component(s) in this plant, 600 mg of the chloroform fraction was fractionated using silica column flash CC (PuriFlash column 30 silica HP 40G 20 bar) with a mobile phase gradient of $CHCl_3$/MeOH/H_2O (36.54 mins 98%:2%:0%; 36.94 mins 90%:9%:1%; 36.94 mins 80%:17%:3%; 36.94 mins 70%:25%:5%; 18.94 mins 60%:35%:5%) to yield 301 fractions pooled thereafter based on the similarities in their TLC profile to give 9 fractions (FCZ1 to FCZ9).The fractions were evaporated to dryness under reduced pressure with Buchi rotary evaporator at 40 $^{\circ}$C. The fractions were placed in desiccator to remove residual solvents. The amounts of the fractions were determined and they were kept in a cool and dry place till needed for analysis.

The elution, detection and collection procedures for the separation are shown in Figure 3.9.

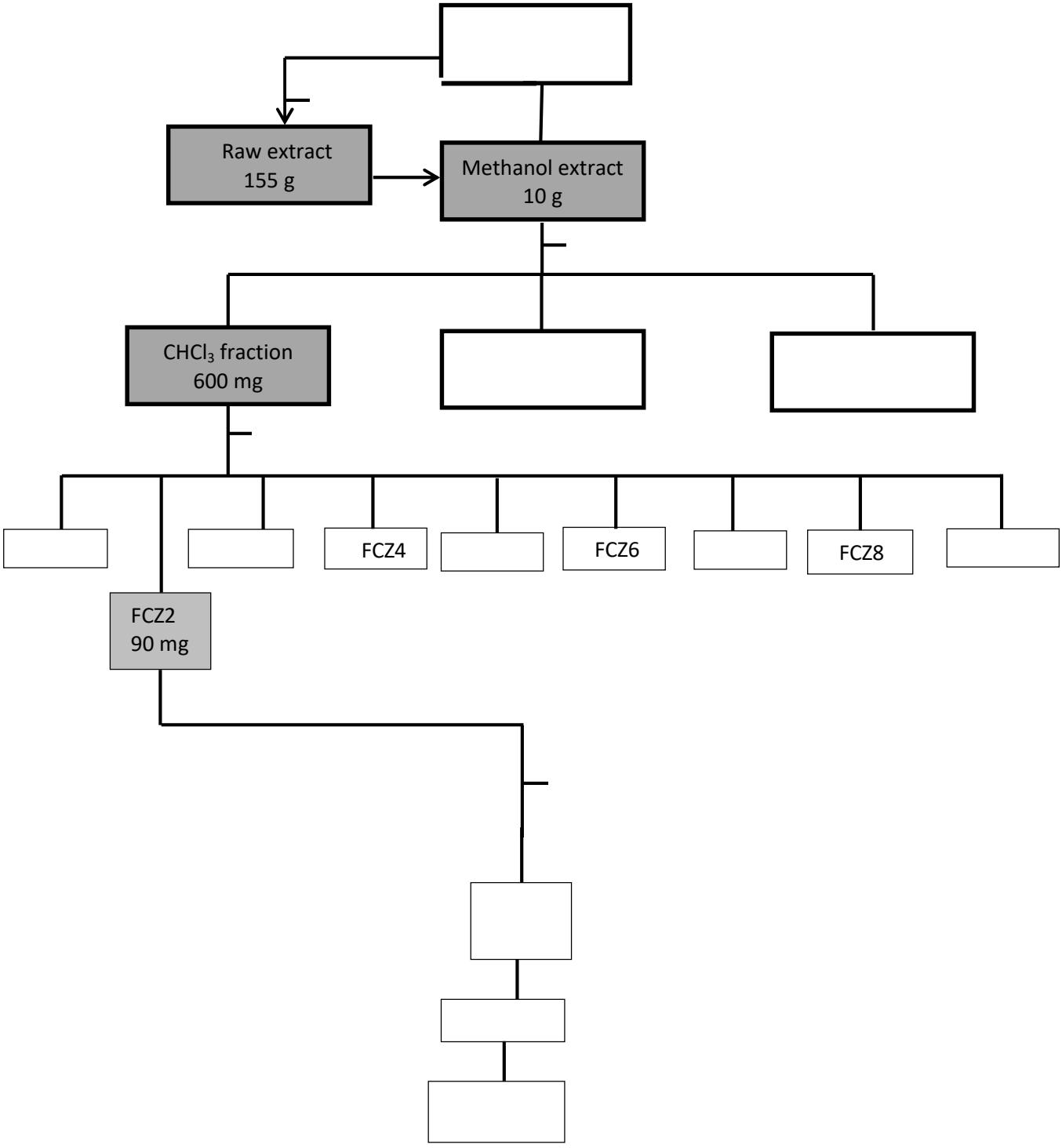

Figure 3.8: Diagramatic representation of extraction and fractionation of *C. zenkeri*

Elution Steps

N°	Time	Flow Rate	%A	%B	%C	B.Flush
01	00 s	26.0	98	02	00	Dir.
02	18:27	26.0	98	02	00	Dir.
03	36:54	26.0	90	09	01	Dir.
04	55:21	26.0	90	09	01	Dir.
05	01:13:48	26.0	80	17	03	Dir.
06	01:32:15	26.0	80	17	03	Dir.
07	01:50:42	26.0	70	25	05	Dir.
08	02:18:23	26.0	70	25	05	Dir.
09	02:27:36	26.0	60	35	05	Dir.
10	02:46:03	26.0	60	35	05	Dir.

Detection Steps

N°	Time	Parameter	Collect	Threshold	F1
01	00 s	UV600:SIG1 ==> 254 nm	No	10	1
		UV600:SCAN ==> 200-600	Yes	10	1
		ELSD ==> 30°-1	Yes	10	1
		UV600:SIG2 ==> 330 nm	No	15	5

Collection Steps

N°	Time	Local	Volume	Mode	Action
01	00 s	Yes	15.0	All	None

Figure 3.9: Procedure steps for separation of *C. zenkeri* chloroform fraction

3.18 Chromatographic isolation of compound CZ-A

The FCZ2 (90 mg) was investigated further by means of chromatographic separation on a silica glass column (1cm x 60cm; 250 mL column vol.) filled with silica gel 60 (70-230 mesh) (Merck) and separated by isocratic elution with mixture of mobile phase ratio 95/1.5/0.1 of $CHCl_3$/MeOH/H_2O. The collection tubes were arranged inside automatic electronic fraction collector with the flow rate set at 2 mL per 30 minutes for the collection of fractions. This produced 21 fractions (F1-F21). The fractions were dried by evaporation under reduced pressure with Buchi rotary evaporator at 40 $^{\circ}$C. The fractions were placed in desiccator to remove residual solvents. These were weighed to determine their amount and they were stored in a cool and dry place till needed for analysis. The TLC of all 21 fractions was carried out. The fractions (5 µL) each were loaded on pre-coated TLC plates F_{254} silica gel 60. Mobile phase chloroform/methanol 97/3 was used to develop the fractions inside TLC chambers. Anisaldehyde-sulphuric acid detecting reagent was used to spray the TLC plate and was subjected to heat at 110 $^{\circ}$C for optimal visualisation of the chromatograms at visible light. From the TLC profiles, F12-F15 as a result of their similarities in TLC pattern afforded compound CZ-A.

3.19Chemical characterization and structure elucidation

The determination of the structures of the compounds was through extensive spectroscopic methods including 1D NMR (^{1}H, ^{13}C and DEPT), 2D NMR (HMBC, HSQC, COSY, NOESY and TOCSY), ESI-MS and HR-ESIMS, and also by comparingdata generated with related reported literature.

3.19.1 Nuclear magnetic resonance (NMR) spectroscopy

One dimensional (1D) and 2D Nuclear Magnetic Resonance (NMR) data were obtained by using an Avance III HDX 700 MHz NMR spectrometer (Bruker BioSpin, Germany), equipped with an inverse quadruple helium cooled cryoprobe (QCI-F, ^{1}H, ^{13}C, ^{19}F, ^{15}N)with z-axis gradients and automatic tuning and matchingaccessory. The samples were measured at 298 K in fully deuterated chloroform or methanolwith TMS as internal standard. The resonance frequency for ^{1}H was 700.40 MHz, and for ^{13}C NMR 176.12 MHz. Standard 1D and gradient-enhanced 2D experiments, such as DEPTq, DQF-COSY, TOCSY, NOESY, HSQC and HMBC were used. All spectra were processed in TopSpin (Bruker BioSpin, Germany) and referenced for ^{1}H on the residual solvent signal (δ = 3.31 ppm for MeOH-d_4, (δ = 7.26 ppm for

$CDCl_3$), and for ^{13}C on the solvent signal (δ = 49.0 ppmfor MeOH-d_4, (δ = 77.0 ppm for $CDCl_3$). Chemical shifts were measured in δ ppm and coupling constants *J* were measured in Hertz (Hz). The multiplicity of signals were given as s (singlet), d (doublet), t (triplet), m (multiplet), q (quartet), qt (quintet) or br (broad).

3.19.2 Mass Spectrometry (MS)

Low-resolution electrospray ionisation - multistage mass spectrometry (ESI-MS^n) experiments were performed on an amaZon speed 3D ion trap instrument and high-resolution ESI mass spectra (*m/z* 50-1900) were obtained on a maXis UHR ESI-Qq-TOF mass spectrometer (both Bruker Daltonics, Bremen, Germany) by direct infusion. The sum formulas of the detected ions were determined using Bruker Compass DataAnalysis 4.1 based on the mass accuracy ($\Delta m/z \leq 5$ ppm) and isotopic pattern matching (SmartFormula algorithm).

3.20 Antiplasmodial activity investigation of the compounds isolated

In vitro culture of the strains of *Plasmodium falciparum* was done according to procedure reported earlier in session 3.6.1.

3.20.1 Sensitivity assay of compounds isolated

For the sensitivity assay of compounds isolated, a colorimetric method was employed based on the parasite LDH detection (Markler *et al*., 1993). Isolated compoundswere dissolved in DMSO becoming 10mg/mL concentration. The compounds were placed in 96 wells flat-bottom micro-well plates in duplicate (Costar) and seven 1:2 serial dilutions were made directly into the plate in a volume of 100 µL (1.6 to 200 µg/mL were the final concentrations used for the fractions and ≤1% was final concentration of DMSO used, which showedno toxicity to the parasite). Asynchronous cultures with parasitemia of 1–1.5% and 2% hematocrit (1% final) were aliquoted into the plates and incubated for 72 h, in a final volume of 200 µL/well. The negative control was cultures without drugs while chloroquine (CQ) was utilised as reference compound. Using a modified method (Markler *et al*., 1993), the parasite growth was determined by measuring the *P. falciparum* lactate dehydrogenase (pfLDH) activity. By the use of 3-acetyl pyridine adenine dinucleotide (APAD) to be a co-factor, the pfLDH activity could be easily distinguished from that of the host LDH.Briefly, the cultures were carefully re-suspendedat the end of the incubation, and aliquots of 20 µL were taken out and added to a 96-well microplate that contained 100 µL ofthe Malstat reagent and 25 µL of NBT/PES (Nitro

Blue Tetrazolium/ Phenazineethylsulphate). The Malstat reagent is made of 0.125% v/v Triton X-100, 130 mM L-lactate, 30 mM Tris buffer and 0.62 mM APAD and controlled to pH 9 using 1 M HCl. The NBT/PES reagent is made up of 1.96 mM NBT and 0.24 mM PES. Nitro Blue Tetrazolium is reduced to blue formazan and is spectrophotometrically (OD_{650}) read as a measure of pLDH activity and thus of parasite viability. The values of the % parasite growth against their concentrations were plotted. The IC_{50}were determined by curve-fitting analysis which was achieved using non-linear regression equation of the sigmoidal dose-response data through a four-parameter variable slope method. The analysis was performed on a Graphpad prism® (7.0). Antiplasmodial activities were determined and demonstratedto be 50% inhibitory concentrations (that is concentrations of drug that can achievethe inhibition of parasite growth by 50%). Each IC_{50} value was calculatedto be mean ± standard deviation of no less than three different analyses measured in duplicate. Statistical analyses were determined by means ofa two-tailed Student t test and statistical significance was set at $\alpha_{0.05}$.

CHAPTER FOUR

4.0RESULTS

4.1Antimalarial activity of selected medicinal plants of Combretaceae family

4.1.1 Qualitative inhibition of beta-hematin formation

The resultsof the qualitative experimentation of antimalarial activities of extracts of selected members of Combretaceae family by β-hematin formation inhibition is shown in Table 4.1 and Figure 4.1. At the 25 mg/mL concentration used, methanol and acetone extracts of*Combretum confertum* and *Terminalia mentalis*among otherstested showed no activity. The *Terminalia ivorensis* methanol extract was more active than the corresponding acetone extract. Only *C. racemosum* showed the same degree of activity for both extracts. Chloroquine tested at 10 mg/mL showed activity, but out of the eighteen extracts tested in this assay, six (*C. platypterum*, *C. hispidum*, *C. racemosum*, *C. sordidum* acetone extracts and *C. racemosum*, *T. ivorensis* methanol extracts) showed higher activity than chloroquine.

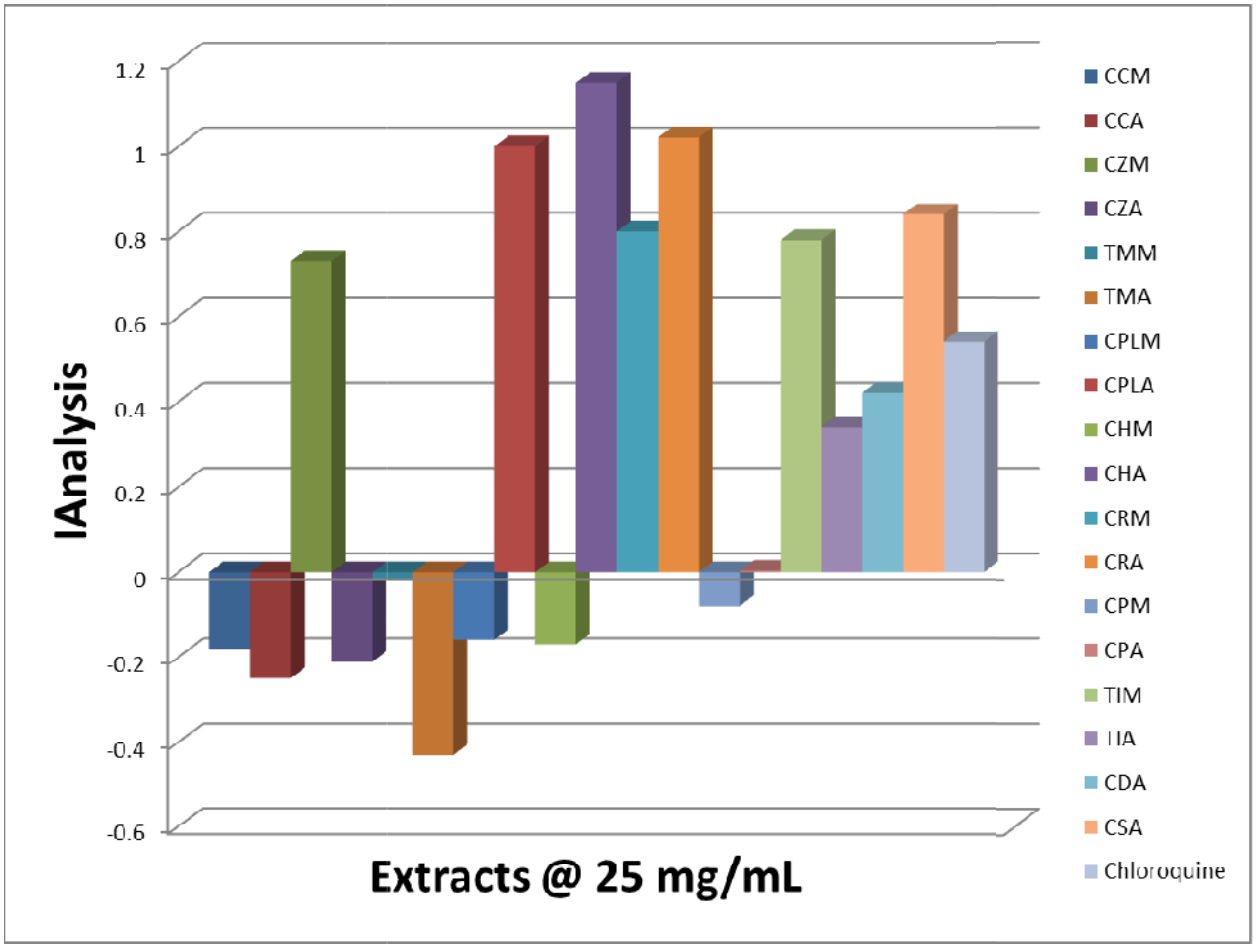

Figure 4.1: Qualitative beta-hematin formation inhibition of extract and chloroquine

Legend: CCM- *Combretum confertum* methanol, CCA- *Combretum confertum* acetone, CZM- *Combretum zenkeri* methanol, *Combretum zenkeri* acetone, *Terminalia mentalis* methanol, *Terminalia mentalis* acetone, *Combretum platypterum* methanol, *Combretum platypterum* acetone, *Combretum hispidum* methanol, *Combretum hispidum* acetone, *Combretum racemosum* methanol, *Combretum racemosum* acetone, *Combretum paniculatum* methanol, *Combretum paniculatum* acetone, *Terminalia ivorensis* methanol, *Terminalia ivorensis* acetone, *Combretum dolicopetalum* acetone, and *Combretum sordidum* acetone, extracts

Table 4.1: Results of Antimalarial β-hematin synthesis inhibition and yield of plant extract

Samples	Extraction solvent		% yield	
	Acetone	Methanol	Acetone (%)	Methanol (%)
C. confertum	-	-	8.4	6.2
C. zenkeri	-	+++	19.1	17.4
C. platypterum	+++	-	9.5	7.3
C. hispidum	+++	-	3.3	2.7
C. racemosum	+++	+++	12.5	10.9
C. paniculatum	+	-	4.0	2.9
C. sordidum	+++	NT	7.2	NA
C. dolicopetalum	++	NT	7.3	NA
T. mentalis	-	-	7.3	5.1
T. ivorensis	++	+++	12.5	8.0
Chloroquine (10 mg/mL)	++			

Legend: +++ = High activity, ++ = Moderate activity, + = Low activity, - = No activity

NT = Not Tested, NA = Not Available.

4.1.2 Quantitative inhibition of beta-hematin formation (IC_{50})

The result of the quantitative determination of inhibition of β-hematin formation at different concentrations is presented in Figure 4.2. *Terminalia ivorensis* methanol extract (TIM) had the significantly highest inhibition at all concentrations compared to other plant extracts. Its inhibition was also higher than that of chloroquine even at the lowest concentration (0.39 mg/mL). *Combretum zenkeri* and *C. racemosum* methanol extracts (CZM and CRM) had medium activity but the activity was significant in comparison with chloroquine.

The results of the IC_{50} values and P-values measured, which show how effective the extracts are, are shown in Table 4.2. As shown in Table 4.2 and Figure 4.2, in the quantitative testing of β-hematin formation inhibition at different concentrations, CPLA, CHA, CRA and CSA had no antimalarial activity while CZM, CRM and TIM showed appreciable antimalarial activity. *Combretum zenkeri* methanol, TIM and CRM showed highly significant antimalarial activity (IC_{50} = 2.92 ± 0.846 mg/mL, IC_{50} = 2.58 ± 0.447 mg/mL and IC_{50} = 3.96 ± 0.132 mg/mL respectively) comparable to the antimalarial standard drug, chloroquine (IC_{50} = 0.55 mg/mL). Butonly TIM was not significantly different when compared with chloroquine. Generally in this study, TIM (IC_{50} =2.58 ± 0.447 mg/mL) demonstrated remarkable the most pronounced effect among all the extracts tested.

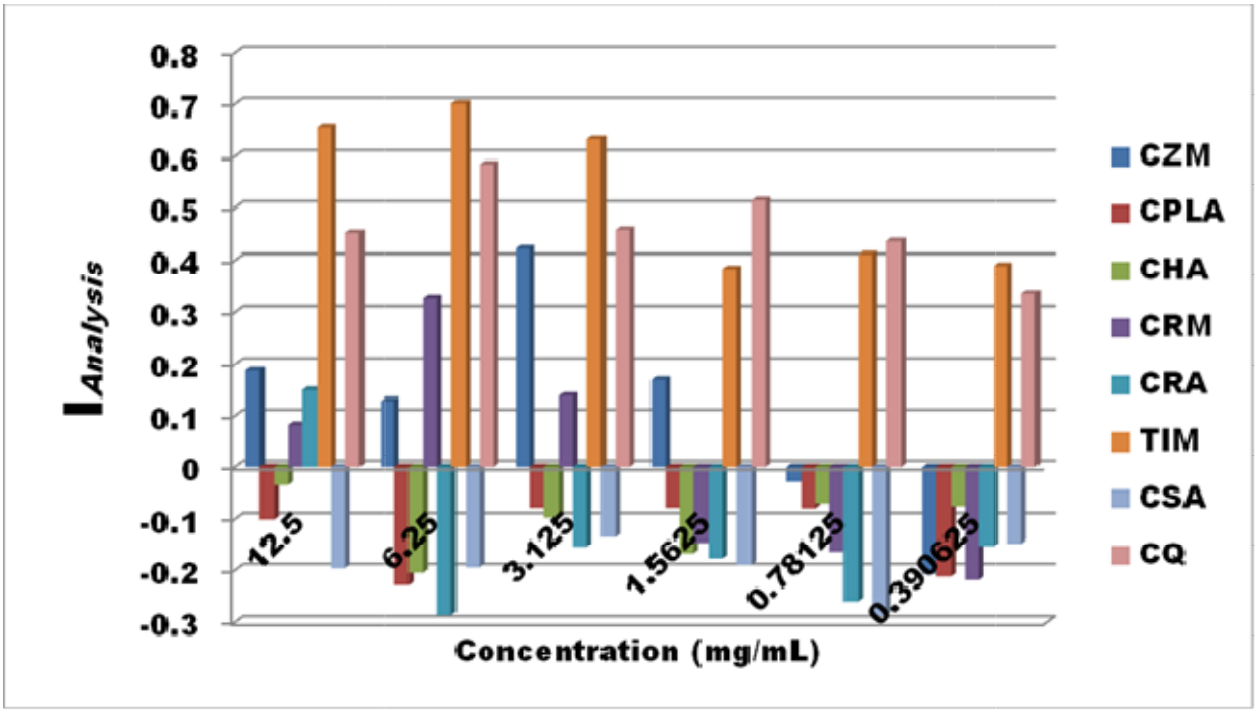

Figure 4.2: The inhibition of β-hematin formation at different concentrations determined spectrophotomically at 405 nm.

Legend: CZM = *C. zenkeri* methanol extract, CPLA = *C. platypterum* acetone extract, CHA = *C. hispidum* acetone extract, CRM = *C. racemosum* methanol extract, CRA = *C. racemosum* acetone extract, TIM = *T. ivorensis* methanol extract, CSA = *C. sordidum* acetone extract, CQ = Chloroquine

Table 4.2: IC_{50} determination of β-hematin formation inhibition

Extract	IC_{50}mg/mL Mean ± SEM	T-test P value
CZM	2.92 ± 0.846	0.0514
CPLA	**	**
CHA	**	**
CRM	3.96 ± 0.132	0.0081
CRA	**	**
TIM	2.58 ± 0.447	0.0736
CSA	**	**
CQ	0.55 ± 0.179	

Experiments were carried out in triplicate and shown as Mean±SEM.

** Not effective

Legend: CZM = *C. zenkeri* methanol extract, CPLA = *C. platypterum* acetone extract, CHA = *C. hispidum* acetone extract, CRM = *C. racemosum* methanol extract, CRA = *C. racemosum* acetone extract, TIM = *T. ivorensis* methanol extract, CSA = *C. sordidum* acetone extract, CQ = Chloroquine.

4.2The TLC fingerprints of*C. racemosum* and *C. zenkeri*methanol extracts

The result of the TLC chromatogram of the methanol extracts of *C. racemosum* and *C. zenkeri* are shown in Figure 4.3 on page 81. It revealed the presence of terpenoids with R_f ranging from 0.2-0.55 (Figure 4.3 A1 to A4) and flavonoids with R_f ranging from 0.3-0.6 (Figure 4.3 B1 to B4) unambiguously. The flavonoids were revealed more conspicuously in chromatogramB4 where ethyl acetate/methanol/water 40:5.4:4 was the mobile phase. The chromatograms of *C. racemosum* (CRM) and *C. zenkeri* (CZM) are both characterized in UV-366 nm by prominent yellow and yellow-green fluorescent zones. Flavonoids are polar compounds and their TLC chromatograms are more obvious in polar solvent systems. On the contrary, in the chromatogram of A4 where the solvent system was apolar- toluene/ethyl acetate 45:5 the flavonoid compounds in the extracts remained on the base line.

4.3 Antiplasmodial activity of *C. racemosum* and *C. zenkeri*methanol extracts

Antiplasmodial test was carried out to check the activities of *C.zenkeri*methanol (CZM) and *C. racemosum* methanol (CRM) extracts. They were quantitatively tested on *P. falciparum* lactate dehydrogenase (pLDH) andthe values of the 50% inhibition (IC_{50}) resulted from a range of concentrations used in the experiment for the extracts. The plots of their percentage parasite growth against concentrations resulted in a sigmoidal curve, specific to *P. falciparum* lactate dehydrogenase (pLDH) activity inhibition (Figures 4.6 and 4.7). The crude extracts of *C. racemosum*(IC_{50}= 64.18±2.69 µg/mL) and *C. zenkeri* (IC_{50}= 68.98±1.00 µg/mL) was active against *P. falciparum* chloroquine-sensitive D10 in concentration-response data which fitted a sigmoidal equation satisfactorily with the statistical treatment results (at 95% confidence interval 56.1-65.7 µg/mL, R^2 = 0.99, Sy.x = 4.9) and (at 95% confidence interval 48.3-75.5 µg/mL, R^2 = 0.95, Sy.x = 9.2), respectively (Table 4.3, Figure 4.6). *Combretum racemosum* (IC_{50}= 65.80±14.85 µg/mL) and *C. zenkeri* (IC_{50}= 69.68±3.09 µg/mL) methanol extractalso showed activity against *P. falciparum* chloroquine-resistant W2 in concentration-response data which fitted a sigmoidal equation satisfactorily with the statistical treatment results (at 95% confidence interval 52.8-84.0 µg/mL, R^2 = 0.96, Sy.x = 7.9) and (at 95% confidence interval 56.4-68.8 µg/mL, R^2 = 0.99, Sy.x = 3.4), respectively (Table 4.4, Figure 4.7).*Combretum*

racemosum methanol extract showed to be slightly more activethan the methanol extract of *C. zenkeri* in both D10 and W2*P. falciparum* srains (Figures 4.6 and 4.7; Tables 4.3 and 4.4).

The chloroquine standard drug was also quantitatively tested on the *P. falciparum* lactate dehydrogenase (pLDH) andthe 50% inhibition (IC_{50}) values were carried out from a range of concentrations in ng/mL tested for the drug. The plots of their percentage parasite growth against concentrations resulted in a sigmoidal curve, specific to *P. falciparum* lactate dehydrogenase (pLDH) activity inhibition (Figures 4.4 and 4.5). Chloroquine tested against the sensitive strain D10 gave satisfactory statistical treatment results as the concentration-response data fitted a sigmoidal equation (R^2 = 0.98, Sy.x = 7.5) with IC_{50}= 0.013 ± 0.002 µg/mL at 95% confidence interval 0.01-0.02 µg/mL (Table 4.3 and Figure 4.4), while against the resistant strain W2, the statistical treatments satisfactorily resulted in (R^2 = 0.97, Sy.x = 7.8) with IC_{50}= 0.22 ± 0.03µg/mL at 95% confidence interval 0.16-0.25 µg/mL (Table 4.4, Figure 4.5). The chloroquine standard drug exhibited to substantially inhibit the activity of lactate dehydrogenase (pLDH) in both*P. falciparum* strains used.

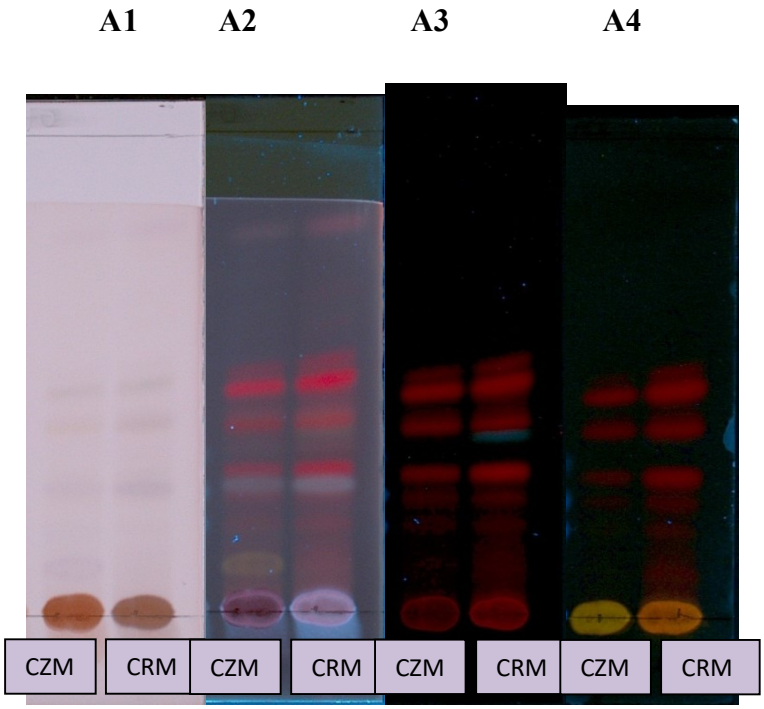

Legend:

CZM- *Combretum zenkeri* methanol extract

CRM- *Combretum racemosum* methanol extract

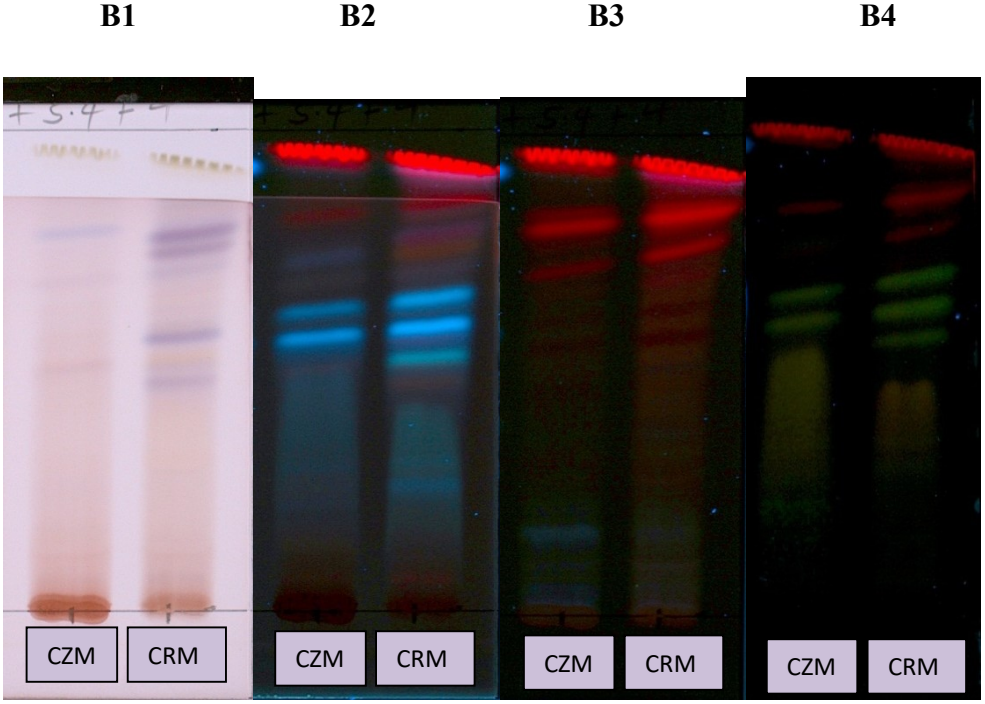

Figure 4.3: TLC of *C. racemosum* and *C. zenkeri*methanol extracts developed in (A) toluene/ethyl acetate 45:5 and (B) ethyl acetate/methanol/water 40:5.4:4; (1) derivatized with anisaldehyde/H_2SO_4 reagent and viewed under visible light (2) derivatized with anisaldehyde/H_2SO_4 reagent and viewed under UV 366 nm (3) not derivatized but viewed under UV 366 nm (4) derivatized with natural product/polyethylene glycol 4000 reagent and viewed under UV 366 nm

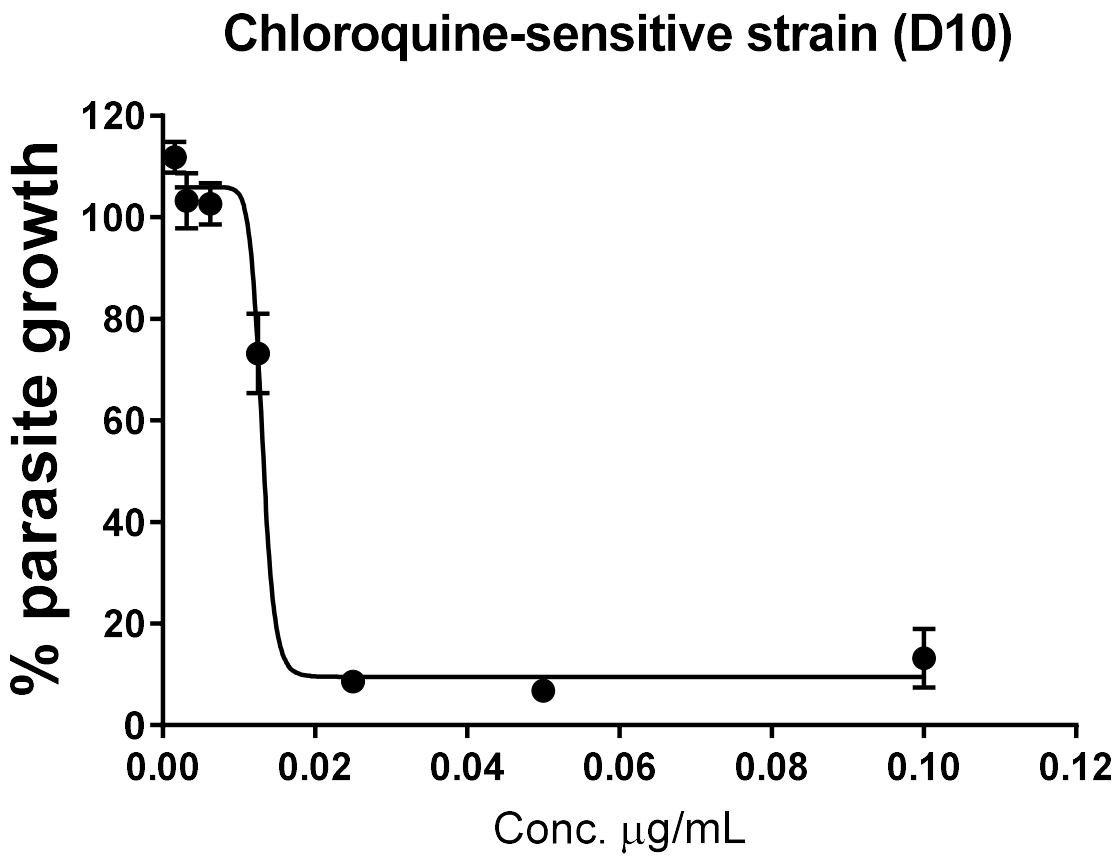

Figure 4.4: Inhibition of *Plasmodium falciparum* chloroquine sensitive strain by chloroquine standard drug

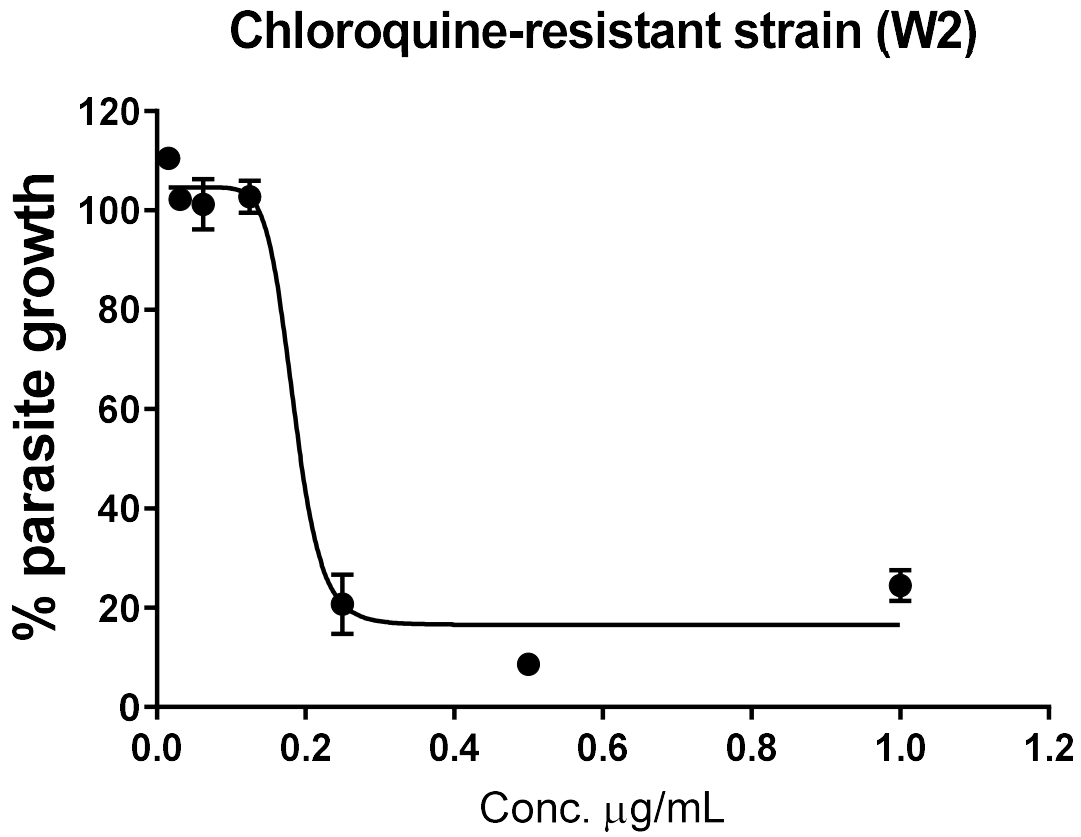

Figure 4.5: Inhibition of *Plasmodium falciparum* chloroquine resistant strain by chloroquine standard drug

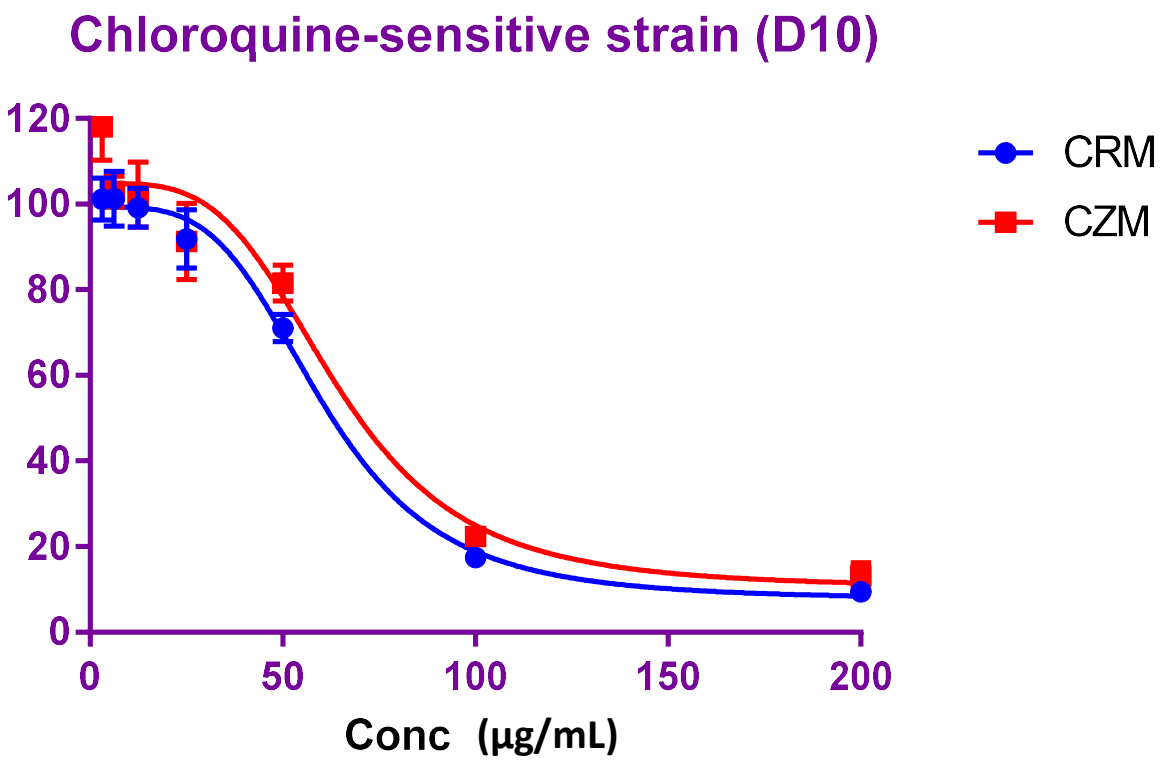

Figure 4.6: Inhibition of *P. falciparum* parasite (D10 strain) by the crude extracts

Legend: CRM- *Combretum racemosum* methanol extract, CZM- *Combretum zenkeri* methanol extract

Table 4.3: Antiplasmodial activity of *C. zenkeri* and *C. racemosum* methanol extracts in *P. falciparum*D10 strain

	D10 (IC_{50} µg/mL)[a]	C.I (µg/mL)	R^2	Sy.x
***C. zenkeri* MeOH extract**	68.98 ± 1.00	48.3-75.5	0.95	9.2
***C. racemosum*MeOH extract**	64.18 ± 2.69	56.1-65.7	0.99	4.9
Chloroquine	0.013 ± 0.002	0.01-0.02	0.98	7.5

[a]IC_{50} values were generated, from duplicate results of three separate experiments, as mean±SD

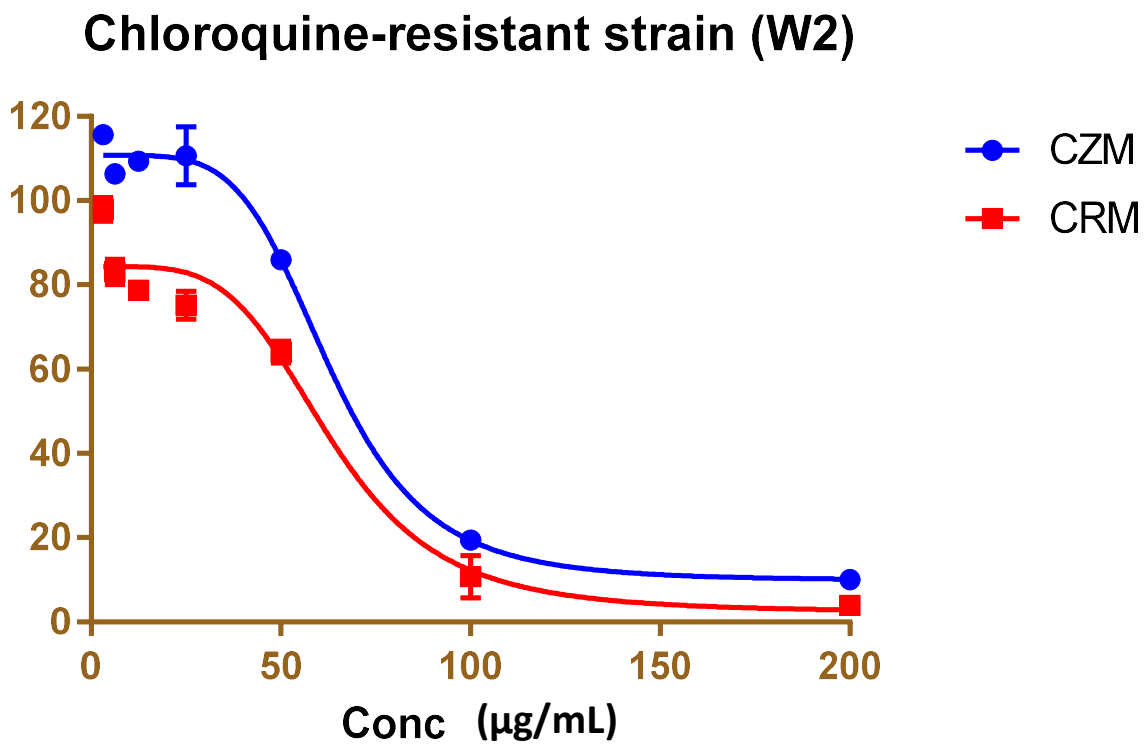

Figure 4.7: *Plasmodium falciparum* inhibition (W2 strain) by the crude extracts

Legend: CRM- *Combretum racemosum* methanol extract, CZM- *Combretum zenkeri* methanol extract

Table 4.4: Antiplasmodial activity of *C. zenkeri* and *C. racemosum* methanol extracts in *P. falciparum*W2 strains

	W2 (IC_{50} µg/mL)[a]	C.I (µg/mL)	R^2	Sy.x
***C. zenkeri* MeOH extract**	69.68 ± 3.09	56.4-78.8	0.99	3.4
***C. racemosum* MeOH extract**	65.80 ± 14.85	52.8-84.0	0.96	7.9
Chloroquine	0.22 ± 0.03	0.16-0.25	0.97	7.8

[a]IC_{50} values were generated, from duplicate results of three separate experiments, as mean±SD

4.4Preliminary solvent-solvent partitioning fractions

Each of the extracts (5 g) were partitioned to produce four fractionsand the amounts of fractions are shown on the next page in Table 4.5.*Combretum zenkeri* showed percentage yield

of 2.2% for chloroform, 6.8% for ethyl acetate, 12.4% for n-butanolalso 42.6% for aqueous fractions. Also, *C. racemosum* showed percentage yield of 12% for chloroform, 9% for ethyl acetate, 32% for n-butanol also 41.2% for aqueous fractions. All the fractions of *C. racemosum*, except aqueous, showed higher amount fractionated than the *C. zenkeri*.

4.5The TLC fingerprints of partitioned fractions of *C. racemosum* and *C. zenkeri*

The TLC profiles of the partitioned fractions of *C. zenkeri* and *C. racemosum* were conducted and shown below in Figures 4.5, 4.6 and 4.7. From the chromatogram B in Figure 4.6, the ethyl acetate and n-butanol fractions of*C. zenkeri* as well as *C. racemosum*extracts showed to be enriched with flavonoids and phenolic compounds. This is evident by the intense green and yellow zones ranging from R_f 0.6-0.8 in both ethyl acetate and n-butanol fractions of *C. racemosum* extract. In the ethyl acetate and n-butanol fractions of *C. zenkeri*, both are characterised by the prominent yellow-green and green fluorescent zones ranging from R_f 0.6-0.9.

Table 4.5: Yield of solvent-solvent partitioned fractions

Fractions	***C.zenkeri* (mg)**	***C.racemosum* (mg)**

Chloroform	110	600
Ethyl acetate	340	450
n-butanol	620	1600
Water	2130	2060

[B] [A]

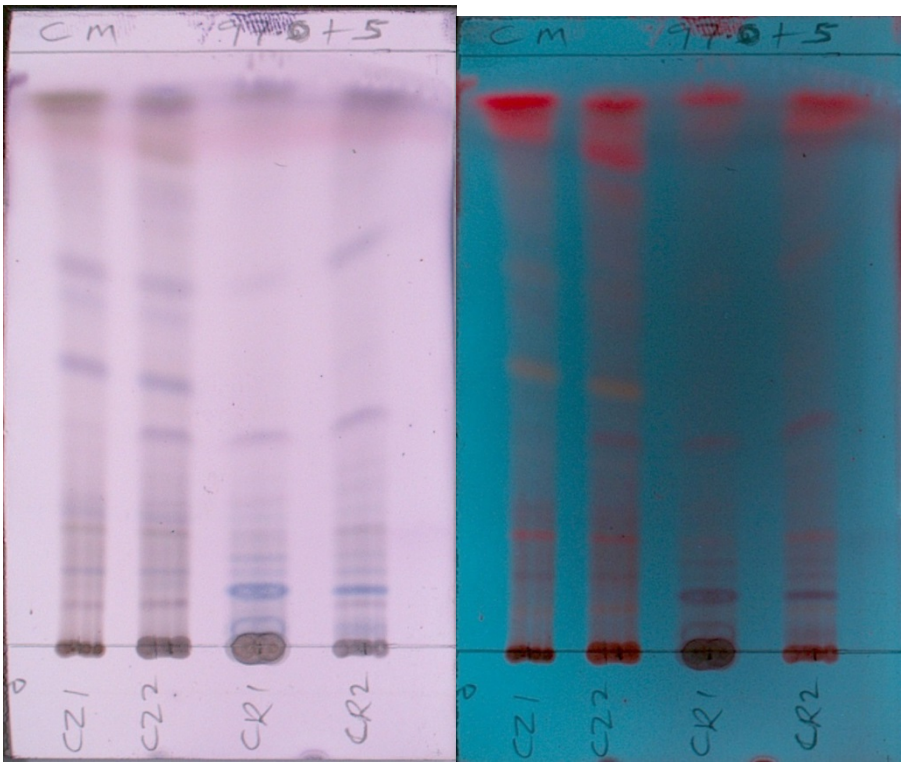

Figure 4.8:TLC of *C. zenkeri* and *C. racemosum* chloroform fractions developed in chloroform/methanol 97/5; (A)with anisaldehyde-sulphuric acid spray reagentviewed at 365nm and (B) with anisaldehyde-sulphuric acid spray reagent viewed at visible light

Legend: CZ- *Combretum zenkeri*, CR- *Combretum racemosum*

(A)(B)

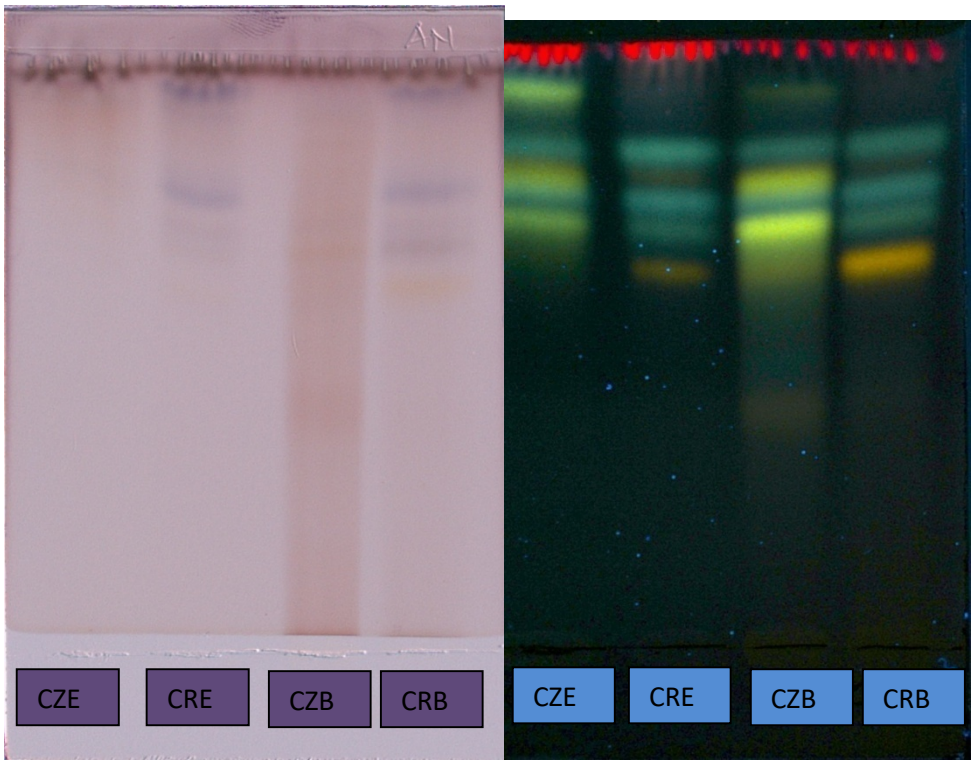

Figure 4.9:TLC of *C. zenkeri* and *C. racemosum* ethyl acetate and n-butanol fractions developed in ethyl acetate/acetic acid/formic acid/water 100/11/11/24; (A) with anisaldehyde-sulphuric acid spray reagent, (B) with natural product/polyethylene glycol 4000spray reagent

Legend: CZE- *Combretum zenkeri* ethyl acetate, CRE- *Combretum racemosum* ethyl acetate, CZB- *Combretum zenkeri* n-butanol, CRB- *Combretum racemosum* n-butanol

[A] [B]

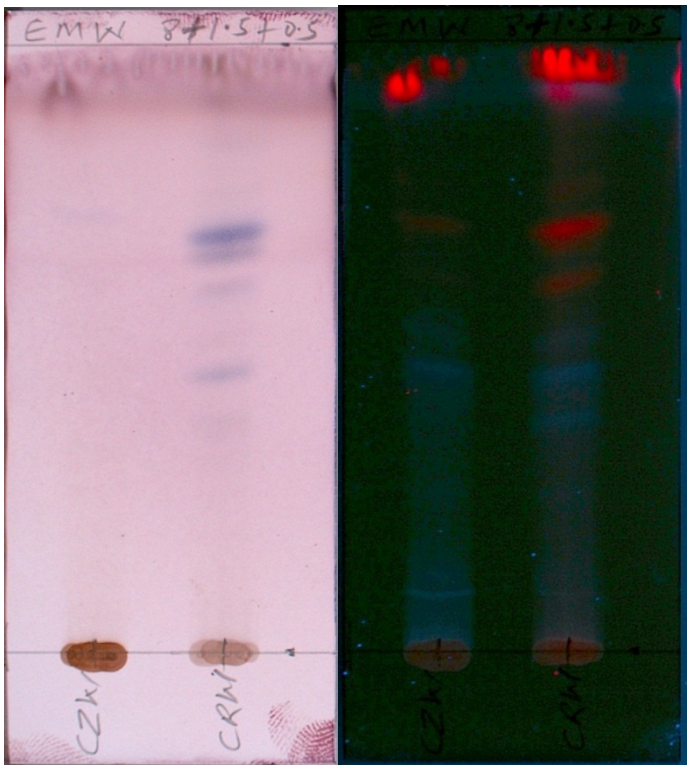

Figure 4.10: TLC of *C. zenkeri* and *C. racemosum* water fractions developed in ethyl acetate/methanol/water 8/1.5/0.5; (A) sprayed with anisaldehyde-sulphuric acid reagent viewed at visible light (B) viewed at 365nm before spraying

4.6*In vitro* antiplasmodial activityof the *C. racemosum* and *C. zenkeri* fractions

The fractions from *C. racemosum* and *C. zenkeri* methanol extracts were screened against D10 and W2 strains of *P. falciparum*for antiplasmodial actions. The fractions were quantitatively

tested on the *P. falciparum* lactate dehydrogenase (pLDH) and the 50% inhibition (IC_{50}) values were derived from a range of concentrations tested for the fractions.The plots of their percentage parasite growth against concentrations resulted in a sigmoidal curve, specific to *P. falciparum* lactate dehydrogenase (pLDH) activity inhibition (Figures 4.11, 4.12, 4.13 and 4.14). The result of the bioactivity investigation of fractions from solvent-solvent partition showed that chloroform fraction (D10: IC_{50}= 33.80±1.52 µg/mL and W2: IC_{50}= 27.82±2.85 µg/mL) was more potent related to n-butanol (D10: IC_{50}= 78.08±7.29 µg/mL and W2: IC_{50}= 78.12±14.98 µg/mL) in *C. racemosum* at 95% confidence interval (D10: 29.0-38.4 µg/mL; W2: 27.1-30.6 µg/mL) and (D10: 73.4-95.0 µg/mL; W2: 75.4-92.0 µg/mL), respectively for the chloroform and n-butanol fractions. Their statistical treatments gave satisfactory outcome with (D10: R^2 = 0.99, Sy.x = 5.3; W2: R^2 = 0.99, Sy.x = 2.9) for the chloroform fraction and (D10: R^2 = 0.99, Sy.x = 4.2; W2: R^2 = 0.98, Sy.x = 5.2) for the n-butanol fraction (Tables 4.6 and 4.7; Figures 4.12 and 4.14). Likewise in *C. zenkeri*, the chloroform fraction (D10: IC_{50}= 12.57±1.57 µg/mL) and (W2: IC_{50}= 12.14±0.95 µg/mL) showed higher activity relative to n-butanol fraction (D10: IC_{50}= 61.98 ± 3.25 µg/mL) and (W2: IC_{50}= 61.26 ± 8.64 µg/mL) at 95% confidence interval for chloroform (D10: 12.6-14.9 µg/mL; W2: 12.0-15.8 µg/mL) and n-butanol (D10: 47.6-75.0 µg/mL; W2: 52.0-70.4 µg/mL). Their concentration-response data fitted a sigmoidal equation satisfactorily with (D10: R^2 = 0.99, Sy.x = 4.8; W2: R^2 = 0.98, Sy.x = 6.8) for the chloroform fraction and (D10: R^2 = 0.96, Sy.x = 8.5; W2: R^2 = 0.99, Sy.x = 4.4) for the n-butanol fraction (Tables 4.6 and 4.7; Figures 4.11 and 4.13).

The water fraction was not testedin this experiment.The chloroform fractions of both *C. zenkeri* and *C. racemosum*generally demonstrated significant inhibitory activities than the n-butanol fractions and as well showed promising activities more than the crude extracts against(pLDH) activity in both D10 and W2 strains of *P. falciparum*.

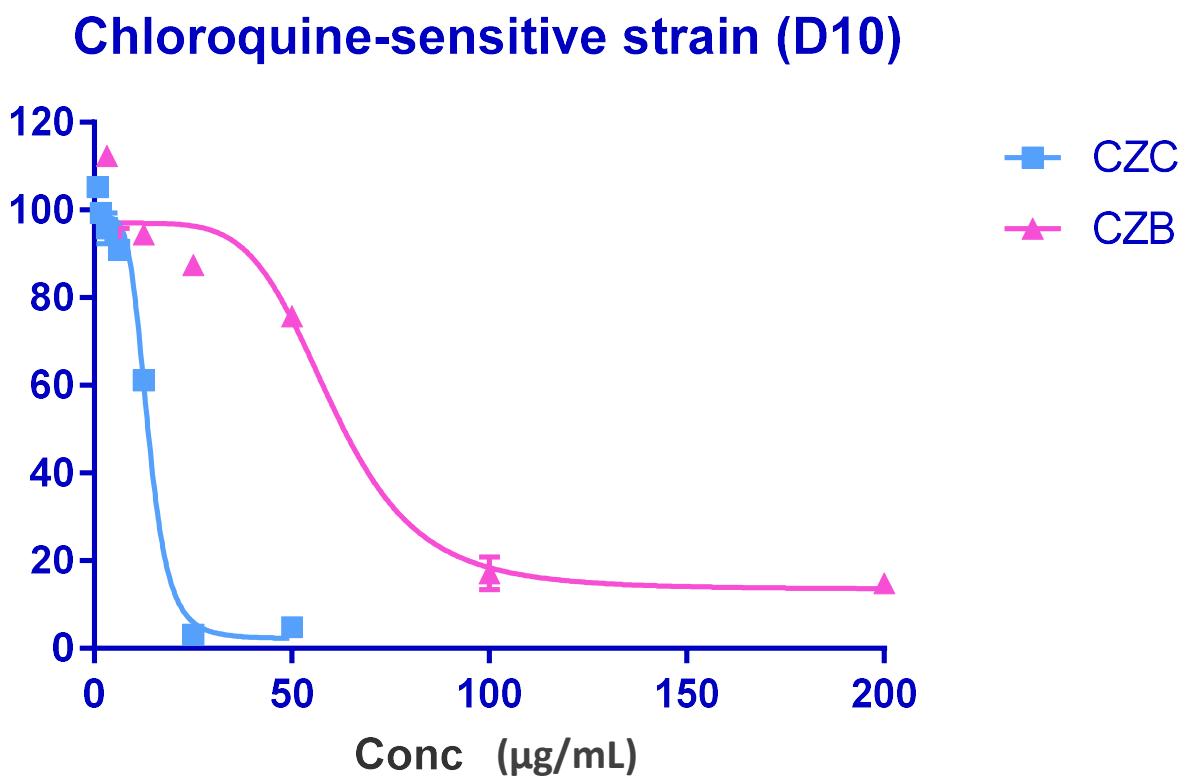

Figure 4.11: *Plasmodium falciparum* (D10 strain) inhibition by the fractions

Legend: CZC- *Combretum zenkeri* chloroform fraction, CZB- *Combretum zenkeri* n-butanol fraction

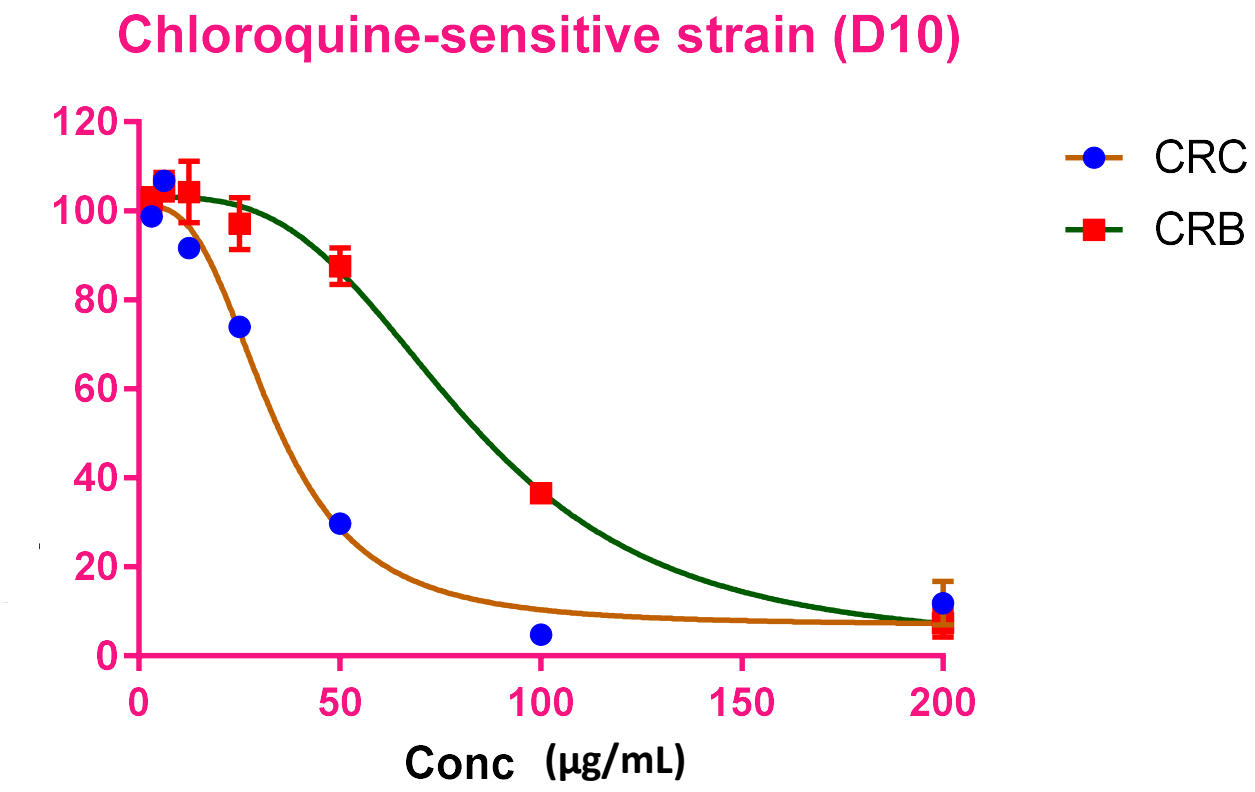

Figure 4.12: *Plasmodium falciparum* (D10 strain) inhibition by the fractions

Legend: CRC- *Combretum racemosum* chloroform fraction, CRB- *Combretum racemosum* n-butanol fraction

Table 4.6: Antiplasmodial activity of *C. zenkeri* and *C. racemosum* partitioned fractions in *P. falciparum*D10strains

	D10 (IC_{50} µg/mL)[a]	C.I (µg/mL)	R^2	Sy.x

C. zenkeri **$CHCl_3$ (CZC) fraction**	12.57 ± 1.57	12.6-14.9	0.99	4.8
C. zenkeri **n-BuOH (CZB) fraction**	61.98 ± 3.25	47.6-75.0	0.96	8.5
C. racemosum **$CHCl_3$ (CRC) fraction**	33.80 ± 1.52	29.0-38.4	0.99	5.3
C. racemosum **n-BuOH (CRB) fraction**	78.08 ± 7.29	73.4-95.0	0.99	4.2

[a]IC_{50} values were generated, from duplicate results of three separate experiments, as mean±SD

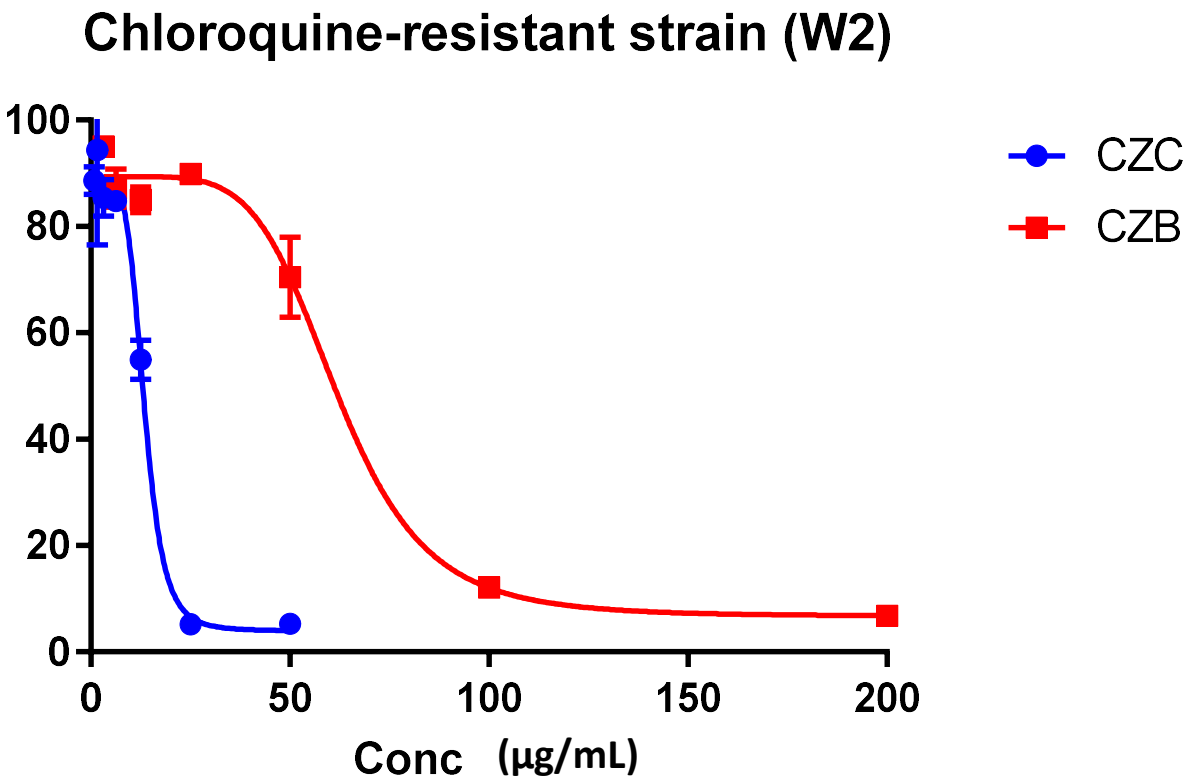

Figure 4.13: Inhibition of *P. falciparum* parasite (W2 strain) by the fractions

Legend:CZC- *Combretum zenkeri* chloroform fraction, CZB- *Combretum zenkeri* n-butanol fraction

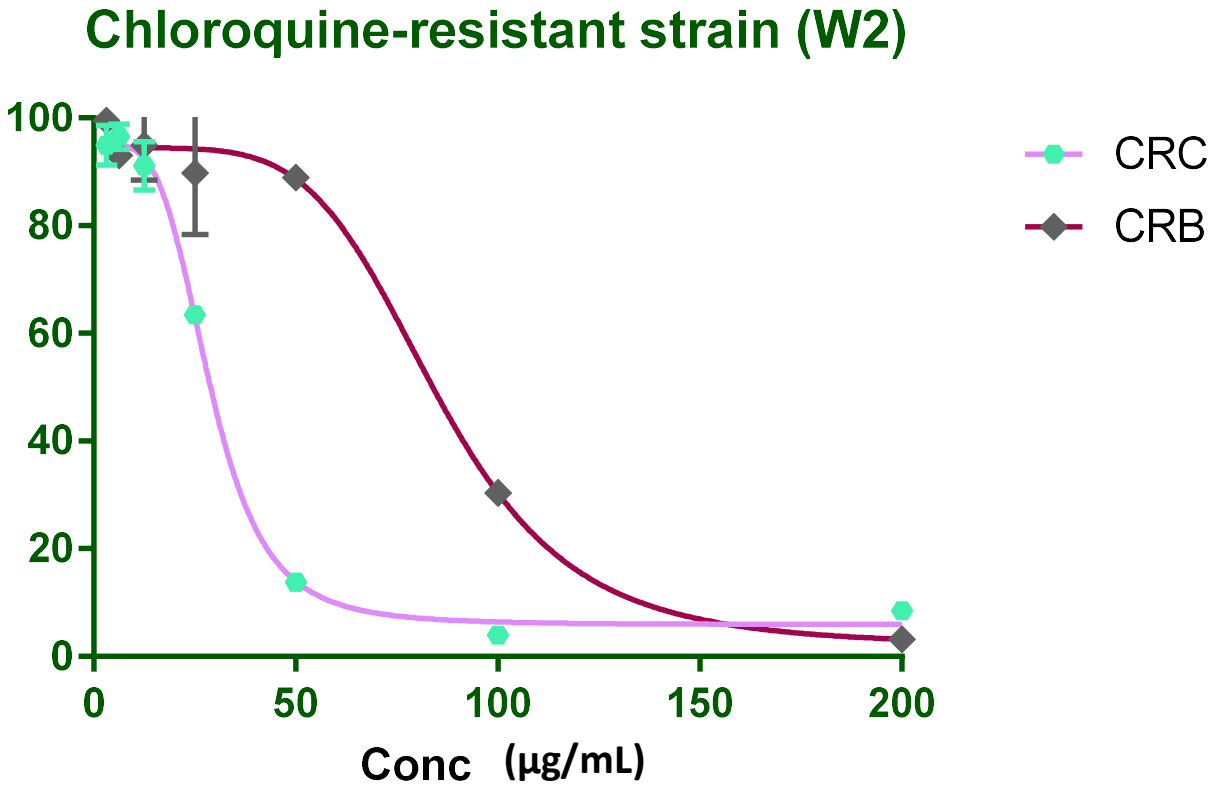

Figure 4.14: Inhibition of *P. falciparum* parasite (W2 strain) by the fractions

Legend: CRC- *Combretum racemosum* chloroform fraction, CRB- *Combretum racemosum* n-butanol fraction

Table 4.7: Antiplasmodial activity of *C. zenkeri* and *C. racemosum* partitioned fractions in *P. falciparum*W2 strains

	W2 (IC_{50} µg/mL)[a]	C.I (µg/mL)	R^2	Sy.x
***C. zenkeri* $CHCl_3$ (CZC) fraction**	12.14 ± 0.95	12.0-15.8	0.98	6.8
***C. zenkeri* n-BuOH (CZB) fraction**	61.26 ± 8.64	52.0-70.4	0.99	4.4
***C. racemosum* $CHCl_3$ (CRC) fraction**	27.82 ± 2.85	27.1-30.6	0.99	2.9
***C. racemosum* n-BuOH (CRB) fraction**	78.12 ± 14.98	75.4-92.0	0.98	5.2

[a]IC_{50} values were generated, from duplicate results of three separate experiments, as mean±SD

4.8Chromatographic fractionation of *C. racemosum* chloroform fraction

The chromatogram of the separation of *C. racemosum* chloroform fraction on flash chromatograph showed compounds ranging from non-polar to intermediate polarity between 5

to 50 minutes of elution (Figure 4.18). The fractions collected, the amounts and their TLC chromatogram are presented in Table 4.6 and Figure 4.19a, b and c.

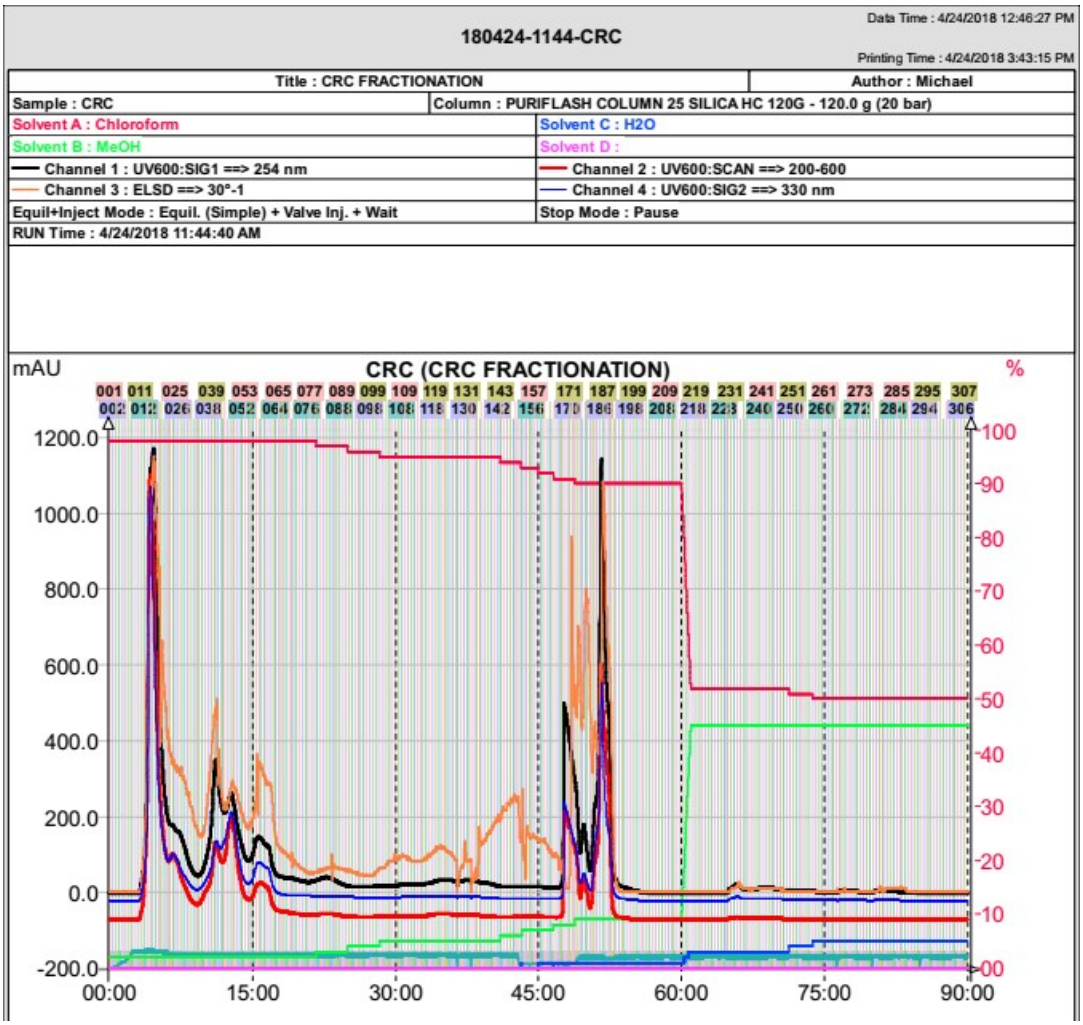

Figure 4.15: Flash chromatogram of *C. racemosum* chloroform fraction

Table 4.8: Fractions collected and the amount from flash chromatographic separation of *C. racemosum* chloroform fraction

Fractions	Combined fractions	Amounts

		(mg)
FCRC1	F1-12	35
FCRC2	F13-24	968
FCRC3	F25-34	218
FCRC4	F35-44	324
FCRC5	F45-54	197
FCRC6	F55-64	242
FCRC7	F65-74	74
FCRC8	F75-84	53
FCRC9	F85-94	51
FCRC10	F95-104	59
FCRC11	F105-114	82
FCRC12	F115-124	89
FCRC13	F125-134	67
FCRC14	F135-167	368
FCRC15	F168-174	237
FCRC16	F175-184	489
FCRC17	F185-189	530
FCRC18	F190-240	36
FCRC19	F241-300	94
FCRC20	F301-307 + column wash	22
Total		**4235**

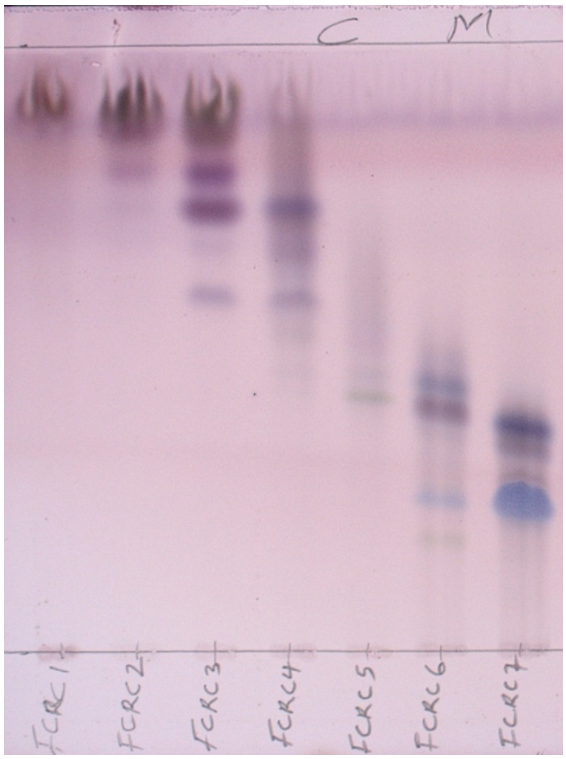

Figure 4.16a: TLC of combined FCRC1-7 (*C. racemosum*) fractionated on flash chromatography (Interchim Puriflash)

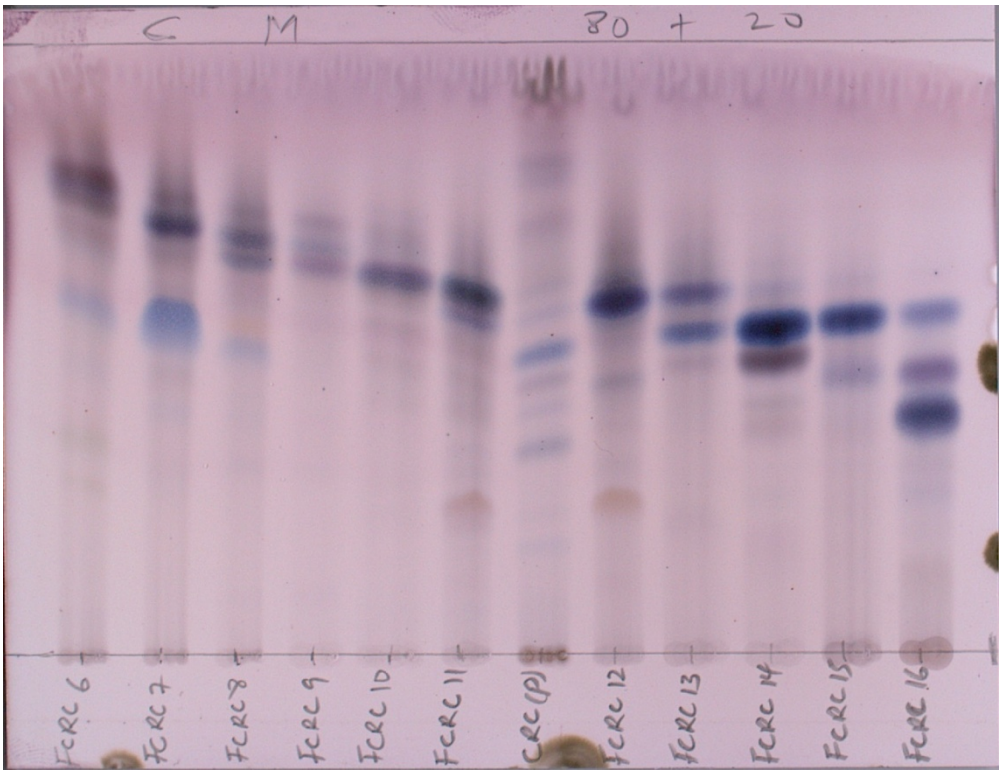

Figure 4.16b: TLC of combined FCRC6-16 (*C. racemosum*) fractionated on flash chromatography (InterchimPuriflash)

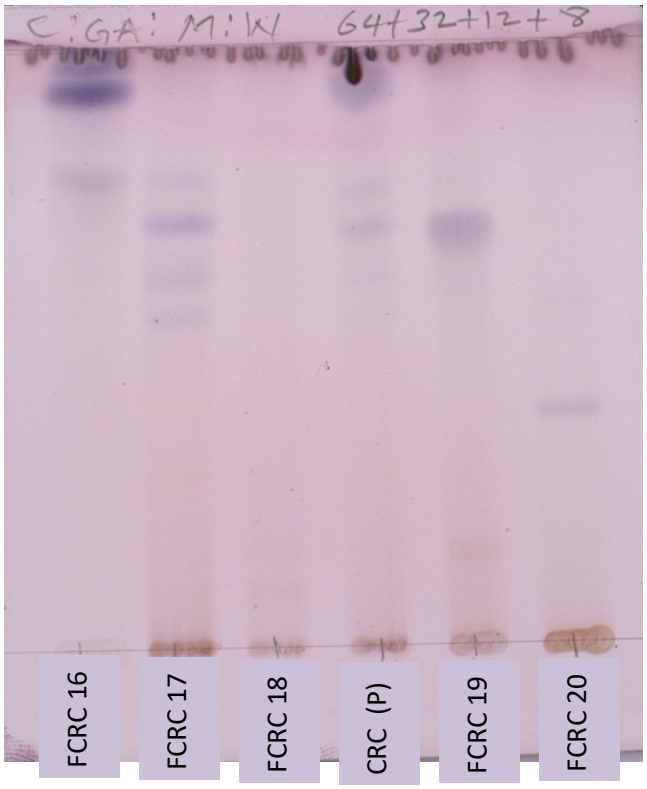

Figure 4.16c:TLC of combined FCRC16-20 (*C. racemosum*) fractionated on flash chromatography (InterchimPuriflash)

4.9Isolation of compound CR-A

The chromatographic separation of FCRC14 afforded 18 fractions (FCRC14_1 to FCRC14_18). All fractions, amount yielded and their TLC chromatogram are presented in Table 4.9 and Figure 4.17. FCRC14_12 (10.67 mg) became **CR-A**, and this isolate showed single spot on the TLC in Figure 4.18.

4.10 Isolation of compound CR-C

The flash chromatographic separation of FCRC16 afforded 5 fractions (FCRC16_1 to FCRC16_5). All fractions, amount yielded and their TLC chromatogram are presented in Table 4.10 and Figure 4.19. FCRC16_3 further fractionated on column chromatograph afforded 17 fractions (FCRC16_3_1 to FCRC16_3_17). All 17 fractions, amount yielded and their TLC chromatogram are presented in Table 4.11 and Figure 4.20. FCRC16_3_10 to FCRC16_3_14 (44.6 mg) became CR-C, and the TLC chromatogram of this compound shown in Figure 4.21.

Table 4.9: Column chromatographic separation sub-fractions collected and amounts from FCRC14

Fractions	Combined fractions	Amounts (mg)
FCRC14_1	F1-93	2.56
FCRC14_2	F94-234	1.36
FCRC14_3	F235-243	0.96
FCRC14_4	F244-262	1.28
FCRC14_5	F263-267	0.89
FCRC14_6	F268-276	1.91
FCRC14_7	F277-288	5.4
FCRC14_8	F289-296	4.77
FCRC14_9	F297-299	4.04
FCRC14_10	F300-312	49.21
FCRC14_11	F313-317	16.47
FCRC14_12	F318-321	10.67
FCRC14_13	F322-325	6.86
FCRC14_14	F326-332	7.23
FCRC14_15	F333-385	16.67
FCRC14_16	F386-408	3.38
FCRC14_17	F409-424	3.64
FCRC14_18	F425-442	7.37
Total		**144.67**

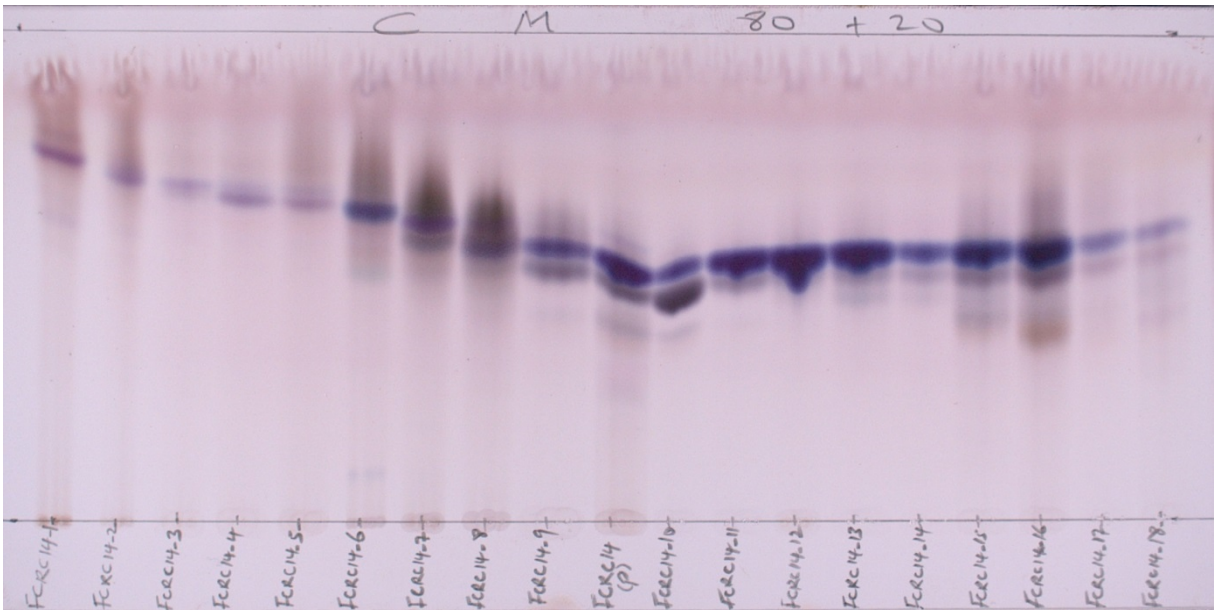

Figure 4.17: TLC of column chromatographic separation sub-fractions of FCRC14

Figure 4.18: TLC of compound CR-A

Table 4.10: Fractions collected and the amount from flash chromatographic separation of sub-fraction FCRC16

Fractions	Combined fractions	Amounts (mg)
FCRC16_F1	F1-12	3.42
FCRC16_F2	F13-17	6.88
FCRC16_F3	F18-68	256.9
FCRC16_F4	F69-88	2.21
FCRC16_F5	F89-128	10.14
Total		**279.55**

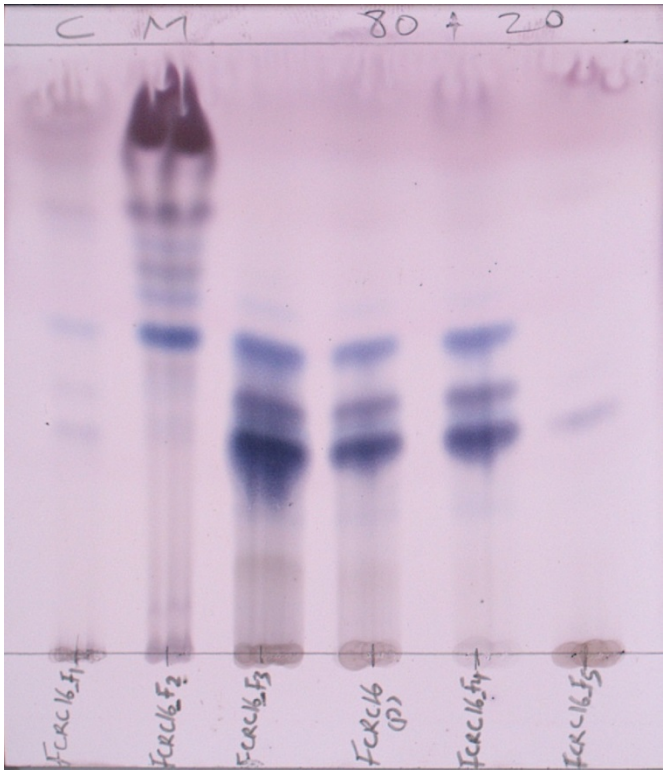

Figure 4.19:TLC of FCRC16 sub-fractions fractionated on flash chromatography (InterchimPuriflash)

Table 4.11: Column chromatographic separation sub-fractions collected and amounts from FCRC16_3

Fractions	Combined fractions	Amounts (mg)
FCRC16_3_F1	F1-30	8.6
FCRC16_3_F2	F31-46	2.6
FCRC16_3_F3	F47-61	1.6
FCRC16_3_F4	F62-72	4.4
FCRC16_3_F5	F73-95	15.3
FCRC16_3_F6	F96-115	5.9
FCRC16_3_F7	F116-128	5.2
FCRC16_3_F8	F129-136	2.9
FCRC16_3_F9	F137-147	4.9
FCRC16_3_F10	F148-158	5.8
FCRC16_3_F11	F159-176	15.2
FCRC16_3_F12	F177-220	15.4
FCRC16_3_F13	F221-247	4.2
FCRC16_3_F14	F248-274	4
FCRC16_3_F15	F275-294	1.6
FCRC16_3_F16	F295-357	5.1
FCRC16_3_F17	F358-380	5.6
Total		**108.3**

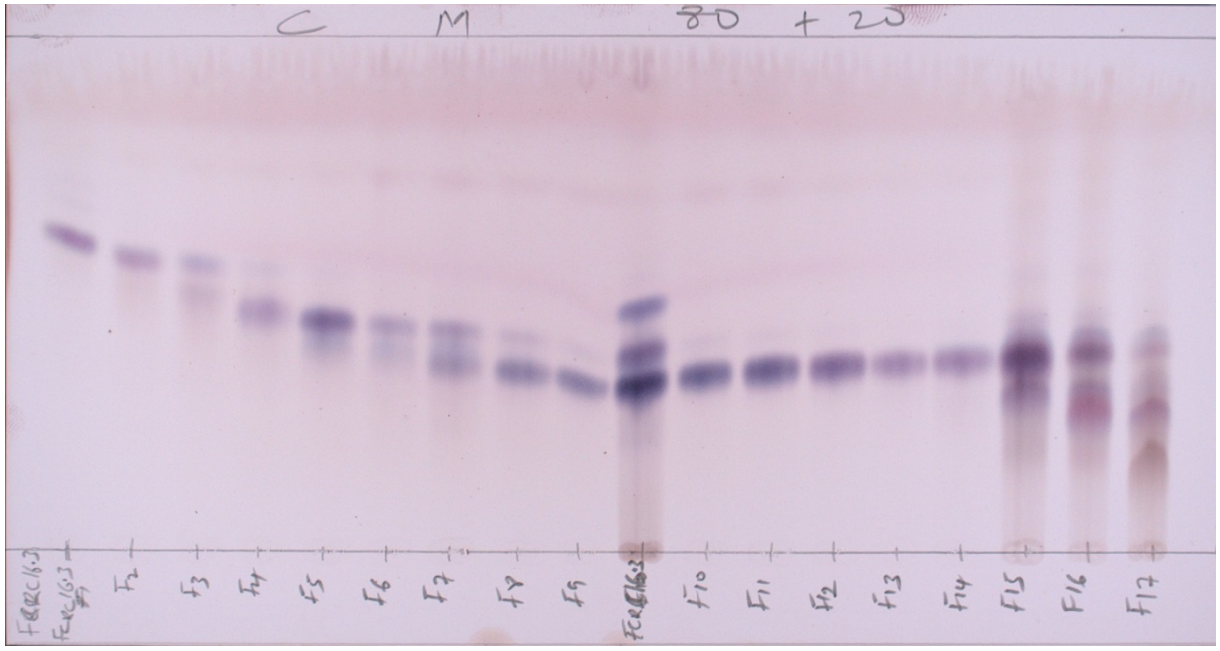

Figure 4.20: TLC of column chromatographic separation sub-fractions of FCRC16_3

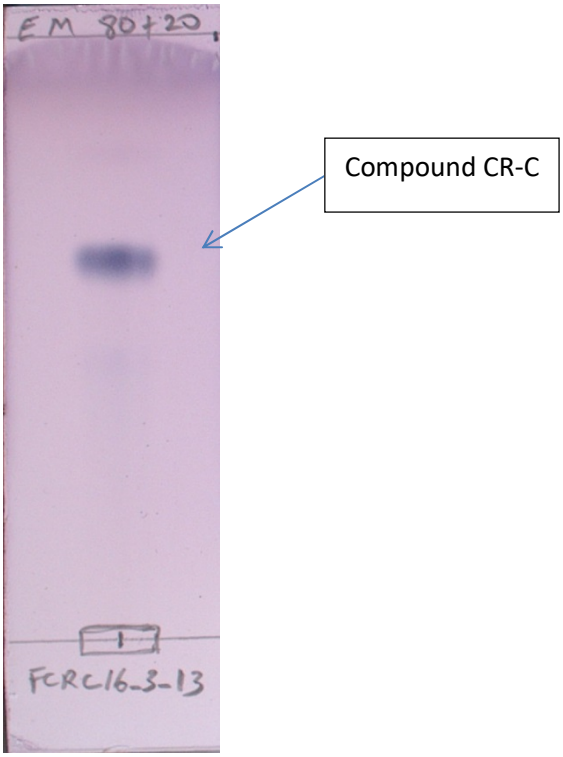

Figure 4.21: TLC of compound CR-C

4.12 Isolation of compound CR-E

Compound CR-E was afforded from preparative TLC. The chromatogram of this isolate showed a single spot on TLC(Figure 4.23). The CR-E was also developed in a TLC side by side the semi-pure fraction from where it was isolated (Figure 4.22).

4.13 Isolation of compound CR-G

The chromatographic separation of FCRC7 afforded 11 fractions (FCRC7_1 to FCRC7_11). All fractions, amount yielded and their TLC chromatogram are presented in Table 4.12 and Figure 4.24. FCRC7_9 to FCRC7_11 (8.4 mg) became CR-G, and the TLC chromatogram of this compound shown in Figure 4.25.

4.14 Isolation of compound CR-H

The chromatographic separation of FCRC17 afforded 14 fractions (FCRC17_1 to FCRC17_14). All fractions, amount yielded and their TLC chromatogram are presented in Table 4.13 and Figure 4.26a. FCRC17_4 to FCRC17_6 (32.9 mg) became CR-H, and shown in Figure 4.27 is the TLC chromatogram for this compound.

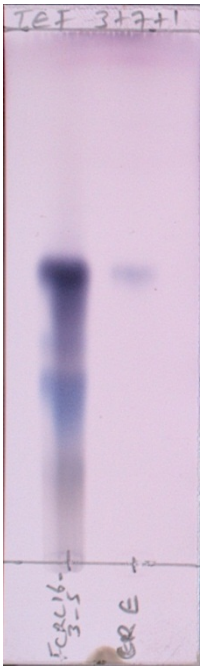

Figure 4.22: TLC of FCRC16_3_5 with compound CR-E

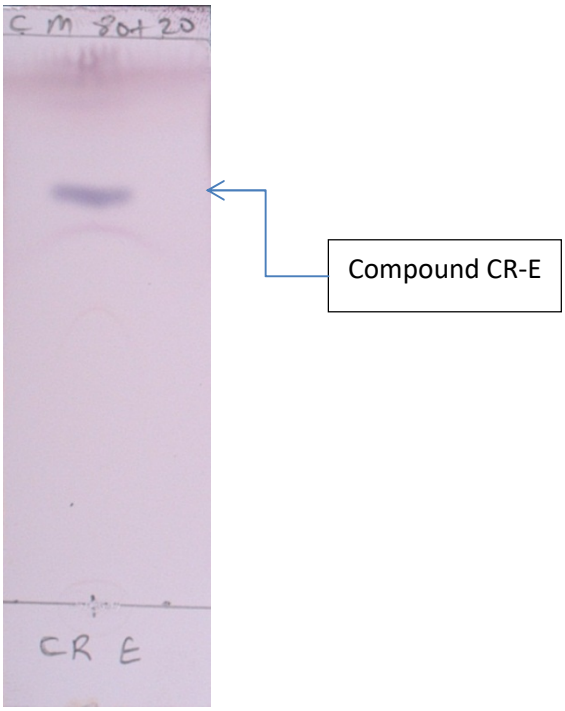

Figure 4.23: TLC of compound CR-E

Table 4.12: Column chromatographic separation sub-fractions collected and amounts from FCRC7

Fractions	Combined fractions	Amounts (mg)
FCRC7_F1	F1-40	2.2
FCRC7_F2	F41-49	19.8
FCRC7_F3	F50-57	2.4
FCRC7_F4	F58-92	4.1
FCRC7_F5	F93-122	1.2
FCRC7_F6	F123-136	0.9
FCRC7_F7	F137-152	1.8
FCRC7_F8	F153-155	1.6
FCRC7_F9	F156-159	2.4
FCRC7_F10	F160-179	4.8
FCRC7_F11	F180-186	1.2
Total		**42.4**

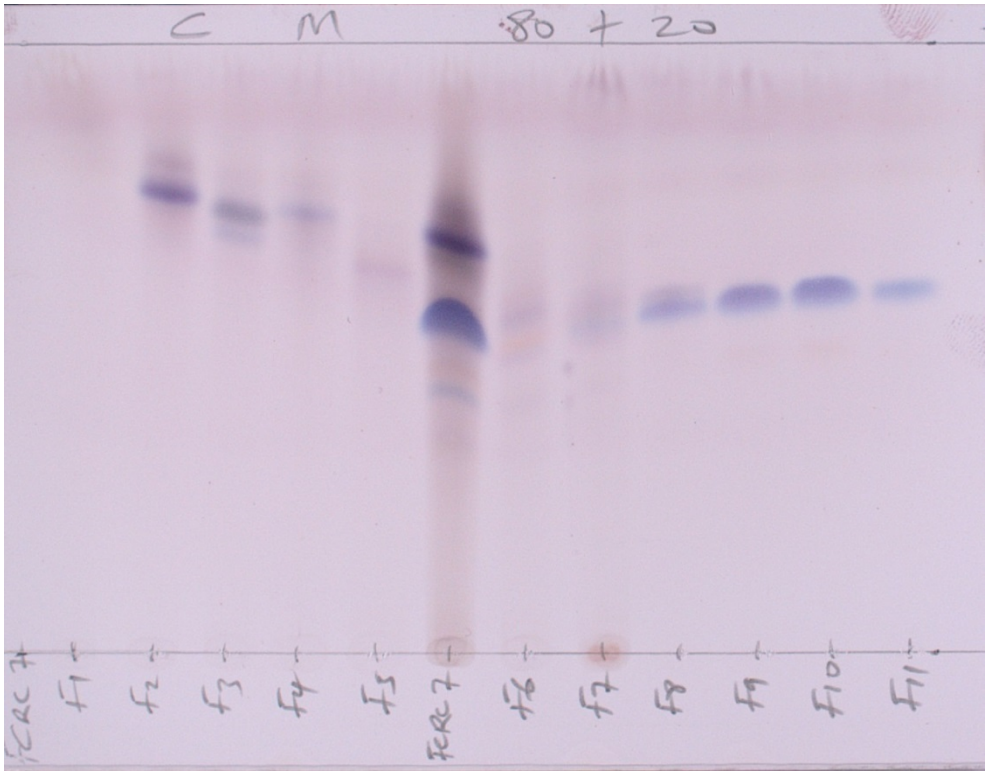

Figure 4.24: TLC of column chromatographic separation sub-fractions of FCRC7

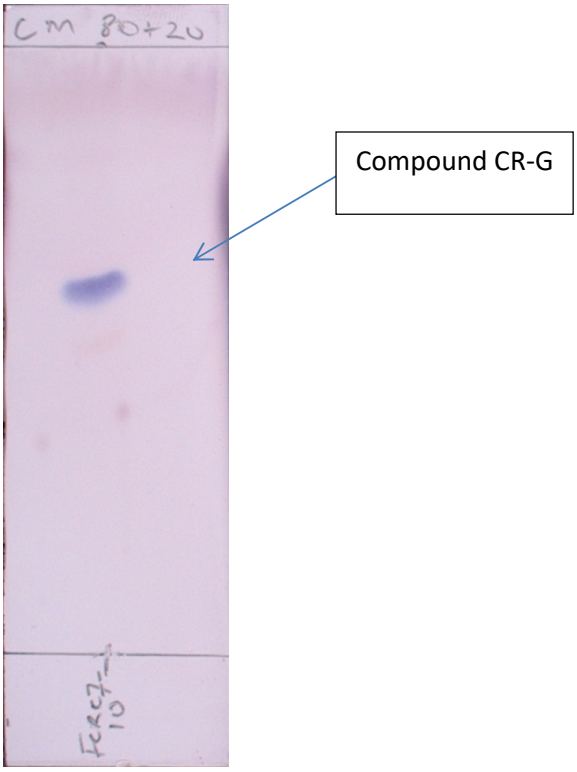

Figure 4.25: TLC of compound CR-G

Table 4.13: Column chromatographic separation sub-fractions collected and amounts from FCRC17

Fractions	Combined fractions	Amounts (mg)
FCRC17_F1	F1-90	6.9
FCRC17_F2	F91-109	1
FCRC17_F3	F110-138	5.1
FCRC17_F4	F139-142	16.5
FCRC17_F5	F143-153	15.4
FCRC17_F6	F154-156	1
FCRC17_F7	F157-177	33.7
FCRC17_F8	F178-220	22.1
FCRC17_F9	F221-232	5.3
FCRC17_F10	F233-260	21.5
FCRC17_F11	F261-283	42.9
FCRC17_F12	F284-302	10.4
FCRC17_F13	F303-335	34.8
FCRC17_F14	Column wash	152.2
Total		**368**

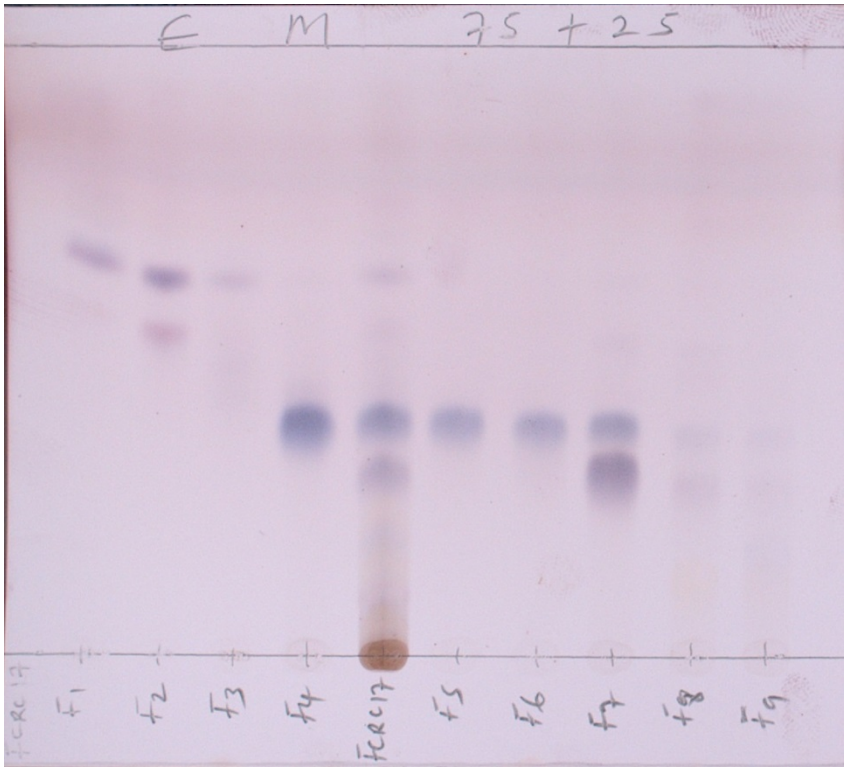

Figure 4.26a: TLC of column chromatographic separation sub-fractions of FCRC17 (1-9)

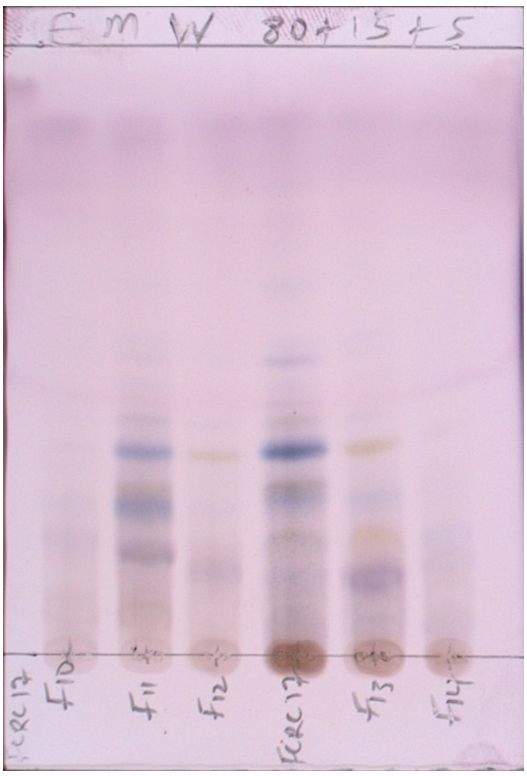

Figure 4.26b: TLC of column chromatographic separation sub-fractions of FCRC17 (10-14)

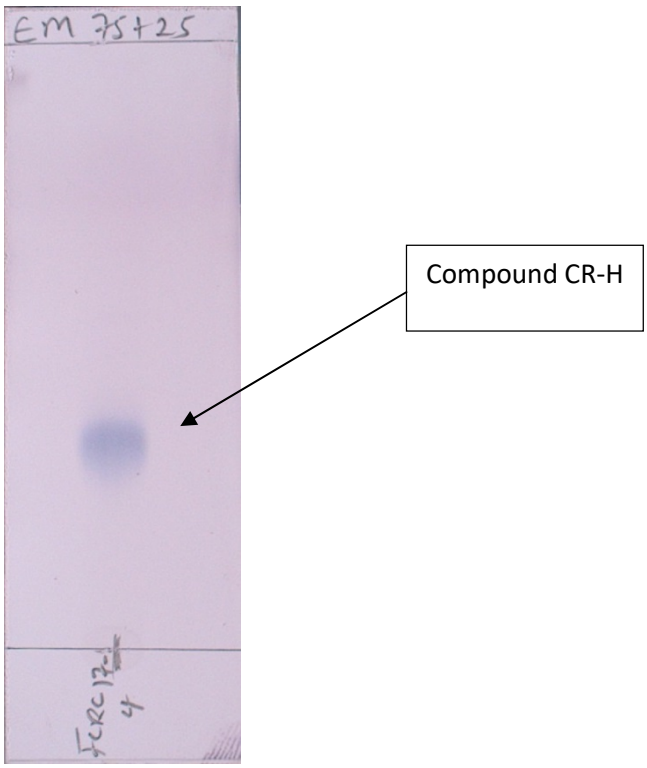

Figure 4.27: TLC of compound CR-H

4.15 Chromatographic fractionation of *C. zenkeri* chloroform fraction

The chromatogram of the *C. zenkeri* chloroform fraction separated with flash chromatograph is shown in Figure 4.28. This showed a lot of non-polar compounds between 5-27 minutes, which signified early elution. Some compounds shown around intermediate polarity between 95-100 minutes while the polar compounds showed around 132-152 minutes of elution. The TLC of collected fractions is shown in Figure 4.29 and amounts yielded for each fraction shown in Table 4.14.

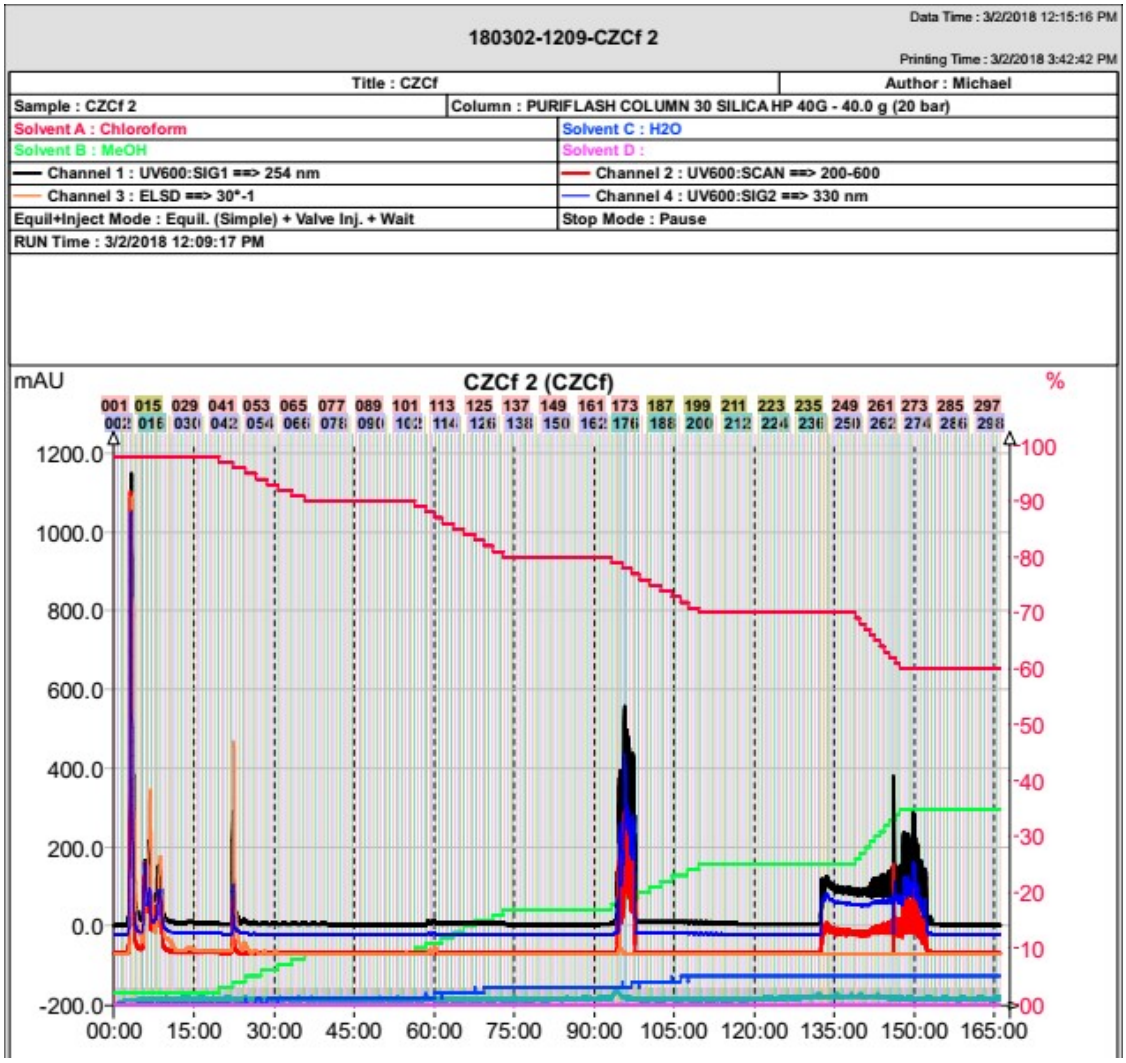

Figure 4.28: Flash chromatogram of *C. zenkeri* chloroform fraction

Table 4.14: Fractions collected and the amount from flash chromatographic separation of *C. zenkeri* chloroform fraction

Fractions	Combined fractions	Amounts (mg)
FCZC 1	F1-10	168
FCZC 2	F11-15	90
FCZC 3	F16-18	23.6
FCZC 4	F19-33	84
FCZC 5	F34-42	13.5
FCZC 6	F43-58	64.7
FCZC 7	F59-164	21.9
FCZC 8	F165-179	13.1
FCZC 9	F180-301	10.4
Total		**489.2**

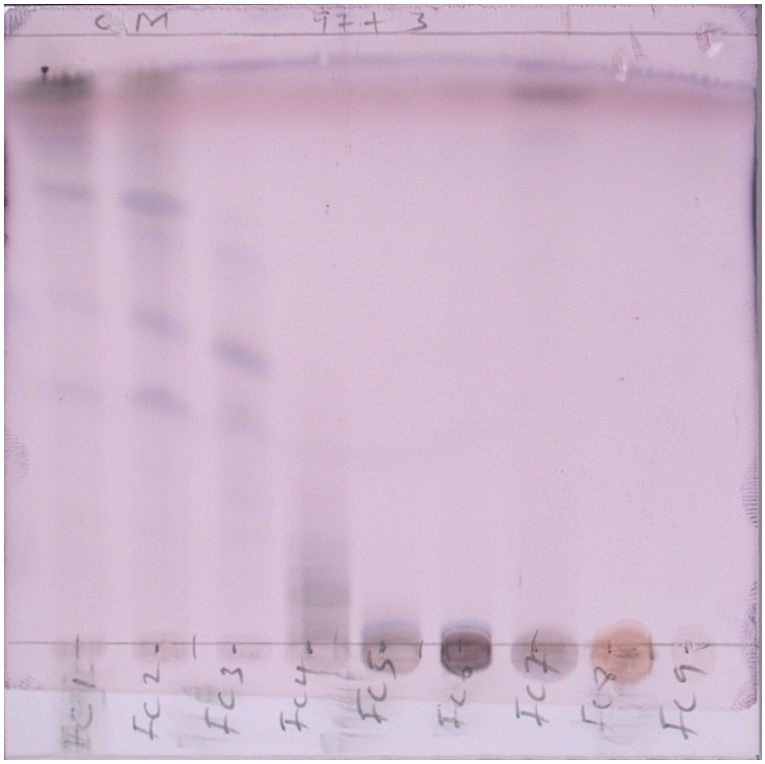

Figure 4.29: TLC of flash chromatographic separation fractions of *C. zenkeri* chloroform

4.16 Isolation of compound CZ-A

The combined fractions and amount of each fraction collected in the column separation is shown on Table 4.15. The TLC chromatogram of all the column fractions is shown in Figure 4.30. FCZC2_12 to FCZC2_15 became **CZ-A** (5 mg). The isolated**CZ-A** showed single spot on TLC in Figure 4.31.

Table 4.15: Column chromatographic separation of fractions collected and amounts from FCZC2

Fractions	Combined fractions	Amounts (mg)
FCZC2_F1	F1-23	15.5
FCZC2_F2	F24-29	3.9
FCZC2_F3	F30-34	4.1
FCZC2_F4	F35-39	3
FCZC2_F5	F40-44	3.4
FCZC2_F6	F45-49	10.6
FCZC2_F7	F50-54	1.8
FCZC2_F8	F55-58	0.8
FCZC2_F9	F59-72	1.8
FCZC2_F10	F73-83	0.9
FCZC2_F11	F84-94	0.8
FCZC2_F12	F95-98	2.1
FCZC2_F13	F99-103	1
FCZC2_F14	F104-108	1
FCZC2_F15	F109-113	1
FCZC2_F16	F114-122	1.1
FCZC2_F17	F123-138	0.8
FCZC2_F18	F139-158	0.7
FCZC2_F19	F159-205	3.1
FCZC2_F20	F206-228	5.2
FCZC2_F21	F229-285	3
Total		**65.6**

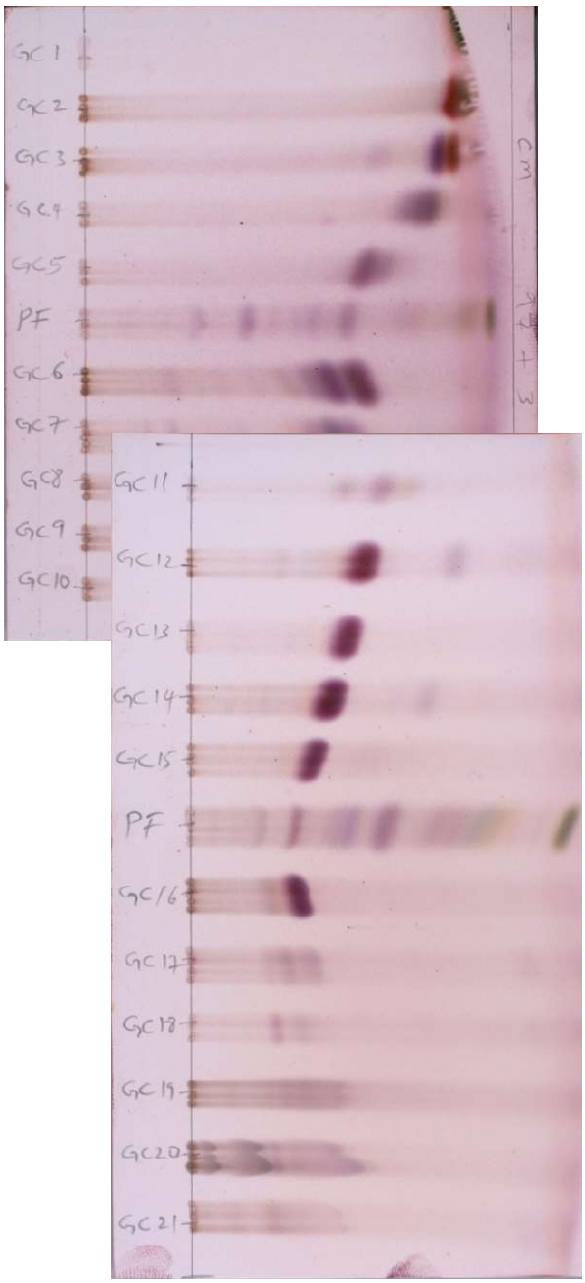

Figure 4.30: TLC of column chromatographic separation sub-fractions of FCZC2

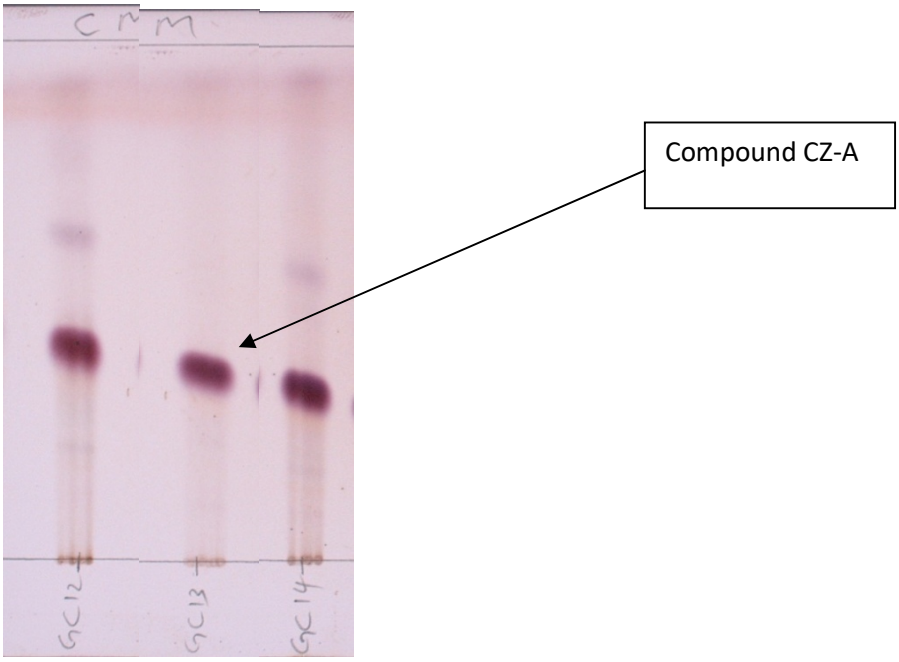

Figure 4.31: TLC of compound CZ-A

4.17 Structure elucidation of compounds isolated from *C. racemosum*

4.17.1 Structure elucidation of CR-A

CR-A (10.7 mg) which showed to be a mixture (1:0.7) of compounds **1** and **2**(Figure 4.32) was identified as colourless powder.HRESIMS indicated a $[M-H]^-$ ion at *m/z* 503.3388, consistent with a molecular formula of $C_{30}H_{48}O_6$(calculatedas $C_{30}H_{47}O_6^-$,with *m/z*showing 503.3378, Δ = 2.0 ppm).

From Table 4.16, compounds **1** and**2** showed signal patterns very alike witheach other for^{1}H- as well as^{13}C-NMR experiments. They showed signal patterns with some characteristic chemical shifts for both ^{1}H and ^{13}C experiments (Tables 4.16). The presence of olefinic proton in **1** and **2** resulted in the chemical shift for the proton at C-12(δ_{H-12} 5.296and δ_{H-12}5.324, respectively).The^{13}C-NMR spectra signals for the olefinic carbons were δ_{C-12}129.23 and δ_{C-13}140.15for **1** and δ_{C-12}124.70 and δ_{C-13}144.75 for **2**. Furthermore, based on the DEPTq analyses, **1** and **2**displayed the occurrence of 30 carbon atoms (Table 4.16). Six methyl (CH_3), nine methylene (CH_2), seven methine (CH) and eight quartenary carbon atoms (C) groups were identified in **1** and **2**.Moreover, **1** and **2**exhibited distinctive chemical shifts in^{1}H-NMR δ_H 2.50 (H-18), δ_H1.35 (H-20) and δ_H 3.06 (H-18), δ_H 3.26 (H-19), respectively and ^{13}C-NMR δ_{C-18} 55.08, δ_{C-19}73.57, δ_{C-20} 43.09 and δ_{C-18} 45.18, δ_{C-19} 82.43, δ_{C-20} 36.03 of **1** and **2**,respectively (Table 4.16). This difference was particularly influenced by the different substitution between positions 19 and 20. The chemical shifts of the olefinic signalsin**1**and **2**and saturation of up-field signals (between 0 and 2 ppm) in their spectra was a preliminary indication of a pentacyclic triterpene skeleton (Table 4.16, Appendices 2a and 2b).

Detailed analysis of 1D NMR as well as 2D NMR including HMBC, HSQC and COSY help resolved **1** as 19α-hydroxyasiatic acid and **2** arjungenin. Compound **1**and **2**(Figure 4.32) from corresponding literature reports(Zebiri *et al*., 2017) and (Gossan *et al*., 2016) displayed spectra information similar to 19α-hydroxyasiatic acid and arjungenin respectively.

Table 4.16:Spectroscopic data from ^{1}H- and ^{13}C-NMR of CR-A(1 &2)in CD_3OD solvent

Position	1			2		
	^{1}H (δ)*^{HH}J-coupling (Hz)		^{13}C (δ)**	^{1}H (δ)*^{HH}J-coupling (Hz)		^{13}C (δ)**
1	1.937 0.908	dd, J=12.4,4.6 (m)	47.9, CH_2	1.906 0.9	dd, J=12.4, 4.6 (m)	47.72, CH_2
2	3.696	ddd, J=11.5, 9.6, 4.6	69.7, CH	3.693	ddd, J=11.6, 9.6, 4.6	69.68, CH
3	3.361	d, J=9.6	78.26, CH	3.358	d, J=9.6	78.25, CH
4		-	44.13, C		-	44.14, C
5	1.311	(m)	48.18, CH	1.310	(m)	48.33, CH
6	1.469 1.414	(m) (m)	19.22, CH_2	1.469 1.414	(m) (m)	19.25, CH_2
7	1.672 1.279	(m) (m)	33.53, CH_2	1.624 1.261	(m) (m)	33.33, CH_2
8		-	41.06, C		-	40.73, C
9	1.8	(m)	48.5, CH	1.844	t, J=8.8	49.1, CH
10		-	39.99, C		-	39.17, C
11	2.021	(m)	24.76, CH_2	2.001	(m)	24.89, CH_2
12	5.296	t, J=3.7	129.23, CH	5.324	(t, 3.7)	124.7, CH
13		-	140.15, C		-	144.75, C
14		-	42.72, C		-	42.71, C
15	1.807 1.006	(m) (m)	29.57, CH_2	1.634 1.005	(m) (m)	29.43, CH_2
16	2.580 1.513	td, J=13.3, 4.7	26.59, CH_2	2.292 1.599	(m)	28.58, CH_2
17		-	49, C		-	46.69, C
18	2.504	(s)	55.08, CH	3.057	(m)	45.18, CH
19		-	73.57, C	3.256	dd, J=3.9, 0.8	82.43, CH
20	1.352	(m)	43.09, CH		-	36.03, C

21	1.732	(m)	27.28, CH_2	1.578	(m)	29.49, CH_2
	1.232	(m)		1.003	(m)	
22	1.731	(m)	39.02, CH_2	1.786	(m)	34.03, CH_2
	1.621	(m)		1.615	(m)	
23	3.505	d, J=11.1	66.34, CH_2	3.505	d, J=11.1	66.33, CH_2
	3.257	d, J=11.1		3.275	d, J=11.1	
24	0.704	(s)	13.87, CH_3	0.704	(s)	13.8, CH_3
25	1.035	(s)	17.51, CH_3	1.026	(s)	17.38, CH_3
26	0.799	(s)	17.53, CH_3	0.770	(s)	17.8, CH_3
27	1.352	(s)	24.88, CH_3	1.314	(s)	25.11, CH_3
28		-	182.31, C		-	181.36, C
29	1.197	(s)	27.05, CH_3	0.966	(s)	28.68, CH_3
30	0.932	d, J=6.8	16.61, CH_3	0.908	(s)	25.11, CH_3

*^{1}H spectra data was generated at 700.40 MHz

** ^{13}C NMR spectra data was generated at 176.12 MHz

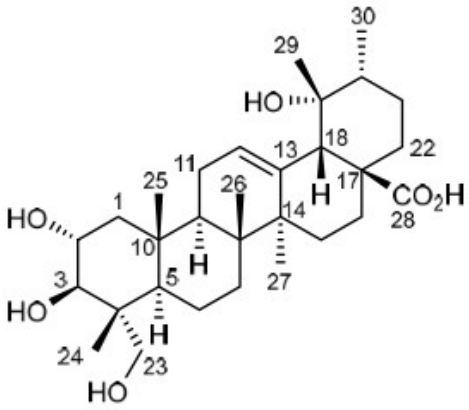

1

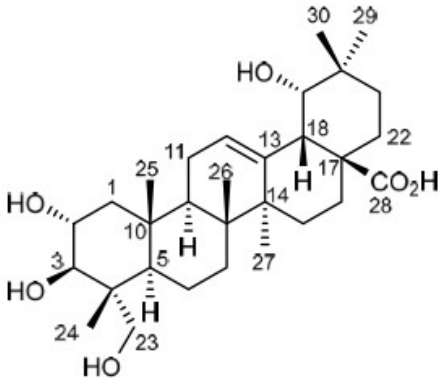

2

Figure 4.32: Compounds 1 and 2, isomeric mixture identified in CR-A isolated from *C. racemosum*

4.17.3 Structure elucidation of CR-C

CR-C (35 mg) which showed to be a mixture (1:0.9) of compounds **3** and **4** (Figure 4.33)was identified as colourless powder.HRESI-MS generated a $[M-H]^-$ ion at *m/z*519.3329, consistent with a molecular formula of $C_{30}H_{48}O_7$(calculated as $C_{30}H_{47}O_7^-$,with *m/z*showing 519.3327, Δ = 0.3 ppm).

From Table 4.17, compounds**3** and **4** showed signal patterns with some characteristic chemical shifts in both ^1H and ^{13}C experiments. The occurrence of olefinic proton in **3** and **4** resulted in the chemical shift for the proton at C-12(δ_{H-12} 5.332and δ_{H-12}5.362, respectively).The^{13}C-NMR spectra signals for the olefinic carbons were δ_{C-12}129.54 and δ_{C-13}139.46for **3** and δ_{C-12}124.95 and δ_{C-13}144.07 for **4**. Additionally, according to the DEPTq experiments, **3** and **4** showed the presence of 30 carbon atoms (Table 4.17). Six methyl (CH_3), eight methylene (CH_2), eight methine (CH) and eight quartenary carbon atoms (C)groups were identified in **3** and **4**. In the ^1H and ^{13}C there were notable differences between **3** (δ_{C-19} 73.61; δ_{H-20} 1.358 (m), δ_{C-20} 43.11) and **4** (δ_{H-19} 3.271 (dd, J=3.9, 0.9 Hz), δ_{C-19} 82.47; δ_{C-20} 36.05)detected in their chemical shifts.

The chemical shifts of the olefinic signals in **3** and **4** and saturation of up-field signals (between 0 and 2 ppm) in their spectra was a preliminary indication of a pentacyclic triterpene skeleton (Table 4.17, Appendices 4a and 4b).

From extensive analysis of 1D NMR as well as 2D NMR including HMBC, HSQC and COSY, **3** and **4**(Figure 4.33) were unambiguously identified as 6β, 23-dihydroxytormentic acidcorresponding to the literature data (Dijoux *et al*., 1993) and combregeninalso corresponding to the literature data (Ponou *et al*., 2008), respectively.

Table 4.17:Spectroscopic data from ^{1}H- and ^{13}C-NMRofCR-C(3 & 4) in CD_3OD solvent

Position	3			4		
	^{1}H (δ)*^{HH}J-coupling (Hz)		^{13}C (δ)**	^{1}H (δ)*^{HH}J-coupling (Hz)		^{13}C (δ)**
1	1.895 0.896	dd, J=12.4, 4.6 (m)	50.09, CH_2	1.864 0.876	(dd, 12.4, 4.6) (m)	49.86, CH_2
2	3.742	ddd, J=11.5, 9.6, 4.6	69.71, CH	3.74	(ddd, 11.5, 9.6, 4.6)	69.69, CH
3	3.3	d, J=9.6	78.24, CH	3.297	d, J=9.6	78.26, CH
4		-	44.81, C		-	44.83, C
5	1.307	d, J=2.0	48.95, CH	1.307	d, J=2.0	49.28, CH
6	4.39	(m)	68.69, CH	4.39	(m)	68.75, CH
7	1.833 1.501	(m) (dd, 14.5, 2.7)	41.4, CH_2	1.792 1.494	(m) (dd, 14.5, 2.7)	41.27, CH_2
8		-	40.29, C		-	40, C
9	1.828	(m)	48.93, CH	1.864	(m)	49.56, CH
10		-	38.53, C		-	38.73, C
11	2.07	(m)	24.72, CH_2	2.09 2.026	(m)	24.81, CH_2
12	5.332	t, J=3.7	129.54, CH	5.362	t, J=3.7	124.95, CH
13		-	139.46, C		-	144.07, C
14		-	43.16, C		-	43.18, C
15	1.885 1.0	(m) (m)	29.54, CH_2	1.711 1.005	(m) (m)	29.39, CH_2
16	2.566 1.505	td, J=13.3, 4.6	26.62, CH_2	2.277 1.604	td, J=13.3, 3.8)	28.62, CH_2
17		-	49.07, C		-	46.74, C
18	2.525	(s)	55.15, CH	3.079	(m)	45.21, CH
19		-	73.61, C	3.271	dd, J=3.9, 0.9	82.47, CH
20	1.358	(m)	43.11, CH		-	36.05, C
21	1.732	(m)	27.3, CH_2	1.75	(m)	29.58, CH_2

	1.237	(m)		1.003	(m)	
22	1.73	(m)	39.03, CH_2	1.789	(m)	34.06, CH_2
	1.627	(m)		1.616	(m)	
23	3.583	(d, 11.1)	65.93, CH_2	3.583	(d, 11.1)	65.93, CH_2
	3.446	(d, 11.1)		3.452	(d, 11.1)	
24	1.068	(s)	15.23, CH_3	1.068	(s)	15.16, CH_3
25	1.386	(s)	19.01, CH_3	1.377	(s)	18.82, CH_3
26	1.084	(s)	18.49, CH_3	1.07	(s)	18.45, CH_3
27	1.328	(s)	24.88, CH_3	1.288	(s)	25.07, CH_3
28		-	182.32, C		-	182.36, C
29	1.206	(s)	27.06, CH_3	0.94	(s)	28.66, CH_3
30	0.933	d, J=6.7	16.6, CH_3	0.973	(s)	25.2, CH_3

*^{1}H spectra data was generated at 700.40 MHz

** ^{13}C NMR spectra data was generated at 176.12 MHz

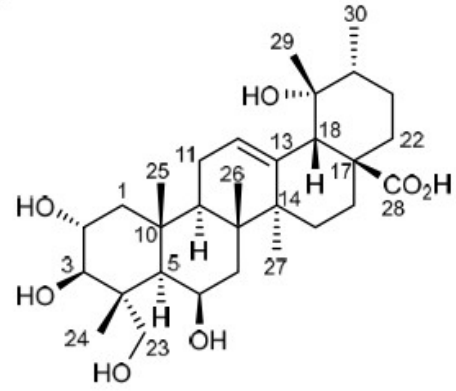

3

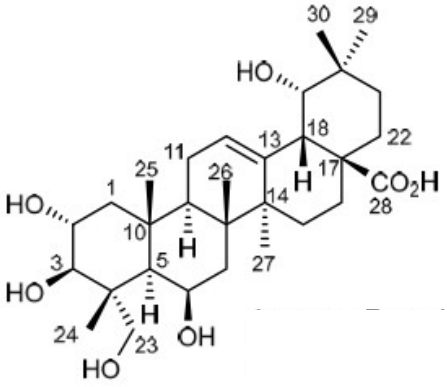

4

Figure 4.33: Compounds 3 and 4, isomeric mixture identified in CR-C isolated from *C. racemosum*

4.17.5 Structure elucidation of CR-E

CR-E (2 mg) was identified ascolourlesspowderand showed to be a mixture (1:0.74) of compounds **5** and **6**(Figure 4.34).These isomeric compounds displayed a $[M-H]^-$ ion at *m/z*503.3384related to a molecular formula of $C_{30}H_{48}O_6$(calculated as $C_{30}H_{47}O_6^-$,with *m/z*showing 503.3378, Δ = 1.2 ppm).

From Table 4.18,compounds **5** and **6** showed signal patternsthat were similar to each other in ^1H as well as^{13}C analysis, with the carbon spectra displaying 30 signals in both. Through DEPT analysis, they were assigned as follows: eight and seven non-hydrogenated carbon (C), seven and nine methine carbons (CH), nine and eight methylene carbons (CH_2), for **6** and **5**, respectively, while showing six methyl substituents (CH_3) for each of the two compounds (Table 4.18). The signals of ^1H and ^{13}Canalyses indicated distinctive shifts between **6** (δ_{H-18} 2.876 (dd, J=13.8, 3.9 Hz), δ_{C-18} 42.82; δ_{H-19} 1.71, 1.145 (m, m), δ_{C-19} 47.25; δ_{C-20} 31.61) and **5**(δ_{H-18} 2.225 (d, J=11.2 Hz), δ_{C-18} 54.47; δ_{H-19} 1.389 (m), δ_{C-19} 40.43; δ_{H-20} 0.99 (m), δ_{C-20} 40.44) (Table 4.20). The signal patterns of **5** and **6** showed some characteristic chemical shifts in both ^1H and ^{13}C experiments (Tables 4.18). The presence of olefinic proton in **5** and **6** resulted in the chemical shift for the proton at C-12(δ_{H-12} 5.279and δ_{H-12}5.295, respectively).The^{13}C-NMR spectra signals for the olefinic carbons were δ_{C-12}127.01 and δ_{C-13}139.13for **5** and δ_{C-12}123.72 and δ_{C-13}144.70 for **6**.

The chemical shifts of the olefinic signals in **5** and **6** and saturation of up-field signals (between 0 and 2 ppm) in their spectra was a preliminary indication of a pentacyclic triterpene skeleton (Table 4.18, Appendices 6a and 6b).

From detailed examination of 1D NMR as well as 2D NMR including HMBC, HSQC and COSY, **5** and **6**(Figure 4.34) were unambiguously identified as madecasic acid which corresponded with literature data (Van Loc *et al*., 2018) and terminolic acid which as well corresponded with literature data (Runyoro *et al*., 2013), respectively.

Table 4.18:Spectroscopic data from ^{1}H- and ^{13}C-NMRofCR-E (5 & 6) in CD_3OD solvent

Position	5			6		
	^{1}H (δ)* ^{HH}J-coupling (Hz)		^{13}C (δ)**	^{1}H (δ)* ^{HH}J-coupling (Hz)		^{13}C (δ)**
1	1.917 0.89	dd, J=12.5, 4.7 (m)	50.28, CH_2	1.885 0.87	dd, J=12.4, 4.6 (m)	50.11, CH_2
2	3.737	ddd, J=11.4, 9.7, 4.6	69.71, CH	3.73	ddd, J=11.4, 9.6, 4.6	69.68, CH
3	3.294	d, J=9.7	78.15, CH	3.289	d, J=9.6	78.15, CH
4		-	44.79, C		-	44.81, C
5	1.289	(m)	48.83, CH	1.289	(m)	48.83, CH
6	4.381	(m)	68.43, CH	4.381	(m)	68.48, CH
7	1.799 1.513	(dd, 14.5, 4.3) (dd, 14.5, 2.6)	41.32, CH_2	1.772 1.492	dd, J=14.5, 4.3 dd, J=14.5, 2.5	41.12, CH_2
8		-	39.99, C		-	39.81, C
9	1.684	(m)	49.24, CH	1.716	(m)	49.33, CH
10		-	38.52, C		-	38.59, C
11	2.016 2.065	(m)	24.47, CH_2	2.07 1.959	(m) ddd, J=18.2 6.4, 4.1	24.58, CH_2
12	5.279	dd, J=3.2, 4.1	127.01, CH	5.295	t, J=3.6	123.72, CH
13		-	139.13, C		-	144.7, C
14		-	43.85, C		-	43.5, C
15	2.002 1.097	(m) (m)	29.17, CH_2	1.852 1.081	(m) (m)	28.8, CH_2
16	2.022 1.644	(m)	25.35, CH_2	2.008 1.599	(m)	24.08, CH_2
17		-	47.24, C		-	?, C
18	2.225	d, J=11.2	54.47, CH	2.876	dd, J=13.8, 3.9	42.82, CH
19	1.389	(m)	40.43, CH	1.71 1.145	(m) (m)	47.25, CH_2

20	0.99	(m)	40.44, CH		-	31.61, C
21	1.508	(m)	31.81, CH_2	1.394	(m)	34.93, CH_2
	1.346	(m)		1.207	(m)	
22	1.693	(m)	38.16, CH_2	1.749	(m)	33.88, CH_2
	1.636	(m)		1.537	(m)	
23	3.582	(d, 11.1)	65.86, CH_2	3.582	(d, 11.1)	65.86, CH_2
	3.436	(d, 11.1)		3.436	(d, 11.1)	
24	1.06	(s)	15.26, CH_3	1.06	(s)	15.21, CH_3
25	1.396	(s)	19.18, CH_3	1.384	(s)	19.03, CH_3
26	1.113	(s)	19.11, CH_3	1.094	(s)	18.81, CH_3
27	1.103	(s)	24.18, CH_3	1.147	(s)	26.47, CH_3
28		-	181.69, C		-	181.92, C
29	0.898	d, J=6.5	17.63, CH_3	0.912	(s)	33.56, CH_3
30	0.966	(m)	21.56, CH_3	0.95	(s)	23.97, CH_3

*^{1}H spectra data was generated at 700.40 MHz

** ^{13}C NMR spectra data was generated at 176.12 MHz

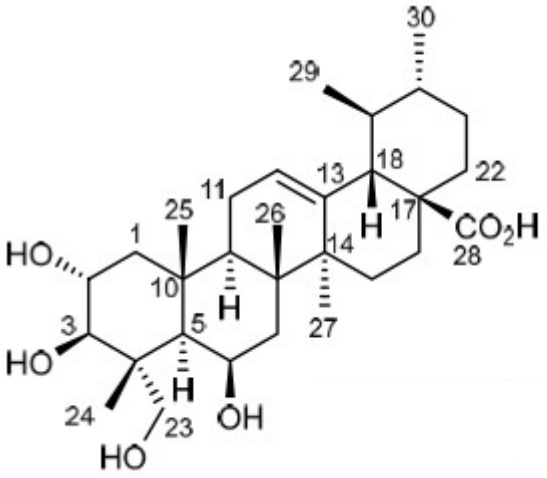

5

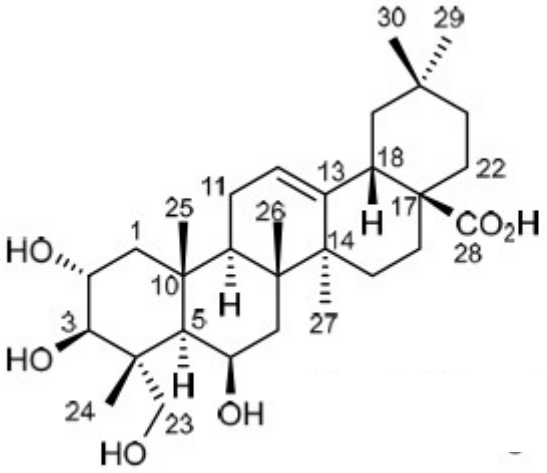

6

Figure 4.34: Compounds 5 and 6, isomeric mixture identified in CR-E isolated from *C. racemosum*

4.17.6 Structure elucidation of CR-G

CR-G (7.2 mg) shown as compound **7** (Figure 4.35) is a colourless amorphous powder. The MS showed molecular ion peak as m/z 264.32 [M-H] related to $C_{15}H_{20}O_4$. By means of DEPTq experiment, there were shown the presence of four methyl (CH_3), one methylene (CH_2), four methine (CH) and six quartenary carbon atoms (C) groups. Its ^{1}H-NMR spectrum showed the occurrence of signals due to four tertiary methyl substituents δ_{H-6} 2.022, $\delta_{H-7'}$ 1.934, $\delta_{H-8'}$ 1.064, $\delta_{H-9'}$ 1.029; a methylene group $\delta_{H-5'}$ 2.537 and $\delta_{H-5'}$ 2.182; two olefinic protons δ_{H-2} 5.759 and $\delta_{H-3'}$ 5.919; and two trans-double bond protons δ_{H-4} 7.748 and δ_{H-5} 6.206. Likewise in the ^{13}C-NMR experiment, the signals due to the occurrence of an α, β-unsaturation ketone carbon $\delta_{C-4'}$ 201.05 and a carboxylic carbon δ_{C-1} 170.29 were observed. In addition, there was occurrence of three double bond groups accounting for six carbon signals (δ_{C-2} 120.75, δ_{C-3} 149.68, δ_{C-4} 129.58, δ_{C-5} 137.33, $\delta_{C-2'}$ 166.69 and $\delta_{C-3'}$ 127.52), also an oxygenated quartenary carbon $\delta_{C-1'}$ 80.60 showed (Table 4.21). The NMR data of compound **7** correlated with literature report for abscisic acid which was previously isolated and reported from Phomopsis amygdali (Ma *et al*., 2016).

Table 4.19:Spectroscopic data from ^{1}H- and ^{13}C-NMR ofCR-G(7) in $CDCl_3$ solvent

Position	7		
	^{1}H (δ)*^{HH}J-coupling (Hz)		^{13}C (δ)**
1		-	170.29, C
2	5.759	s, br	120.75, CH
3		-	149.68, C
4	7.748	d, J=16.1	129.58, CH
5	6.206	dd, J=16.1, 0.4	137.33, CH
6	2.022	d, J=1.3	21.15, CH_3
1‘		-	80.6, C
2‘		-	166.69, C
3‘	5.919	(m)	127.52, CH
4‘		-	201.05, C
5‘	2.537	d, J=15.8 br	50.68, CH_2
	2.182	d, J=15.8, br	
6‘		-	42.85, C
7‘	1.934	d, J=1.4	19.62, CH_3
8‘	1.064	(s)	23.55, CH_3
9‘	1.029	(s)	24.66, CH_3

*^{1}H spectra data was generated at 700.40 MHz

** ^{13}C NMR spectra data was generated at 176.12 MHz

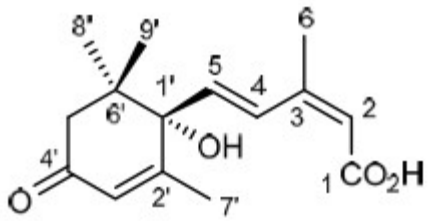

7

Figure 4.35: Compound 7 identified in CR-G from *C. racemosum*

4.17.7 Structure elucidation of CR-H

CR-H (31 mg) which showed to be a mixture (1:0.47) of compounds **8** and **9**(Figure 4.36) was identified as pale yellowish powder.The detected $[M-H]^-$ ion at *m/z*665.3929 correlatedwith a molecular formula of $C_{36}H_{58}O_{11}$(calculated as $C_{36}H_{57}O_{11}^-$, with*m/z*showing 665.3906, Δ = 3.4 ppm) also the MS^n spectra of the $[M+Na]^+$ ion at *m/z*689.5 displayed the consecutive loss of a hexosyl moiety and CO_2.

From Table 4.20, the signals of **8**as well as**9** showed some characteristic chemical shifts in both ^1H and ^{13}C experiments. The presence of olefinic proton in **8** and **9** resulted in the chemical shift for the proton at C-12(δ_{H-12} 5.312and δ_{H-12}5.336, respectively).The^{13}C-NMR spectra for the olefinic carbons signals were δ_{C-12}129.49 and δ_{C-13}139.75for **8** and δ_{C-12}124.78 and δ_{C-13}144.48 for **9**.The signal patterns of the anomeric protons in **8** and **9**($\delta_{H-1'}$ 5.322and $\delta_{H-1'}$5.375, respectively) indicated the integration of glycosides. The sugar moiety attached in**8** and **9** are connected to the oxygen of the hydroxyl moiety at position C-28.

The chemical shifts of the olefinic and anomeric proton signals in **8** and **9** and saturation of up-field signals (between 0 and 2 ppm) in their spectra was a preliminary indication of a pentacyclic triterpene skeleton with sugar moiety linkages (Table 4.20, Appendices 11a and 11b).

Based on detailed examination of the 1D NMR as well as 2D NMR including HMBC, HSQC and COSY information, **8** and **9** were unambiguously identified as nigaichigoside F1 corresponding to literature data (Wu *et al*., 2007) and arjunglucoside 1 corresponding to literature data (Gossan *et al*., 2016), respectively (Figure 4.36), which are the glycosides of **1**and **2** respectively.

Table 4.20:Spectroscopic data from ^{1}H- and ^{13}C-NMRof CR-H(8 & 9) in CD_3OD solvent

Position	8			9		
	^{1}H (δ)*	^{HH}J-coupling (Hz)	^{13}C (δ)**	^{1}H (δ)*	^{HH}J-coupling (Hz)	^{13}C (δ)**
1	1.942 0.909	dd, J=12.6, 4.5 (m)	47.97, CH_2	1.909 0.9	dd, J=12.6, 4.5 (m)	47.79, CH_2
2	3.699	ddd, J=11.5, 9.6, 4.6	69.71, CH	3.695	ddd, J=11.6, 9.6, 4.6	69.69, CH
3	3.358	d, J=9.6	78.3, CH	3.358	(m)	78.3, CH
4		-	44.12, C		-	44.13, C
5	1.297	(m)	48.23, CH	1.297	(m)	48.37, CH
6	1.446 1.391	(m) (m)	19.24, CH_2	1.426 1.386	(m) (m)	19.26, CH_2
7	1.653 1.289	(m) (m)	33.51, CH_2	1.658 1.268	(m) (m)	33.26, CH_2
8		-	41.26, C		-	40.88, C
9	1.777	(m)	48.53, CH	1.831	(m)	49.14, CH
10		-	38.99, C		-	39.16, C
11	2.022	(m)	24.8, CH_2	2.006	(m)	24.92, CH_2
12	5.312	t, J=3.7	129.49, CH	5.336	t, J=3.7	124.78, CH
13		-	139.75, C		-	144.48, C
14		-	42.78, C		-	42.75, C
15	1.837 1.01	(m) (m)	29.63, CH_2	1.671 1.005	(m) (m)	29.43, CH_2
16	2.613 1.629	td, J=13.4, 4.6	26.51, CH_2	2.326 1.722	td, J=13.3, 3.5	28.43, CH_2
17		-	49.46, C		-	47.11, C
18	2.518	(m)	54.96, CH	3.054	(m)	45.07, CH
19		-	73.63, C	3.272	(m)	82.43, CH
20	1.351	(m)	42.94, CH		-	35.95, C

21	1.734	(m)	27.21, CH_2	1.766	(m)	29.5, CH_2
	1.232	(m)		1.005	(m)	
22	1.783	(m)	38.31, CH_2	1.784	(m)	33.29, CH_2
	1.624	(m)		1.603	(m)	
23	3.504	d, J=11.1	66.41, CH_2	3.504	d, J=11.1	66.39, CH_2
	3.269	d, J=11.1		3.269	d, J=11.1	
24	0.703	(s)	13.87, CH_3	0.703	(s)	13.79, CH_3
25	1.038	(s)	17.6, CH_3	1.028	(s)	17.46, CH_3
26	0.781	(s)	17.67, CH_3	0.751	(s)	17.82, CH_3
27	1.344	(s)	24.73, CH_3	1.304	(s)	25.03, CH_3
28		-	178.54, C		-	178.58, C
29	1.205	(s)	27.06, CH_3	0.94	(s)	28.61, CH_3
30	0.932	d, J=6.7	16.6, CH_3	0.951	(s)	25.16, CH_3
1‘	5.322	d, J=8.2	95.78, CH	5.375	d, J=8.2	95.81, CH
2‘	3.318	(m)	73.86, CH	3.322	(m)	73.92, CH
3‘	3.398	dd, J=9.2, 8.7	78.32, CH	3.404	(m)	78.32, CH
4‘	3.36	(m)	71.12, CH	3.36	(m)	71.08, CH
5‘	3.341	(m)	78.59, CH	3.341	(m)	78.73, CH
6‘	3.798	dd, J=12.0, 2.3	62.42, CH_2	3.82	dd, J=12.0, 2.0	62.38, CH_2
	3.68	dd, J=12.0, 4.8		3.682	dd, J=12.0, 4.6	

*^{1}H spectra data was generated at 700.40 MHz

** ^{13}C NMR spectra data was generated at 176.12 MHz

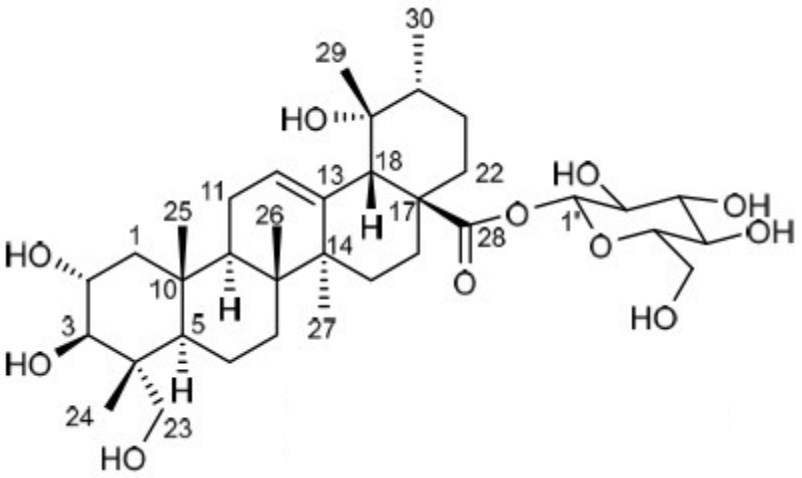

8

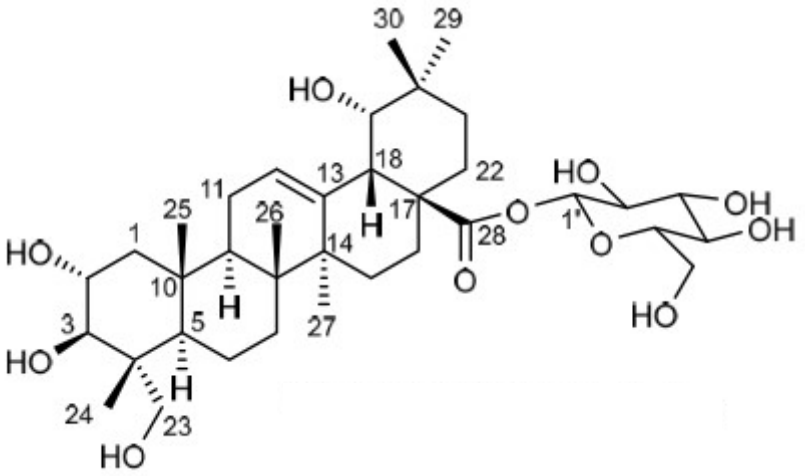

9

Figure 4.36:Compounds 8 and 9, isomeric mixture identified in CR-H isolated from *C. racemosum*

4.18 Structure elucidation of compounds isolated from *Combretum zenkeri*

4.18.1 Structure elucidation of CZ-A

The structure of **CZ-A** (5 mg) was unambiguously determined and elucidated by spectroscopic experiments including 1D NMR (^{1}H and ^{13}C), 2D NMR (HMBC, HSQC, COSY, NOESY and TOCSY), ESI-MS and HR-ESIMS, as well asthroughliterature reports comparison. Compound **CZ-A** was found to be an isomeric mixture (1:0.4) as revealed from the spectroscopic information. The HRESIMS displayed molecular ion peak $[M-H]^-$ ion at m/z 455.3535 relating to a molecular formula of $C_{30}H_{48}O_3$. The isomers were identified as ursolic acid (3β-hydroxyurs-12-en-28-oic acid) (**12**) (Venditti *et al*., 2016) and oleanolic acid (3β-hydroxyolean-12-en-28-oic acid) (**13**) (Kipchakbaeva *et al*., 2016) (Figure 4.37).

In both ^{1}H and ^{13}C experiments,compound **11** showed signal pattern related to the ones in**10**(Table 4.21), but the difference lied in the DEPTq analysis, where **10** and **11** had seven and eight non-hydrogenated carbons(C), seven and six methine carbons (CH), nine and ten methylene carbons (CH_2), respectively, while each compoundhad seven methyl (CH_3) groups. For compound **10**,^{13}C NMR experiment showed at postions C-12 and C-13olefinic signals δ_C 126.88 and δ_C 139.66 respectively. On the other hand for compound **11**, the olefinic signals at postions C-12 and C-13in^{13}C experiment showed δ_C 123.62 and δ_C 145.25 respectively. The spectrum also showed for compound **10** (δ_H 3.154; dd, J=11.7, 4.6) and compound **11** (δ_H 3.147, m) at position 3. Also showed at position 18, compound **10** (δ_H 2.203; dd, J=11.5, 1.0; δ_C 54.38) and compound **11** (δ_H 2.851, m; δ_C 42.75). The chemical shifts of olefinic carbons revealed on ^{13}C NMR signals help to unambiguously identify compounds **10** and **11**. Previous report has confirmed that the chemical shifts of the double bond C_{12} and C_{13} for the olean-12-ene type are around 122.0 and 144.0, respectively, while those of its isomer urs-12-ene are around 125.0 and 139.0, respectively, for the same carbons (Mahato and Kundu, 1994). This characteristic chemical sifts of oleanane and ursane triterpenes are consistent with ^{13}C NMR signals generated in this study; help to establish the difference between compound 1 and 2 and elucidate their structures in the mixture.

Table 4.21: Spectroscopic information from ^{1}H- and ^{13}C-NMR generated for CZ-A (10 & 11)in $CDCl_3$

Position	10			11		
	^{1}H (δ)*	^{HH}J-coupling (Hz)	^{13}C (δ)**	^{1}H (δ)*	^{HH}J-coupling (Hz)	^{13}C (δ)**
1	1.67	m, m	39.99	1.63	m, m	39.83
	1.01			0.99		
2	1.63	m	27.90	1.63	m	27.87
	1.56			1.56		
3	3.15	dd, J=11.7, 4.6	79.70	3.15	m	79.71
4	-		39.84	-		40.55
5	0.75	dd, J=11.8, 1.6	56.74	0.76	m	56.76
6	1.56	m, m	19.47	1.56	m, m	19.50
	1.42			1.42		
7	1.55	m, m	34.33	1.51	m, m	34.02
	1.34			1.32		
8	-		40.78	-		40.78
9	1.55	m	49.06	1.59	m	49.10
10	-		38.10	-		38.17
11	1.93	m	24.36	1.93	m	24.52
12	5.23	t, J=3.7	126.88	5.24	t, J=3.7	123.62
13	-		139.66	-		145.25
14	-		43.25	-		42.89
15	1.93	m, m	29.22	1.78	m, m	28.85
	1.09			1.08		
16	2.04	m	25.33	1.74	m	24.06
	1.65			1.26		
17	-		49.10	-		47.67
18	2.20	dd, J=11.5, 1.0	54.38	2.85	m	42.75
19	1.38	m	40.44	1.69	m, m	47.27

				1.12		
20	0.99	m	40.42	-		31.62
21	1.50	m, m	31.79	1.39	m, m	34.91
	1.35			1.20		
22	1.70	m, m	38.13	1.74	m, m	33.84
	1.63			1.54		
23	0.98	s	28.76	0.97	s	28.73
24	0.78	s	16.37	0.78	s	16.31
25	0.96	d, J=0.6	16.02	0.95	d, J=0.6	15.88
26	0.85	s	17.81	0.82	s	17.73
27	1.12	d, J=0.7	24.08	1.16	d, J=0.7	26.38
28	-		181.74	-		181.96
29	0.88	d, J=6.5	17.64	0.94	s	23.98
30	0.96	m	21.57	0.91	s	33.57

*^{1}H spectra data was generated at 700.40 MHz

** ^{13}C NMR spectra data was generated at 176.12 MHz

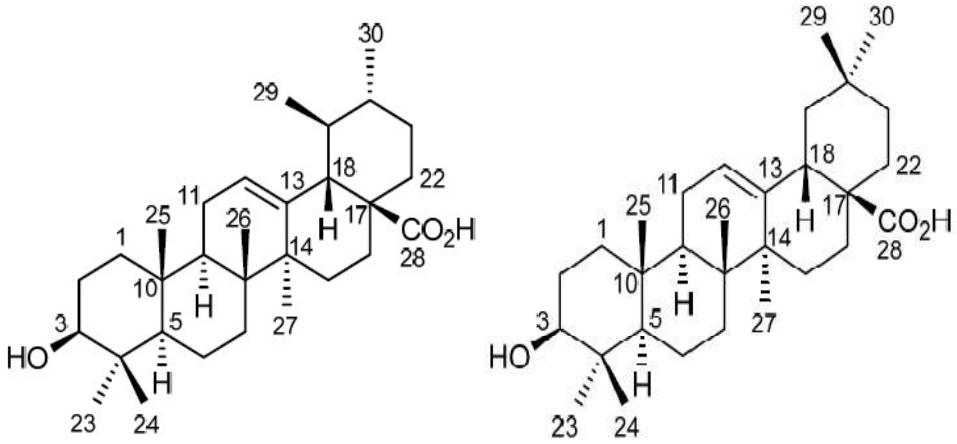

10 **11**

Figure 4.37: Compounds 10 and 11, isomeric mixture identified in CZ-A isolated from *C. zenkeri*

4.20 Antiplasmodial activity of isolated compounds

The compounds isolated from*C. racemosum* methanol extract, **CR-A**, **CR-C**, **CR-H**as well as single compounds arjungenin, abscisic acid, madecassic acid, were screenedagainst D10 and W2

strains forantiplasmodial action.The compounds were quantitatively tested on the *P. falciparum* lactate dehydrogenase (pLDH) and the values for the 50% inhibition (IC_{50}) were derived from a range of concentrations tested for the compounds.The plots of their percentage parasite growth against concentrations resulted in a sigmoidal curve, specific to *P. falciparum* lactate dehydrogenase (pLDH) activity inhibition (Figures 4.38 and 4.39). Compounds from *C. zenkeri* methanol extract, **CZ-A** were not tested in this experiment because the ursolic and oleanolic acidsantiplasmodial effects identified from this extract was previously reported (Cimanga *et al*., 2006). The isolates CR-A (IC_{50}=33.52±12.41 µg/mL), CR-C (IC_{50}= 49.71±18.88 µg/mL) and CR-H (IC_{50}= 41.96±15.73 µg/mL)was active against D10 strain of *P. falciparum* at 95% confidence interval 32.0-44.6 µg/mL, 46.9-71.0 µg/mL and 29.1-54.1 µg/mL, respectively, in concentration-response data which fitted a sigmoidal equation wellwith the statistical treatment results (R^2 = 0.98, Sy.x =7.1), (R^2 = 0.98, Sy.x = 4.9) and (R^2 = 0.98, Sy.x = 7.5), respectively(Table 4.22, Figure 4.38).The isolates CR-A (IC_{50}=23.08±8.17 µg/mL), CR-C (IC_{50}= 61.07±23.15 µg/mL) and CR-H (IC_{50}= 33.84±12.53 µg/mL)indicated activity against W2 strain of *P. falciparum* as well,at 95% confidence interval 13.0-24.5 µg/mL, 25.3-66.7 µg/mL and 16.2-38.0 µg/mL, respectively, their concentration-response data as well fitted a sigmoidal equation well (R^2 = 0.95, Sy.x =10.1), (R^2 = 0.91, Sy.x = 9.8) and (R^2 = 0.97, Sy.x = 6.5), respectively(Table 4.23, Figure 4.39). CR-A displayed the highest inhibitory action against D10 and W2 strains. The single compounds tested showed inhibition of*P. falciparum* D10 growth, with IC_{50} values ranging from 27.62±11.56 µg/mL to 57.04±21.81 µg/mL and they also inhibited*P. falciparum* W2 growth resulted in IC_{50} values ranging from 17.19±4.34 µg/mL to 134.70±13.21 µg/mL.Madecassic acid was the most active compounds and its statistical treatment gave satisfactory results with R^2 = 0.96, Sy.x = 8.3 with IC_{50}= 27.62±11.56 µg/mL at 95% confidence interval 20.3-36 µg/mL against the strain D10 (Table 4.22), and R^2 = 0.98, Sy.x = 6.6 with IC_{50}= 17.19±4.34 µg/mL at 95% confidence interval 13.9-19.5 µg/mL against the strain W2 (Tables 4.23).CR-C, abscisic acid and arjungenin showedmore potency against the D10 than against the W2, while CR-A, CR-H and madecassic acid showed less activity against D10 strain as compared to theW2 (Tables 4.22 and 4.23).

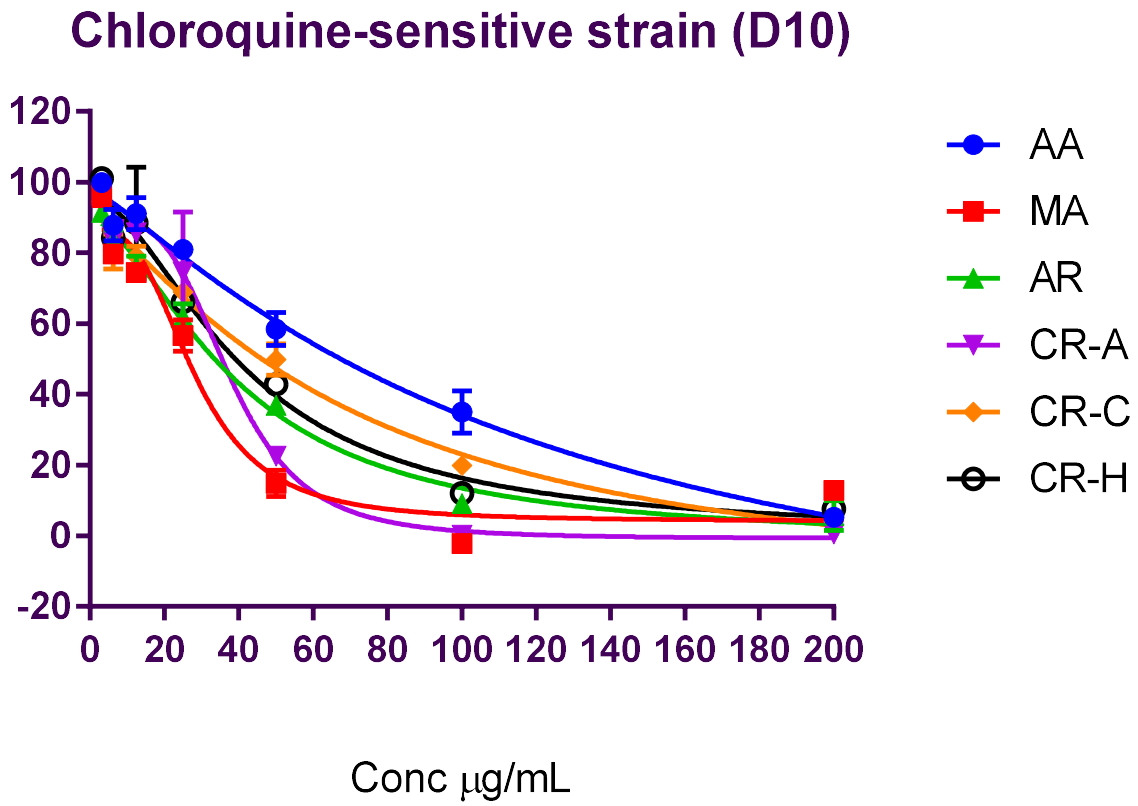

Figure 4.38: Inhibition of *P. falciparum* parasite (D10 strain) by the isolated compounds

Legend:AA- absisic acid, MA- madecasic acid, AR- arjungenin, CR-A- isomeric mix of 19α-hydroxyasiatic acid and arjungenin, CR-C- isomeric mix of 6β, 23-dihydroxytormentic acid+ combregenin, CR-H- isomeric mix of arjunglucoside I and nigaichigoside F1

Table 4.22: Antiplasmodial activity of compounds from *C. racemosum* against D10

	D10 (IC_{50} µg/mL)[a]	C.I (µg/mL)	R^2	Sy.x

CR-A	33.52 ± 12.41	32.0-44.6	0.98	7.1
CR-C	49.71 ± 18.88	46.9-71	0.98	4.9
CR-H	41.96 ± 15.73	29.1-54.1	0.98	7.5
Abscisic Acid	57.04 ± 21.81	63.6-119	0.98	4.9
Madecassic Acid	27.62 ± 11.56	20.3-36.0	0.96	8.3
Arjungenin	41.06 ± 16.92	32.4-50.4	0.99	4.0

[a]IC_{50} values were generated, from duplicate results of three separate experiments, as mean±SD

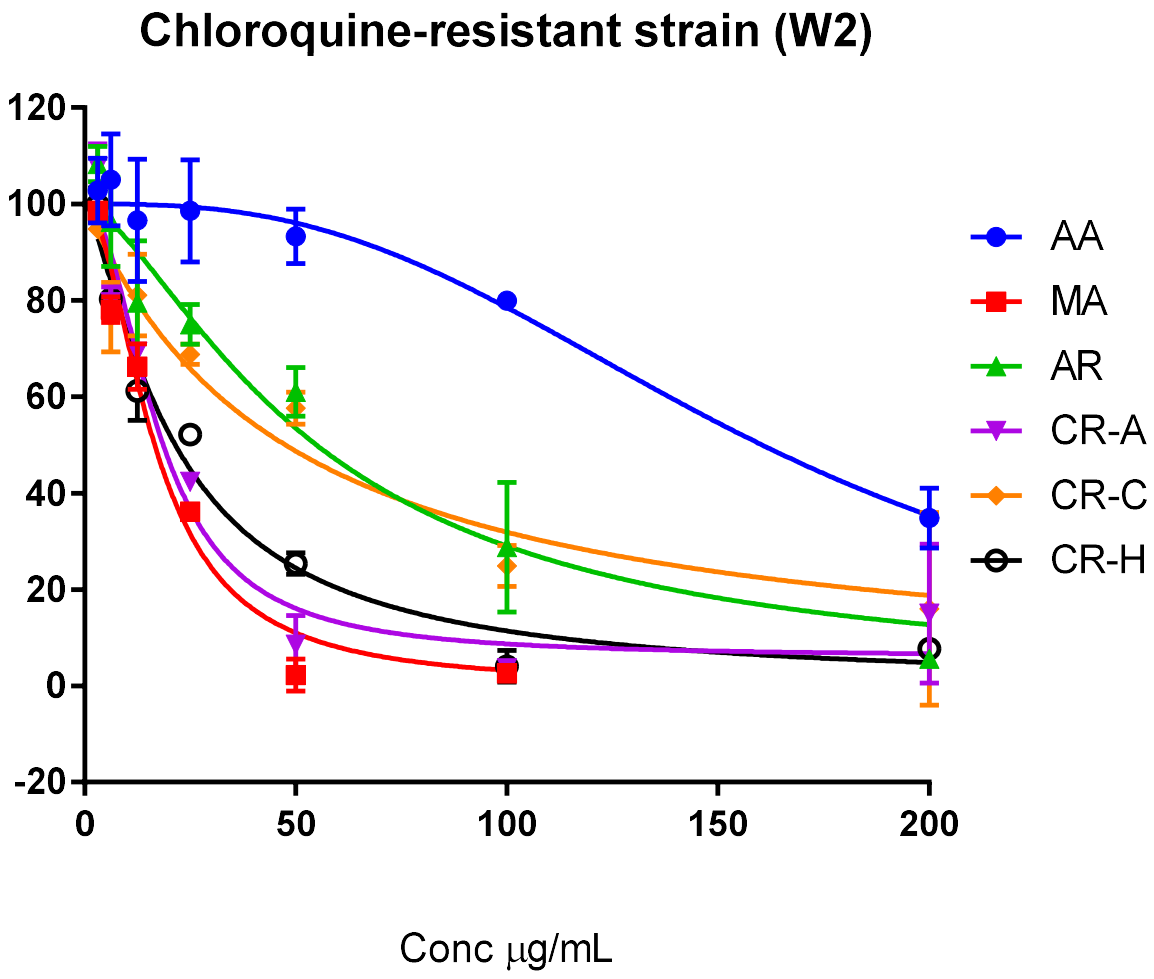

Figure 4.39: Inhibition of *P. falciparum* parasite (W2 strain) by the isolated compounds

Legend: AA- absisic acid, MA- madecasic acid, AR- arjungenin, CR-A- isomeric mix of 19α-hydroxyasiatic acid and arjungenin, CR-C- isomeric mix of 6β, 23 dihydroxytormentic acid and combregenin, CR-H- isomeric mix of arjunglucoside I and nigaichigoside F1

Table 4.23: Antiplasmodial activity of compounds from *C. racemosum* against W2 strain

	W2 (IC_{50}	C.I (µg/mL)	R^2	Sy.x

	µg/mL)[a]			
CR-A	23.08 ± 8.17	13.0-24.5	0.95	10.1
CR-C	61.07 ± 23.15	25.3-66.7	0.91	9.8
CR-H	33.84 ± 12.53	16.2-38.0	0.97	6.6
Abscisic Acid	134.70 ± 13.21	123.0-188.1	0.93	7.4
Madecassic Acid	17.19 ± 4.34	13.9-19.5	0.98	6.6
Arjungenin	64.36 ± 9.31	37.3-71.5	0.96	8.5

[a]IC_{50} values were generated, from duplicate results of three separate experiments, as mean±SD

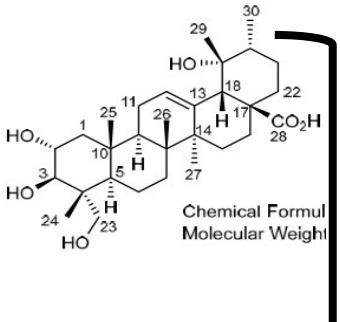

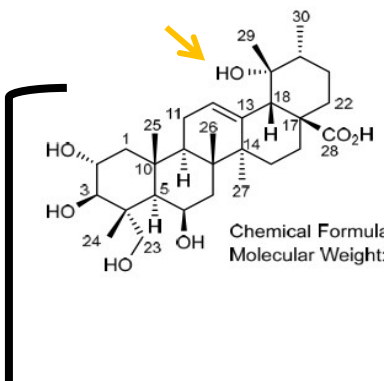

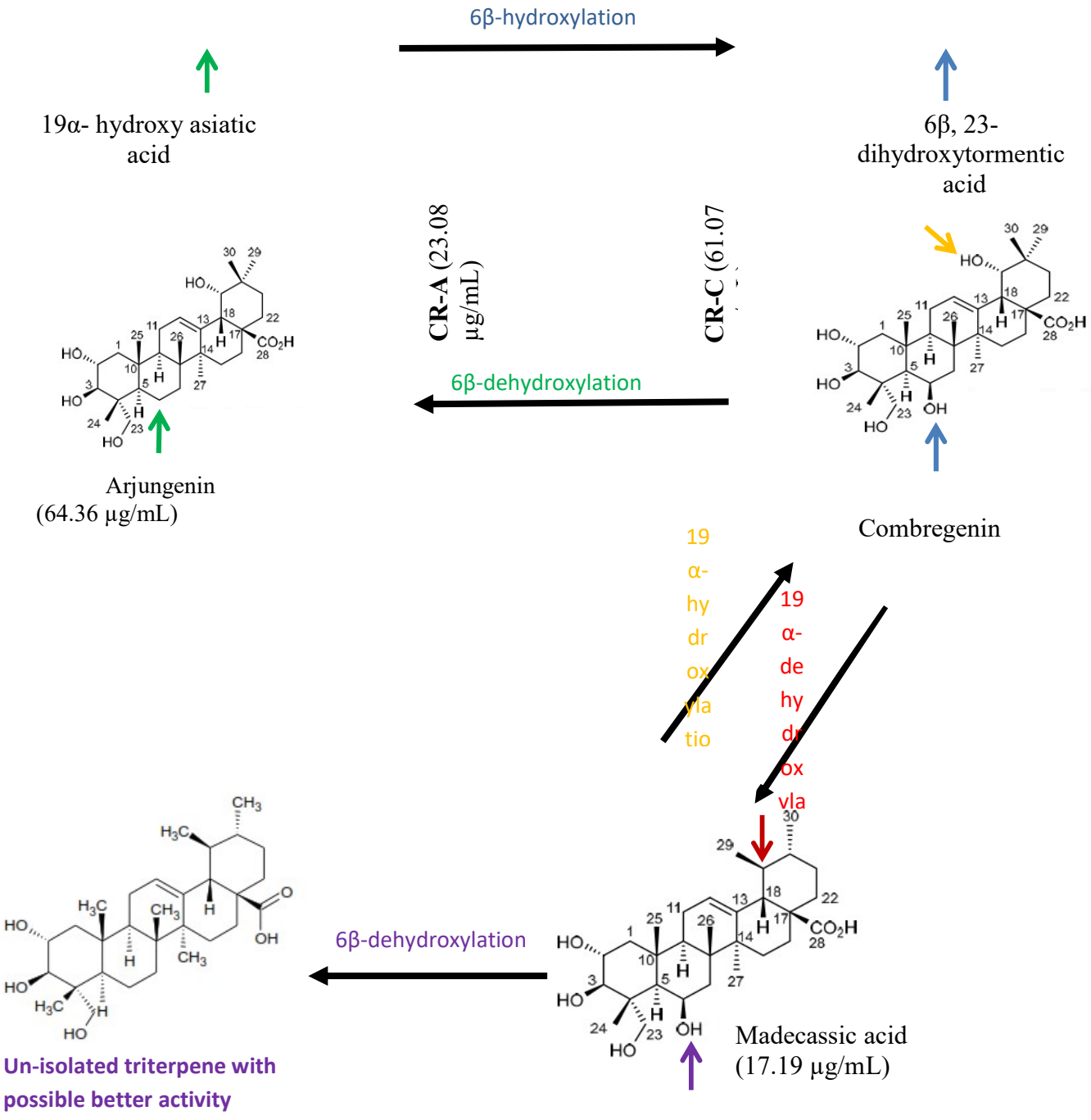

Figure 4.40: Schematic representation of structure-activity relationship (SAR) of compounds isolated

CHAPTER FIVE

5.0DISCUSSIONS

5.1 Antimalarial activity of selected medicinal plants from Combretaceae family

Antimalarial activities of different medicinal plants using the *in vitro* β-hematin (hemozoin) synthesisinhibition has been described by Vargas *et al*.(2011). All medicinal plants screened in this work are all from the plant family Combretaceae.

Malaria infectionis as a result of the invasion of human host by*Plasmodium*parasite through mosquito bites.Considerable amount of heme is produced in the course of intra-erythrocytic cycleas a toxic by-product due to more than 75% of the host hemoglobin being ingested by the parasite (Tekwani and Walker, 2005). Afterwards, insoluble hemozoin is bio-synthesized through an in-built mechanism of detoxification developed by the parasite inorderto protect itself from the self-formed toxicity (Mojarrab *et al*., 2014). β-hematincomprises of cyclic heme dimers, same as hemozoin, having intermolecular hydrogen bonding configured in awell-organized crystalline structure. It is presumed to be the most confirmed sitefor detoxification. This pathway is confirmedfor a number ofantimalarials such as the 4-aminoquinolines:chloroquine,quinine, amodiaquine,mefloquine; therefore considered a suitable drug target (Egan, 2003).To evaluate antimalarial activities on the basis of difference in solubility of heme and *β*-hematin,lots of different*in vitro* methods have been exploited (Tekwani and Walker, 2005; Vargas *et al*., 2011). Eighteen leaf extracts of ten Combretaceae species were investigated in this study for antimalarial activities using *in vitro* method. Our findings showed that theextracts of eight plants demonstratedhemozoin (β-hematin) formation inhibition, suggesting presence of antimalarial compounds. The results showed that extracts with different mode of extraction exhibit different degrees of antimalarial activities as shown in Table 4.1.

Many of the plants studied are prepared in ethnomedicine by alcoholic decoction, hence, the reason for the extraction methods adopted in this work (Atindehou *et al*., 2004); also solvents of intermediate polarity have been shown to possess the highest extraction capacity for both non-polar and polar constituents of plants (Eloff *et al*., 2005). Thus,it was revealed that the percentage yield of all the acetone extracts are higher than that of the methanol (Table 4.1),

which suggests that acetone (intermediate polar solvent) extract more phytocompounds than methanol (polar solvent) which supports the report of Eloff *et al*. (2005).

The monitoring ofthe complex formed in the course of the assay between pyridine and heme (Py-Fe(III)PPIX) resulting to a red colouration, was doneusing UV/visible spectrophotometer at different concentrations. The procedure for the β-hematin synthesis suitable for screening of extracts from plants, as carried out in the present study, was adapted from Vargas *et al*. (2011). Antimalarial potential is shown by the β-hematin synthesisinhibition of an extract, wherea high absorbance value of the sample is indicative of increasedβ-hematin synthesis inhibition. The inhibition of β-hematin synthesis by the extracts is dose independent as revealedin Figure4.2.Among the seven extracts experimented for their activity using the β-hematin model, *Terminalia ivorensis* methanol extract (TIM) showed the highest activity(IC_{50}: 2.58 ± 0.447 mg/mL) (Figure 4.2 and Table 4.2). Other polar extracts, *Combretum zenkeri* (CZM) and *Combretum racemosum* (CRM) methanol extracts were also determined as significantly potent antimalarial extracts (IC_{50}: 2.92 ± 0.846 and 3.96 ± 0.132 mg/mL, respectively). An earlier report by Komlaga *et al*. (2016) has also showed the potency of *Terminalia ivorensis* in an antiplasmodial assay indicating the occurrence of antimalarial agents in the plant. But information regarding theantimalarial activities of the other two promising Combretaceae plants is still scanty.

Cobbinah(2008) showed thattriterpenoids,saponins, steroids, flavonoids, anthraquinone glycosides,polyphenols and tanninsare present in various extracts of *Terminalia ivorensis*. Alsoreported in the leaves of *Combretum zenkeri*were flavonoids, saponins, alkaloids as well as tannins(Ujowundu *et al*., 2010). Onocha *et al*., 2005 reported that alkaloids, steroids, saponins and tannins were shownin different extracts of *Combretum racemosum*. Samuel *et al*. (2014) in a separate study isolated a flavonoid from the acetone extract of *C. racemosum*. This correlate with the report of Rodrigues *et al*. (2012), which described some of the identified phytochemicals in some *Combretum* species. Dibua *et al*. (2013) identified saponins, terpenoids, steroids, glycosides, and acidic compounds as possible antimalarial agents in plants used as antimalarials in ethnomedicine. Thus, it is plausible to assume that all the aforementionedclass of secondary metabolites present in these plants could contribute to the high antimalarial activity observed and maybe also in other Combretaceae used traditionally in

treating malaria. The outcomes of the preliminary study validated the traditional use of these plants as revealed from earlier reports (Atindehou *et al*., 2004).

The mode of action responsible for antimalarial activity in beta-hematin assay can be evaluated, therefore, giving it an advantage to be informative (Vargas *et al*., 2011).

The most suitable and regular methods for bioactive moleculesdiscovery from plants is reported to be ethnopharmacological screening(Kuria, 2001). Furthermore, the ethnopharmocological informations gathered from this study could permit forjustification in relation to the bio-prospect of the plants used in treating malaria.

5.2*Combretum racemosum*

The outcomes of the antiplasmodial screening of the fractions were earlier reported in Chapter 4(Table 4.6 and 4.7), and according to these results,$CHCl_3$ fraction was selectedand subjected to fractionation, sub-fractionation and purification stepsusing different chromatographic techniquesleading to unequivocally identifying fourursane-type pentacyclic triterpenoids:19α-hydroxyasiatic acid **(1)**, 6β, 23-dihydroxytormentic acid **(3)**,madecassic acid **(5)**,nigaichigoside F1 **(8)**; four oleanane-type pentacyclic triterpenoids: arjungenin **(2)**, combregenin **(4)**, terminolic acid **(6)**, and arjunglucoside I **(9)**and one plant hormone: abscisic acid **(7)**. Mixtures of two isomeric triterpenes were contained in each of the isolates**CR-A**, **CR-C**, **CR-E**, **CR-G**as well as**CR-H**.

5.2.1 Isolation of compounds

Fractionation and isolation of phytochemicals are always preceeded by the development of TLC chromatograms of extracts or fractions of interest. This is an important step to aid the selection of most appropriate solvent system for subsequent column separation. The TLC chromatogram of *C. racemosum* methanol extract in this study has shown the presence of terpenoids (R_f 0.2-0.55) when developed with toluene/ethyl acetate 90:10 (Figure 4.3A1) and when developed with ethyl acetate/methanol/water 40:4.5:4 (R_f 0.5-0.8) (Figure 4.3B1) as mobile phases. This was obvious by the characteristic violet colour of the chromatograms afterspraying of anisaldehyde-sulphuric acid reagent to visualise in the visible. This is in agreement with previous report that anisaldehyde-sulphuric acid spray reagent is suitable derivatisation reagent for optimal colour detection (violet or violet red) of TLC spots due to triterpenes (Wagner and Bladt, 1996).

The non-polar toluene/ethyl acetate 90:10 mobile phase obviously could not move some compounds up from the base line; using ethyl acetate/methanol/water 40:4.5:4 which is a relatively more polar mobile phase became necessary. This system was able to reveal the presence of compounds with prominent yellow and green fluorescent zones which indicated flavonoids by spraying with natural product/polyethylene glycol 400 detection reagent and characterised under UV-365 nm (Figure 4.3 B4). The chromatogram of *C. racemosum* n-butanol fraction showed similar pattern in its TLC synopsis evident by the intense green and yellow fluorescence, thereby revealing flavonoids (Figure 4.6 B). These characteristics support earlier report that flavonoids are characterized on TLC with the presence of green, yellow and/or orange fluorescent zones when sprayed with natural product/polyethylene glycol 400 as detection reagent and view under UV-365 nm (Wagner and Bladt, 1996). However, further investigation on these flavonoids was not included in this report as it became not the focus of this study due to the direction of the bioactivity towards chloroform fraction.

Consequent upon the bioactivity of the fractions tested, the chloroform fraction enriched with triterpenes was selected for further fractionation on silica column flash chromatography, which employs pressure, much more higher thanopen column chromatography, for elution ofthefractions down the column. It gives chance for higher amounts of sample to be used and time of fractionation step reduces significantly (Roge *et al*., 2011). This liquid chromatographic technique using medium-pressure coupled with ELSD and DAD was used in this study to separate the fractions before further purifying on open column chromatography to afford pentacyclic triterpenes.For the selection ofmost suitable mobile phase for flash chromatography on silica gel,TLC is considered as the first-line and most appropriate approach (Wei *et al*., 2013). More reason the TLC of the chloroform fraction was carried out (Figure 4.5), and chloroform/methanol was chosen as suitable starting solvent system in the subsequent flash chromatography.Separation and purification of compounds present in plants by the use of flash column chromatography has been reported by many studies. Using chloroform/methanol as eluent, bioactive principles such as scopoletin and triterpenoids demonstratingantioxidant as well as antimicrobial activities were isolated from *Acmella oleracea* methanol extract (Prachayasittikul *et al*. 2009). Flash chromatography was used to carry out isolation of spilanthol from fractions using hexane/ethyl acetate as mobile phase (Mbeunkui*et al*., 2011).Purifications were also carried out using open-column chromatography

with silica gel.This was achieved by the use of 2 mL/30 minutes (0.1 mL/min) on an automatic fraction collector. This very low flow rate was necessary to avail the compounds the opportunity for extended time of interaction with the stationary phase. This is because the TLC profiles of some of the semi-purified compounds in their respective fractions showed spots that were too close, therefore, increasing their solute-stationary phase percolation time increased their retention time thereby afforded better resolution of the various components. In cases where there were a little more complex mixtures of compounds in the fractions, the length of the column used was inceased to allow more distance travelled by the solutes by the mobile phases; this is believed to be an important factor that may influence increased separation and resolution of compounds in a mixture.

Fractions 12, 13 and 14 became the isolate CR-A (24.76 mg), a white amorphous powder obtained from a gradient elution of increasing polarity order starting from chloroform/methanol/water95:1.5:0.1 and ended at chloroform/methanol/water60:30:2.5 in a total run time of 221 hours. But CR-A was produced from F318 (FCRC14_12) to F325 (FCRC14_14) (Table 4.9, Figure 4.17); and isolation was achieved at the gradient mobile phase $CHCl_3$/MeOH/H_2O 85:8:0.5 between 42-45 hours 30 minutes of this gradient (Table 3.1). The TLC analysis showed it to have single spot (mobile phase chloroform/methanol 80:20; R_f 0.75; see Figure 4.18). The violet colour of the single spot was an indication of triterpene when sprayed with anisaldehyde-sulphuric acid detection reagent (Wagner and Bladt, 1996).

Fractions 10-14 (from FCRC16_3) became the isolate CR-C (44.6 mg), a white amorphous powder obtained from a gradient elution of increasing polarity order starting from $CHCl_3$/MeOH/H_2O 85:8:0.5 and ended at $CHCl_3$/MeOH/H_2O 75:15:1.5 in a total run time of 190 hours. But CR-C was produced from F148 (FCRC16_3_10) to F274 (FCRC16_3_14) (Table 4.11, Figure 4.20); and isolation was achieved at the gradient mobile phase $CHCl_3$/MeOH/H_2O 85:8:0.5 between 74-137 hours of this gradient (Table 3.2). TLC analysis showed it to have single spot (mobile phase ethyl acetate/methanol 80:20; R_f 0.63; see Figure 4.21). The violet colour of the single spot was a confirmation of triterpene when sprayed with anisaldehyde-sulphuric acid detection reagent (Wagner and Bladt, 1996).

CR-E was obtained from FCRC16_3_5 as a white amorphous powder from a preparative TLC. Acetone was used instead of methanol to extract CR-E from its mixture with silica gel that was

scrapped from the TLC plate.This was because using methanol may dissolve some amount of silica as impurity into the isolate. TLC analysis showed it to have single spot (mobile phase chloroform/methanol 80:20; R_f 0.7; see Figure 4.23). The violet colour of the single spot was an indication of triterpene when sprayed with anisaldehyde-sulphuric acid detection reagent (Wagner and Bladt, 1996).

Fractions 9-11 became the isolate CR-G (8.4 mg), a white amorphous powder obtained from a gradient elution of increasing polarity order starting from chloroform/methanol/water 95:1.5:0.1 and ended at chloroform/methanol/water 85:8:0.5 in a total run time of 110 hours. But CR-G was produced from F156 (FCRC7_10) to F186 (FCRC7_11) (Table 4.12, Figure 4.24); and isolation was achieved at the gradient mobile phase $CHCl_3$/MeOH/H_2O 85:8:0.5 between 32-47 hours of this gradient (Table 3.3). The TLC analysis showed it to have single spot (mobile phase chloroform/methanol 80:20; R_f 0.63; see Figure 4.25). The violet-blue colour of the single spot was an indication of triterpene when sprayed with anisaldehyde-sulphuric acid detection reagent (Wagner and Bladt, 1996).

Fractions 4-6 (from FCRC17) became the isolate CR-H (32.9 mg), a pale yellow amorphous powder obtained from a gradient elution of increasing polarity order starting from EtoAc/MeOH/H_2O 97.5:2.5:0 and ended at EtoAc/MeOH/H_2O 65:30:0.2 in anoverall run period of 167 hours 30 minutes. But CR-H was produced from F139 (FCRC17_4) to F156 (FCRC17_6) (Table 4.13, Figure 4.26a); and isolation was achieved at the gradient mobile phase EtoAc/MeOH/H_2O 85:15:0.1 between 15-23 hours 30 minutes of this gradient (Table 3.4). The TLC analysis showed it to have single spot (mobile phase ethyl acetate/methanol 75:25; R_f 0.38; see Figure 4.27). The violet-blue colour of the single spot was an indication of triterpene when anisaldehyde-sulphuric acid spray reagent was used for detection (Wagner and Bladt, 1996).

5.2.2 Structure elucidation of compounds isolated

The NMR with the MS had been useful tools in the elucidation of structures of natural compounds for many decades. The application of these techniques had been useful for identifying of compounds from several classes of secondary metabolites including triterpenoids.

The NMR and MS spectra information generated for all compounds from *C. racemosum* in this study revealed eight pentacyclic triterpenes: four ursane-type and four oleanane-type, as

well as a plant hormone. The similarities in the NMR spectra of the compounds of pentacyclic triterpenes showed that they belong to a class of chemical compounds- pentacyclic triterpenoids. They consist of six isoprene units $(C_5H_8)_6$ formed by the cyclization of the linear squalene molecule. The pentacyclic triterpenes contain five rings: A, B, C, D and E; based on their structural backbone, also are categorised intolupane, ursane and oleananetypes (Figure 5.1). The stereochemistry of these class of compounds shows the general trans-linked formation of A/B, B/C, C/D rings in oleananes as well as ursanes, whereascis-linked form are revealed in D/E rings (Alqahtani*et al*., 2013). The lupanes shows trans-fusedrings in A, B, C, D, E; the ring E is present as a five-membered. The molecules have all their rings saturated with too many methyl (CH_3), methylene (CH_2) and methine (CH) groups with one or more olefinic (C=C) signals present, and this is the reason for the increased degree of hydrophobicity related with these class of compounds.Polyhydroxylation at positions C -2, -3, -6, -7, -11, -15, -16, -19; the unsaturation present at C-12/13; functionalisation of the methyl substituents at positions C -23, -28 or -30 (hydroxymethylene, esters, carboxyl, aldehyde or sugar moieties)and many others, are all the main structural characterisation of these classes.The occurrence of carboxyl moiety in the aglycones orin the glycosides confers acidic properties on several of the pentacyclic triterpenoids. The compounds identified in this study demonstrated a number of these characterisation which supported their identification as triterpenes. The compounds in the pentacyclic triterpenoid group show a lot of similarities in their NMR spectra, but differ by their characteristic signals peculiar to each type under the group. In this study, only ursane and oleanane types were clearly identified. The oleananes possess a geminal-dimethyl groups onposition C-20, while the ursane-types possess methyl substituents atpostions C-19 as well as C-20. The chemical shifts of the C12/C13 double bond for oleananes are always around 122.0 and 144.0, respectively, while those of the ursanes are around 125.0 and 139.0, respectively, for the same carbons (Mahato and Kundu, 1994).

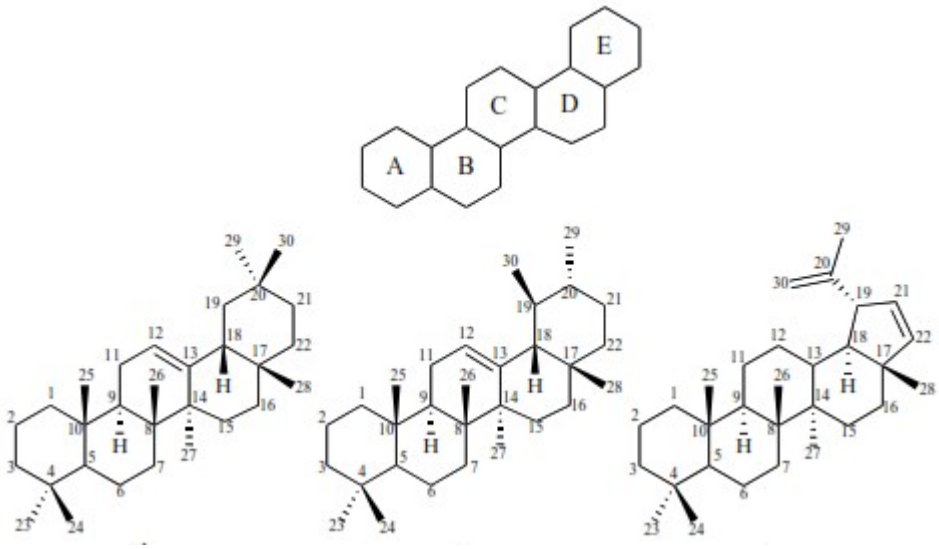

Oleanane Ursane Lupane

Figure 5.1: Skeletal structure of the main pentacyclic triterpenes

Compound CR-A (Figure 4.32), a colourless amorphous powder, was elucidated as isomeric mixture of 19α-hydroxyasiatic acid (**1**) and arjungenin (**2**) by comparingwith literatures(Zebiri *et al*., 2017; Gossan *et al*., 2016) its NMR and MS spectra information.

The HRESI-MS displayed an [M-1] peak at m/z 503.3388, consistent with a molecular formula of $C_{30}H_{48}O_6$ (calculated as $C_{30}H_{47}O_6^-$, with m/z showing 503.3378) (Appendix 1b).Also, $[M+Na]^+$ and $[M+COO]^-$ molecular ions were detected at m/z 527.3337 and m/z 549.3443, respectively. Fragmentation pattern at m/z 485 indicated loss of H_2O from m/z 503 in $[M-H]^-$ molecular ion. From the molecular formula, seven degrees of unsaturation were obviouswith one among them as a result of the occurrence of carbonyl group at C-28, and another one also as a result ofone double bond in ring C and five among them as a result of pentacyclic ring system.

Compounds**1**and **2** showed very similar signal patterns in their ^1H NMR spectra information(Table 4.16; Appendix 2a). Theyexhibited the same doublet signals (each d, J= 11.1 Hz) which integrated for 2H-atoms at δ_{H-23} 3.505 and 3.275,and accounted for the hydrogen atoms of an oxymethylene groupattached to a quartenary sp^3 carbon atom. Another similar signal pattern in the ^1H NMR experiment for **1** and **2** is shown in the triple-doublet signal at δ_{H-2} 3.696 (each d, J= 11.5, 9.6 and 4.6 Hz, integrated for 1H-atom), doublet signal at δ_{H-3} 3.361 (J= 9.6 Hz, integrated for 1H-atom) in compound **1**and triple-doublet signal at δ_{H-2} 3.693 (each d, J= 11.5, 9.6 and 4.6 Hz, integrated for 1H-atom), doublet signal at δ_{H-3} 3.358 (J= 9.6 Hz, integrated for 1H-atom) in compound **2**, which are attributableto a hydrogen attached to an oxygenated sp^3 carbon in a cyclic system for both **1** and **2**. Five tertiary methyl substituents, singlet signals at (δ_H0.704, 1.035, 0.799, 1.352 and 1.197) which were attributable to methyl groups attached to quartenary carbon atoms were shown in the spectrum of **1**, and detection of one doublet signal at δ_H0.932 (J= 6.8) of secondary methyl groupattached to a methine carbon; which indicated ursane-type triterpenes. However, the spectrum of **2** showed the detection of six singlet signals (δ_H0.704, 1.026, 0.770, 1.314, 0.966 and 0.908) of tertiary methyl groups which is attributable to methyl groups attached to quartenary carbon atoms which is indicative of oleanane-type triterpenes. The geminal-dimethyl groups at position-20 in **2** is an indication of oleanane-type triterpenes.

One double bond system displayed in C-ring of both **1** and **2** corresponded to the presence of one olefinic proton signal(δ_{H-12} 5.296 and δ_{H-12} 5.324) respectively and is attributable to a

hydrogen atom attached to a vinyl carbon. This signal is indicative of both oleanane- and ursane-type triterpenes (Gossan *et al*., 2016).

The spectra of^{13}C as welldisplayed similarities in the signal pattern of compounds **1** and **2**(Tables 4.16 and 5.1 and Appendix 2b). They exhibited signals for 30 carbons in the DEPTq experiment: Compound **1**showed one carboxyl at low field (δ_{C-28} 182.31), one double bond (δ_{C-12} 129.23; δ_{C-13} 140.15), one sp^3 oxygenated methylene (δ_{C-23} 66.34), two sp^3oxygenated methine (δ_{C-2} 69.7 and δ_{C-3} 78.26), one sp^3 oxygenated quartenary carbon (δ_{C-19} 73.57), six methyl groups, eight sp^3methylene groups, four sp^3 methine groups and five quartenary carbons, and compound **2**likewise showed one carboxyl at low field (δ_{C-28} 181.36), one double bond (δ_{C-12} 124.7; δ_{C-13} 144.75), one sp^3 oxygenated methylene (δ_{C-23} 66.33), three sp^3oxygenated methine (δ_{C-2} 69.68, δ_{C-3} 78.25 and δ_{C-19} 82.43), six methyl groups, eight sp^3 methylene groups, four sp^3 methine groups and five quartenary carbons. But the actualdissimilarity in the DEPTq analysis showed that**1**had quartenary carbon at position 19 while **2**had a methine carbon at same position, also **1** had a methine carbon at position 20 while **2**possessed a quartenary carbon at this position (Table 4.16, Figure 4.32). Compound **1** and **2**, based on the spectra data in this study, were proposed to belong to the ursane-and oleanane-types triterpene (Mahato and Kundu, 1994). In rings A-D, there were presence of superimposable signals in both **1** and **2** by comparing their ^{1}H and ^{13}C data, but with differences shown only in ring E. Furthermore, **1** and **2**exhibited substantial differencein chemical shifts for^{1}H signals δ_H 2.50 (H-18), δ_H1.35 (H-20) and δ_H 3.06 (H-18), δ_H 3.26 (H-19) respectively, and ^{13}C-NMR signals δ_{C-18} 55.08, δ_{C-19}73.57, δ_{C-20} 43.09 and δ_{C-18} 45.18, δ_{C-19} 82.43, δ_{C-20} 36.03 of **1** and **2**respectively (Table 4.16). This difference was particularly influenced by the different substitution between positions 19 and 20.The HMBC correlations between H-18/C-19, H_2-21/C-19, H_3-30/C-19 and H_3-29/C-19 in compound **1** and **2**, also H-19/C-18, H-19/C-21, H-19/C-29 and H-19/C-30 in only **2**established the location of the α-hydroxyl substituent at position C-19 (Appendix 2d). Moreso between δ_{H-18} (3.057) and δ_{H-19} (3.256),observation of ^{1}H-^{1}H COSY correlationin compound **2**(Appendix 2c) whichadditionallyestablished the occurrence of the hydroxyl moietypositioned at C-19. The α-axial direction of hydroxyl moiety located at C-19 in **2**was inferred by the strong NOESY correlations at the 19-β-H position with 18-β-H and 18-β-H position with 30-β-methyl position,and the small coupling constant at H-19 [δ_H3.256 (1H, dd, J= 3.9, 0.8 Hz)], while the

hydroxyl at C-19 in **1**was deduced to be α-orientation by NOESY correlation at 29-β-methyl position with 18-β-H position and 18-β-H position with 20-β-H position.

The deshielding effect observed in **2**at C-19 (δ_C82.43) relative to **1**(δ_{C-19} 73.57) is believed to be due to the decrease in electron density at C-19 after the methyl substitution has moved to C-20.

The^{13}C-NMR data ofring A-D signals in**1**showed similarities with those of asiatic acid (Masoko *et al*., 2008) but differ in the signals of ring E, likewise, compound **2**with those of arjunolic acid were similar in ring A-D but differ also in the signals of ring E carbon atoms (Masoko *et al*., 2008). This is suggested to be as a result of the occurrence of α-hydroxyl substitution at C-19 in ring E in both **1** and **2**;and the downfield signals of δ_{C-18}55.08, δ_{C-19}73.57 and δ_{C-20}43.09 in **1**compared to asiatic acid, and δ_{C-18}45.18, δ_{C-19}82.43, δ_{C-20}36.03 in **2**compared to arjunolic acid was in agreement with this.

In HMBC spectra data, the correlations between H_2-11 (δ_H2.021) and the two vinylic carbons at C-12 and C-13 suggested a Δ^{12}-unsaturated double bond. The HSQC correlations (Appendix 2e) between H-18/ C-13 and H_2-11/C12 with also the data of^{1}H-^{1}H COSY which revealed that it was only H_2-11 that had direct correlation with the olefinic proton (H-12) further affirmed the double bond to be located at C-12 (Figure 4.32). Also, the location of double bond at C-12 was inferred by HMBC correlations between the carbons C-9, C-11, C-14, C18 and olefinic proton H-12.

In the HMBC experiment, the observation of cross-peaks in the spectra between H_3-24 and signals at C-3 as well as C-23 showed the occurrence of a secondary hydroxyl moiety at C-3 and a C-4 hydroxymethylene. The chemical shift of C-24 confirmed that this primary hydroxyl moietywas located at C-23.Also by comparing the spectra of^{13}C with the ones of asiatic acid as well as arjunolic acid (hydroxyl present at C-23) together with hyptatic acid A (hydroxyl present at C-24) (Mahato and Kundu, 1994), further agreed with the C-23 hydroxyl location.

The correlations in the HMBC between H-2/C-1, H-2/C-3, H-2/C-5, H-2/C-9, H-2/C-10, H-2/C-25 and H_2-1/C-2 with also the data of^{1}H-^{1}H COSY showingcorrelation between H-2 and H-3 all proposed the location of hydroxyl moiety at C-2.

In the HSQC spectrum, H-2/C-3 and H-3/C-2 exhibited correlations; and also the large vicinal couplingin the data of ^{1}H-^{1}H COSY spectrum between H-2 (J= 11.5, 9.6 Hz) and H-3 (J= 9.6 Hz), all together proposed a *quasitrans*-diaxial relationship between them. In the

NOESYspectrum (Appendix 2f), H-3 and H-5 as well as H-9 and H-27 showed correlations which confirmed the β-axial direction of the secondary hydroxyl at postion C-3. The NOESY correlations shown between H-2 and protons at H-24 and H-25 as well as between H-25 and H-26, established the α-orientation of the C-2 hydroxyl moiety.

From a different species of the genus *Combretum* (*Combretum quadrangulare*),Adnyana *et al*. (2001) had previously identified 19α-hydroxyasiatic acid (**1**), also Zebiri *et al*. (2017) reported it to be isolated from species of another genus(*Poraqueiba sericea*), but this study is the first report of it in *Combretum racemosum*.Arjungenin(**2**)was formerly identifiedby Ponou *et al*. (2008) from the stem bark of *Combretum molle*,andit was also identifiedby Gossan *et al*. (2016) from the root of *Combretum racemosum*, however, this is the first time it is identified from *Combretum racemosum* leaves.

Table 5.1: The ^{13}C-NMR of experimental and literature data for compounds 1 and 2 in CD_3OD solvent

Position	1		2	
	^{13}C experimental	^{13}C literature *	^{13}C experimental	^{13}C literature **
1	47.9	47.9	47.72	47.7
2	69.7	69.7	69.68	69.7
3	78.26	78.3	78.25	78.3
4	44.13	44.1	44.14	44.1
5	48.18	48.2	48.33	48.4
6	19.22	19.2	19.25	19.3
7	33.53	33.5	33.33	33.3
8	41.06	41.1	40.73	40.7
9	48.5	48.5	49.1	49.1
10	39.99	39.0	39.17	39.2
11	24.76	24.8	24.89	24.9
12	129.23	129.2	124.7	124.7
13	140.15	140.2	144.75	144.8
14	42.72	42.7	42.71	42.7
15	29.57	29.6	29.43	29.4
16	26.59	26.6	28.58	28.6
17	49	48.9	46.69	46.7
18	55.08	55.1	45.18	45.2
19	73.57	73.6	82.43	82.5
20	43.09	43.1	36.03	36.0
21	27.28	27.3	29.49	29.5
22	39.02	39.0	34.03	34.0
23	66.34	66.4	66.33	66.4
24	13.87	13.9	13.8	13.8
25	17.51	17.5	17.38	17.4
26	17.53	17.6	17.8	17.8
27	24.88	24.9	25.11	25.1

28	182.31	182.3	181.36	182.4
29	27.05	27.1	28.68	28.7
30	16.61	16.6	25.11	25.1

*Zebiri *et al*., 2017

**Gossan *et al*., 2016

Compound CR-C (Figure 4.33), a colourless amorphous powder, was elucidated as isomeric mixture of 6β, 23-dihydroxytormentic acid **(3)** and combregenin (**4**) by comparing with literatures (Dijoux *et al*., 1993; Gossan *et al*., 2016)its NMR and MS spectra information.

The HRESI-MS (Appendix 3b)displayed an [M-1] peak at m/z 519.3329, consistent with a molecular formula of $C_{30}H_{48}O_7$ (calculated as $C_{30}H_{47}O_7^-$, with m/z showing 519.3327). Also, $[M+Na]^+$ and $[M+COO]^-$ molecular ions were detected at m/z 543.3273 and m/z 565.3381 respectively. From the molecular formula, seven degrees of unsaturation were obvious with one among them as a result of the occurrence of carbonyl group at C-28, and another one also as a result of one double bond in ring C and five among them as a result of pentacyclic ring system.

From Table 4.17, ^{1}H information of compound **3**revealed very similar signal pattern to compound **4**(Appendix 4a). ^{1}H-NMR spectra of **3** and **4**revealed similar doublet signals at (δ_{H-23} 3.583, 3.446) and (δ_{H-23} 3.583, 3.452),respectively, (each d, J= 11.1 Hz, which integrated for 2H-atoms), and characterized the hydrogen atoms of a oxymethylene groupattached to a quartenary sp^3 carbon atom. Another similar signal pattern in the ^{1}H NMR experiment for **3** and **4** is shown in the triple-doublet signal at δ_{H-2} 3.742 (each d, J= 11.5, 9.6 and 4.6 Hz, which integrated for 1H-atom), doublet signal at δ_{H-3} 3.300 (J= 9.6 Hz, which integrated for 1H-atom) in compound **3**,and triple-doublet signal at δ_{H-2} 3.740 (each d, J= 11.5, 9.6 and 4.6 Hz, which integrated for 1H-atom), doublet signal at δ_{H-3} 3.297 (J= 9.6 Hz, which integrated for 1H-atom) in compound **4**, which are attributable to a hydrogen attached to an oxygenated sp^3 carbon in a cyclic system for both **3** and **4**.Five tertiary methyl substituents, singlet signals at (δ_H1.068, 1.386, 1.084, 1.328 and 1.206) which were attributable to methyl groups attached to quartenary carbon atoms were shown in the spectrum of **3**, and the detection of one doublet signal at δ_H0.933 (J= 6.7 Hz) of a secondary methyl substituentattributable to a methylattached to a methine carbon; which indicated ursane-type triterpenes. However, the spectrum of **4** showed the detection of six singlet signals at (δ_H1.068, 1.377, 1.070, 1.288, 0.940 and 0.973) of tertiary methyl groups which were attributable to methyl groups attached to quartenary carbon atoms which is indicative of oleanane-type triterpenes. The geminal-dimethyl groups at position-20 in **4** is an indication of oleanane-type triterpenes.

The presence of one olefinic proton (δ_{H-12} 5.332) and (δ_{H-12} 5.362) in both **3** and **4**, respectively corresponded to the occurrence of one double bond system in ring Cwhich was attributable to

a hydrogen atom attached to a vinyl carbon. This signal is indicative of both oleanane- and ursane-type triterpenes (Gossan *et al*., 2016).

The spectra of ^{13}C(Appendix 4b) as wellindicated similarities in the signal pattern of compounds **3** and **4**(Tables 4.17 and 5.2). They exhibited signals for 30 carbons in the DEPTq experiment: Compound **3** showed one carboxyl at low field (δ_{C-28} 182.32), one double bond (δ_{C-12} 129.54; δ_{C-13} 139.46), one sp^3 oxygenated methylene carbon (δ_{C-23} 65.93) attributed to carbon attached to a primary hydroxyl group, three sp^3oxygenated methine carbon (δ_{C-2} 69.71,δ_{C-3} 78.24 and δ_{C-6} 68.69) attributed to carbons attached to secondary hydroxyl groups, one sp^3 oxygenated quartenary carbon (δ_{C-19} 73.61) attributed to a carbon attached to tertiary hydroxyl group, six methyl, seven sp^3 methylene, four sp^3 methine and five quartenary carbons, and compound **4**likewise showed one carboxyl at low field (δ_{C-28} 182.36), one double bond (δ_{C-12} 124.95; δ_{C-13} 144.07), one sp^3 oxygenated methylene carbon (δ_{C-23} 65.93) attributed to a carbon attached to a primary hydroxyl group, four sp^3oxygenated methine carbon (δ_{C-2} 69.68, δ_{C-3} 78.25, δ_{C-6} 68.75 and δ_{C-19} 82.43), six methyl, seven sp^3 methylene, four sp^3 methine and five quartenary carbons. But with the actual dissimilarity in the DEPTq analysis showing that **3** had quartenary carbon at position 19 while **4** had a methine carbon at same position, also **3** had a methine carbon at position 20 while **4** possessed a quartenary carbon at this position(Table 4.1; Figure 4.33). These spectra data in this study suggested that compound **3** was an ursane-type triterpenoid and compound **4** was an oleanane-type triterpenoid (Mahato and Kundu, 1994).In rings A-D, there were presence of superimposable signals in both **3** and **4** by comparing their ^{1}H and ^{13}C data, but with differences shown only in ring E. Additionally, **3** and **4**indicated considerable difference in chemical shifts for^{1}H[δ_H 2.525 (H-18), δ_H1.358 (H-20)] and [δ_H 3.079 (H-18), δ_H 3.271 (H-19)] respectively, and ^{13}C-NMR signals[δ_{C-18} 55.15, δ_{C-19}73.61, δ_{C-20} 43.11] and [δ_{C-18} 45.21, δ_{C-19} 82.47, δ_{C-20} 36.05] of **3** and **4**respectively (Table 4.17). This difference was particularly influenced by the different substitution between positions 19 and 20.The HMBC correlations (Appendix 4d) between H-18/C-19, H_2-21/C-19, H_3-30/C-19 and H_3-29/C-19 in compound **3** and **4**, also H-19/C-18, H-19/C-21, H-19/C-29 and H-19/C-30 in only **4** established the location of α-hydroxyl group at position C-19. Moreso, the observed correlation in the^{1}H-^{1}H COSYspectrum (Appendix 4c) between δ_{H-18} (3.079) and δ_{H-19} (3.271) in compound **4**additionallyestablished the occurrence of hydroxyl moietypositioned at C-19. The α-axial direction of hydroxyl moiety located at C-19 in **4** was

inferred by the strong NOESY correlations at the 19-β-H position with 18-β-H and 18-β-H position with 30-β-methyl position, and the small coupling constant at H-19 [δ_H3.271 (1H, dd, J= 3.9, 0.8 Hz)], while the hydroxyl at C-19 in **3**was deduced to be α-orientation by NOESY correlation at 29-β-methyl position with 18-β-H position and 18-β-H position with 20-β-H position.

The deshielding effect observed in **4**at C-19 (δ_C82.47) relative to **3**($\delta_{C\text{-}19}$ 73.61) is believed to be due to the decrease in electron density at C-19 after the methyl substitution has moved to C-20.

In HMBC spectra data, the correlations between H_2-11 for **3**(δ_H2.070),H_2-11 for **4** (δ_H2.090) and the two vinylic carbons at C-12 and C-13 suggested a Δ^{12}-unsaturated double bond in both **3** and **4**. The HSQC correlations between H-18/ C-13 and H_2-11/C12with also the data of ^{1}H-^{1}H COSY showing that it was only H_2-11 that had direct correlation with the olefinic proton (H-12) further established the double bond is C-12 positioned (Figure 4.33). Also, the location of double bond at position C-12 was inferred by HMBC correlations between the carbons C-9, C-11, C-14, C-18, C-27 and olefinic proton H-12. The observation of the cross-peaks in the spectra of the HMBC experiment, between H_3-24 and signals at C-3 as well as C-23 showed the occurrence of a secondary hydroxyl moiety at C-3 also a hydroxymethylene at C-4. The chemical shift of C-24 confirmed that this primary hydroxyl moiety was located at C-23.

The HMBC correlations between H-2/C-1, H-2/C-3, H-2/C-5, H-2/C-9, H-2/C-10, H-2/C-25 and H_2-1/C-2 with the observed correlations in the ^{1}H-^{1}H COSY spectrum between H-1 and H-2; taken all togetherproposed a hydroxyl moiety was positioned at C-2.

In the HSQC spectrum (Appendix 4e), H-2/C-3 and H-3/C-2 exhibited correlations; and also the large vicinal coupling in the data of ^{1}H-^{1}H COSY spectrum between H-2 (J= 11.5, 9.6 Hz) and H-3 (J= 9.6 Hz), all together proposed a *quasitrans*-diaxial relationship between them. In the NOESY spectrum, H-3 and H-5 as well as H-9 and H-27 showed correlations which confirmed the β-axial orientation of the secondary hydroxyl at C-3. The NOESY correlations shown between H-2 and protons at H-24 and H-25, between H-25 and H-26, confirmed the α-orientation of the hydroxyl at C-2.

Compounds**3** and **4**showedthat their signal patterns have respective similarities with the ones of **1** and **2** in^{1}H and ^{13}C analyses (Tables 4.17 and 4.16). The ^{13}C-NMR information of compound **3**compared with 19α-hydroxyasiatic acid also isolated in this study as compound

1,showed similarities in rings A and C-E signals but differ in some signals of ring B, likewise, compound **4**with those of arjungeninwhich was also isolated in this study as compound **2** were similar in rings A and C-E but differ also in some signals of ring B carbon atoms. This is suggested to be as a result of α-hydroxyl substitution present at C-6 in ring B in both **3** and **4**. The occurrence of hydroxyl moiety in this location in **3** and **4** is responsible for substantial increase in the chemical shifts for the protons at C-6 from $\delta_{H\text{-}6}$ 1.469 (**1**) and 1.414 (m, m) (**2**) to $\delta_{H\text{-}6}$ 4.39 (m) (**3** and **4**).The resonances at C-6 postion in ^{13}C moved from $\delta_{C\text{-}6}$ 19.22 (**1**)and $\delta_{C\text{-}6}$ 19.25 (**2**) to $\delta_{C\text{-}6}$ 68.69 (**3**) and $\delta_{C\text{-}6}$ 68.75 (**4**). Also, based on the DEPTq analyses, a methylene carbon was indicated for **1** and **2**at C-6 position (Table 4.16) while methine carbon occurred at same location for **3** and **4** (Table 4.17).

The HMBC cross peaks showing the correlations between H-6/C-4, H-6/C-5, H-6/C-7, H-6/C-8, H-6/C-10, and H_2-7/C-6 with the observed correlation in the ^{1}H-^{1}H COSY spectrum between H-7 and H-6 all proposedthe location of a hydroxyl moiety was at C-6. The HSQC spectra data showed correlations H-6/C-7 as well as H-7/C-6; also the large vicinal coupling constant at H-7 [δ_H1.501 (J= 14.5)]additionally inferred the presence of hydroxyl moiety at C-6 postion in both **3** and **4**.

In the NOESY spectrum, H-6 and H-5 as well as H-9 and H-27 showed correlations which confirmed the β-axial orientation of the secondary hydroxyl at C-6.

Compound **3** identified as 6β, 23-dihydroxytormentic acid was formerly isolated from leaves of *Aphloia madagascariensis* (Dijoux *et al*., 1993). Compound **4**identified as combregenin was earlier isolated from stem bark of *Combretum molle* (Ponou *et al*., 2008), and also Gossan *et al*. (2016) identified it from the root of *Combretum racemosum*.

The genus *Combretum* as well as the Combretaceae family has generated several pentacyclic triterpenes, but this study represent the first time, to the best of my knowledge,6β, 23-dihydroxytormentic acid**(3)** is reported to have been identified from the genus or the family. Its isomer, combregenin**(4)**, though has already been isolated from the root of *Combretum racemosum*, but this is the first time it is identified from the leaves of *Combretum racemosum*.

Table 5.2: The ^{13}C-NMR experimental and literature data for compounds 3 and 4 in CD_3OD solvent

Position	3		4	
	^{13}C experimental	^{13}C literature *	^{13}C experimental	^{13}C literature **
1	50.09	50.4	49.86	49.9
2	69.71	69.7	69.69	69.7
3	78.24	78.3	78.26	78.3
4	44.81	44.8	44.83	44.8
5	48.95	49.4	49.28	49.3
6	68.69	68.7	68.75	68.7
7	41.4	40.4	41.27	41.3
8	40.29	41.4	40.0	40.0
9	48.93	48.9	49.56	49.5
10	38.53	38.6	38.73	38.7
11	24.72	24.7	24.81	24.8
12	129.54	129.5	124.95	125.0
13	139.46	139.5	144.07	144.0
14	43.16	43.2	43.18	43.2
15	29.54	29.6	29.39	29.4
16	26.62	26.7	28.62	28.6
17	49.07	49.5	46.74	46.7
18	55.15	55.1	45.21	45.2
19	73.61	73.6	82.47	82.5
20	43.11	43.1	36.05	36.0
21	27.3	27.3	29.58	29.6
22	39.03	39.0	34.06	34.0
23	65.93	66.0	65.93	66.0
24	15.23	15.2	15.16	15.2
25	19.01	19.0	18.82	18.4
26	18.49	18.5	18.45	18.2
27	24.88	24.9	25.07	25.1

28	182.32	182.5	182.36	182.3
29	27.06	27.1	28.66	28.7
30	16.6	16.6	25.2	25.2

*Dijoux *et al*., 1993

**Ponou *et al*., 2008; Gossan *et al*., 2016

Compound CR-E (Figure 4.34), a colourless amorphous powder, was elucidated as isomeric mixture of madecassic acid (**5**) and terminolic acid **(6)** by comparing with literatures(Van Loc *et al*., 2018; Gossan *et al*., 2016) its NMR and MS spectra data information.

The HRESI-MS (Appendix 5b) displayed [M-1] peak at m/z 503.3384, consistent with a molecular formula of $C_{30}H_{48}O_6$ (calculated as $C_{30}H_{47}O_6^-$, with m/z showing 503.3378). Also, $[M+Na]^+$ as well as $[M+COO]^-$ molecular ions were detected at m/z 527.33 and m/z 549.3439 respectively. From the molecular formula, seven degrees of unsaturation were obvious with one among them as a result of the occurrence of carbonyl group at C-28, and another one also as a result of one double bond in ring C and five among them as a result of pentacyclic ring system.

From Table 4.18,^{1}H NMR spectra information (Appendix 6a) of compound **5**and **6**displayed very similar signal patterns. ^{1}H-NMR spectra of **5** and **6**showed the same doublet signals(each d, J= 11.1 Hz) which integrated for 2H-atoms at δ_{H-23} 3.582 and 3.436,and were accounted for the hydrogen atoms of a oxymethylene groupattached to a quartenary sp^3 carbon atom. Another similar signal pattern in the ^{1}H NMR experiment for **5** and **6**; is shown in the triple-doublet signal at δ_{H-2} 3.737 (each d, J= 11.4, 9.7and 4.6 Hz, integrated for 1H-atom), doublet signal at δ_{H-3} 3.294 (J= 9.7 Hz, integrated for 1H-atom) in compound **5**,and triple-doublet signal at δ_{H-2} 3.730 (each d, J= 11.4, 9.6 and 4.6 Hz, integrated for 1H-atom), doublet signal at δ_{H-3} 3.289 (J= 9.6 Hz, integrated for 1H-atom) in compound **6**, which aretypical of a hydrogen attached to an oxygenated sp^3 carbon in a cyclic system for both **5** and **6**.Four tertiary methyl groups, singlet signals at (δ_H1.061, 1.396, 1.113 and 1.103) which were attributable to methyl groups attached to quartenary carbon atoms were shown in the spectrum of **5**, and the detection of two signals [δ_H0.898 (d, J= 6.7) and δ_H0.966, m] of secondary methyl substituentsascribedto methyl groups attached to methine carbons; which indicated ursane-type triterpenes. However, the spectrum of **6** showed the detection of six singlet signals of tertiary methyl substituents at (δ_H1.060, 1.384, 1.094, 1.147, 0.912 and 0.950) which areascribed to methyl groups attached to quartenary carbon atoms which is indicative of oleanane-type triterpenes. The geminal-dimethyl groups at position-20 in **6** is an indication of oleanane-type triterpenes.

The presence of one olefinic proton (δ_{H-12} 5.279) and (δ_{H-12} 5.295) in both **5** and **6** respectively corresponded to the occurrence of one double bond system in ring C which accounted for a

hydrogen atom attached to a vinyl carbon. This signal is indicative of both oleanane- and ursane-type triterpenes (Gossan *et al*., 2016).

The ^{13}C-NMR spectra (Appendix 6b) also showed similarities in the signal pattern of compounds **5** and **6**(Tables 4.18 and 5.3). They exhibited signals for 30 carbons in the DEPTq experiment: Compound **5** showed one carboxyl at low field (δ_{C-28} 181.69), one double bond (δ_{C-12} 127.01; δ_{C-13} 139.13), one sp^3 oxygenated methylene carbon (δ_{C-23} 65.86) attributed to carbon attached to a primary hydroxyl group, three sp^3oxygenated methine carbon (δ_{C-2} 69.71, δ_{C-3} 78.15 and δ_{C-6} 68.43) attributed to carbons attached to secondary hydroxyl groups, six methyl, seven sp^3 methylene, five sp^3 methine and five quartenary carbons, and compound **6**likewise showed one carboxyl at low field (δ_{C-28} 181.92), one double bond (δ_{C-12} 123.72; δ_{C-13} 144.70), one sp^3 oxygenated methylene carbon (δ_{C-23} 65.86) attributed to a carbon attached to a primary hydroxyl group, three sp^3oxygenated methine carbon (δ_{C-2} 69.68, δ_{C-3} 78.15 andδ_{C-6} 68.48), six methyl, eight sp^3 methylene, three sp^3 methine and six quartenary carbons. But the actual dissimilarity in the DEPTq analysis showed that **5**had methine group at position 19 while **6** had a methylene group at same position, also **5** had a methine carbon at position 20 while **6** possessed a quartenary carbon at this position(Table 4.18 and Figure 4.34). These spectra data in this study suggested that compound **5** was an ursane-type triterpenoid and compound **6** was an oleanane-type triterpenoid (Mahato and Kundu, 1994). In rings A-D, there were presence of superimposable signals in both **5** and **6** by comparing their ^{1}H and ^{13}C data, but with differences shown only in ring E. Additionally, **5** and **6** showed slightly different chemical shifts in both ^{1}H-NMR spectra [δ_{H-18} 2.225 (d, J= 11.2 Hz),δ_{H-19}1.389, δ_{H-20}0.990] and [δ_H 2.876 (dd, J= 13.8, 3.9 Hz) (H-18), δ_H 1.710, 1.145(H-19)] respectively, and ^{13}C-NMR spectra [δ_{C-18} 54.47, δ_{C-19}40.43, δ_{C-20} 40.44] and [δ_{C-18} 42.82, δ_{C-19} 47.25, δ_{C-20} 31.61] of **5** and **6**respectively (Table 4.18). This difference was particularly influenced by the methyl substitution between positions 19 and 20.

The deshielding effect observed in **6**at C-19 (δ_C47.25) relative to **5**(δ_{C-19} 40.43) is believed to be due to the decrease in electron density at C-19 after the methyl substitution has moved to C-20.

In HMBC spectra data, the correlations between H_2-11 for **5** (δ_H2.016), H_2-11 for **6** (δ_H2.070) and the two vinylic carbons at C-12 and C-13 suggested a Δ^{12}-unsaturated double bond in both **5** and **6**. The HSQC correlations between H-18/ C-13 and H_2-11/C12 along with the data of^{1}H-

^{1}H COSY spectrum which showed that it was only H_2-11 that had direct correlation with the olefinic proton (H-12) further established the double bond is positioned at C-12 (Figure 4.34). Also, the correlations in the HMBC data between the carbons C-9, C-11, C-14, C18, C-27 and olefinic proton H-12 inferred C-12 as the location of the double bond.

In the HMBC experiment (Appendix 6d), the cross-peaks observed in the spectra between H_3-24 and signals at C-3 and C-23 showed the occurrence of a secondary hydroxyl moiety at C-3 and a hydroxymethylene at C-4. The chemical shift of C-24 confirmed that this primary hydroxyl moiety was located at C-23. The HMBC correlations between H-2/C-1, H-2/C-3, H-2/C-5, H-2/C-9, H-2/C-10, H-2/C-25 as well as H_2-1/C-2 together with the observed correlation in the data of ^{1}H-^{1}H COSY spectrum between H-1 and H-2; and the large vicinal coupling constant at H-1 [δ_H1.917 (J= 12.5)] and [δ_H1.917 (J= 12.4)] respectively for **5** and **6**, taken all together proposed a hydroxyl moiety was positioned at C-2.

The correlations of H-2/C-3 and H-3/C-2displayed in the HSQC spectrum proposed a *quasitrans*-diaxial relationship between them. In the NOESY spectrum, H-3 and H-5 as well as H-9 and H-27 showed correlations which confirmed the β-axial orientation of the secondary hydroxyl at C-3. The NOESY correlations shown between H-2 and protons at H-24 and H-25, as well as H-25 and H-26, established the α-orientation of the hydroxyl at C-2.

Compounds**5** and **6**showed signal patterns with respective similarities to the ones of **3** and **4** in^{1}H as well as^{13}C analyses (Tables 4.18 and 4.17). The ^{13}C-NMR information of compound **5**compared with6β, 23-dihydroxytormentic acid also isolated in this study as compound **3**, showed similarities in rings A-D signals butdiffer in some signals of ring E, likewise, compound **6**with those of combregenin which was also isolated in this study as compound **4** were similar in rings A-D but differ also in some signals of ring E carbon atoms. This is suggested to be as a result of the occurrence of α-hydroxyl substitution at C-19 in ring E in both **3** and **4**. The occurrence of hydroxyl moiety at this position in **3**as well as**4** led to substantialchemical shift increase for the C-19position from $\delta_{H\text{-}19}$ 1.389 (m), $\delta_{C\text{-}19}$ 40.43 and $\delta_{H\text{-}19}$ 1.71, 1.145 (m, m), $\delta_{C\text{-}19}$47.25 respectively for **5** and **6** to $\delta_{C\text{-}19}$ 73.61 and $\delta_{H\text{-}19}$ 3.271, (dd, J=3.9, 0.9 Hz); $\delta_{C\text{-}19}$ 82.47 respectively for **3** and **4**. Furthermore, based on the DEPTq analyses, **3** and **4** showed the occurrence of quartenary carbonand methine carbon respectively at C-19 position(Table 4.17, Figure 4.33) whereas**5** and **6** inthis same locationdisplayed the occurrence of methine carbon and methylene group respectively (Table 4.18, Figure 4.34).

The HMBC cross peaks showing the correlations of H-6/C-4, H-6/C-5, H-6/C-7, H-6/C-8, H-6/C-10, and H_2-7/C-6 with the observed correlation in the data of ^{1}H-^{1}H COSY spectrum between H-7 and H-6 all proposedthe location of a hydroxyl moiety wasC-6. HSQC spectra data showed correlations H-6/C-7 as well as H-7/C-6; also large vicinal coupling constant at H-7 ([δ_H1.799 (J= 14.5)] and [δ_H1.772 (J= 14.5)])establishedfurther the presence of hydroxyl moiety at C-6 postion in both **3** and **4**respectively.

In the NOESY spectrum, H-6 and H-5 as well as H-9 and H-27 showed correlations which confirmed the β-axial orientation of the secondary hydroxyl at C-6.

Compound **5** identified as madecassic acid was formerly isolated from*Centella asiatica* (Van Loc *et al*., 2018).From*Combretum zeyheri* leaves, compound **6** identified as terminolic acidwas earlier isolated (Runyoro *et al*., 2013), and was more recently identified from *Combretum racemosum*root (Gossan *et al*., 2016).

This is the first report, to the best of my knowledge,of madecassic acid**(5)** to have been identified from the genus *Combretum* and the Combretaceae family and its isomer, terminolic acid**(6)**, though has already been isolated from the root of *Combretum racemosum*, but this is the first time it is identified from the leaves of *Combretum racemosum*.

Table 5.3: The ^{13}C-NMR showing experimental and literature data for compounds 5 and 6 in CD_3OD solvent

Position	5		6	
	^{13}C experimental	^{13}C literature *	^{13}C experimental	^{13}C literature **
1	50.28	50.08	50.11	50.1
2	69.71	69.68	69.68	69.7
3	78.15	78.14	78.15	78.2
4	44.79	44.77	44.81	44.8
5	48.83		48.83	48.8
6	68.43	68.45	68.48	68.5
7	41.32	41.29	41.12	41.1
8	39.99	39.96	39.81	39.8
9	49.24		49.33	49.3
10	38.52	38.97	38.59	38.6
11	24.47	24.45	24.58	24.6
12	127.01	127.0	123.72	123.7
13	139.13	139.08	144.7	144.7
14	43.85	43.82	43.5	43.5
15	29.17	29.15	28.8	28.8
16	25.35	25.33	24.08	24.6
17	47.24		?	48.5
18	54.47	54.42	42.82	42.8
19	40.43	40.40	47.25	47.3
20	40.44	40.40	31.61	31.6
21	31.81	31.79	34.93	34.9
22	38.16	38.13	33.88	33.9
23	65.86	65.86	65.86	65.9
24	15.26	15.26	15.21	15.2
25	19.18	19.19	19.03	18.9
26	19.11	19.09	18.81	19.1
27	24.18	24.20	26.47	26.5

28	181.69	182.64	181.92	181.9
29	17.63	17.65	33.56	33.6
30	21.56	21.59	23.97	24.0

*Van Loc *et al*., 2018

**Gossan *et al*., 2016; Runyoro *et al*., 2013

Compound CR-G (Figure 4.35), a colourless powder, was elucidated as absisic acid by comparing with literature its NMR and MS spectra information (Ma*et al*., 2016).
The HRESI-MS (Appendix 7b) displayed a [M-1] peak at m/z 263.1288 relating to a molecular formula of $C_{15}H_{20}O_4$.From the molecular formula, six degrees of unsaturation were obvious with one among them as a result of the occurrence of lone ring, and another one also as a result of double bond in ring, two due to carbonyl group at C-1 and C-4', and two among them as a result of double bonds in the aliphatic chain.

By means of DEPTq experiment, there were shown the presence of four methyl (CH_3), one methylene (CH_2), four methine (CH) and six quartenary carbon atoms (C). Its ^{1}H-NMR spectrum showed the occurrence of signals due to four tertiary methyl substituents δ_{H-6} 2.022, $\delta_{H-7'}$ 1.934, $\delta_{H-8'}$ 1.064, $\delta_{H-9'}$ 1.029; a methylene group $\delta_{H-5'}$ 2.537, (d, J=15.8 Hz, br) and $\delta_{H-5'}$ 2.182, (d, J=15.8 Hz, br); two trans-double bond protons δ_{H-4} 7.748, (d, J=16.1 Hz) and δ_{H-5} 6.206, (dd, J=16.1, 0.4 Hz); and two olefinic protons δ_{H-2} 5.759, (s, br) and $\delta_{H-3'}$ 5.919, (m). Likewise in the data of^{13}C-NMR spectrum, the resonance due to the occurrence of an α, β-unsaturation ketone carbon $\delta_{C-4'}$ 201.05 and a carboxylic carbon δ_{C-1} 170.29 were observed. In addition, six olefinic carbons attributedto three double bonds (δ_{C-2} 120.75, δ_{C-3} 149.68, δ_{C-4} 129.58, δ_{C-5} 137.33, $\delta_{C-2'}$ 166.69 and $\delta_{C-3'}$ 127.52) were present, including one oxygenated quartenary carbon $\delta_{C-1'}$ 80.60 shown (Table 4.19). NMR information of compound **7** correlated with the ones reported in literature for abscisic acid (Table 5.4) which was previously identified and reported from *Phomopsis amygdali* (Ma *et al*., 2016).

Although the NMR spectrum of CR-G (Appendice 8a to 8h) showed mixture of other signals suggested to be due to triterpenoid isomers, but complete assignment of these signals were not possible (Appendix 9) as a result of signals were very broad, no carbon signals in the direct ^{13}C NMR, very broad cross peaks in the HSQC and HMBC spectra. Nevertheless, the signals due to abscisic acid were unambiguously identified and assigned completely.

Table 5.4: The ^{13}C NMR of experimental and literature data for compound 7 in $CDCl_3$ solvent

Position	Compound 7	
	^{13}C experimental	^{13}C literature *
1	170.29	167.2
2	120.75	118.6
3	149.68	151.1
4	129.58	128.6
5	137.33	138.4
6	21.15	19.2
1‘	80.6	80.0
2‘	166.69	163.2
3‘	127.52	127.3
4‘	201.05	197.4
5‘	50.68	50.3
6‘	42.85	42.2
7‘	19.62	21.2
8‘	23.55	23.5
9‘	24.66	24.7

*Ma *et al*., 2016

Compound CR-H (Figure 4.36), a pale yellow powder, was elucidated as isomeric mixture of nigaichigoside F1 (**8**) and arjunglucoside I (**9**) by comparing with literatures(Wu *et al*., 2007; Gossan *et al*., 2016) its NMR and MS spectra information.

The HRESI-MS (Appendix 10b) displayed a [M-1] peak at m/z 665.3929, consistent with a molecular formula of $C_{36}H_{58}O_{11}$ (calculated as $C_{36}H_{57}O_{11}^{-}$, with m/z showing 665.3906). Also, $[M+Na]^{+}$ as well as $[M+COO]^{-}$ molecular ions were detected at m/z 689.38 and m/z 711.3983 respectively. From the molecular formula, seven degrees of unsaturation were obvious with one among them as a result of the occurrence of carbonyl group at C-28, and another one also as a result of one double bond in ring C and five among them as a result of pentacyclic ring system. The ^{1}H-NMR spectra (Appendix 11a) information of compound **8**exhibited very similar signal patterns to compound **9** (Table 4.20). ^{1}H NMR spectra of **8** and**9**showed the same doublet signal (each d, J= 11.1 Hz) which integrated for 2H-atoms at δ_{H-23} 3.504 and 3.269 and were attributable to hydrogen atoms of a oxymethylene groupattached to a quartenary sp^3 carbon atom. Another similar signal pattern in the ^{1}H NMR experiment for **8** and **9** is shown in the triple-doublet signal at δ_{H-2} 3.699 (each d, J= 11.5, 9.6 and 4.6 Hz, which integrated for 1H-atom), doublet signal at δ_{H-3} 3.358 (J= 9.6 Hz, which integrated for 1H-atom) in compound **8**,and triple-doublet signal at δ_{H-2} 3.695 (each d, J= 11.6, 9.6 and 4.6 Hz, which integrated for 1H-atom), doublet signal at δ_{H-3} 3.358 (J= 9.6 Hz, which integrated for 1H-atom) in compound **9**, and aretypical of a hydrogen attached to an oxygenated sp^3 carbon in a cyclic system for both **8** and **9**. Five tertiary methyl substituents, singlet signals at (δ_H0.703, 1.038, 0.781, 1.344 and 1.205) which were attributable to methyl groups attached to quartenary carbon atoms were shown in the spectrum of **8**,and detection of one doublet signalat δ_H0.932 (J= 6.7) of secondary methyl group accountablefor a methyl substituentattached to a methine carbon; which indicated ursane-type triterpenes. However, the spectrum of **9** showed the detection of six singlet signals at (δ_H0.703, 1.028, 0.751, 1.304, 0.940 and 0.951) of tertiary methyl substituentswhich were attributable to methyl substituentsattached to quartenary carbon atoms which is indicative of oleanane-type triterpenes. The geminal-dimethyl groups at position-20 in **9** is an indication of oleanane-type triterpenes.

The presence of one olefinic proton (δ_{H-12} 5.312) and (δ_{H-12} 5.336) in both **8** and **9** respectively corresponded to the occurrence of one double bond system in ring C, also were typical of a

hydrogen atom attached to a vinyl carbon. This signal is indicative of both oleanane- and ursane-type triterpenes (Gossan *et al*., 2016).

The spectra of ^{13}C(Appendix 11b) as welldisplayed similarities in the signal pattern of compounds **8** and **9**(Tables 4.20 and 5.5). They exhibited signals for 36 carbons in the DEPTq experiment: Compound **8** showed one carboxyl at low field (δ_{C-28} 178.54), one double bond (δ_{C-12} 129.49; δ_{C-13} 139.75), one sp^3 oxygenated methylene (δ_{C-23} 66.41), two sp^3oxygenated methine carbon (δ_{C-2} 69.71 and δ_{C-3} 78.30), one sp^3 oxygenated quartenary carbon (δ_{C-19} 73.63), six methyl, eight sp^3 methylene, four sp^3 methine, five quartenary carbons, one glycosidic methylene carbon and five glycosidic methine carbons, and compound **9**likewise showed one carboxyl at low field (δ_{C-28} 178.58), one double bond (δ_{C-12} 124.78; δ_{C-13} 144.48), one sp^3 oxygenated methylene (δ_{C-23} 66.39), three sp^3oxygenated methine carbon (δ_{C-2} 69.69, δ_{C-3} 78.30 and δ_{C-19} 82.43), six methyl, eight sp^3 methylene, four sp^3 methine, five quartenary carbons, one glycosidic methylene carbon and five glycosidic methine carbons. But the actual dissimilarity in the DEPTq analysis showed that **8** had quartenary carbon at position 19 while **9** had a methine carbon at same position, also **8** had a methine carbon at position 20 while **9** possessed a quartenary carbon at this position(Table 4.20; Figure 4.36). These spectra data in this study suggested that compound **8** was an ursane-type triterpenoid and compound **9** was an oleanane-type triterpenoid (Mahato and Kundu, 1994). In rings A-D, there were presence of superimposable signals in both **8** and **9** by comparing their ^{1}H and ^{13}C data, but with differences shown only in ring E. Additionally, **8** and **9**exhibited substantial difference in chemical shifts for^{1}Hsignals δ_H 2.518 (H-18), δ_H1.351 (H-20) and δ_H 3.054 (H-18), δ_H 3.272 (H-19) respectively, then^{13}C-NMR signals δ_{C-18} 54.96, δ_{C-19}73.63, δ_{C-20} 42.94 and δ_{C-18} 45.07, δ_{C-19} 82.43, δ_{C-20} 35.95 of **8** and **9**respectively (Table 4.20). This difference was particularly influenced by the different substitution between positions 19 and 20.The HMBC (Appendix 11d) correlations between H-18/C-19, H_2-21/C-19, H_3-30/C-19 and H_3-29/C-19 in compound **8** and **9**, also H-19/C-18, H-19/C-21, H-19/C-29 and H-19/C-30 in only **9** confirmed the location of α-hydroxyl group at C-19. Moreso, the observed correlation of the data of ^{1}H-^{1}H COSY spectrum between δ_{H-18} (3.054) and δ_{H-19} (3.272) in compound **9**additionallyestablished the occurrence of hydroxyl moietypositioned at C-19. The α-axial direction of hydroxyl moiety located at C-19 in**9** was inferred by the strong NOESY correlations at the 19-β-H position with 18-β-H and 18-β-H position with 30-β-methyl position, while the hydroxyl at C-

19, while the hydroxyl at C-19 in**8**was deduced to be α-orientation by NOESY correlation at 29-β-methyl position with 18-β-H position and 18-β-H position with 20-β-H position.

The^{13}C-NMR information of**8**with asiatic acid (Masoko *et al*., 2008) showed similarities in ring A-D signals but differ in the signals of ring E, likewise, compound **9**with those of arjunolic acid were similar in ring A-D but differ also in the signals of ring E carbon atoms (Masoko *et al*., 2008). This is suggested to be as a result of the occurrence of α-hydroxyl substitution at C-19 in ring E in both **8** and **9**.The downfield signals of $\delta_{C\text{-}18}$ 54.96, $\delta_{C\text{-}19}$ 73.63 and $\delta_{C\text{-}20}$ 42.94 in **8**compared to asiatic acid, and $\delta_{C\text{-}18}$ 45.07, $\delta_{C\text{-}19}$ 82.43, $\delta_{C\text{-}20}$ 35.95 in **9**compared to arjunolic acid was in agreement with this.

In HMBC spectra data, the correlations between H_2-11 (δ_H2.022) and the two vinylic carbons at C-12 and C-13 suggested a Δ^{12}-unsaturated double bond. The HSQC correlations between H-18/ C-13 and H_2-11/C12along with the ^{1}H-^{1}H COSY data which showed that it was only H_2-11 that had direct correlation with the olefinic proton (H-12) further inferred double bond is situated at C-12 (Figure 4.36). Also, the correlations observed in the HMBC spectrum between carbons C-9, C-11, C-14, C18 and the olefinic proton H-12 inferred the location of the double bond at C-12.

In the HMBC experiment, the cross-peaks observed in the spectra between H_3-24 and signals at C-3 and C-23 showed the occurrence of a secondary hydroxyl moiety at C-3 as well as a hydroxymethylene at C-4. The chemical shift of C-24 confirmed that this primary hydroxyl moiety was located at C-23.

The HMBC correlations of H-2/C-1, H-2/C-3, H-2/C-5, H-2/C-9, H-2/C-10, H-2/C-25 and H_2-1/C-2 with the ^{1}H-^{1}H COSY correlation observed between H-1 and H-2, also large vicinal coupling constant present at H-1 (J= 12.6), all proposed a hydroxyl moiety was positioned at C-2.

In the NOESY spectrum, H-3 and H-5 as well as H-9 and H-27 showed correlations which confirmed the β-axial orientation of the secondary hydroxyl at C-3. The NOESY correlations shown between H-2 and protons at H-24 and H-25, between H-25 and H-26, established the α-orientation of the hydroxyl at C-2.

From all the spectra analyses discussed above, it was evident that compounds**8**and **9**showed signal patterns with considerable similarities to the ones of **1** and **2**, resepectivelyin^{1}H and ^{13}C analyses (Tables 4.20and 4.16), except for the glycoside linkages present in **8** and **9**(Figure

4.36). Analysis of ^{1}H and ^{13}C spectra of **8**and **9**showed the occurrence of anomeric protons at $\delta_{H\text{-}1}$,5.322 (d, J=8.2) and $\delta_{H\text{-}1}$,5.375 (d, J= 8.2) whichin the HSQC spectrum showed correlation with anomeric carbons at $\delta_{C\text{-}1}$, 95.78 and $\delta_{C\text{-}1}$,95.81, respectively (Table 4.20). Complete assignment of the glycoside protons and carbons in **8** and **9**leading to a β-D-glucopyranoside unit was possible by analysis of the COSY and HSQC experiments (Gossan *et al*., 2016; Agrawal, 1992).

The ^{1}H signals of oxymethine groups $\delta_{H\text{-}2}$, 3.318, $\delta_{H\text{-}3}$, 3.398, $\delta_{H\text{-}4}$, 3.360, $\delta_{H\text{-}5}$, 3.341 and oxymethylene group $\delta_{H\text{-}6}$, 3.798, $\delta_{H\text{-}6}$, 3.680 (dd, J=12.0, 4.8 Hz) as well as ^{13}C signals of the oxygenated methine ($\delta_{C\text{-}2}$, 73.86, $\delta_{C\text{-}3}$, 78.32, $\delta_{C\text{-}4}$, 71.12 and $\delta_{C\text{-}5}$, 78.59) and oxygenated methylene ($\delta_{C\text{-}6}$, 62.42), all together established the possibility of a glycosidic linkage in compound **8**. Likewise, the ^{1}H signals of oxymethine groups $\delta_{H\text{-}2}$, 3.322, $\delta_{H\text{-}3}$, 3.404, $\delta_{H\text{-}4}$, 3.360, $\delta_{H\text{-}5}$, 3.341 and oxymethylene group $\delta_{H\text{-}6}$, 3.820, $\delta_{H\text{-}6}$, 3.682 as well as ^{13}C signals of the oxygenated methine ($\delta_{C\text{-}2}$, 73.92, $\delta_{C\text{-}3}$, 78.32, $\delta_{C\text{-}4}$, 71.08 and $\delta_{C\text{-}5}$, 78.73) and oxygenated methylene ($\delta_{C\text{-}6}$, 62.38), all together established also the possibility of a glycosidic linkage in compound **9**. From the ^{13}C-NMR information ($\delta_{C\text{-}3}$ 78.30; $\delta_{C\text{-}28}$ 178.54) and ($\delta_{C\text{-}3}$ 78.30; $\delta_{C\text{-}28}$ 178.58), C-28 glycosylation of **8** and **9** was proposed as a result of C-3 as well as C-28 of aglycone resonance signals (Mahato and Kundu, 1994).Theobserved correlation in the HMBC spectrum between the anomeric proton of thesugar moiety and the C-28 of the aglycone further confirmed a C-28 glycosylation of **8**and **9**.

Compound **8**(Figure 4.36) identified asnigaichigoside F1 was formerly isolated from leaves of *Ilex oblonga* (Wu *et al*., 2007).Previous work by Adnyana *et al*. (2001) isolated from seeds of *Combretum quadrangulare*, compound **9**(Figure 4.36) identified asarjunglucoside 1,also Gossan *et al*. (2016) isolated it of recentfrom*Combretum racemosum* root.

From other species of the genus *Combretum* (*Combretum quadrangulare*),nigaichigoside F1**(8)**, had been formerly isolated (Adnyana *et al*. 2001), but this is the first report showing its occurrence in *Combretum racemosum*, and its isomer, arjunglucoside 1**(9)**, though has already been isolated from the root of *Combretum racemosum*, but this is the first time it is identified from the leaves of *Combretum racemosum*.

Table 5.5: The ^{13}C NMR for experimental and literature data for compounds 8 and 9 in CD_3OD solvent

Position	8		9	
	^{13}C experimental	^{13}C literature *	^{13}C experimental	^{13}C literature **
1	47.97	47.1	47.79	47.8
2	69.71	69.7	69.69	69.7
3	78.3	78.7	78.3	78.7
4	44.12	41.3	44.13	44.1
5	48.23	55.0	48.37	48.4
6	19.24	19.2	19.26	19.3
7	33.51	33.5	33.26	33.3
8	41.26	42.8	40.88	40.9
9	48.53	49.0	49.14	49.0
10	38.99	39.0	39.16	39.2
11	24.8	24.8	24.92	24.9
12	129.49	129.5	124.78	124.8
13	139.75	139.7	144.48	144.5
14	42.78	42.9	42.75	42.8
15	29.63	29.6	29.43	29.4
16	26.51	26.4	28.43	28.4
17	49.46	49.8	47.11	47.1
18	54.96	55.0	45.07	45.1
19	73.63	73.8	82.43	82.4
20	42.94	44.1	35.95	36.0
21	27.21	27.2	29.5	29.5
22	38.31	38.3	33.29	33.3
23	66.41	66.6	66.39	66.5
24	13.87	13.8	13.79	13.8
25	17.6	17.4	17.46	17.5
26	17.67	17.7	17.82	17.8
27	24.73	24.7	25.03	25.0

28	178.54	178.6	178.58	178.6
29	27.06	27.1	28.61	28.6
30	16.6	16.6	25.16	25.2
1‘	95.78	95.8	95.81	95.8
2‘	73.86	73.9	73.92	73.9
3‘	78.32	78.3	78.32	78.3
4‘	71.12	71.2	71.08	71.1
5‘	78.59	78.6	78.73	78.4
6‘	62.42	62.5	62.38	62.4

*Wu *et al*., 2007

**Gossan *et al*., 2016

Triterpenes, which was proposed to show oxidativeproperties comparable to artemisinin and its antimalarial derivatives,are a kind of pentacyclic phytochemicals that occur in several plants (Etkin, 2003). This way, as alluded to by Ruwende and Hill (1998), triterpenes may mimic the haemoglobinopathies effects on the red blood cells' surroundings that destroy the parasite by way of its oxidative status alteration. From the current work,*C. racemosum*leaves methanol extract exhibited antiplasmodial actionagainst *P. falciparum* strains of chloroquine-sensitive and chloroquine-resistance. This showed a correlation with our previous report (Wande and Babatunde, 2017) of same extract in the assay on formation of beta-hematin inhibition, hence, thesuccessive partition, between chloroform/water, n-butanol/water, of the methanol extract for this current study. The chloroform fraction showed good antiplasmodial action against both*P. falciparum*strains(D10 and W2) which was more potentrelative to n-butanol fraction. But the activity showed better effect in the W2 strain than in the D10 strain; thus, the activity margin was wider between the fractions tested in the W2 compared to D10 (Figure 4.12 and 4.14). The aqueous fraction was not tested in this work. The result suggested that the occurrence of triterpenes, which are non-polar secondary metabolites, present in greater amounts inside chloroform fraction could be responsible for itsantimalarial actionrelated to the remaining fractions. Moreover, the chloroform fraction possessed antiplasmodial actiontwo-fold higher than the crude extract against the two*P. falciparum* strains. This as well suggested that the activity was enhanced due to the fractionation. Therefore, it is doubtful that the water fraction (which is also from the crude methanol extract) would have been more active than the chloroform. Thus, enrichment of active compounds in the chloroform fraction was obvious, hencethe decision to focus on this fraction.

19α-hydroxyasiatic acid **(1)**and arjungenin **(2)**, 6β, 23-dihydroxytormentic acid **(3)**and combregenin **(4)**,madecassic acid **(5)**and terminolic acid **(6)** as well as nigaichigoside F1 **(8)**and arjunglucoside I **(9)**were respectively identifiedfrom isolates CR-A, CR-C, CR-E and CR-H as isomeric mixtures.

Reports showed that compounds were previously isolated as isomeric mixtures from species of *Combretum* genus. The work by Masoko *et al*. (2008) reported the isolation of Arjunolic and asiatic acid as isomeric mixtures from *C. nelsonii*. Similarly in a different study, 2α, 3β-dihydroxyurs-12-en-28-oic and maslinic acids as well as oleanolic and ursolic acids were isolated from *C. zeyheri* as isomeric mixtures (Runyoro *et al*. 2013).

Dissimilar degrees of antiplasmodial actionwere possessed by all isolates against both parasite strains used in this study (Tables 4.22 and 4.23). In a previous report by Glennon *et al*. (2016), abscisic acid at low nM doses exhibited antimalarial action *in vivo*, however, it showed a low potency on D10 and absence of activity on W2 in this current work. Though the investigation of activity mechanism of the isolates was not conducted as it was not part of the focus of this present study, but it is proposed that a likely relationship between the chemical structures of the isolates and their activities onspecific strain (D10 or W2) of the parasite may be responsible for the dissimilarity in activity. The CR-A (19α-hydroxyasiatic acid/arjungenin), CR-H (nigaichigoside F1/arjunglucoside 1) and madecasic acid exhibited higher potency against W2 (23.08 ± 8.17, 33.84 ± 12.53 and 17.19 ± 4.34, respectively) but showed lesser activity against D10 (33.52 ± 12.41, 41.96 ± 15.73 and 27.62 ± 11.56, respectively). However, CR-C (6β, 23-dihydroxytormentic acid/combregenin), abscisic acid and arjungenin showed lesser activity against W2 (61.07 ± 23.15, 134.70 ± 13.21 and 64.36 ± 9.31, respectively) when compared to their better activity against D10 (49.71 ± 18.88, 57.04 ± 21.81 and 41.06 ± 16.92, respectively). Also the ursane-type triterpene (madecasic acid) showed stronger inhibition against W2 (17.19 ± 4.34) compared to the D10 (27.62 ± 11.56). Conversely, the oleanane-type triterpene (arjungenin) showed better activity against D10 (41.06 ± 16.92) compared to W2 (64.36 ± 9.31). The differences in chemical structures of the two isomeric groups, ursane- and oleanane-type triterpenes, may be the reason for different degrees of activity against both*Plasmodium falciparum*strains (D10 and W2).

Reports have suggested that the demonstration of the activity in this class of compounds is hinged on the differences in their structures (Suksamrarn *et al*., 2003; Cimanga *et al*., 2006). Consequently, the structure-activity relationship (SAR) of thesepentacyclic triterpenoids**(1, 2, 3, 4, 5, 6, 8, 9)** against D10 and W2 strains of *P. falciparum* was postulated (Figure 4.40). As isolate CR-A showedapproximately three-fold higher activitythan CR-C (Table 4.23),it is assumed that the addition of hydroxyl moiety at position 6βwas responsible for the decrease in CR-C activity. Madecassic acid(**5**) (17.19 ± 4.34) showed to be significantlyhigher (3.5 fold) in activity compared to CR-C (61.07 ± 23.15) containing 6β, 23-dihydroxytormentic acid (**3**) and combregenin(**4**)against the W2 strain. Hence, this increase in activity could be due to dehydroxylation at position C-19. Based on these outcomes, it is suggested that ifhydroxyl moiety is introduced atposition-6β and/or position-19α in these class of pentacyclic

molecules(ursane- and/or oleanane-type triterpenoids), then there will be decreasein the antimalarial activities; while the geminal-dimethyl substitutions at positionC-20 did not significantly impact the bioactivity (Figure 4.40). A related observation was describedby Runyoro *et al*.(2013) where it was shown that the introduction of hydroxyl moiety in 6β-hydroxymaslinic acid at 6β-position decreased its anti-fungi activityrelated to maslinic acid. Based on this, it is presumed that a further removal of hydroxyl moiety at position-6β in madecassic acid might enhance the antiplasmodial effect of the resulting compound to increase significantly. In this work, it is shown that CR-A which is the mixture of 19α-hydroxyasiatic acid and arjungenin was moderately active with better effects on W2 strain (Table 4.23).In contrast, an activity which was over 2.5 folds lesser than that of CR-A was demonstrated by arjungenin tested in this experiment as a single compound. Assingle compound showed lesser activity than the mixture, this could indicate a more active 19α-hydroxyasiatic acid related to arjungenin or an indication of synergismof these isomeric triterpenes against the *P. falciparum*. Based on the antiplasmodial activity result of madecassic acid (an ursane-type) as being the highest among compounds tested in current study.Also,from *Morinda lucida* leaves, Cimanga*et al*. (2006) described the antiplasmodial action of ursolic acid (an ursane-type) to be five-fold higher than oleanolic acid(oleanane-type). Therefore, it is plausible to suggest19α-hydroxyasiatic acid (an ursane-type) as the one largely responsible for the increased activity in CR-A compared to arjungenin as single compound.However,this question could not be clarified in this study as a result of the lack of isolated 19α-hydroxyasiatic(**1**).

In general, it is possible that theursane-class triterpenesmightdemonstrate higher antiplasmodial activity related to their respective oleanane-class counterparts. Madecassic acid demonstrated the highest antipalsmodial actionamongst all single compounds as well as mixtures tested in this study with better activity on W2 strain of *P. falciparum*(Table 4.23). Also, a previous report of Cimanga *et al*. (2006)showed that ursane (an ursane-class triterpene) demonstrated 5-fold higher antiplasmodial effect than oleanane (an oleanane-class triterpene).

Schofield and Hackett (1993) showed in their report that there is initiation of proinflammatory cytokine responsesduring malaria when glycosylphosphatidylinositol (GPI) is released by intraerythrocytic *Plasmodium falciparum*in the course of merogony or death of erythrocytewhen the infected erythrocytes rupture. Prominent factors responsible for severe

malarial anaemia and death from malaria includes high release of tumour necrosis factor-α (TNF-α), IL-6 and interleukin-1β (IL-1β) (Kwiatkowski *et al*., 1989). Report had shown that madecassic acid significantly inhibited TNF-α, IL-1β and IL-6 production (Van Loc *et al*., 2018). It has likewise been revealed from a recent report that asiatic acid, a pentacyclic triterpenoidsimilar to madecassic acid, reduced the production of IL-1β, IL-6 as well as TNF-αand lower anaemia in malaria parasites (*P. berghei*) (Mavondo *et al*., 2016). As a result of the ability of madecassic acid to inhibit the release of cytokines which also showed to be factors in severe malarial anaemia and cerebral malaria,it is therefore suggested that this might be partly responsible for the antiplasmodial action observed. Additionally, the activity of GPI has showed to be crucial to the survival of the *Plasmodium* parasites, simply because several functionally important parasite proteins are attached to the membrane of cells via GPI moieties (Naik *et al*., 2000). Since the enzyme specificity of some mainstages of parasite GPI bio-formationvaries significantly from those of the host; hence the prospect of aiming the parasite GPI structures to enable the blockade of the induction of toxic responses due to the inhibition of *P. falciparum* GPIs. This suggests that GPI-based therapy is possible as another way of treating the *Plasmodium falciparum* infection (Naik *et al*., 2000). Therefore, the inhibitors of proinflammatory cytokines (TNF-α, IL-1β and IL-6) as well as compounds of this class of triterpene might be exerting antimalarial activity through this pathway.

This study reports for the first time the antiplasmodial activities of these pentacyclic triterpenes **1, 2, 3, 4, 5, 7, 8**and **9**.

Among all the compounds isolated, 6β, 23-dihydroxytormentic acid **(3)**, madecassic acid (**5**)as well asabscisic acid (**7**)are reported from the Combretaceae family for the first time. For the nine compounds (**1-9**) identified in this work, a number of bioactivities was reported in previous studies;arjungenin, combregenin, terminolic acid and arjunglucoside 1 demonstrated antioxidant and antibacterial potential (Gossan *et al*., 2016),19α-hydroxyasiatic acid and nigaichigoside F1 showed antileishmanial activities as well as cytotoxic activities on fibroblasts (Zebiri *et al*., 2016), madecassic acid also showed cytotoxic activities against carcinoma, liver and lung cancers (Van Loc *et al*., 2018).

5.3*Combretum zenkeri*

Successive partitioning of the methanol extract of *C. zenkeri* leaveswas carried out using $CHCl_3$, n-BuOH and H_2O. According to its appropriate antiplasmodial activity (lowest IC_{50}), the $CHCl_3$ soluble fraction was selected for silica flash CC followed by a glass column separation done on a silica gel to yield compound **CZ-A** as a mixture of two isomers. The structure of **CZ-A** from *C. zenkeri* was unambiguously determined by spectroscopic experiments including 1D NMR (^1H and ^{13}C), 2D NMR (COSY, TOCSY, NOESY, HSQC and HMBC), ESI-MS and HR-ESIMS, alsocompared with related information reported in literature. The isomers were identified as ursolic acid (3β-hydroxyurs-12-en-28-oic acid) (**10**) (Venditti *et al*., 2016) and oleanolic acid (3β-hydroxyolean-12-en-28-oic acid) (**11**) (Kipchakbaeva *et al*., 2016) (Figure 4.48).

5.3.1 Isolation of compounds

Fractionation and isolation of phytochemicals are always preceeded by the development of TLC chromatograms of extracts or fractions of interest. This is an important step to aid the selection of most appropriate solvent system for subsequent column separation. The TLC chromatogram of *C. zenkeri* methanol extract in this study has shown the presence of terpenoids (R_f 0.2-0.55) when developed with toluene/ethyl acetate 90:10 (Figure 4.3 A1) and when developed with ethyl acetate/methanol/water 40:4.5:4 (R_f 0.5-0.8) (Figure 4.3 B1) as mobile phases. This was obvious by the characteristic violet colour of the chromatograms after applying anisaldehyde-sulphuric acid spray reagent with clear visible light visualisation. This is in agreement with previous report that anisaldehyde-sulphuric acid spray reagent is suitable derivatisation reagent for optimal colour detection (violet or violet red) of TLC spots due to triterpenes (Wagner and Bladt 1996). This observation is clearly similar to those early reported in this study for *C. racemosum* methanol extract, which is a possible indication that the investigated compounds in these two plants could be of the same class of triterpene.

There are presence ofprominent yellow bands at the start line (Figure 4.3 A4) (detection method: natural product/polyethylene glycol 4000) which the nonpolar toluene/ethyl acetate 90:10 mobile phase obviously could not move up from the base line; which necessitated the use of a relatively more polar mobile phase ethyl acetate/methanol/water 40:4.5:4. This more polar system was able to reveal the presence of compounds with prominent yellow and green

fluorescent zones which indicated flavonoids after spraying with natural product/polyethylene glycol 4000 detection reagent and characterised under UV-365 nm (Figure 4.3 B4). The chromatogram of *C. zenkeri* n-butanol fraction showed similar pattern in its TLC synopsis, evident by the intense green and yellow fluorescence, thereby revealing flavonoids (Figure 4.6 B). These characteristics support earlier report that flavonoids are characterised on TLC with the presence of green, yellow and/or orange fluorescent zones when sprayed with natural product/polyethylene glycol 4000 as detection reagent and viewed with UV at 365 nm (Wagner and Bladt, 1996). However, further investigation on these flavonoids was not included in this report as it became not the focus of this study due to the direction of the bioactivity towards chloroform fraction.

Consequent upon the bioactivity of the fractions tested, the chloroform fraction enriched with triterpenes was selected for further fractionation on silica column flash chromatographycoupled with ELSD and DAD where separation of the fractions took place before further purifying on open column chromatography to afford triterpenes.

For mobile phase selection for silica flash chromatographic separation, TLC is considered as the first-line and most appropriate approach (Wei *et al*., 2013). More reason the TLC of the chloroform fraction was carried out (Figure 4.5), and chloroform/methanol was chosen as suitable starting solvent system in the subsequent flash chromatography.

Purifications were also carried out using open-column chromatography with silica gel. This was achieved by the use of 2 mL/30 minutes (0.1 mL/min) on an automatic fraction collector. This very low flow rate was necessary to avail the mixture of compounds the opportunity for extended time of interaction with the stationary phase. This is because the TLC profiles of some of the semi-purified compounds in their respective fractions showed spots that were too close, therefore, increasing their solute-stationary phase percolation time increased their retention time thereby afforded better resolution of the various components. In cases where there were a little more complex mixtures of compounds in the fractions, the length of the column used was increased to allow more distance travelled by the solutes by the mobile phases; this is believed to be an important factor that may influence increased separation and resolution of compounds in a mixture.

Fractions 12, 13, 14 and 15 became the isolate CZ-A (5 mg), a white amorphous powder obtained from an isocratic elution with mixture of mobile phase $CHCl_3$/MeOH/H_2O 95:1.5:0.1. But CR-A was produced from F318 (FCRC14_12) to F325 (FCRC14_14) (Table 4.9, Figure 4.17); and isolation was achieved at the gradient mobile phase $CHCl_3$/MeOH/H_2O 85:8:0.5 between 42-45 hours 30 minutes of this gradient (Table 3.1). TLC analysis showed it to have single spot (mobile phase chloroform/methanol 80:20; R_f 0.75; see Figure 4.18). The violet colour of the single spot was an indication of triterpene when sprayed with anisaldehyde-sulphuric acid detection reagent (Wagner and Bladt, 1996).

5.3.2 Structure elucidation compounds isolated

The NMR and the MS spectra information generated for all compounds from *C. zenkeri* in this study revealed two pentacyclic triterpenes: one ursane-type and one oleanane-type. The stereochemistry and chemical configuration of these compounds is similar to those of the ones discussed above in section 5.2.

Compound CZ-A (Figure 4.37), a colourless powder, was elucidated as isomeric mixture of ursolic acid (**10**) and oleanolic acid (**11**) by comparing with literatureits NMR and MS spectra information (Venditti *et al*., 2016; Kipchakbaeva *et al*., 2016).

The HRESI-MS displayed a [M-1] peak at m/z 455.3536, consistent with a molecular formula of $C_{30}H_{48}O_3$ (calcd for $C_{30}H_{47}O_3^-$, m/z 455.3530). Also, $[M+Na]^+$ and $[M+COO]^-$ molecular ions were detected at m/z 479.3499 and m/z 501.3588 respectively. From the molecular formula, seven degrees of unsaturation were obvious with one among them as a result of the occurrence of carbonyl group at C-28, and another one also as a result of one double bond in ring C and five among them as a result of pentacyclic ring system.

From Table 4.23, the ^{1}H-NMR spectra information of compound **10**revealed a very similar signal pattern to compound **11**. A prominent similar signal pattern in the ^{1}H NMR experiment for **10** and **11** is shown in the double-doublet signal at $\delta_{H\text{-}3}$ 3.154 (each d, J= 11.7 and 4.6 Hz, which integrated for 1H-atom) in compound **10**and multiplet signal at $\delta_{H\text{-}3}$ 3.147 (integrated for 1H-atom) in compound **11**, which characterised hydrogen attached to oxygenated sp^3 carbon in a cyclic system for both **10** and **11**. Five tertiary methyl groups at (δ_H0.977, 0.780, 0.960, 0.851 and 1.119) which were attributable to methyl groups attached to quartenary

carbon atoms were shown in the spectrum of **10** and the detection of secondary methyl groups at $\delta_{H\text{-}29}$0.932 (J= 6.5) and $\delta_{H\text{-}30}$ 0.964which are attributable to methyl substituentsattached to methine carbon, which indicated ursane-type triterpenes. However, seven tertiary methyl groups signals at (δ_H0.974, 0.778, 0.946, 0.819, 1.161, 0.943 and 0.908) showed in the spectrum of **11**which are attributable to methyl substituentsattached to quartenary carbon atoms which is indicative of oleanane-type triterpenes. The geminal-dimethyl groups at position-20 in **11** is an indication of oleanane-type triterpenes.

The presence of one olefinic proton ($\delta_{H\text{-}12}$ 5.228) and ($\delta_{H\text{-}12}$ 5.243) in both **10** and **11** respectively corresponded to the occurrence of one double bond system in ring C which was attributable to a hydrogen atom attached to a vinyl carbon. This signal is indicative of both oleanane- and ursane-type triterpenes (Gossan *et al*., 2016).

The ^{13}C-NMR spectra also showed similarities in the signal pattern of compounds **10** and **11**(Tables 4.23 and 5.6). They exhibited signals for 30 carbons in the DEPTq experiment: Compound **10** showed one carboxyl at low field ($\delta_{C\text{-}28}$ 181.74), one double bond ($\delta_{C\text{-}12}$ 126.88; $\delta_{C\text{-}13}$ 139.66), one sp^{3}oxygenated methine carbon ($\delta_{C\text{-}3}$ 79.70), seven methyl, nine sp^{3}methylene carbons, five sp^3 methine carbons and five quartenary carbons, and compound **11**likewise showed one carboxyl at low field ($\delta_{C\text{-}28}$ 181.96), one double bond ($\delta_{C\text{-}12}$ 123.62; $\delta_{C\text{-}13}$ 145.25), one sp^{3}oxygenated methine carbon ($\delta_{C\text{-}3}$ 79.71), seven methyl carbons, ten sp^3 methylene carbons, three sp^3 methine carbons and six quartenary carbons. But the actual dissimilarity in the DEPTq analysis showed that **10**had methine group at position 19 while **11** had a methylene group at same position, also **10** had a methine carbon at position 20 while **11** possessed a quartenary carbon at this position(Table 4.23 and Figure 4.48). These spectra data in this study suggested that compound **10** was an ursane-type triterpenoid and compound **11** was an oleanane-type triterpenoid (Mahato and Kundu, 1994). In rings A-D, there were presence of superimposable signals in both **10** and **11** by comparing their ^{1}H and ^{13}C data, but with differences shown only in ring E. Additionally, **10** and **11** showed some different chemical shifts in both ^{1}H-NMR spectra $\delta_{H\text{-}18}$ 2.203, $\delta_{H\text{-}19}$ 1.379, $\delta_{H\text{-}20}$0.996 and $\delta_{H\text{-}18}$ 2.851, $\delta_{H\text{-}19}$ 1.695, 1.125 respectively, and ^{13}C-NMR spectra $\delta_{C\text{-}18}$ 54.38, $\delta_{C\text{-}19}$40.44, $\delta_{C\text{-}20}$ 40.42 and $\delta_{C\text{-}18}$ 42.75, $\delta_{C\text{-}19}$ 47.27, $\delta_{C\text{-}20}$ 31.62 of **10** and **11**respectively (Table 4.23). This difference was particularly influenced by the different substitution between positions 19 and 20. The^{13}C-NMR information of compound **10**compared to α-amyrin (Vázquez*et al*., 2012) showed similarities

in ring A-E signals but differ by the signals at C-28 (carboxyl in **10**, but methyl group in α-amyrin) likewise, compound **11**with those of β-amyrin were similar in ring A-E but differ also by the signals at C-28 (carboxyl in **11**, but methyl group in β-amyrin) (Vázquez*et al*., 2012). This was agreed to by the lowfield signal of C-28 (δ_C181.74) in **10**compared to α-amyrin, and C-28 (δ_C181.96) in **11**compared to β-amyrin.

In HMBC spectra data, the correlations between H_2-11 (δ_H1.931) and the two vinylic carbons at C-12 and C-13 suggested a Δ^{12}-unsaturated double bond. The HSQC correlations between H-18/ C-13 and H_2-11/C12together withdata of the ^{1}H-^{1}H COSY spectrum (Appendix 13c) which showed that it was only H_2-11 that had direct correlation with the olefinic proton (H-12) further established the double bond is positioned at C-12 (Figure 4.37). Also, the observed correlations in the HMBC spectrum (Appendix 13d) between the carbons C-9, C-11, C-14, C18 and the olefinic proton H-12 establishedC-12 as the location of the double bond.

In the HMBC experiment, the cross-peaks observed in the spectra between H_3-23 and signals at C-3 showed the occurrence of a secondary hydroxyl moiety at C-3. In the NOESY spectrum, H-3 and H-5 as well as H-9 and H-27 showed correlations which confirmed the β-axial orientation of the secondary hydroxyl at C-3. Compound **10**(Figure 4.37) identified as ursolic acid was formerly identified from*Morinda lucida*leaves (Cimanga *et al*. 2006) also more recently from*Helichrysum microphyllum*subsp. *tyrrhenicum* (Venditti *et al*. 2016). Compound **11**(Figure 4.41) identified as oleanolic acid was previously identified from*Morinda lucida*leaves (Cimanga *et al*. 2006) also recently isolated from*Climacoptera subcrassa* (Kipchakbaeva*et al*., 2016).

From other species of the genus *Combretum* (*Combretum zeyheri*), ursolic acid **(10)**and oleanolic acid **(11)**had been formerly isolated (Runyoro *et al*. 2013), but this is their first report in*Combretum zenkeri*.

Table 5.6: The ^{13}C NMR of experimental and literature data for compounds 10 and 11 in $CDCl_3$ solvent

Position	10		11	
	^{13}C experimental	^{13}C literature *	^{13}C experimental	^{13}C literature **
1	39.99	39.0	39.83	37.6
2	27.90	27.6	27.87	26.7
3	79.70	78.4	79.71	78.5
4	39.84	39.4	40.55	39.2
5	56.74	55.3	56.76	55.5
6	19.47	18.1	19.50	18.3
7	34.33	32.9	34.02	32.6
8	40.78	41.9	40.78	39.6
9	49.06	47.6	49.10	48.1
10	38.10	38.5	38.17	37.0
11	24.36		24.52	22.7
12	126.88	125.4	123.62	122.4
13	139.66	138.1	145.25	144.1
14	43.25	41.9	42.89	42.0
15	29.22	29.4	28.85	27.7
16	25.33	25.5	24.06	22.8
17	49.10	47.5	47.67	46.7
18	54.38	52.8	42.75	41.5
19	40.44	38.9	47.27	46.1
20	40.42	38.6	31.62	30.4
21	31.79	30.5	34.91	33.7
22	38.13	36.7	33.84	32.3
23	28.76	27.8	28.73	28.8
24	16.37	16.5	16.31	14.7
25	16.02	15.2	15.88	15.1
26	17.81	20.5	17.73	16.5
27	24.08	24.0	26.38	25.2

28	181.74	180.3	181.96	180.4
29	17.64	16.6	23.98	32.8
30	21.57	23.0	33.57	23.3

*Venditti *et al*., 2016

**Kipchakbaeva *et al*., 2016

Some genus *Combretum*had been studied where ursolic and oleanolic acidsas isomeric mixtures were similarly isolated. In a separate work, ursolic acid with oleanolic acid were identified by Runyoro *et al*.(2013)as isomeric mixturefrom *C. zeyheri*. From a different genus, ursolic acid with oleanolic acid as isomeric mixture were as well identified from *Salvia buchananii* where they synergistically demonstrated a significant inhibitory activity on numerous Gram-positive species (Bisio *et al*., 2015). Compound **10** and **11** is almost ubiquitous among all species of plant. Ursolic acid is widely spread, especially in higher plants such as *Rosmarinus officinalis*, *Glechona hederaceae*, *Salvia officinalis*, *Thymus vulgaris*, *Eucalyptus teretocornis*, *Morinda lucida* and many others (Wozniak *et al*., 2015; Cimanga *et al*., 2006), but from the *Combretum* genus, its isolation was only reported from *Combretum zeyheri*, *Combretum quadrangulare* and *Combretum vendee* (Runyoro *et al*., 2013).Oleanolic acid is also spread across many plant species such as ginseng root, *Sambucus chinensis*, *Viburnum nervosum*, *Morinda lucida*, and found in more than 120 plants (Cimanga *et al*., 2006; Awan *et al*., 2013), but from genus *Combretum* it was only reported from *Combretum zeyheri* (Runyoro *et al*., 2013).This work is the first report showing the identification of these two compounds from *Combretum zenkeri*. The antiplasmodial activity test was not conducted for these two known compounds identified in this study as their antimalarial activities were previously investigated (Cimanga *et al*., 2006; Innocente *et al*., 2012; Awan *et al*., 2013). Ursolic acid from *Morinda lucida* was shown to exhibit good*in vivo* and *in vitro* antimalarial activities (Cimanga *et al*., 2006), due to its presence in the extract of *C. zenkeri*, it is suggested that it could be partly or majorly implicated in the observed potency in this work. In the earlier report, ursolic acid (IC_{50}: 3.1±1.3 µg/mL) exhibited good*in vitro* antiplasmodial activitiesagainst a *P. falciparum* chloroquine-sensitive strain, about 5-folds active more than oleanolic acid (IC_{50}: 15.2±3.4 µg/mL) (Cimanga *et al*., 2006). Likewise in the *in vivo* test from same study, ursolic acid produced 97.7% parasitemia chemosuppression, greater reduction in parasitemia compared to oleanolic acid 37.5% in *Plasmodium berghei berghei*infected mice. Although work is currently ongoing in our research group for other compounds from the chloroform fraction to be isolated and purified, as there may be other principles having similar activities from this extract. The activity test of their mixture (ursolic acid/oleanolic acid) was not possible in this study as a result of insufficient amount isolated. Although, the activity of their mixture is higher in few other pharmacological activities compared to the single

compounds (Bisio *et al*., 2015), also broad data concerning the synergistic antimalarial action of these two isomers is unavailable. Ursolic acid has recently been described as pentacyclic triterpene having broad spectrum of pharmacological actions including protecting effect on brain, liver, kidneys and lungs, anti-inflammation, anabolic effect on skeletal muscles, anti-osteoporosis, antimicrobial effect against several bacteria strains, anti-virus against HIV and HCV and antimalarial among others (Wozniak *et al*., 2015; Liu, 2005). Consequently, it is plausible to suggest that the presence of ursolic acid in *C. zenkeri* contribute hugely to the different pharmacological actions (Ogbonna *et al*., 2016; Wande and Babatunde, 2017; Ujowundu *et al*., 2015; Okwu *et al*., 2014) exerted by the plant. However, it is important to widely explore *C. zenkeri* for its other bioactive constituents which may be useful lead compounds or scaffolds necessary for their synthesis for many other pharmacological investigations important. Meanwhile in a recent study, analogue of ursolic acid, N-{3-[4-(3-aminopropyl)piperazinyl]propyl}-3-O-acetylursolamide, which showed better antiplasmodial activity (175 nM) than the aglycone was synthesized (Innocente *et al*., 2012). This report showed that the ursolic acid derivative which showed to be non-toxic demonstrated a novel effective antiplasmodial prototype that interrupts plasmodium calcium homeostasis.

CHAPTER SIX

6 CONCLUSION

TheCombretaceae family has demonstrated to be a valuable source of medicinal plants possessing broad spectrum of activities against several diseases, therefore, its exploration is vital in the search for biologically active principle useful in malaria treatment. The antimalarial potential of *Combretumzenkeri*is shown in this study from a good antiplasmodial action exhibited by its chloroform fraction, and thereby justifying its use in ethnomedicine. The antimalarial potential of *Combretumracemosum* and its use in traditional medicine has also been justified with this study through the antiplasmodial effects of its chloroform fraction and the compounds elicited from it. Apparently, triterpenoids are largely responsible for the antimalarial effects manifested in theses plants as a result of the significant potency of their chloroform fractions compared to other fractions.On the other hand, future investigation should involve*in vivo* antimalarial effect of *Combretum racemosum*methanol extract as well as the compounds isolated from it as a required recommendation to further authenticate its usage in ethnomedicine. The genus *Combretum*has afforded many triterpenoids from several previous reports, which made it an imperative group when searching for biologically active molecules useful in treatingseveral diseases including malaria.

Two closely related triterpenes, ursolic and oleanolic acids were identified as known antimalarial principles from *Combretumzenkeri*.The antimalarial effect exerted by the extractmight be largely as a result of the existence of ursolic acid therein. Earlier studies have shown isolation of similar isomeric mixture from other species (Runyoro *et al*., 2013; Bisio *et al*., 2015). This is the first report of the identification of any bioactive principles from *Combretum zenkeri*.

Madecassic acid demonstrated the most significant antiplasmodial action among all compounds derived from *C. racemosum*, even better activity was observedagainst the *P. falciparum*chloroquine-resistant strain (W2). Similarly, based on antiplasmodial result of

isolate CR-A in this work, 19α-hydroxyasiatic acid or in synergism with arjungenin could presumably contribute to the observed activity in*C racemosum*. Though the modes of action of isolated compounds were not conducted in this work, but it is proposedbased on literature data that the ability of these class of triterpenes for the inhibition of cytokines release which are also significantly involved in the development of cerebral malaria as well assevere malarial anaemia might be partly attributedto the observed antiplasmodial action. The inhibition of cytokines´ pathways could be a mechanism of action of the antimalarial effect of this compounds. However, a further investigation into the mechanism of action of isolated compounds could help validate this claim. Madecassic acid has shown from this study potential for antimalarial drug development; and this is presentedas the first reportof its occurrence in the Combretaceae family.

REFERENCES

Adebayo, J.O.and Krettli, A.U. 2011. Potential antimalarials from Nigerian plants: A review. *Journal of Ethnopharmacology* 133: 289-302

Adedotun, A.A., Morenikeji, O.A., and Odaibo, A.B. 2010. Knowledge,attitudes and practices about malaria in an urban community in south-western Nigeria. *Journal of Vector Borne Diseases* 47: 155–159.

Adhami, V.M., Syed, D.N., Khan, N. and Mukhtar, H. 2012. Dietary flavonoid fisetin: a novel dual inhibitor of PI3K/Akt and mTOR for prostate cancer management. *Biochemical Pharmacology*84.10:1277–1281.

Adnyana, K., Tezyka, Y., Banskota, A.H., Tran, K.Q. and Kadota, S. 2001. Three new triterpenes from the seeds of *Combretum quadrangulare* and their hepatoprotective activity. *Journal of Natural Products* 64: 360-363.

Afonso, A., Hunt, P., Cheesman, S., Alves, A.C., Cunha, C.V., do Rosario, V. and Cravo, P. 2006. Malaria parasites can develop stable resistance to artemisinin but lack mutations in candidate genes atp6 (encoding the sarcoplasmic and endoplasmic reticulum Ca^{2+} ATPase), tctp, mdr1, and cg10. *Antimicrobial Agents Chemotherapy* 50: 480–489.

Agbedahunsi, J.M., Elujoba, A.A., Makinde, J.M. and Oduola, A.M.J. 1998. Antimalarial activity of *Khaya grandifoliola* stem-bark. *Pharmaceutical Biology* 36: 8–12.

Ajaiyeoba, E.O., Abalogu, U.I., Krebs, H.C., Oduola, A.M.J. 1999. *In vivo* antimalarial activities of *Quassia amara* and *Quassia undulata* plant extracts in mice. *Journal of Ethnopharmacology* 67: 321–325.

Ajaiyeoba, E.O., Abiodun, O.O., Falade, M.O., Ogbole, N.O., Ashidi, J.S., Happi, C.T. and Akinboye, D.O. 2006a. *In vitro* cytotoxicity studies of 20 plants used in Nigerian antimalarial ethnomedicine.*Phytomedicine* 13: 295–298.

Ajaiyeoba, E., Falade, M., Ogbole, O., Okpako, L. and Akinboye, D. 2006b.*In vivo* antimalarial and Cytotoxic properties of *Annona senegalensis* extract. *African Journal of Traditional, Complementary and alternative Medicine*3.1: 137 – 141.

Allaoua, Z., Benkhaled, M., Dibi, A., Long, C., Aberkane, M.C., Bouzidi, S., Kassah-Laouar, A. and Haba, H. 2016. Chemical composition, antioxidant and antibacterial properties of *Pteranthus dichotomus* from Algerian Sahara.*Natural Products Research* 30: 700-704.

Alqahtani, A., Hamid, K., Kam, A., Wong, K.H., Abdelhak, Z., Razmovski-Naumovski, V., Chan, K.,Li, K.M., Groundwater, P.W. and Li, G.Q. 2013. The Pentacyclic Triterpenoids in Herbal Medicines and Their Pharmacological Activities in Diabetes and Diabetic Complications.*Current Medicinal Chemistry*20:908-931.

Amusan, O.O.G., Adesogan, E.K. and Makinde, J.M. 1996. Antimalarial active principles of *Spathodea campanulata* stem bark.*Phytotherapy Research* 10: 692–693.

Anderson, W. K. 1927. Malarial psychoses and neuroses. Oxford University Press, London, United Kingdom.

Angeh, J.E., Huang, X., Sattler, I., Swan, G.E., Dahse, H., Hartl, A. and Eloff, J.N. 2007.Antimicrobial and anti-inflammatory activity of four known and one new triterpenoid from *Combretum imberbe* (Combretaceae).*Journal of Ethnopharmacology* 110: 56–60.

Ansa-Asamoah, R., Kapadia, G.J., Lloyd, H.A. and Sokoloski, E.A. 1990.Picratidine, a new indole alkaloid from *Picralima nitida* seeds.*Journal of Natural Products* 53: 975–977.

Arif, T., Bhosale, J. D., Kumar, N., Mandal, T. K., Bendre, R.S., Lavekar, G.S. and Dabur, R. 2009. Natural products – antifungal agents derived from plants.*Journal of Asian Natural Products Research* 11.7: 621–638.

Atindehou, K.K., Schmid, C., Brun, R., Koné, M.W. and Traore, D. 2004. Antitrypanosomal and antiplasmodial activity of medicinal plants from Côte d'Ivoire. *Journal of Ethnopharmacology*90: 221–227.

Attioua, B., Lagnika, L., Yeo, D., Antheaume, C., Kaiser, M., Weniger, B., Lobstein, A. and Vonthron-Sénécheau, C. 2011.*In vitro* antiplasmodial and antileishmanial activities of flavonoids from *anogeissus leiocarpus* (Combretaceae). *International Journal of Pharmaceutical Sciences Review and Research* 11.2: 1-6.

Austarheim, I., Pham, A.T., Nguyen, C., Zou, Y., Diallo, D., Malterud, K.E. and Wangensteen, H.2016. Antiplasmodial, anti-complement and anti-inflammatory *in vitro* effects of *Biophytumumbraculum* welw. Traditionally used against cerebral malaria in Mali. *Journal of Ethnopharmacology* 190:159-164.

Avwioro, O.G., Aloamaka, P.C., Ojianya, N.U., Oduola, T. and Ekpo, E.O. 2005.Extracts of *Pterocarpus osun* as a histological stain for collagen fibres.*African Journal of Biotechnology* 5: 460–462.

Awan, Z.I., Habib-Ur-Rehman, Minhas, F.A. and Awan, A.A. 2013.Antiplasmodial activity of compounds isolated from *Viburnum nervosum*. *International Journal of Pharmaceutical Science and Invention*2.5: 19-24.

Babamale, O.A., Adenekan, T.A. and Ugbomoiko, U.S. 2015. Communityknowledge on Transmission of malaria and its management practice inOorelope local government, southwestern region, Nigeria. *AnimalResearch International* 12: 2203-2211

Baird, J.K., Caneta-Miguel, E., Masba, S., Bustos, D.G., Abrenica, J.A., Layawen, A.V., Calulut, J.M., Leksana, B. and Wignall, F.S. 1996.Survey of resistance to chloroquine of *falciparum* and *vivax* malaria in Palawan, The Philippines.*Transactions of the Royal Society of Tropical Medicine and Hygiene* 90: 413–414.

Balick, M.J., Elizabetsky, E. and Laird, S.A. 1996.*Medicinal Resources of the Tropical Rain Forest*. Columbia University Press, New York.

Balunas, M. J. and Kinghorn, A. 2005. Drug discovery from medicinal plants.*Life Sciences* 78.5: 31-41.

Bell, A. and Boehm, D. 2013. Anti-disease therapy for malaria – 'resistance proof '?*Current Pharmaceutical Design* 19:300–306. doi:10.2174/138161213804070366

Bertani, S., Houël, E., Stien, D., Chevolot, L., Jullian, V., Garavito, G., Bourdy, G. and Deharo, E. 2006. Simalikalactone D is responsible for the antimalarial properties of an Amazonian traditional remedy made with *Quassia amara* L. (Simaroubaceae). *Journal of Ethnopharmacology* 108: 155–157.

Bhutani, K. K. and Gohil, V. M. 2010. Natural Products Drug Discovery Research in India: Status and Appraisal. *IndianJournalofExperimentalBiology* 48: 199-207.

Bickii, J., Nijifutie, N., Foyere, J.A., Basco, L.K. and Ringwald, P. 2000. *In vitro* antimalarial activity of limonoids from *Khaya grandifoliola* C.D.C (Meliaceae).*Journal of Ethnopharmacology* 69: 27–33.

Bisio, A., Schito, A.M., Parricchi, A., Mele, G., Romussi, G., Malafronte, N., Oliva, P. and Tommasi, N. 2015.Antibacterial activity of constituents from *Salvia buchananii* Hedge (Lamiaceae).*Phytochemistry letters* 14: 170-177.

Bousema, T., Okell, L., Felger, I. and Drakeley, C. 2014. Asymptomatic malaria infections: detectability, transmissibility and public health relevance. *Nature Reviews Microbiology* 12:833–40. doi:10.1038/nrmicro3364

Bray, D.H., Warhurst, D.C., Connolly, J.D., O'Neill, M.J. and Phillipson, J.D. 1990. Plants as sources of antimalarial drugs. Part 7. Activity of some species of Meliaceae and their constituent limonoids. *Phytotherapy Research* 4: 29–35.

Bringmann, G., Saeb, W., Assi, L.A., François, G., Sankara Narayanan, A.S., Peters, K. andPeters, E.M. 1997. Betulinic acid: Isolation from *Triphyophyllum peltatum* and *Ancistrocladus heyneanus*, antimalarial activity, and crystal structure of the benzyl ester. *Planta Medica*63: 255–257. DOI:10.1055/s-2006-957666

Bumah, V.V., Essien, E.U., Agbedahunsi, J.M. and Ekah, O.U. 2005.Effects of *Khaya grandifoliola* (Meliaceae) on some biochemical parameters in rats.*Journal of Ethnopharmacology* 102: 446–449.

Butler, M.S. 2004. The role of natural product chemistry in drug Discovery. *Journal of Natural Products*67.12: 2141–2153.

Butterworth, J.H. and Morgan, E.D. 1968. Isolation of a substance that suppresses feeding in locusts. *Chemical Communication*1968: 23–24.

Cabral, J.A., McChesney, J.D. and Milhous, W.K. 1993.A new antimalarial Quassinoid from *Simaba guianensis*.*Journal of Natural Products*56: 1954-1961.

Campanale, N., Nickel, C., Daubenberger, C.A., Wehlan, D.A., Gorman, J.J., Klonis, N., Becker, K. and Tilley, L. 2003. Identification and characterization of heme interacting proteins in the malaria parasite, *Plasmodium falciparum*.*Journal of Bioligical Chemistry*278: 27354-27361.

Chanphen, R., Thebtaranonth, Y., Wanauppathamkul, S.andYuthavong, Y. 1998. Antimalarial principles from *Artemisia indica. Journal of Natural Products*61: 1146–1147. DOI:10.1021/np980041x

Chen, M., Theander, T.G., Christensen, S.B., Hviid, L., Zhai, L. andKharazmi, A. 1994. Licochalcone A, a new antimalarial agent, inhibits *in vitro* growth of the human malaria parasite *Plasmodium falciparum* and protects mice from *P. yoelii* infection. *Antimicrobial Agents and Chemotherapy* 38.7: 1470-1475.

Chong, C.R. and Sullivan, D.J. 2003. Inhibition of heme crystal growth by antimalarials and other compounds: implications for drug discovery. *Biochemical Pharmacology*66: 2201–2212.

Church, J.A., Nyamako, L., Olupot-Olupot, P., Maitland, K. and Urban, B.C. 2016. Increased adhesion of *Plasmodium falciparum* infected erythrocytes to ICAM-1 in children with acute intestinal injury. *Malaria Journal* 15:1–6. doi:10.1186/s12936-016-1110-3

Cimanga, R.K., Tona, G.L., Mesia, G.K., Kambu, O.K., Bakana, D.P., Kalenda, P.D.T., Penge, A.O., Muyembe, J.T., Totte, J., Pieters, L. and Vlietinck, A.J. 2006. Bioassay-guided isolation of triterpenoid acids from the leaves of *Morinda lucida*. *Pharmaceutical Biology* 44.9: 677-681.

Cobbinah, E.A. 2008. Antioxidant and antibacterial activities of the chemical constituents of *Terminalia ivorensis chev.*,*MSc thesis submitted to the department of Chemistry,*

Kwame Nkrumah University of Science and Technology. Retrieved Nov. 12, 2016, from www.pdffiller.com/48140246.

Colegate, S. M. and Molyneux, R. J. 2008.*Bioactive Natural Products: Detection, Isolation and Structure Determination*; CRC Press: Boca Raton,FL, USA, pp. 421–437.

Cowman, A.F., Berry, D. and Baum, J. 2012.The cellular and molecular basis for malaria parasite invasion of the human red blood cell.*Journal of Cell Biology* 198:961–971. doi:10.1083/jcb.201206112

Cragg, G. M. and Newman, D. J. 2005. Biodiversity: A continuing source of novel drug leads. *Pure and Applied Chemistry* 77: 7–24.

Cruz, L.N., Wu, Y., Craig, A.G. and Garcia, C.R. 2012. Signal transduction in *Plasmodium* red Blood cells interactions and in cytoadherence. *Anais da Academia Brasileira de Ciências* 84.2:555–72. doi:10.1590/S0001-37652012005000036

de Monbrison, F.,Maitrejean, M., Latour, C., Bugnazet, F., Peyron, F., Barron, D. andPicot, S.2006.*In vitro* antimalarial activity of flavonoid derivatives dehydrosilybin and 8-(1;1)-DMA-kaempferide. *Acta Tropica* 97.1:102–107. DOI: 10.1016/j.actatropica.2005.09.004

De Morais Lima, G.R., Praxedes de Sales, I.R. , Dutra Caldas Filho, M.R., Taveira de Jesus, N.Z., De Sousa Falcão, H., Barbosa-Filho, J.M., Silveira Cabral, A.G., Lopes Souto, A., Tavares, J.F. and Batista, L.M., 2012. Bioactivities of the Genus *Combretum* (Combretaceae): A Review. *Molecules* 17: 9142-9206.

Deleu, D., Hanssens, Y. and Northway, M. G. 2004. Subcutaneous apomorphine: An evidence-based review of its use in Parkinson's disease. *Drugs Aging* 21: 687–709.

Deng, W. and Baker, D.A. 2002. A novel cyclic GMP-dependent protein kinase is expressed in the ring stage of the *Plasmodium falciparum* life cycle. *Molecular Microbiology* 44:1141–1151. doi:10.1046/j.1365-2958.2002.02948.x

Dewick, P. M. 2002. *Medicinal Natural Products: A Biosynthentic Approach*, 2nd ed.; John Wiley and Son: West Sussex, UK, pp. 520.

Dias, D. A., Urban, S. and Roessner, U. 2012. A Historical Overview of Natural Products in Drug Discovery.*Metabolites* 2:303-336.

Dibua, U.M., Okeke, C.C., Ugwu, C., Kenechukwu, F.C. and Okorie, A. 2013.*In vivo* antimalarial and cytotoxicity activity of ethanolic stem bark of *Petersianthus macrocarpus* and leaf of *Astonia boonei* in experimental mice model. *International Journal of Current Microbiology and Applied Science*2.12: 354-368

Dijoux, M.-G., Lavaud, C., Massiot, G., Le Men-Olivier, L. and Sheeley, D.M. 1993.A Saponin from Leaves of *Aphloia madagascariensis*.*Phytochemistry* 34: 497-499.

Dixon, R. and Paiva, N. 1995.Stress-induced phenylpropanoid metabolism.*Plant Cell* 7: 1085-1097.

Dobson, M. J. 1994. Malaria in England: a geographical and historical perspective. *Parassitologia*36: 35–60.

Dondorp, A.M., Kager, P.A., Vreeken, J. and White, N.J. 2000. Abnormal blood flow and red blood cell deformability in severe malaria. *Parasitology Today*16:228–232.doi:10.1016/S0169-4758(00)01666-5

Dondorp, A.M., Nosten, F., Yi, P., Das, D., Phyo, A.P., Lwin, J.T.K.M., Ariey, F., Hanpithakpong, W., Lee, S.J., Ringwald, P., Silamut, K., Imwong, M., Chotivanich, K., Lim, P., Herdman, T., An, S.S., Yeung, S., Singhasivanon, P., Day, N.P.J., Lindegardh,N., Socheat, D. and White, N.J. 2009. Artemisinin resistance in *Plasmodium falciparum* malaria.*New England Journal of Medicine*361: 455–467.

Eaton, J.W. and Brewer, G.J. 1969.Red cell ATP and malaria infection.*Nature*222:389–390. doi:10.1038/222389a0

Efange, S.M.N. 2002. Natural products: a continuing source of inspiration for the medicinal chemist. *In Advances in phytomedicine.* Edited by Iwu M.M. and Wootton J.C. Amsterdam*: Elsevier Science;* 61–69.

Egan, T.J. 2003. Haemozoin (malaria pigment): a unique crystalline drug target. *Targets* 2.3:115-124.

Ehiagbonare, J.E. 2007. Vegetative propagation on some key malaria medicinal plants in Nigeria. *Scientific Research and Essay* 2: 37–39.

Eisenreich, W., Bacher, A., Arigoni, D. and Rohdich, F. 2004.Biosynthesis of isoprenoids via the non-mevalonate pathway.*Cell Molecular Life Sciences* 61.12:1401-1426.DOI:10.1007/s00018-004-3381-z

Elford, B.C. 1986.l-Glutamine influx in malaria-infected erythrocytes: a Target for antimalarials?*ParasitologyToday* 2: 309.

Eloff, J. 1998. Which extractant should be used for the screening and isolation of antimicrobial components from plants? *Journal ofEthnopharmacology* 60: 1–8.

Eloff, J.N. 1999. The antibacterial activity of 27 Southern African members of the Combretaceae.*South African Journal of Science* 95: 148–152.

Eloff, J.N., Famakin, J.O. and Katerere, D.R. 2005. Isolation of an antibacterial stilbene from *Combretum woodii* (combretaceae) leaves. *African Journal of Biotechnology*4.10: 1167-1171.

Eloff, J.N., Katerere, D.R.P. and McGaw, L.J. 2008.The biological activity and chemistry of the southern African Combretaceae.*Journal of Ethnopharmacology* 119: 686–699.

Elufioye, T.O. and Agbedahunsi, J.M. 2004.Antimalarial activities of *Tithonia diversifolia* (Asteraceae) and *Crossopteryx febrifuga* (Rubiaceae) on mice *in vivo*.*Journal of Ethnopharmacology* 93: 167–171.

Erhun, W.O., Agbani, E.O., and Adesanya, S.O. 2005. Malaria Prevention: Knowledge, Attitude and Practice in a Southwestern Community. *African Journal of Biomedical Research* 8: 25–29.

Etkin, N.L. 2003. Co-evolution of people, plants, and parasites: biological and cultural adaptations to malaria. *Proceedings of the Nutrition Society* 62.2: 311-317.DOI: 10.1079/pns2003244

Ezeamuzie, K., Ojinnaka, M.C., Uzogara, E.O. and Orji, S.E. 1994. Antiinflammatory, antipyretic and antimalarial activities of West African medicinal plant, *Picralima nitida*.*African Journal of Medicine and Medical Sciences* 23: 85–90.

Fabricant, D. S. and Farnsworth, N. R. 2001. The value of plants used in traditional medicine for drug discovery. *Environmental Health Perspectives* 109: 69–75.

Facchini, P. 2001. Alkaloids biosythesis in plants: biochemistry, cell biology, molecular regulation, and metabolic engineering application. *AnnualReview of Plant Physiology and Plant MolecularBiology* 52: 29-66.

Falae, A., Combe, A., Amaladoss, A., Carvalho, T., Menard, R. and Bhanot, P. 2010. Role of *Plasmodium berghei* cGMP-dependent protein kinase in late liver stage development.*Journal of Biological Chemistry*285:3282–3288. doi:10.1074/jbc.M109.070367

Fidock, D.A., Rosenthal, P.J., Croft, S.L., Brun, R. and Nwaka, S. 2004. Antimalarial drug discovery: efficacy models for compound screening. *Nature Reviews Drug Discovery* 3:509-520. Doi:10.1038/nrd1416

Francis, S.E., Sullivan, D.J. Jr. and Goldberg, D.E. 1997. Hemoglobin metabolism in the malaria parasite *Plasmodium falciparum*.*Annual Review of Microbiology*51: 97–123

François, G., Passreiter, C.M., Woerdenbag, H.J.andVan Looveren, M. 1996. Antiplasmodial activities and cytotoxic effects of aqueous extracts and sesquiterpene lactones from *Neurolaena lobata*. *Planta Medica*62: 126-129.

Francois, G., Timperman, G., Eling, W., Assi, L.A., Holenz, J. and Bringmann, G. 1997. Naphthylisoquinoline alkaloids against malaria: Evaluation of the curative potentials of dioncophylline C and dioncopeltine A against *Plasmodium bergheiin vivo*. *Antimicrobial Agents and Chemotherapy*41.11: 2533-2539.

Fyhrquist, P., Mwasumbi, L., Haeggstrom, C.A., Vuorela, H., Hiltunen, R. and Vuorela, P. 2002. Microscopic diagnosis of tumors of the central nervous system by phase contrast microscopy. *Journal of Ethnophamacology*79: 169–177.

Gakunju, D.M.N., Mberu, E.K., Dossaji, S.F., Gray, A.I., Waigh, R.D., Waterman, P.G. andWatkins, W.M. 1995.Potent antimalarial activity of the alkaloid nitidine, isolated from a Kenyan herbal remedy. *Antimicrobial Agents and Chemotherapy*39: 2606–2609. DOI: 10.1128/AAC.39.12.2606

Ganesh, D., Fuehrer, H.P., Starzengruber, P., Swoboda, P., Khan, W.A., Reismann, J.A., Mueller, M.S., Chiba, P. and Noedl, H. 2012. Antiplasmodial activity of flavonol quercetin and its analogues in *Plasmodium falciparum*: evidence from clinical isolates in Bangladesh and standardized parasite clones. *Parasitology Research* 110.6: 2289–2295.

Garnham, P.C.C. 1966. Malaria parasites and other Haemosporidia. Oxford Blackwell Scientific publication.

Gbolade, A.A., Ogbole, O.O. and Ajaiyeoba, E.O. 2010. Ethnobotanical Survey of Plants used in Treatment of Inflammatory Diseases in Ogun State of Nigeria. *European Journal of Scientific Research* 43.2: 183-191.

Ghosh, A., Das, B., Roy, A., Mandal, B. and Chandra, G. 2008. Antibacterial activity of some medicinal plant extracts. *Journal of Natural Medicines* 62: 259–262.

Glennon, E.K.K., Adams, L.G., Hicks, D.R., Dehesh, K., Luckhart, S., 2016. Supplementation with Abscisic Acid Reduces Malaria Disease Severityand Parasite Transmission. *American Journal of Tropical Medicine and Hygiene* 94.6: 1266–1275.Retrieved Jun. 14, 2019, from https://doi.org/10.4269/ajtmh.15-0904

Glushakova, S., Lizunov, V., Blank, P.S., Melikov, K., Humphrey, G., Zimmerberg, J. 2013. Cytoplasmic free Ca^{2+} is essential for multiple steps in malaria parasite egress from infected erythrocytes. *Malaria Journal*12:41. doi:10.1186/1475-2875-12-41

Goffin, E., Ziemons, E., De Mol, P., de Ceu de Madureira, M., Martins, A.P., Proenca da Cunha, A., Philippe, G., Tits, M., Angenot, L. and Frederich, M. 2002.*In vitro* antiplasmodial activity of *Tithonia diversifolia* and identification of its main active constituent: tagitinin C. *Planta Medica* 68: 543–545.

Gopiesh Khanna, V., Kannabiran, K., Rajakumar, G., Rahuman, A.A. and Santhoshkumar, T. 2011. Biolarvicidal compound gymnemagenol isolated from leaf extract of miracle fruit plant, *Gymnema sylvestre* (Retz) Schult against malaria and filariasis vectors. *Parasitology Research* 109.5:1373–1386.

Gossan, A.D.P.A.,Magid, A.A., Yao-Kouassi, P.A., Josse, J., Gangloff, S.C., Morjani, H. and Voutquenne-Nazabadioko, L. 2016. Antibacterial and cytotoxic triterpenoids from the roots of *Combretum racemosum*. *Fitoterapia* 110: 89-95.

Gowda, D.C. 2007.TLR-mediated cell signaling by malaria GPIs.*Trends in Parasitology* 23:596–604. doi:10.1016/j.pt.2007.09.003

Gray, C., McCormick, C., Turner, G. and Craig, A. 2003. ICAM-1 can play a major role in mediating *Plasmodium falciparum* adhesion to endothelium under flow. *Molecular and Biochemical Parasitology* 128:187–193. doi:10.1016/S0166-6851(03)00075-6

Gurib-Fakim, A. 2006.Medicinal plants: traditions of yesterday and drugs of tomorrow.*Molecular Aspects of Medicine* 27.1: 1-93. DOI:10.1016/j.mam.2005.07.008

Hallock, Y.F., Manfredi, K.P., Dai, J-R., Cardellina, J.H., Gulakowski, R.J., McMahon, J.B., Schäffer, M., Stahl, M., Gulden, K-P., Bringmann, G., François, G. and Boyd, M.R. 1997. Michellamines D−F, New HIV-Inhibitory Dimeric Naphthylisoquinoline Alkaloids, and Korupensamine E, a New Antimalarial Monomer, from *Ancistrocladus korupensis*. *Journal of Natural Products* 60.7: 677-683.

Hamburger, M. and Hostettmann, K. 1991. Bioactivity in plants: the link between phytochemistry and medicine. *Phytochemistry* 30.12: 3864-3874.

Harborne, J.B. 1986. Nature, distribution and function of plant flavonoids.*Progress in Clinical and Biological Research* 213: 15–24.

Harvey, A. L. 2008.Natural products in drug discovery.*DrugDiscoveryToday* 13: 894-901.

Harwaldt, P., Rahlfs, S., Becker, K. 2002. Glutathione S-transferase of the malaria parasite *Plasmodium falciparum*: characterization of a potential drug target. *Biological Chemistry*383: 821-830.

Havsteen, B.H. 2002.The biochemistry and medical significance of the flavonoids.*Pharmacology and Therapeutics*96.2–3:67–202.

Ho, M. and White, N.J. 1999. Molecular mechanisms of cytoadherence in malaria.*American Journal of Physiology* 276:C1231–1242.

Hostettmann, K., Marston, A., Ndjoko, K. and Wolfender, J.L. 2000.The potential of African plants as a source of drugs.*Current Organic Chemistry* 4.10: 973-1010.

Ilboudo, D.P., Basilico, N., Parapini, S., Corbett, Y., D'Alessandro, S., Dell'Agli, M., Coghi, P., Karou, S.D., Sawadogo, R., Gnoula, C., Simpore, J., Nikiema, J.B., Monti, D., Bosisio, E., Taramelli, D., 2013. Antiplasmodial and anti-inflammatory activities of *Canthium henriquesianum* (K. Schum), a plant used in traditional medicine in Burkina Faso.*Journal of Ethnopharmacology* 148.3: 763-769. https://doi:10.1016/j.jep.2013.04.049.

Innocente, A.M., Silva, G.N.S., Cruz, L.N., Moraes, M.S., Nakabashi, M., Sonnet, P., Gosmann, G., Garcia, C.R.S. and Gnoatto, S.C.B. 2012.Synthesis and antiplasmodial activity of betulinic acid and ursolic acid analogues.*Molecules* 17: 12003-12014.

Isah, A.B., Ibrahim, Y.K. and Iwalewa, E.O. 2003. Evaluation of the antimalarial properties and standardization of tablets of *Azadirachta indica* (Meliaceae) in mice.*Phytotherapy Research* 17: 807–810.

Joshi, S.P., Rojatkar, S.R. and Nagasampagi, B.A. 1998. Antimalarial activity of neem (*Azadirachta indica*).*Journal of Medicinal and Aromatic Plant Sciences* 20: 1000–1004.

Kabanywanyi, A.M., Mwita, A., Sumari, D., Mandike, R., Mugittu, K. and Abdulla, S.2007. Efficacy and safety of artemisinin-based antimalarial in the treatment of uncomplicated malaria in children in southern Tanzania.*Malaria Journal*6:146.DOI: 10.1186/1475-2875-6-146

Kassim, O.O., Loyevsky, M., Elliott, B., Geall, A., Amonoo, H. and Gordeuk, V.R. 2005.Effects of root extracts of *Fagara zanthoxyloides* on the *in vitro* growth and stage distribution of *Plasmodium falciparum*.*Antimicrobial Agents and Chemotherapy* 49: 264–268.

Kayode, J. 2006. Conservation of indigenous medicinal botanicals in Ekiti State, Nigeria.*Journal of Zhejiang University Science B* 7: 713–718.

Kayser, O., Kiderlen, A.F. and Croft, S.L. 1998. *In: Proceedings of the 9 International Congress of Parasitology, Monduzzi Editore:* Bologna, Italy, Pp. 925-9.

Kedei, N., Lundberg, D. J., Toth, A., Welburn, P., Garfield, S. H. and Blumberg, P.M. 2004.Characterization of the interaction of ingenol 3-angelate with protein kinase C. *Cancer Research* 64: 3243–3255.

Khalid, S.A., Friedrichsen, G.M., Kharazmi, A., Theander, T.G., Olsen, C.E. and Christensen, S.B. 1998.Limonoids from *Khaya senegalensis*.*Phytochemistry* 49: 1769–1772.

Kipchakbaeva, A.K., Eskalieva, B.K., Burasheva, G.Sh., Adikari, A., Aisa, H.A.and Choudhary, M.I. 2016. Saponins from *Climacopterasubcrassa*.*Chemistry of Natural Compounds* 52.2: 363-364.

Klayman, D.L. 1985. Qinghaosu (artemisinin): an antimalarial drug from China. *Science* 228: 1049–1055.

Köhler, I., Jenett-Siems, K., Kraft, C., Siems, K., Abbiw, D., Bienzle, U. andEich, E. 2002. Herbal remedies traditionally used against malaria in Ghana: Bioassay-guided fractionation of *Microglossa pyrifolia* (Asteraceae). *Zeitschrift fur Naturforschung C* 57.11-12: 1022-1027. DOI: 10.1515/znc-2002-11-1212

Komlaga, G., Cojean, S., Dickson, R.A., Beniddir, M.A., Suyyagh-Albouz, S., Mensah, M.L.K., Agyare, C., Champy, P. and Loiseau, P.M. 2016. Antiplasmodial activity of selected medicinal plants used to treat malaria in Ghana. *Parasitol. Res.*DOI 10.1007/s00436-016-5080-8

Kozawa, M., Baba, K. and Matsuyama, Y. 1982.Components of the root of *Anthriscussylvestris* Hoffm.2.insecticidal activity. *Chemicaland Pharmaceutical Bulletin* 30: 2885-2888.

Kraft, C., Jenett-Siems, K., Siems, K., Gupta, M.P., Bienzle, U., Eich, E.2000.Antiplasmodial activity of isoflavones from *Andira inermis*.*Journal of Ethnopharmacology* 73.1–2:131–135

Krane, B.D., Fagbule, O.M. and Shamma, M. 1984. The benzophenanthridine alkaloids.*Journal of Natural Products*47: 1-43.

Kren, V. and Walterova, D.2005.Silybin and silymarin—new effects and applications.*Biomedical papers of the Medical Faculty of the University Palacky, Olomouc, Czechoslovakia* 149.1:29–41

Kumar, S., Paul, S., Walia, Y.K., Kumar, A. and Singhal, P. 2015. Therapeutic Potential of Medicinal Plants: A Review. *Journal of Biological and Chemical Chronicles*1.1:46-54

Kuria, K.A.M., De Coster, S., Muriuki, G., Masengo, W., Kibwage, I., Hoogmartens, J. and Laekeman, G.M. 2001. Antimalarial activity of *Ajuga remota* Benth (Labiatae) and *Caesalpinia volkensii* Harms (Caesalpiniaceae): *in vitro* confirmation of ethnopharmacological use. *Journal of Ethnopharmacology*74:141-148.

Kwiatkowski, D., Cannon, J., Manogue, K., Cerami, A., Dinarello, C. and Greenwood, B. 1989. Tumour necrosis factor production in *falciparum* malaria and its association with schizont rupture. *Clinical and Experimental lmmunology* 77: 361-366.

Lahlou, M. 2007.Screening of Natural Products for Drug Discovery.*Expert Opinion on Drug Discovery* 2.5: 697-705.

Lahlou, M. 2013.The Success of Natural Products in Drug Discovery.*Pharmacology & Pharmacy* 4: 17-31.

Lehane, A.M. and Saliba, K.J. 2008.Common dietary flavonoids inhibit the growth of the intraerythrocytic malaria parasite. *BMC Research Notes* 1:26–31.DOI: 10.1186/1756-0500-1-26

Likhitwitayawuid, K., Phadungcharoen, T. and Krungkrai, J. 1998.Antimalarial xanthones from *Garcinia cowa*.*Planta Medica* 64: 70-72. DOI: 10.1055/s-2006-957370

Lin, L.C., Yang, L.L. and Chou, C.J. 2003. Cytotoxic naphtho-quinones and plumbagic acid glucosides from *Plumbago zeylanica*.*Phytochemistry* 62: 619–622.

Liu, J. 2005. Oleanolic acid and ursolic acid: Research perspectives. *Journal of Ethnopharmacology*100: 92-94.

Liu, W., Li, Y., Learn, G.H., Rudicell, R.S., Robertson, J.D., Keele, B.F., Ndjango, J.B., Sanz, C.M., Morgan, D.B., Locatelli, S., Gonder, M.K., Kranzusch, P.J., Walsh, P.D., Delaporte, E., Mpoudi-Ngole, E., Georgiev, A.V., Muller, M.N., Shaw, G.M., Peeters, M., Sharp, P.M., Rayner, J.C., and Hahn, B.H.2010. Origin of the human malaria parasite Plasmodium falciparum in gorillas. *Nature* 467: 420–425

Lu, X., Zheng, Z., Miao, S., Li, H., Guo, Z., Zheng, Y., Zheng, B.andXiao, J. 2017. Separation of Oligosaccharides from Lotus Seeds via Medium pressure Liquid Chromatography Coupled with ELSD and DAD. *Scientific reports* 7: 44174

Ma, X., Wang, W., Li, E., Gao, F., Guo, L. and Pei, Y. 2016. A new sesquiterpene from the entomogenous fungus *Phomopsis amygdali*. *Natural Products Research* 30: 276-280.

MacKinnon, S., Durst, T., Arnason, J.T., Angerhofer, C., Pezutto, J., Sanchez-Vindas, P.E., Poveds, L.J. and Gbeassor, M. 1997.Antimalarial activity of tropical Meliaceae extracts and gedunin derivatives.*Journal of Natural Products* 60: 336–341.

MacKinnon, S., Durst, T., Arnason, J.T., Angerhofer, C., Pezzuto, J., Sanchez-Vindas, P.E., Poveda, L.J. andGbeassor, M. 1997. Antimalarial activity of tropical Meliaceae extracts and gedunin derivatives. *Journal of Natural Products*60: 336–341.

Mahato, S.B. and Kundu, A.P. 1994. ^{13}C NMR spectra of pentacyclictriterpenoids-a compilation and some salient features.*Phytochemistry* 37.6: 1517-1575.

Makhafola, T.J., Samuel, B.B., Elgorashi, E.E. and Eloff, J.N. 2012.Ochnaflavone and Ochnaflavone 7-*O*-methyl Ether: two Antibacterial Biflavonoids from *Ochnapretoriensis*(Ochnaceae). *Natural Products Communication* 7.12: 1601-1604.

Makinde, J.M., Amusan, O.G. and Adesogan, E.K. 1988. The antimalarial activity of *Spathodea campanulata* stem bark extract on *Plasmodium berghei berghei* in mice. *Planta Medica* 54.2: 122–125.

Makinde, J.M., Awe, S.O. and Salako, L.A. 1994. Seasonal variation in the antimalarial activity of *Morinda lucida* on *Plasmodium berghei* in mice.*Fitoterapia* 65: 124–130.

Maplestone, R. A., Stone, M. J. and Williams, D. H. 1992.The evolutionary role of secondary metabolites-A review.*Gene* 115: 151–157.

Markler, M.T., Ries, J.M., Williams, J.A., Bancroft, J.E., Piper, R.C., Gibbins, B.L., Hinrichs, D.J., 1993. Parasite Lactate Dehydrogenase as an Assay for *Plasmodium falciparum* Drug Sensitivity.*American Journal of Tropical Medicine and Hygiene* 48.6: 739–741.https://doi.org/10.4269/ajtmh.1993.48.739

Masoko, P., Mdee, L.K., Mampuru, L.J. and Eloff J.N. 2008. Biological activity of two related triterpenes isolated from *Combretum nelsonii* (Combretaceae) leaves. *Natural Products Research* 22.12: 1074-1084.

Mavondo, G.A. and Kasvosve, I. 2017. Antimalarial Phytochemicals: Delineation of the Triterpene Asiatic Acid Malarial Anti-Disease and Pathophysiological Remedial Activities - Part II. *Journal of Infectious Diseases and Pathogenesis*1: 104.

Mavondo, G.A., Mkhwananzi, B.N. and Mabandla, M.V. 2016. Pre-infection administration of asiatic acid retards parasitaemia induction in *Plasmodium berghei* murine malaria infected Sprague-Dawley rats. *Malaria Journal* 15: 226. Retrieved Jan. 16, 2019, from https://doi.org/10.1186/s12936-016-1278-6

Mbeunkui, F., Grace, M.H., Lategan, C., Smith, P.J., Raskin, I. and Lila, M.A. 2011. Isolation andidentification of antiplasmodial N-alkylamides from *Spilanthes acmella* flowersusing centrifugal partition chromatography and ESI-IT-TOF-MS. *Journal of Chromatography B* 879: 1886–1892.Retrieved May 22, 2019, from https://doi.org/10.1016/j.jchromb.2011.05.013.

McGaw, L.J., Rabe, T., Sparg, S.G., Jäger, A.K., Eloff, J.N. and Van Staden, J. 2001.An investigation on the biological activity of *Combretum*species.*Journal of Ethnopharmacology* 75: 45–50.

McRae, J., Yang, Q., Crawford, R. and Palombo, W. 2007. Review of the methods used for isolating pharmaceutical lead compounds from traditional medicinal plants. *Environmentalist* 27: 165–174.

Mgbemena, I. C., Allison, L. N., Udensi, U. J., Nweke, K. E., Nwachukwu, A.A. and Ezea, C.O. 2016. Screening of Ethanol extract of *Combretum racemosum*and *Euphorbia hirta*leaves for possible activity on *Trypanosoma brucei brucei* infected mice. *Scholars Academic Journal of Biosciences* 4.9:725-731.

Miller, L.H., Baruch, D.I., Marsh, K. and Doumbo, O.K. 2002.The pathogenic basis of malaria.*Nature* 415:673–679. doi:10.1038/415673a

Mojarrab, M., Shiravand, A., Delazar, A. and Afshar, F.H. 2014. Evaluation of *in vitro* antimalarial activity of different extracts of *Artemisia aucheri* Boiss. and*A. armeniaca*

L and fractions of the most potent extracts. *Scientific World Journal*2014: 1-6. Retrieved Sept. 16, 2018, from http://dx.doi /10.1155/2014/825370

Mokuolu, O.A., Okoro, E.O., Ayetoro, S.O. and Adewara, A.A. 2007. Effect of artemisininbased treatment policy on consumption pattern of antimalarials. *American Journal of Tropical Medicine and Hygiene* 76: 7–11.

Mosaffa-Jahromi, M., Lankarani, K.B., Pasala, M., Afsharypuor, S. and Tamaddon, A.M. 2016.Efficacy and safety of enteric coated capsules of anise oil to treat irritable bowel syndrome.*Journal of Ethnopharmacology*194: 937-946.

Mustafa, N. R. and Verpoorte, R. 2007.Phenolic compounds in *Catharanthus roseus*. *Phytochemistry Reviews*6.2:243-258. DOI: 10.1007/s11101-006-9039-8

Mutabingwa, T.K. 2005. Artemisinin based combination therapy (ACTs): Best hope for malaria treatment but inaccessible to the needy! *Acta Tropica* 95:305-315

National Center of Infectious Diseases 2006.

Naik, R.S.,Branch, O.H.,Woods, A.S.,Vijaykumar, M.,Nahlen, B.L., Lal, A.A.,Perkins, D.J.,Cotter, R.J.,Costello, C.E., Ockenhouse, C.F.,Davidson, E.A., and Gowda, D.C. 2000. Glycosylphosphatidylinositol Anchors of*Plasmodium falciparum*: Molecular Characterizationand Naturally Elicited Antibody Response That May Provide Immunity to Malaria Pathogenesis. *The Journal of Experimental Medicine* 192.11: 1563-1575.

Newman, D. J. and Cragg, G. M. 2007.Natural products as sources of new drugs over the last 25 years.*Journal of Natural Products* 70: 461–477.

Ngemenya, M.N., Tane, P., Berzins, K. and Titanji, V.P.K. 2004. Antiplasmodial Activity of some Medicinal Plants used in Cameroon:- preliminary toxicity studies of highly active extracts . *XIth Annual Conference of The Cameroon Bioscience Society*16-18 December, 2004.

Nicolaou, K. C., Yang, Z., Liu, J. J., Ueno, H., Nantermet, P. G., Guy, R. K., Claiborne, C.F., Renaud, J., Couladouros, E. A., Paulvannan, K. and Sorensen, E.J. 1994.Total synthesis of taxol.*Nature* 367: 630–634.

Njoroge, G. N. and Bussmann, R. W. 2006.Diversity and Utilization of antimalarial ethnophytotherapeutic remedies among Kikuyus (Central Kenya).*Journal of Ethnobiology and Ethnomedicine* 2: 8. doi:10.1186/1746-4269-2-8.

Noedl, H., Se, Y., Schaecher, K., Smith, B.L., Socheat, D. and Fukuda, M.M.2008. Evidence of artemisinin-resistant malaria in western Cambodia.*New England Journal of Medicine*359.24: 2619-2620.DOI: 10.1056/NEJMc0805011

Obih, P.O. and Makinde, J.M. 1985. Effect of *Azadirachta indica* on *Plasmodium berghei berghei* in mice.*African Journal of Medicine and Medical Science* 14: 51–54.

Ogan, A.U. 1972. Alkaloids in leaves of *Combretum micranthum*.Studies on West African medicinal plants.*Planta medica* 21.2:210-217.

Ogbonna, C.U., Ujowundu, C.O., Okwu, G.N., Emejulu, A.A., Alisi, C.S. and Igwe, K.O. 2016.Biochemical and histological evaluation of benzo[a]pyrene induced nephrotoxicity and therapeutic potentials of *C. zenkeri* leaf extract. *African Journal of Pharmacy and Pharmacology* 10.41: 873-882.

Ogbourne, S. M., Suhrbier, A. and Jones, B. 2004. Antitumour activity of ingenol 3-angelate: Plasma membrane and mitochondrial disruption and necrotic cell death. *CancerResearch* 64: 2833–2839.

Oketch-Rabah, H. A., Dossaji, S.F., Christensen, S.B., Frydenvang, K., Lemmich, E., Cornett, C., Carl Erik Olsen, C.E., Chen, M., Kharazmi, A. and Theander, T.G.1997a. Antiprotozoal compounds from *Asparagus africanus*. *Journal of Natural Products*60: 1017-1022.

Oketch-Rabah, H. A., Lemmich, E., Dossaji, S.F., Theander, T.G., Olsen, C.E., Cornett, C., Kharazmi, A. andChristensen, S.B. 1997b. Two New Antiprotozoal 5-

Methylcoumarins from *Vernonia brachycalyx* .*Journal of Natural Products*60.5: 458-461. DOI:10.1021/np970030o

Oketch-Rabah, H.A., Brøgger Christensen, S., Frydenvang, K., Dossaji, S.F., Theander, T.G., Cornett, C., Watkins, W.M., Kharazmi, A. andLemmich, E. 1998. Antiprotozoal properties of 16,17-dihydrobrachycalyxolide from *Vernonia brachycalyx*. *Planta Medica* 64.6: 559-562. DOI:10.1055/s-2006-957514

Okunji, C.O., Iwu, M.M., Ito, Y. and Smith, P.L. 2005.Preparative separation of indole alkaloids from the rind of *Picralima nitida* (Stapf) T. Durand and H. Durand by pH-Zone-Refining Countercurrent chromatography.*Journal of Liquid Chromatography and Related Technology* 28: 775–783.

Okwu, G.N., Ogbonna, C.U., Ujowundu, C.O., Igwe, K.O., Igwe, C.U. and Emejulu, A.A. 2014. Protective effect of ethanol leaf extract of *C. zenkeri* on liver functions of Albino rats following benzo[a]pyrene exposure. *Biological and Chemical Research*2014: 16-25.

Oluyole, K.A., Ogunlade, M.O., and Agbeniyi, S.O. 2011. Socio-economic Burden of Malaria Disease on Farm Income among Cocoa Farming Households in Nigeria. *American-Eurasian J. Agric. & Environ. Science* 10: 696–701.

Onocha, P.A., Audu, E.O., Ekundayo, O. and Dosumu, O.O. 2005.Phytochemical and antimicrobial properties of extracts of *Combretum racemosum*.*Acta Horticulturae* 675.12: 97-101

Onwujekwe, O.E., Chima, R., and Okonkwo, P.O. 2000. The Economic burden of malaria illness versus that of a combination of all other illnesses: A study in five malaria holo-endemic communities. *Health Policy* 54: 143–159.

Parker, P.D., Tilley, L. and Klonis, N. 2004.*Plasmodium falciparum* induces reorganization of host membrane proteins during intraerythrocytic growth. *Blood* 103:2404–2406.doi:10.1182/blood-2003-08-2692

Perez, H.A., De La Rosa, M. and Apitz, R. 1994.*In vivo* activity of ajoene against rodent malaria.*Antimicrobial Agents Chemotherapy* 38: 337–339.

Pettit, G.R., Singh, S.B., Boyd, M.R., Hamel, E., Pettit, R.K., Schmidt, J.M. and Hogan, F. 1995. Antineoplastic agents. 291. Isolation and synthesis of combretastatins A-4, A-5, and A-6(1a).*Journal of Medicinal Chemistry* 38.10: 1666-1672.

Pettit, G.R., Singh, S.B., Niven, M.L. and Schimdt, J.M. 1988. Cell growth inhibitory dihydrophenanthrene and phenanthrene constituents of the African tree *Combretum caffrum*.*Canadian Journal of Chemistry* 66: 406–413.

Pettit, G.R., Singh, S.B., Niven, M.L., Hamel, E. and Schmidt, J.M. 1987. Isolation, Structure, and Synthesis of Combretastatins A-1 and B-1, Potent New Inhibitors of Microtubule Assembly, Derived from *Combretum caffrum*.*Journal of Natural Products*50.1: 119-131.

Phillipson, J. D. 2007.Phytochemistry and pharmacognosy.*Phytochemistry*68.22-24: 2960-2972.

Ponou, B.K., Barboni, L., Teponno, R.B., Mbiantcha, M., Nguelefack, T.B., Park, H.-J., Lee, K.-T. and Tapondjou, L.A. 2008. Polyhydroxyoleanane-type triterpenoids from *Combretum molle* and their anti-inflammatory activity. *Phytochemistry Letters* 1: 183-187.

Prachayasittikul, S., Suphapong, S., Worachartcheewan, A., Lawung, R., Ruchirawat, S. and Prachayasittikul, V. 2009. Bioactive Metabolites from *Spilanthes acmella* Murr. *Molecules* 14: 850–867.Retrieved Jun. 12, 2019, from https://doi.org/10.3390/molecules14020850

Prole, D.L. and Taylor, C.W. 2011.Identification of intracellular and plasma membrane calcium channel homologues in pathogenic parasites.*PLoS One*6.10:e26218. doi:10.1371/journal.pone.0026218

Raina, H., Soni, G., Jauhari, N., Sharma, N. and Bharadvaja, N. 2014.Phytochemical importance of medicinal plants as potential sources of anticancer agents.*Turkish Journal of Botany* 38: 1027-1035.

Ramawat, K. G. 2007.*Secondary metabolites in nature*. In: Ramawat K.G., Merillon J.M. (eds) Biotechnology: Secondary Metabolites. Science Publishers, Enfield, CT, p 21

Ramawat, K.G ., Dass, S. and Mathur, M. 2009.The Chemical Diversity of Bioactive Molecules and Therapeutic Potential of Medicinal Plants. In: Ramawat, K.G. (ed.) *Herbal Drugs:Ethnomedicine to Modern Medicine*. Springer-Verlag Berlin Heidelberg.

Raskin, I., Ribnicky, D., Komarnytsky, S., Ilic, N., Poulev, A., Borisjuk, N., Brinker, A., Moreno, A., Ripoll, C., Yakoby, N., Cornwell, T., Pastor, I. and Fridlender, B. 2002 Plants and human health in the twenty-first century.*Trends In Biotechnology* 20.12: 522-531.

Rochanakij, S., Thebtaranonth, Y., Yenjai, C.andYuthavong, Y. 1985. A constituent of *Azadirachta indica,*inhibits *Plasmodium falciparum* in culture. *South East Asian Journal Tropical Medicine and Public Health*16: 66-72.

Rodrigues, I. and Naehrer, K. 2012. Prevalence of mycotoxins in feedstuffs and feed surveyed worldwide in 2009 and 2010. *Phytopathologia Mediterranea*51: 175-192

Roge, A.B., Firke, S.N., Kawade, R.M., Sarje, S.K. and Vadvalkar, S.M. 2011. Brief review on:flash chromatography. *International Journal of Pharmaceutical Sciences and Research* 2: 1930–1937.

Roll Black Malaria, World Health Organization (RBM, WHO) 2006. Facts on ACTs Artemisinin-based Combination Therapies. Retrieved Oct. 26, 2016, from www.rbm.who.int.

Roll back malaria 2008. Malaria consortium roll back malaria needs assessment report, pp 8-12.

Roll Back Malaria, Action and investment to defeat malaria 2016-2030. For a malaria-free world. Geneva: World Health Organisation (WHO) 2015. Retrieved Oct. 26, 2016, from http://www.rollbackmalaria.org/files/aim/RBM_AIM_Report_A4_EN-Sept2015.pdf

Runyoro, D.K.B., Srivastava, S.K., Darokar, M.P., Olipa, N.D., Joseph, C.C. and Matee, M.I.N. 2013. Anticandidiasis agents from a Tanzanian plant, *C. zeyheri*. *Medicinal Chemistry Research* 22: 1258-1262.

Ruwende, N.R. and Hill, A. 1998. Review: Glucose-6-phosphate dehydrogenase deficiency and malaria. *Journal of Molecular Medicine* 76: 581-588.

Sachs, J.D. and Malaney, P. 2002. The economic and social burden of malaria. *Nature* 415: 680-685.

Salim, A. A., Chin, Y. W. and Kinghorn, A. D. 2008.Drug Discovery from Plants. In: Ramawat, G., Merillon, J. M. (eds) *Bioactive Molecules andMedicinal Plants.* Springer, Berlin Heidelberg New York.

Samuel, B., Oluyemi, W.M. and Abiodun, O. 2015. Bio-guided investigation of the antimalarial activities of *Trema orientalis*(L.) Blume leaves. *African Journal of Biotechnology* 14.43: 2966-2971.

Samuel, B.B., Owolabi, O.M., Adaramoye, O., Williams, E. and Jain, K.S. 2014.Bioguided isolation of an antioxidant compound from *Combretum racemosum* P.Beav leaf.*International Journal of Biological and Chemical Science* 6.5:2339-2346. Retrieved Feb. 17, 2017, from http://dx.doi.org/10.4314/ijbcs.v8i5.36

Samy, R. P. and Gopalakrishnakone, P. 2007.Current status of herbal and their future perspectives.*NaturePrecedings*: 1-13.

Santos, S.N., Oliveira, L.K.X., Melo, I.S., Velozo, E.S. and Roque, M.R.A. 2011.Antifungal activity of bacterial strains from the rhizosphere of *Stachytarpheta crassifólia*.*African Journal of Biotechnology*10.25: 4996-5000.

Saxena, S., Pant, N., Jain, D.C. and Bhakuni, R.S. 2003.Antimalarial agents from plant sources.*Current Science* 85: 1314–1329.

Schofield, L. and Grau, G.E. 2005.Immunological processes in malaria pathogenesis. *Nature Reviews Immunology* 5:722–735. doi:10.1038/nri1686

Schofield, L. and Hackett, F. 1993. Signal transduction in host cells by a glycosylphosphatidylinositoltoxin of malaria parasites. *Journal of Experimental Medicine* 177: 145-53.

Sherman, I.W. 1998. A brief history of malaria and discovery of the parasite's life cycle. In: Sherman I.W., editor. , ed. Malaria: Parasite Biology, Pathogenesis and Protection.*ASM press,* Washington, DC.

Sherman, I.W., Eda, S. and Winograd, E. 2004.Erythrocyte aging and malaria.*Cellular and Molecular Biology (Noisy-le-grand)*50.2:159–169.

Sicard, A., Semblat, J-P., Doerig, C., Hamelin, R., Moniatte, M., Dorin-Semblat, D., Spicer, J.A., Srivastava, A., Retzlaff, S., Heussler, V., Waters, A.P. and Doerig, C. 2011.Activation of a PAK-MEK signalling pathway in malaria parasite-infected erythrocytes.*Cellular Microbiology* 13:836–845. doi:10.1111/j.1462-5822.2011.01582.x

Sittie, A.A., Lemmich, E., Olsen, C.E., Hviid, L., Kharazmi, A., Nkrumah, F.K. and Christensen, S.B. 1999. Structure–activity studies: *in vitro* antileishmanial and antimalarial activities of anthraquinones from *Morinda lucida*. *Planta Medica* 65: 259–261.

Slater, A.F. and Cerami, A. 1992.Inhibition by chloroquine of a novel haem polymerase enzyme activity in malaria trophozoites.*Nature*355: 167-169.

Smith, W.B., Deavenport, D.L., Swanzy, J.A. and Pate, G.A. 1973. Steroid ^{13}C chemical shifts.Assignments via shift reagents.*Journal of Magnetic Resonance* 12.1:15-19.

Sneader, W. 1996.Drug Prototypes and Their Exploitation.Published by John Wiley and Sons, UK.

Sneader, W. 2005. Drug Discovery: a History. Published by John Wiley and Sons limited, 1st edition, Chichester, UKPp 88-105. DOI:10.1002/0470015535

Sobota, R.S., Dara, A., Manning, J.E., Niangaly, A., Bailey, J.A., Kone, A.K., Thera, M.A., Djimdé, A.A., Vernet, G., Leissner, P., Williams, S.M., Plowe, C.V. and Doumbo, O.K. 2016.Expression of complement and toll-like receptor pathway genes is associated with malaria severity in Mali: a pilot case control study. *Malaria Journal* 15:1–12. doi:10.1186/s12936-016-1189-6

Solis, P.N., Lang'at, C., Gupta, M.P., Kirby, G.C., Warhusrst, D.C. andPhillipson, J.D. 1995. Bioactive compounds from *Psychotria camponutans*.*Planta Medica*61: 62–65. DOI:10.1055/s-2006-958001

Sowemimo, A., Van de Venter, M., Baatjies, L. and Koekemoer, T. 2009.Cytotoxic activity of selected Nigerian plants.*African Journal of Traditional Complimentary and Alternative Medicine* 6.4: 526-528.

Spelman, K., Depoix, D., McCray, M., Mouray, E. and Grellier, P. 2011. The Traditional Medicine*Spilanthes acmella*, and the Alkylamides Spilanthol and Undeca-2E-ene-8,10-diynoic acid Isobutylamide, Demonstrate In Vitro and In Vivo Antimalarial Activity. *Phytotherapy Research* 25: 1098–1101. Retrieved Nov. 13, 2018, fromhttps://doi.org/10.1002/ptr.3395.

Suksamrarn, A., Tanachatchairatana, T. and Kanokmedhakul, T. 2003.Antiplasmodial triterpenes from twigs of *Gardenia saxatilis*.*Journal of Ethnopharmacology* 88: 275–277.

Sullivan, D.J. 2002.Theories on malarial pigment formation and quinoline action.*International Journal of Parasitology*32: 1645–1653

Tan, F.X., Shi, S.H., Zhong, Y., Gong, X. and Wang, Y.G. 2002. Phylogenetic relationships of *Combretoideae* (Combretaceae) inferred from plastid, nuclear gene and spacer sequences. *Journal of Plant Research*115: 475–481.

Tanneur, V., Duranton, C., Brand, V.B., Sandu, C.D., Akkaya, C., Kasinathan, R.S.,Gachet, C., Sluyter, R., Barden, J.A., Wiley, J.S., Lang, F. and Huber, S.M. 2006. Purinoceptors are involved in the induction of an osmolyte permeability in malaria-infected and oxidized human erythrocytes. *FASEB Journal* 20:133–5. doi:10.1096/fj.04-3371fje

Tantry, M. A. 2009. Plant natural products and drugs: a comprehensive study. *Asian Journal ofTraditional Medicines* 4.6: 241-249.

Tasdemir, D., Gabriela, L., Brun, R., Rüedi, P., Scapozza, L. and Perozzo, R. 2006. Inhibition of *Plasmodium falciparum* fatty acid biosynthesis: evaluation of FabG. FabZ, and FabI as drug targets for flavonoids.*Journal of Medicinal Chemistry* 49:3345–3353.

Tasdemir, D., Kaiser, M., Brun, R., Yardley, V., Schmidt, T.J., Tosun, F. and Ruedi, P. 2006. Antitrypanosomal and antileishmanial activities of flavonoids and their analogues.*In vitro, in vivo*, structure activity relationship and quantitative structure activity relationship studies.*Antimicrobial Agents and Chemotherapy*49: 1352–1364.

Tekwani, B.L. and Walker, L.A. 2005. Targeting the hemozoin synthesis pathway for new antimalarial drug discovery: technologies for *in vitro* beta-hematin formation assay.*Combinatorial Chemistryand High Throughput Screening*8.1: 63-79. doi: 10.2174/1386207053328101

Tor-Anyiin, T.A., Shaato, R. and Oluma, H.O.A. 2003.Ethnobotanical survey of antimalarial medicinal plants amongst the Tiv people of Nigeria.*Journal of Herbs, Spices and Medicinal Plants* 10: 61–74.

Trager, W. and Jensen, J.B. 1976.Human malaria parasites in continuous culture. Science 193, 673– 675.https://doi.org/10.1126/science.781840

Trapp, S. and Corteau, R. 2001.Defensive resin biosynthesis in conifers.*Annual Review of PlantPhysiology and Plant Molecular Biology*52: 689-724.

Trease, G.E. and Evans, W.C. 1997. Phytochemicals In: (Eds). *Pharmacognosy Textbook Four edition, Harcourt Brace and Company Asia PTE Limited, India* Pp.269 – 275.

Ujowundu, C.O., Ogbonna, C.U., Okwu, G.N. and Alisi, C.S. 2015.Free radicals scavenging and neuroprotective effects of ethanolic leaf extract of *Combretum zenkeri*. *Annual Research and Review in Biology* 6.2: 133-141.

Ujowundu, C.O., Okafor, O.E., Agha, N.C., Nwaogu, L.A., Igwe, K.O. and Igwe, C.U. 2010. Phytochemical and chemical composition of *Combretum zenkeri* leaves. *Journal of Medicinal Plants Research* 4.10:965-968

Van Dam, R.M., Naidoo, N. and Landberg, R. 2013. Dietary flavonoids and the development of type 2 diabetes and cardiovascular diseases: review of recent findings. *Current Opinion on Lipidology*24.1:25–33.

Van Loc, T., Nhu, V.T.Q., Van Chien, T., Ha, L.T.T., Thao, T.T.P. and Sung, T.V. 2018. Synthesis of madecassic acid derivatives and their cytotoxic activity.*Zeitschrift für Naturforschung B*73.2: 91-98.

Vargas, S., Ndjoko Ioset, K., Hay, A.E., Ioset, J.R., Wittlin, S. and Hostettmann, K. 2011. Screening medicinal plants for the detection of novel antimalarial products applying the inhibition of β-hematin formation. *Pharmaceutical and Biomedical Analysis*56:880-886.

Vázquez, L.H., Palazon, J. and Navarro-Ocaña, A. 2012. The Pentacyclic Triterpenes α, β-amyrins: A Review of Sources and Biological Activities, Phytochemicals – A Global Perspective of Their Role in Nutrition and Health, Dr Venketeshwer Rao (Ed.), ISBN: 978-953-51-0296-0. Retrieved Jun. 12, 2019, fromhttp://www.intechopen.com/books/phytochemicals-a-global-perspective-of-their-role-in-nutrition-andhealth/the-pentacyclic-triterpenes-amyrins-a-review-of-sources-and-biological-activities

Venditti, A., Lattanzi, C., Ornano, L., Maggi, F., Sanna, C., Ballero, M., Alvinao, A., Serafini, M. and Bianco, A. 2016.A new glucosidicphthalide from *Helichrysummicrophyllum*subsp. *Tyrrhenicum* from La Maddalena Island (Sardinia, Italy).*Natural Product Research* 30.7: 789-795.

Vennerstrom, J.L. andKlayman, D.L. 1988. Protoberberine alkaloids as antimalarials.*Journal of Medicinal Chemistry* 31.6: 1084–1087. DOI: 10.1021/jm00401a006

Wagner, H. and Bladt, S. 1996. Plant drug analysis- A thin layer chromatography atlas. 2nd edition, Published by Springer, New York.

Wande, O.M. and Babatunde, S.B. 2017. In vitro screening of ten Combretaceae plants for antimalarial activities applying the inhibition of beta-hematin formation. *International Journal of Biological and Chemical Science* 11.6: 2971-2981.

Wei, Z., Luo, M., Zhao, C., Wang, W., Zhang, L., Zu, Y., Li, C., Li, T. and Fu, Y. 2013. An efficientpreparative procedure for main flavone aglycones from Equisetumpalustre L. using macroporous resin followed by gel resin flash chromatography.*Separation and Purification Technology* 118: 680–689.

White, N. J., Pukrittayakamee, S., Hien, T. T., Faiz, M. A., Mokuolu, O. A., and Dondorp, A. M. 2014. Malaria. *Lancet*383.9918: 723–735. Retrieved Sept. 23, 2018, from http://doi.org/10.1016/S0140-6736(13)60024-0

White, N.J.2004. Antimalarial drug resistance.*Journal of Clinical Investigation*113:1084-1092.

WHO Global technical strategy for malaria 2016-2030. Geneva: World Health Organisation (WHO) 2015. Retrieved Oct. 15, 2018, from http://www.int/malaria/areas/global_technical_strategy/en

WHO, 2015.World Malaria Report 2015. World Health Organization, Geneva, pp. 2–57.

WHO, 2018.World Health Statistics. Retrieved Mar. 04, 2019,from http://www.who.int/gho/publications/world_health_statistics/2018/en/.

Willcox, M. 2011.Improved traditional phytomedicines in current use for the clinical treatment of malaria.*Planta Medica* 77.6:662–671. doi:10. 1055/s-0030-1250548

Willcox, M.L. and Bodeker, G. 2004. Traditional herbal medicines for Malaria.*BMJ*329:1156-1159

Wood-Sheldon, J., Balick, M. and Laird, S. 1997. *Medicinal Plants: Can Utilization and ConservationCoexist*?.The New York Botanical Ga*rden,USA.*

World Health Organization, Global report on antimalarial drug efficacy and drug resistance: 2000–2010.

World Health Organization 2015.Guidelines for the treatment of malaria 3rd edn, (World Health Organization, Geneva, 2015).

World Health Organization 2018.First malaria vaccine in Africa: A potential new tool for child health and improved malaria control (World Health Organization, Geneva, April 2018). WHO reference number: WHO/CDS/GMP/2018.05 Retrieved Mar. 04, 2019, from http://www.who.int/malaria/publications/atoz/first-malaria-vaccine/en/

World malaria report 2017. Geneva: World Health Organisation (WHO); 2017. Licence: CC BY-NC-SA 3.0 IGO Retrieved Mar. 04, 2019, from http://www.who.int/malaria/publications/world-malaria-report-2017/en/

Wozniak, L., Skapska, S. and Marszalek, K. 2015. Ursolic acid- A pentacyclictriterpenoid with a wide spectrum of pharmacological activities.*Molecules* 20: 20614-20641

Wu, Z.-J., Ouyang, M.-A., Wang, C.-Z., Zhang, Z.-K.and Shen, J.-G. 2007. Anti-Tobacco Mosaic Virus (TMV) Triterpenoid Saponins from the Leaves of *Ilex oblonga*. *Journal of Agriculture and Food Chemistry* 55: 1712-1717.

Yao, L.H., Jiang, Y.M., Shi, J., Tomás-Barberán, F.A., Datta, N., Singanusong, R.,Chen, S.S. 2004.Flavonoids in food and their health benefits.*Plant Foods for Human Nutrition* 59.3:113–122.

Yenesew, A., Derese, S., Irungu, B., Midiwo, J.O., Waters, N.C., Liyala, P., Akala, H., Heydenreich, M. and Peter, M.G. 2003.Flavonoids and isoflavonoids with antiplasmodial activities from the root bark of *Erythrina abyssinica*. *Planta Medica* 69.7:658–661. DOI: 10.1055/s-2003-41119

Zebiri, I., Haddad, M., Duca, L., Sauvain, M., Paloque, L., Cabanillas, B., Rengifo, E., Behr, J.-B.and Voutquenne-Nazabadioko, L. 2017. Biological activities of triterpenoids from *Poraqueiba sericea* stems.*Natural Products Research* 31: 1333-1338.

APPENDICES

Appendix 1: Mass spectra of CR-A

Appendix 1a: ESI-MS of CR-A

Generic Display Report

Analysis Info

Analysis Name	D:\MZ\amaZon_data\1806\CR_A_amaZon_aMSn.d	Acquisition Date	26/06/2018 14:45:43
Method	DI_MSMS.m	Operator	MSC
Sample Name	CR A NMR sample	Instrument	amaZon speed ETD
Comment	Kaehlig/Krenn/Zehl ACN/MeOH + 1% H2O		

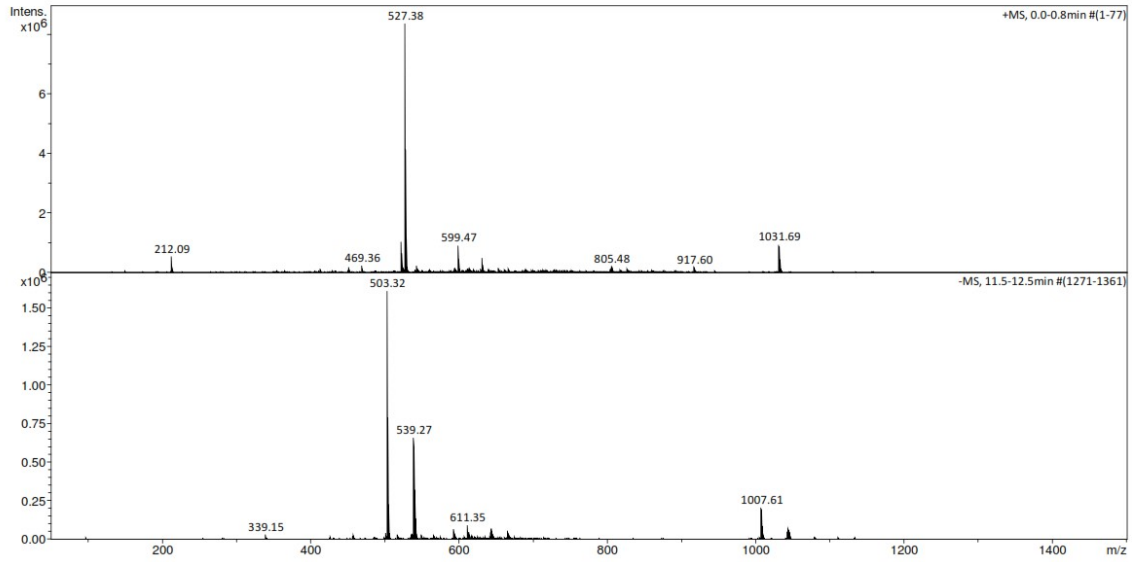

Bruker Compass DataAnalysis 4.1 printed: 15/05/2019 18:13:41 by: MSC Page 1 of 1

Generic Display Report

Analysis Info

Analysis Name	D:\MZ\amaZon_data\1806\CR_A_amaZon_aMSn.d	Acquisition Date	26/06/2018 14:45:43
Method	DI_MSMS.m	Operator	MSC
Sample Name	CR A NMR sample	Instrument	amaZon speed ETD
Comment	Kaehlig/Krenn/Zehl ACN/MeOH + 1% H2O		

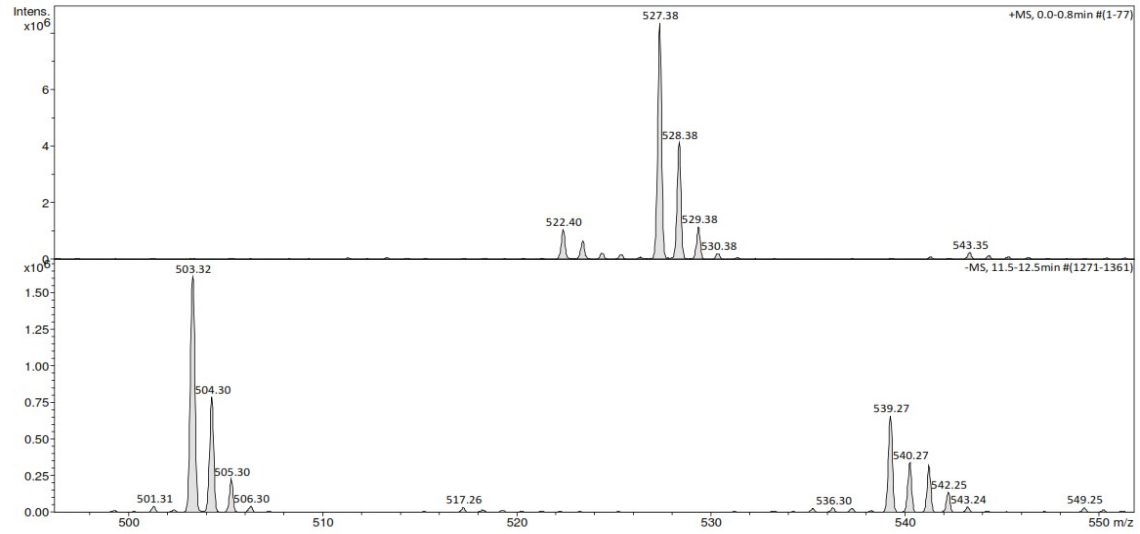

Generic Display Report

Analysis Info

Analysis Name	D:\MZ\amaZon_data\1806\CR_A_amaZon_aMSn.d	Acquisition Date	26/06/2018 14:45:43
Method	DI_MSMS.m	Operator	MSC
Sample Name	CR A NMR sample	Instrument	amaZon speed ETD
Comment	Kaehlig/Krenn/Zehl ACN/MeOH + 1% H2O		

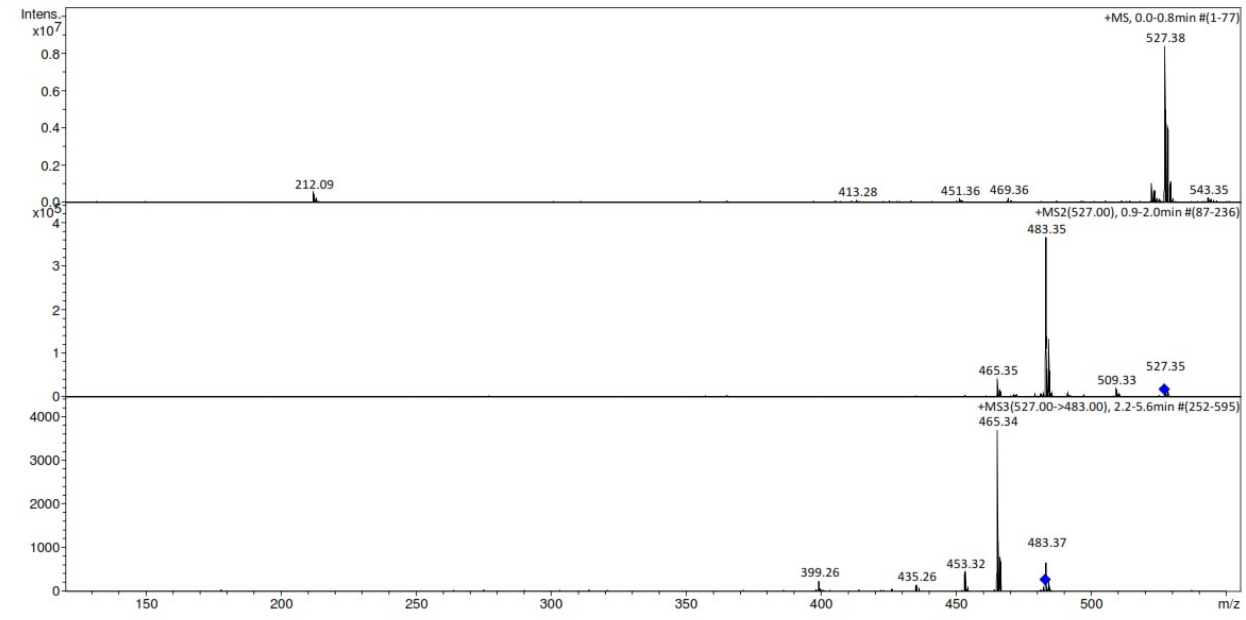

Generic Display Report

Analysis Info

Analysis Name	D:\MZ\amaZon_data\1806\CR_A_amaZon_aMSn.d	Acquisition Date	26/06/2018 14:45:43
Method	DI_MSMS.m	Operator	MSC
Sample Name	CR A NMR sample	Instrument	amaZon speed ETD
Comment	Kaehlig/Krenn/Zehl ACN/MeOH + 1% H2O		

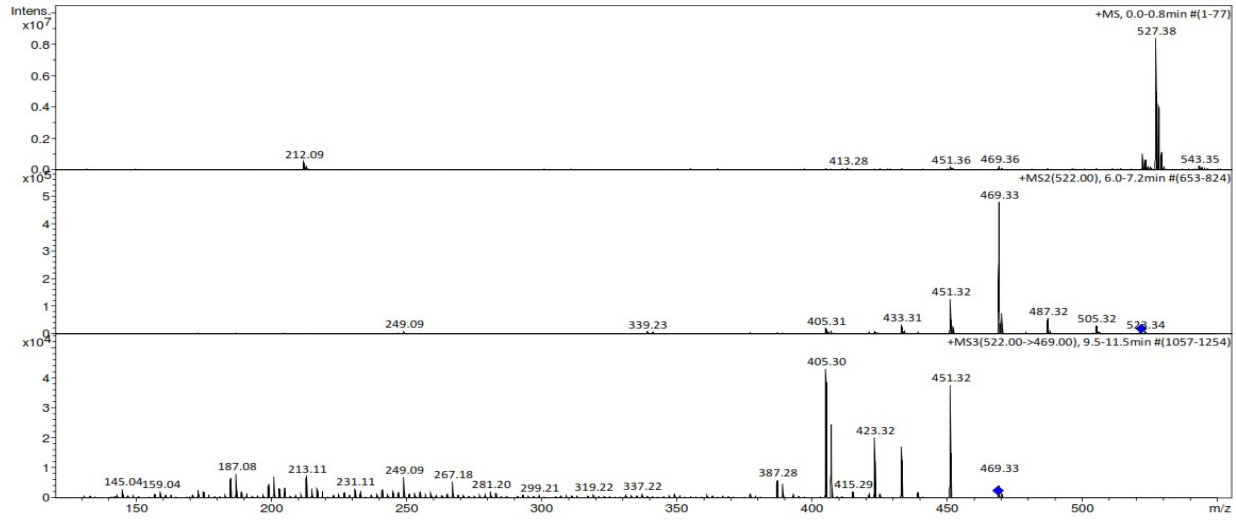

Generic Display Report

Analysis Info

Analysis Name	D:\MZ\amaZon_data\1806\CR_A_amaZon_aMSn.d	Acquisition Date	26/06/2018 14:45:43
Method	DI_MSMS.m	Operator	MSC
Sample Name	CR A NMR sample	Instrument	amaZon speed ETD
Comment	Kaehlig/Krenn/Zehl ACN/MeOH + 1% H2O		

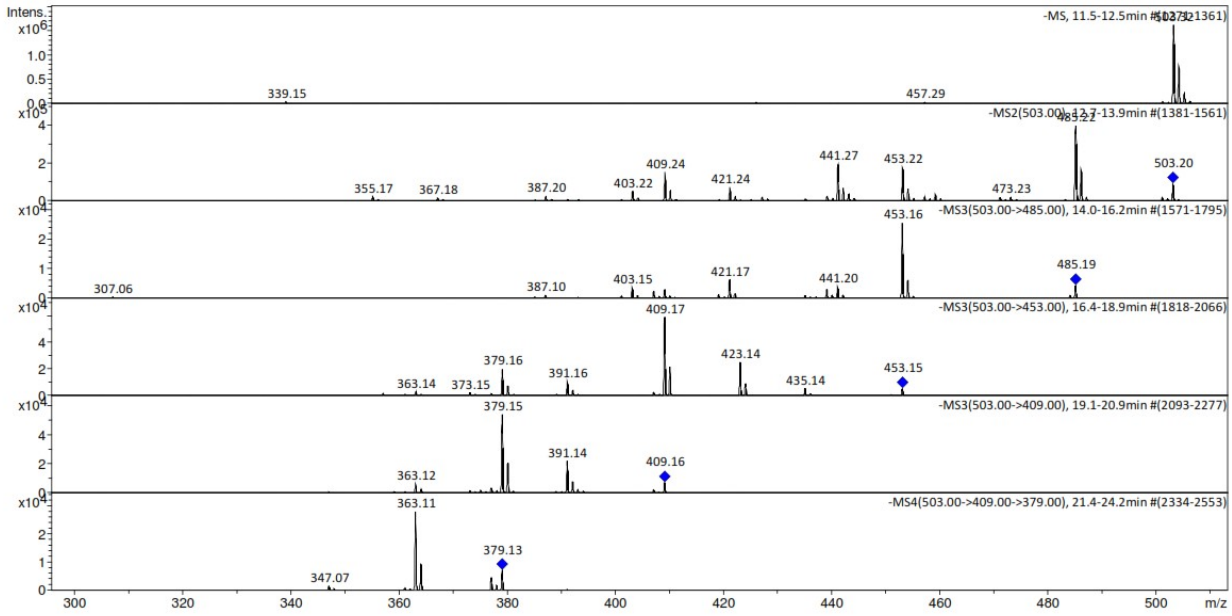

Appendix 1b: HRESI-MS of CR-A

Display Report

Analysis Info

Analysis Name	D:\MZ\maXis_data\Kaehlig_1806\CR_A_maXis_nHRESIMS.d	Acquisition Date	27/06/2018 13:38:48
Method	tune_low_MS_Service_06_18_neg.m	Operator	msc
Sample Name	CR A	Instrument	maXis 255552.00016
Comment	Kaehlig/Krenn/Zehl Ergebnis: +/- 2ppm ACN/MeOH + 1% H2O		

Acquisition Parameter

Source Type	ESI	Ion Polarity	Negative	Set Nebulizer	0.4 Bar
Focus	Not active	Set Capillary	4500 V	Set Dry Heater	180 °C
Scan Begin	50 m/z	Set End Plate Offset	-500 V	Set Dry Gas	4.0 l/min
Scan End	1900 m/z	n/a	n/a	Set Divert Valve	Source
		Set Corona	0 nA	Set APCI Heater	0 °C

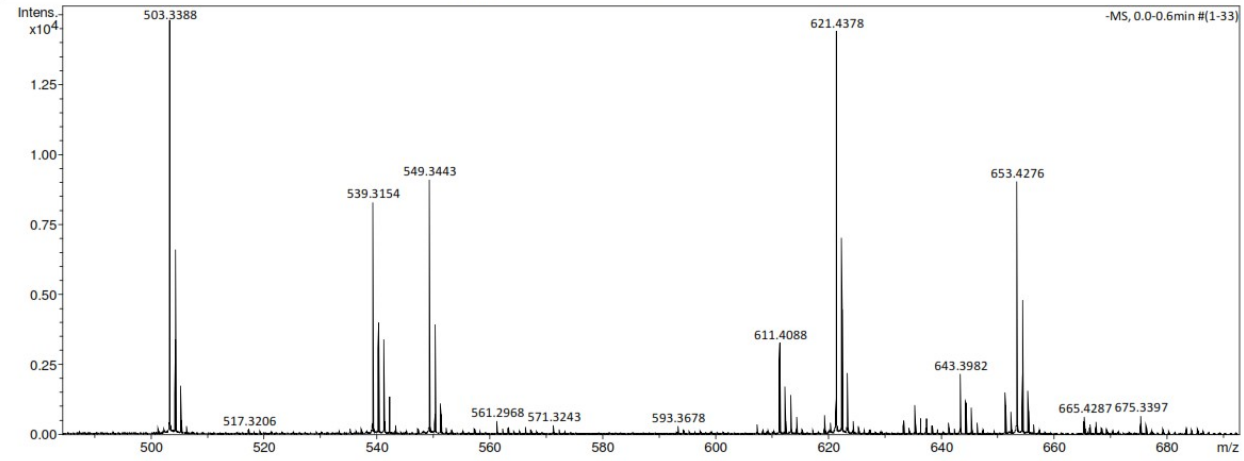

CR_A_maXis_nHRESIMS.d

Bruker Compass DataAnalysis 4.1 printed: 14/05/2019 19:26:32 by: MSC Page 1 of 1

Mass Spectrum SmartFormula Report

Analysis Info

Acquisition Date	27/06/2018 13:38:48		
Analysis Name	D:\MZ\maXis_data\Kaehlig_1806\CR_A_maXis_nHRESIMS.d		
Method	tune_low_MS_Service_06_18_neg.m	Operator	msc
Sample Name	CR A	Instrument	maXis 255552.00016
Comment	Kaehlig/Krenn/Zehl Ergebnis: +/- 2ppm ACN/MeOH + 1% H2O		

Acquisition Parameter

Source Type	ESI	Ion Polarity	Negative	Set Nebulizer	0.4 Bar
Focus	Not active	Set Capillary	4500 V	Set Dry Heater	180 °C
Scan Begin	50 m/z	Set End Plate Offset	-500 V	Set Dry Gas	4.0 l/min
Scan End	1900 m/z	n/a	n/a	Set Divert Valve	Source
		Set Corona	0 nA	Set APCI Heater	0 °C

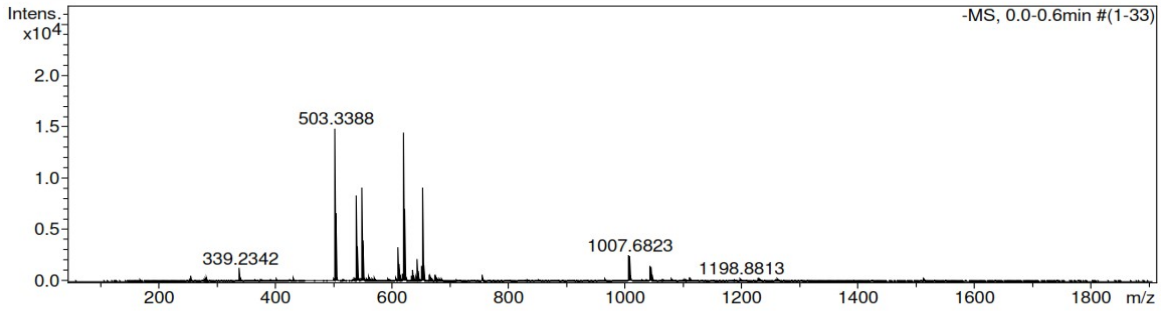

Meas. m/z	#	Ion Formula	Score	m/z	err [mDa]	err [ppm]	mSigma	rdb	e⁻ Conf	N-Rule
503.338824	1	C31H43N4O2	100.00	503.339150	0.3	0.6	52.9	12.5	even	ok
	2	C30H47O6	50.14	503.337813	1.0	2.0	63.2	7.5	even	ok
	3	C27H39N10	17.84	503.336465	2.4	4.7	65.7	13.5	even	ok

Generic Display Report

Analysis Info

		Acquisition Date	27/06/2018 12:40:35
Analysis Name	D:\MZ\maXis_data\Kaehlig_1806\CR_A_maXis_pHRESIMS.d		
Method	tune_low_MS_Service_06_18.m	Operator	msc
Sample Name	CR A	Instrument	maXis
Comment	Kaehlig/Krenn/Zehl Ergebnis: +/- 2ppm ACN/MeOH + 1% H2O		

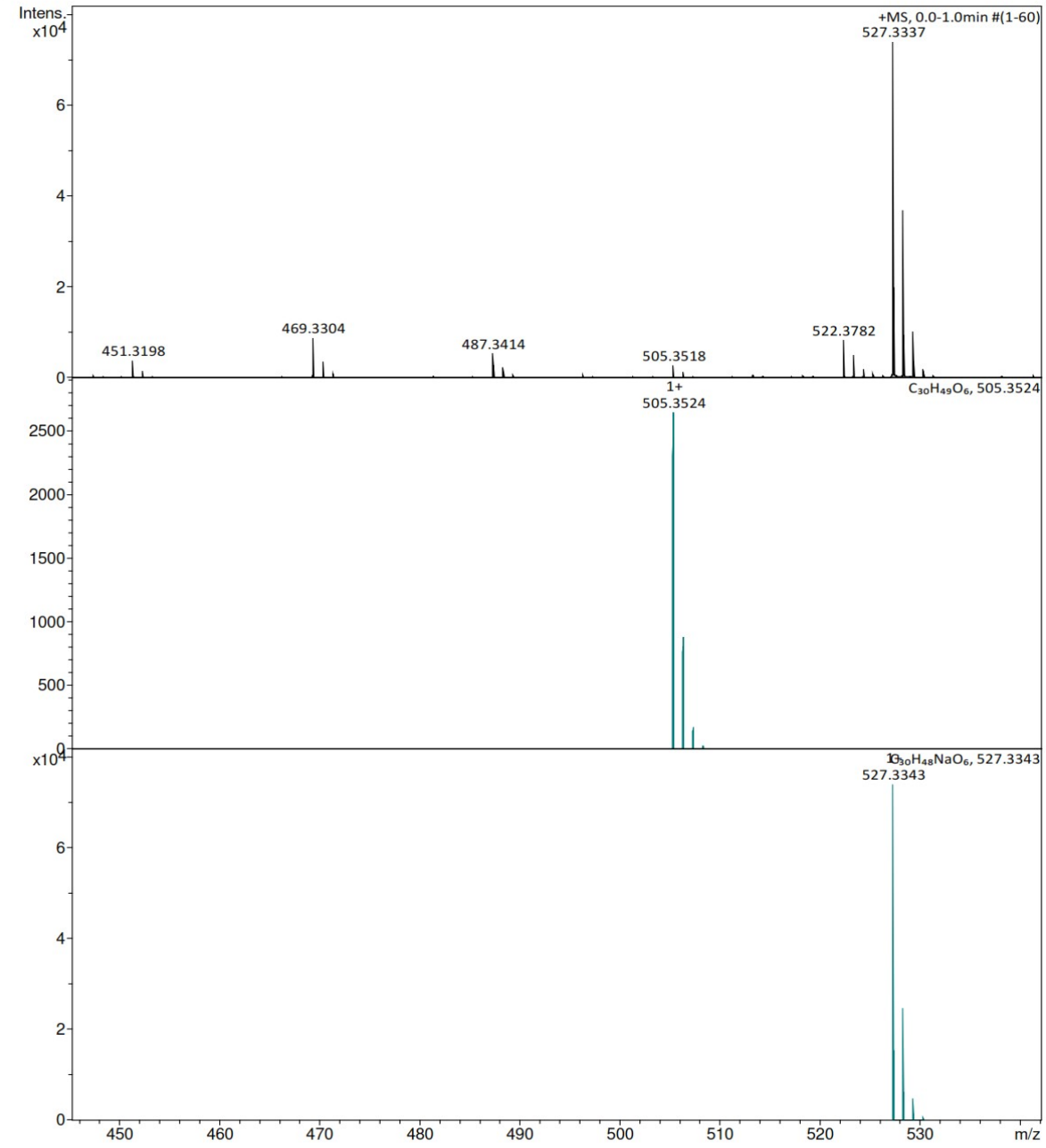

Mass Spectrum SmartFormula Report

Analysis Info

		Acquisition Date	27/06/2018 12:40:35	
Analysis Name	D:\MZ\maXis_data\Kaehlig_1806\CR_A_maXis_pHRESIMS.d			
Method	tune_low_MS_Service_06_18.m	Operator	msc	
Sample Name	CR A	Instrument	maXis	255552.00016
Comment	Kaehlig/Krenn/Zehl Ergebnis: +/- 2ppm ACN/MeOH + 1% H2O			

Acquisition Parameter

Source Type	ESI	Ion Polarity	Positive	Set Nebulizer	0.4 Bar
Focus	Not active	Set Capillary	4500 V	Set Dry Heater	180 °C
Scan Begin	50 m/z	Set End Plate Offset	-500 V	Set Dry Gas	4.0 l/min
Scan End	1900 m/z	n/a	n/a	Set Divert Valve	Source
		Set Corona	0 nA	Set APCI Heater	0 °C

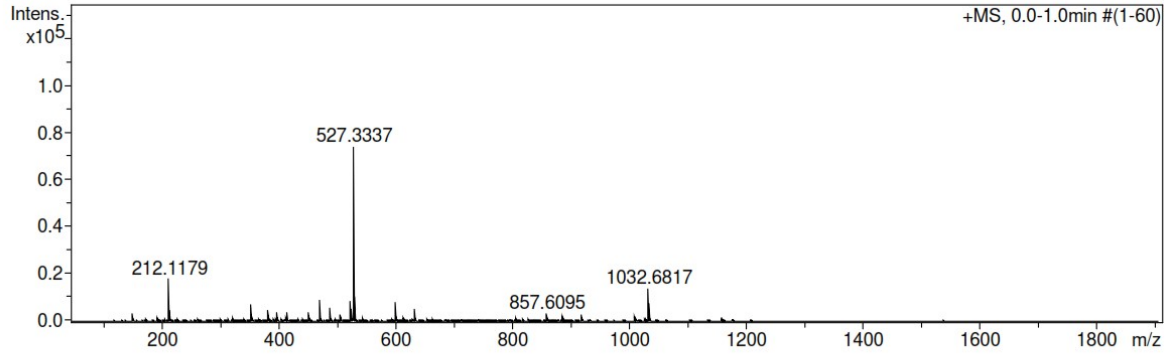

Meas. m/z	#	Ion Formula	Score	m/z	err [mDa]	err [ppm]	mSigma	rdb	e⁻ Conf	N-Rule
505.351767	1	C31H45N4O2	63.23	505.353703	-1.9	-3.8	58.8	11.5	even	ok
	2	C30H49O6	100.00	505.352366	-0.6	-1.2	69.4	6.5	even	ok
	3	C27H41N10	85.96	505.351018	-0.7	-1.5	71.4	12.5	even	ok

Appendix 2: 1D and 2D NMR of CR-A

Appendix 2a: ^{1}H NMR of CR-A

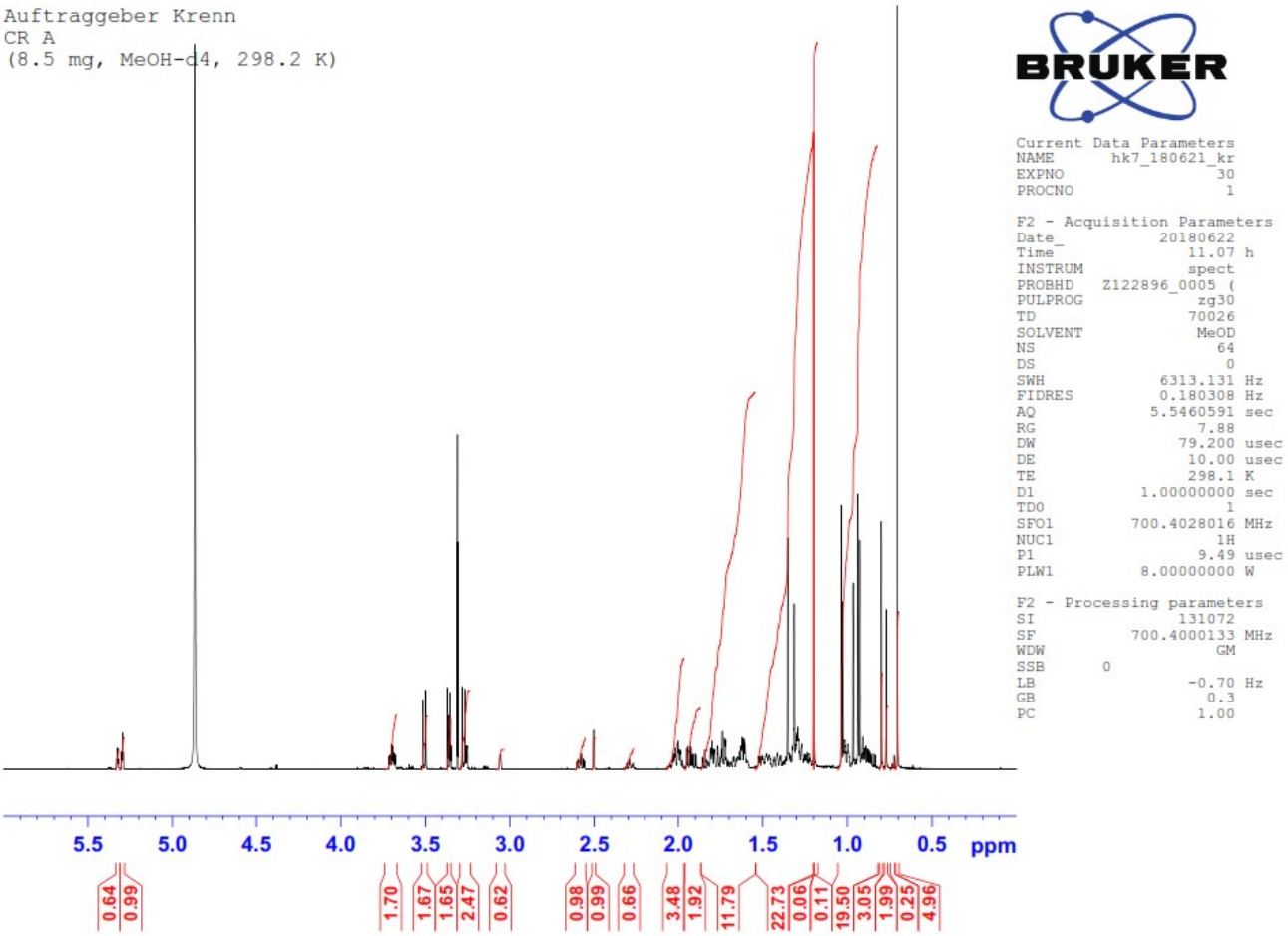

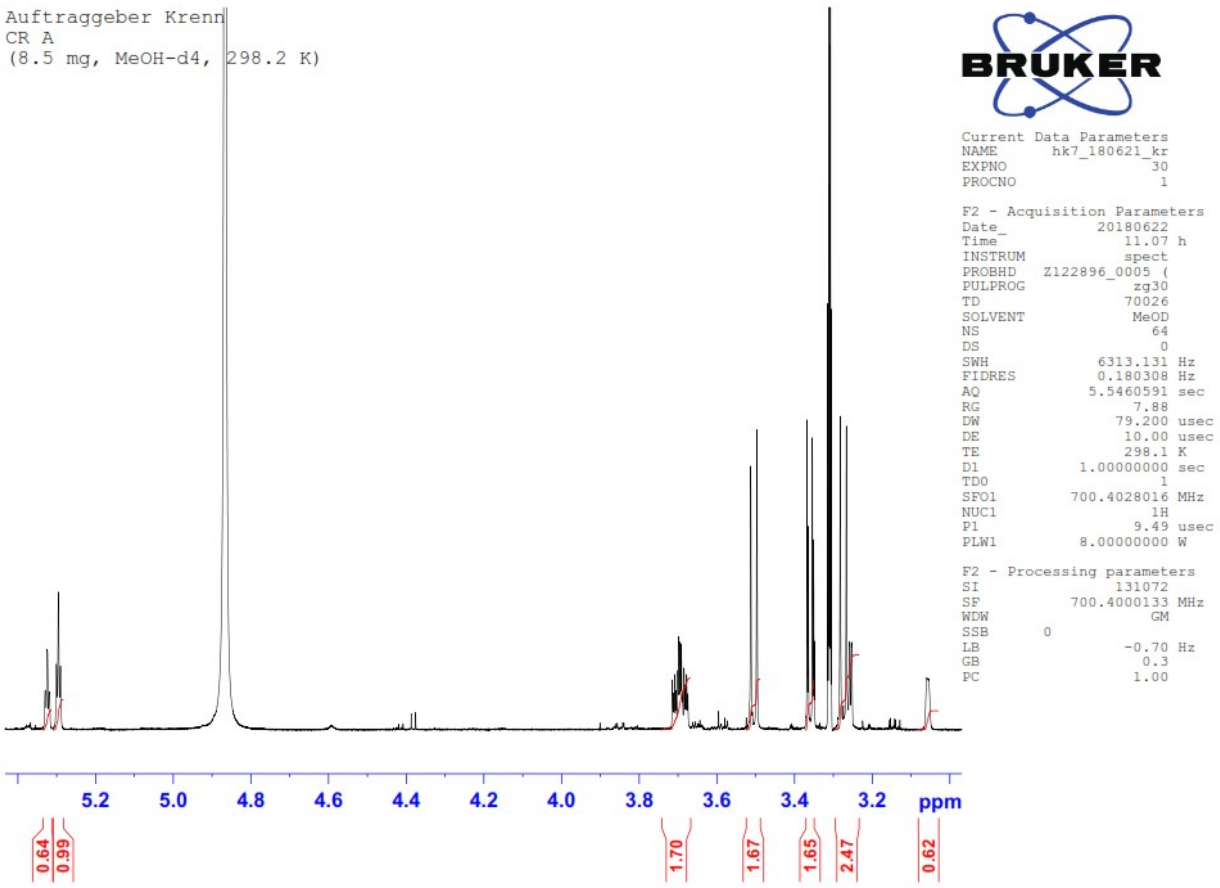
Auftraggeber Krenn
CR A
(8.5 mg, MeOH-d4, 298.2 K)
BRUKER
Current Data Parameters
NAME hk7_180621_kr
EXPNO 30
PROCNO 1
F2 - Acquisition Parameters
Date_ 20180622
Time 11.07 h
INSTRUM spect
PROBHD Z122896_0005 (
PULPROG zg30
TD 70026
SOLVENT MeOD
NS 64
DS 0
SWH 6313.131 Hz
FIDRES 0.180308 Hz
AQ 5.5460591 sec
RG 7.88
DW 79.200 usec
DE 10.00 usec
TE 298.1 K
D1 1.00000000 sec
TD0 1
SFO1 700.4028016 MHz
NUC1 1H
P1 9.49 usec
PLW1 8.00000000 W
F2 - Processing parameters
SI 131072
SF 700.4000133 MHz
WDW GM
SSB 0
LB -0.70 Hz
GB 0.3
PC 1.00
5.2
5.0
4.8
4.6
4.4
4.2
4.0
3.8
3.6
3.4
3.2
ppm
0.64
0.99
1.70
1.67
1.65
2.47
0.62

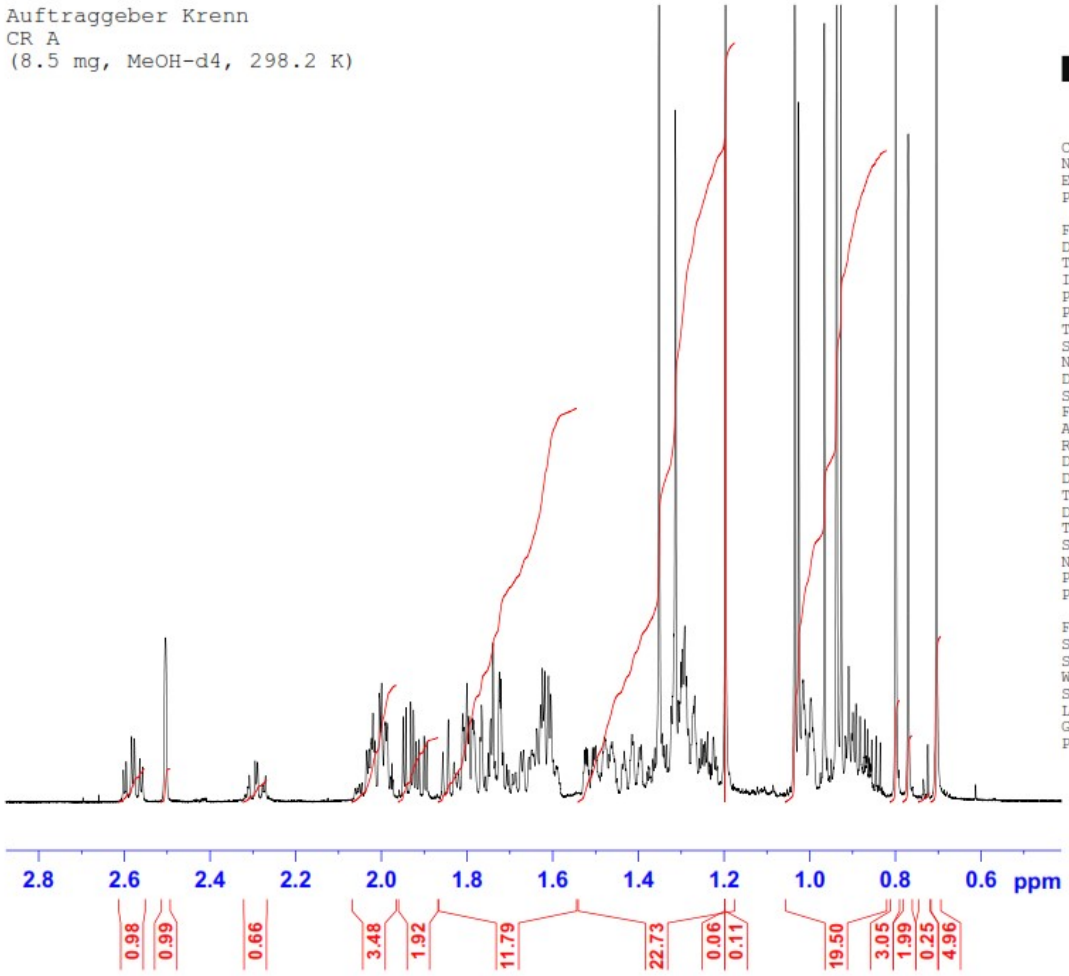


```
Current Data Parameters
NAME       hk7_180621_kr
EXPNO                 30
PROCNO                 1

F2 - Acquisition Parameters
Date_           20180622
Time              11.07 h
INSTRUM            spect
PROBHD   Z122896_0005 (
PULPROG            zg30
TD                70026
SOLVENT            MeOD
NS                   64
DS                    0
SWH            6313.131 Hz
FIDRES        0.180308 Hz
AQ            5.5460591 sec
RG                 7.88
DW               79.200 usec
DE               10.00 usec
TE               298.1 K
D1            1.00000000 sec
TD0                   1
SFO1        700.4028016 MHz
NUC1                 1H
P1                9.49 usec
PLW1         8.00000000 W

F2 - Processing parameters
SI               131072
SF          700.4000133 MHz
WDW                  GM
SSB       0
LB               -0.70 Hz
GB                  0.3
PC                 1.00
```

Appendix 2b:^{13}C NMR of CR-A

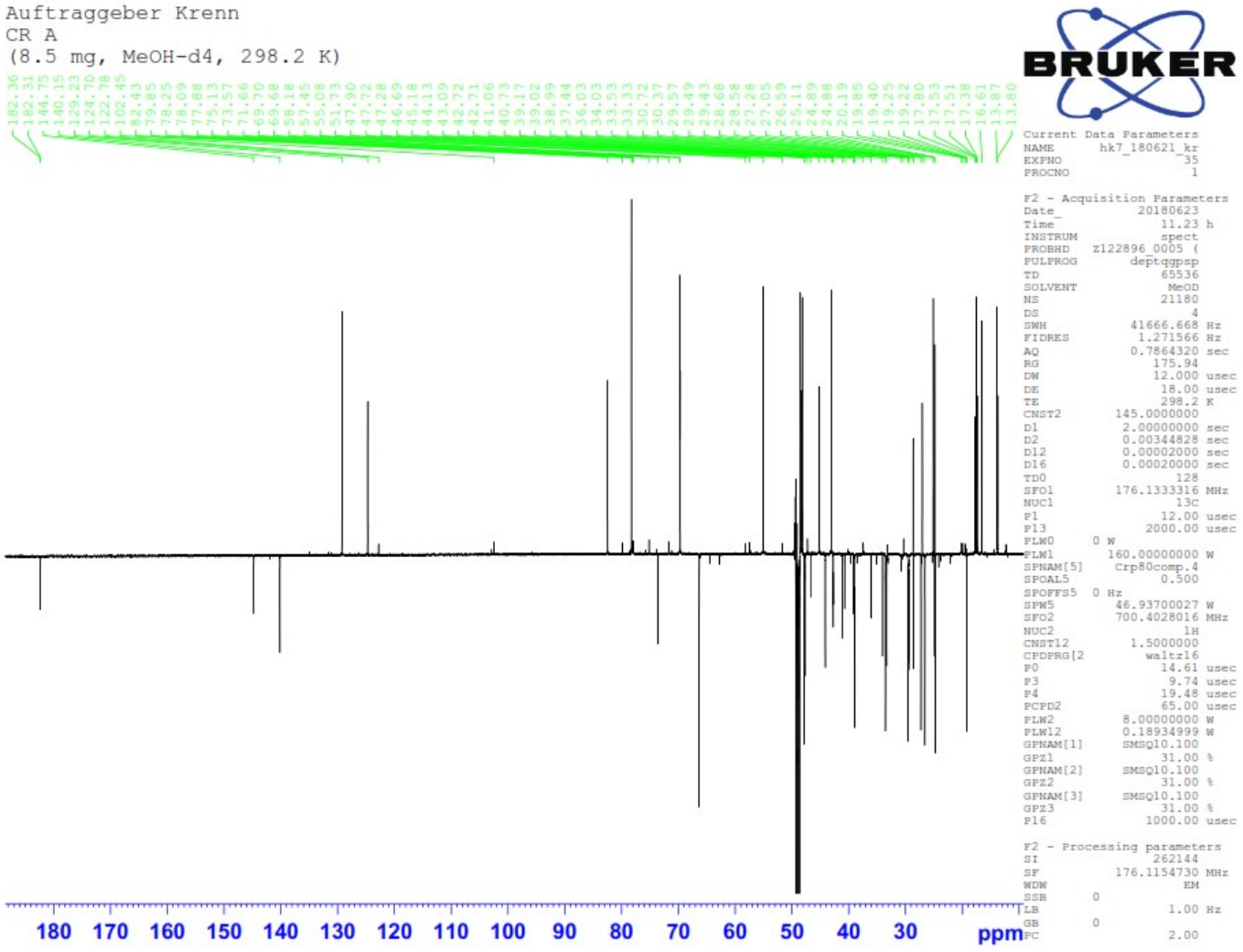

Appendix 2c: COSY of CR-A

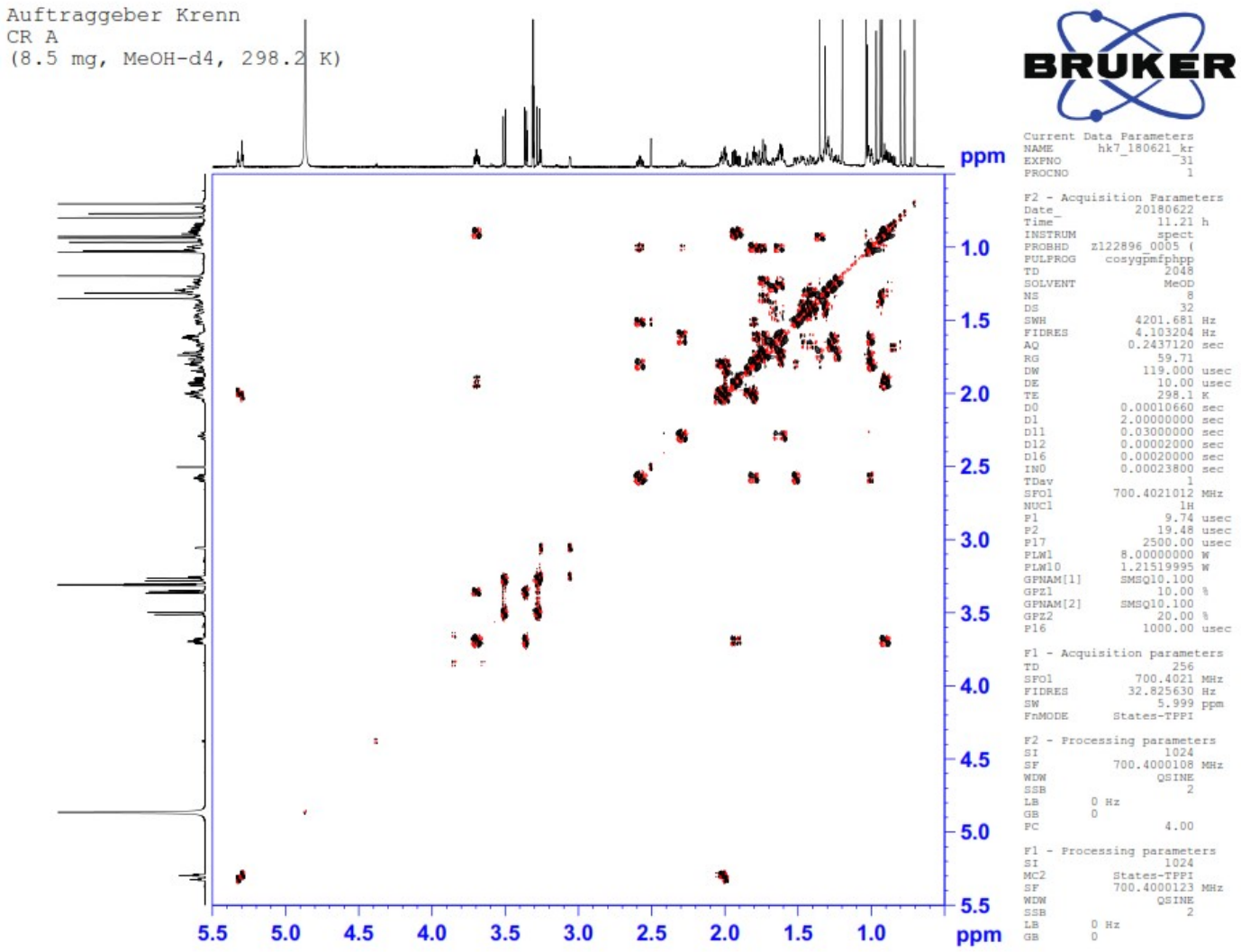

Appendix 2d: HMBC of CR-A

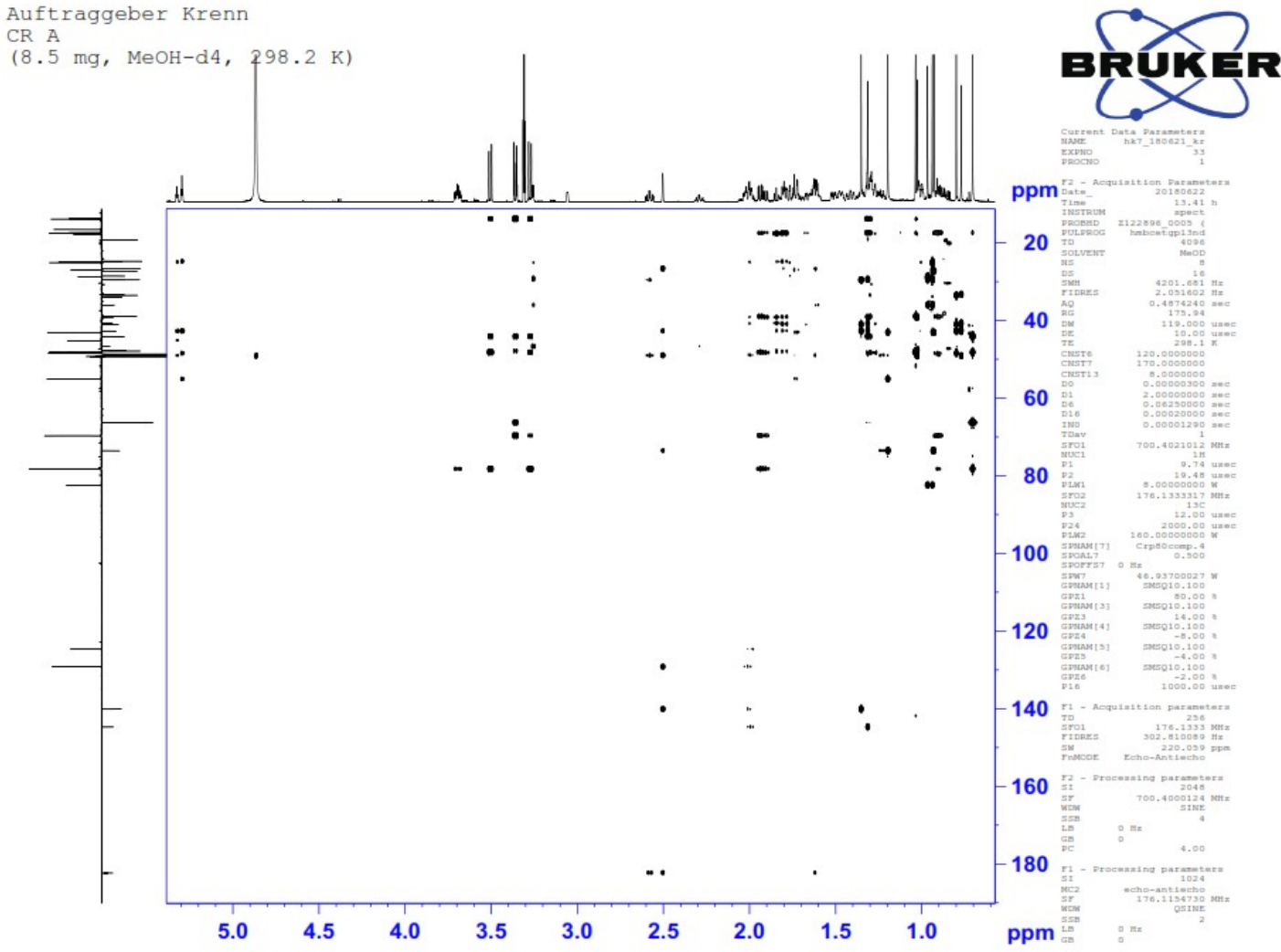

Appendix 2e: HSQC of CR-A

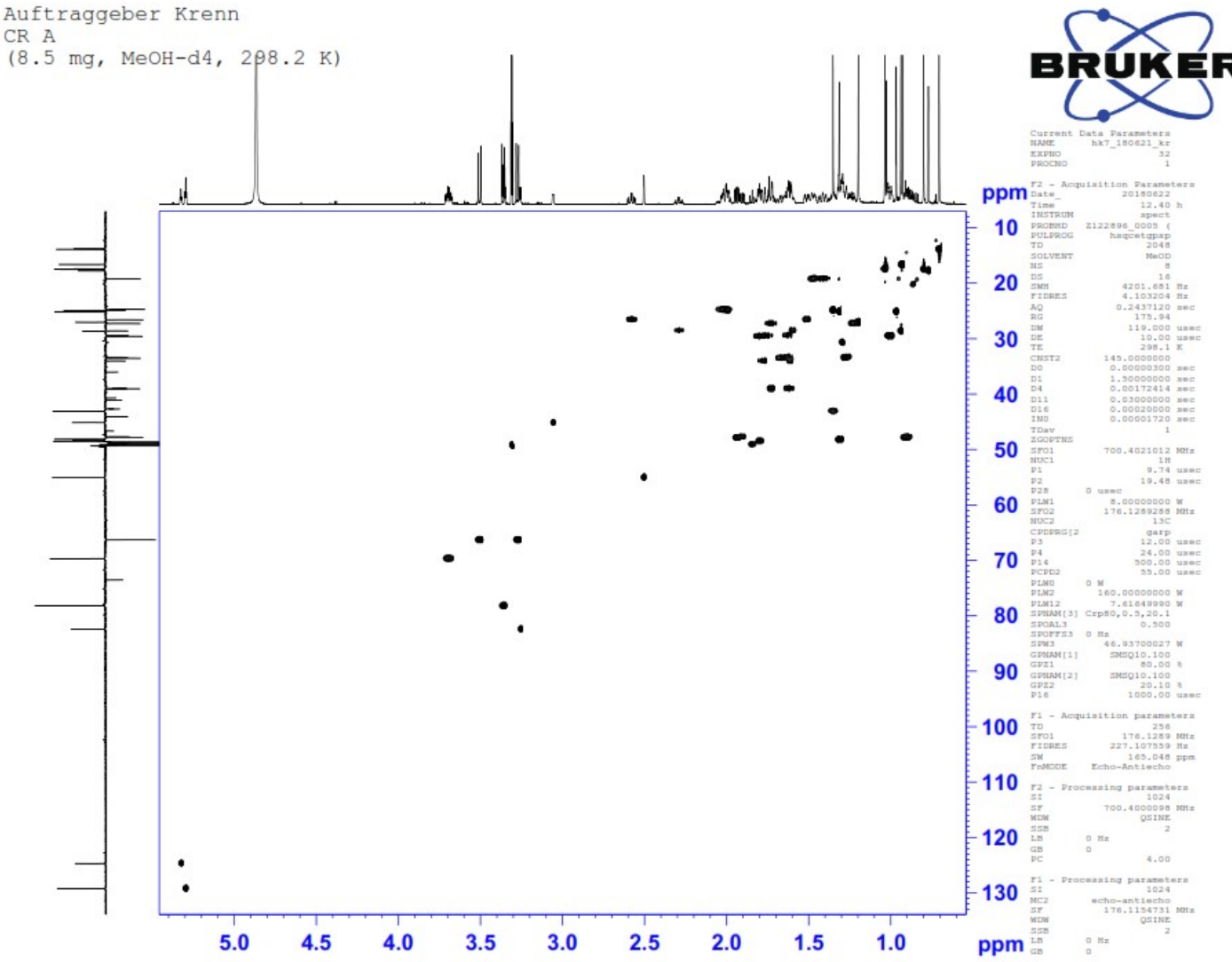

Appendix 2f: NOESY of CR-A

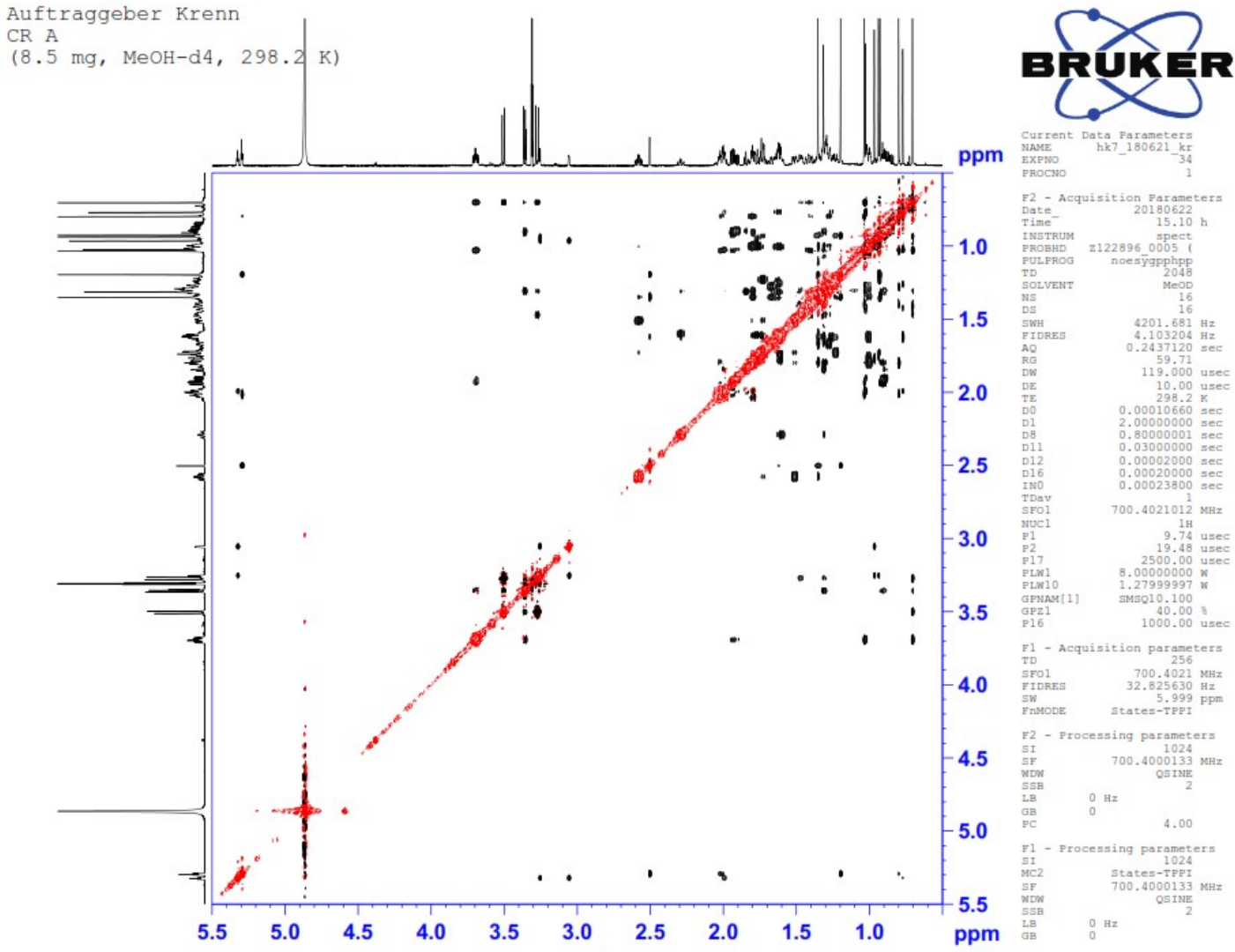

Appendix 3: Mass spectra of CR-C

Appendix 3a: ESI-MS of CR-C

Analysis Info

Acquisition Date	8/27/2018 4:37:38 PM		
Analysis Name	D:\MZ\maXis_data\1808\Krenn_Kaehlig\CR_C_amaZon_aMSn.d		
Method	DI_MSMS.m	Operator	MSC
Sample Name	CR C	Instrument	amaZon speed ETD
Comment	Kaehlig/Krenn/Zehl ACN / MeOH + 1% H2O		

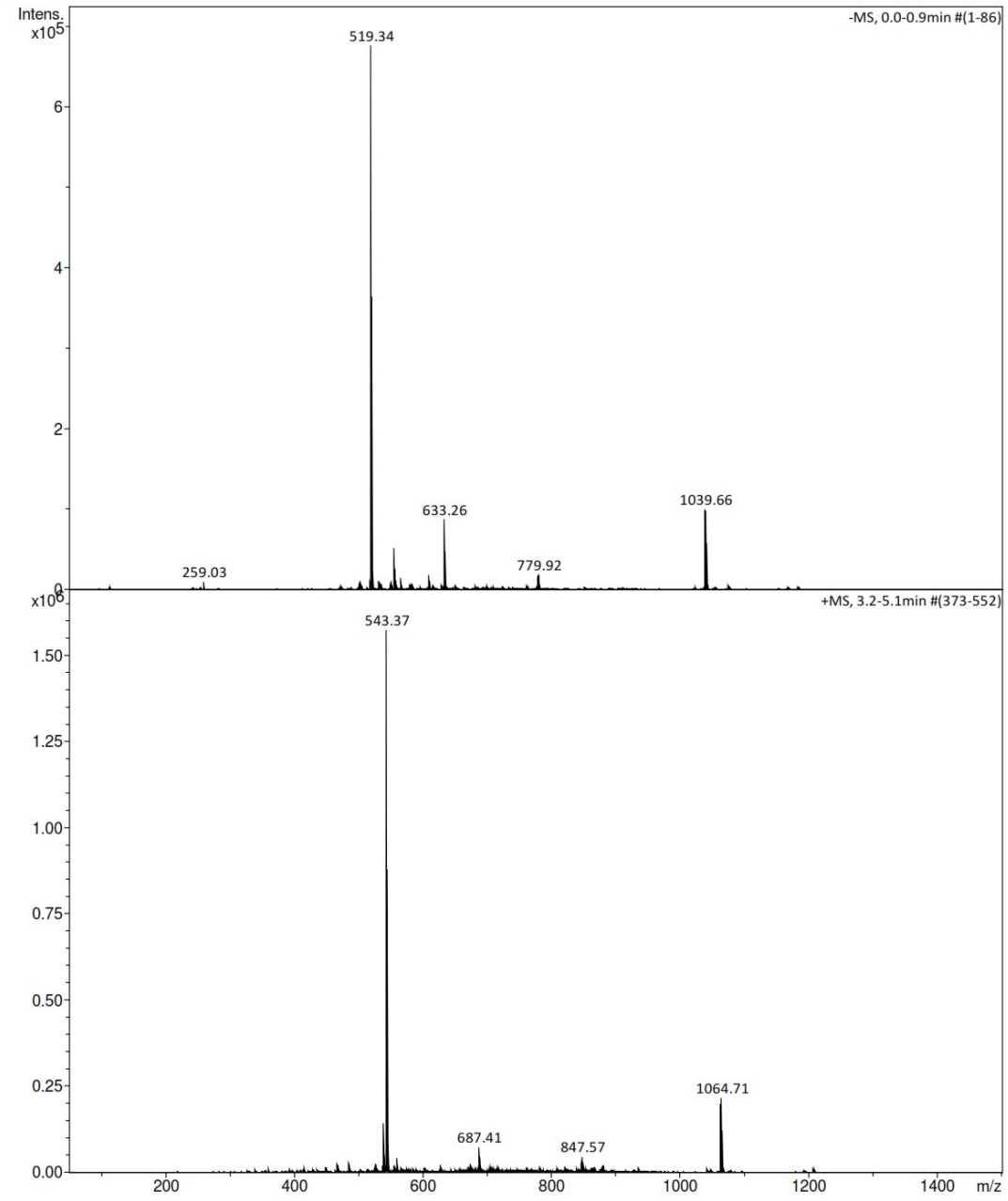

Bruker Compass DataAnalysis 4.1 printed: 8/28/2018 10:23:45 AM by: MSC Page 1 of 1

Analysis Info

Acquisition Date	8/27/2018 4:37:38 PM		
Analysis Name	D:\MZ\maXis_data\1808\Krenn_Kaehlig\CR_C_amaZon_aMSn.d		
Method	DI_MSMS.m	Operator	MSC
Sample Name	CR C	Instrument	amaZon speed ETD
Comment	Kaehlig/Krenn/Zehl ACN / MeOH + 1% H2O		

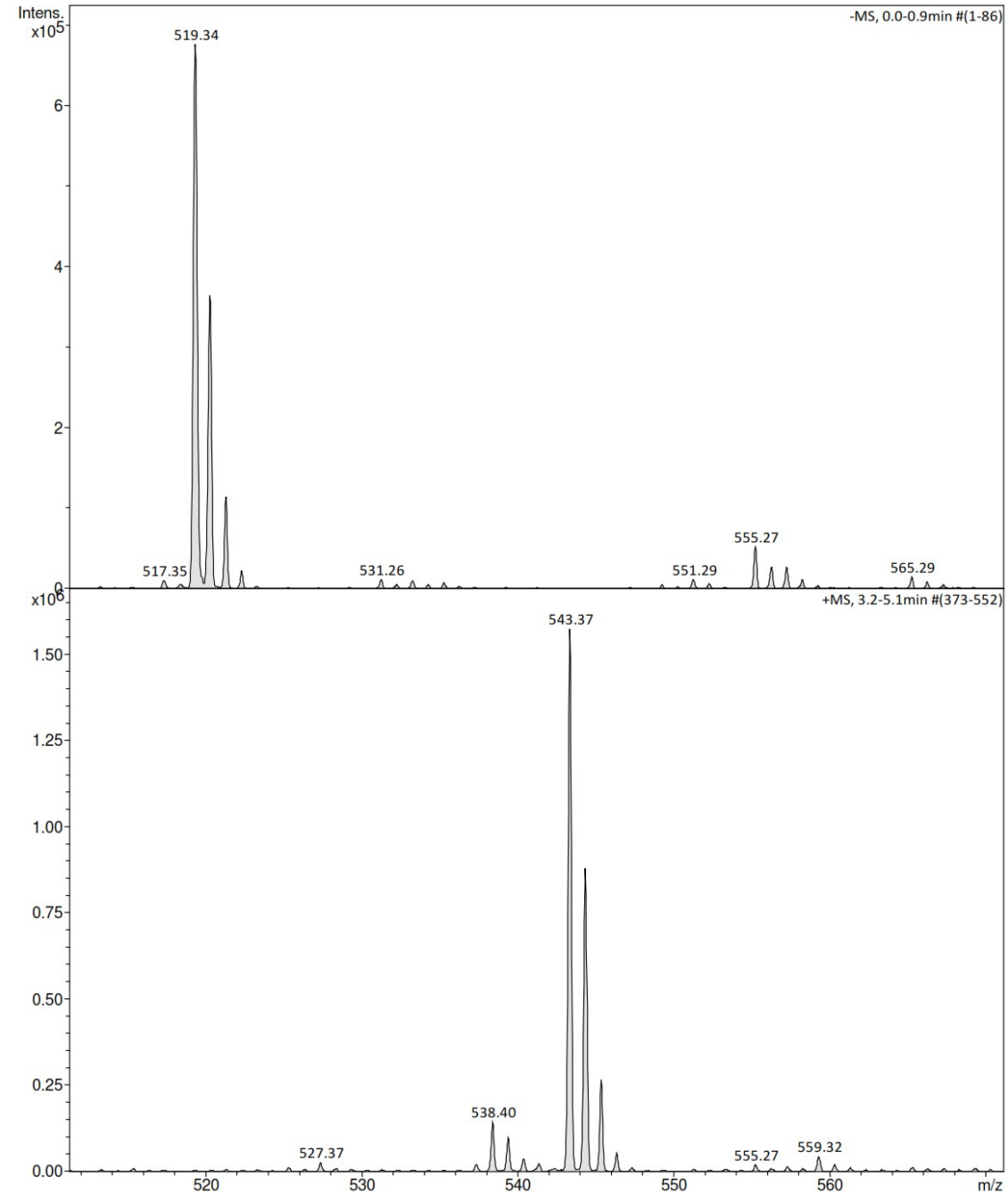

Analysis Info

Analysis Name	D:\MZ\maXis_data\1808\Krenn_Kaehlig\CR_C_amaZon_aMSn.d	Acquisition Date	8/27/2018 4:37:38 PM
Method	DI_MSMS.m	Operator	MSC
Sample Name	CR C	Instrument	amaZon speed ETD
Comment	Kaehlig/Krenn/Zehl ACN / MeOH + 1% H2O		

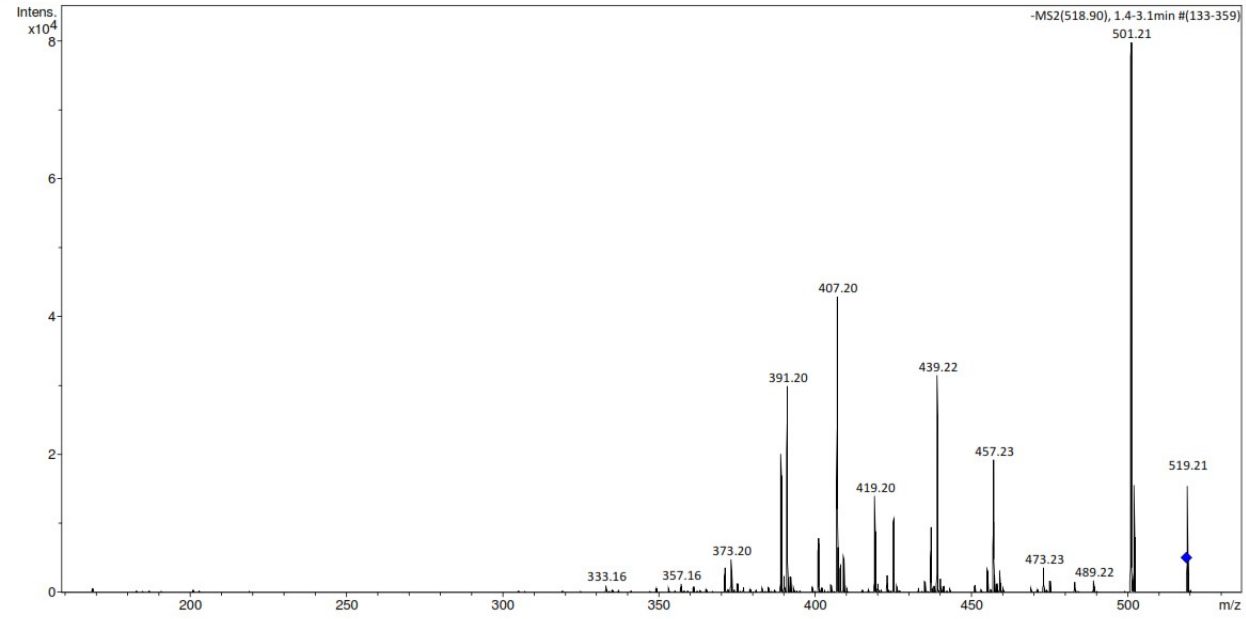

Analysis Info

Analysis Name	D:\MZ\maXis_data\1808\Krenn_Kaehlig\CR_C_amaZon_aMSn.d	Acquisition Date	8/27/2018 4:37:38 PM
Method	DI_MSMS.m	Operator	MSC
Sample Name	CR C	Instrument	amaZon speed ETD
Comment	Kaehlig/Krenn/Zehl ACN / MeOH + 1% H2O		

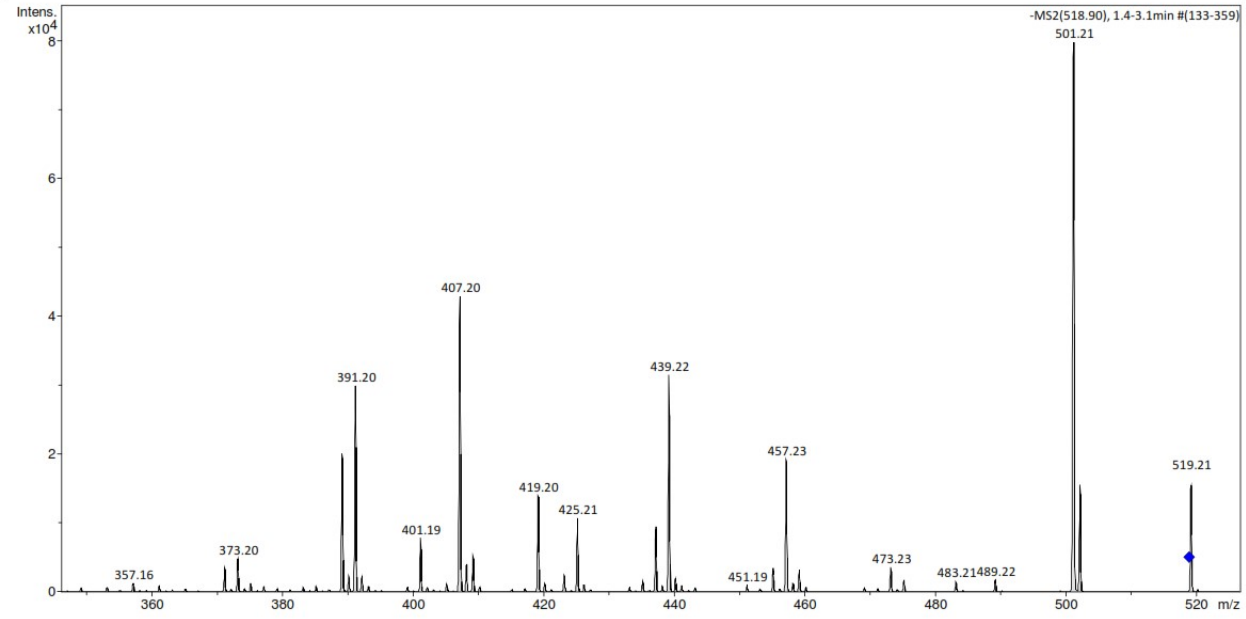

Analysis Info

Analysis Name	D:\MZ\maXis_data\1808\Krenn_Kaehlig\CR_C_amaZon_aMSn.d	Acquisition Date	8/27/2018 4:37:38 PM
Method	DI_MSMS.m	Operator	MSC
Sample Name	CR C	Instrument	amaZon speed ETD
Comment	Kaehlig/Krenn/Zehl ACN / MeOH + 1% H2O		

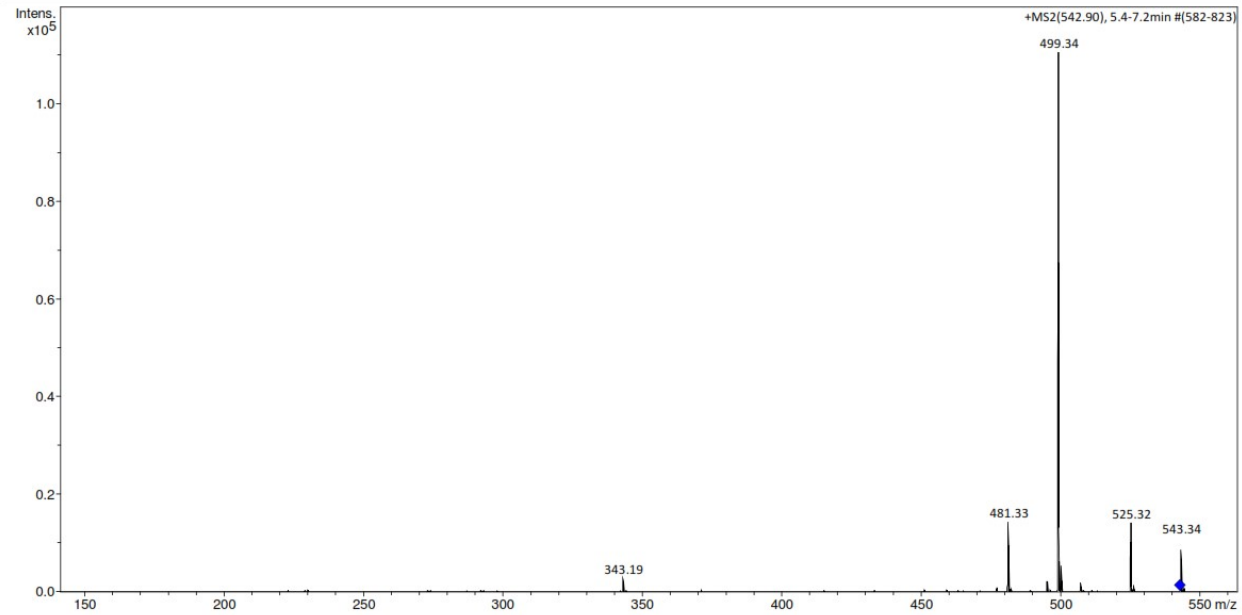

Appendix 3b: HRESI-MS of CR-C

Analysis Info

Analysis Name	D:\MZ\maXis_data\1808\Krenn_Kaehlig\59023000001.d	Acquisition Date	8/20/2018 12:01:10 PM
Method	tune_low_MS_Service_08_18.m	Operator	msc
Sample Name	CRC	Instrument	maXis
Comment	Kaehlig-Zehl/Anorg.Chem Ergebnis: +/- 5ppm ACN/MeOH +1%H2O		

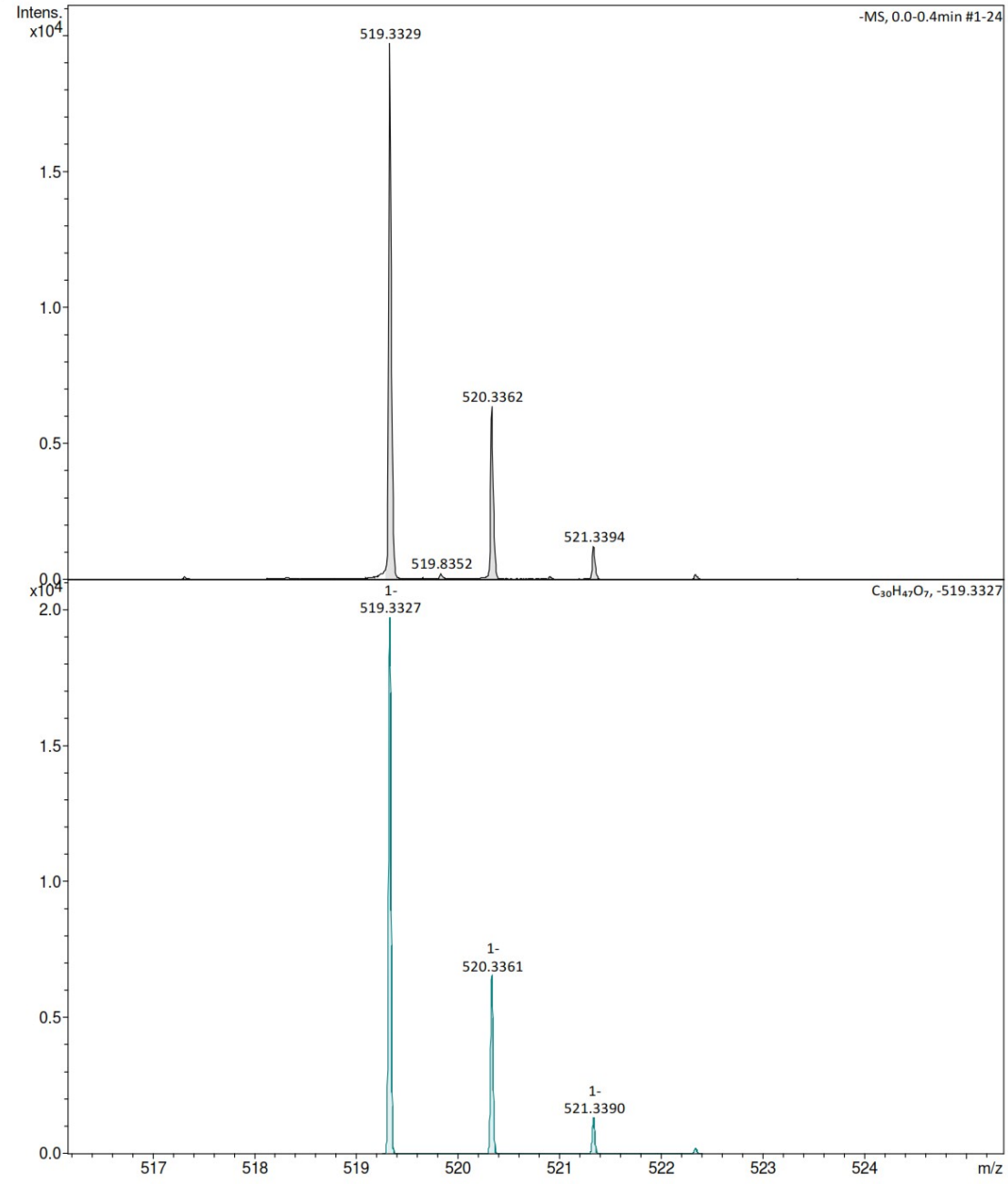

Bruker Compass DataAnalysis 4.1 printed: 8/27/2018 2:53:19 PM by: MSC Page 1 of 1

Mass Spectrum SmartFormula Report

Analysis Info

Analysis Name	D:\MZ\maXis_data\1808\Krenn_Kaehlig\59023000001.d	Acquisition Date	8/20/2018 12:01:10 PM
Method	tune_low_MS_Service_08_18.m	Operator	msc
Sample Name	CRC	Instrument	maXis 255552.00016
Comment	Kaehlig-Zehl/Anorg.Chem Ergebnis: +/- 5ppm ACN/MeOH +1%H2O		

Acquisition Parameter

Source Type	ESI	Ion Polarity	Negative	Set Nebulizer	0.4 Bar
Focus	Not active	Set Capillary	4500 V	Set Dry Heater	180 °C
Scan Begin	50 m/z	Set End Plate Offset	-500 V	Set Dry Gas	4.0 l/min
Scan End	1900 m/z	Set Charging Voltage	0 V	Set Divert Valve	Source
		Set Corona	0 nA	Set APCI Heater	0 °C

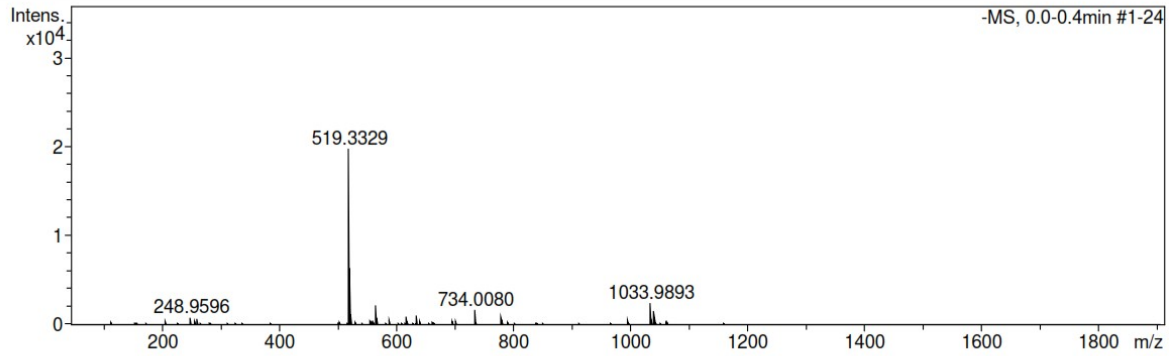

Meas. m/z	#	Ion Formula	Score	m/z	err [mDa]	err [ppm]	mSigma	rdb	e⁻ Conf	N-Rule
519.3329	1	C30H47O7	100.00	519.3327	0.2	0.3	5.5	7.5	even	ok
	2	C27H39N10O	47.65	519.3314	1.5	2.9	6.2	13.5	even	ok
	3	C31H43N4O3	47.84	519.3341	1.2	2.3	16.6	12.5	even	ok
565.3381	1	C31H49O9	100.00	565.3382	0.2	0.3	8.0	7.5	even	ok

Analysis Info

Analysis Name	D:\MZ\maXis_data\1808\Krenn_Kaehlig\59023000002.d	Acquisition Date	8/20/2018 12:54:03 PM
Method	tune_low_MS_Service_08_18.m	Operator	msc
Sample Name	CRC	Instrument	maXis
Comment	Kaehlig-Zehl/Anorg.Chem Ergebnis: +/- 5ppm ACN/MeOH +1%H2O		

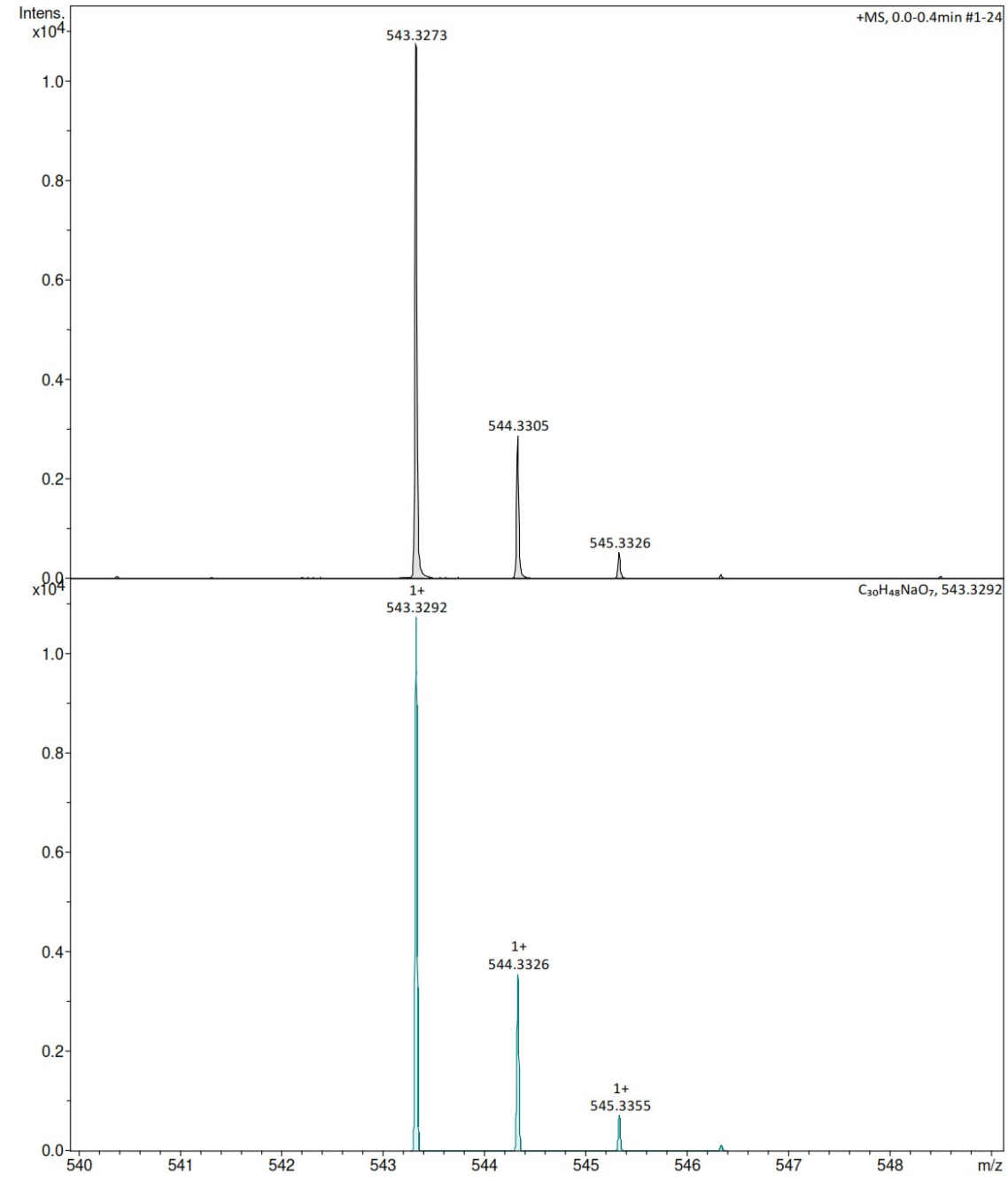

Mass Spectrum SmartFormula Report

Analysis Info

Analysis Name	D:\MZ\maXis_data\1808\Krenn_Kaehlig\59023000002.d	Acquisition Date	8/20/2018 12:54:03 PM	
Method	tune_low_MS_Service_08_18.m	Operator	msc	
Sample Name	CRC	Instrument	maXis	255552.00016
Comment	Kaehlig-Zehl/Anorg.Chem Ergebnis: +/- 5ppm ACN/MeOH +1%H2O			

Acquisition Parameter

Source Type	ESI	Ion Polarity	Positive	Set Nebulizer	0.4 Bar
Focus	Not active	Set Capillary	4500 V	Set Dry Heater	180 °C
Scan Begin	50 m/z	Set End Plate Offset	-500 V	Set Dry Gas	4.0 l/min
Scan End	1900 m/z	Set Charging Voltage	0 V	Set Divert Valve	Source
		Set Corona	0 nA	Set APCI Heater	0 °C

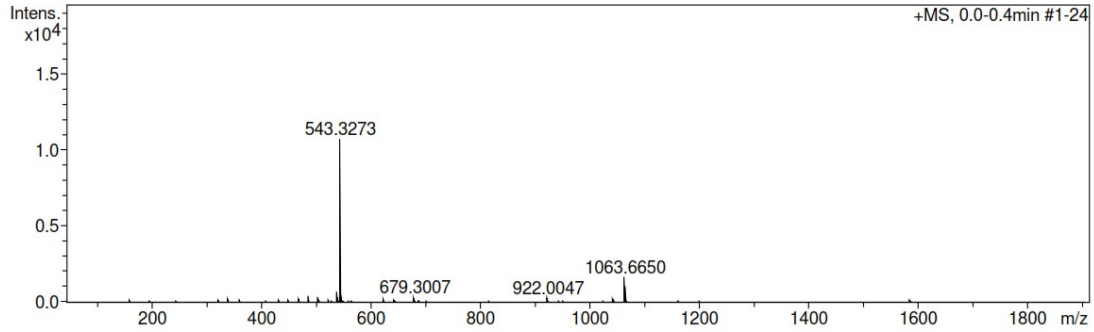

Meas. m/z	#	Ion Formula	Score	m/z	err [mDa]	err [ppm]	mSigma	rdb	e⁻ Conf	N-Rule
543.3273	1	C25H48N2NaO9	51.82	543.3252	2.1	3.8	11.1	2.5	even	ok
	2	C26H44N6NaO5	100.00	543.3265	-0.8	-1.4	21.5	7.5	even	ok
	3	C27H40N10NaO	83.41	543.3279	-0.6	-1.1	32.9	12.5	even	ok
	4	C30H48NaO7	35.29	543.3292	-1.9	-3.6	33.9	6.5	even	ok

Appendix 4: 1D and 2D NMR of CR-C

Appendix 4a: ^{1}H NMR of CR-C

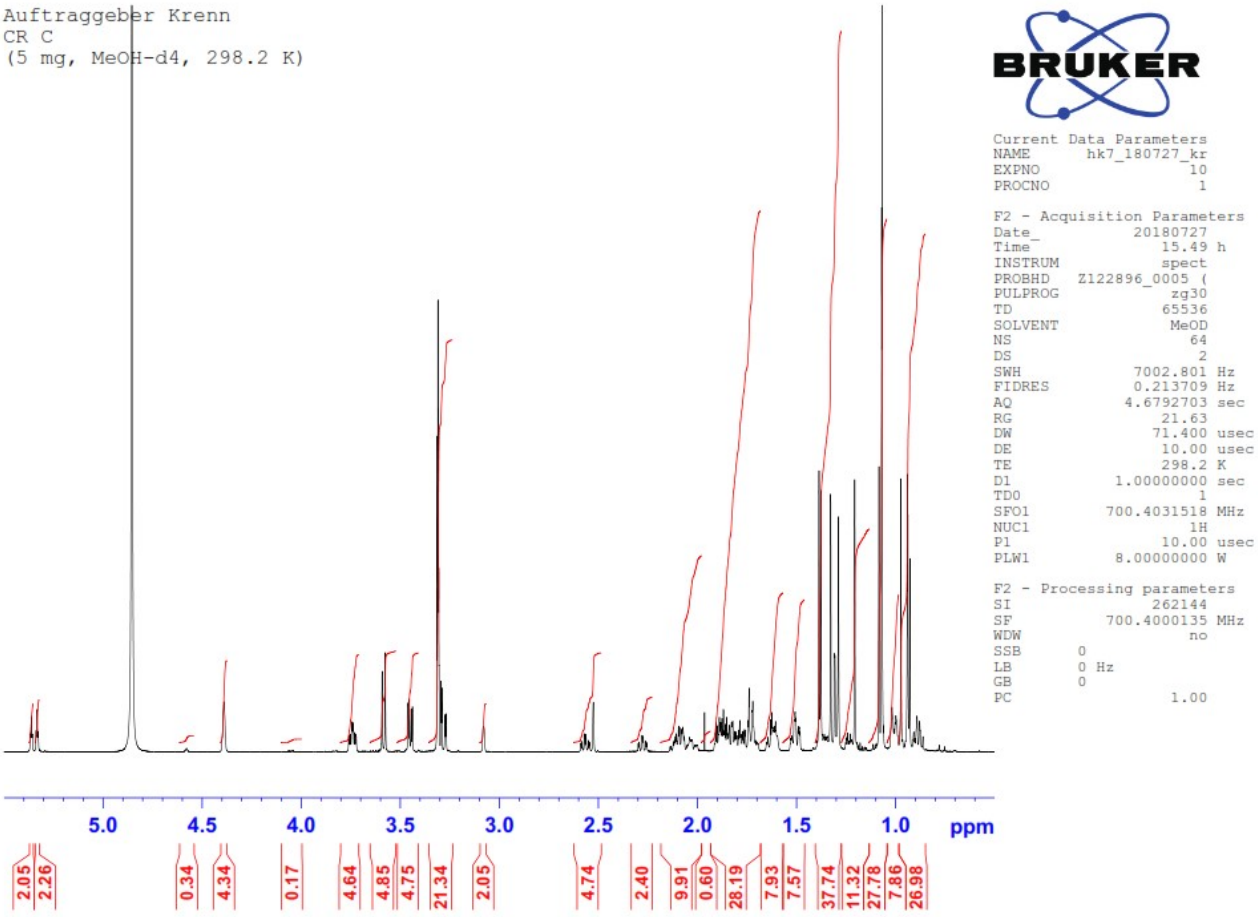

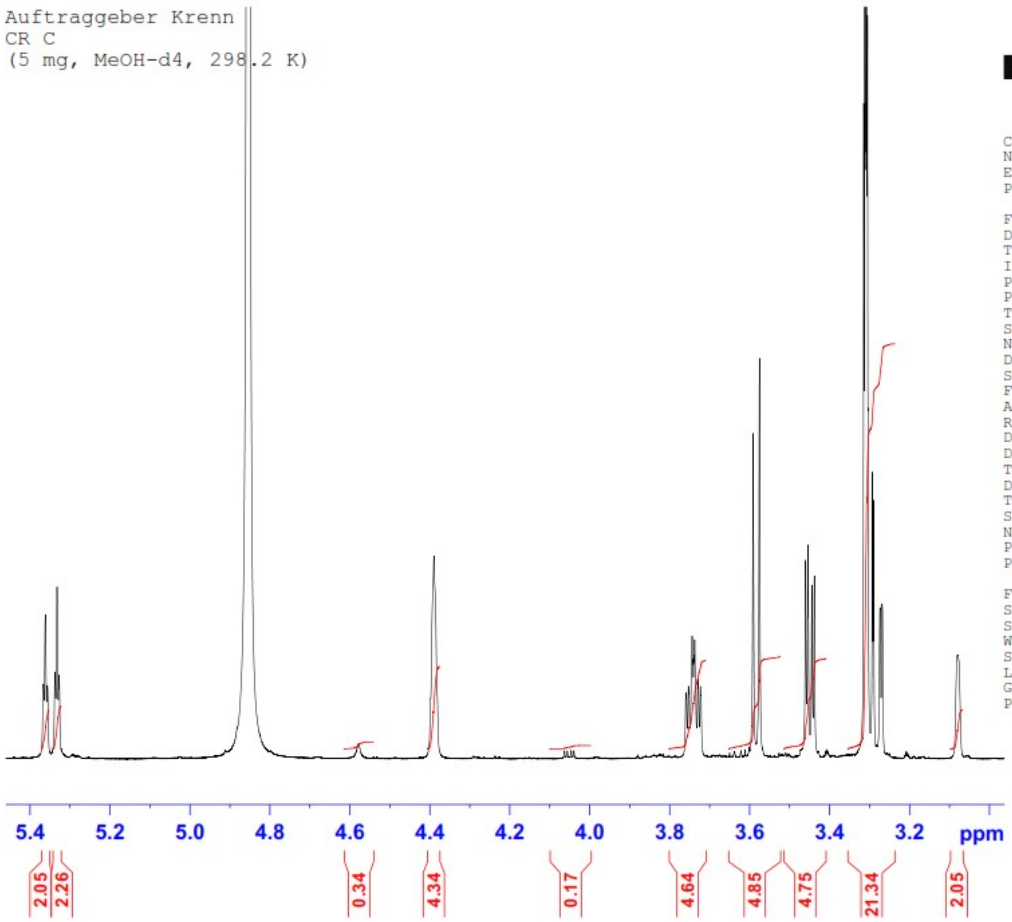

BRUKER

Current Data Parameters
NAME hk7_180727_kr
EXPNO 10
PROCNO 1

F2 - Acquisition Parameters
Date_ 20180727
Time 15.49 h
INSTRUM spect
PROBHD Z122896_0005 (
PULPROG zg30
TD 65536
SOLVENT MeOD
NS 64
DS 2
SWH 7002.801 Hz
FIDRES 0.213709 Hz
AQ 4.6792703 sec
RG 21.63
DW 71.400 usec
DE 10.00 usec
TE 298.2 K
D1 1.00000000 sec
TD0 1
SFO1 700.4031518 MHz
NUC1 1H
P1 10.00 usec
PLW1 8.00000000 W

F2 - Processing parameters
SI 262144
SF 700.4000135 MHz
WDW no
SSB 0
LB 0 Hz
GB 0
PC 1.00

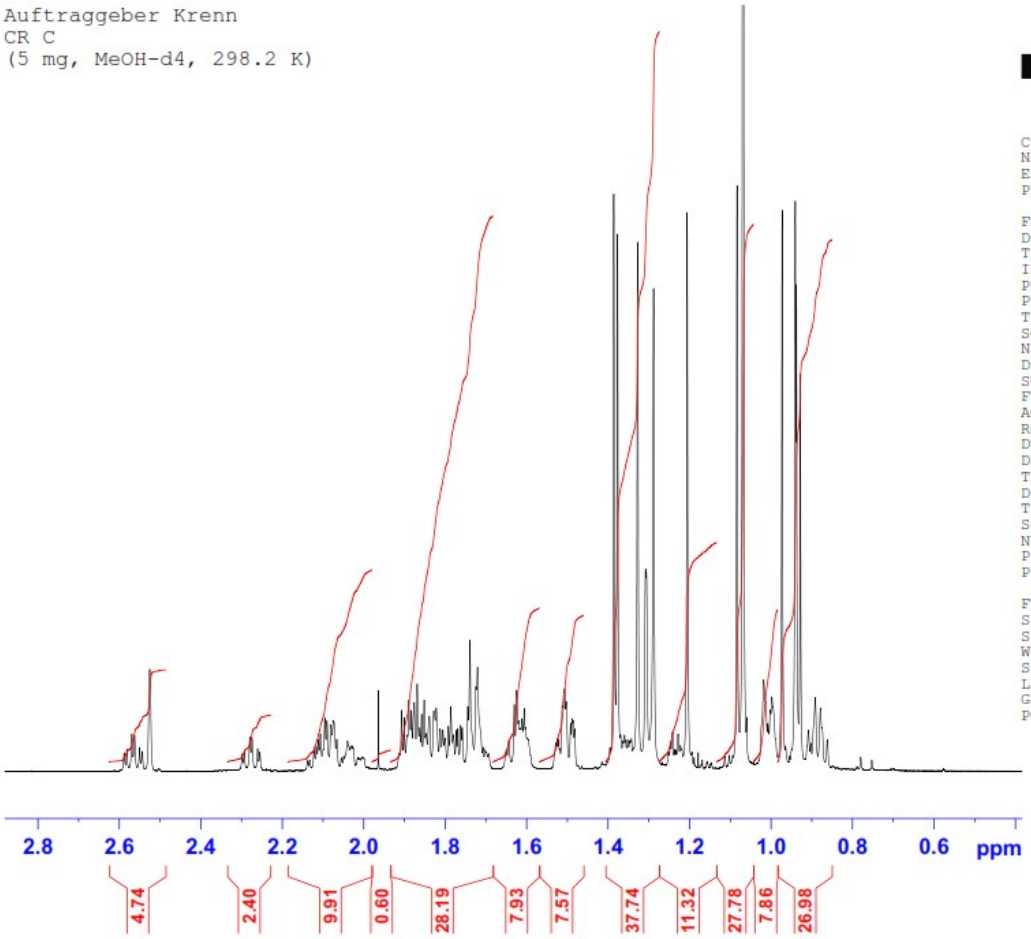

BRUKER

```
Current Data Parameters
NAME       hk7_180727_kr
EXPNO                 10
PROCNO                 1

F2 - Acquisition Parameters
Date_           20180727
Time              15.49 h
INSTRUM             spect
PROBHD   Z122896_0005 (
PULPROG             zg30
TD                 65536
SOLVENT             MeOD
NS                    64
DS                     2
SWH             7002.801 Hz
FIDRES          0.213709 Hz
AQ              4.6792703 sec
RG                 21.63
DW                71.400 usec
DE                10.00 usec
TE                298.2 K
D1             1.00000000 sec
TD0                    1
SFO1         700.4031518 MHz
NUC1                  1H
P1                 10.00 usec
PLW1          8.00000000 W

F2 - Processing parameters
SI                262144
SF           700.4000135 MHz
WDW                   no
SSB       0
LB        0 Hz
GB        0
PC                  1.00
```

Appendix 4b: ^{13}C NMR of CR-C

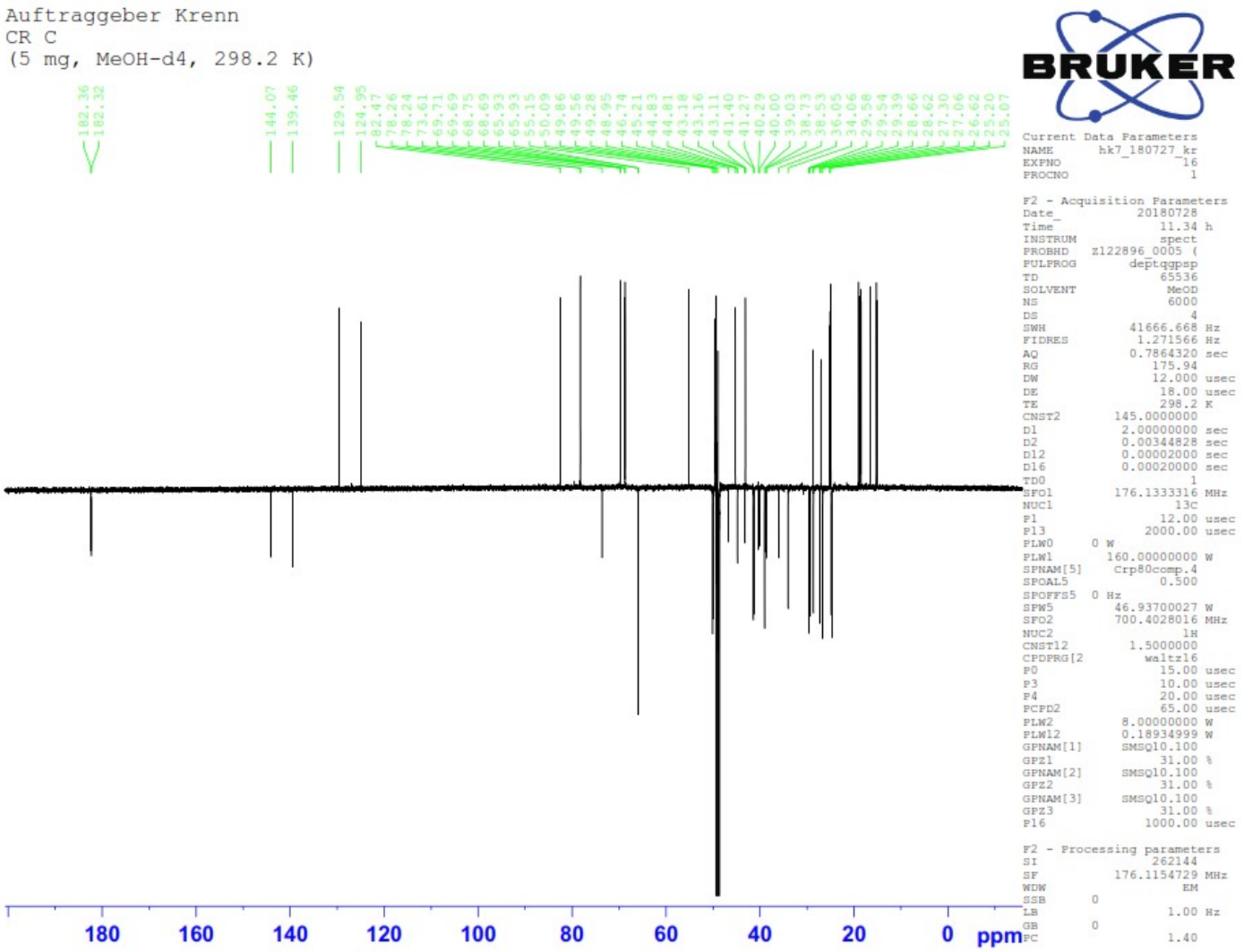

Appendix 4c: COSY of CR-C

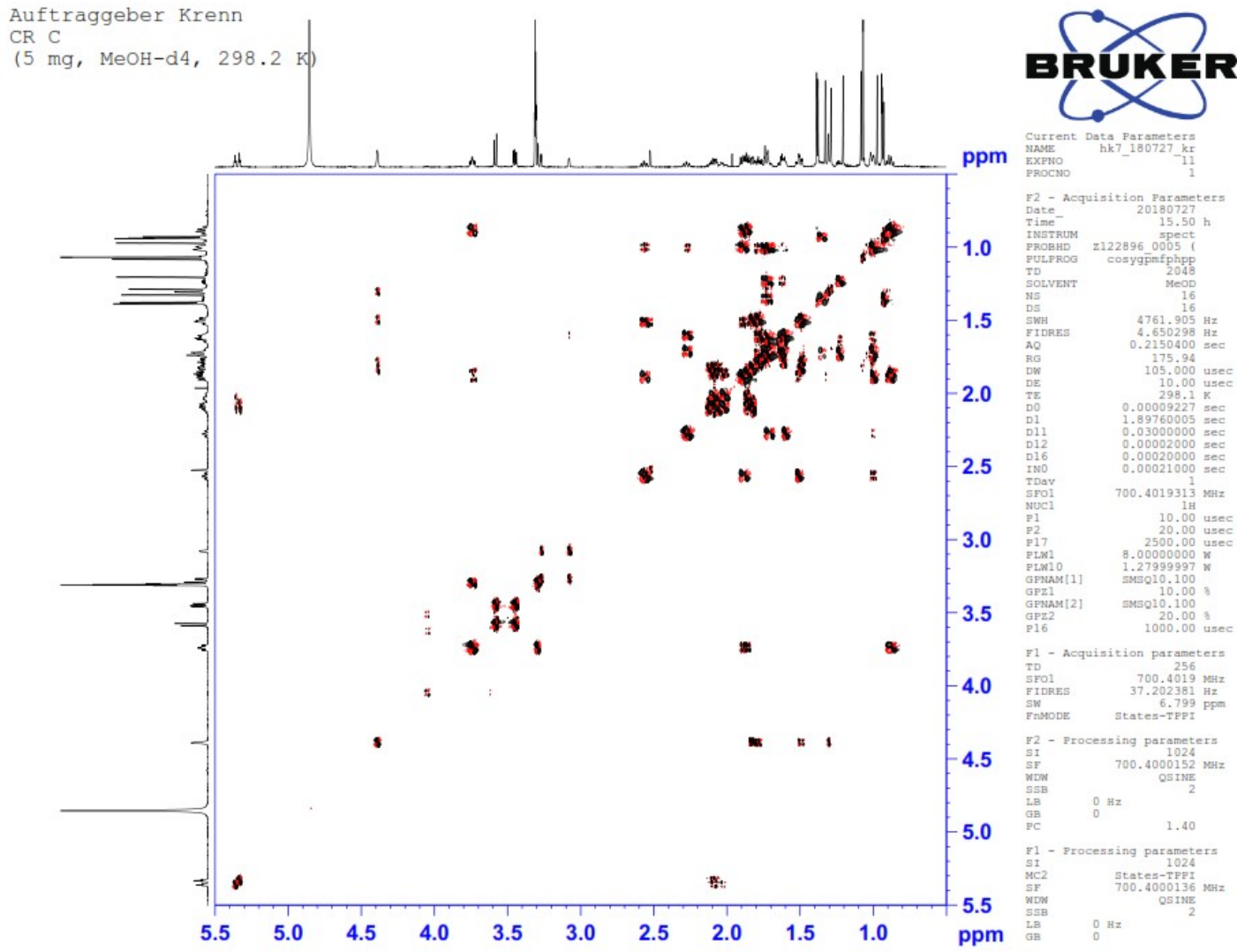

Appendix 4d: HMBC of CR-C

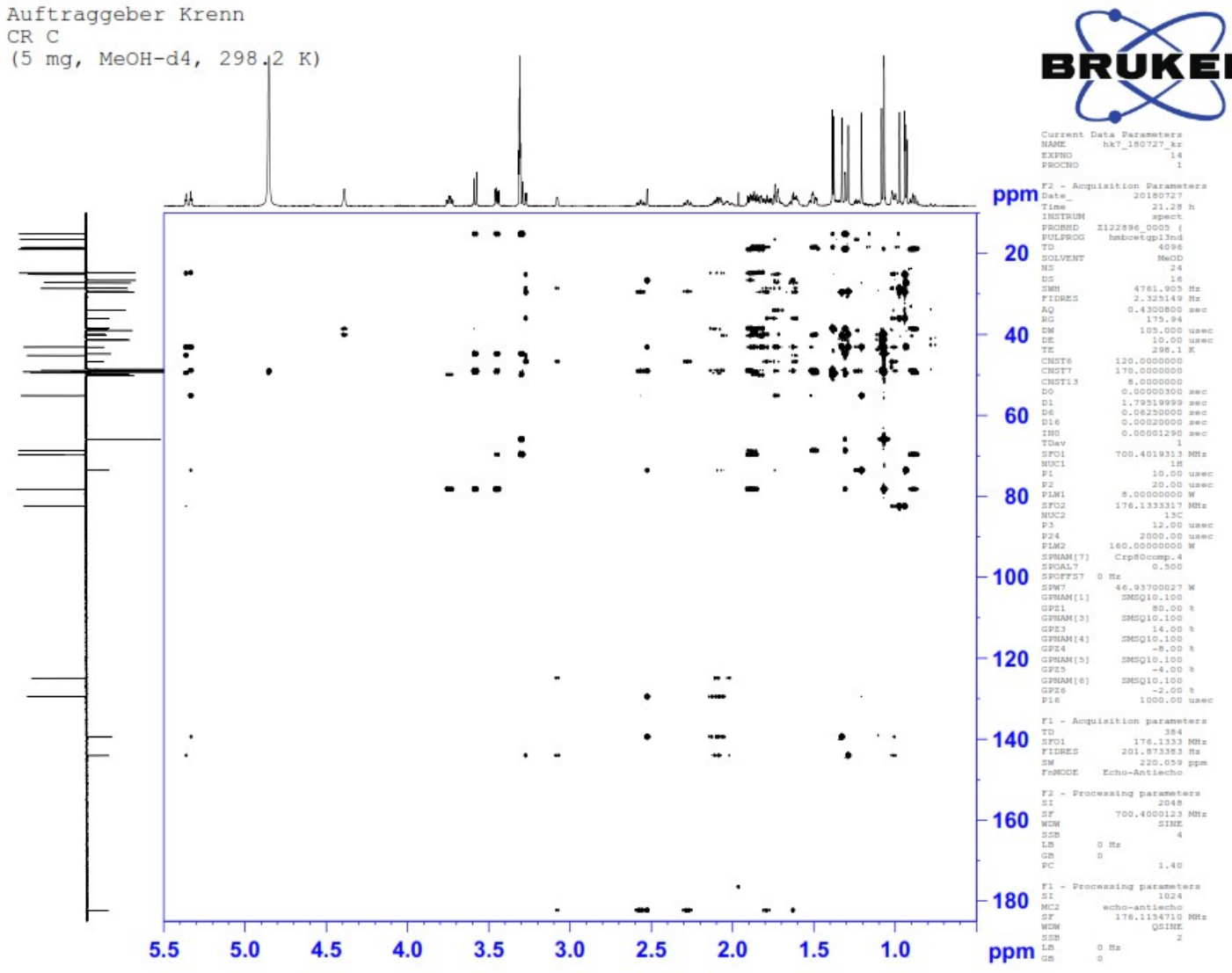

Appendix 4e: HSQC of CR-C

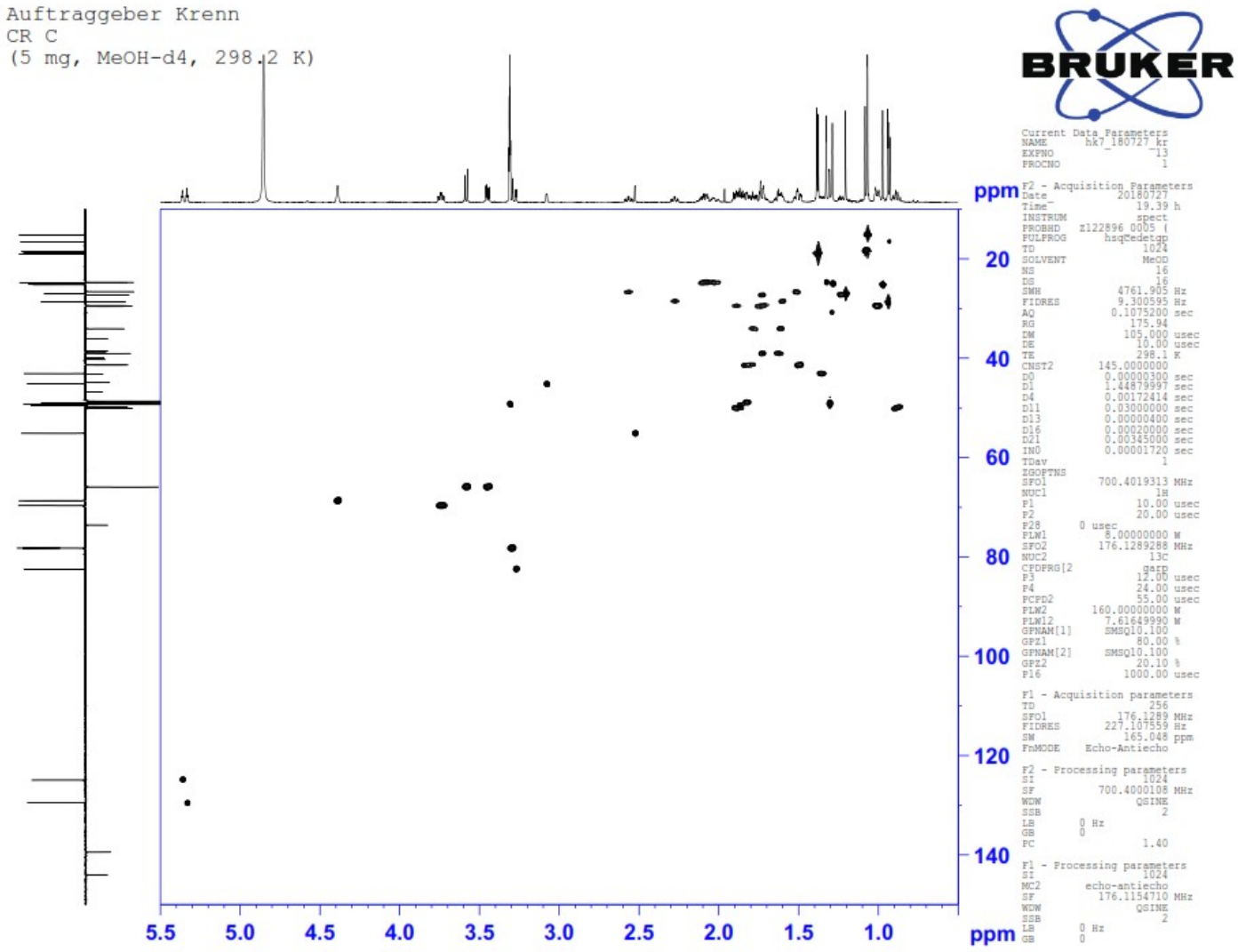

Appendix 4f: NOESY of CR-C

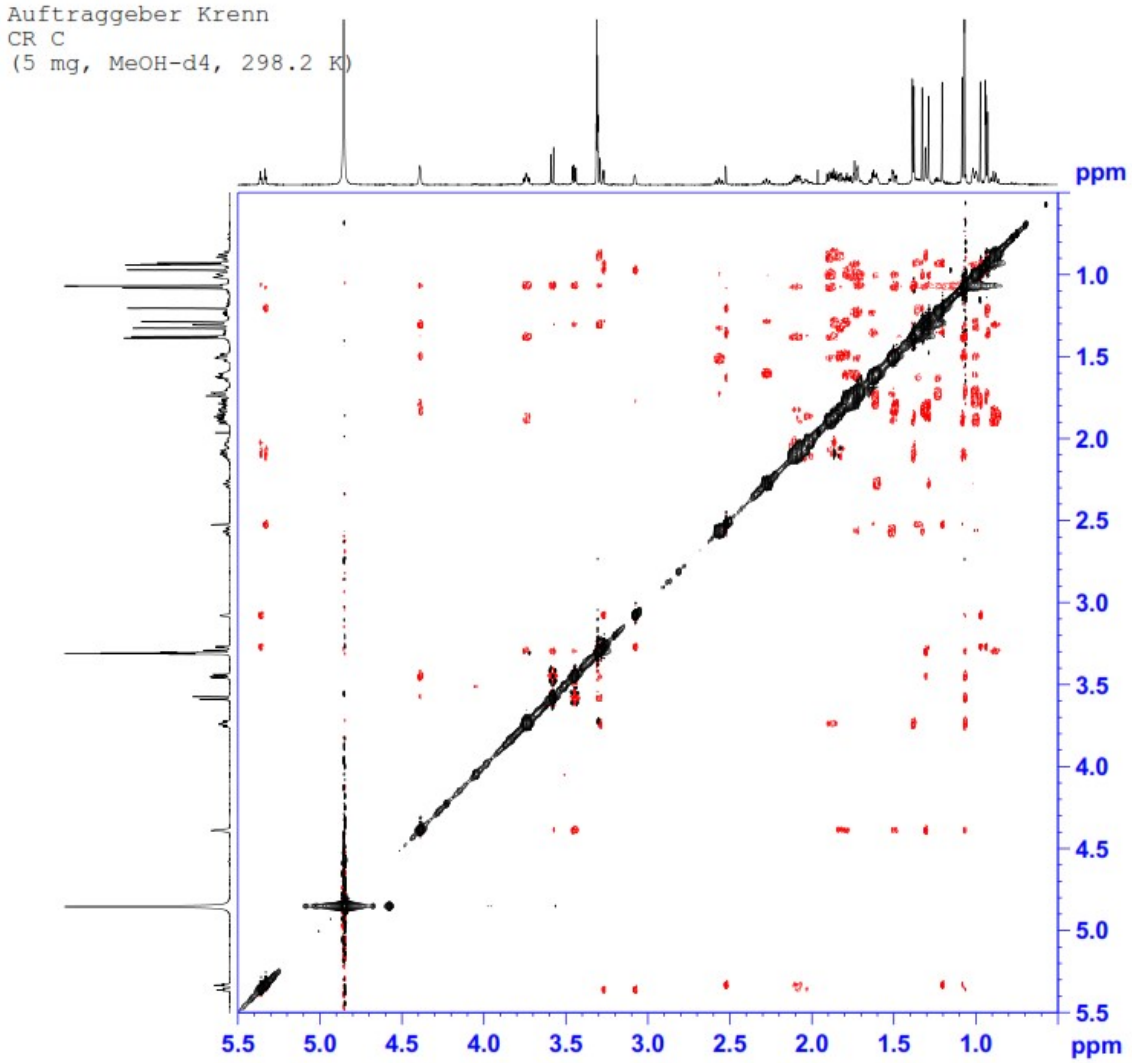

BRUKER

```
Current Data Parameters
NAME        hk7_180727_kr
EXPNO                  15
PROCNO                  1

F2 - Acquisition Parameters
Date_            20180728
Time                3.25 h
INSTRUM             spect
PROBHD    z122896_0005 (
PULPROG      noesygpphpp
TD                   2048
SOLVENT              MeOD
NS                     16
DS                     32
SWH            4761.905 Hz
FIDRES         4.650298 Hz
AQ             0.2150400 sec
RG                 19.06
DW              105.000 usec
DE               10.00 usec
TE               298.2 K
D0            0.00009227 sec
D1            1.93118703 sec
D8            0.80000001 sec
D11           0.03000000 sec
D12           0.00002000 sec
D16           0.00020000 sec
IN0           0.00021000 sec
TDav                   1
SFO1         700.4019313 MHz
NUC1                1H
P1               10.00 usec
P2               20.00 usec
P17            2500.00 usec
PLW1          8.00000000 W
PLW10         1.27999997 W
GPNAM[1]      SMSQ10.100
GPZ1             40.00 %
P16            1000.00 usec

F1 - Acquisition parameters
TD                   256
SFO1          700.4019 MHz
FIDRES       37.202381 Hz
SW               6.799 ppm
FnMODE       States-TPPI

F2 - Processing parameters
SI                  1024
SF           700.4000135 MHz
WDW                 QSINE
SSB                     2
LB         0 Hz
GB         0
PC                  1.00

F1 - Processing parameters
SI                  1024
MC2          States-TPPI
SF           700.4000137 MHz
WDW                 QSINE
SSB                     2
LB         0 Hz
GB         0
```

Appendix 4g: TOCSY of CR-C

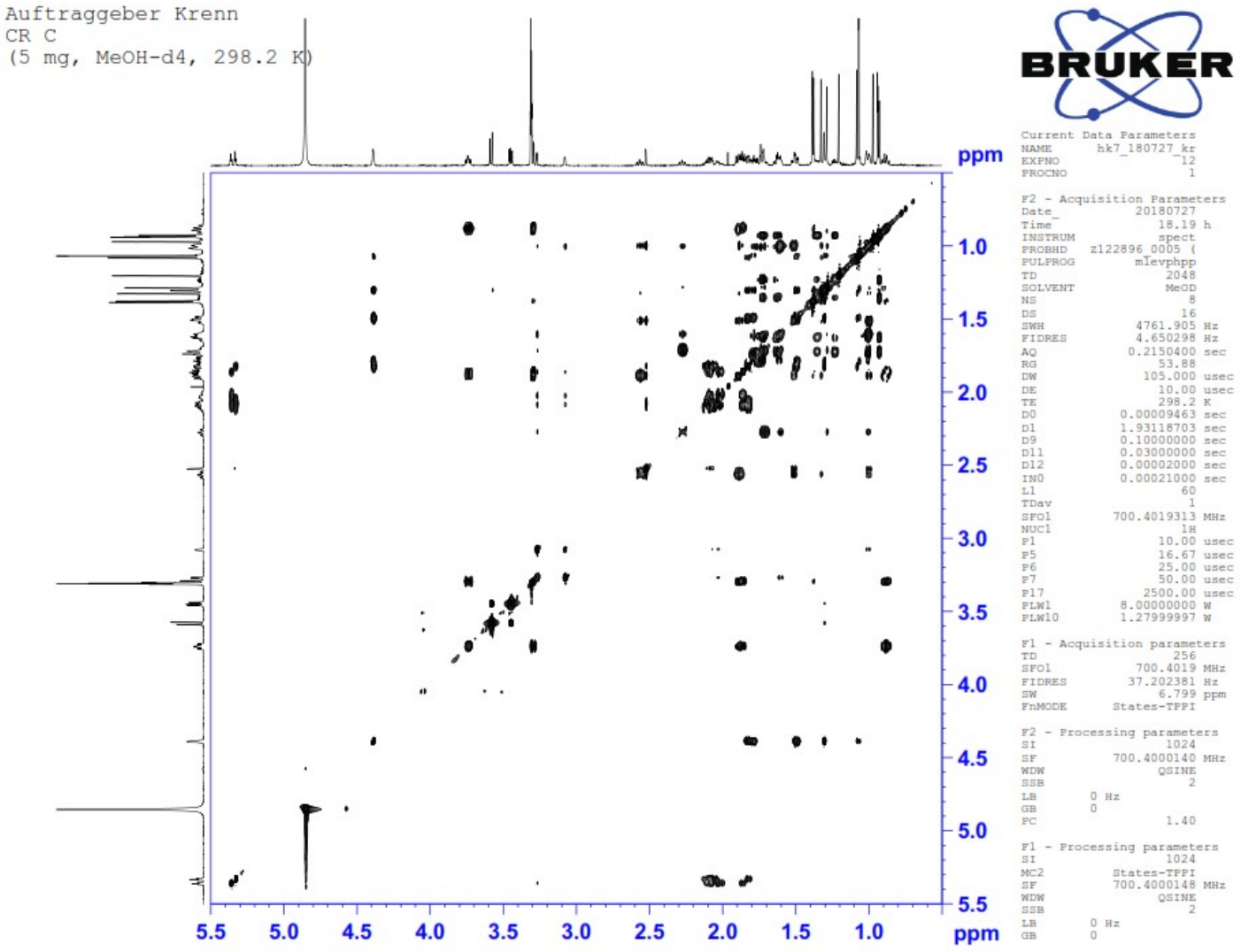

Appendix 5: Mass spectra of CR-E

Appendix 5a: ESI-MS of CR-E

Analysis Info

Analysis Name	D:\MZ\maXis_data\1808\Krenn_Kaehlig\CR_E_amaZon_aMSn.d	Acquisition Date	8/27/2018 4:55:37 PM
Method	DI_MSMS.m	Operator	MSC
Sample Name	CR E	Instrument	amaZon speed ETD
Comment	Kaehlig/Krenn/Zehl ACN / MeOH + 1% H2O		

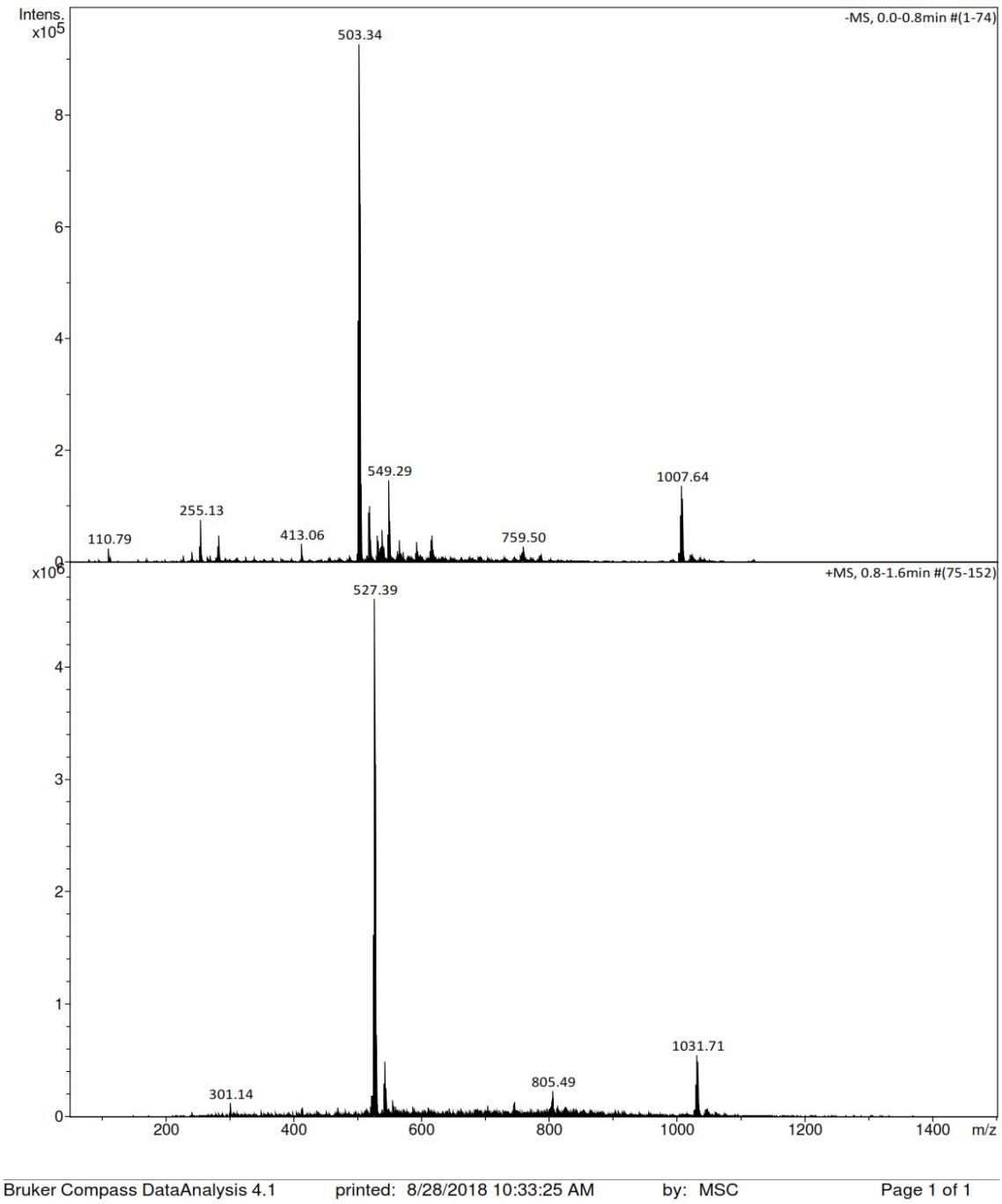

Bruker Compass DataAnalysis 4.1 printed: 8/28/2018 10:33:25 AM by: MSC Page 1 of 1

Analysis Info

Analysis Name	D:\MZ\maXis_data\1808\Krenn_Kaehlig\CR_E_amaZon_aMSn.d	Acquisition Date	8/27/2018 4:55:37 PM
Method	DI_MSMS.m	Operator	MSC
Sample Name	CR E	Instrument	amaZon speed ETD
Comment	Kaehlig/Krenn/Zehl ACN / MeOH + 1% H2O		

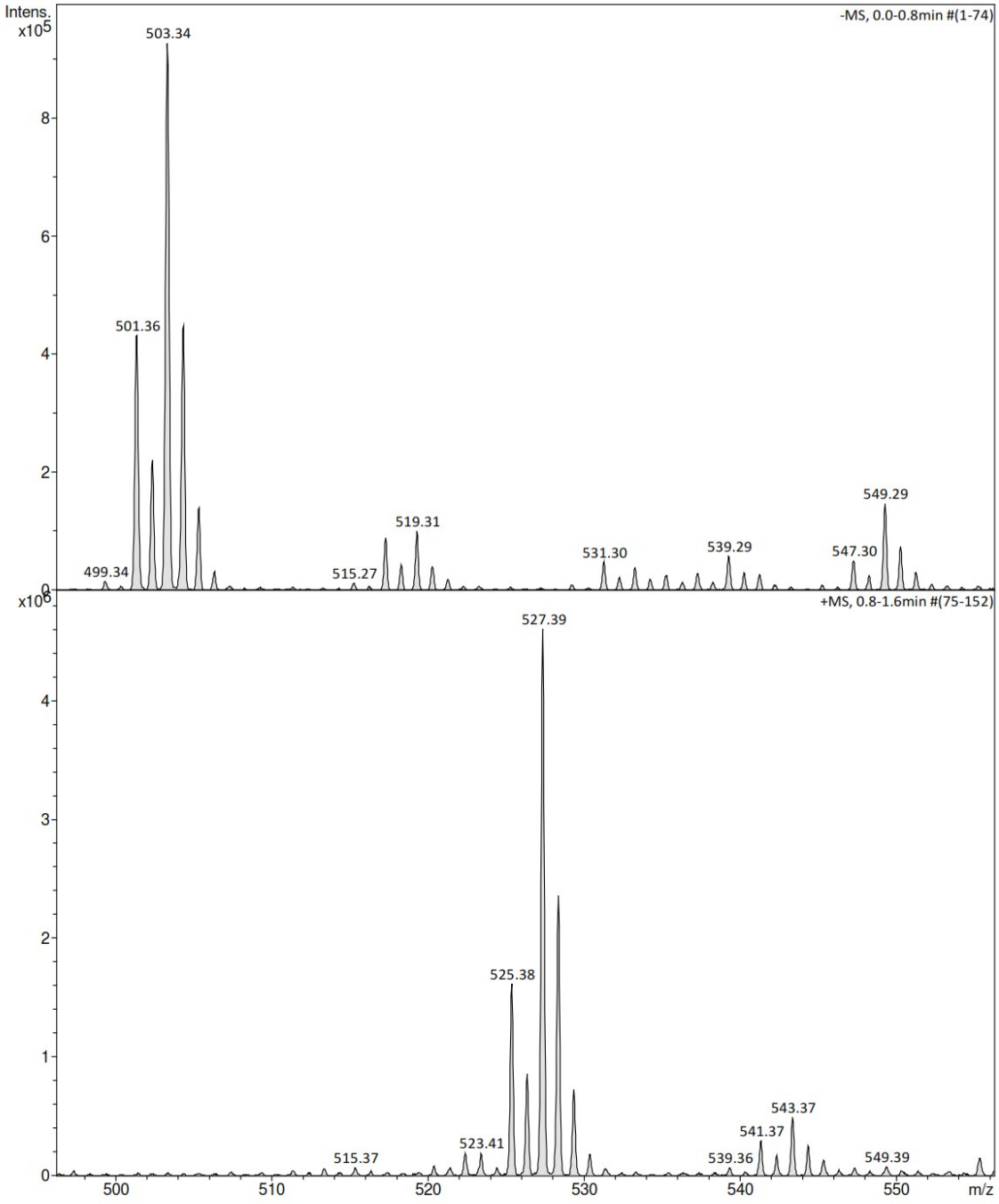

Bruker Compass DataAnalysis 4.1 printed: 8/28/2018 10:33:54 AM by: MSC Page 1 of 1

Analysis Info

Analysis Name	D:\MZ\maXis_data\1808\Krenn_Kaehlig\CR_E_amaZon_aMSn.d	Acquisition Date	8/27/2018 4:55:37 PM
Method	DI_MSMS.m	Operator	MSC
Sample Name	CR E	Instrument	amaZon speed ETD
Comment	Kaehlig/Krenn/Zehl ACN / MeOH + 1% H2O		

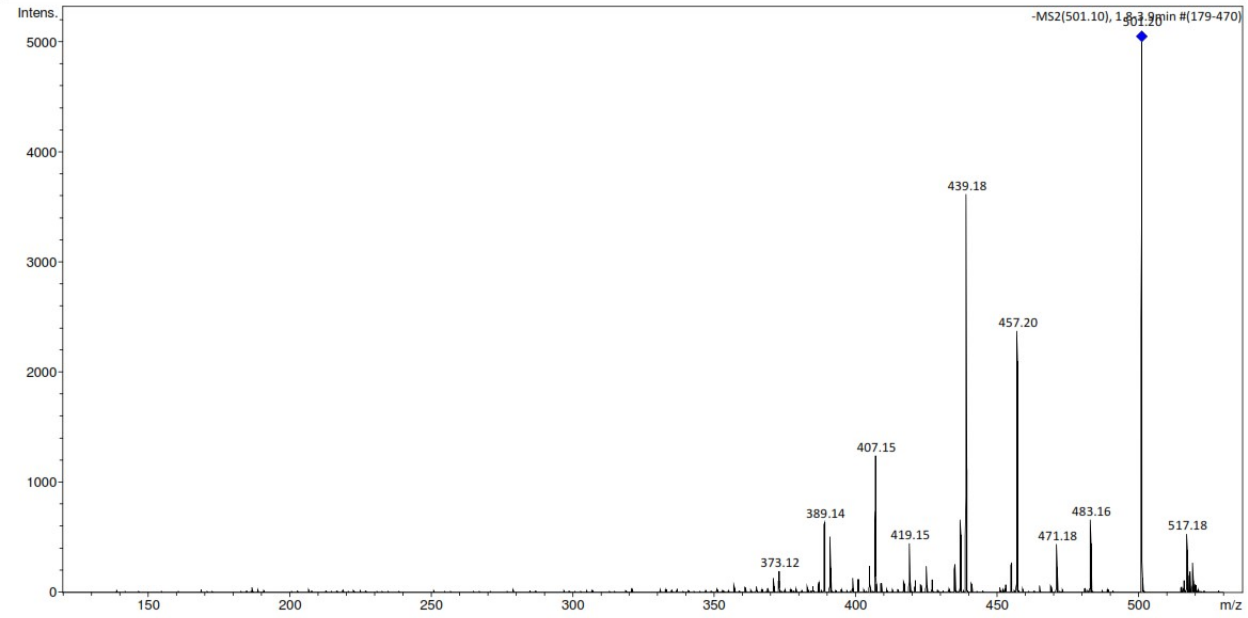

Bruker Compass DataAnalysis 4.1 printed: 8/28/2018 10:36:48 AM by: MSC Page 1 of 1

Analysis Info

Analysis Name	D:\MZ\maXis_data\1808\Krenn_Kaehlig\CR_E_amaZon_aMSn.d	Acquisition Date	8/27/2018 4:55:37 PM
Method	DI_MSMS.m	Operator	MSC
Sample Name	CR E	Instrument	amaZon speed ETD
Comment	Kaehlig/Krenn/Zehl ACN / MeOH + 1% H2O		

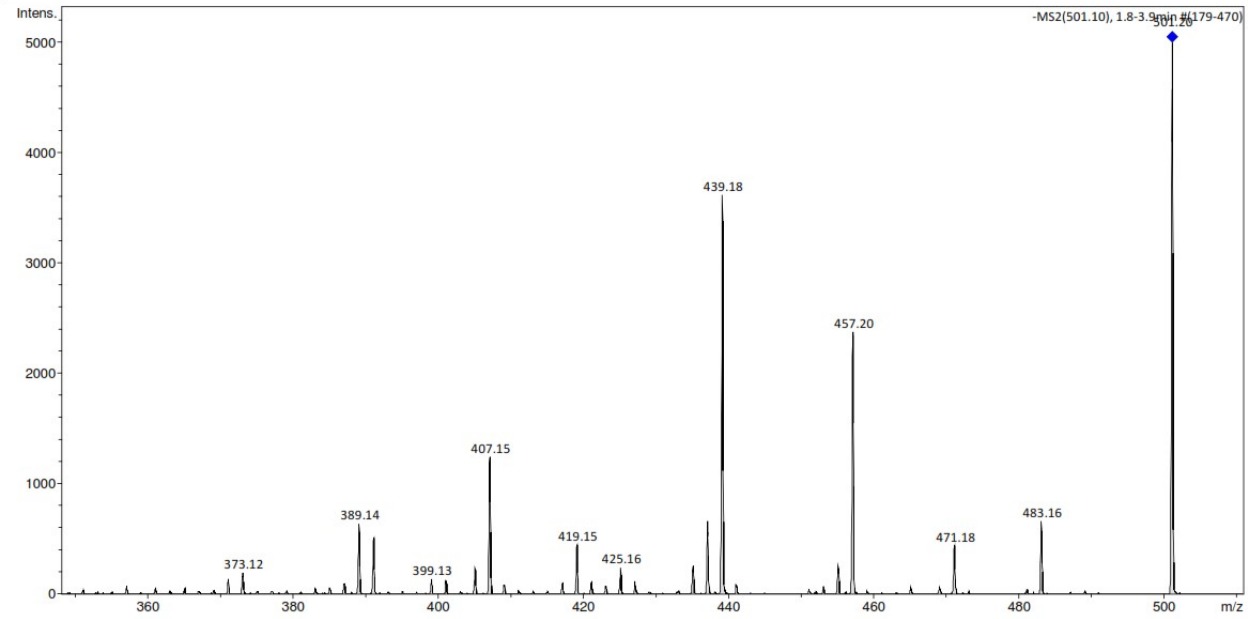

Bruker Compass DataAnalysis 4.1 printed: 8/28/2018 10:36:57 AM by: MSC Page 1 of 1

Analysis Info

Analysis Name	D:\MZ\maXis_data\1808\Krenn_Kaehlig\CR_E_amaZon_aMSn.d	Acquisition Date	8/27/2018 4:55:37 PM
Method	DI_MSMS.m	Operator	MSC
Sample Name	CR E	Instrument	amaZon speed ETD
Comment	Kaehlig/Krenn/Zehl ACN / MeOH + 1% H2O		

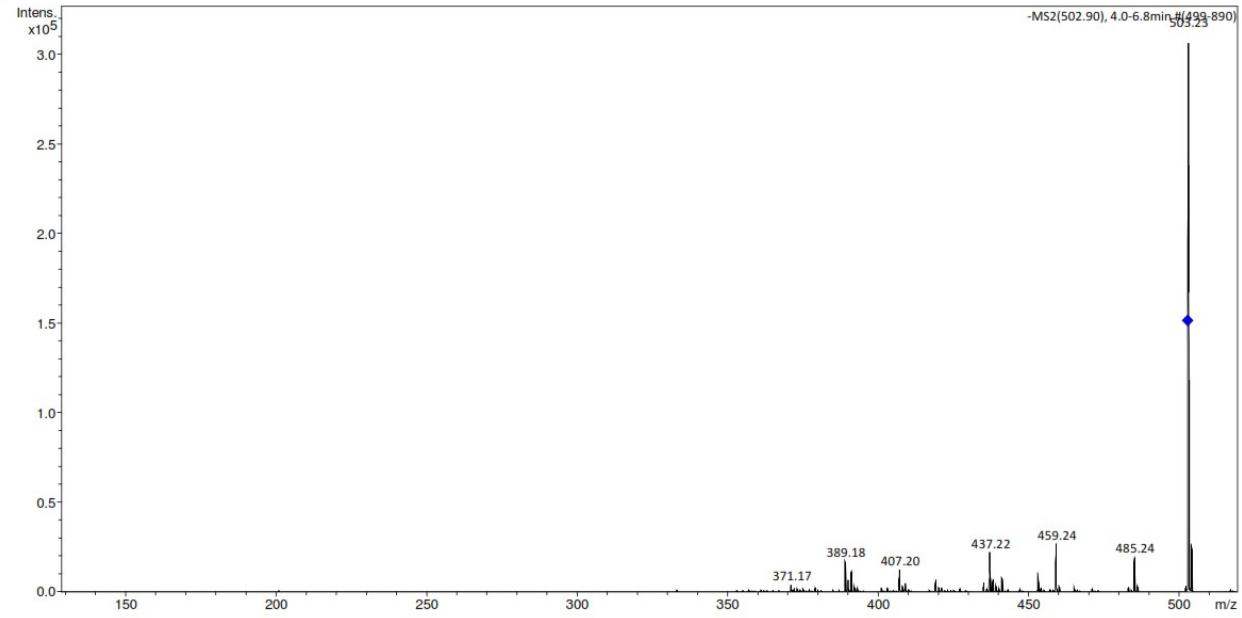

Analysis Info

Analysis Name	D:\MZ\maXis_data\1808\Krenn_Kaehlig\CR_E_amaZon_aMSn.d	Acquisition Date	8/27/2018 4:55:37 PM
Method	DI_MSMS.m	Operator	MSC
Sample Name	CR E	Instrument	amaZon speed ETD
Comment	Kaehlig/Krenn/Zehl ACN / MeOH + 1% H2O		

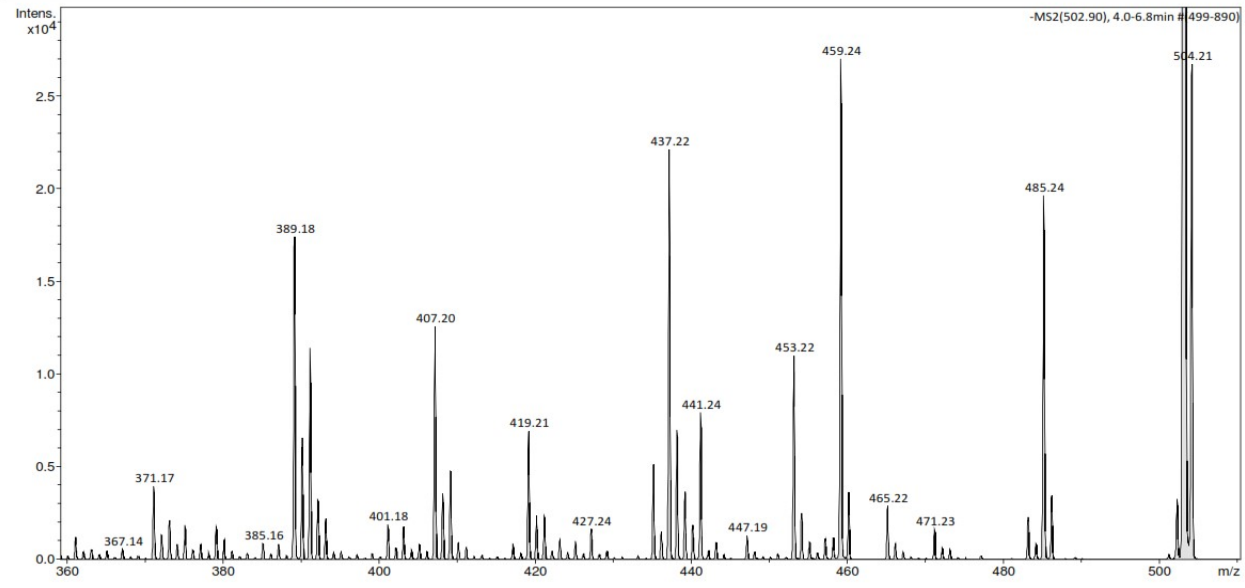

Analysis Info

Analysis Name	D:\MZ\maXis_data\1808\Krenn_Kaehlig\CR_E_amaZon_aMSn.d	Acquisition Date	8/27/2018 4:55:37 PM
Method	DI_MSMS.m	Operator	MSC
Sample Name	CR E	Instrument	amaZon speed ETD
Comment	Kaehlig/Krenn/Zehl ACN / MeOH + 1% H2O		

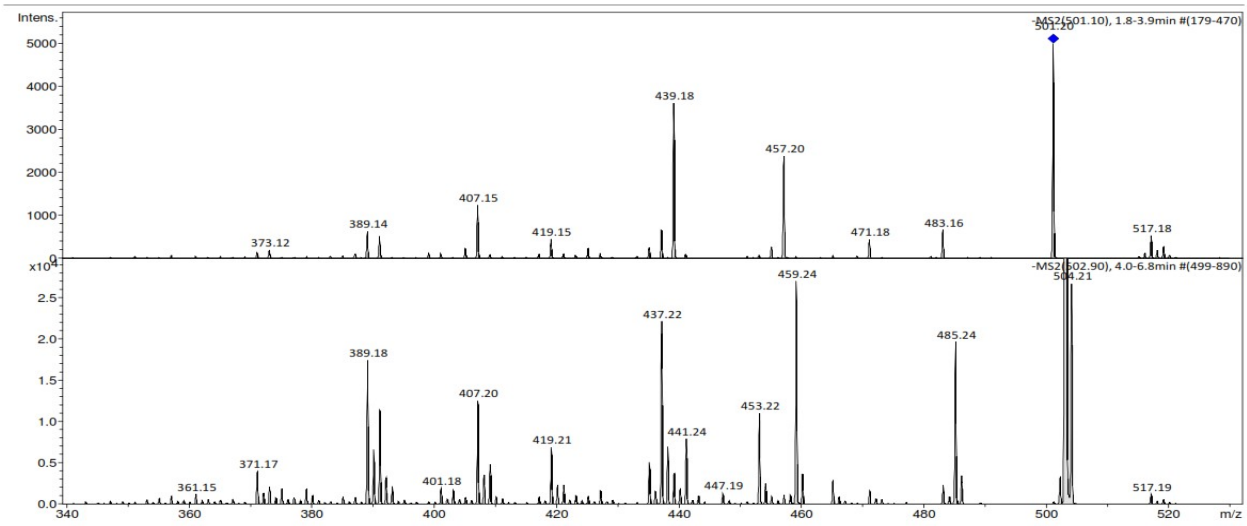

Analysis Info

Analysis Name	D:\MZ\maXis_data\1808\Krenn_Kaehlig\CR_E_amaZon_aMSn.d	Acquisition Date	8/27/2018 4:55:37 PM
Method	DI_MSMS.m	Operator	MSC
Sample Name	CR E	Instrument	amaZon speed ETD
Comment	Kaehlig/Krenn/Zehl ACN / MeOH + 1% H2O		

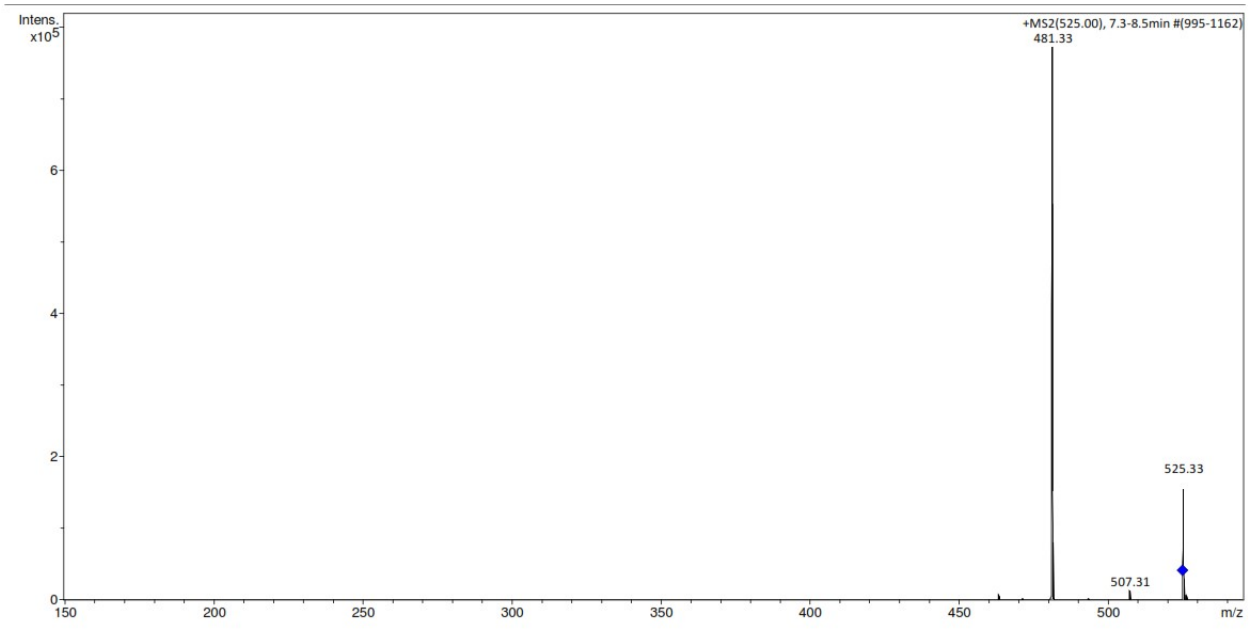

Analysis Info

Analysis Name	D:\MZ\maXis_data\1808\Krenn_Kaehlig\CR_E_amaZon_aMSn.d	Acquisition Date	8/27/2018 4:55:37 PM
Method	DI_MSMS.m	Operator	MSC
Sample Name	CR E	Instrument	amaZon speed ETD
Comment	Kaehlig/Krenn/Zehl ACN / MeOH + 1% H2O		

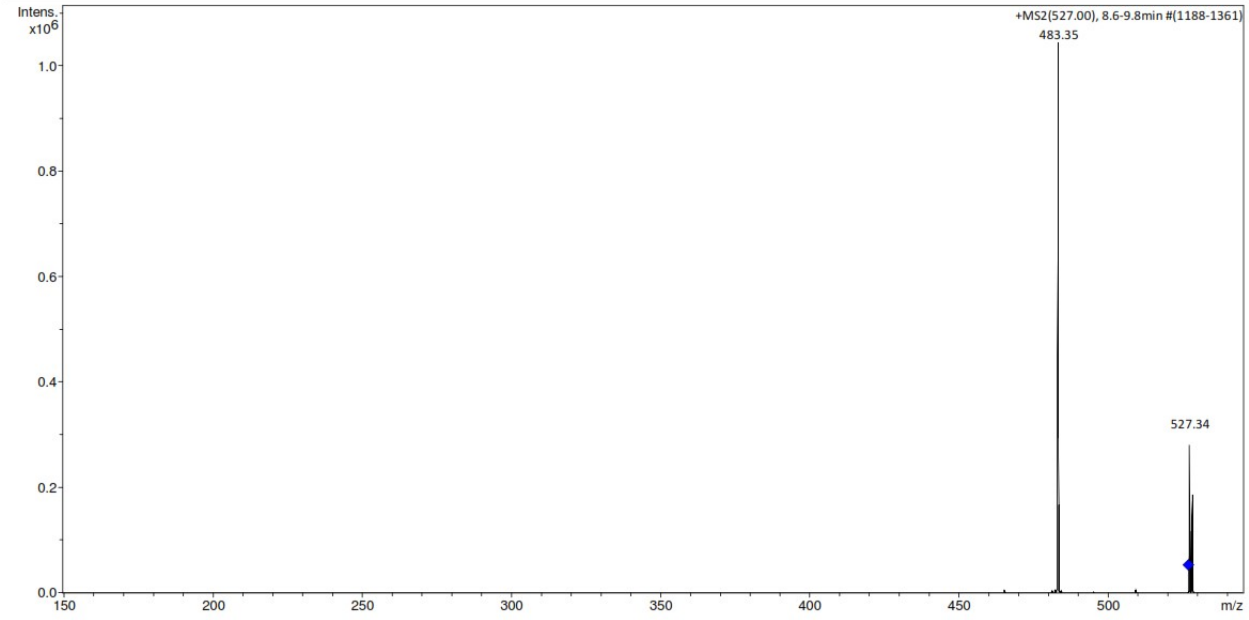

Appendix 5b: HRESI-MS of CR-E

Analysis Info

Analysis Name	D:\MZ\maXis_data\1808\Krenn_Kaehlig\59025000001.d	Acquisition Date	8/20/2018 12:08:11 PM
Method	tune_low_MS_Service_08_18.m	Operator	msc
Sample Name	CRE	Instrument	maXis
Comment	Kaehlig-Zehl/Anorg.Chem Ergebnis: +/- 5ppm ACN/MeOH +1%H2O		

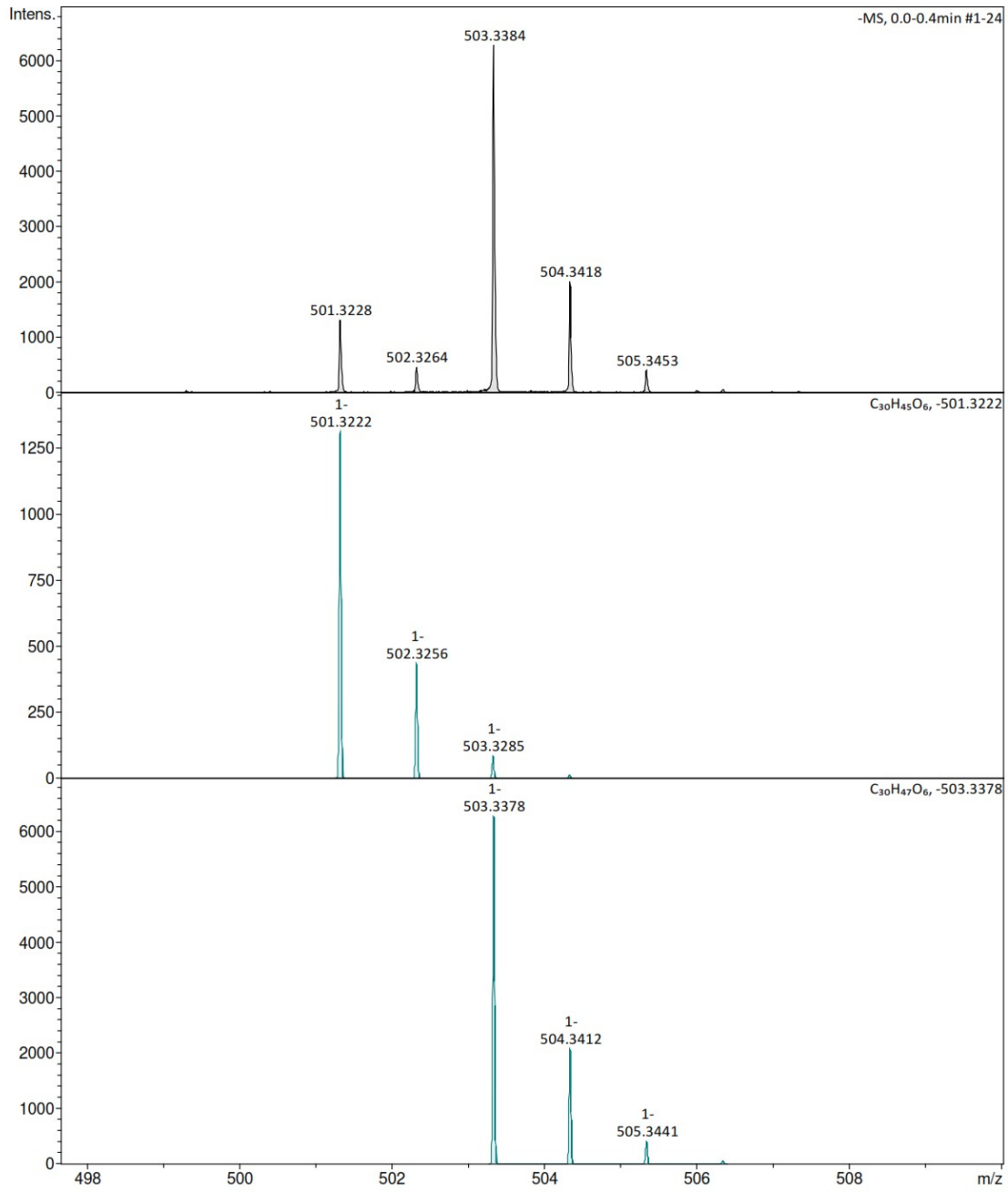

Bruker Compass DataAnalysis 4.1 printed: 8/27/2018 2:55:41 PM by: MSC Page 1 of 1

Mass Spectrum SmartFormula Report

Analysis Info

Analysis Name	D:\MZ\maXis_data\1808\Krenn_Kaehlig\59025000001.d	Acquisition Date	8/20/2018 12:08:11 PM
Method	tune_low_MS_Service_08_18.m	Operator	msc
Sample Name	CRE	Instrument	maXis 255552.00016
Comment	Kaehlig-Zehl/Anorg.Chem Ergebnis: +/- 5ppm ACN/MeOH +1%H2O		

Acquisition Parameter

Source Type	ESI	Ion Polarity	Negative	Set Nebulizer	0.4 Bar
Focus	Not active	Set Capillary	4500 V	Set Dry Heater	180 °C
Scan Begin	50 m/z	Set End Plate Offset	-500 V	Set Dry Gas	4.0 l/min
Scan End	1900 m/z	Set Charging Voltage	0 V	Set Divert Valve	Source
		Set Corona	0 nA	Set APCI Heater	0 °C

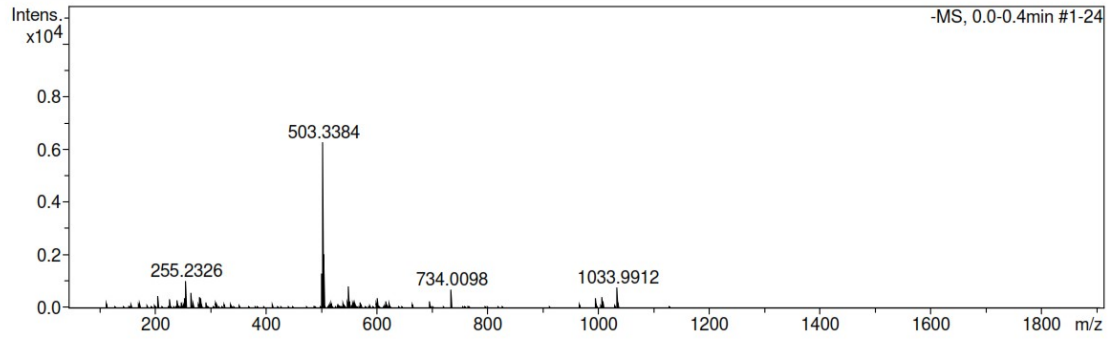

Meas. m/z	#	Ion Formula	Score	m/z	err [mDa]	err [ppm]	mSigma	rdb	e⁻ Conf	N-Rule
501.3228	1	C30H45O6	100.00	501.3222	-0.6	-1.3	644.4	8.5	even	ok
	2	C31H41N4O2	48.28	501.3235	-0.7	-1.4	647.1	13.5	even	ok
	3	C27H37N10	11.92	501.3208	2.0	4.0	649.3	14.5	even	ok
503.3384	1	C30H47O6	100.00	503.3378	-0.6	-1.2	7.7	7.5	even	ok
	2	C27H39N10	42.23	503.3365	2.0	3.9	8.8	13.5	even	ok
	3	C31H43N4O2	77.06	503.3392	-0.7	-1.4	18.2	12.5	even	ok

Appendix 6: 1D and 2D NMR of CR-E

Appendix 6a: ^{1}H NMR of CR-E

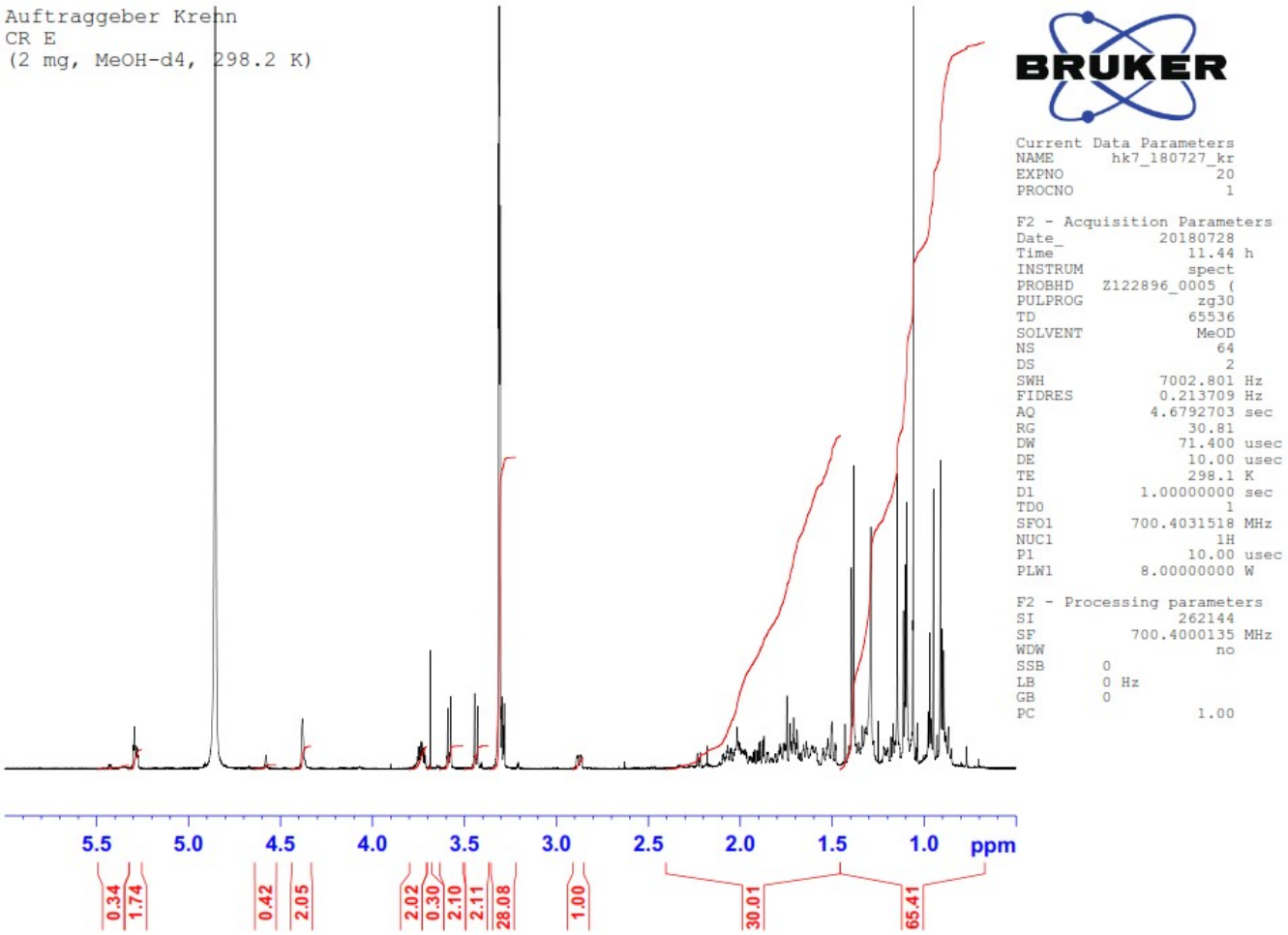

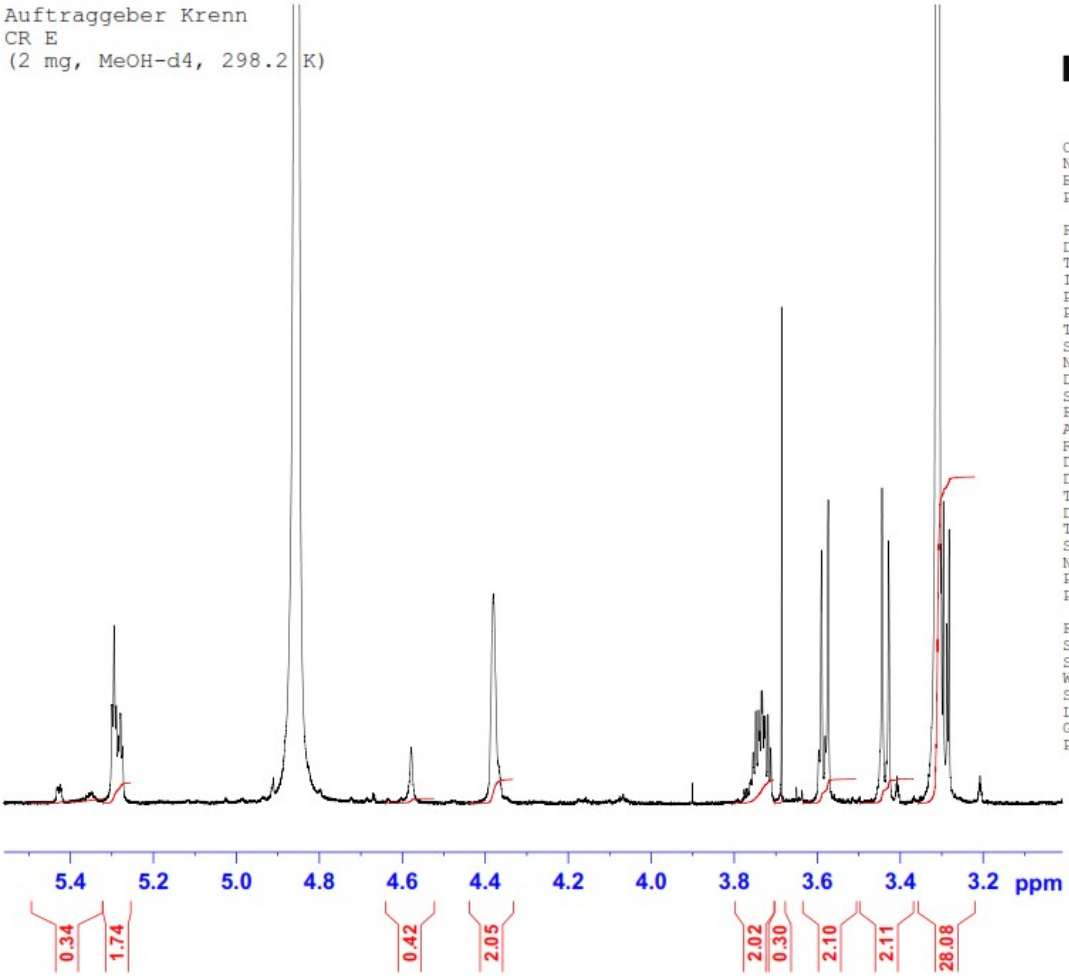

BRUKER

```
Current Data Parameters
NAME      hk7_180727_kr
EXPNO                20
PROCNO                1

F2 - Acquisition Parameters
Date_          20180728
Time              11.44 h
INSTRUM           spect
PROBHD   Z122896_0005 (
PULPROG             zg30
TD                 65536
SOLVENT             MeOD
NS                    64
DS                     2
SWH            7002.801 Hz
FIDRES        0.213709 Hz
AQ            4.6792703 sec
RG                 30.81
DW                71.400 usec
DE                10.00 usec
TE                298.1 K
D1           1.00000000 sec
TD0                    1
SFO1        700.4031518 MHz
NUC1                  1H
P1                10.00 usec
PLW1         8.00000000 W

F2 - Processing parameters
SI                262144
SF        700.4000135 MHz
WDW                   no
SSB       0
LB        0 Hz
GB        0
PC                  1.00
```

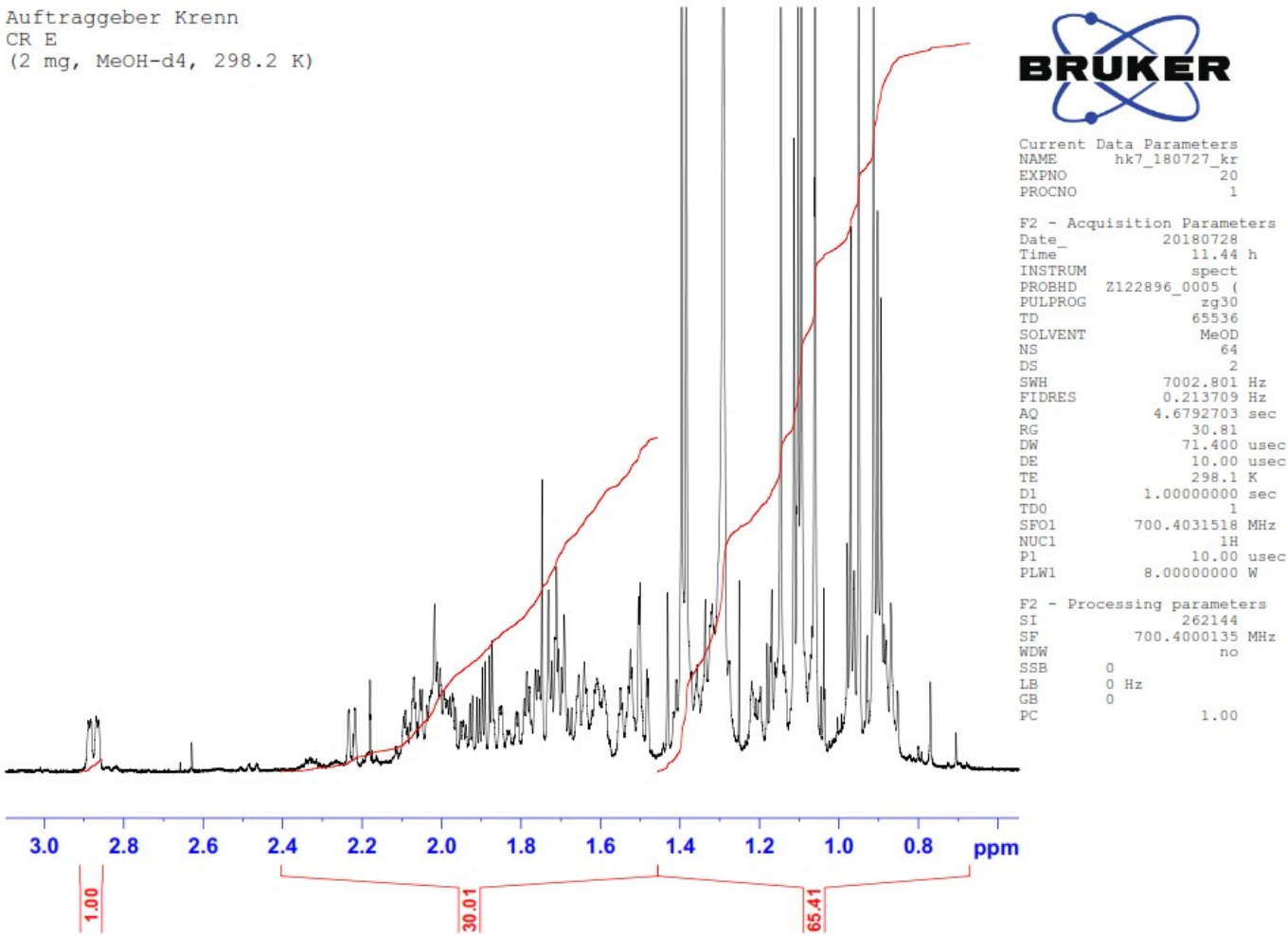
Auftraggeber Krenn
CR E
(2 mg, MeOH-d4, 298.2 K)
BRUKER
Current Data Parameters
NAME hk7_180727_kr
EXPNO 20
PROCNO 1
F2 - Acquisition Parameters
Date_ 20180728
Time 11.44 h
INSTRUM spect
PROBHD Z122896_0005 (
PULPROG zg30
TD 65536
SOLVENT MeOD
NS 64
DS 2
SWH 7002.801 Hz
FIDRES 0.213709 Hz
AQ 4.6792703 sec
RG 30.81
DW 71.400 usec
DE 10.00 usec
TE 298.1 K
D1 1.00000000 sec
TD0 1
SFO1 700.4031518 MHz
NUC1 1H
P1 10.00 usec
PLW1 8.00000000 W
F2 - Processing parameters
SI 262144
SF 700.4000135 MHz
WDW no
SSB 0
LB 0 Hz
GB 0
PC 1.00
3.0
2.8
2.6
2.4
2.2
2.0
1.8
1.6
1.4
1.2
1.0
0.8
ppm
1.00
30.01
65.41

Appendix 6b: ^{13}C NMR of CR-E

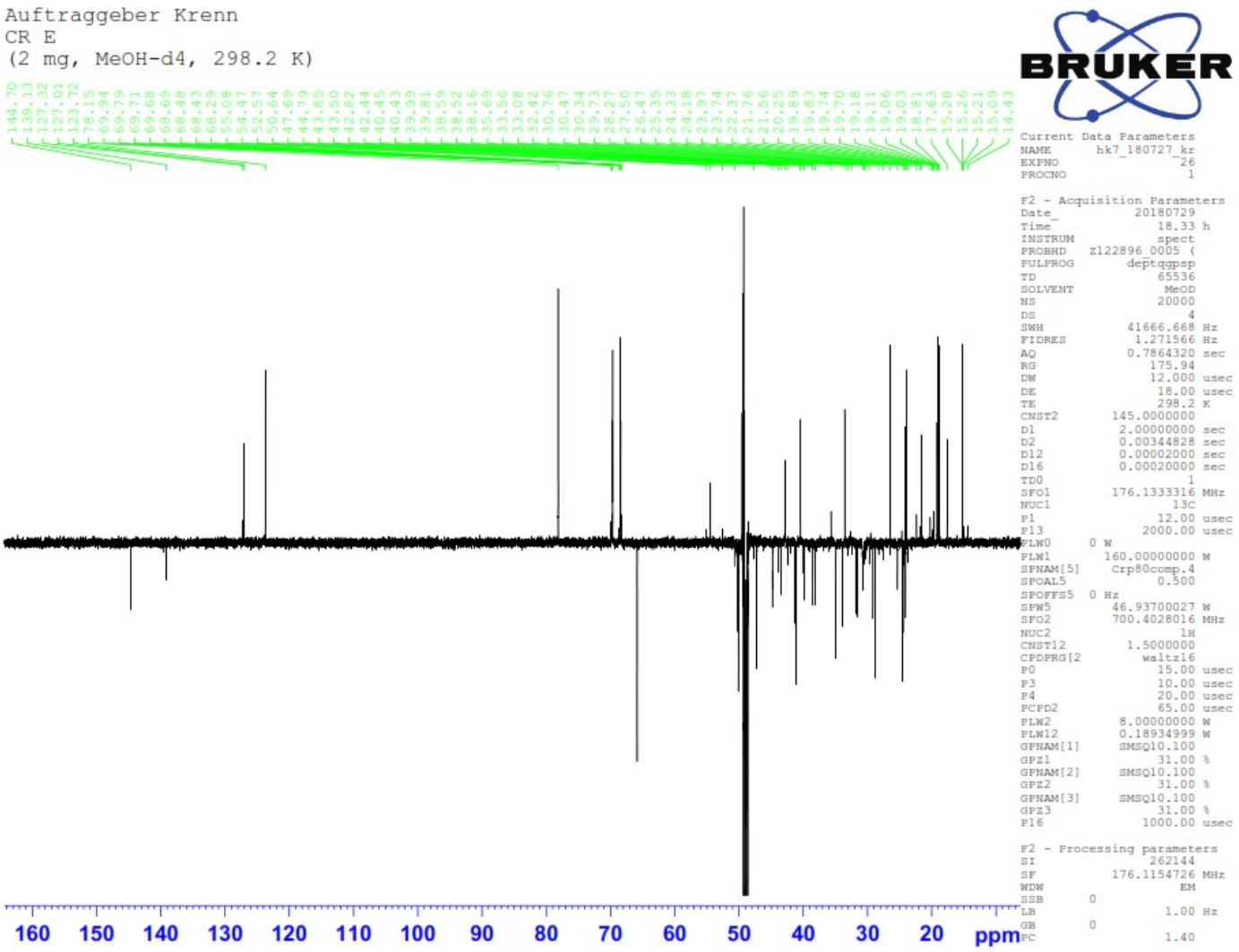

Appendix 6c: COSY of CR-E

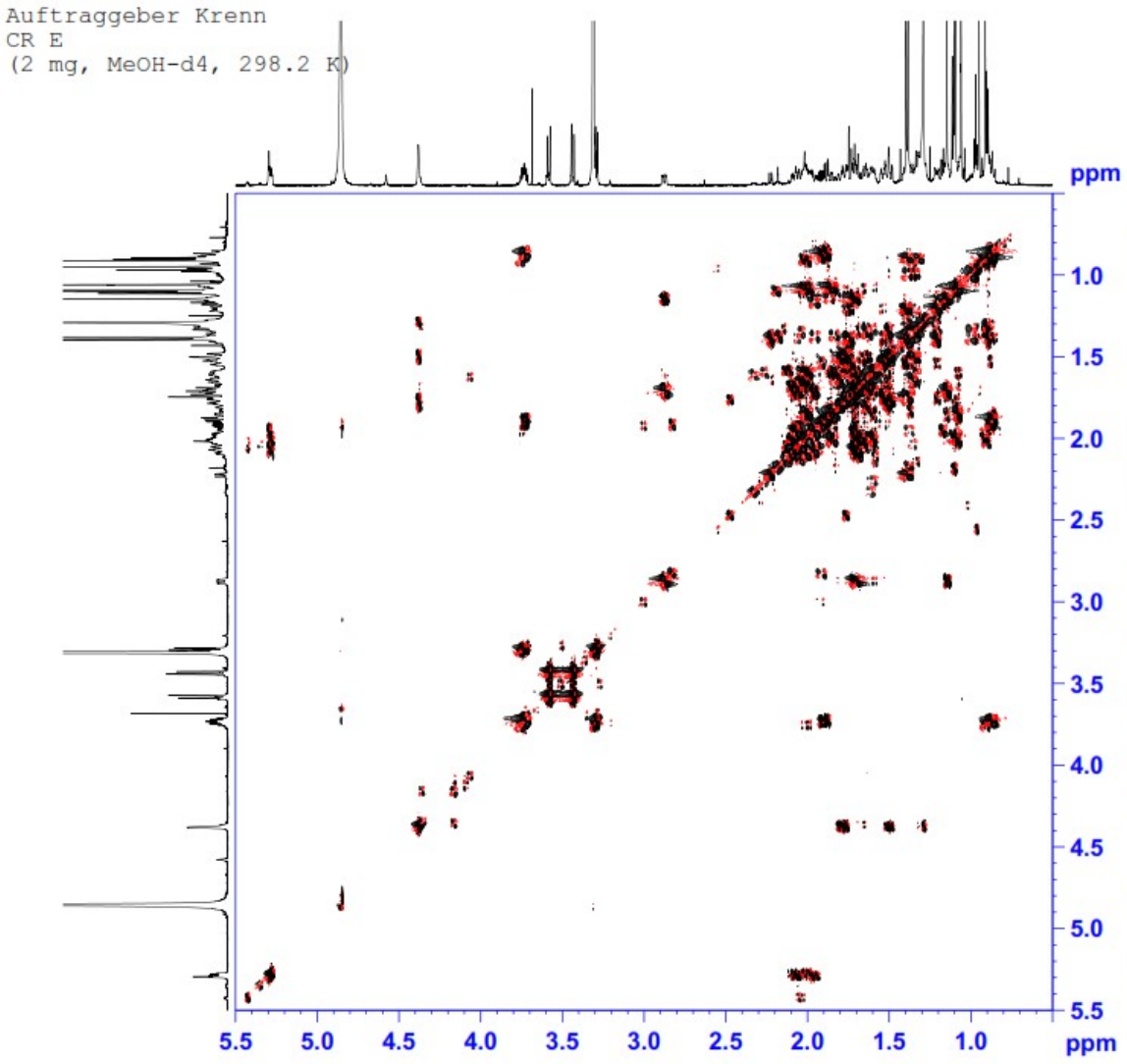

Current Data Parameters
NAME hk7_180727_kr
EXPNO 21
PROCNO 1

F2 - Acquisition Parameters
Date_ 20180728
Time 11.46 h
INSTRUM spect
PROBHD z122896_0005 (
PULPROG cosygpmfphpp
TD 2048
SOLVENT MeOD
NS 16
DS 16
SWH 4587.156 Hz
FIDRES 4.479644 Hz
AQ 0.2232320 sec
RG 175.94
DW 109.000 usec
DE 10.00 usec
TE 298.2 K
D0 0.00009627 sec
D1 1.88940799 sec
D11 0.03000000 sec
D12 0.00002000 sec
D16 0.00020000 sec
IN0 0.00021800 sec
TDav 1
SFO1 700.4019643 MHz
NUC1 1H
P1 10.00 usec
P2 20.00 usec
P17 2500.00 usec
PLW1 8.00000000 W
PLW10 1.27999997 W
GPNAM[1] SMSQ10.100
GPZ1 10.00 %
GPNAM[2] SMSQ10.100
GPZ2 20.00 %
P16 1000.00 usec

F1 - Acquisition parameters
TD 256
SFO1 700.402 MHz
FIDRES 35.837154 Hz
SW 6.549 ppm
FnMODE States-TPPI

F2 - Processing parameters
SI 1024
SF 700.4000148 MHz
WDW QSINE
SSB 2
LB 0 Hz
GB 0
PC 1.40

F1 - Processing parameters
SI 1024
MC2 States-TPPI
SF 700.4000136 MHz
WDW QSINE
SSB 2
LB 0 Hz
GB 0

Appendix 6d:HMBC of CR-E

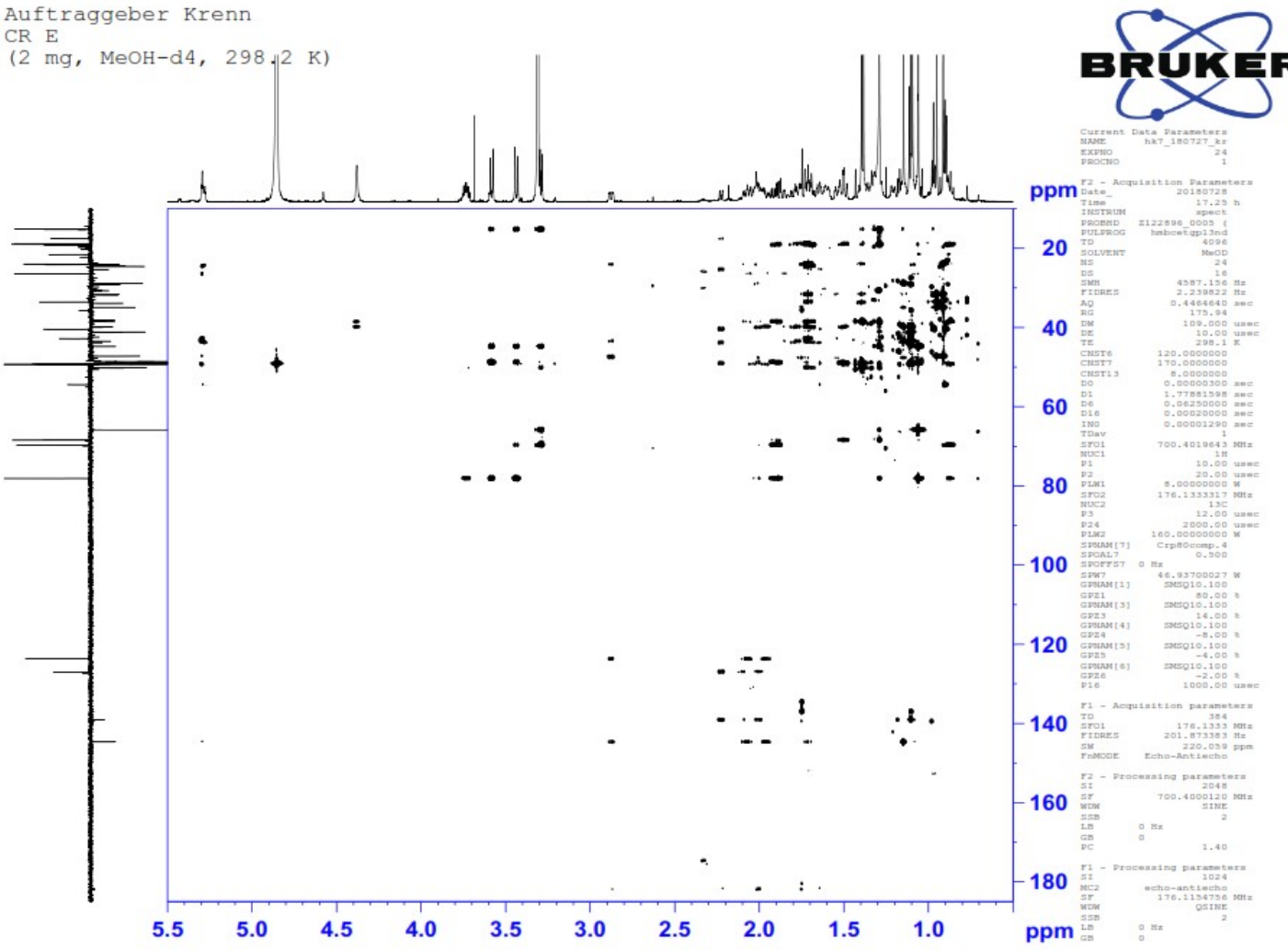

Appendix 6e: HSQC of CR-E

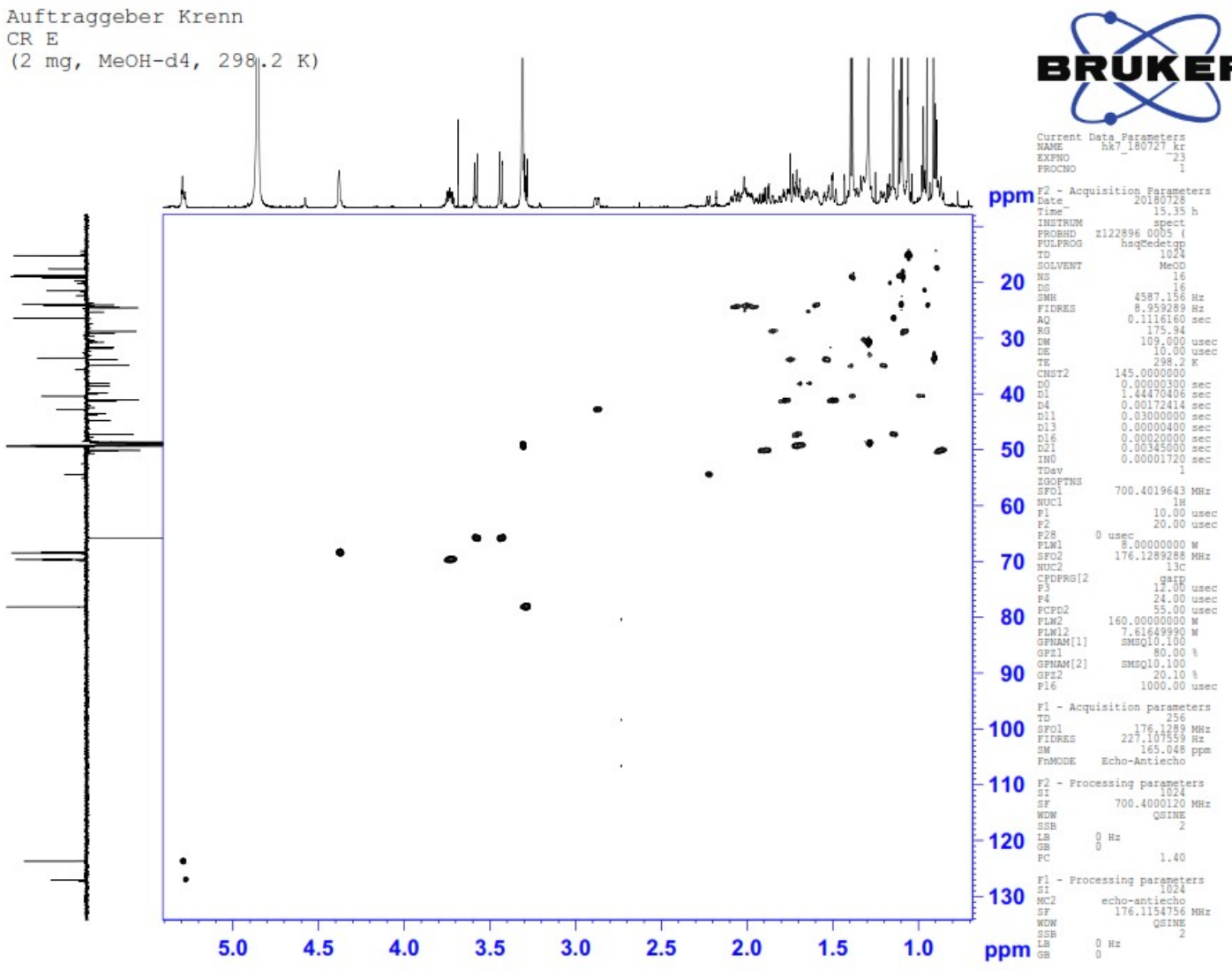

Appendix 6f: NOESY of CR-E

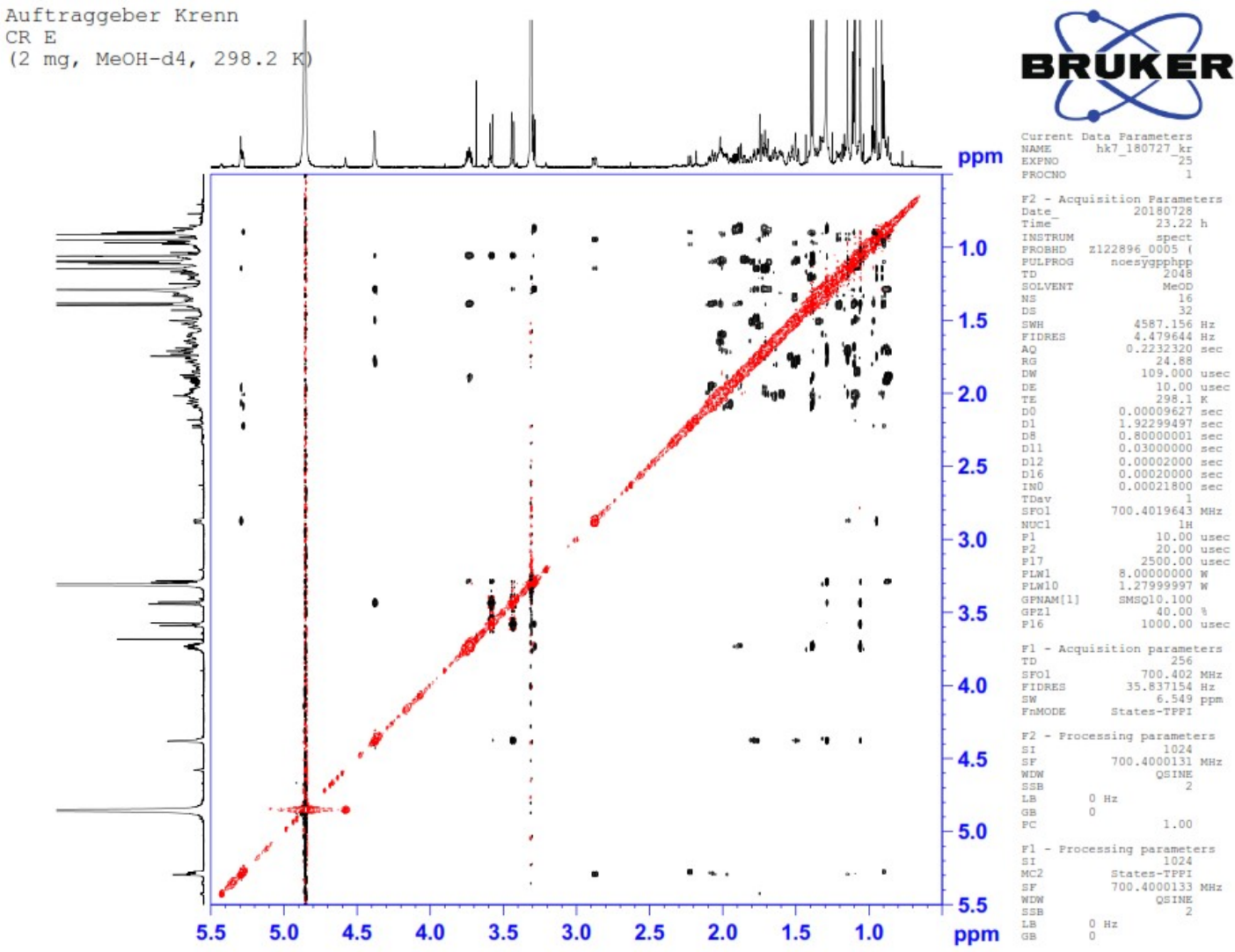

Appendix 6g: TOCSY of CR-E

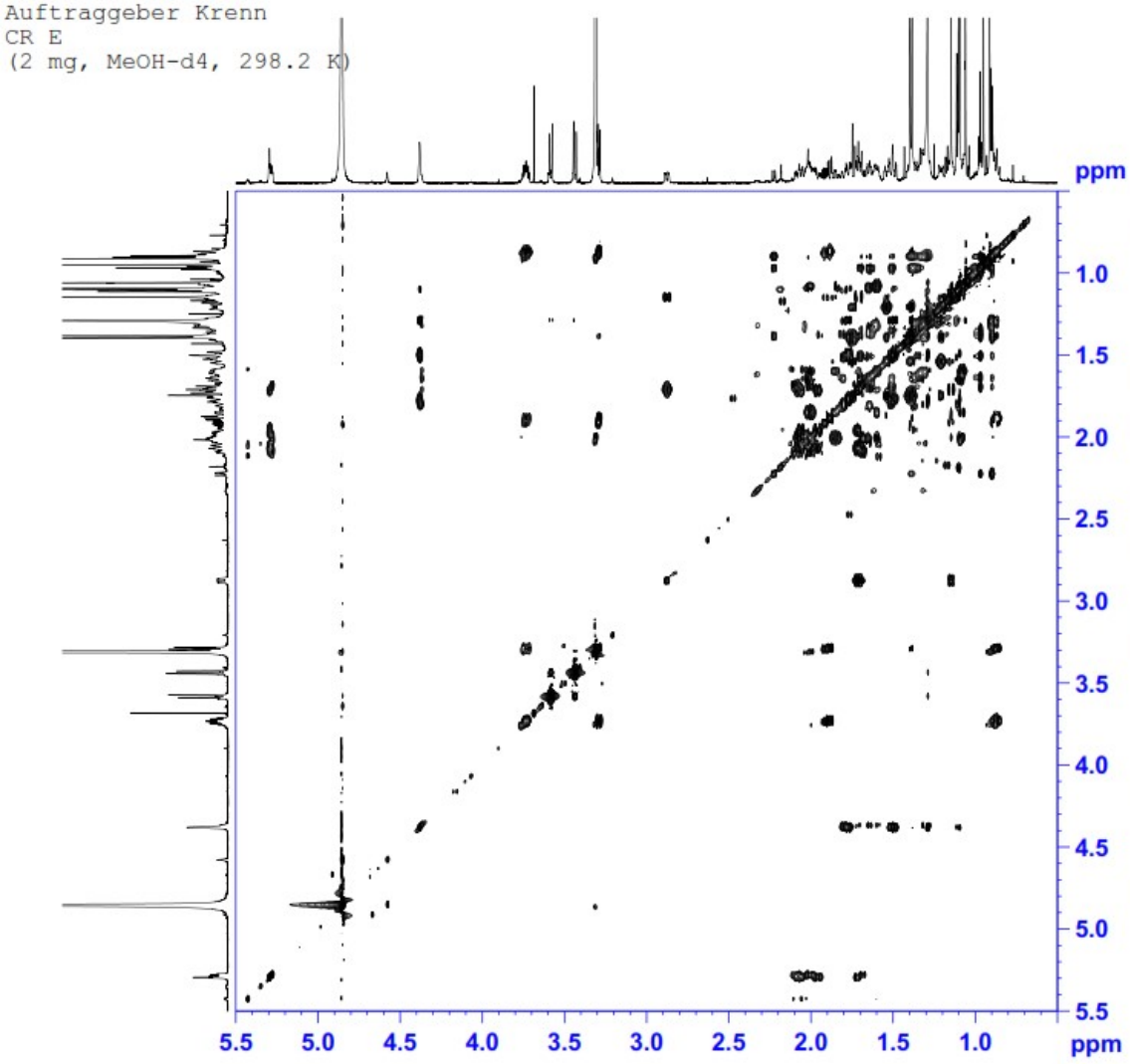

BRUKER

Current Data Parameters
NAME hk7_180727_kr
EXPNO 22
PROCNO 1

F2 - Acquisition Parameters
Date_ 20180728
Time 14.15 h
INSTRUM spect
PROBHD z122896_0005 (
PULPROG mlevphpp
TD 2048
SOLVENT MeOD
NS 8
DS 16
SWH 4587.156 Hz
FIDRES 4.479644 Hz
AQ 0.2232320 sec
RG 34.11
DW 109.000 usec
DE 10.00 usec
TE 298.1 K
D0 0.00009863 sec
D1 1.92299497 sec
D9 0.10000000 sec
D11 0.03000000 sec
D12 0.00002000 sec
IN0 0.00021800 sec
L1 60
TDav 1
SFO1 700.4019643 MHz
NUC1 1H
P1 10.00 usec
P5 16.67 usec
P6 25.00 usec
P7 50.00 usec
P17 2500.00 usec
PLW1 8.00000000 W
PLW10 1.27999997 W

F1 - Acquisition parameters
TD 256
SFO1 700.402 MHz
FIDRES 35.837154 Hz
SW 6.549 ppm
FnMODE States-TPPI

F2 - Processing parameters
SI 1024
SF 700.4000130 MHz
WDW QSINE
SSB 2
LB 0 Hz
GB 0
PC 1.40

F1 - Processing parameters
SI 1024
MC2 States-TPPI
SF 700.4000124 MHz
WDW QSINE
SSB 2
LB 0 Hz
GB 0

Appendix 7: Mass spectra of CR-G

Appendix 7a: ESI-MS of CR-G

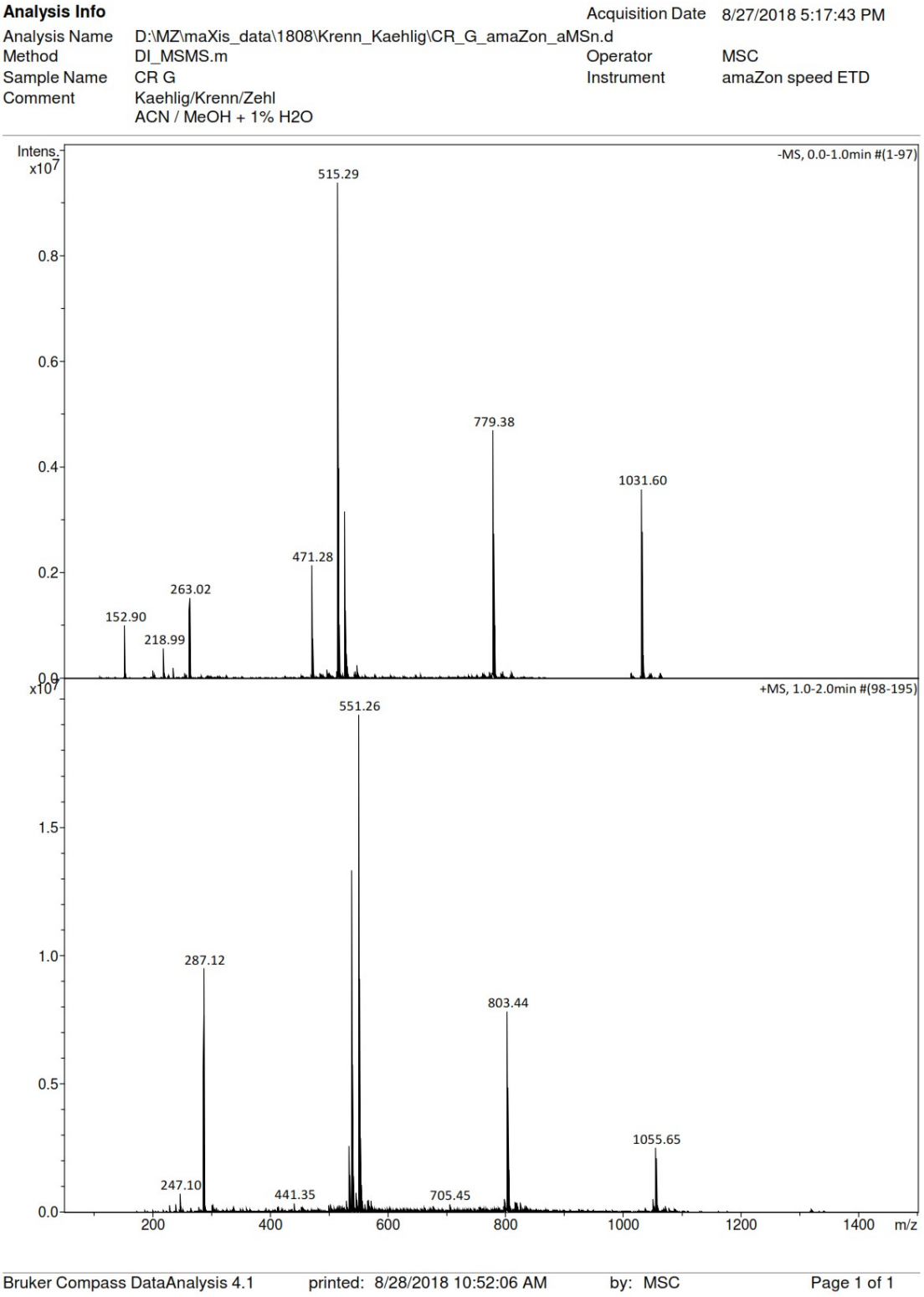

Analysis Info

Analysis Name	D:\MZ\maXis_data\1808\Krenn_Kaehlig\CR_G_amaZon_aMSn.d	Acquisition Date	8/27/2018 5:17:43 PM
Method	DI_MSMS.m	Operator	MSC
Sample Name	CR G	Instrument	amaZon speed ETD
Comment	Kaehlig/Krenn/Zehl ACN / MeOH + 1% H2O		

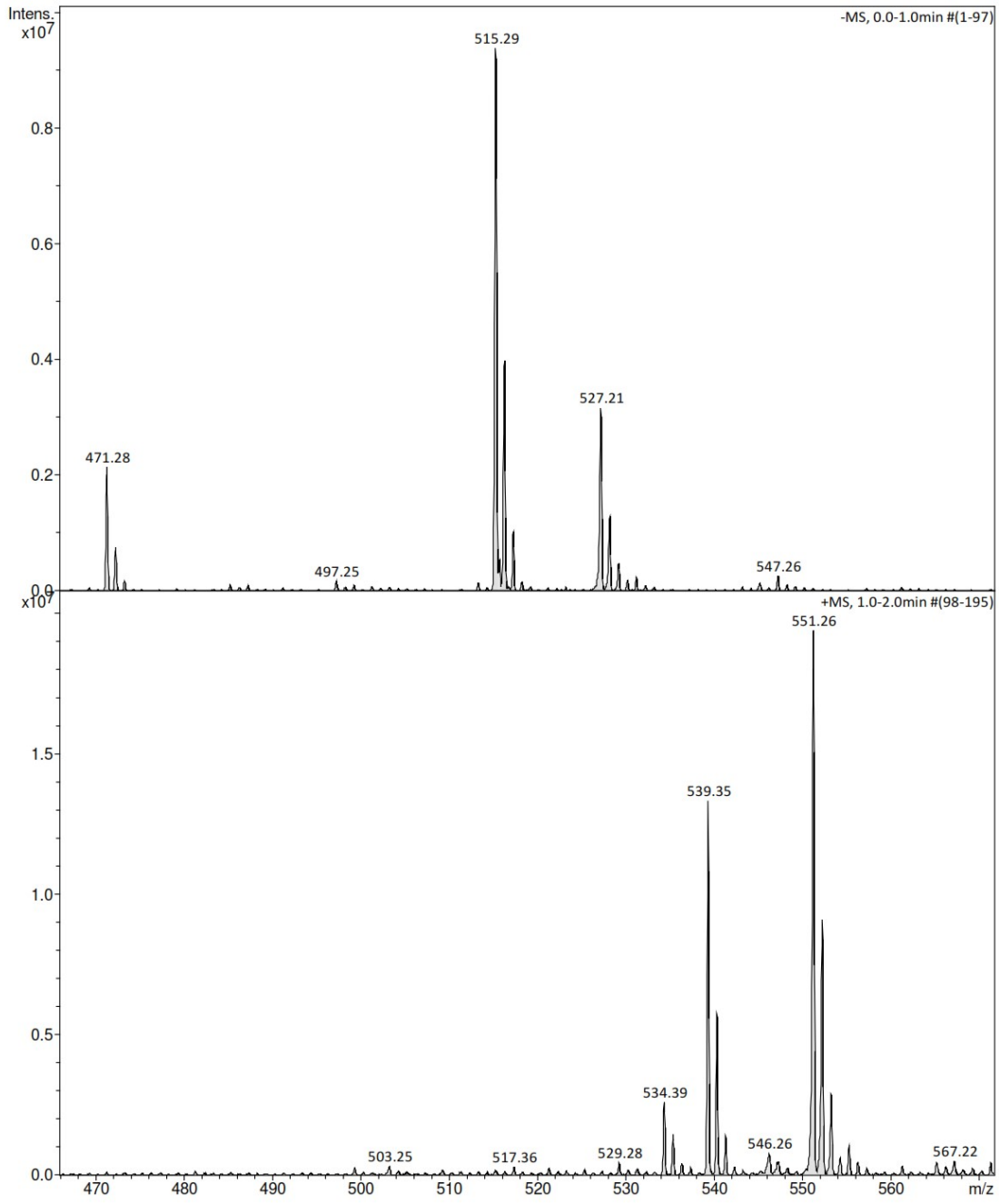

Analysis Info

Acquisition Date	8/27/2018 5:17:43 PM		
Analysis Name	D:\MZ\maXis_data\1808\Krenn_Kaehlig\CR_G_amaZon_aMSn.d		
Method	DI_MSMS.m	Operator	MSC
Sample Name	CR G	Instrument	amaZon speed ETD
Comment	Kaehlig/Krenn/Zehl ACN / MeOH + 1% H2O		

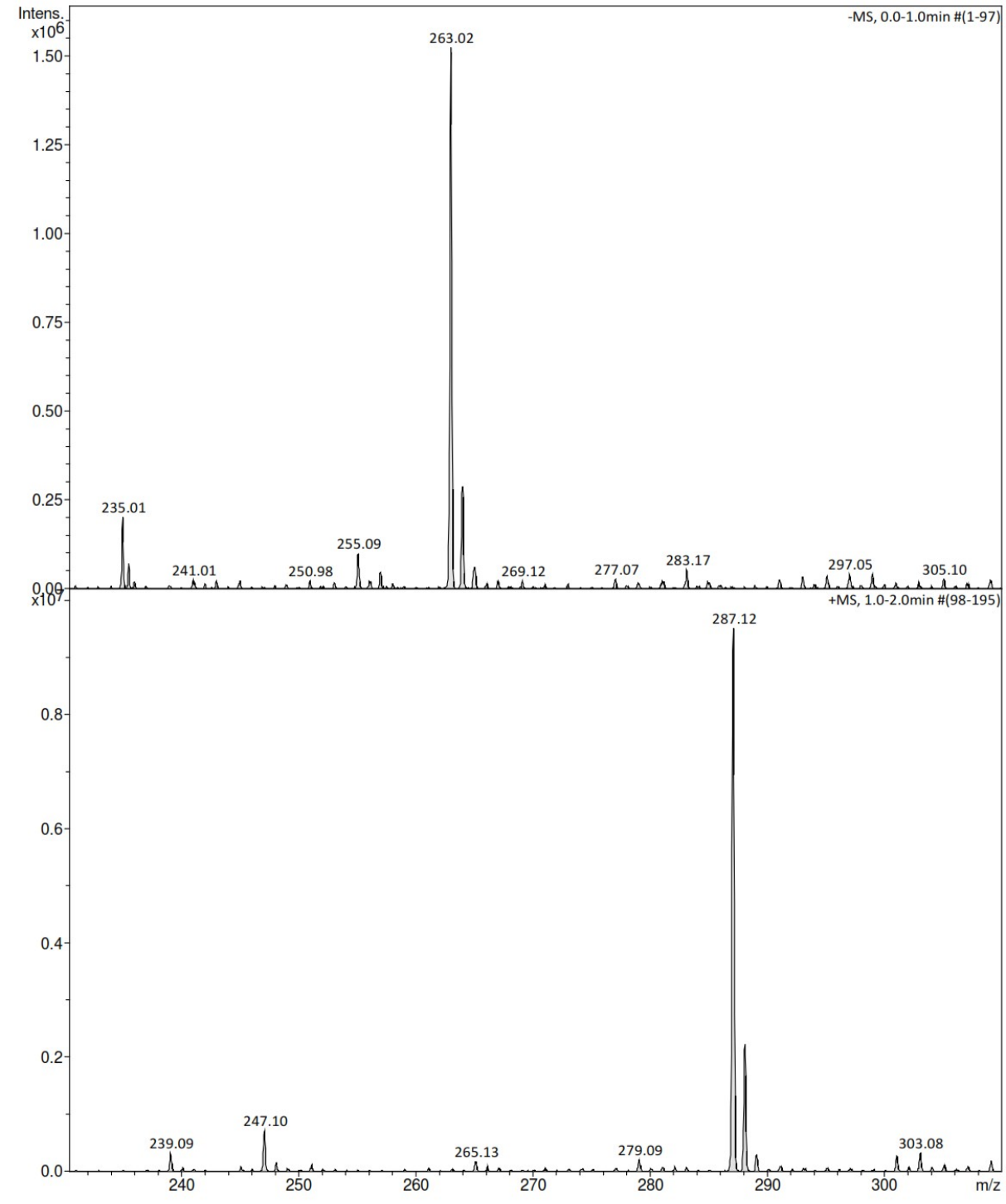

Analysis Info

Analysis Name	D:\MZ\maXis_data\1808\Krenn_Kaehlig\CR_G_amaZon_aMSn.d	Acquisition Date	8/27/2018 5:17:43 PM
Method	DI_MSMS.m	Operator	MSC
Sample Name	CR G	Instrument	amaZon speed ETD
Comment	Kaehlig/Krenn/Zehl ACN / MeOH + 1% H2O		

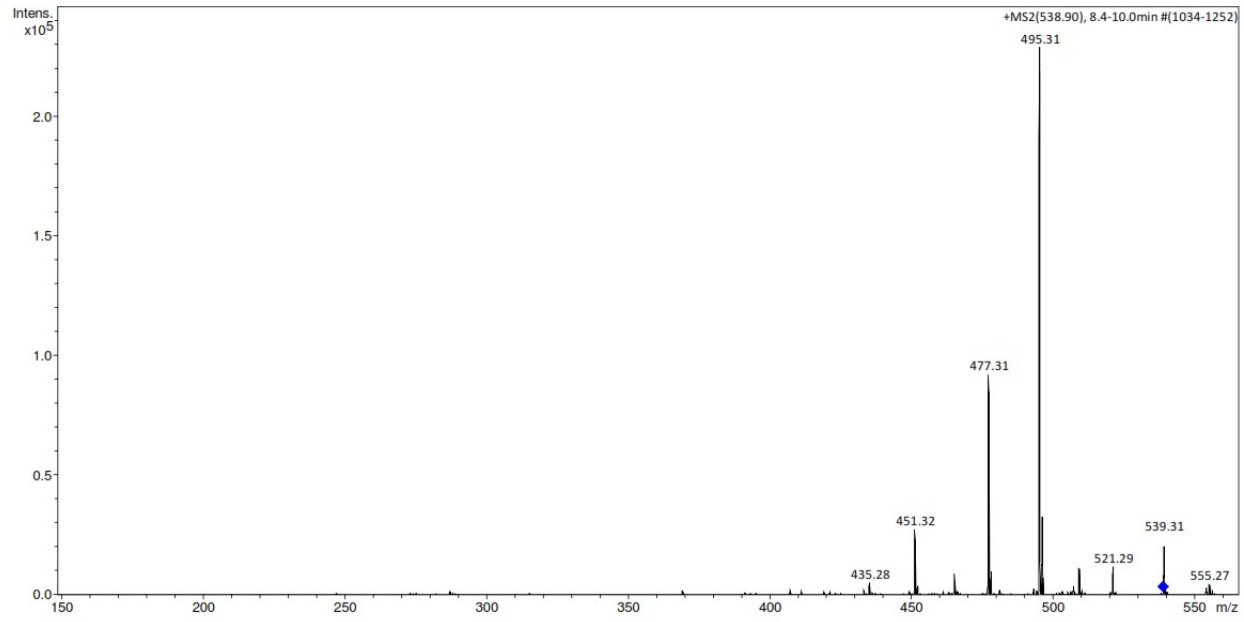

Analysis Info

Analysis Name	D:\MZ\maXis_data\1808\Krenn_Kaehlig\CR_G_amaZon_aMSn.d	Acquisition Date	8/27/2018 5:17:43 PM
Method	DI_MSMS.m	Operator	MSC
Sample Name	CR G	Instrument	amaZon speed ETD
Comment	Kaehlig/Krenn/Zehl ACN / MeOH + 1% H2O		

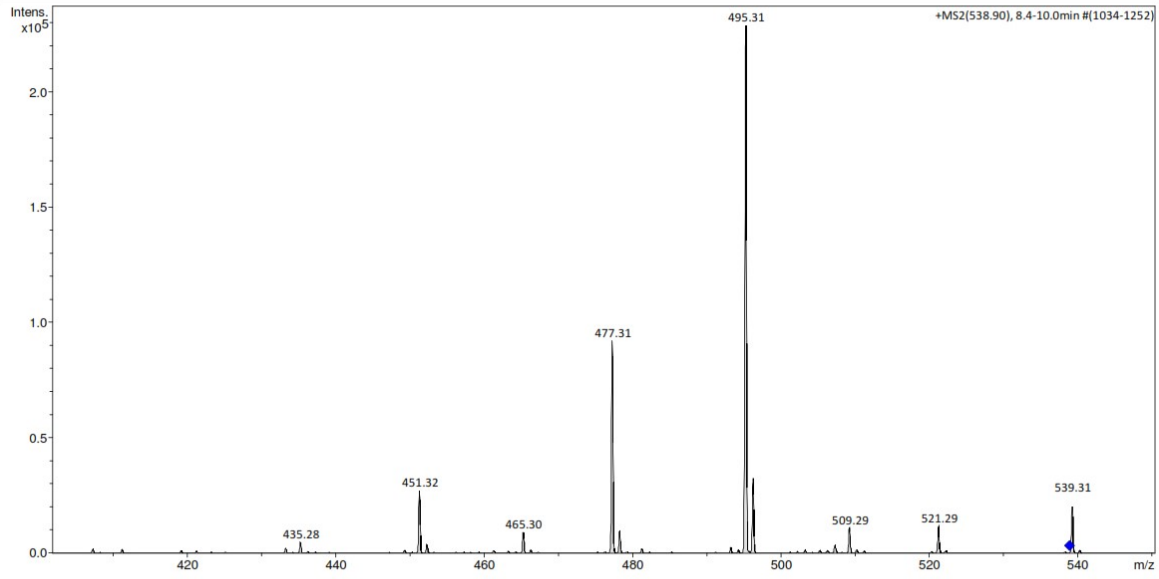

Analysis Info

Analysis Name	D:\MZ\maXis_data\1808\Krenn_Kaehlig\CR_G_amaZon_aMSn.d	Acquisition Date	8/27/2018 5:17:43 PM
Method	DI_MSMS.m	Operator	MSC
Sample Name	CR G	Instrument	amaZon speed ETD
Comment	Kaehlig/Krenn/Zehl ACN / MeOH + 1% H2O		

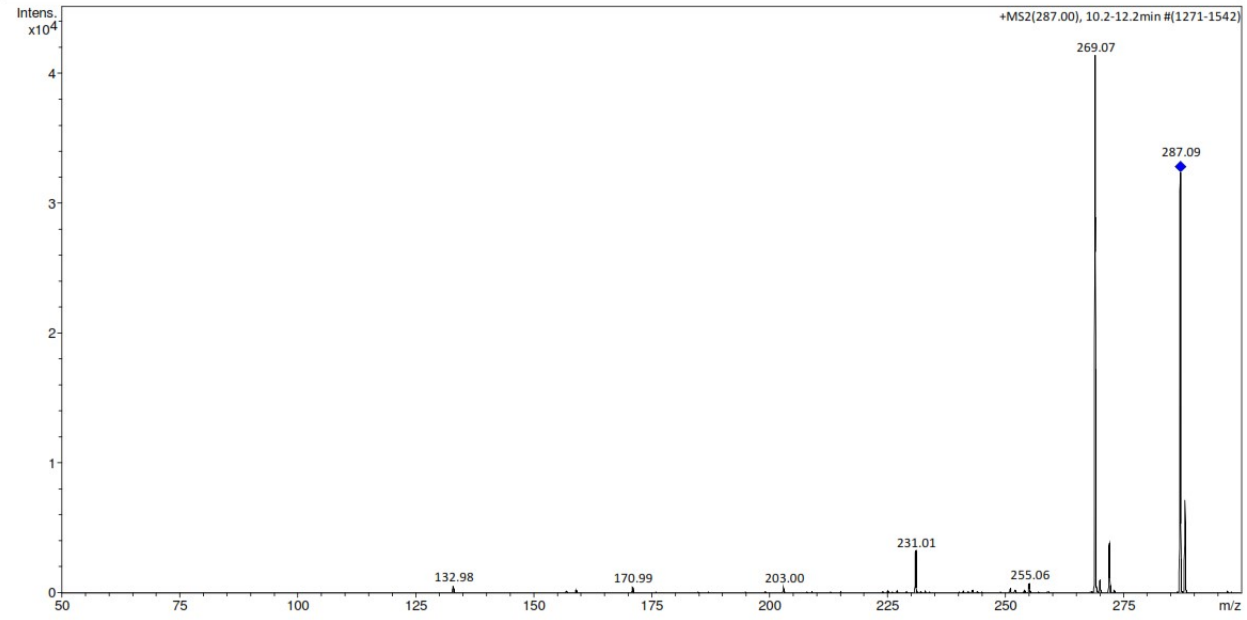

Analysis Info

Analysis Name	D:\MZ\maXis_data\1808\Krenn_Kaehlig\CR_G_amaZon_aMSn.d	Acquisition Date	8/27/2018 5:17:43 PM
Method	DI_MSMS.m	Operator	MSC
Sample Name	CR G	Instrument	amaZon speed ETD
Comment	Kaehlig/Krenn/Zehl ACN / MeOH + 1% H2O		

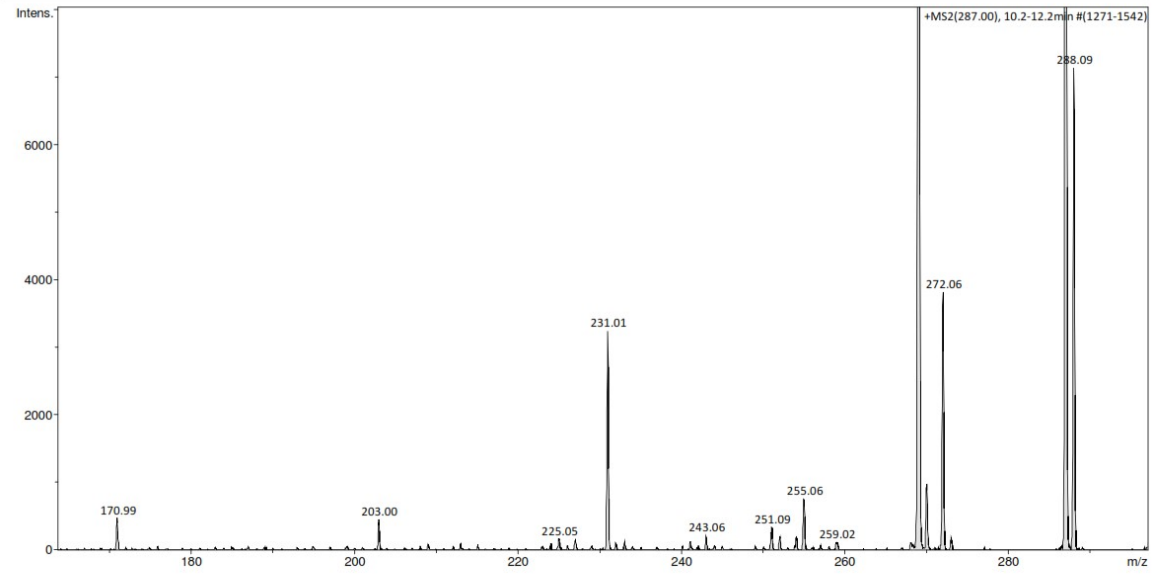

Analysis Info

Analysis Name	D:\MZ\maXis_data\1808\Krenn_Kaehlig\CR_G_amaZon_aMSn.d	Acquisition Date	8/27/2018 5:17:43 PM
Method	DI_MSMS.m	Operator	MSC
Sample Name	CR G	Instrument	amaZon speed ETD
Comment	Kaehlig/Krenn/Zehl ACN / MeOH + 1% H2O		

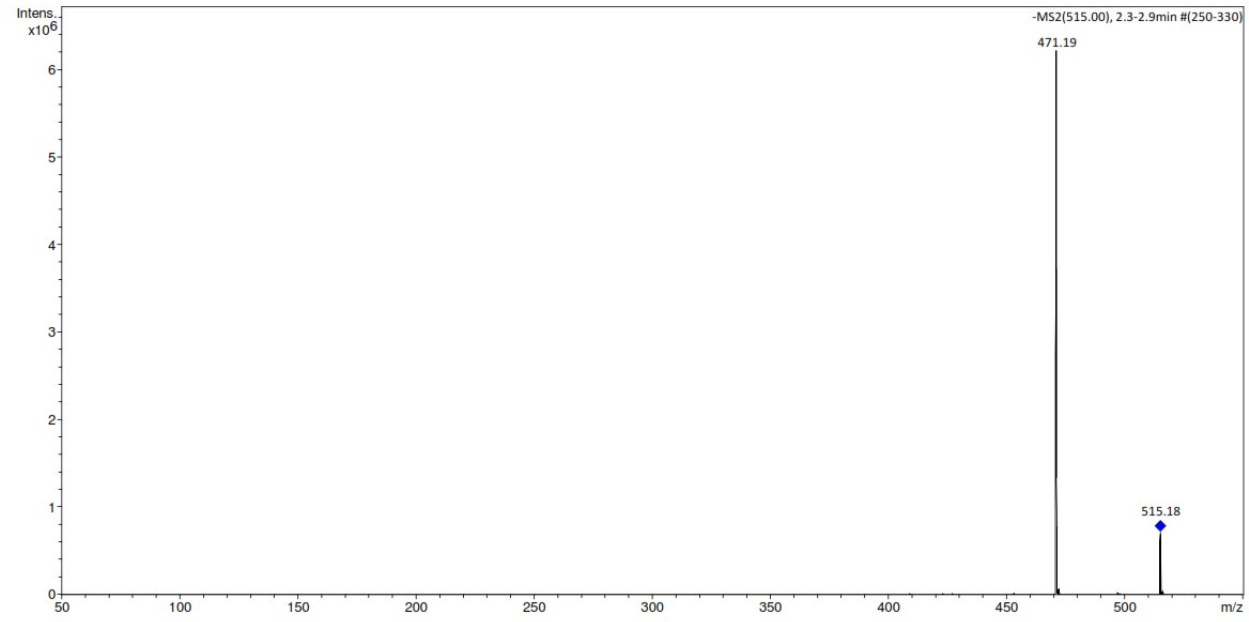

Bruker Compass DataAnalysis 4.1 printed: 8/28/2018 10:55:33 AM by: MSC Page 1 of 1

Analysis Info

Analysis Name	D:\MZ\maXis_data\1808\Krenn_Kaehlig\CR_G_amaZon_aMSn.d	Acquisition Date	8/27/2018 5:17:43 PM
Method	DI_MSMS.m	Operator	MSC
Sample Name	CR G	Instrument	amaZon speed ETD
Comment	Kaehlig/Krenn/Zehl ACN / MeOH + 1% H2O		

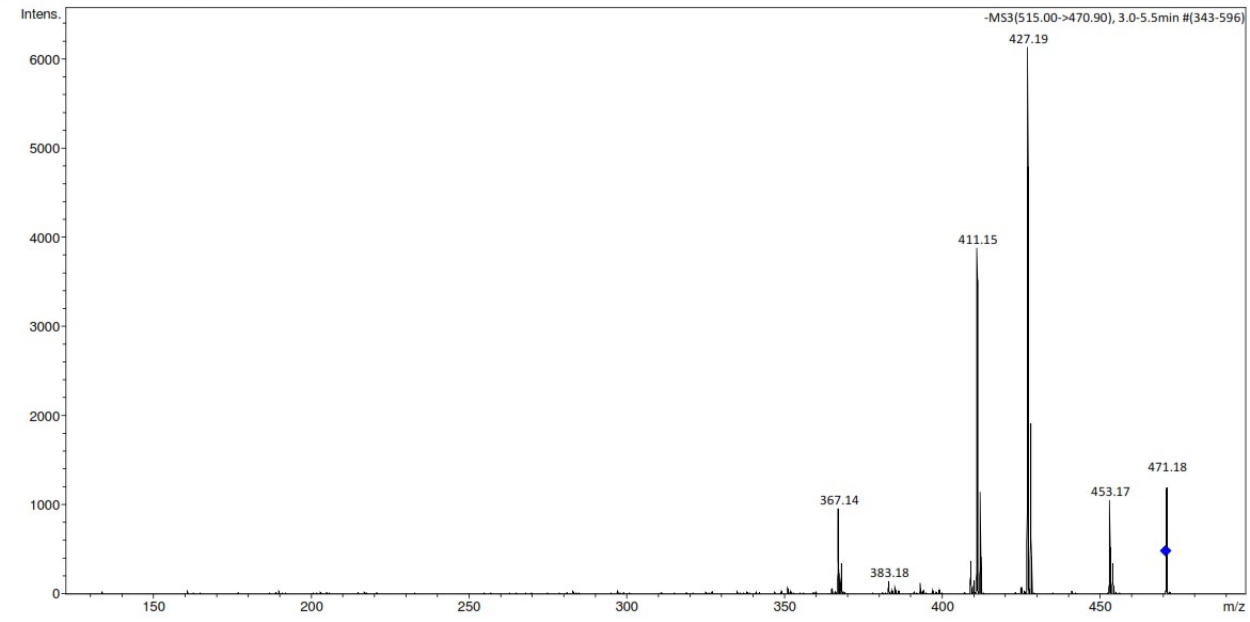

Bruker Compass DataAnalysis 4.1 printed: 8/28/2018 10:56:19 AM by: MSC Page 1 of 1

Analysis Info

Analysis Name	D:\MZ\maXis_data\1808\Krenn_Kaehlig\CR_G_amaZon_aMSn.d	Acquisition Date	8/27/2018 5:17:43 PM
Method	DI_MSMS.m	Operator	MSC
Sample Name	CR G	Instrument	amaZon speed ETD
Comment	Kaehlig/Krenn/Zehl ACN / MeOH + 1% H2O		

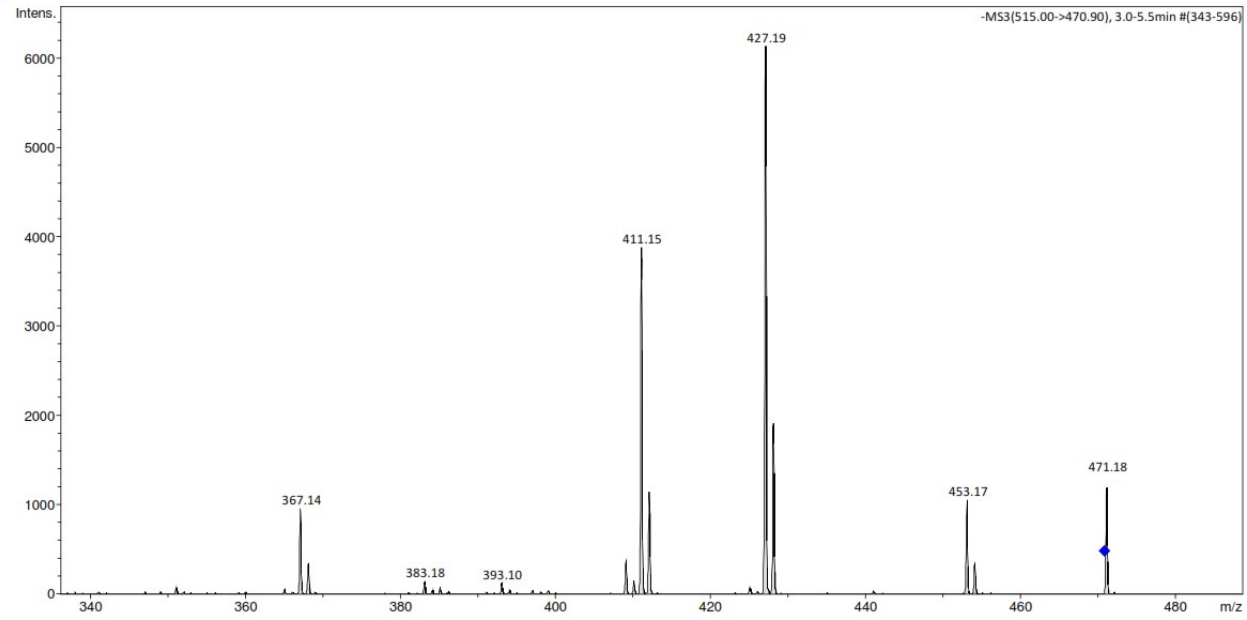

Analysis Info

Analysis Name	D:\MZ\maXis_data\1808\Krenn_Kaehlig\CR_G_amaZon_aMSn.d	Acquisition Date	8/27/2018 5:17:43 PM
Method	DI_MSMS.m	Operator	MSC
Sample Name	CR G	Instrument	amaZon speed ETD
Comment	Kaehlig/Krenn/Zehl ACN / MeOH + 1% H2O		

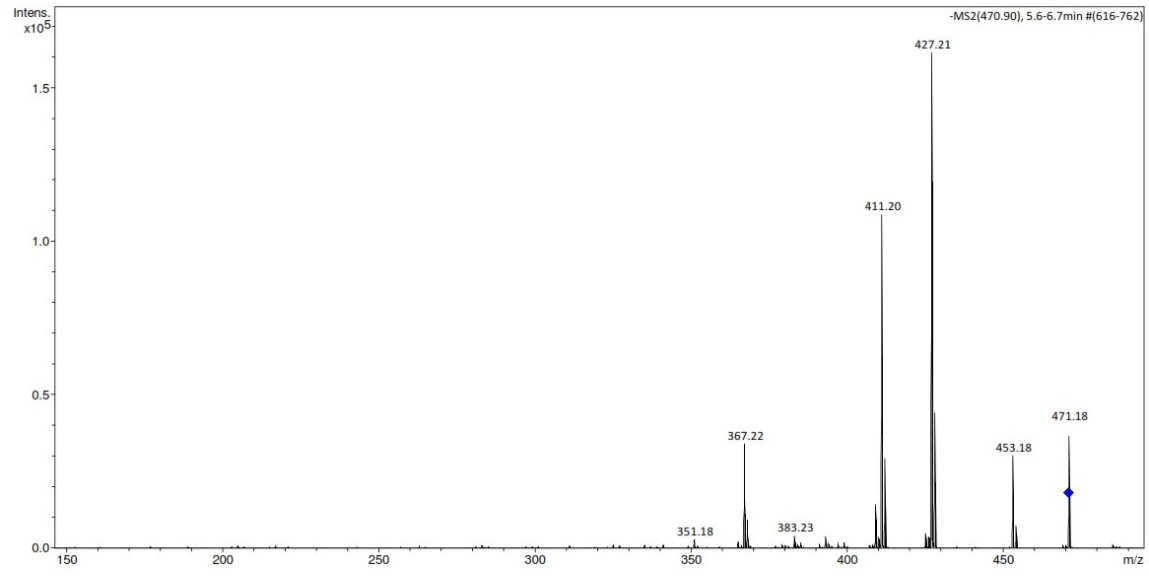

Analysis Info

Analysis Name	D:\MZ\maXis_data\1808\Krenn_Kaehlig\CR_G_amaZon_aMSn.d	Acquisition Date	8/27/2018 5:17:43 PM
Method	DI_MSMS.m	Operator	MSC
Sample Name	CR G	Instrument	amaZon speed ETD
Comment	Kaehlig/Krenn/Zehl ACN / MeOH + 1% H2O		

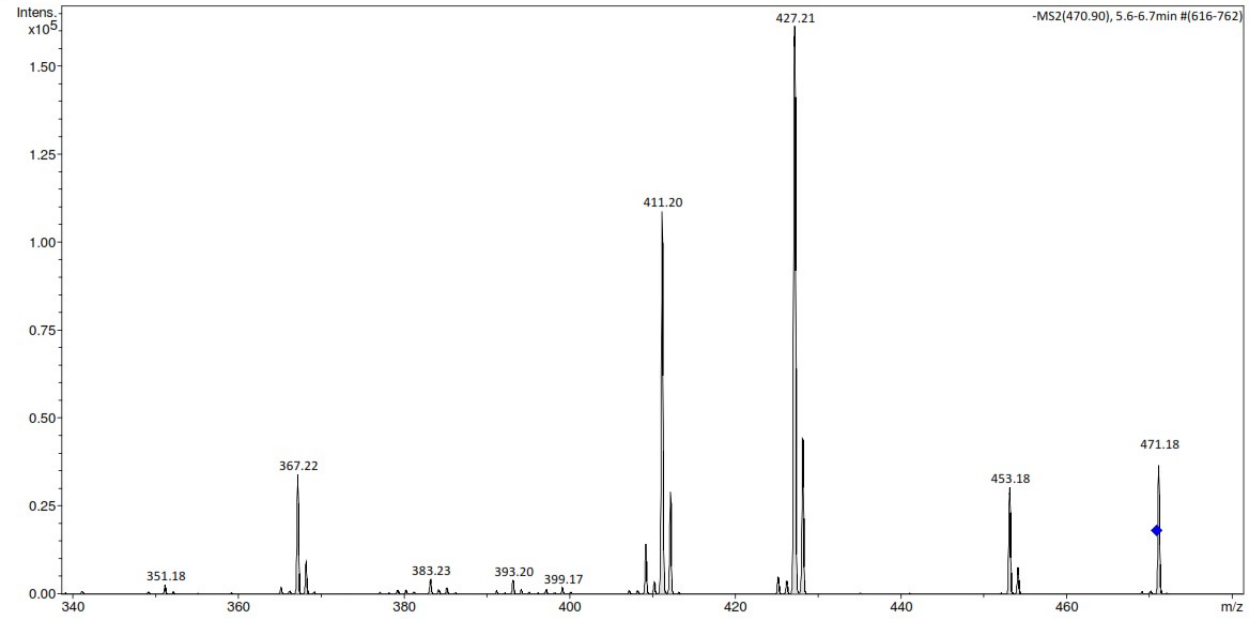

Analysis Info

Analysis Name	D:\MZ\maXis_data\1808\Krenn_Kaehlig\CR_G_amaZon_aMSn.d	Acquisition Date	8/27/2018 5:17:43 PM
Method	DI_MSMS.m	Operator	MSC
Sample Name	CR G	Instrument	amaZon speed ETD
Comment	Kaehlig/Krenn/Zehl ACN / MeOH + 1% H2O		

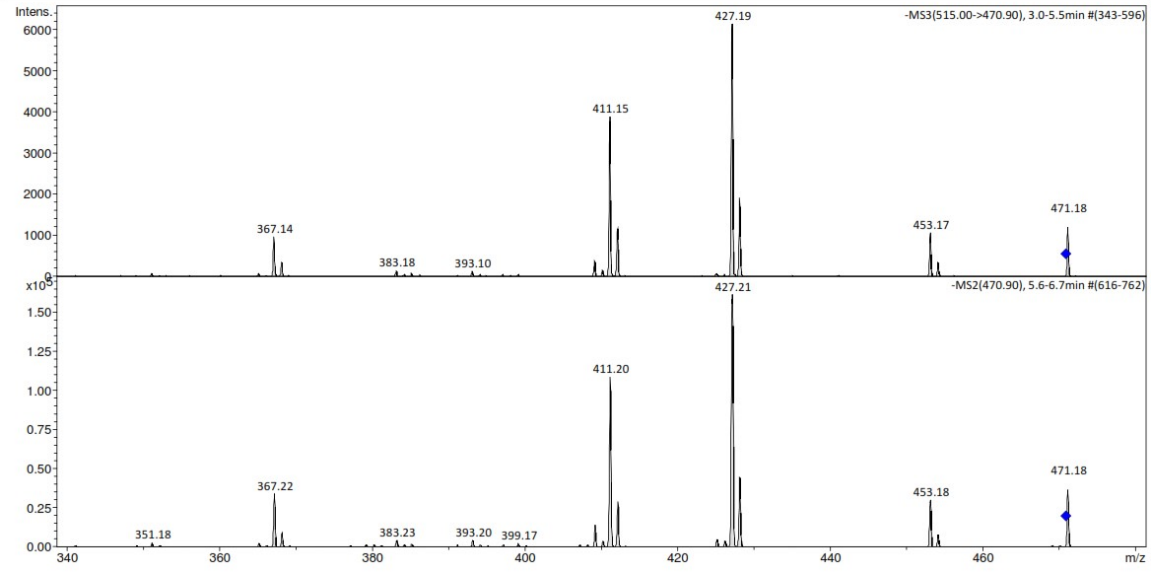

Analysis Info

Analysis Name	D:\MZ\maXis_data\1808\Krenn_Kaehlig\CR_G_amaZon_aMSn.d	Acquisition Date	8/27/2018 5:17:43 PM
Method	DI_MSMS.m	Operator	MSC
Sample Name	CR G	Instrument	amaZon speed ETD
Comment	Kaehlig/Krenn/Zehl ACN / MeOH + 1% H2O		

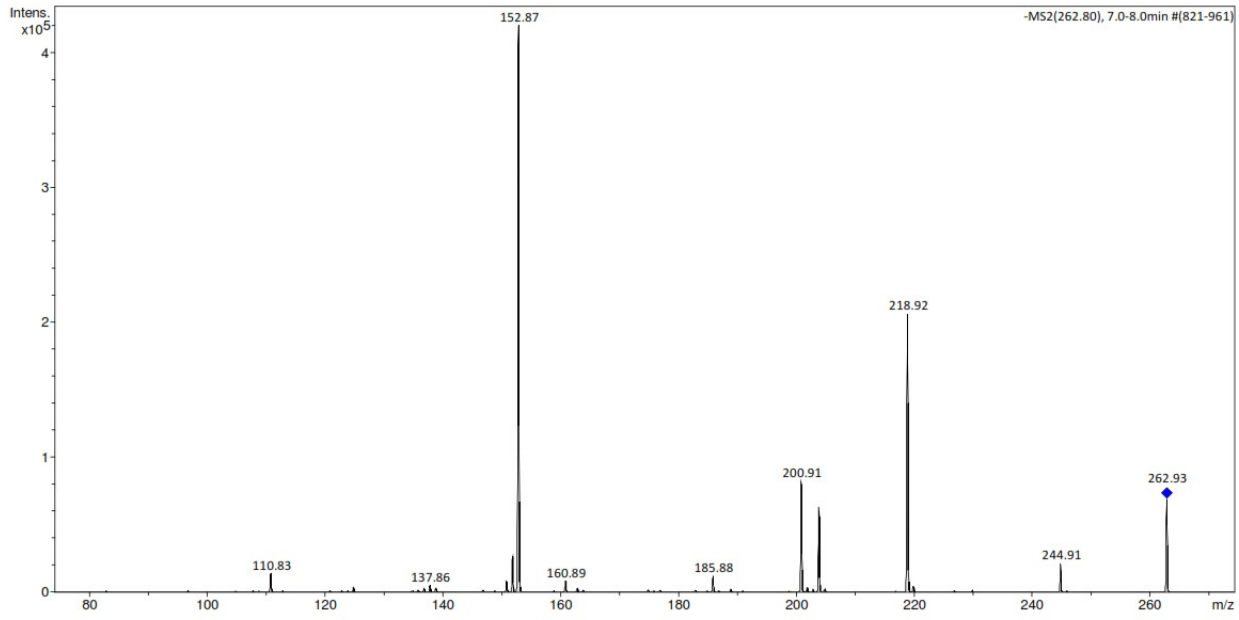

Bruker Compass DataAnalysis 4.1 printed: 8/28/2018 10:57:24 AM by: MSC Page 1 of 1

Appendix 7b: HRESI-MS of CR-G

Analysis Info

Analysis Name	D:\MZ\maXis_data\1808\Krenn_Kaehlig\59027000001.d	Acquisition Date	8/20/2018 12:13:25 PM
Method	tune_low_MS_Service_08_18.m	Operator	msc
Sample Name	CRG	Instrument	maXis
Comment	Kaehlig-Zehl/Anorg.Chem Ergebnis: +/- 5ppm ACN/MeOH +1%H2O		

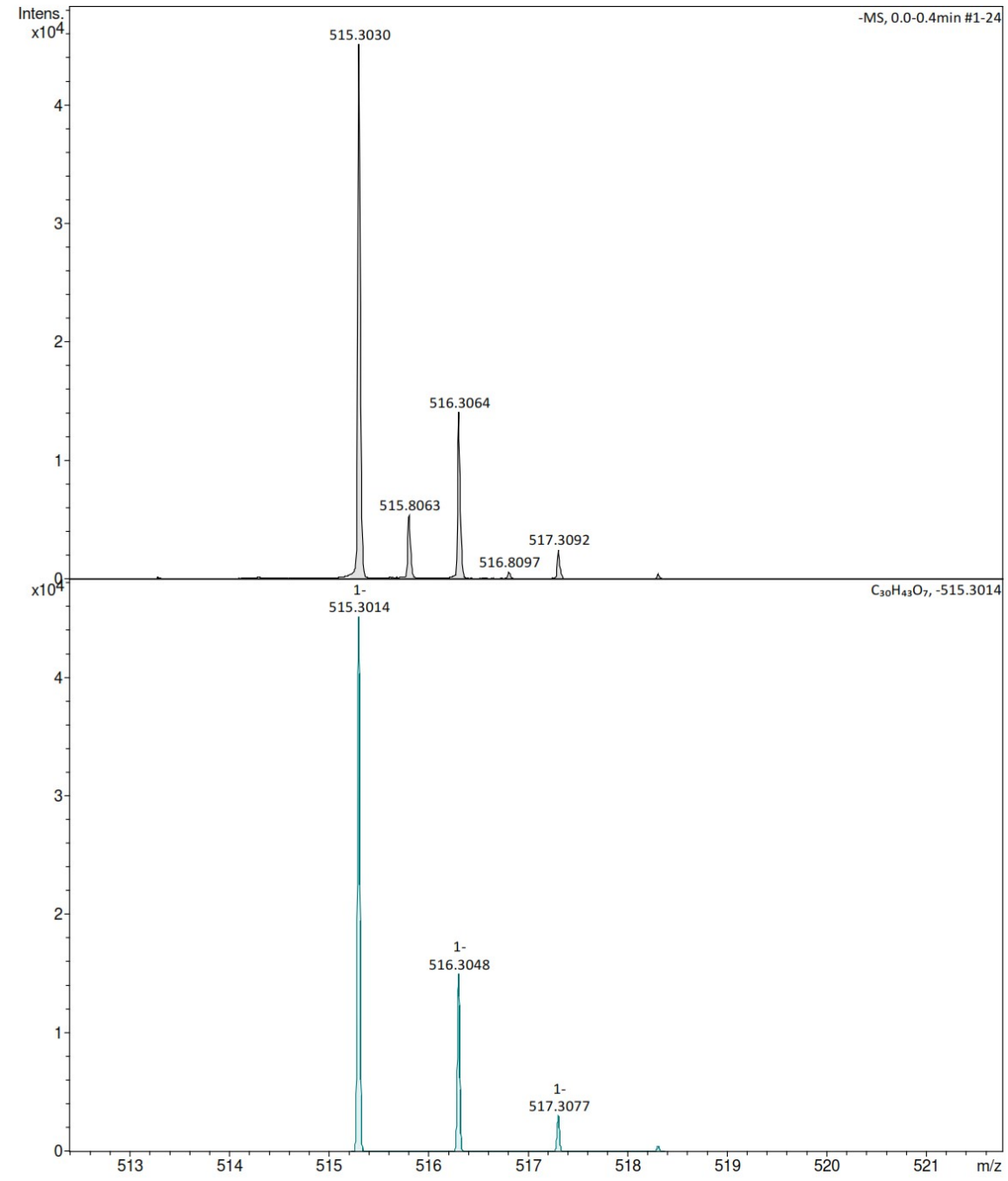

Bruker Compass DataAnalysis 4.1 printed: 8/28/2018 10:47:38 AM by: MSC Page 1 of 1

Analysis Info

Analysis Name	D:\MZ\maXis_data\1808\Krenn_Kaehlig\59027000001.d	Acquisition Date	8/20/2018 12:13:25 PM
Method	tune_low_MS_Service_08_18.m	Operator	msc
Sample Name	CRG	Instrument	maXis
Comment	Kaehlig-Zehl/Anorg.Chem Ergebnis: +/- 5ppm ACN/MeOH +1%H2O		

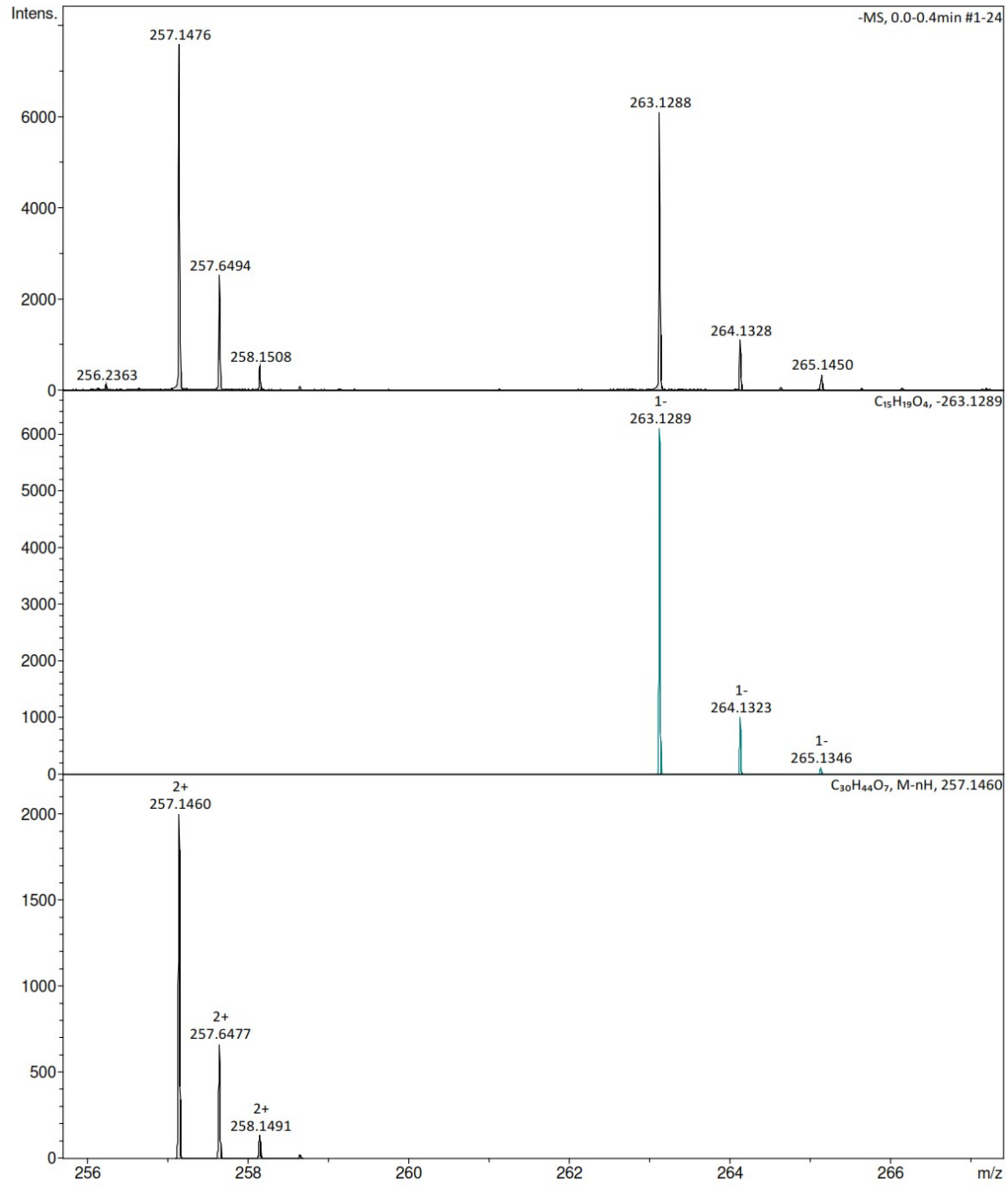

Mass Spectrum SmartFormula Report

Analysis Info

Analysis Name	D:\MZ\maXis_data\1808\Krenn_Kaehlig\59027000001.d	Acquisition Date	8/20/2018 12:13:25 PM
Method	tune_low_MS_Service_08_18.m	Operator	msc
Sample Name	CRG	Instrument	maXis 255552.00016
Comment	Kaehlig-Zehl/Anorg.Chem Ergebnis: +/- 5ppm ACN/MeOH +1%H2O		

Acquisition Parameter

Source Type	ESI	Ion Polarity	Negative	Set Nebulizer	0.4 Bar
Focus	Not active	Set Capillary	4500 V	Set Dry Heater	180 °C
Scan Begin	50 m/z	Set End Plate Offset	-500 V	Set Dry Gas	4.0 l/min
Scan End	1900 m/z	Set Charging Voltage	0 V	Set Divert Valve	Source
		Set Corona	0 nA	Set APCI Heater	0 °C

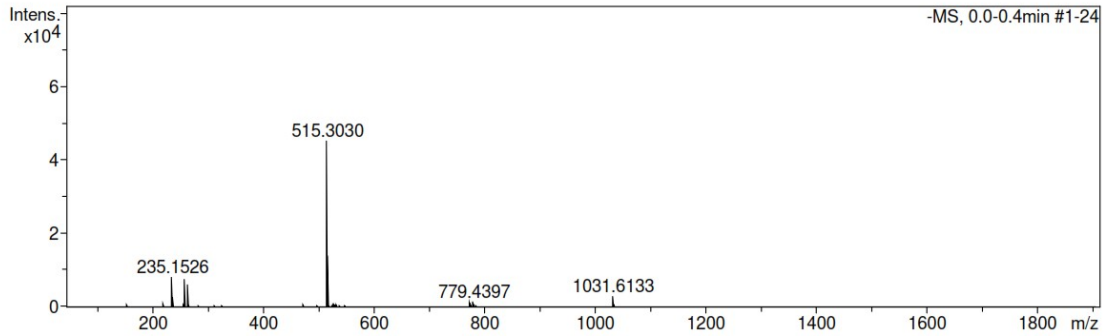

Meas. m/z	#	Ion Formula	Score	m/z	err [mDa]	err [ppm]	mSigma	rdb	e⁻ Conf	N-Rule
257.1476	1	C30H42O7	91.28	257.1471	-0.6	-2.2	5.5	10.0	even	ok
	2	C27H34N10O	60.16	257.1464	-1.2	-4.8	8.0	16.0	even	ok
	3	C31H38N4O3	100.00	257.1477	0.1	0.4	11.5	15.0	even	ok
	4	C17H30N20	26.10	257.1487	-1.0	-4.0	48.0	13.0	even	ok
	5	C19H42N6O10	24.00	257.1487	-1.0	-4.0	50.7	2.0	even	ok
	6	C16H34N16O4	32.76	257.1480	0.4	1.4	51.9	8.0	even	ok
	7	C15H38N12O8	23.65	257.1473	-0.3	-1.2	62.7	3.0	even	ok
	8	C12H30N22O2	11.14	257.1467	-1.0	-3.8	73.9	9.0	even	ok
263.1288	1	C15H19O4	100.00	263.1289	-0.1	-0.5	15.4	6.5	even	ok
	2	C8H19N6O2S	38.09	263.1296	-0.8	-3.1	42.0	2.5	even	ok
515.3030	1	C30H43O7	59.84	515.3014	-1.5	-3.0	11.7	9.5	even	ok
	2	C31H39N4O3	100.00	515.3028	0.2	0.4	22.4	14.5	even	ok

Appendix 8: 1D and 2D NMR of CR-G

Appendix 8a: ^{1}H NMR of CR-G

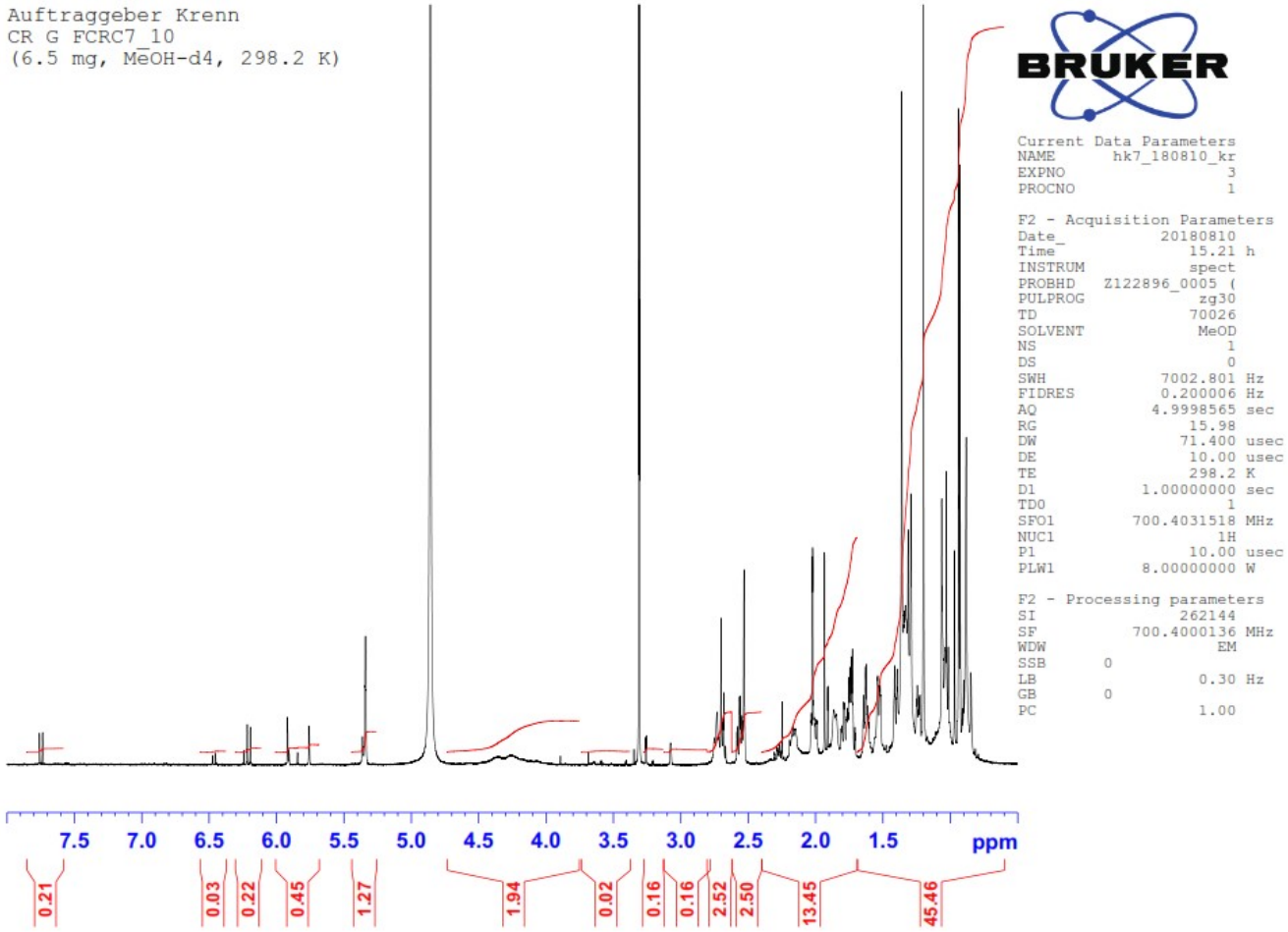

Auftraggeber Krenn
CR G FCRC7_10
(6.5 mg, MeOH-d4, 298.2 K)

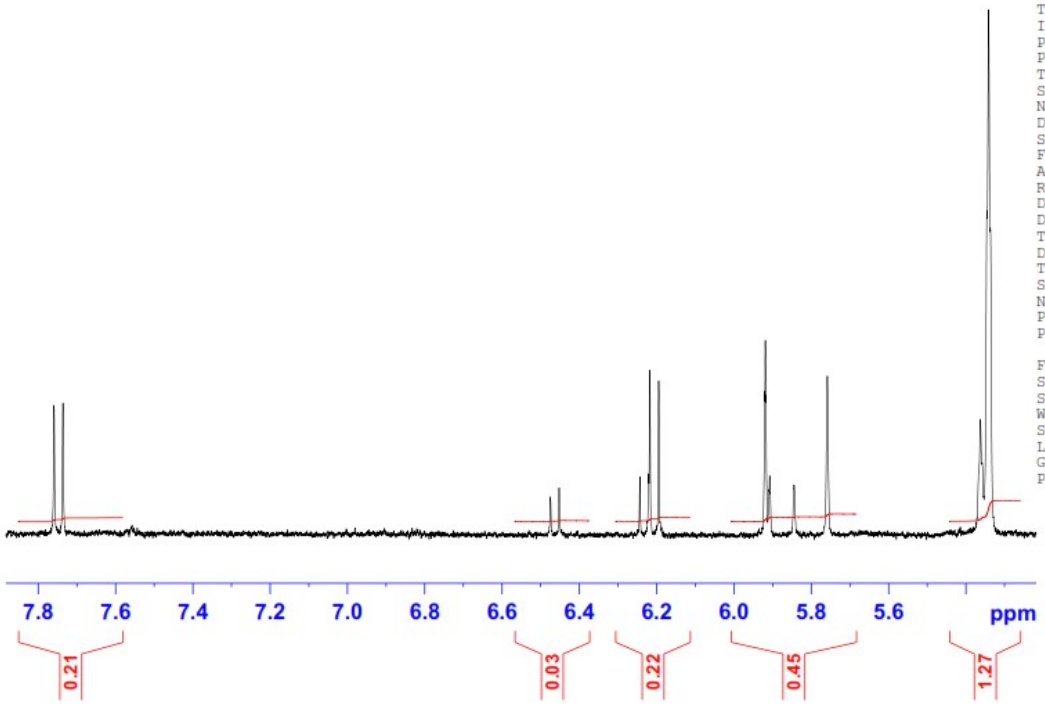


```
Current Data Parameters
NAME      hk7_180810_kr
EXPNO                 3
PROCNO                1

F2 - Acquisition Parameters
Date_          20180810
Time              15.21 h
INSTRUM            spect
PROBHD   Z122896_0005 (
PULPROG            zg30
TD                70026
SOLVENT            MeOD
NS                    1
DS                    0
SWH            7002.801 Hz
FIDRES        0.200006 Hz
AQ            4.9998565 sec
RG                15.98
DW               71.400 usec
DE               10.00 usec
TE               298.2 K
D1           1.00000000 sec
TD0                   1
SFO1        700.4031518 MHz
NUC1                 1H
P1               10.00 usec
PLW1          8.00000000 W

F2 - Processing parameters
SI                262144
SF          700.4000136 MHz
WDW                 EM
SSB       0
LB               0.30 Hz
GB        0
PC               1.00
```

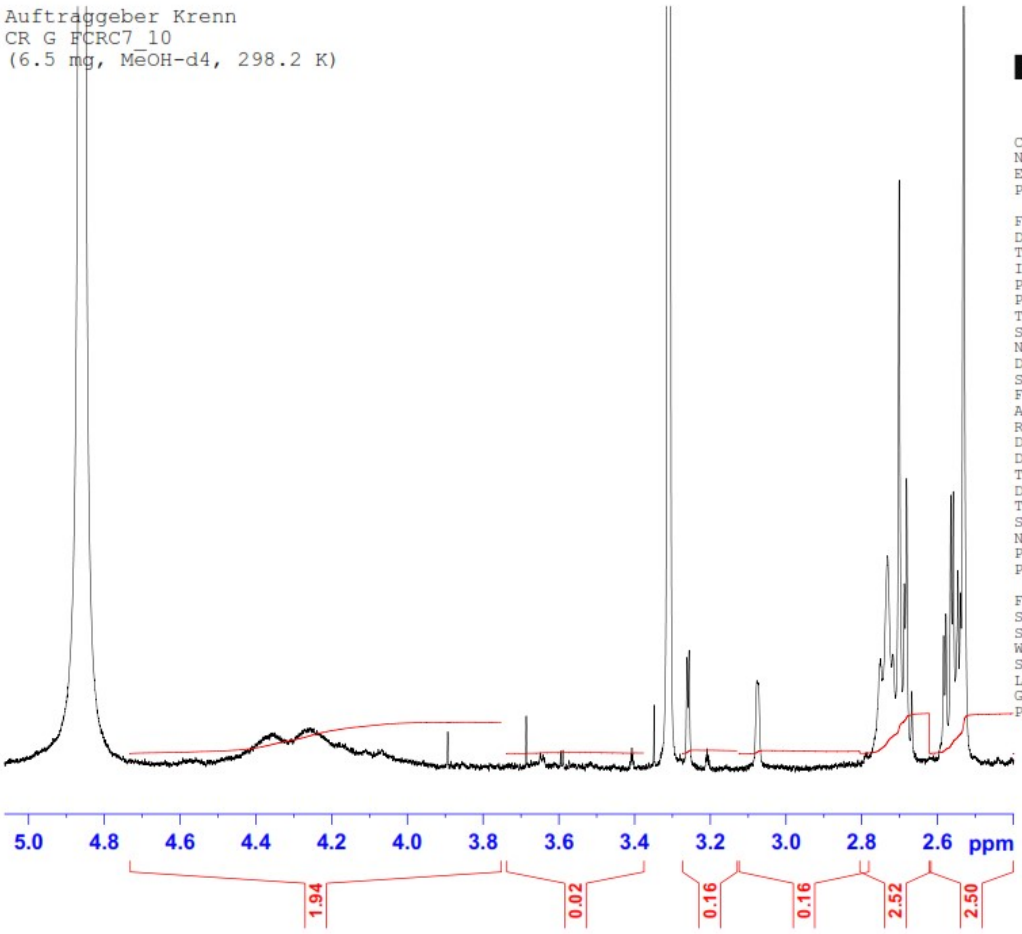

BRUKER

Current Data Parameters
NAME hk7_180810_kr
EXPNO 3
PROCNO 1

F2 - Acquisition Parameters
Date_ 20180810
Time 15.21 h
INSTRUM spect
PROBHD Z122896_0005 (
PULPROG zg30
TD 70026
SOLVENT MeOD
NS 1
DS 0
SWH 7002.801 Hz
FIDRES 0.200006 Hz
AQ 4.9998565 sec
RG 15.98
DW 71.400 usec
DE 10.00 usec
TE 298.2 K
D1 1.00000000 sec
TD0 1
SFO1 700.4031518 MHz
NUC1 1H
P1 10.00 usec
PLW1 8.00000000 W

F2 - Processing parameters
SI 262144
SF 700.4000136 MHz
WDW EM
SSB 0
LB 0.30 Hz
GB 0
PC 1.00

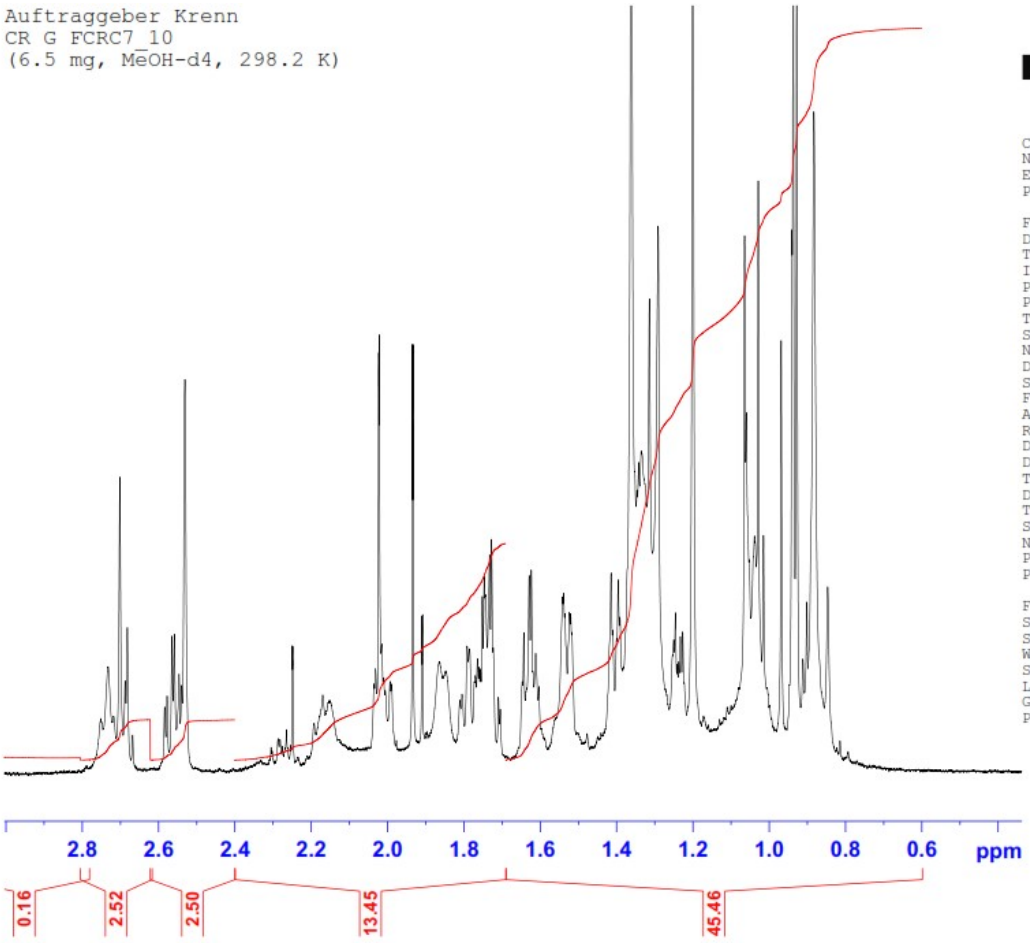

Current Data Parameters
NAME hk7_180810_kr
EXPNO 3
PROCNO 1

F2 - Acquisition Parameters
Date_ 20180810
Time 15.21 h
INSTRUM spect
PROBHD Z122896_0005 (
PULPROG zg30
TD 70026
SOLVENT MeOD
NS 1
DS 0
SWH 7002.801 Hz
FIDRES 0.200006 Hz
AQ 4.9998565 sec
RG 15.98
DW 71.400 usec
DE 10.00 usec
TE 298.2 K
D1 1.00000000 sec
TD0 1
SFO1 700.4031518 MHz
NUC1 1H
P1 10.00 usec
PLW1 8.00000000 W

F2 - Processing parameters
SI 262144
SF 700.4000136 MHz
WDW EM
SSB 0
LB 0.30 Hz
GB 0
PC 1.00

Appendix 8b: ^{13}C NMR of CR-G

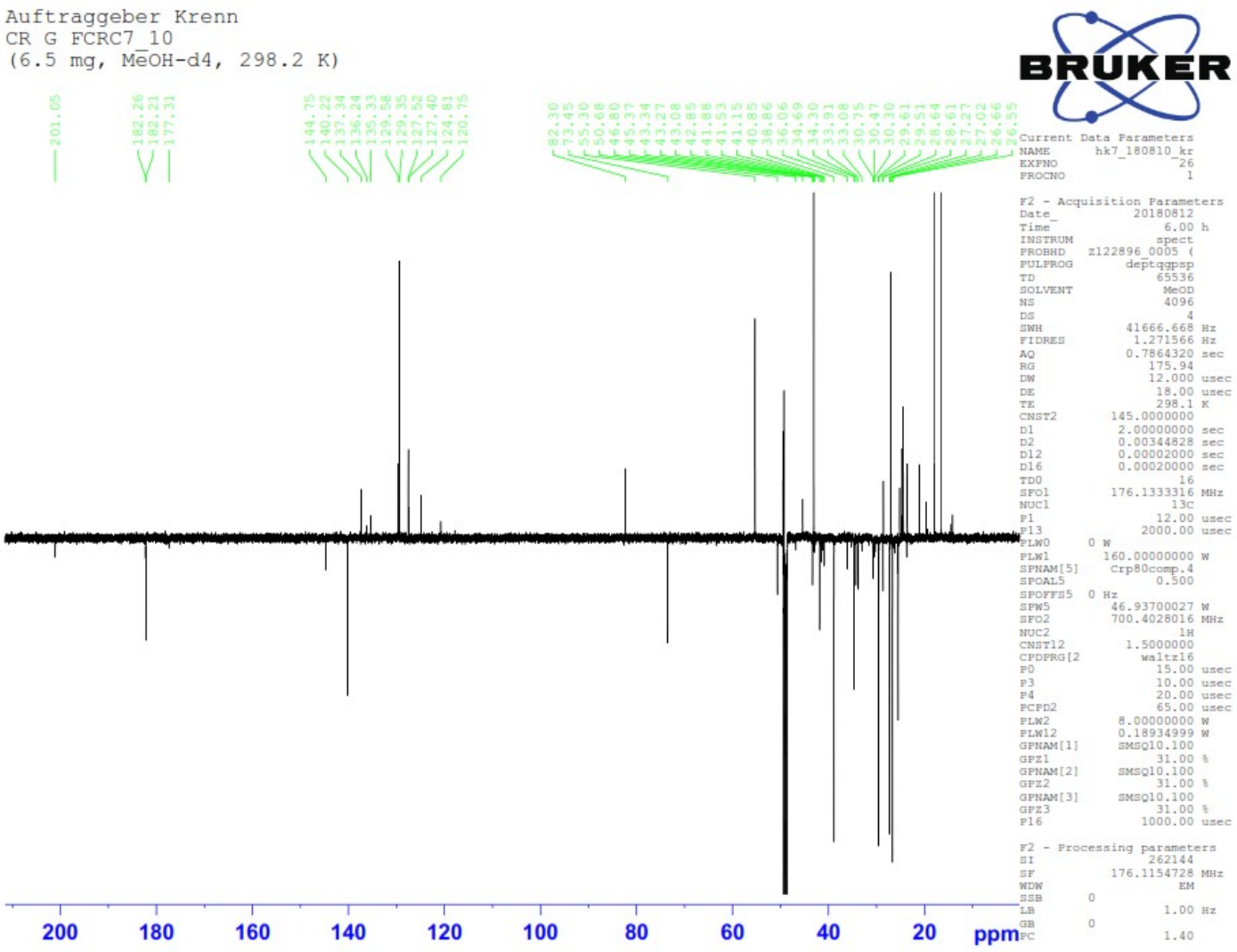

Auftraggeber Krenn
CR G FCRC7_10
(6.5 mg, MeOH-d4, 298.2 K)

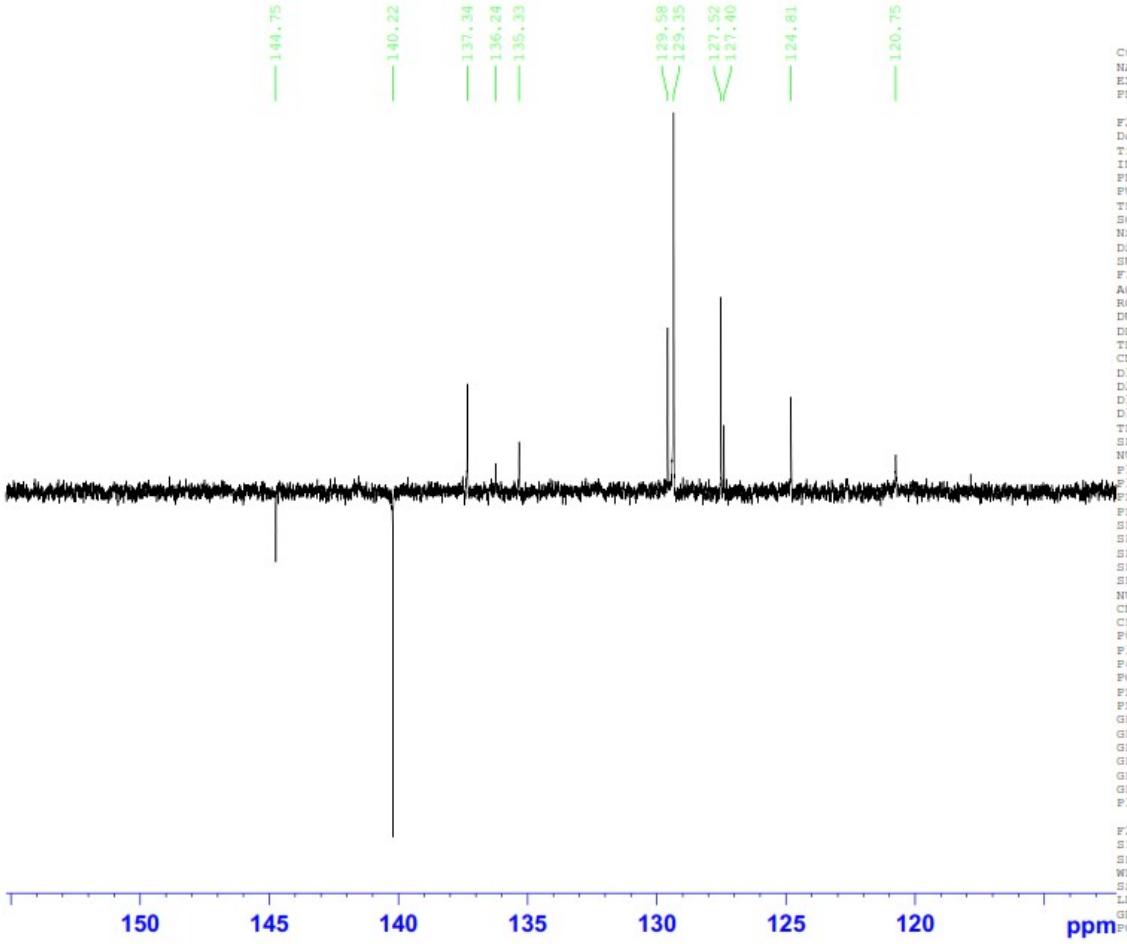

Current Data Parameters
NAME hk7_180810_kr
EXPNO 26
PROCNO 1

F2 - Acquisition Parameters
Date_ 20180812
Time 6.00 h
INSTRUM spect
PROBHD z122896_0005 (
PULFROG deptqgpsp
TD 65536
SOLVENT MeOD
NS 4096
DS 4
SWH 41666.668 Hz
FIDRES 1.271566 Hz
AQ 0.7864320 sec
RG 175.94
DW 12.000 usec
DE 18.00 usec
TE 298.1 K
CNST2 145.0000000
D1 2.00000000 sec
D2 0.00344828 sec
D12 0.00002000 sec
D16 0.00020000 sec
TD0 16
SFO1 176.1333316 MHz
NUC1 13C
P1 12.00 usec
P13 2000.00 usec
PLW0 0 W
PLW1 160.00000000 W
SFNAM[5] Crp80comp.4
SPOAL5 0.500
SPOFFS5 0 Hz
SPW5 46.93700027 W
SFO2 700.4028016 MHz
NUC2 1H
CNST12 1.5000000
CPDPRG[2 waltz16
P0 15.00 usec
P3 10.00 usec
P4 20.00 usec
PCPD2 65.00 usec
PLW2 8.00000000 W
PLW12 0.18934999 W
GPNAM[1] SMSQ10.100
GPZ1 31.00 %
GPNAM[2] SMSQ10.100
GPZ2 31.00 %
GPNAM[3] SMSQ10.100
GPZ3 31.00 %
P16 1000.00 usec

F2 - Processing parameters
SI 262144
SF 176.1154728 MHz
WDW EM
SSB 0
LB 1.00 Hz
GB 0
PC 1.40

Auftraggeber Krenn
CR G FCRC7_10
(6.5 mg, MeOH-d4, 298.2 K)

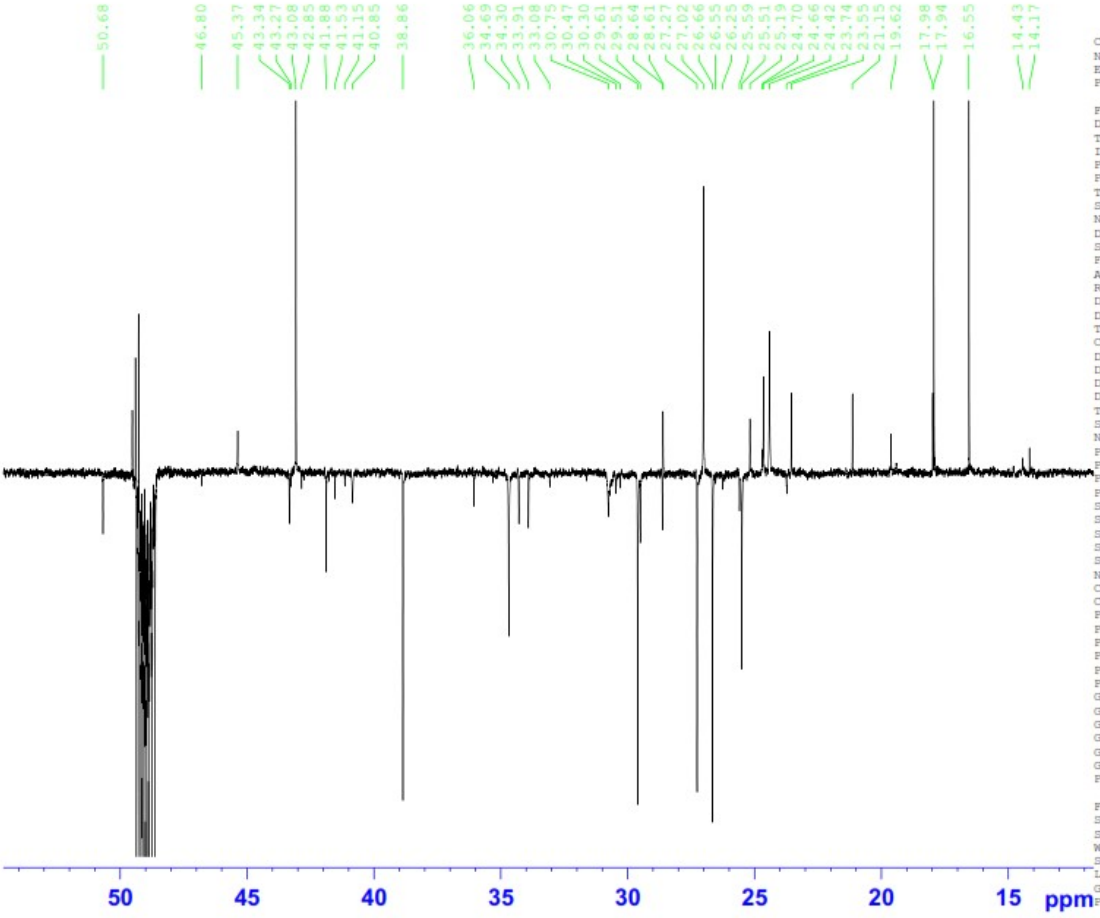


```
Current Data Parameters
NAME      hk7_180810_kr
EXPNO               26
PROCNO               1

F2 - Acquisition Parameters
Date_          20180812
Time               6.00 h
INSTRUM           spect
PROBHD   z122896_0005 (
PULPROG       deptqgpsp
TD                65536
SOLVENT            MeOD
NS                 4096
DS                    4
SWH           41666.668 Hz
FIDRES         1.271566 Hz
AQ            0.7864320 sec
RG                175.94
DW                12.000 usec
DE                18.00 usec
TE                298.1 K
CNST2        145.0000000
D1            2.00000000 sec
D2            0.00344828 sec
D12           0.00002000 sec
D16           0.00020000 sec
TD0                  16
SFO1         176.1333316 MHz
NUC1                13c
P1                12.00 usec
P13             2000.00 usec
PLW0      0 W
PLW1       160.00000000 W
SPNAM[5]     Crp80comp.4
SPOAL5             0.500
SPOFFS5   0 Hz
SPW5        46.93700027 W
SFO2         700.4028016 MHz
NUC2                1H
CNST12         1.5000000
CPDPRG[2          waltz16
P0                15.00 usec
P3                10.00 usec
P4                20.00 usec
PCPD2             65.00 usec
PLW2          8.00000000 W
PLW12         0.18934999 W
GPNAM[1]      SMSQ10.100
GPZ1                31.00 %
GPNAM[2]      SMSQ10.100
GPZ2                31.00 %
GPNAM[3]      SMSQ10.100
GPZ3                31.00 %
P16               1000.00 usec

F2 - Processing parameters
SI                  262144
SF           176.1154728 MHz
WDW                    EM
SSB       0
LB                 1.00 Hz
GB        0
PC                 1.40
```

Appendix 8c: COSY of CR-G

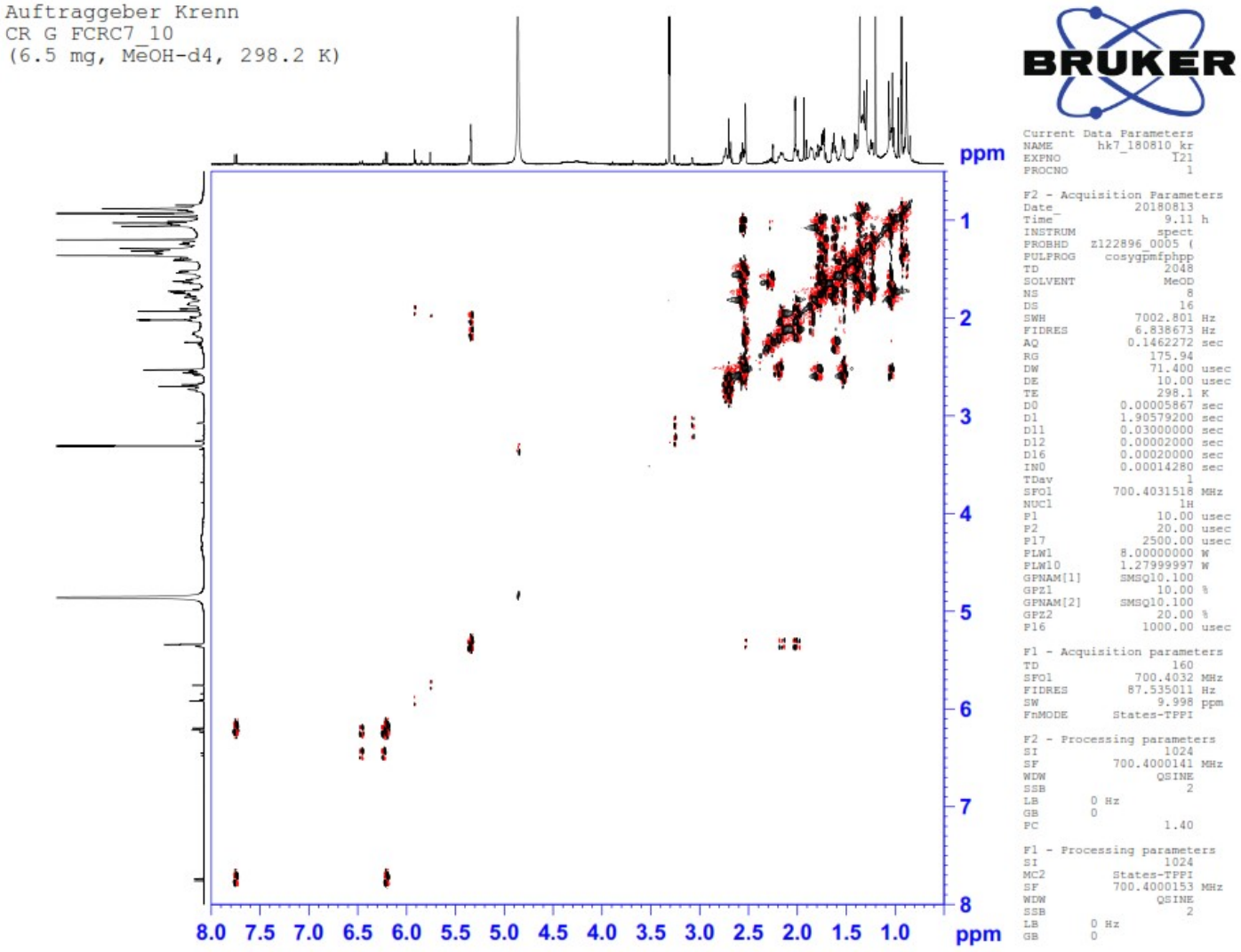

Appendix 8d: HMBC of CR-G

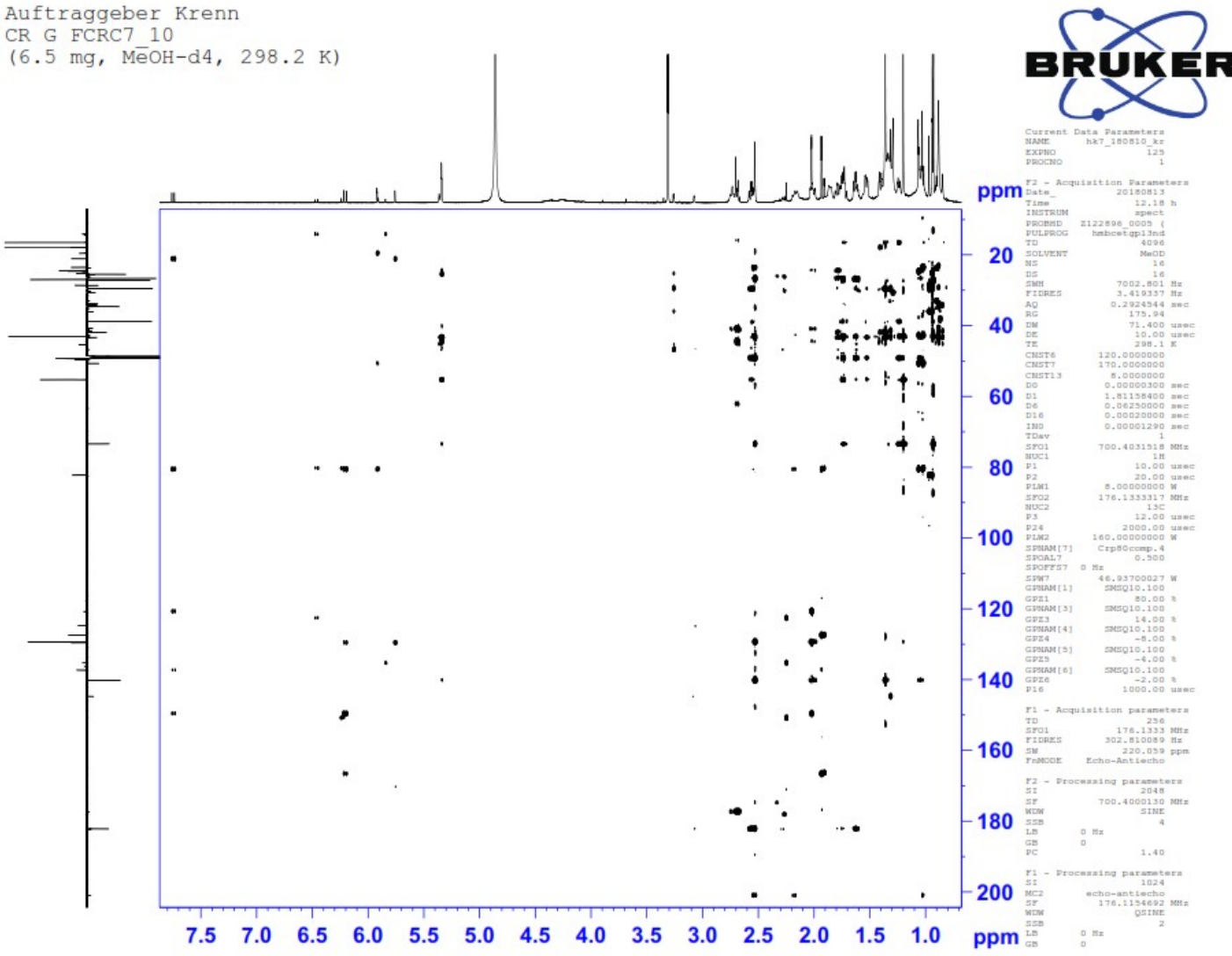

Appendix 8e: HSQC of CR-G

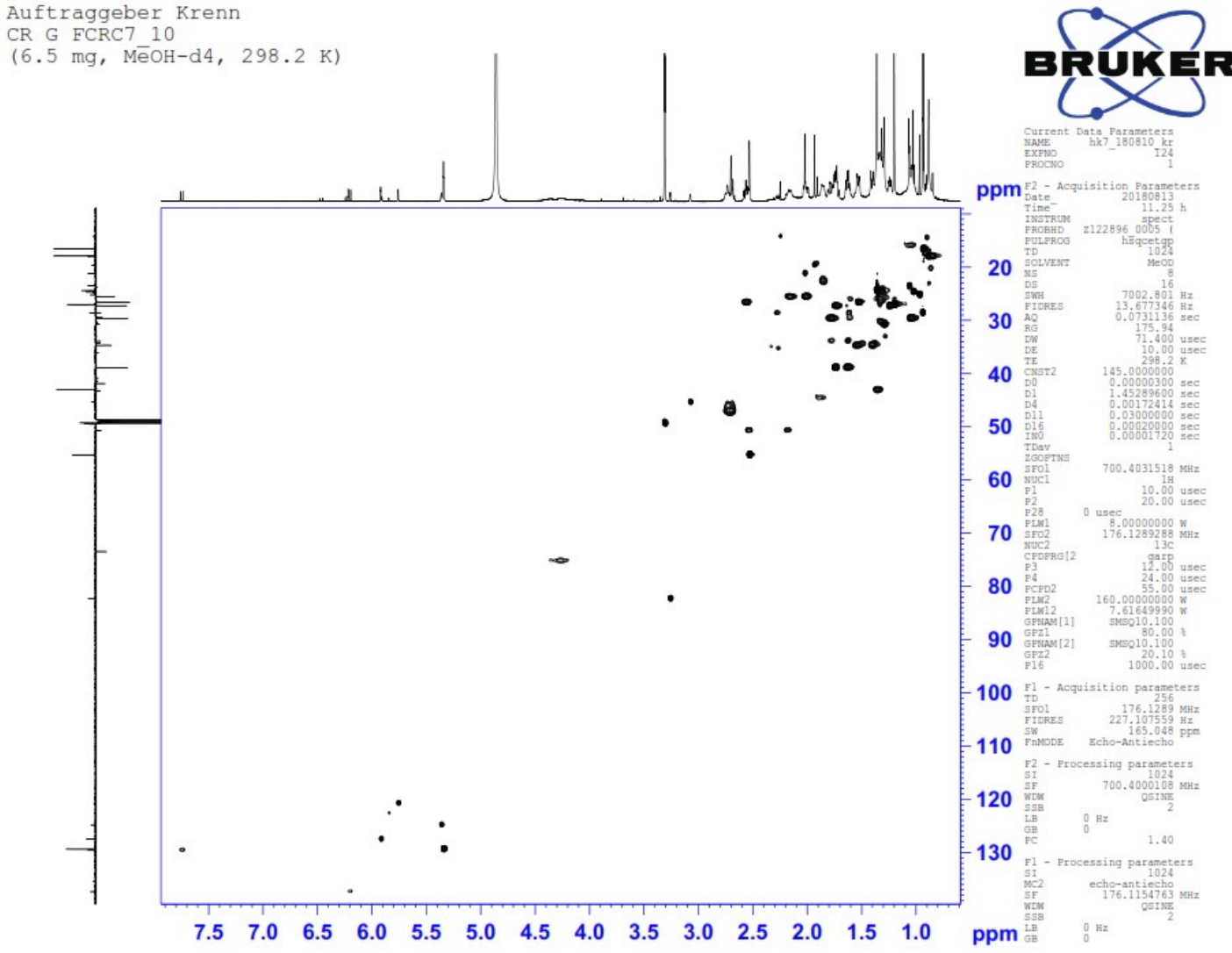

Appendix 8f: HSQC of CR-G

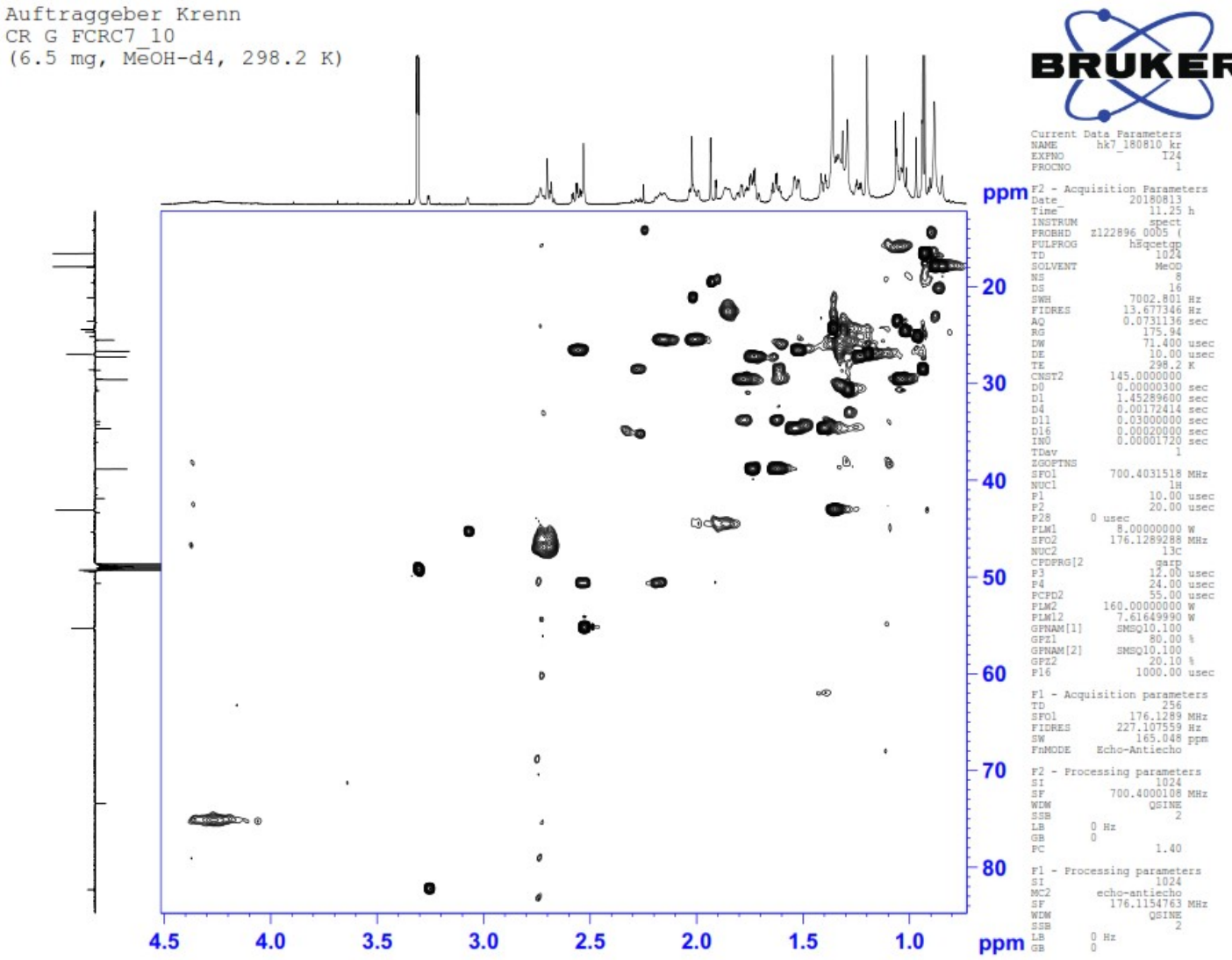

Appendix 8g: NOESY of CR-G

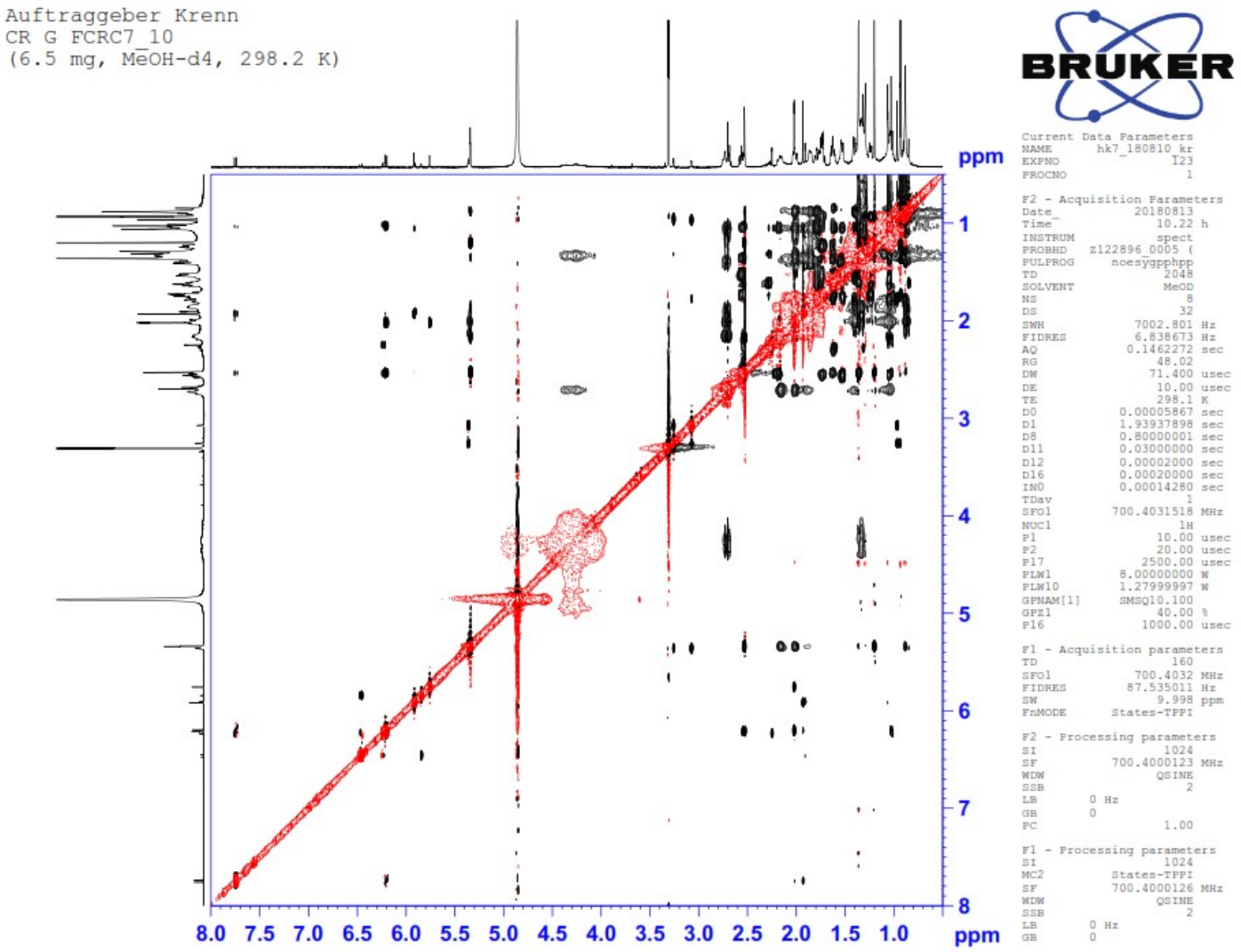

Appendix 8h: TOCSY of CR-G

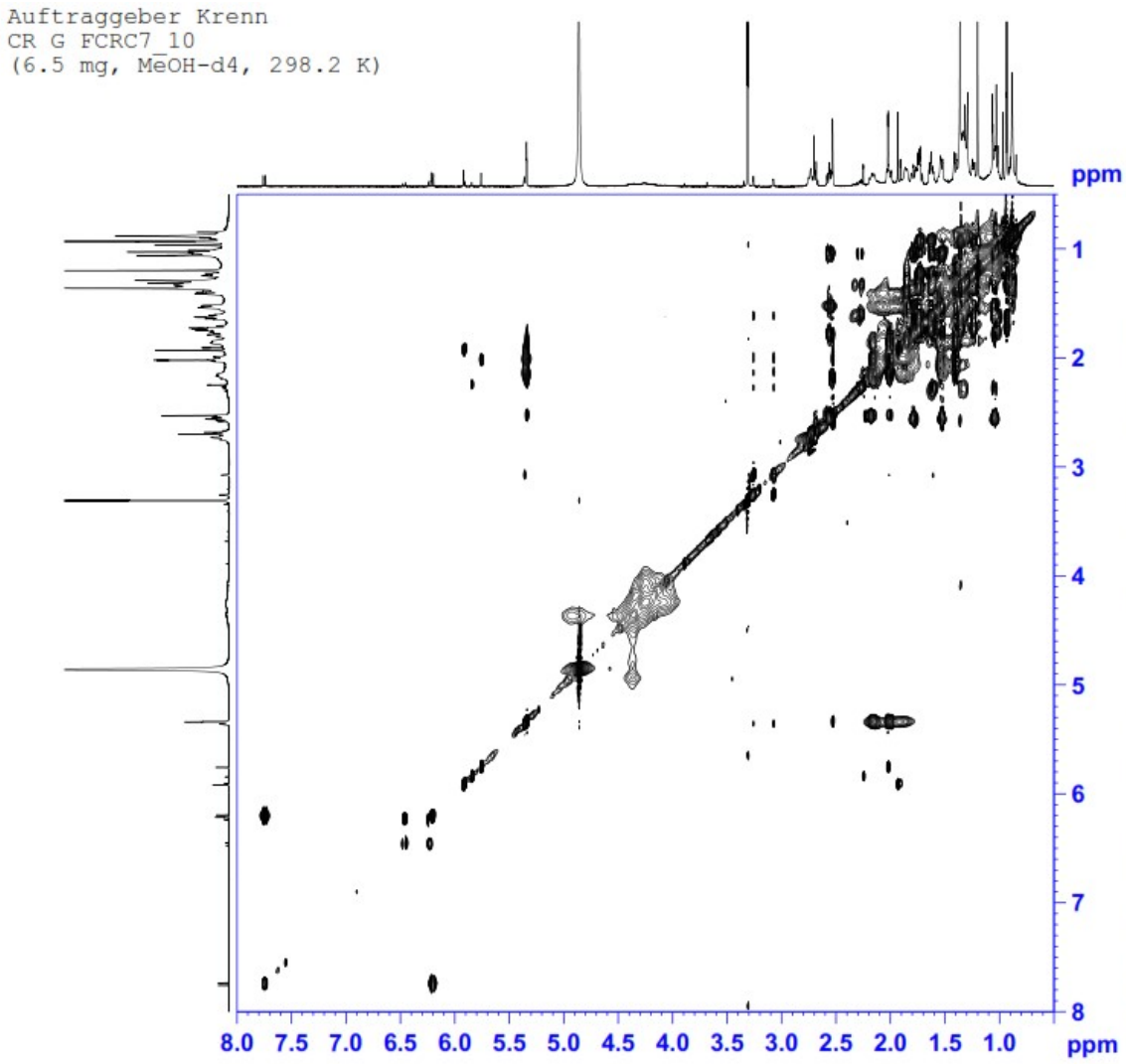

BRUKER

```
Current Data Parameters
NAME        hk7_180810_kr
EXPNO                 T22
PROCNO                  1

F2 - Acquisition Parameters
Date_            20180813
Time                9.56 h
INSTRUM            spect
PROBHD    z122896_0005 (
PULPROG         mlevphpp
TD                  2048
SOLVENT             MeOD
NS                     4
DS                    16
SWH             7002.801 Hz
FIDRES          6.838673 Hz
AQ              0.1462272 sec
RG                 48.02
DW                71.400 usec
DE                10.00 usec
TE                298.1 K
D0           0.00006103 sec
D1           1.93937898 sec
D9           0.08000000 sec
D11          0.03000000 sec
D12          0.00002000 sec
IN0          0.00014280 sec
L1                     48
TDav                    1
SFO1         700.4031518 MHz
NUC1                   1H
P1                10.00 usec
P5                16.67 usec
P6                25.00 usec
P7                50.00 usec
P17             2500.00 usec
PLW1         8.00000000 W
PLW10        1.27999997 W

F1 - Acquisition parameters
TD                    160
SFO1           700.4032 MHz
FIDRES         87.535011 Hz
SW                 9.998 ppm
FnMODE       States-TPPI

F2 - Processing parameters
SI                   1024
SF           700.4000131 MHz
WDW                 QSINE
SSB                     2
LB         0 Hz
GB         0
PC                   1.40

F1 - Processing parameters
SI                   1024
MC2          States-TPPI
SF           700.4000134 MHz
WDW                 QSINE
SSB                     2
LB         0 Hz
GB         0
```

Appendix 9: Incomplete spectra data assignment of CR-G

CR G

hk7_180810_kr 3, 20-26, 120-125
(6.5 mg, MeOH-d_4, 298.2 K)

Mixture, several signals in ^{1}H and/or ^{13}C-NMR broad, some ^{13}C shifts only from HSQC or HMBC

1) the red part could not be assigned, signals are very broad, no carbon signals in the direct ^{13}C NMR, very broad cross peaks in the HSQC and HMBC spectra

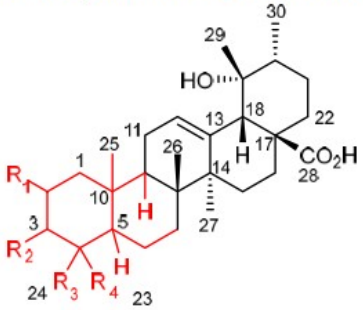

		^{1}H (ppm)	$J_{H,H}$ (Hz)	^{13}C (ppm)
7	CH_2	1.540	m	34.69
		1.404	m	
8	C	-	-	41.88
11	CH_2	2.164	m	25.51
		2.012		
12	CH	5.332	t 3.2, br	129.35
13	C	-	-	140.22
14	C	-	-	43.34
15	CH_2	1.785	m	29.61
		1.046	m	
16	CH_2	2.562	t 13.3 / d 4.6	26.66
		1.530		
17	C	-	-	49.18
18	CH	2.531	s	55.30
19	C	-	-	73.45
20	CH	1.354	m	43.08
21	CH_2	1.733	m	27.27
		1.236	m	
22	CH_2	1.740	m	38.86
		1.622	m	
26	CH_3	0.883	s, br	17.94

27	CH_3	1.362	s	24.42
28	C	-	-	182.21
29	CH_3	1.200	s	27.02
30	CH_3	0.933	d 6.8	16.55

2) seems to be the isomer of 1), even less signals assigned due to low amount

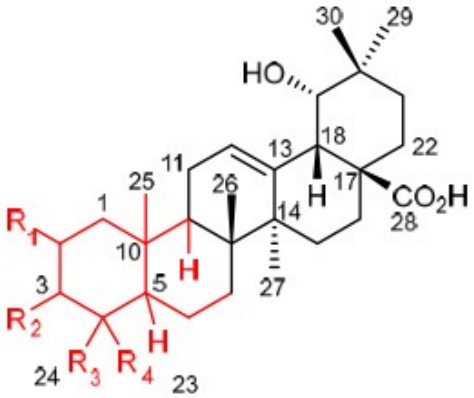

		^1H (ppm)	$J_{H,H}$ (Hz)	^{13}C (ppm)
12	CH	5.362	t 3.2, br	124.81
13	C	-	-	144.75
14	C	-	-	43.27
17	C	-	-	46.70
18	CH	3.075	m	45.37
19	CH	3.259	d 3.5	82.30
20	C	-	-	36.06
21	CH_2	1.758	m	29.51
		1.005	m	
22	CH_2	1.781	m	33.91
		1.631	m	
28	C	-	-	181.26
29	CH_3	0.941	s	28.61
30	CH_3	0.969	s	25.19

Appendix 10: Mass spectra of CR-H

Appendix 10a: ESI-MS of CR-H

Analysis Info

Analysis Name	D:\MZ\maXis_data\1808\Krenn_Kaehlig\CR_H_amaZon_aMSn.d	Acquisition Date	8/28/2018 11:56:52 AM
Method	DI_MSMS.m	Operator	MSC
Sample Name	CR H	Instrument	amaZon speed ETD
Comment	Kaehlig/Krenn/Zehl ACN / MeOH + 1% H2O		

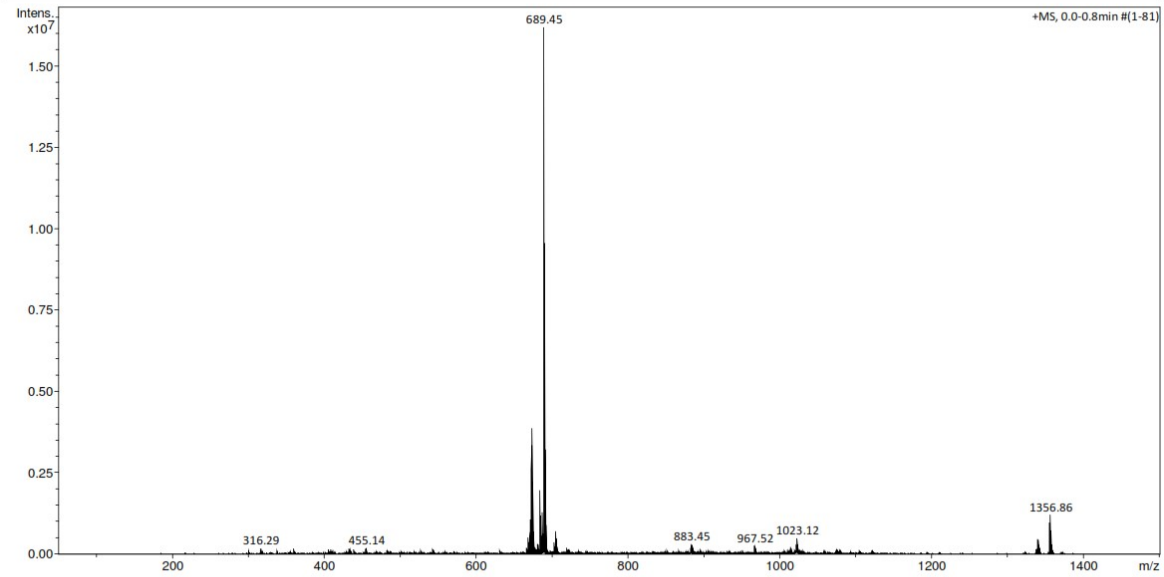

Bruker Compass DataAnalysis 4.1 printed: 8/28/2018 2:04:46 PM by: MSC Page 1 of 1

Analysis Info

Analysis Name	D:\MZ\maXis_data\1808\Krenn_Kaehlig\CR_H_amaZon_aMSn.d	Acquisition Date	8/28/2018 11:56:52 AM
Method	DI_MSMS.m	Operator	MSC
Sample Name	CR H	Instrument	amaZon speed ETD
Comment	Kaehlig/Krenn/Zehl ACN / MeOH + 1% H2O		

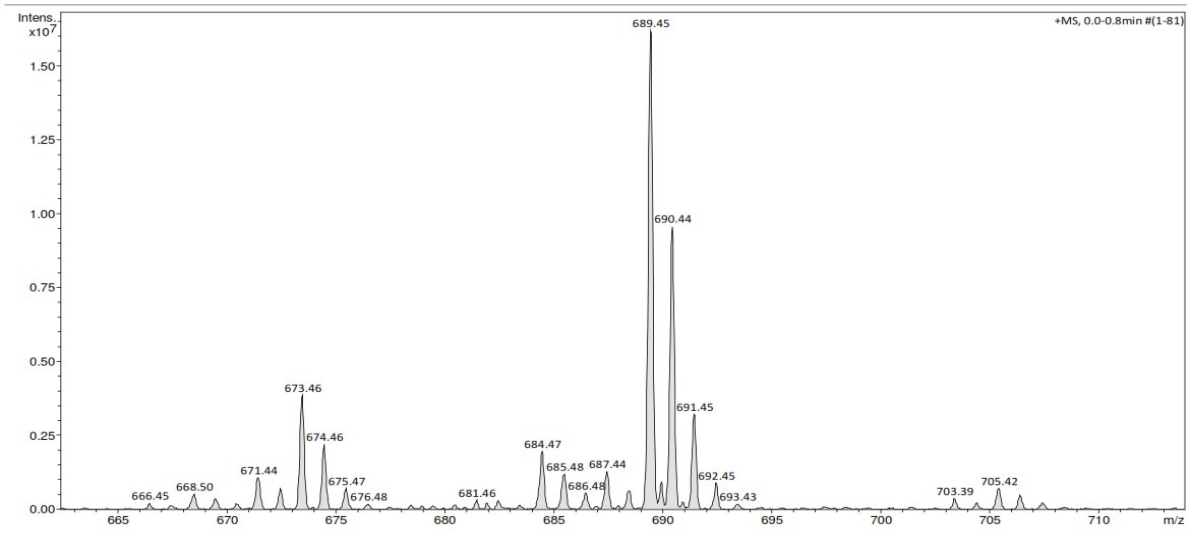

Bruker Compass DataAnalysis 4.1 printed: 8/28/2018 2:05:08 PM by: MSC Page 1 of 1

Analysis Info

Analysis Name	D:\MZ\maXis_data\1808\Krenn_Kaehlig\CR_H_amaZon_aMSn.d	Acquisition Date	8/28/2018 11:56:52 AM
Method	DI_MSMS.m	Operator	MSC
Sample Name	CR H	Instrument	amaZon speed ETD
Comment	Kaehlig/Krenn/Zehl ACN / MeOH + 1% H2O		

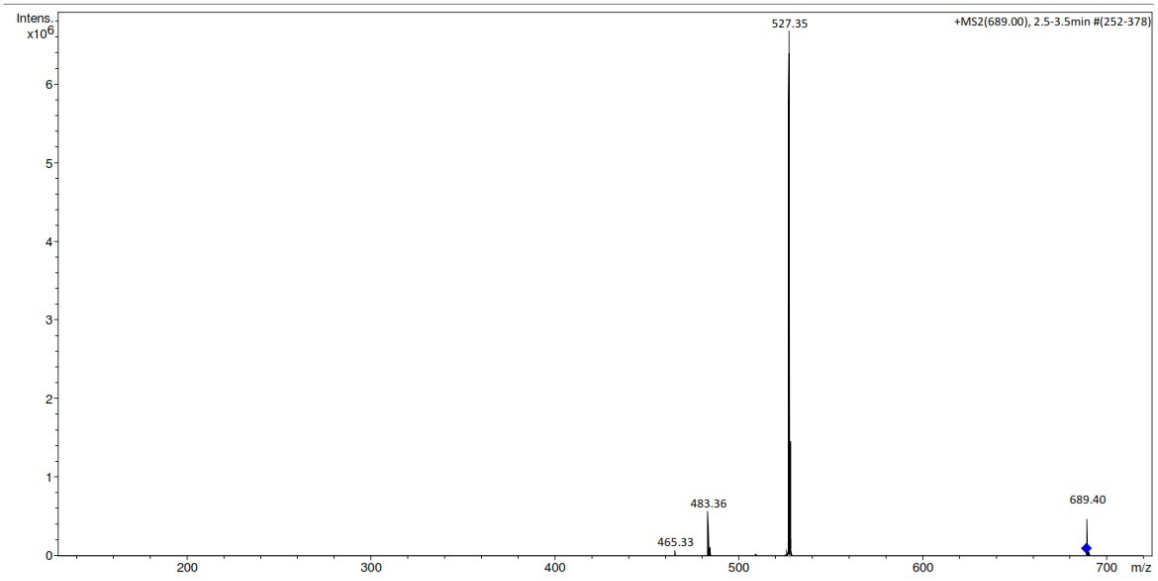

Analysis Info

Analysis Name	D:\MZ\maXis_data\1808\Krenn_Kaehlig\CR_H_amaZon_aMSn.d	Acquisition Date	8/28/2018 11:56:52 AM
Method	DI_MSMS.m	Operator	MSC
Sample Name	CR H	Instrument	amaZon speed ETD
Comment	Kaehlig/Krenn/Zehl ACN / MeOH + 1% H2O		

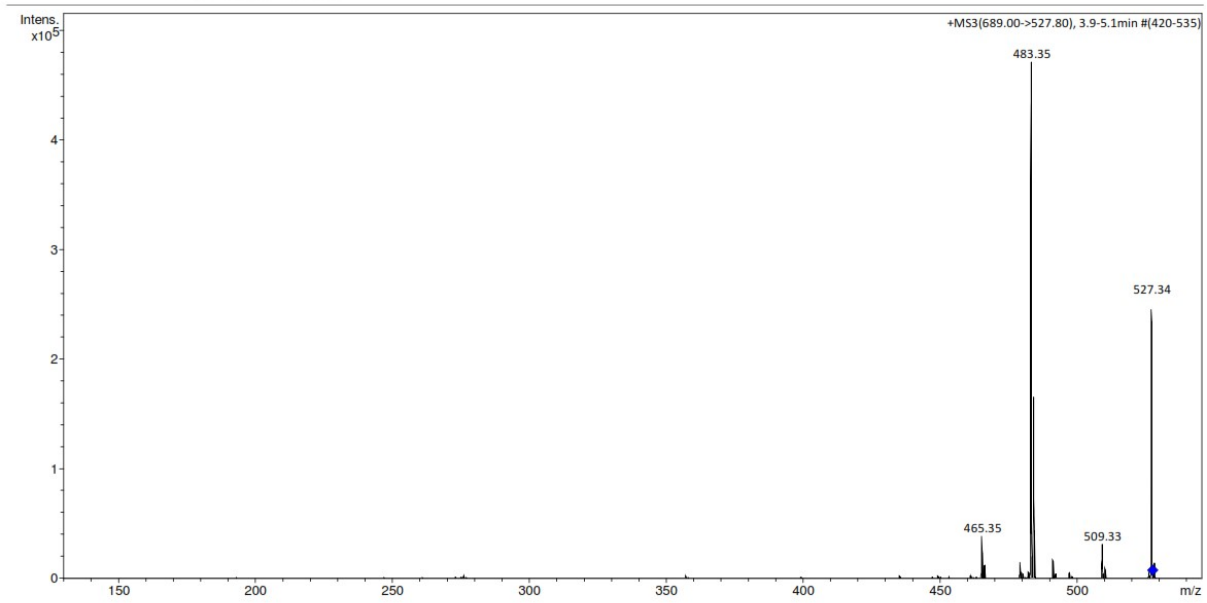

Analysis Info

Analysis Name	D:\MZ\maXis_data\1808\Krenn_Kaehlig\CR_H_amaZon_aMSn.d	Acquisition Date	8/28/2018 11:56:52 AM
Method	DI_MSMS.m	Operator	MSC
Sample Name	CR H	Instrument	amaZon speed ETD
Comment	Kaehlig/Krenn/Zehl ACN / MeOH + 1% H2O		

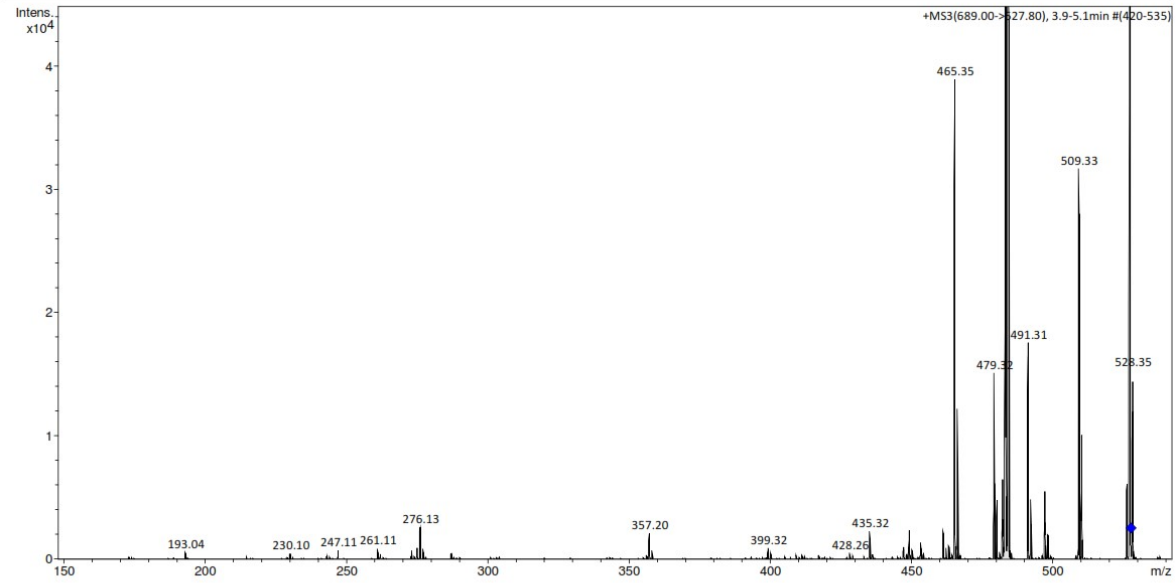

Bruker Compass DataAnalysis 4.1 printed: 8/28/2018 2:06:42 PM by: MSC Page 1 of 1

Analysis Info

Analysis Name	D:\MZ\maXis_data\1808\Krenn_Kaehlig\CR_H_amaZon_aMSn.d	Acquisition Date	8/28/2018 11:56:52 AM
Method	DI_MSMS.m	Operator	MSC
Sample Name	CR H	Instrument	amaZon speed ETD
Comment	Kaehlig/Krenn/Zehl ACN / MeOH + 1% H2O		

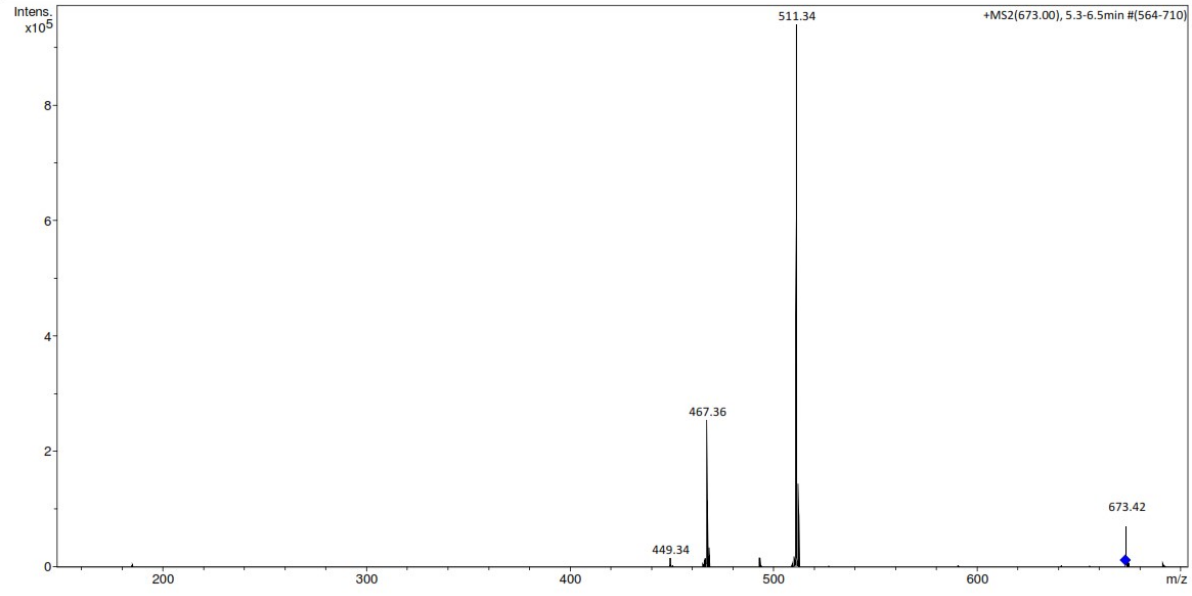

Bruker Compass DataAnalysis 4.1 printed: 8/28/2018 2:06:51 PM by: MSC Page 1 of 1

Appendix 10b: HRESI-MS of CR-H

Analysis Info

Analysis Name	D:\MZ\maXis_data\1808\Krenn_Kaehlig\59028000001.d	Acquisition Date	8/20/2018 12:16:03 PM
Method	tune_low_MS_Service_08_18.m	Operator	msc
Sample Name	CRH	Instrument	maXis
Comment	Kaehlig-Zehl/Anorg.Chem Ergebnis: +/- 5ppm ACN/MeOH +1%H2O		

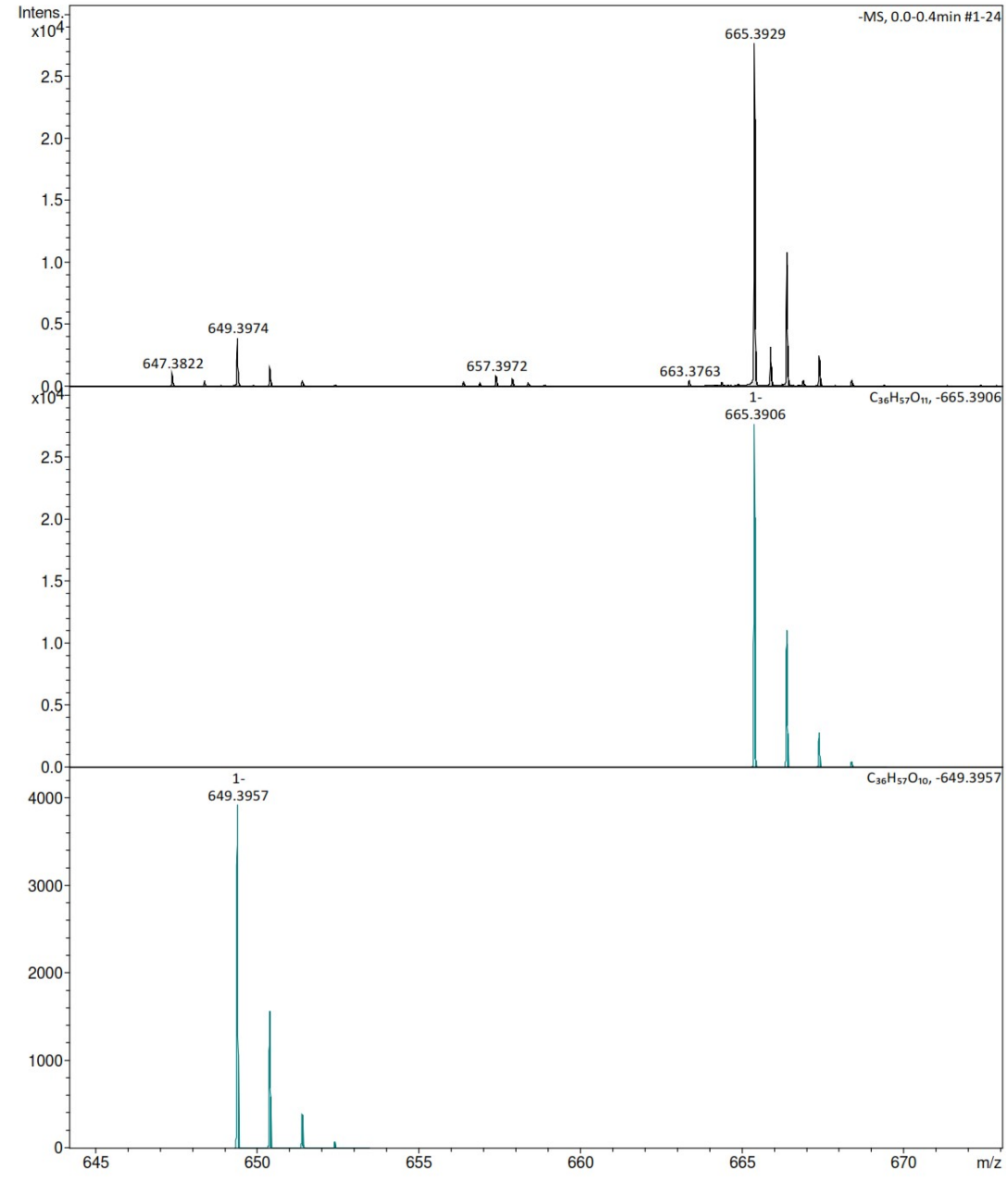

Bruker Compass DataAnalysis 4.1 printed: 8/27/2018 3:42:40 PM by: MSC Page 1 of 1

Mass Spectrum SmartFormula Report

Analysis Info

Analysis Name	D:\MZ\maXis_data\1808\Krenn_Kaehlig\59028000001.d	Acquisition Date	8/20/2018 12:16:03 PM
Method	tune_low_MS_Service_08_18.m	Operator	msc
Sample Name	CRH	Instrument	maXis 255552.00016
Comment	Kaehlig-Zehl/Anorg.Chem Ergebnis: +/- 5ppm ACN/MeOH +1%H2O		

Acquisition Parameter

Source Type	ESI	Ion Polarity	Negative	Set Nebulizer	0.4 Bar
Focus	Not active	Set Capillary	4500 V	Set Dry Heater	180 °C
Scan Begin	50 m/z	Set End Plate Offset	-500 V	Set Dry Gas	4.0 l/min
Scan End	1900 m/z	Set Charging Voltage	0 V	Set Divert Valve	Source
		Set Corona	0 nA	Set APCI Heater	0 °C

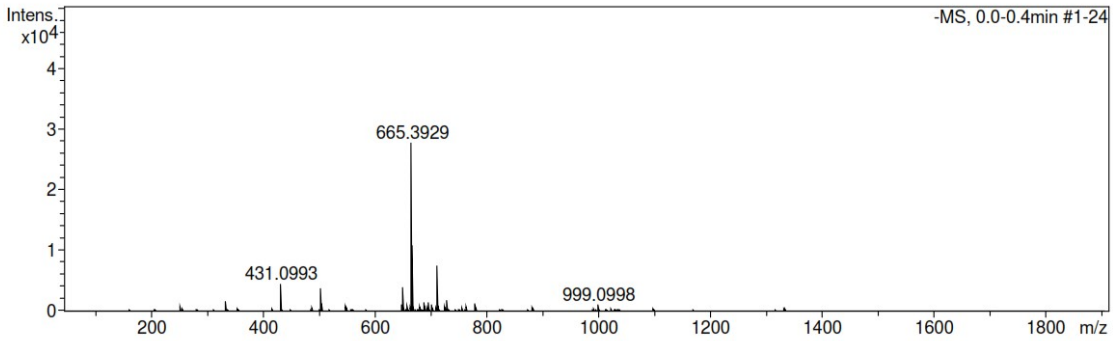

Meas. m/z	#	Ion Formula	Score	m/z	err [mDa]	err [ppm]	mSigma	rdb	e⁻ Conf	N-Rule
649.3974	1	C36H57O10	48.35	649.3957	-1.6	-2.5	12.5	8.5	even	ok
	2	C37H53N4O6	100.00	649.3971	0.3	0.5	14.1	13.5	even	ok
	3	C33H49N10O4	14.01	649.3944	-3.0	-4.6	18.7	14.5	even	ok
	4	C34H45N14	41.28	649.3957	-1.7	-2.5	20.0	19.5	even	ok
	5	C38H49N8O2	57.49	649.3984	-1.0	-1.6	22.7	18.5	even	ok
665.3929	1	C36H57O11	49.26	665.3906	2.2	3.4	7.1	8.5	even	ok

Appendix 11: 1D and 2D NMR of CR-H

Appendix 11a: ^{1}H NMR of CR-H

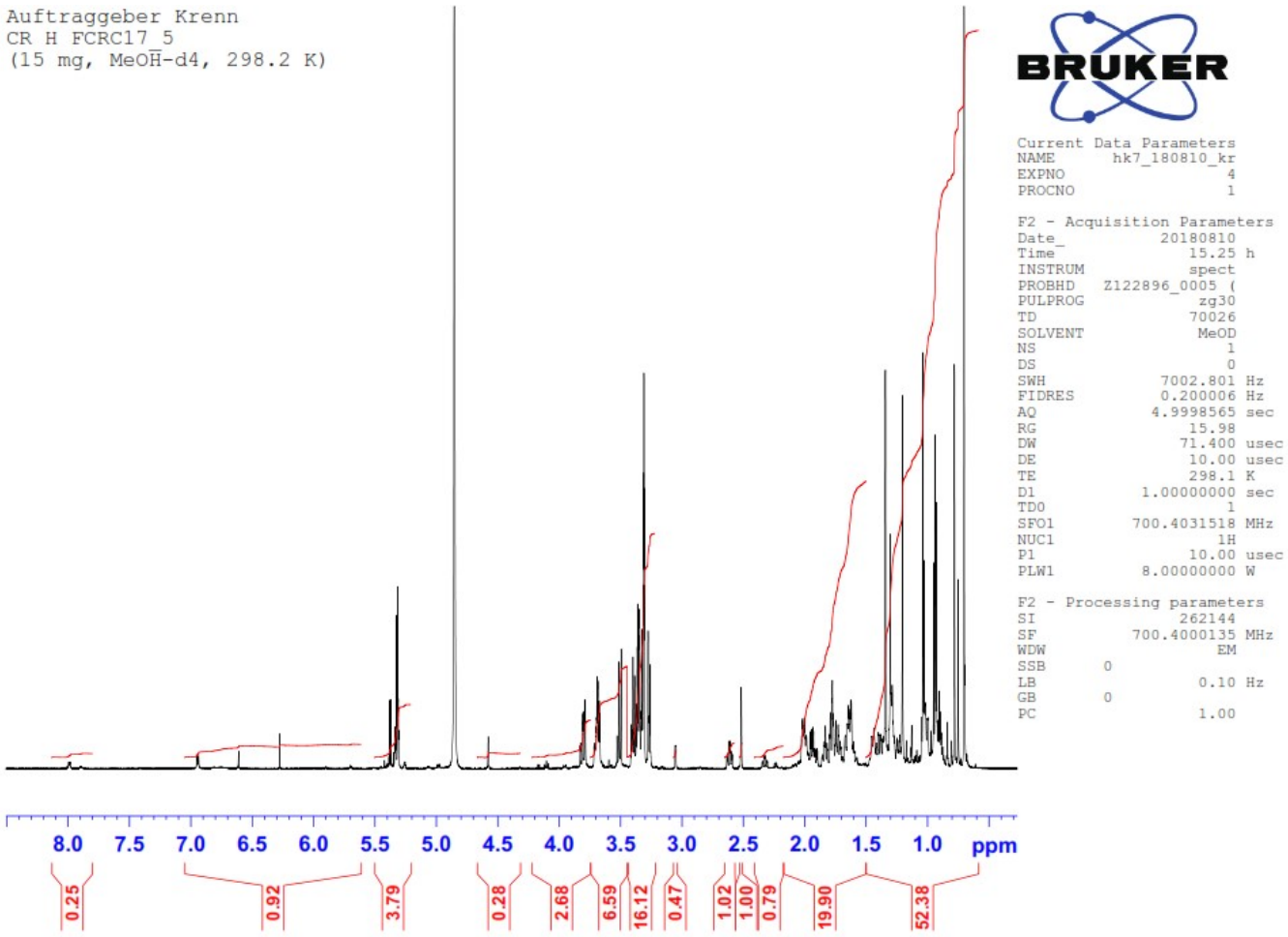

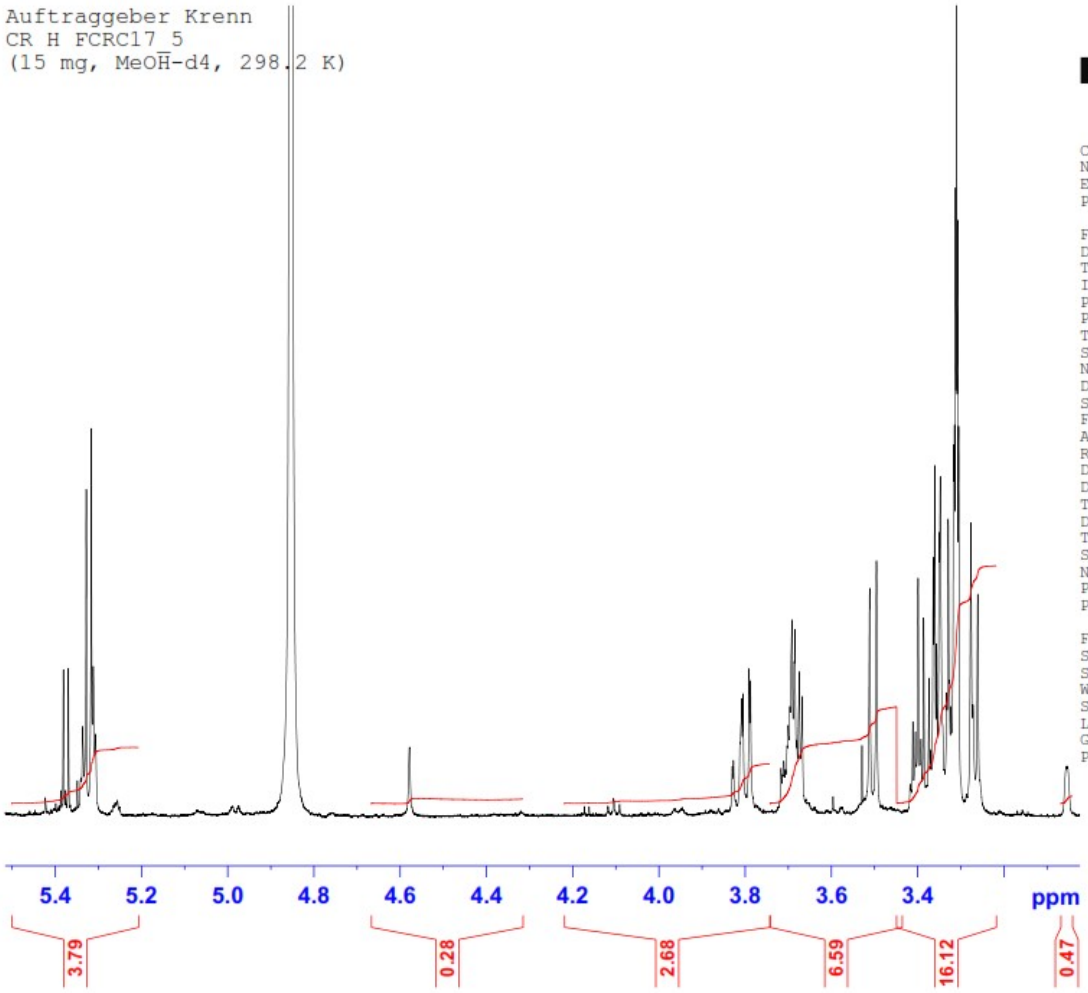


```
Current Data Parameters
NAME       hk7_180810_kr
EXPNO                  4
PROCNO                 1

F2 - Acquisition Parameters
Date_           20180810
Time               15.25 h
INSTRUM             spect
PROBHD   Z122896_0005 (
PULPROG             zg30
TD                 70026
SOLVENT             MeOD
NS                     1
DS                     0
SWH             7002.801 Hz
FIDRES          0.200006 Hz
AQ              4.9998565 sec
RG                 15.98
DW                 71.400 usec
DE                 10.00 usec
TE                 298.1 K
D1             1.00000000 sec
TD0                    1
SFO1          700.4031518 MHz
NUC1                  1H
P1                 10.00 usec
PLW1           8.00000000 W

F2 - Processing parameters
SI                262144
SF          700.4000135 MHz
WDW                   EM
SSB       0
LB                 0.10 Hz
GB        0
PC                 1.00
```

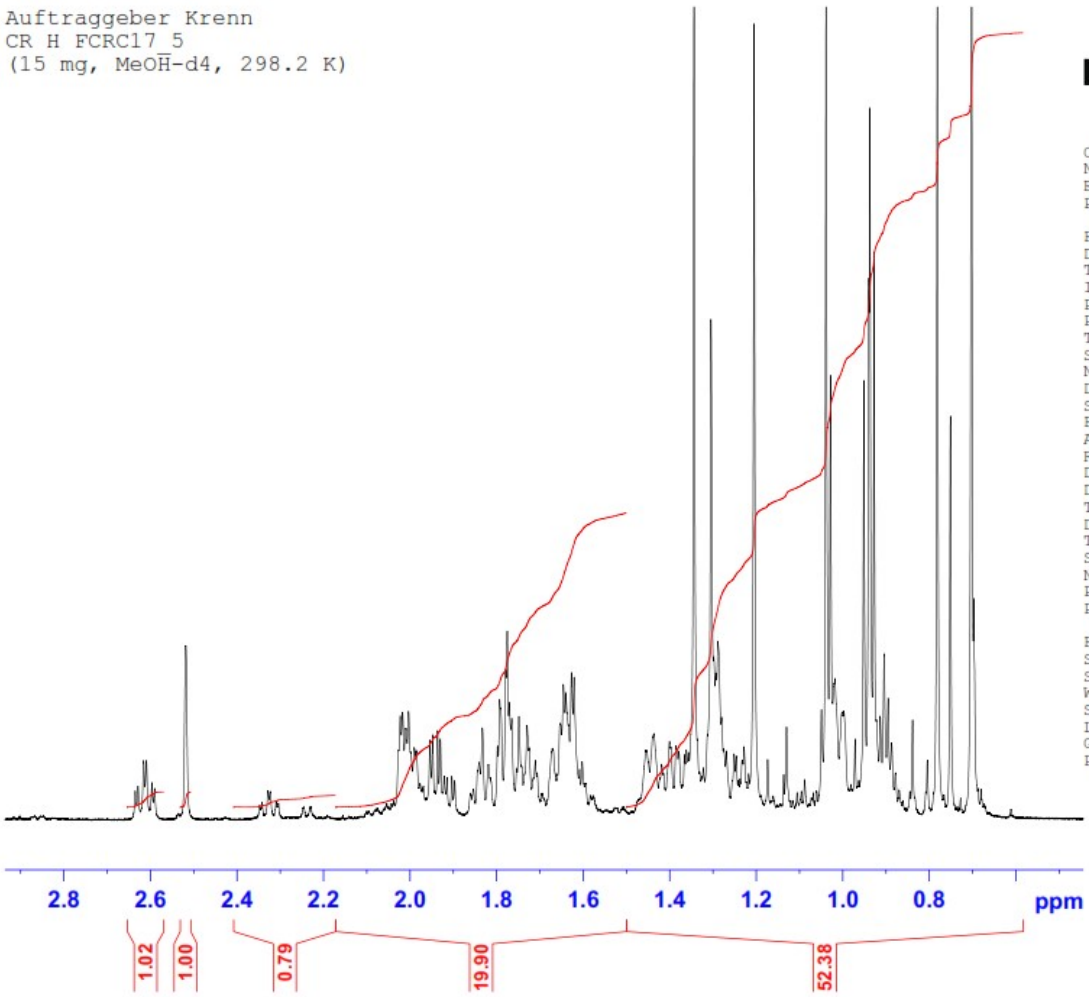

Current Data Parameters
NAME hk7_180810_kr
EXPNO 4
PROCNO 1

F2 - Acquisition Parameters
Date_ 20180810
Time 15.25 h
INSTRUM spect
PROBHD Z122896_0005 (
PULPROG zg30
TD 70026
SOLVENT MeOD
NS 1
DS 0
SWH 7002.801 Hz
FIDRES 0.200006 Hz
AQ 4.9998565 sec
RG 15.98
DW 71.400 usec
DE 10.00 usec
TE 298.1 K
D1 1.00000000 sec
TD0 1
SFO1 700.4031518 MHz
NUC1 1H
P1 10.00 usec
PLW1 8.00000000 W

F2 - Processing parameters
SI 262144
SF 700.4000135 MHz
WDW EM
SSB 0
LB 0.10 Hz
GB 0
PC 1.00

Appendix 11b: ^{13}C NMR of CR-H

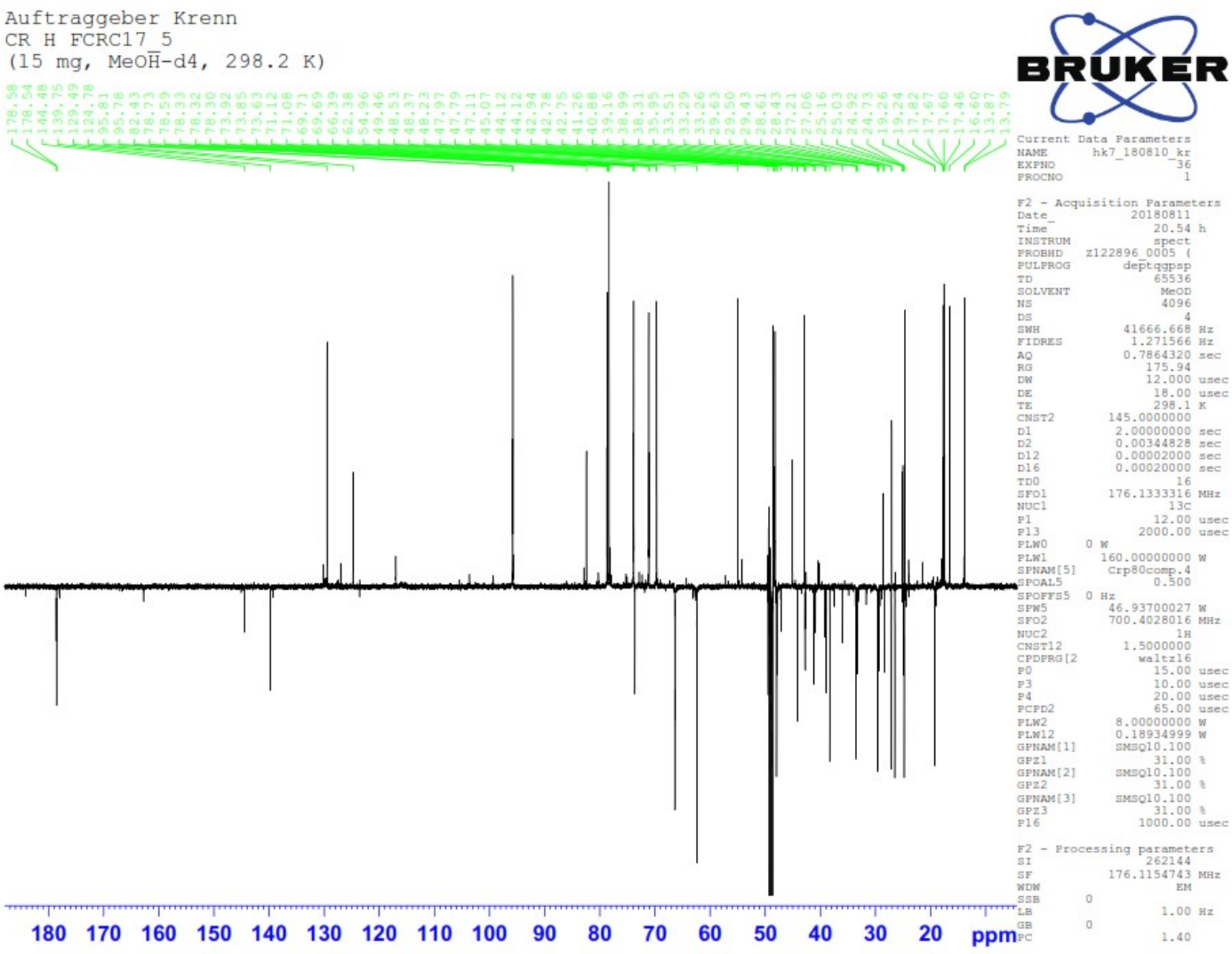

Appendix 11c: COSY of CR-H

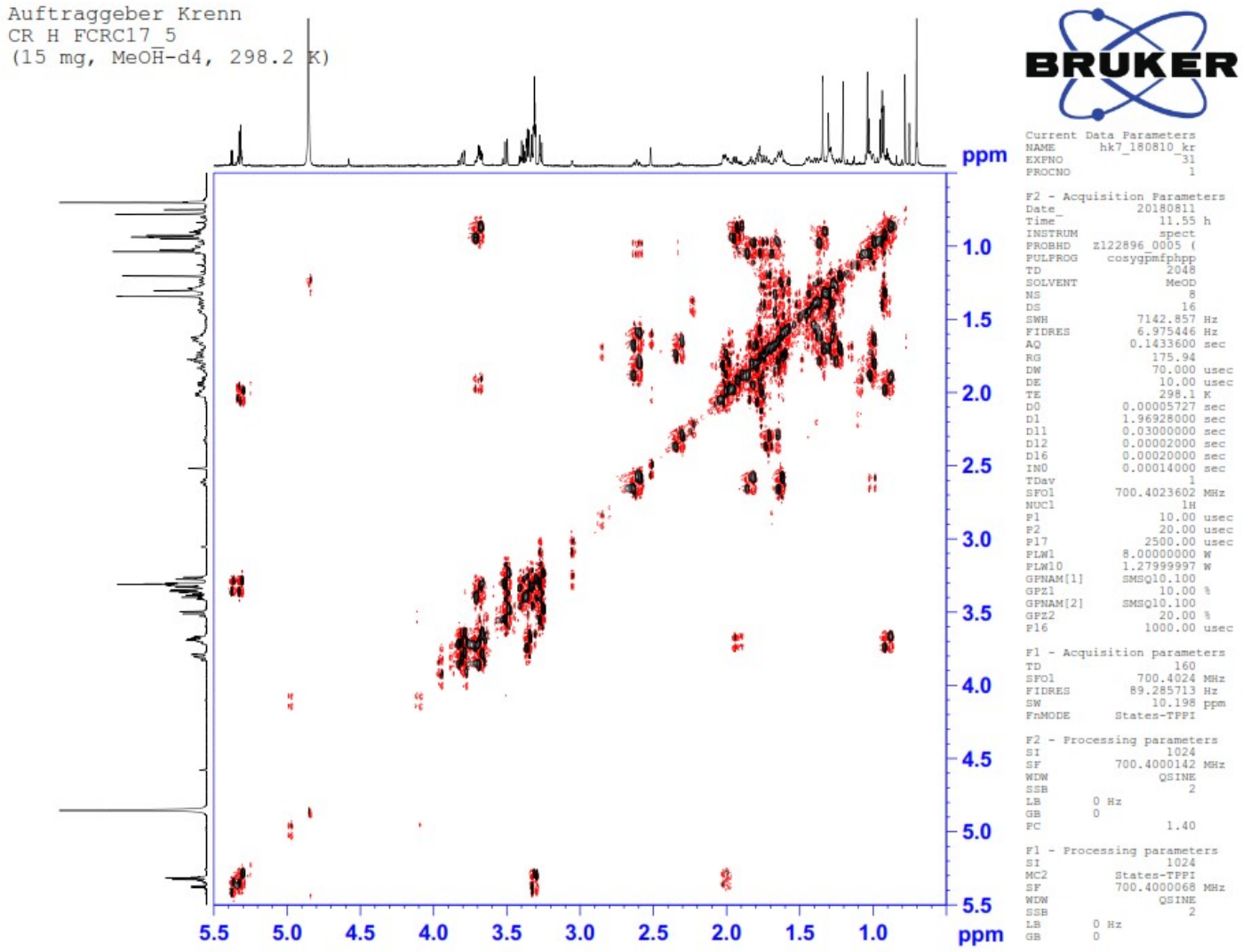

Appendix 11d: HMBC of CR-H

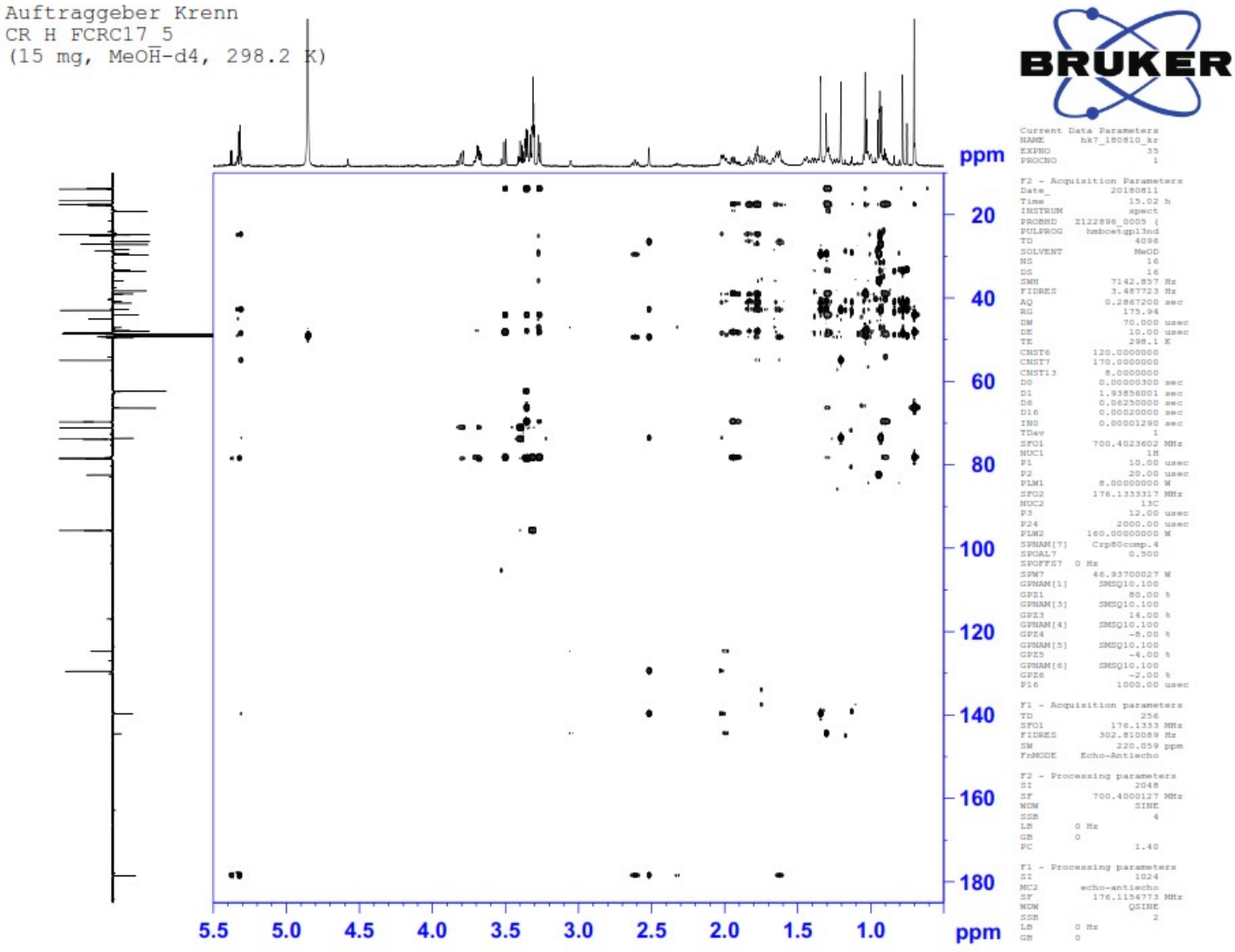

Appendix 11e: HSQC of CR-H

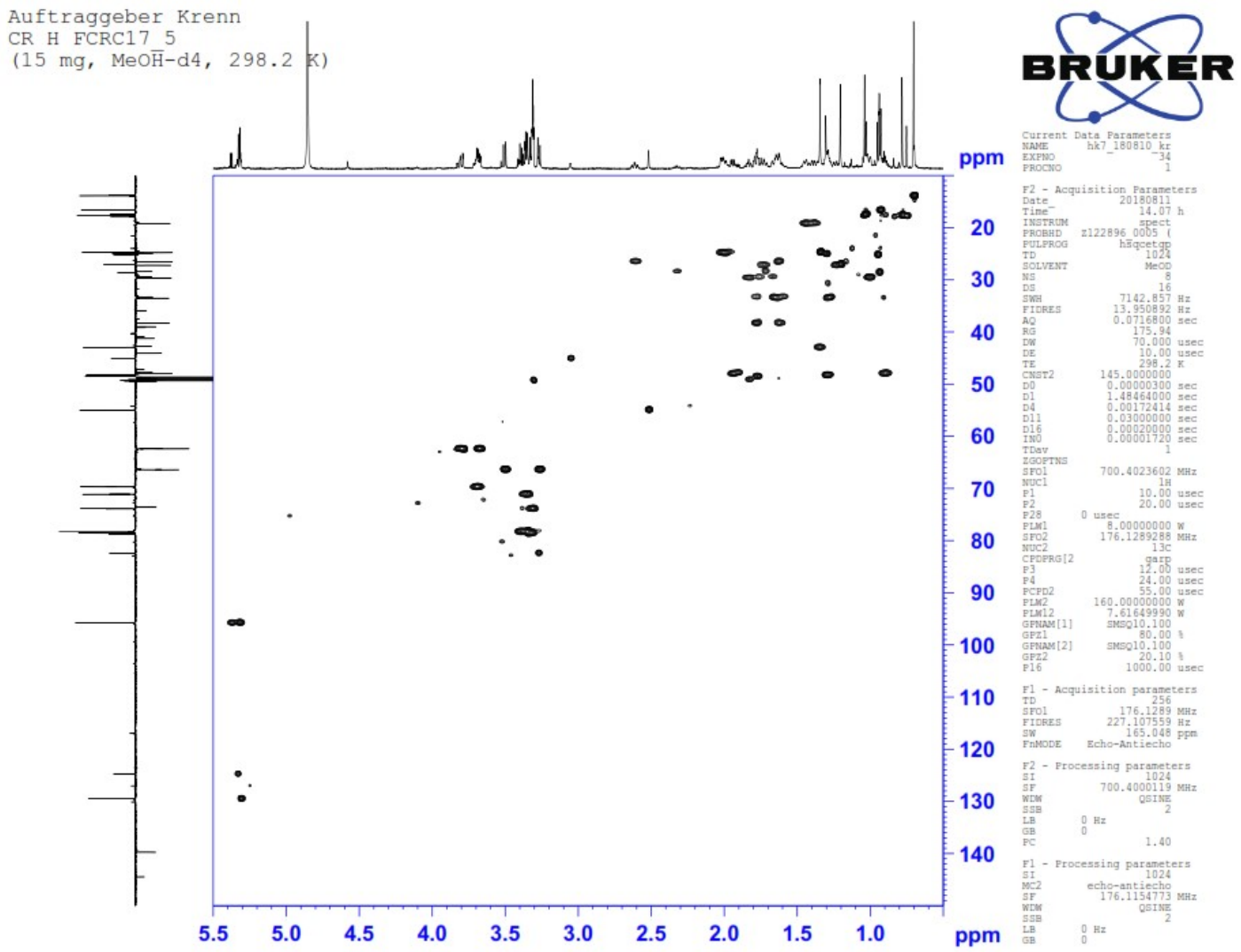

Appendix 11f: NOESY of CR-H

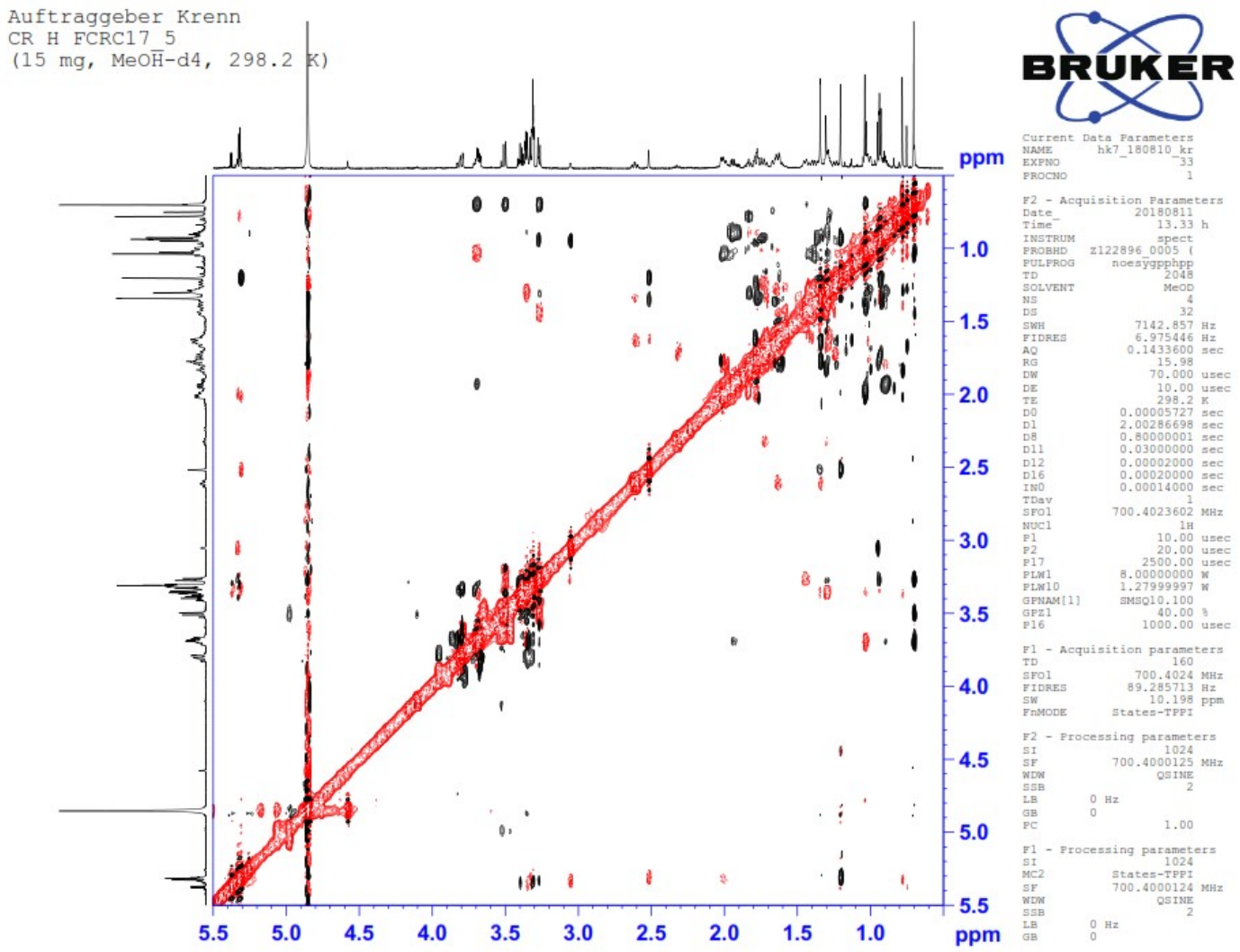

Appendix 11g: TOCSY of CR-H

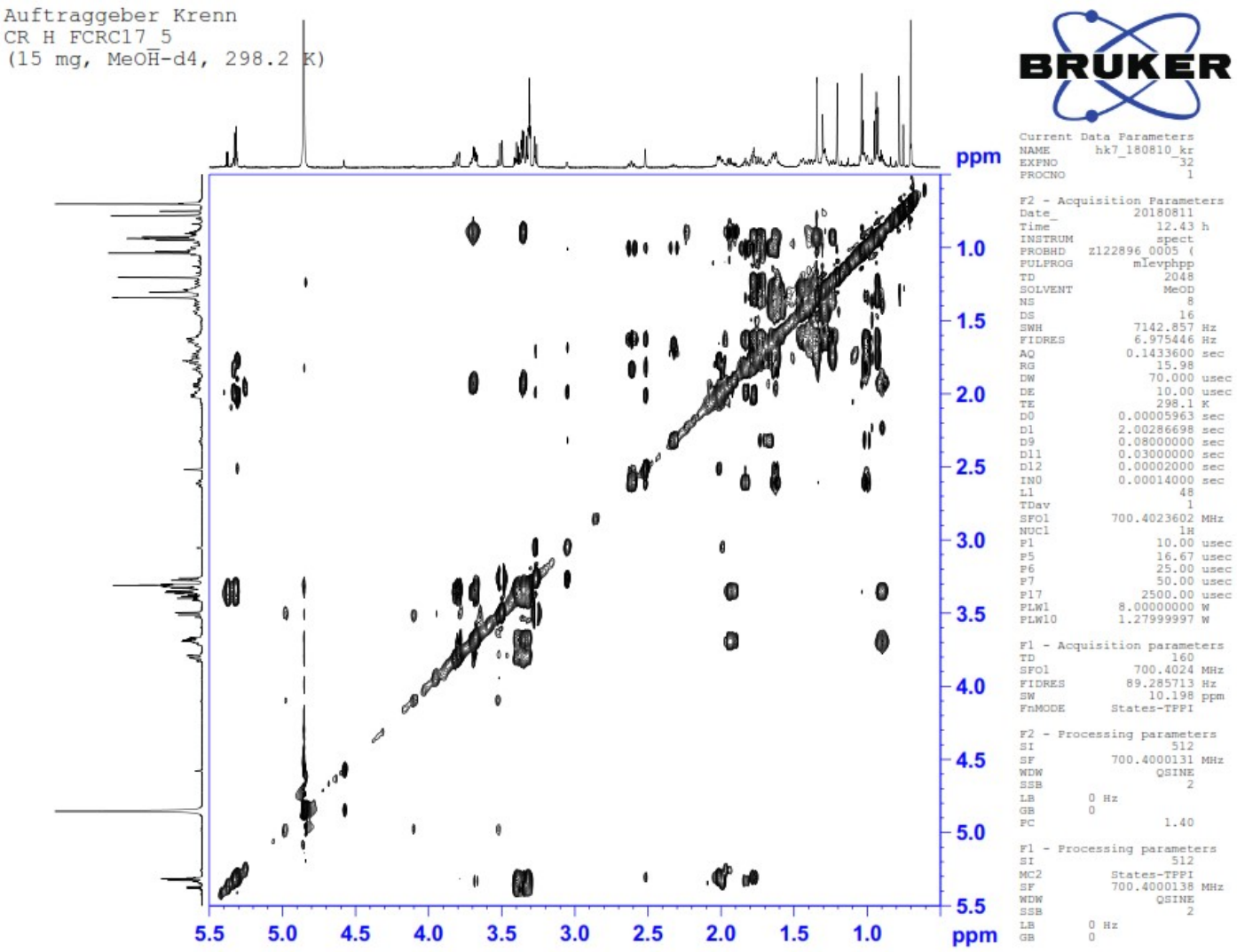

Appendix 11: Mass spectra of CZ-A

Appendix 12a: ESI-MS of CZ-A

Generic Display Report

Analysis Info

Analysis Name	D:\MZ\amaZon_data\1806\CZ_A2_amaZon_aMSn.d	Acquisition Date	26/06/2018 16:25:07
Method	DI_MSMS.m	Operator	MSC
Sample Name	CZ A2 NMR sample	Instrument	amaZon speed ETD
Comment	Kaehlig/Krenn/Zehl ACN/MeOH + 1% H2O		

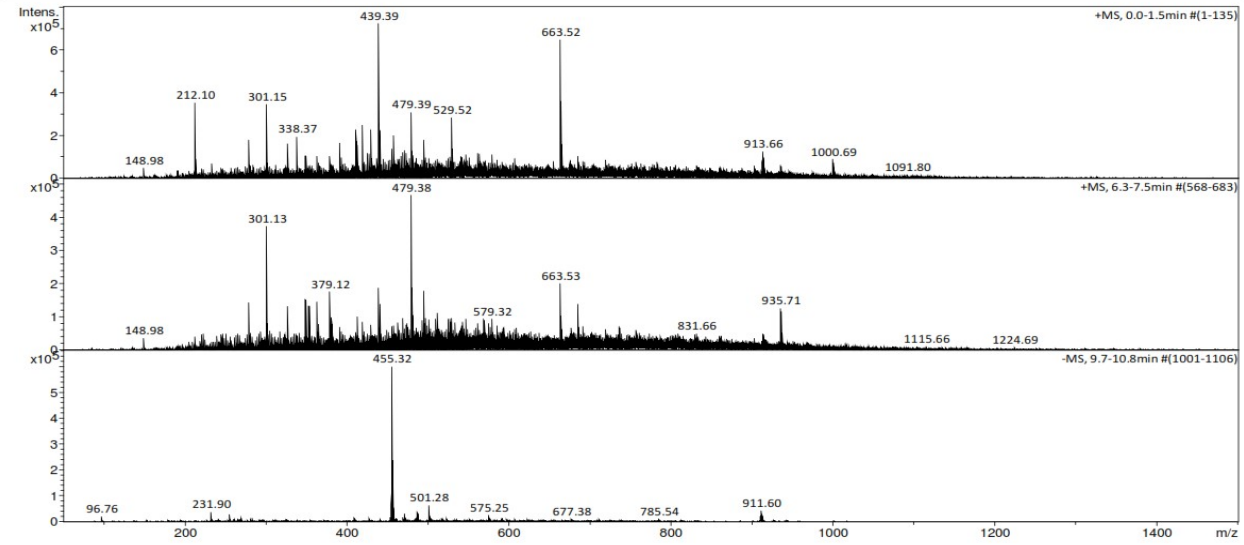

Bruker Compass DataAnalysis 4.1 printed: 15/05/2019 18:19:18 by: MSC Page 1 of 1

Generic Display Report

Analysis Info

Analysis Name	D:\MZ\amaZon_data\1806\CZ_A2_amaZon_aMSn.d	Acquisition Date	26/06/2018 16:25:07
Method	DI_MSMS.m	Operator	MSC
Sample Name	CZ A2 NMR sample	Instrument	amaZon speed ETD
Comment	Kaehlig/Krenn/Zehl ACN/MeOH + 1% H2O		

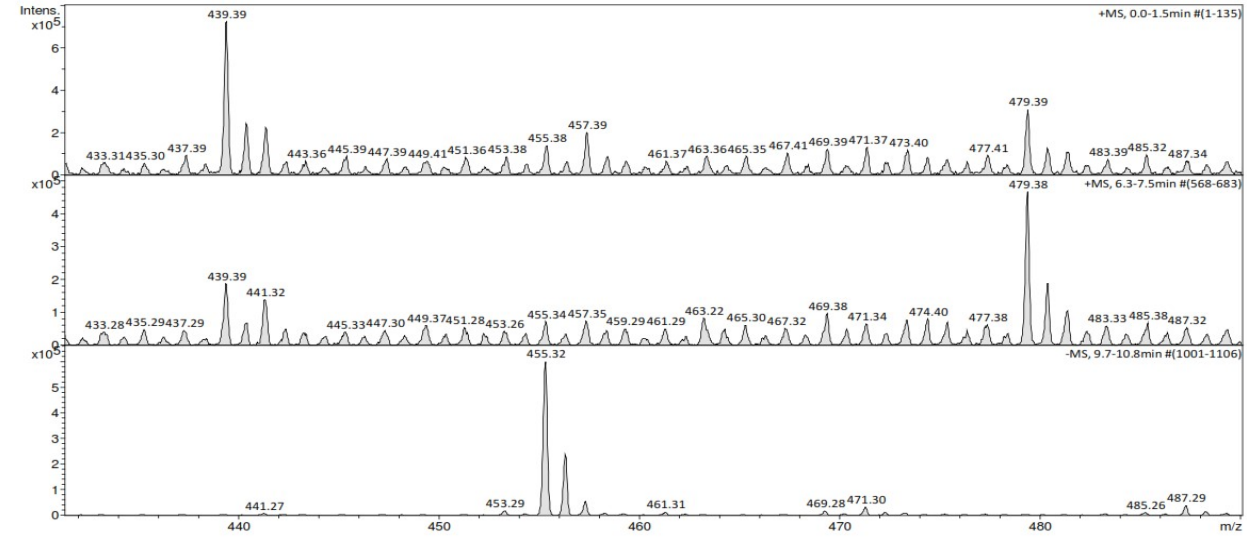

Bruker Compass DataAnalysis 4.1 printed: 15/05/2019 18:19:36 by: MSC Page 1 of 1

Generic Display Report

Analysis Info

Analysis Name	D:\MZ\amaZon_data\1806\CZ_A2_amaZon_aMSn.d	Acquisition Date	26/06/2018 16:25:07
Method	DI_MSMS.m	Operator	MSC
Sample Name	CZ A2 NMR sample	Instrument	amaZon speed ETD
Comment	Kaehlig/Krenn/Zehl ACN/MeOH + 1% H2O		

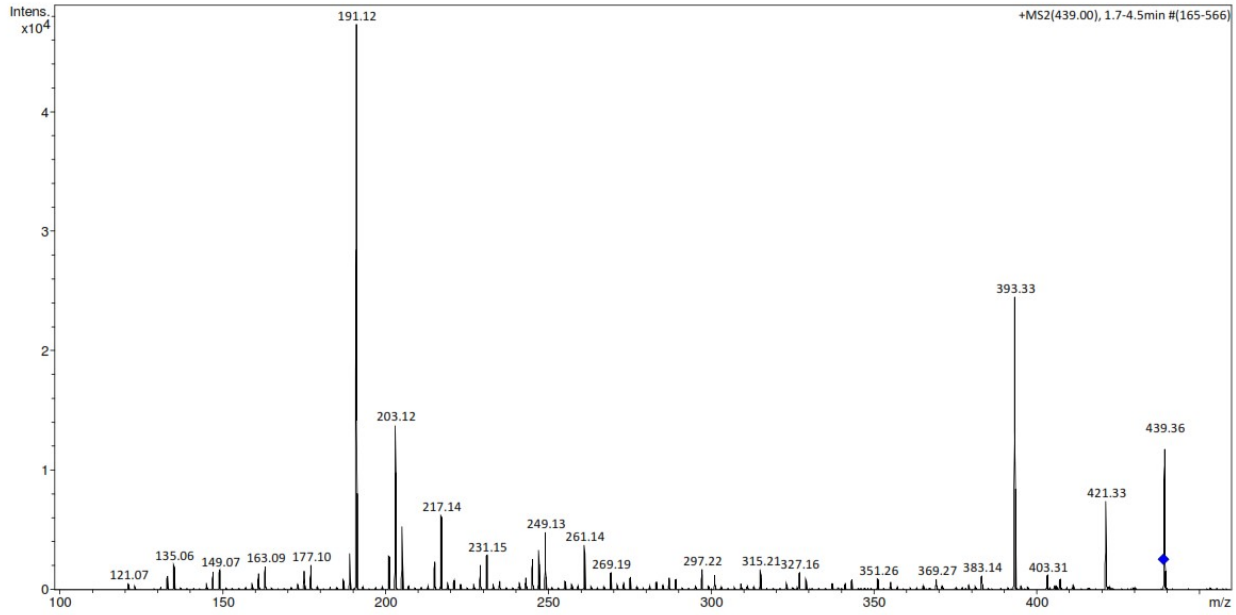

Bruker Compass DataAnalysis 4.1 printed: 15/05/2019 18:20:06 by: MSC Page 1 of 1

Generic Display Report

Analysis Info

Analysis Name	D:\MZ\amaZon_data\1806\CZ_A2_amaZon_aMSn.d	Acquisition Date	26/06/2018 16:25:07
Method	DI_MSMS.m	Operator	MSC
Sample Name	CZ A2 NMR sample	Instrument	amaZon speed ETD
Comment	Kaehlig/Krenn/Zehl ACN/MeOH + 1% H2O		

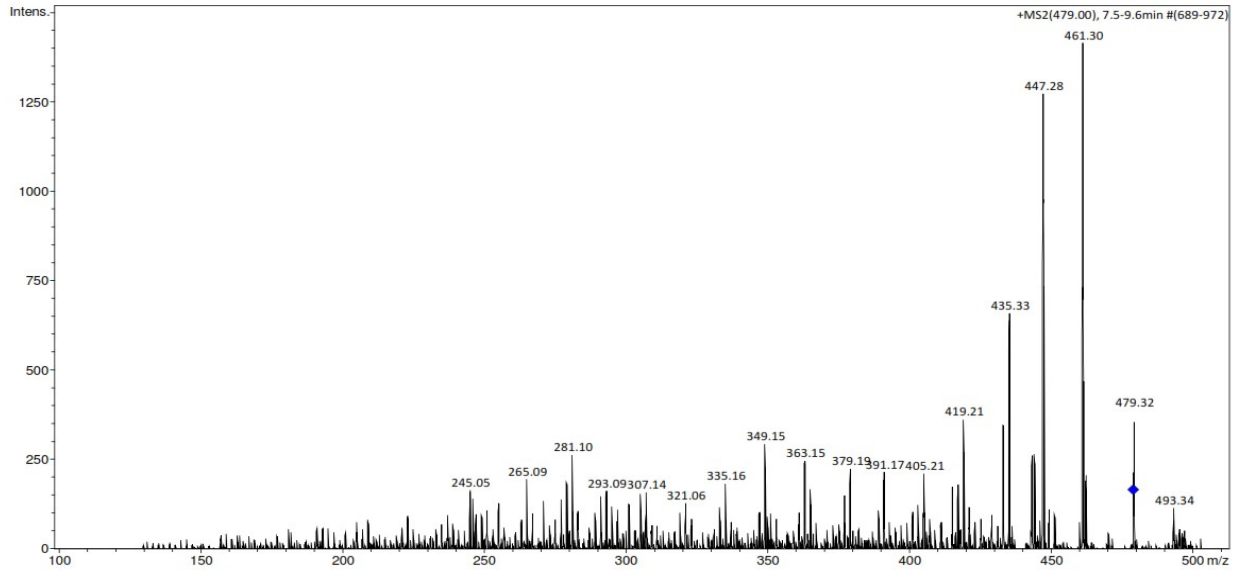

Bruker Compass DataAnalysis 4.1 printed: 15/05/2019 18:20:21 by: MSC Page 1 of 1

Generic Display Report

Analysis Info

Analysis Name	D:\MZ\amaZon_data\1806\CZ_A2_amaZon_aMSn.d	Acquisition Date	26/06/2018 16:25:07
Method	DI_MSMS.m	Operator	MSC
Sample Name	CZ A2 NMR sample	Instrument	amaZon speed ETD
Comment	Kaehlig/Krenn/Zehl ACN/MeOH + 1% H2O		

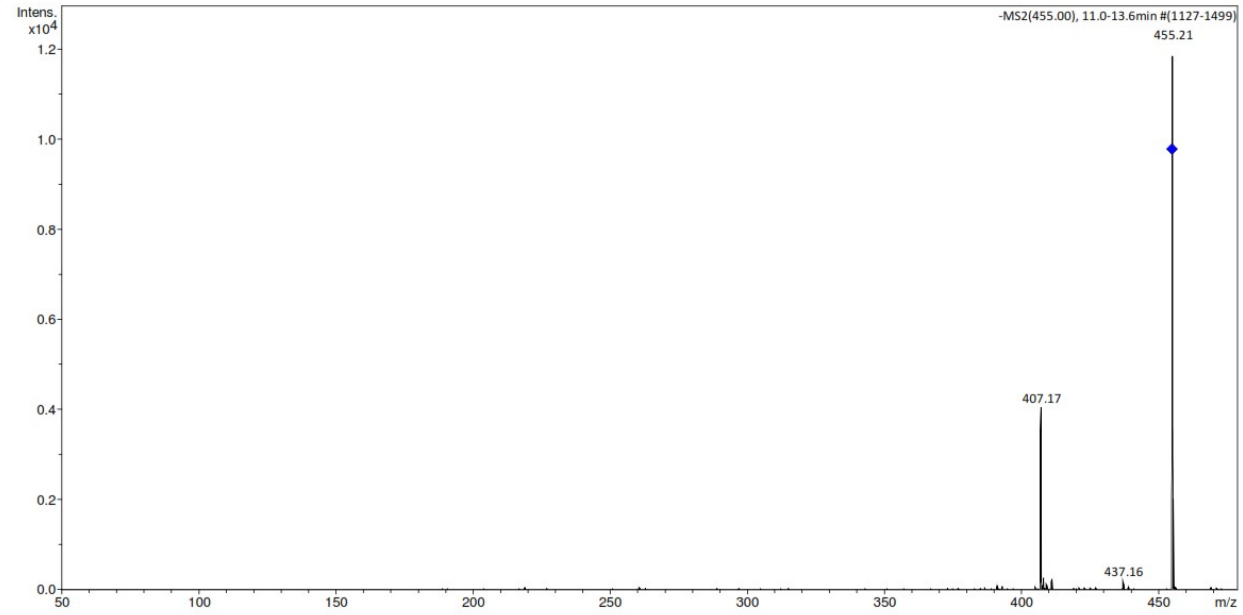

Appendix 12b: HRESI-MS of CZ-A

Generic Display Report

Analysis Info

Acquisition Date	27/06/2018 13:44:55		
Analysis Name	D:\MZ\maXis_data\Kaehlig_1806\CZ_A1_maXis_nHRESIMS.d		
Method	tune_low_MS_Service_06_18_neg.m	Operator	msc
Sample Name	CZ A1	Instrument	maXis
Comment	Kaehlig/Krenn/Zehl Ergebnis: +/- 2ppm ACN/MeOH + 1% H2O		

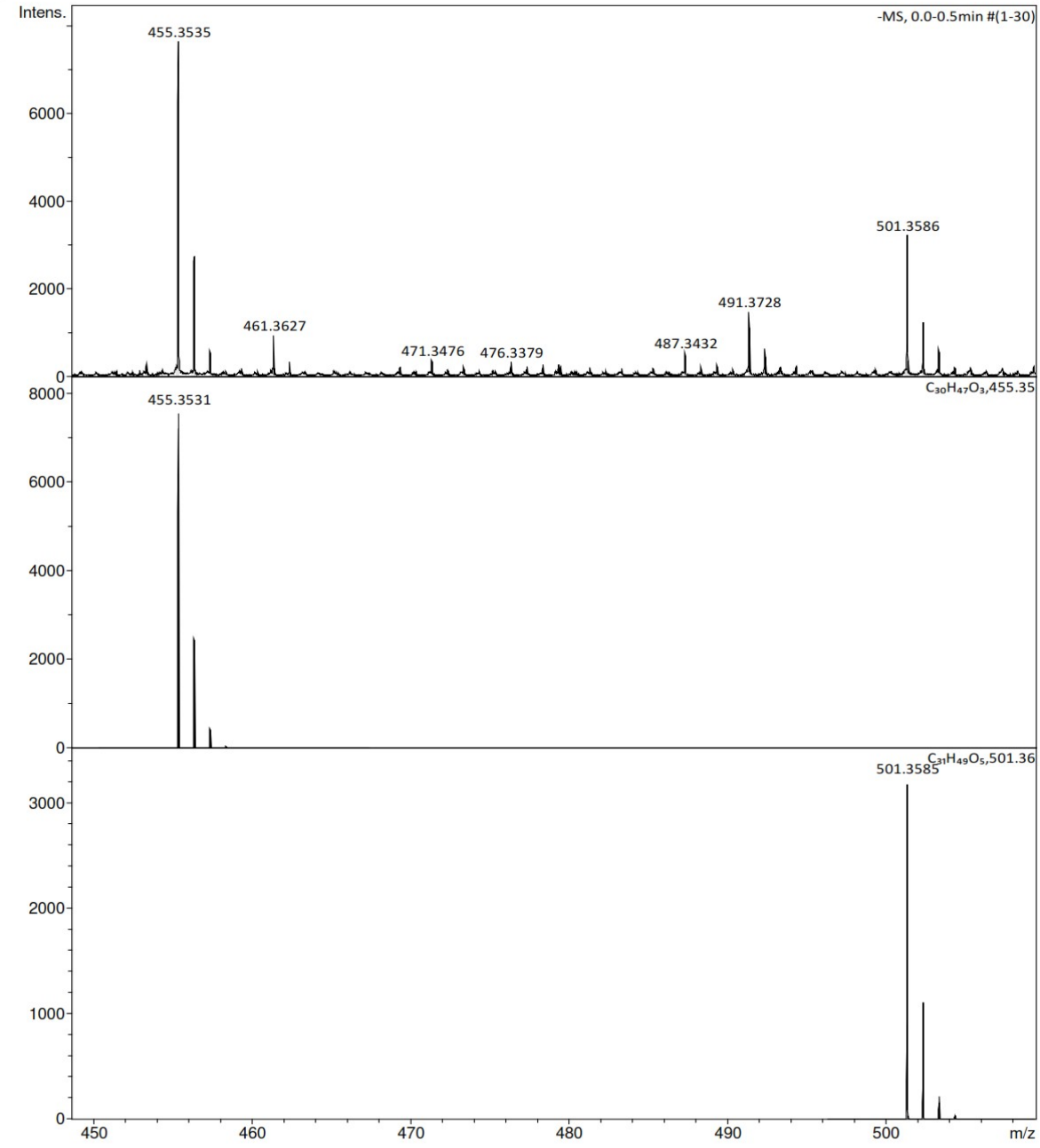

Bruker Compass DataAnalysis 4.1 printed: 14/05/2019 18:52:55 by: MSC Page 1 of 1

Mass Spectrum SmartFormula Report

Analysis Info

		Acquisition Date	27/06/2018 13:44:55	
Analysis Name	D:\MZ\maXis_data\Kaehlig_1806\CZ_A1_maXis_nHRESIMS.d			
Method	tune_low_MS_Service_06_18_neg.m	Operator	msc	
Sample Name	CZ A1	Instrument	maXis	255552.00016
Comment	Kaehlig/Krenn/Zehl Ergebnis: +/- 2ppm ACN/MeOH + 1% H2O			

Acquisition Parameter

Source Type	ESI	Ion Polarity	Negative	Set Nebulizer	0.4 Bar
Focus	Not active	Set Capillary	4500 V	Set Dry Heater	180 °C
Scan Begin	50 m/z	Set End Plate Offset	-500 V	Set Dry Gas	4.0 l/min
Scan End	1900 m/z	n/a	n/a	Set Divert Valve	Source
		Set Corona	0 nA	Set APCI Heater	0 °C

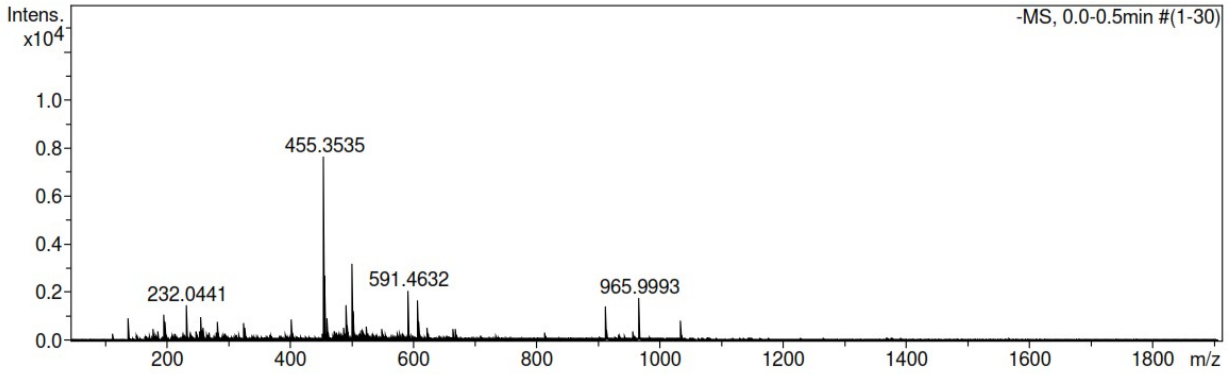

Meas. m/z	#	Ion Formula	Score	m/z	err [mDa]	err [ppm]	mSigma	rdb	e⁻ Conf	N-Rule
455.353509	1	C30H47O3	100.00	455.353069	-0.4	-1.0	17.4	7.5	even	ok
501.358638	1	C31H49O5	100.00	501.358548	-0.1	-0.2	72.5	7.5	even	ok

Generic Display Report

Analysis Info

		Acquisition Date	27/06/2018 12:54:08
Analysis Name	D:\MZ\maXis_data\Kaehlig_1806\CZ_A1_maXis_pHRESIMS.d		
Method	tune_low_MS_Service_06_18.m	Operator	msc
Sample Name	CZ A1	Instrument	maXis
Comment	Kaehlig/Krenn/Zehl Ergebnis: +/- 2ppm ACN/MeOH + 1% H2O		

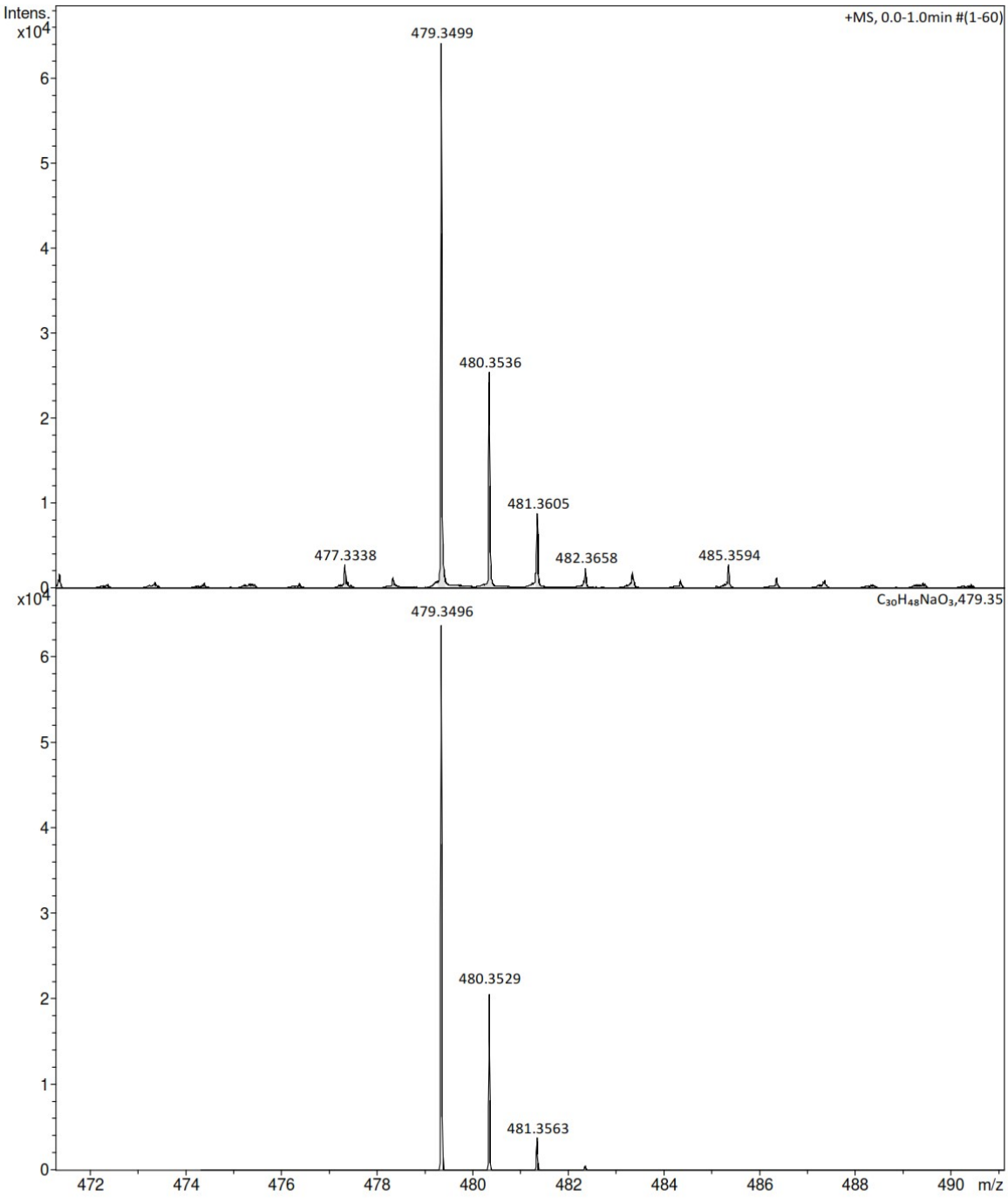

Mass Spectrum SmartFormula Report

Analysis Info

Acquisition Date	27/06/2018 12:54:08		
Analysis Name	D:\MZ\maXis_data\Kaehlig_1806\CZ_A1_maXis_pHRESIMS.d		
Method	tune_low_MS_Service_06_18.m	Operator	msc
Sample Name	CZ A1	Instrument	maXis 255552.00016
Comment	Kaehlig/Krenn/Zehl Ergebnis: +/- 2ppm ACN/MeOH + 1% H2O		

Acquisition Parameter

Source Type	ESI	Ion Polarity	Positive	Set Nebulizer	0.4 Bar
Focus	Not active	Set Capillary	4500 V	Set Dry Heater	180 °C
Scan Begin	50 m/z	Set End Plate Offset	-500 V	Set Dry Gas	4.0 l/min
Scan End	1900 m/z	n/a	n/a	Set Divert Valve	Source
		Set Corona	0 nA	Set APCI Heater	0 °C

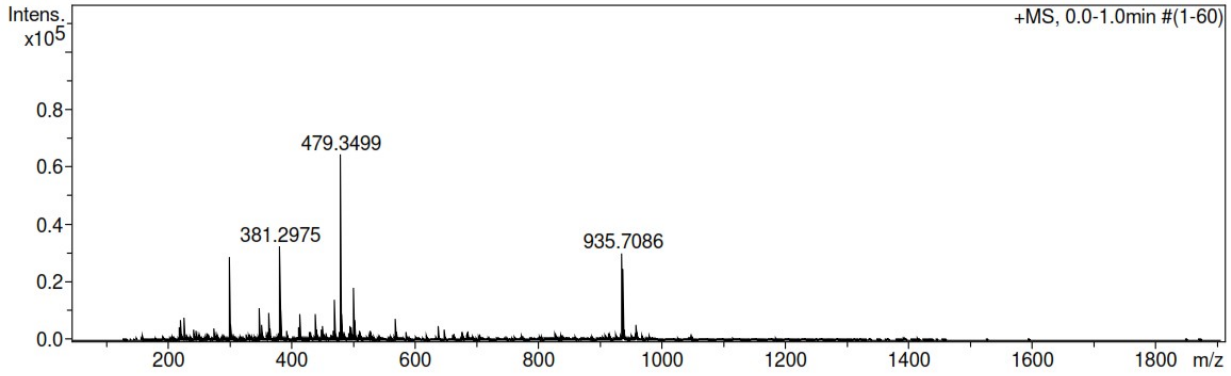

Meas. m/z	#	Ion Formula	Score	m/z	err [mDa]	err [ppm]	mSigma	rdb	e⁻ Conf	N-Rule
479.349889	1	C30H48NaO3	100.00	479.349566	-0.3	-0.7	52.9	6.5	even	ok

Appendix 13: 1D and 2D NMR of CZ-A

Appendix 13a: ^{1}H NMR of CZ-A

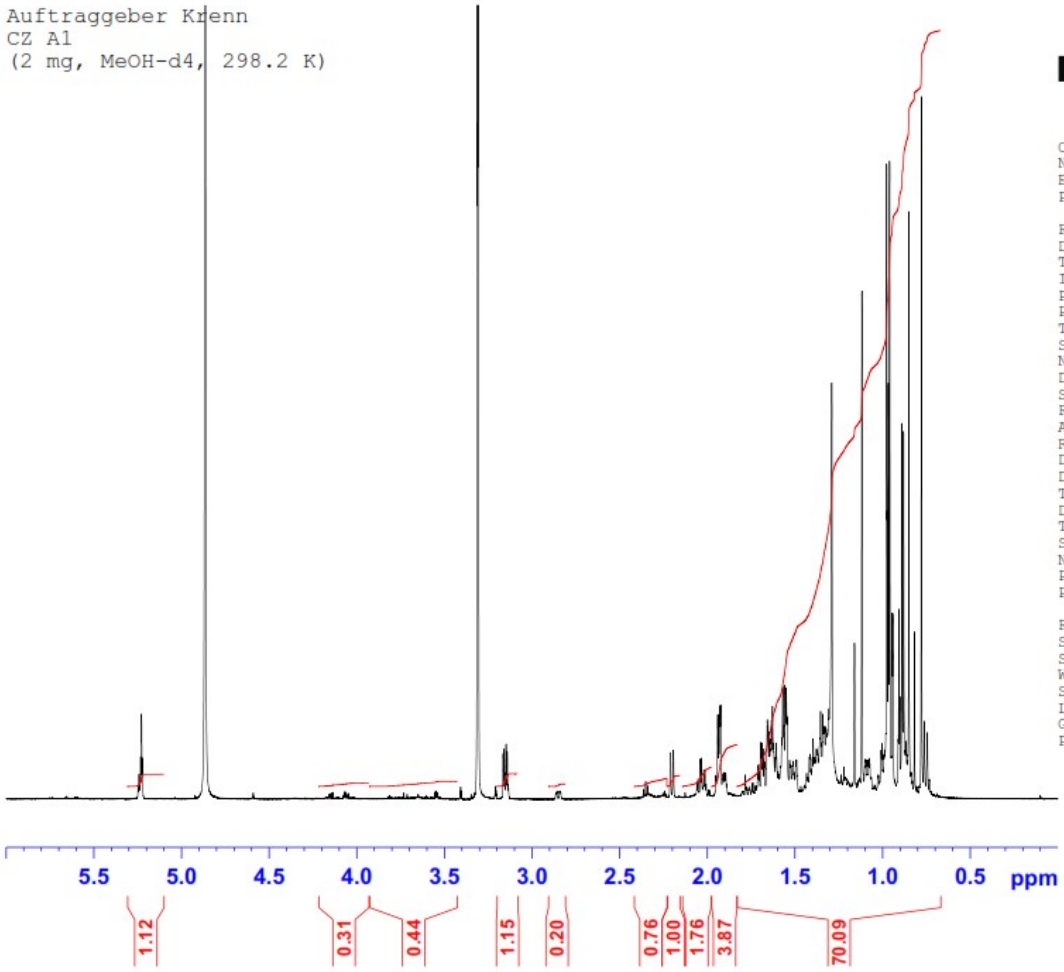

BRUKER

```
Current Data Parameters
NAME       hk7_180621_kr
EXPNO                  1
PROCNO                 1

F2 - Acquisition Parameters
Date_           20180621
Time              17.20 h
INSTRUM            spect
PROBHD   Z122896_0005 (
PULPROG             zg30
TD                 70026
SOLVENT             MeOD
NS                   128
DS                     0
SWH           6313.131 Hz
FIDRES        0.180308 Hz
AQ            5.5460591 sec
RG                  7.88
DW                79.200 usec
DE                10.00 usec
TE                298.2 K
D1          1.00000000 sec
TD0                    1
SFO1        700.4028016 MHz
NUC1                  1H
P1                  9.49 usec
PLW1        8.00000000 W

F2 - Processing parameters
SI                262144
SF          700.4000134 MHz
WDW                   EM
SSB       0
LB                 0.10 Hz
GB        0
PC                 1.00
```

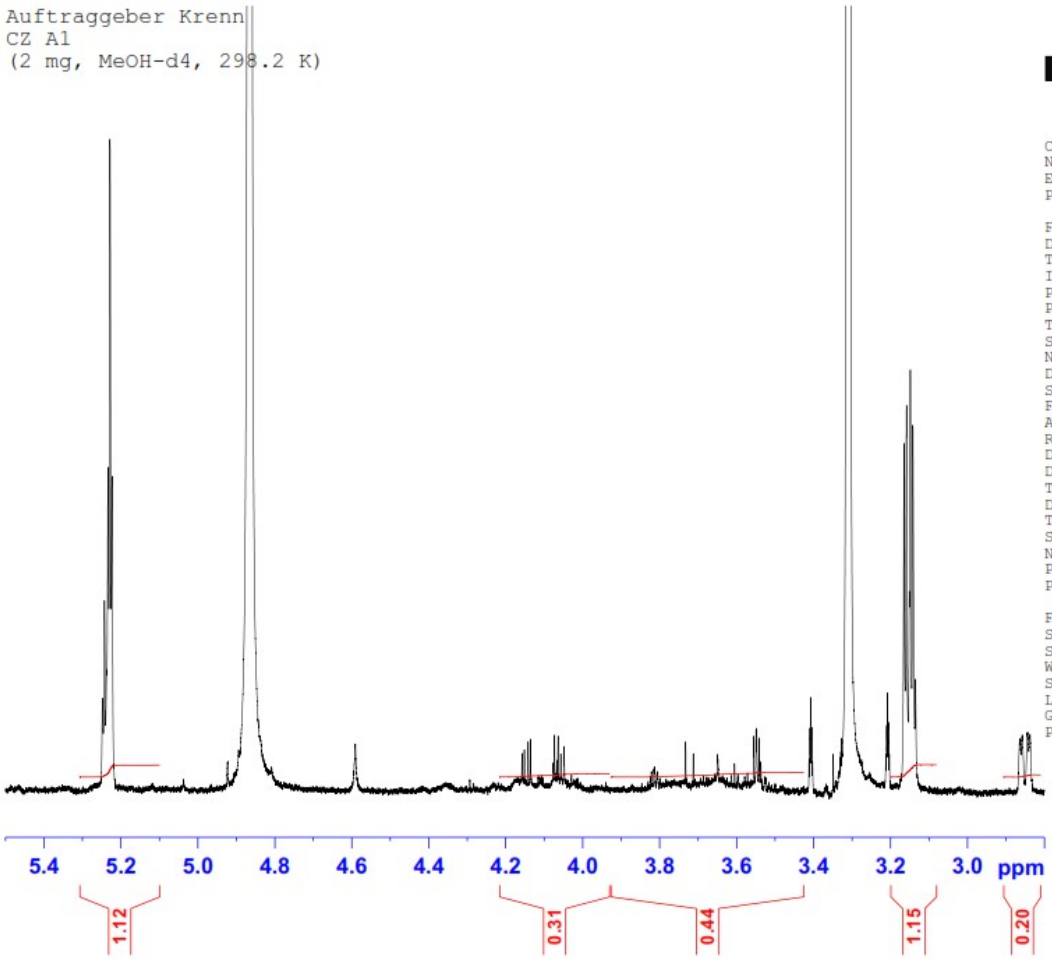

BRUKER

```
Current Data Parameters
NAME       hk7_180621_kr
EXPNO                  1
PROCNO                 1

F2 - Acquisition Parameters
Date_           20180621
Time              17.20 h
INSTRUM            spect
PROBHD   Z122896_0005 (
PULPROG            zg30
TD                70026
SOLVENT            MeOD
NS                  128
DS                    0
SWH            6313.131 Hz
FIDRES        0.180308 Hz
AQ            5.5460591 sec
RG                 7.88
DW               79.200 usec
DE               10.00 usec
TE               298.2 K
D1           1.00000000 sec
TD0                   1
SFO1        700.4028016 MHz
NUC1                1H
P1                9.49 usec
PLW1         8.00000000 W

F2 - Processing parameters
SI                262144
SF          700.4000134 MHz
WDW                 EM
SSB       0
LB             0.10 Hz
GB        0
PC             1.00
```

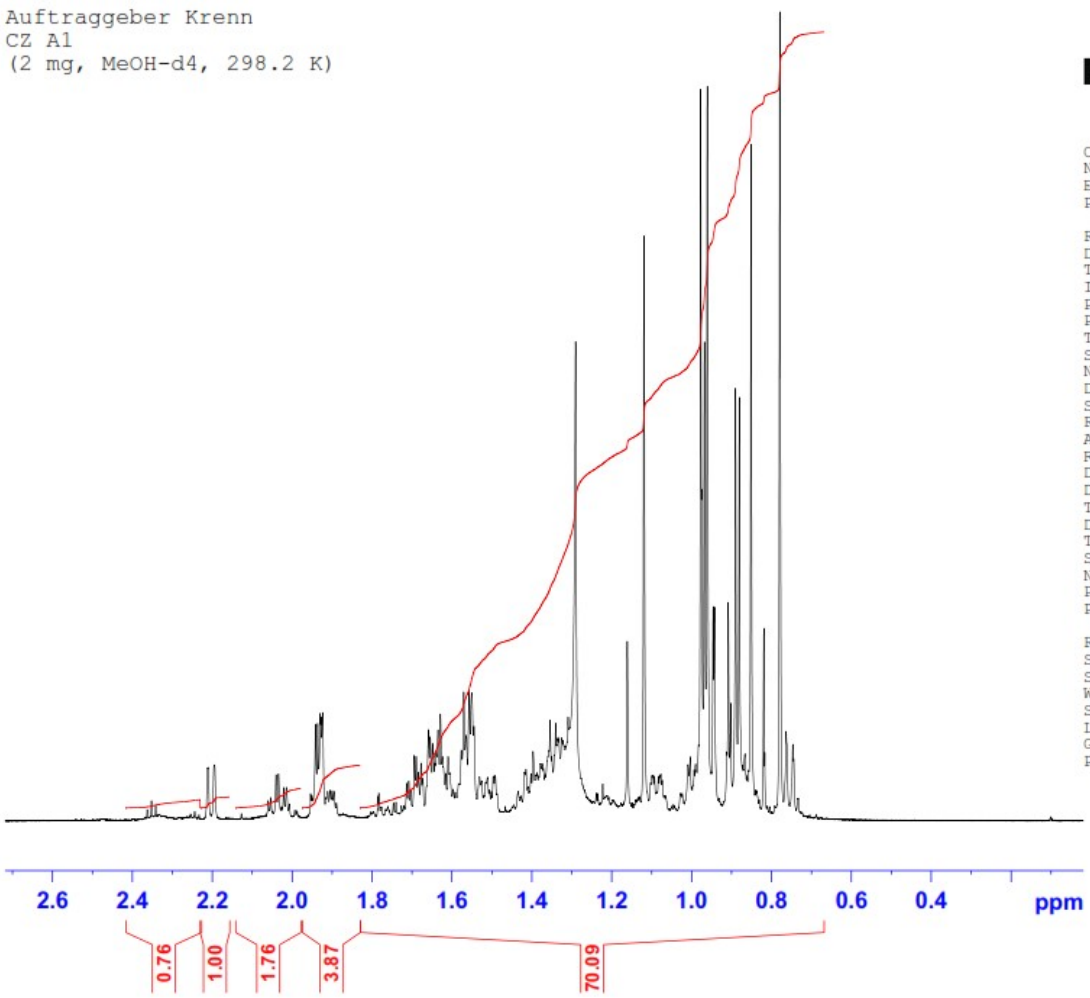

BRUKER

```
Current Data Parameters
NAME       hk7_180621_kr
EXPNO                  1
PROCNO                 1

F2 - Acquisition Parameters
Date_           20180621
Time              17.20 h
INSTRUM            spect
PROBHD   Z122896_0005 (
PULPROG             zg30
TD                 70026
SOLVENT             MeOD
NS                   128
DS                     0
SWH             6313.131 Hz
FIDRES          0.180308 Hz
AQ              5.5460591 sec
RG                  7.88
DW                79.200 usec
DE                10.00 usec
TE                298.2 K
D1             1.00000000 sec
TD0                    1
SFO1          700.4028016 MHz
NUC1                  1H
P1                  9.49 usec
PLW1           8.00000000 W

F2 - Processing parameters
SI                262144
SF          700.4000134 MHz
WDW                   EM
SSB       0
LB                0.10 Hz
GB        0
PC                1.00
```

Appendix 13b: ^{13}C NMR of CZ-A

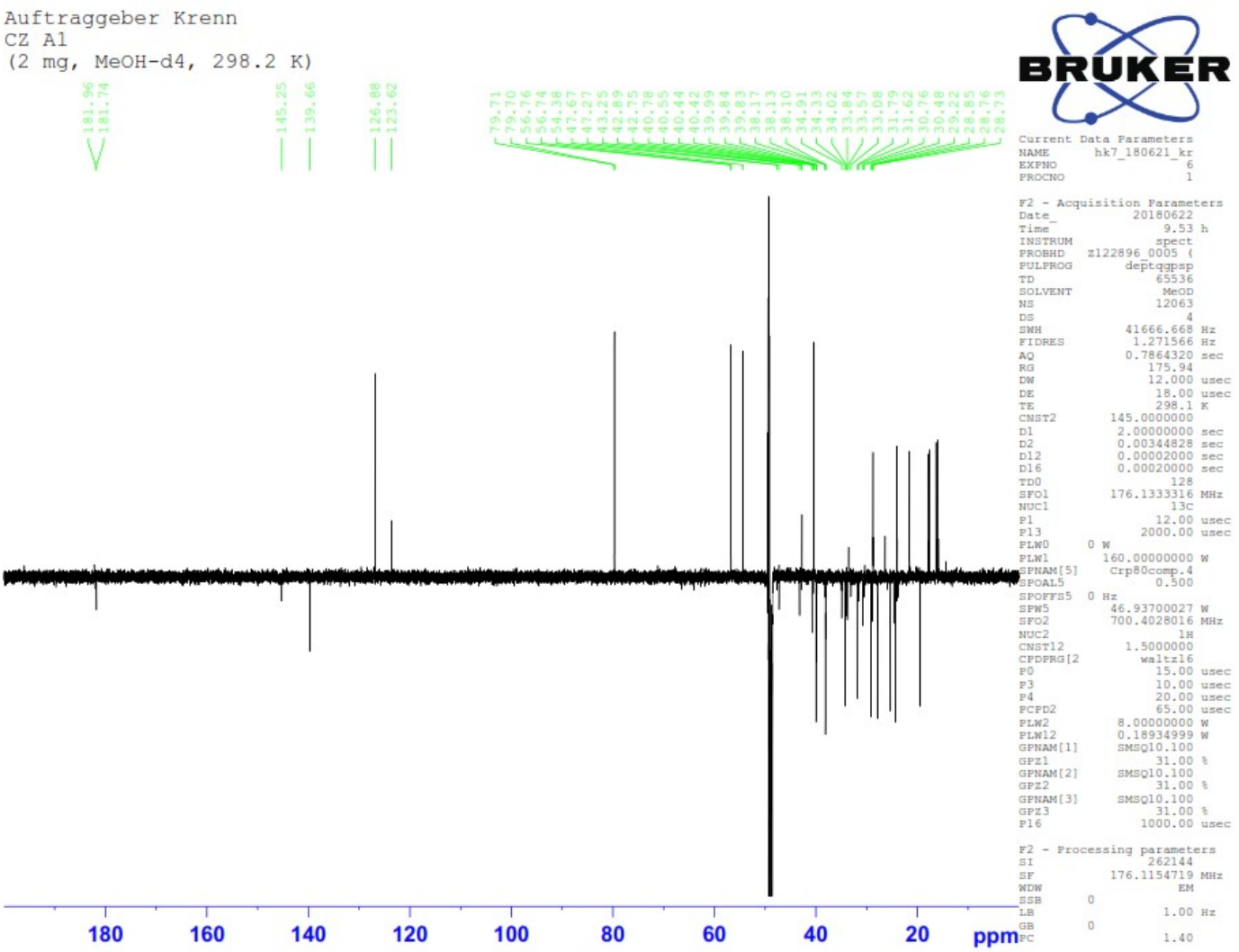

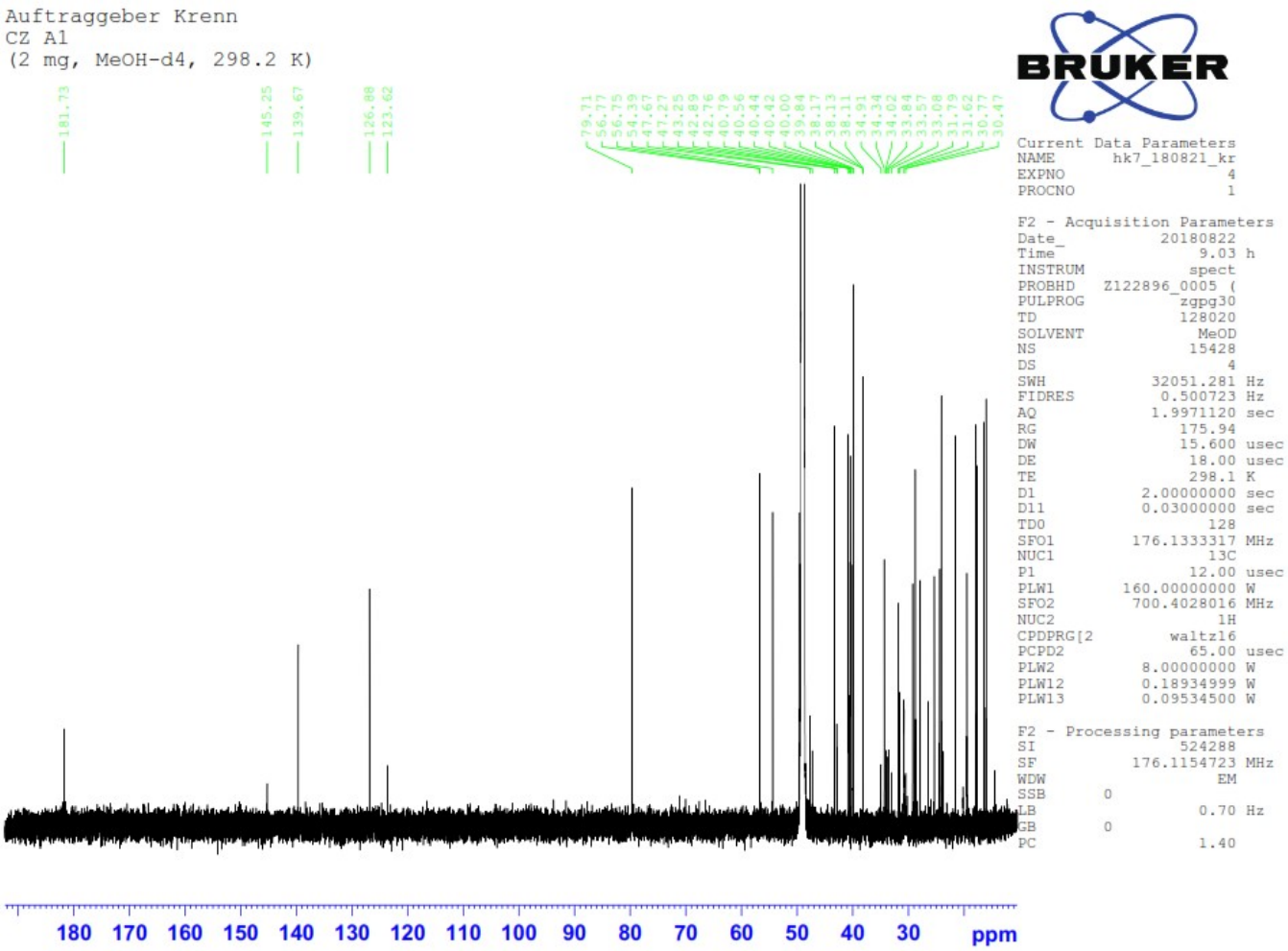
Auftraggeber Krenn
CZ A1
(2 mg, MeOH-d4, 298.2 K)
181.73
145.25
139.67
126.88
123.62
79.71
56.77
56.75
54.39
47.67
47.27
43.25
42.89
42.76
40.79
40.56
40.44
40.42
40.00
39.84
38.17
38.13
38.11
34.91
34.34
34.02
33.84
33.57
33.08
31.79
31.62
30.77
30.47
BRUKER
Current Data Parameters
NAME hk7_180821_kr
EXPNO 4
PROCNO 1
F2 - Acquisition Parameters
Date_ 20180822
Time 9.03 h
INSTRUM spect
PROBHD Z122896_0005 (
PULPROG zgpg30
TD 128020
SOLVENT MeOD
NS 15428
DS 4
SWH 32051.281 Hz
FIDRES 0.500723 Hz
AQ 1.9971120 sec
RG 175.94
DW 15.600 usec
DE 18.00 usec
TE 298.1 K
D1 2.00000000 sec
D11 0.03000000 sec
TD0 128
SFO1 176.1333317 MHz
NUC1 13C
P1 12.00 usec
PLW1 160.00000000 W
SFO2 700.4028016 MHz
NUC2 1H
CPDPRG[2 waltz16
PCPD2 65.00 usec
PLW2 8.00000000 W
PLW12 0.18934999 W
PLW13 0.09534500 W
F2 - Processing parameters
SI 524288
SF 176.1154723 MHz
WDW EM
SSB 0
LB 0.70 Hz
GB 0
PC 1.40
180 170 160 150 140 130 120 110 100 90 80 70 60 50 40 30 ppm

Auftraggeber Krenn
CZ A1
(2 mg, MeOH-d4, 298.2 K)

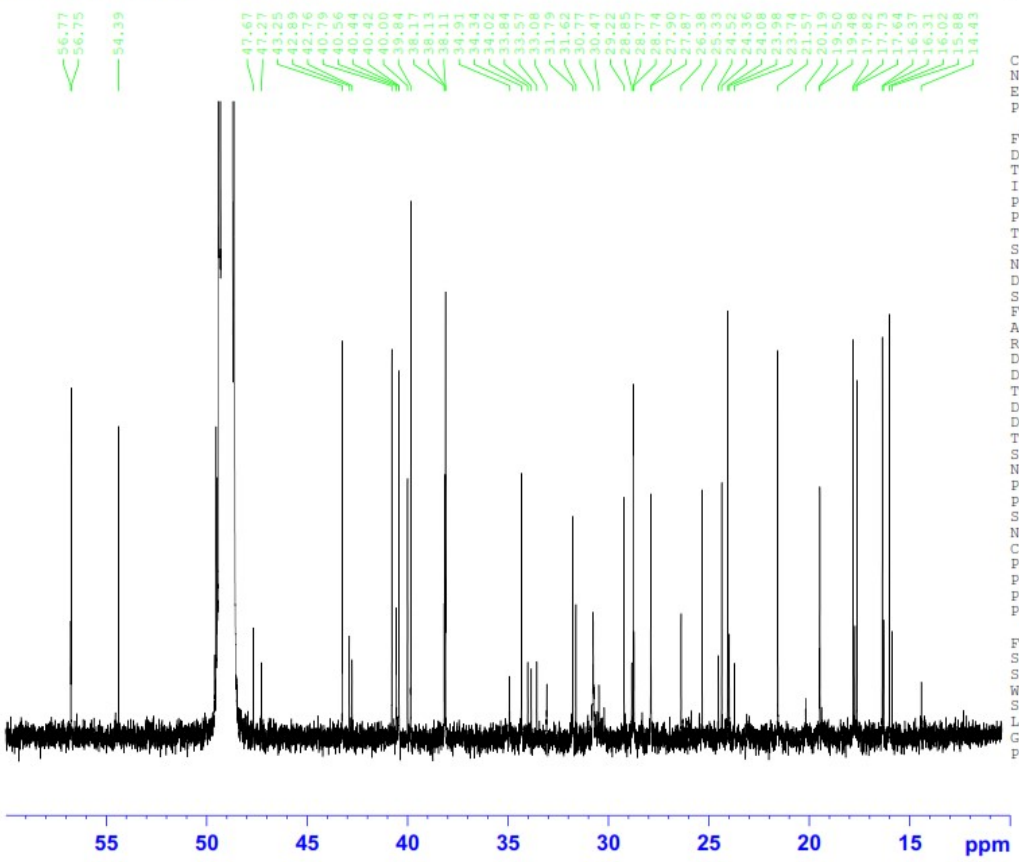

Current Data Parameters
NAME hk7_180821_kr
EXPNO 4
PROCNO 1

F2 - Acquisition Parameters

Date_	20180822	
Time	9.03	h
INSTRUM	spect	
PROBHD	Z122896_0005 (	
PULPROG	zgpg30	
TD	128020	
SOLVENT	MeOD	
NS	15428	
DS	4	
SWH	32051.281	Hz
FIDRES	0.500723	Hz
AQ	1.9971120	sec
RG	175.94	
DW	15.600	usec
DE	18.00	usec
TE	298.1	K
D1	2.00000000	sec
D11	0.03000000	sec
TD0	128	
SFO1	176.1333317	MHz
NUC1	13C	
P1	12.00	usec
PLW1	160.00000000	W
SFO2	700.4028016	MHz
NUC2	1H	
CPDPRG[2	waltz16	
PCPD2	65.00	usec
PLW2	8.00000000	W
PLW12	0.18934999	W
PLW13	0.09534500	W

F2 - Processing parameters

SI	524288	
SF	176.1154723	MHz
WDW	EM	
SSB	0	
LB	0.70	Hz
GB	0	
PC	1.40	

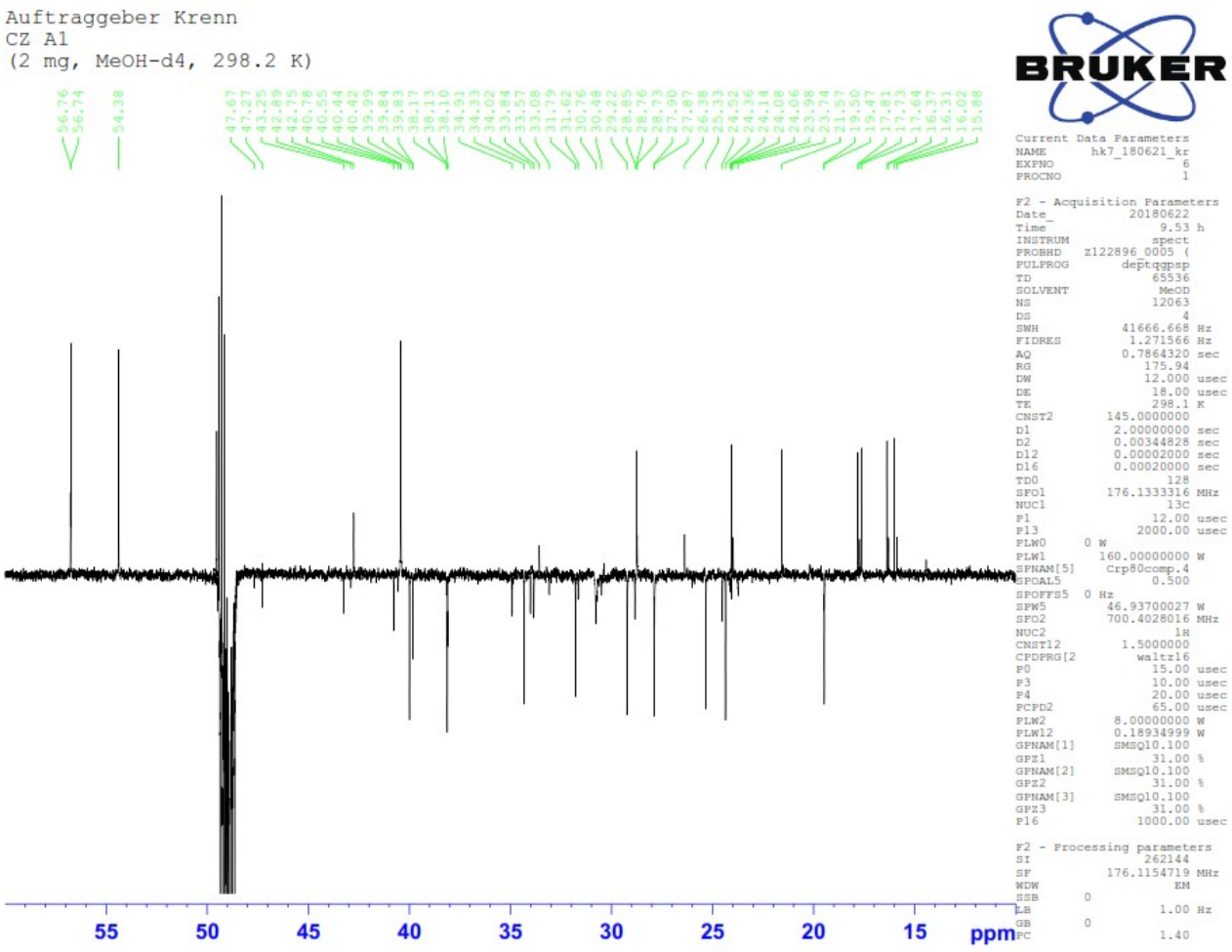
Auftraggeber Krenn
CZ A1
(2 mg, MeOH-d4, 298.2 K)
56.76
56.74
54.38
47.67
47.27
43.25
42.89
42.75
40.78
40.55
40.44
40.42
39.99
39.84
39.83
38.17
38.13
38.10
34.91
34.33
34.02
33.84
33.57
33.08
31.79
31.62
30.76
30.48
29.22
28.85
28.76
28.73
27.90
27.87
26.38
25.33
24.52
24.36
24.14
24.08
24.06
23.98
23.74
21.57
19.50
19.47
17.81
17.73
17.64
16.37
16.31
16.02
15.88
55
50
45
40
35
30
25
20
15
ppm
Current Data Parameters
NAME hk7_180621_kr
EXPNO 6
PROCNO 1
F2 - Acquisition Parameters
Date_ 20180622
Time 9.53 h
INSTRUM spect
PROBHD z122896_0005 (
PULPROG deptqgpsp
TD 65536
SOLVENT MeOD
NS 12063
DS 4
SWH 41666.668 Hz
FIDRES 1.271566 Hz
AQ 0.7864320 sec
RG 175.94
DW 12.000 usec
DE 18.00 usec
TE 298.1 K
CNST2 145.0000000
D1 2.00000000 sec
D2 0.00344828 sec
D12 0.00002000 sec
D16 0.00020000 sec
TD0 128
SFO1 176.1333316 MHz
NUC1 13c
P1 12.00 usec
P13 2000.00 usec
PLW0 0 W
PLW1 160.00000000 W
SPNAM[5] Crp80comp.4
SPOAL5 0.500
SPOFFS5 0 Hz
SPW5 46.93700027 W
SFO2 700.4028016 MHz
NUC2 1H
CNST12 1.5000000
CPDPRG[2 waltz16
P0 15.00 usec
P3 10.00 usec
P4 20.00 usec
PCPD2 65.00 usec
PLW2 8.00000000 W
PLW12 0.18934999 W
GPNAM[1] SMSQ10.100
GPZ1 31.00 %
GPNAM[2] SMSQ10.100
GPZ2 31.00 %
GPNAM[3] SMSQ10.100
GPZ3 31.00 %
P16 1000.00 usec
F2 - Processing parameters
SI 262144
SF 176.1154719 MHz
WDW EM
SSB 0
LB 1.00 Hz
GB 0
PC 1.40

Appendix 13c: COSY of CZ-A

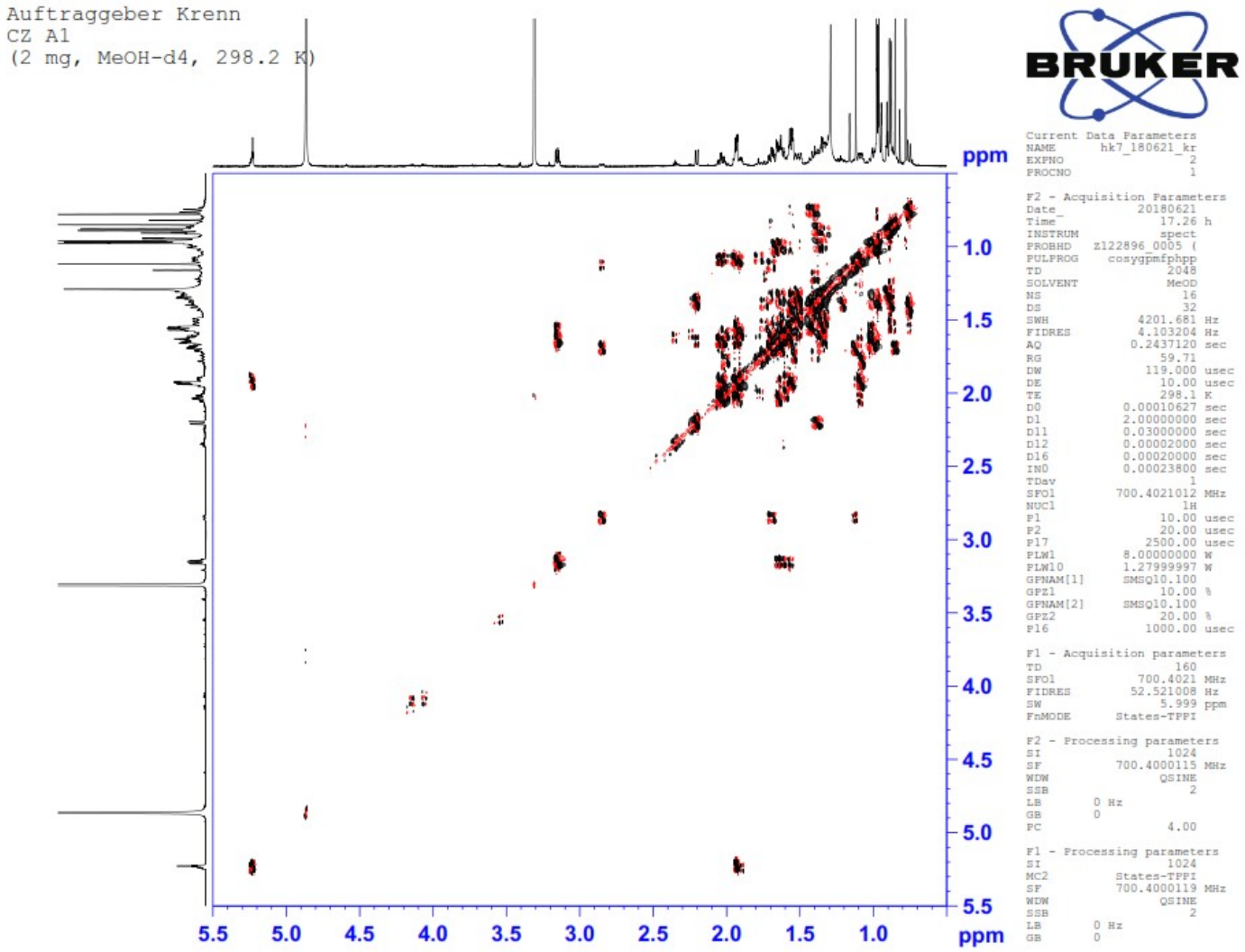

Appendix 13d: HMBC of CZ-A

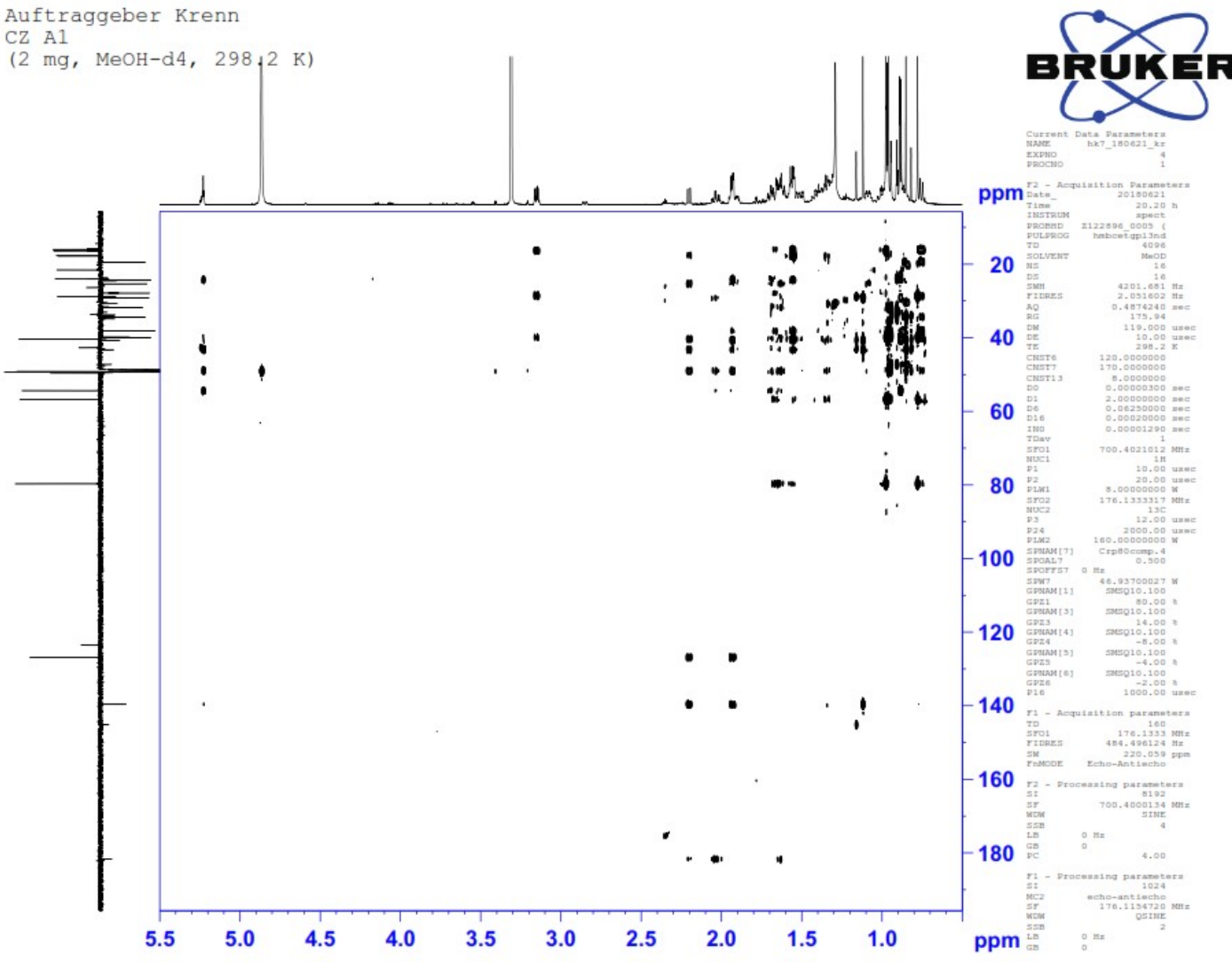

Appendix 13e: HSQC of CZ-A

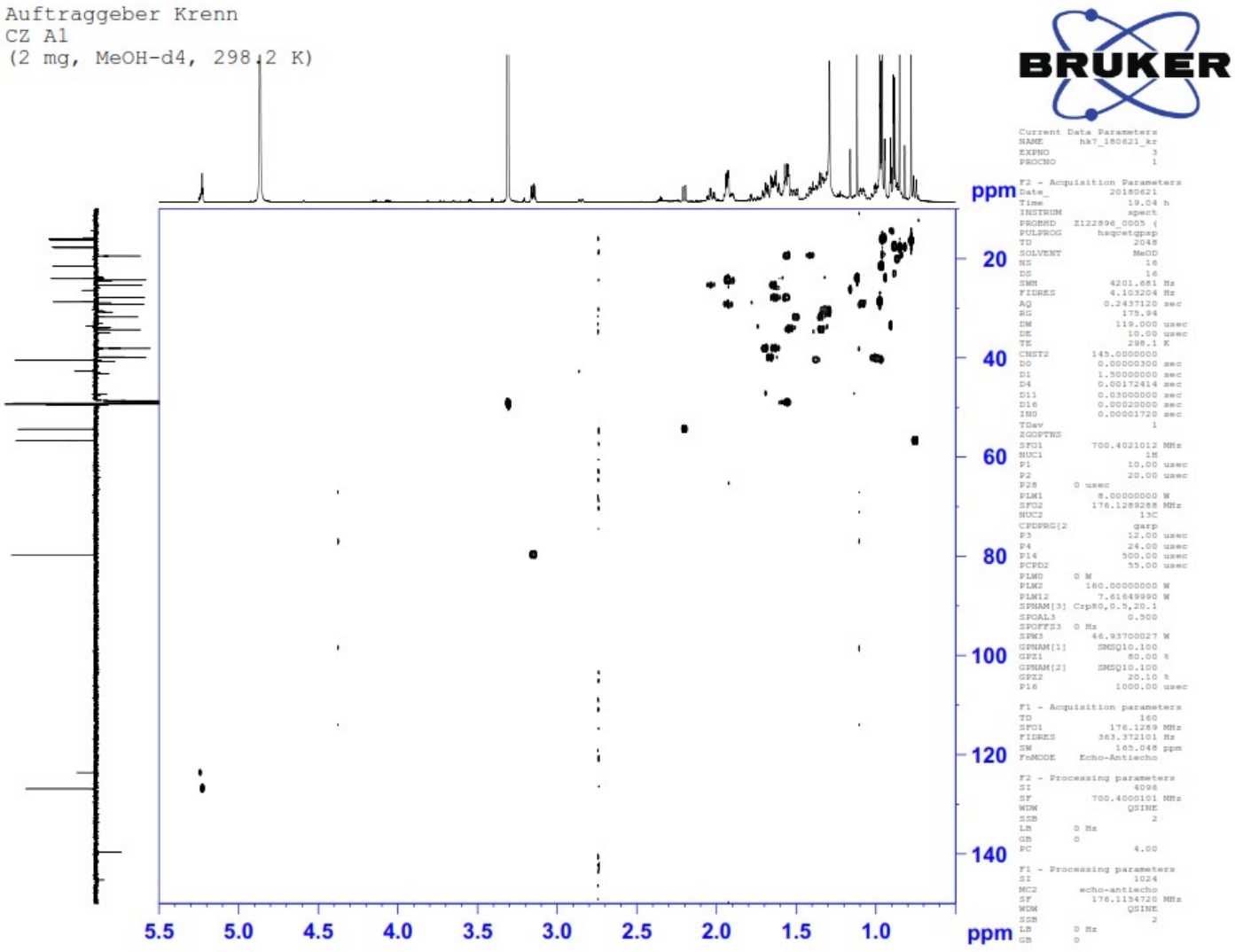

Appendix 13f: NOESY of CZ-A

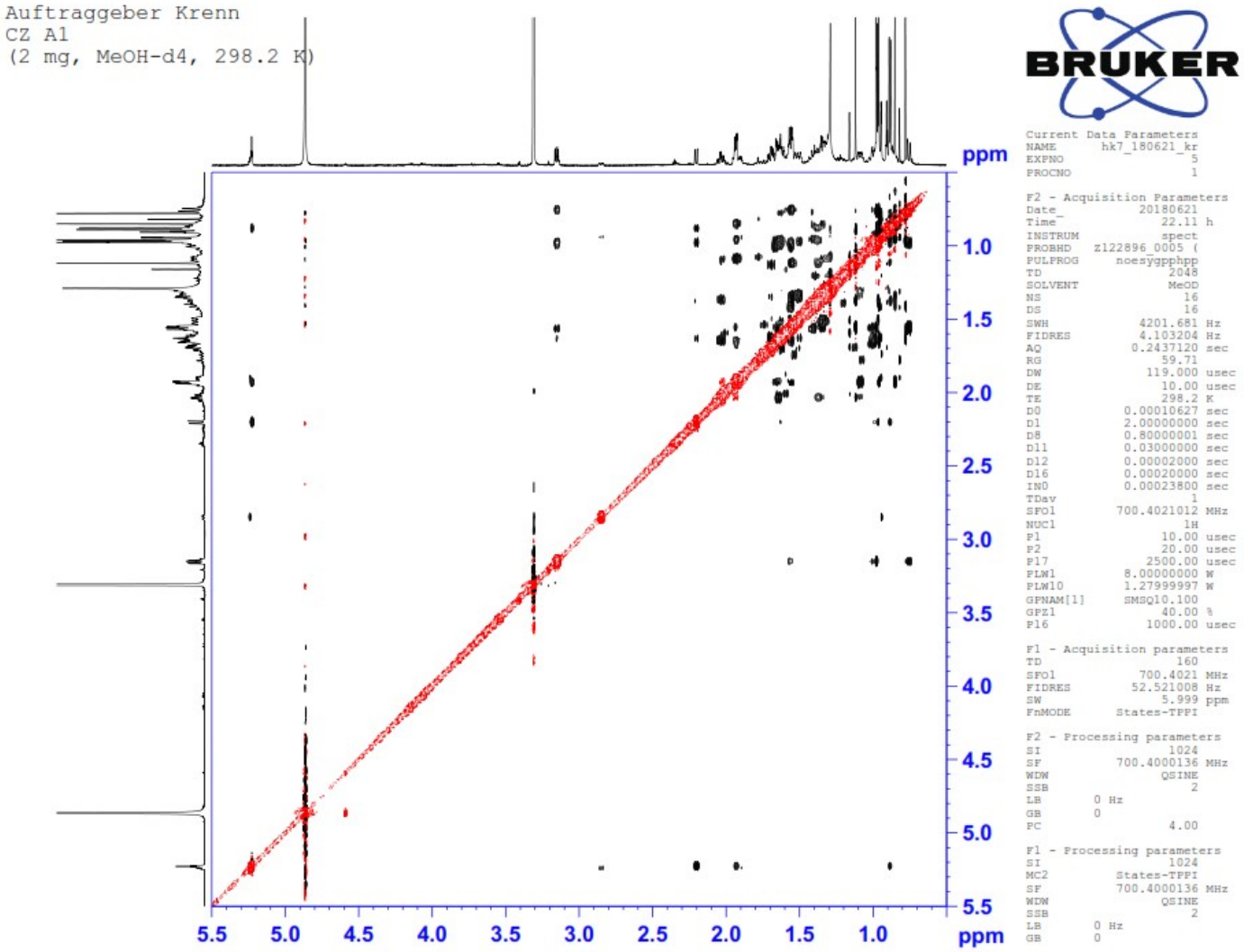

Appendix 14: Statistical analysis details of extracts, fractions and isolated compounds

Madecassic acid vs abscisic acid (D10 strain)

Table Analyzed	D10 strain
Column B	AA
vs.	vs.
Column A	MA
Wilcoxon matched-pairs signed rank test	
P value	0.0469
Exact or approximate P value?	Exact
P value summary	*
Significantly different (P < 0.05)?	Yes
One- or two-tailed P value?	Two-tailed
Sum of positive, negative ranks	26 , -2
Sum of signed ranks (W)	24
Number of pairs	7
Median of differences	
Median	16.79
How effective was the pairing?	
rs (Spearman)	0.9286
P value (one tailed)	0.0034
P value summary	**
Was the pairing significantly effective?	Yes

Madecassic acid vs arjungenin (D10 strain)

Table Analyzed	D10 strain
Column C	AR
vs.	vs.
Column A	MA
Wilcoxon matched-pairs signed rank test	
P value	0.3750
Exact or approximate P value?	Exact
P value summary	ns
Significantly different (P < 0.05)?	No
One- or two-tailed P value?	Two-tailed
Sum of positive, negative ranks	20 , -8
Sum of signed ranks (W)	12
Number of pairs	7
Median of differences	
Median	3.772
How effective was the pairing?	
rs (Spearman)	0.9643
P value (one tailed)	0.0014
P value summary	**
Was the pairing significantly effective?	Yes

Madecassic acid vs CR-A (D10 strain)

Table Analyzed	D10 strain
Column D	CR-A
vs.	vs.
Column A	MA
Wilcoxon matched-pairs signed rank test	
P value	0.2188
Exact or approximate P value?	Exact
P value summary	ns
Significantly different (P < 0.05)?	No
One- or two-tailed P value?	Two-tailed
Sum of positive, negative ranks	22 , -6
Sum of signed ranks (W)	16
Number of pairs	7
Median of differences	
Median	3.691
How effective was the pairing?	
rs (Spearman)	0.9643
P value (one tailed)	0.0014
P value summary	**
Was the pairing significantly effective?	Yes

Madecassic acid vs CR-C (D10 strain)

Table Analyzed	D10 strain
Column E	CR-C
vs.	vs.
Column A	MA
Wilcoxon matched-pairs signed rank test	
P value	0.2188
Exact or approximate P value?	Exact
P value summary	ns
Significantly different (P < 0.05)?	No
One- or two-tailed P value?	Two-tailed
Sum of positive, negative ranks	22 , -6
Sum of signed ranks (W)	16
Number of pairs	7
Median of differences	
Median	4.701
How effective was the pairing?	
rs (Spearman)	0.9643
P value (one tailed)	0.0014
P value summary	**
Was the pairing significantly effective?	Yes

Madecassic acid vs CR-H (D10 strain)

Table Analyzed	D10 strain
Column F	CR-H
vs.	vs.
Column A	MA
Wilcoxon matched-pairs signed rank test	
P value	0.0781
Exact or approximate P value?	Exact
P value summary	ns
Significantly different (P < 0.05)?	No
One- or two-tailed P value?	Two-tailed
Sum of positive, negative ranks	25 , -3
Sum of signed ranks (W)	22
Number of pairs	7
Median of differences	
Median	9.64
How effective was the pairing?	
rs (Spearman)	0.9286
P value (one tailed)	0.0034
P value summary	**
Was the pairing significantly effective?	Yes

Madecassic acid vs abscisic acid (W2 strain)

Table Analyzed	W2 strain
Column B	AA
vs.	vs.
Column A	MA
Wilcoxon matched-pairs signed rank test	
P value	0.0156
Exact or approximate P value?	Exact
P value summary	*
Significantly different (P < 0.05)?	Yes
One- or two-tailed P value?	Two-tailed
Sum of positive, negative ranks	28 , 0
Sum of signed ranks (W)	28
Number of pairs	7
Median of differences	
Median	32.74
How effective was the pairing?	
rs (Spearman)	0.8929
P value (one tailed)	0.0062
P value summary	**
Was the pairing significantly effective?	Yes

Madecassic acid vs arjungenin (W2 strain)

Table Analyzed	W2 strain
Column C	AR
vs.	vs.
Column A	MA
Wilcoxon matched-pairs signed rank test	
P value	0.0156
Exact or approximate P value?	Exact
P value summary	*
Significantly different (P < 0.05)?	Yes
One- or two-tailed P value?	Two-tailed
Sum of positive, negative ranks	28 , 0
Sum of signed ranks (W)	28
Number of pairs	7
Median of differences	
Median	18.1
How effective was the pairing?	
rs (Spearman)	0.9643
P value (one tailed)	0.0014
P value summary	**
Was the pairing significantly effective?	Yes

Madecassic acid vs CR-A (W2 strain)

Table Analyzed	W2 strain
Column D	CR-A
vs.	vs.
Column A	MA
Wilcoxon matched-pairs signed rank test	
P value	0.0156
Exact or approximate P value?	Exact
P value summary	*
Significantly different (P < 0.05)?	Yes
One- or two-tailed P value?	Two-tailed
Sum of positive, negative ranks	28 , 0
Sum of signed ranks (W)	28
Number of pairs	7
Median of differences	
Median	6.209
How effective was the pairing?	
rs (Spearman)	0.8571
P value (one tailed)	0.0119
P value summary	*
Was the pairing significantly effective?	Yes

Madecassic acid vs CR-C (W2 strain)

Table Analyzed	W2 strain
Column E	CR-C
vs.	vs.
Column A	MA
Wilcoxon matched-pairs signed rank test	
P value	0.0781
Exact or approximate P value?	Exact
P value summary	ns
Significantly different (P < 0.05)?	No
One- or two-tailed P value?	Two-tailed
Sum of positive, negative ranks	25 , -3
Sum of signed ranks (W)	22
Number of pairs	7
Median of differences	
Median	14.8
How effective was the pairing?	
rs (Spearman)	0.9286
P value (one tailed)	0.0034
P value summary	**
Was the pairing significantly effective?	Yes

Madecassic acid vs CR-H (W2 strain)

Table Analyzed	W2 strain
Column F	CR-H
vs.	vs.
Column A	MA
Wilcoxon matched-pairs signed rank test	
P value	0.1094
Exact or approximate P value?	Exact
P value summary	ns
Significantly different (P < 0.05)?	No
One- or two-tailed P value?	Two-tailed
Sum of positive, negative ranks	24 , -4
Sum of signed ranks (W)	20
Number of pairs	7
Median of differences	
Median	2.114
How effective was the pairing?	
rs (Spearman)	0.8929
P value (one tailed)	0.0062
P value summary	**
Was the pairing significantly effective?	Yes

D10 strain vs W2 strain (Madecassic acid)

Table Analyzed	(D10 strain vs W2 strain)
Column B	MA (W2)
vs.	vs.
Column A	MA (D10)
Wilcoxon matched-pairs signed rank test	
P value	0.1563
Exact or approximate P value?	Exact
P value summary	ns
Significantly different (P < 0.05)?	No
One- or two-tailed P value?	Two-tailed
Sum of positive, negative ranks	5 , -23
Sum of signed ranks (W)	-18
Number of pairs	7
Median of differences	
Median	-8.141
How effective was the pairing?	
rs (Spearman)	0.8929
P value (one tailed)	0.0062
P value summary	**
Was the pairing significantly effective?	Yes

D10 strain vs W2 strain (Abscisic acid)

Table Analyzed	(D10 strain vs W2 strain)
Column D	AA (W2)
vs.	vs.
Column C	AA (D10)
Wilcoxon matched-pairs signed rank test	
P value	0.0156
Exact or approximate P value?	Exact
P value summary	*
Significantly different (P < 0.05)?	Yes
One- or two-tailed P value?	Two-tailed
Sum of positive, negative ranks	28 , 0
Sum of signed ranks (W)	28
Number of pairs	7
Median of differences	
Median	17.57
How effective was the pairing?	
rs (Spearman)	0.8214
P value (one tailed)	0.0171
P value summary	*
Was the pairing significantly effective?	Yes

D10 strain vs W2 strain (Arjungenin)

Table Analyzed	(D10 strain vs W2 strain)
Column F	AR (W2)
vs.	vs.
Column E	AR (D10)
Wilcoxon matched-pairs signed rank test	
P value	0.0313
Exact or approximate P value?	Exact
P value summary	*
Significantly different (P < 0.05)?	Yes
One- or two-tailed P value?	Two-tailed
Sum of positive, negative ranks	27 , -1
Sum of signed ranks (W)	26
Number of pairs	7
Median of differences	
Median	13.23
How effective was the pairing?	
rs (Spearman)	1
P value (one tailed)	0.0002
P value summary	***
Was the pairing significantly effective?	Yes

D10 strain vs W2 strain (CR-A)

Table Analyzed	(D10 strain vs W2 strain)
Column H	CR-A (W2)
vs.	vs.
Column G	CR-A (D10)
Wilcoxon matched-pairs signed rank test	
P value	0.4688
Exact or approximate P value?	Exact
P value summary	ns
Significantly different (P < 0.05)?	No
One- or two-tailed P value?	Two-tailed
Sum of positive, negative ranks	9 , -19
Sum of signed ranks (W)	-10
Number of pairs	7
Median of differences	
Median	-3.802
How effective was the pairing?	
rs (Spearman)	0.9286
P value (one tailed)	0.0034
P value summary	**
Was the pairing significantly effective?	Yes

D10 strain vs W2 strain (CR-C)

Table Analyzed	(D10 strain vs W2 strain)
Column J	CR-C (W2)
vs.	vs.
Column I	CR-C (D10)
Wilcoxon matched-pairs signed rank test	
P value	0.1563
Exact or approximate P value?	Exact
P value summary	ns
Significantly different (P < 0.05)?	No
One- or two-tailed P value?	Two-tailed
Sum of positive, negative ranks	23 , -5
Sum of signed ranks (W)	18
Number of pairs	7
Median of differences	
Median	1.953
How effective was the pairing?	
rs (Spearman)	0.9643
P value (one tailed)	0.0014
P value summary	**
Was the pairing significantly effective?	Yes

D10 strain vs W2 strain (CR-H)

Table Analyzed	(D10 strain vs W2 strain)
Column L	CR-H (W2)
vs.	vs.
Column K	CR-H (D10)
Wilcoxon matched-pairs signed rank test	
P value	0.0313
Exact or approximate P value?	Exact
P value summary	*
Significantly different (P < 0.05)?	Yes
One- or two-tailed P value?	Two-tailed
Sum of positive, negative ranks	1 , -27
Sum of signed ranks (W)	-26
Number of pairs	7
Median of differences	
Median	-7.883
How effective was the pairing?	
rs (Spearman)	0.9286
P value (one tailed)	0.0034
P value summary	**
Was the pairing significantly effective?	Yes

Appendix 15: Publications in research journals produced from this study